DESIGN AND SYNTHESIS OF QUINOLINE-TRIAZOLE SCHIFF BASE METAL COMPLEXES AS POTENTIAL ANTI-CANCER AGENTS

MASTER OF SCIENCE IN CHEMISTRY

MOKOENA T.P.

2023

DESIGN AND SYNTHESIS OF QUINOLINE-TRIAZOLE SCHIFF BASE METAL COMPLEXES AS POTENTIAL ANTI-CANCER AGENTS

BY

MOKOENA TERRINNE PALESA

A RESEARCH DISSERTATION SUBMITTED FOR THE DEGREE OF MASTER OF SCIENCE IN CHEMISTRY, DEPARTMENT OF CHEMISTRY, SCHOOL OF PHYSICAL AND MINERAL SCIENCES, FACULTY OF SCIENCE AND AGRICULTURE, UNIVERSITY OF LIMPOPO, SOUTH AFRICA

MASTER OF SCIENCE IN CHEMISTRY

SUPERVISOR: PROF R.M. MAMPA

CO-SUPERVISOR: DR M.M. MALULEKA

2023

DECLARATION

I declare that the “Design and synthesis of Quinoline-triazole Schiff base metal complexes as potential anti-cancer agents” hereby submitted to the University of Limpopo, for the degree of Master of Science has not previously submitted by me for a degree at this or any other university; that is my own work in design and execution, and that all material contained herein has been duly acknowledged.

…….. 25/07/2022……

Mokoena, T. P. (Ms) **Date**

DEDICATION

This study is dedicated to my mother Mrs B.T. Mokoena.

ACKNOWLEDGEMENTS

- I would like to thank My supervisors Prof R.M. Mampa and Dr M.M. Maluleka for the supporting and mentoring me throughout the course of my study.

I would also like extent my thanks and gratitude to the following:

- God Almighty, for his constant love and grace.
- The University of Limpopo for allowing me to enroll in this institution.
- The NRF-Sasol Inzalo bursary for the financial support.
- Ms T.G. Ramakadi for teaching me how to operate and to process data on the Nuclear Magnetic Resonance instrument.
- Ms L.A. Raphoko for the High-Resolution Mass spectrometry experimental data.
- Dr B. Monchusi-Khumalo for assisting with cancer experimental data
- The University of the Witwatersrand for the XRD experimental data.
- My family Busisiwe, Mahlogonolo, Tshepe, Thabo, my twin Terrence Mokoena and Theofellus Mavasa (Big Bear) for their constant support and encouragement.

SCIENTIFIC CONTRIBUTION

1. Conference contribution

Oral presentation at: 11th Faculty of Science and Agriculture, University of Limpopo, Research Day 2021

Synthesis of quinoline-1,2,3-triazole hybrids for biological evaluation against cancer

Terrinne Mokoena[1], Marole Maluleka[1], Richard Mampa[1]
University of Limpopo, Department of Chemistry, Private Bag x1106, Sovenga, 0727
e-mail address: 201605381@keyaka.ul.ac.za

Cancer is one of the leading diseases in the world and is responsible for increase in the mortality rate in the world[1]. According to the World Health Organisation (WHO), 9.6 million deaths as results of cancer have been reported in the year 2018 alone[2]. 1,2,3-Triazole derivatives have been found to possess biological activities such as anti-bacterial[3] and anti-cancer[4] properties. Quinolines, on the other hand, exhibit a wide range of biological properties including anti-inflammatory[5], anti-cancer[6] and anti-tubecular[7]. Thus, due to the biological properties of quinolines and 1,2,3-triazoles, this prompted us to synthesize quinoline-1,2,3-triazole hybrids as promising anti-cancer agents. These were achieved by initial Claisen-Schmidt aldol-condensation of 2-amino-3,5-dibromoactophenone with benzaldehyde derivatives to form 2-aminochalones. Followed by an acid mediated-cyclization reaction to form 2-substituted 2,3-dihydro-quinolin-4(*1H*)-ones, which in turn underwent dehydrogenation and oxidative aromatization to afford 2-substituted quinolin-4(*1H*) ones derivatives. The nucleophilic substitution of the latter with sodium azide yielded the 2-substituted 4-azidoquinolines, which will undergo Huisgen cycloaddition reaction to form the 2-substituted 4-triazolo-quinoline derivatives in high yields. All the synthesised compounds were confirmed using a combination of ^{1}H-NMR, ^{13}C-NMR, FT-IR, and mass spectrometry.

Keywords: Cancer, quinoline, click-chemistry, triazole

2. Publications

Spectroscopic, XRD, Hirshfeld surface and density functional theory (DFT) studies of the non-covalent interactions in 2-hydroxy-3-iodo-5-nitroacetophenone

Malose J. Mphahlele[a,*], Marole M. Maluleka[b], Terrinne P. Mokoena[b]

[a] *Department of Chemistry, College of Science, Engineering and Technology, University of South Africa, Private Bag X06, Florida, 1710, South Africa*
[b] *Department of Chemistry, Faculty of Science and Agriculture, School of Physical and Mineral Science, University of Limpopo, Private Bag X1106, Sovenga, 0727, South Africa*

ARTICLE INFO

Article history:
Received 5 May 2022
Revised 5 June 2022
Accepted 6 June 2022
Available online 07 June 2022

Keywords:
2-hydroxy-3-iodo-5-nitroacetophenone (**1**)
Crystal structure
Hirshfeld surface
Non-covalent (hydrogen & halogen) bonding
DFT study

ABSTRACT

2–hydroxy-5-nitroacetophenone (**1**) reacted with *N*-iodosuccinimide in acetic acid at room temperature to afford 2–hydroxy-3-iodo-5-nitroacetophenone (**2**). Structural elucidation was carried out using a combination of spectroscopic and single crystal X-ray diffraction (XRD) techniques complemented with DFT method. The hydroxyl proton resonates significantly downfield at δ_H = 13.80 ppm due to participation in intramolecular hydrogen bonding, which resulted in a not easy to discern low intensity infrared band located in the region of the $\nu_{(CH)}$ vibrations 2800–3000 cm^{-1}. XRD analysis confirmed the presence of a chair-like six-membered hydrogen bonded pseudo aromatic ring involving O–H···O=C interaction. Prediction model (Hirshfeld surface and 2D fingerprint model) was performed to understand the intermolecular interactions responsible for the molecular packing in the crystal of **2**.

Synthesis, crystal, and Hirschfeld surface, DFT and molecular docking studies of 6-(3–chloro-4-fluorophenyl)-4-ethoxy-2-(4-methoxyphenyl)quinazoline derivative

Marole M. Maluleka*, Terrinne P. Mokoena, Richard R. Mampa

Department of Chemistry, Faculty of Science and Agriculture, School of Physical and Mineral Science, University of Limpopo, Private Bag X1106, Sovenga 0727, South Africa

ARTICLE INFO

Article history:
Received 5 October 2021
Revised 15 January 2022
Accepted 17 January 2022
Available online 18 January 2022

Keywords:
6-(3–chloro-4-fluorophenyl)-4-ethoxy-2-(4-methoxyphenyl)quinazoline
Hirshfeld surface analysis
Suzuki cross coupling
X-ray
Molecular docking
MD simulation

ABSTRACT

The 4–chloro-6-iodo-2-(4-methoxyphenyl)quinazoline **2** undergoes nucleophilic substitution with sodium ethoxide followed by the Suzuki–Miyaura reactions to afford novel 6-(3–chloro-4-fluorophenyl)-4-ethoxy-2-(4-methoxyphenyl)quinazoline **4**. Structural elucidation was carried out using a combination of spectroscopic (NMR, IR and MS) and single crystal X-ray diffraction (XRD) techniques. Compound **4** crystallizes in monoclinic space group C2/c with crystal parameters $a = 28.116(4)$ Å, $b = 7.2267(9)$ Å, $c = 20.975(3)$ Å, $\beta = 116.727(4)°$, $V = 3806.6(8)$ Å^3 and $Z = 8$. The crystal packing is stabilized by intermolecular hydrogen bond, C–H···F, C–H···Cl, C–H···π, and π···π interactions. The halogen Cl···Cl contacts were found to be of the type I having the angles $\Theta1$ and $\Theta2 = 154°$. DFT analysis of the optimized geometry is in agreement with the solid phase results. The Hirshfeld surface was used to analyze the properties of the intermolecular interactions of **4**. The energy-framework analysis reveals that π···π and C–H···π interactions energies are mainly dispersive and are the most important forces in the crystal structure. The in-silico evaluation of compounds **4** and vandetanib with the vascular endothelial growth factor receptor-2 (VEGFR-2) was carried out. Molecular docking results showed that **4** has the most favourable binding free energy (−9.39 kcal/mol) compared with that of vandetanib (−8.31 kcal/mol). The MD simulation results reveal there is a presence of hydrogen bonds between compound **4** and the VEGFR-2 protein.

3. In preparation

3.1 Synthesis, crystal structures, spectroscopic characterization, and in vitro evaluation of the 4-sulfono-3-methoxycinnamaldehydes as potential α-glucosidase and/or α-amylase inhibitors. T.P. Mokoena, M.M. Maluleka, R.M. Mampa, M.J. Mphahlele and B.A, Monchusi. 2022. **Submitted for review in ACS Omega Journal**

3.2 Design and synthesis of quinoline-1,2,3-triazolyl hybrids as anti-cancer agents targeting VEGFR-2 receptor. Terrinne P. Mokoena, Marole M. Maluleka, Richard R. Mampa. 2022.

TABLE OF CONTENTS

LIST OF FIGURES

LIST OF SCHEMES

LIST OF TABLES

ABBREVIATIONS

A

ATP	Adenosine Triphosphate

C

$CDCl_3$	Deuterated chloroform
CDK-2	Cyclin-dependent kinase 2
CIS	Coordination Induced Shift
COSY	Homonuclear correlation spectroscopy
COX	Cyclooxygenase

D

d	doublet
dd	doublet of doublet
2D	2-dimensional
DCM	Dichloromethane
DDQ	2,3-Dichloro-5,6-dicyano-1,4-benzoquinone
DMAC	Dimethylacetamide
DMSO	Dimethyl Sulfoxide
DNA	Deoxyribonucleic acid
DPPH	1,1-diphenyl-2-picrylhydrazyl
DTBP	di-tert-butyl-peroxide

F

FDA	Food and Drug Administration
FGI	Functional group interchange
FGR	Functional group removal

FTIR Fourier Transform Infrared Spectroscopy

H

HMBC Heteronuclear Multiple Bond Correlation

HRMS High Resolution Mass Spectrometry

HSQC Heteronuclear single quantum coherence spectroscopy

I

IC_{50} 50 % Inhibitory Concentration

IR Infrared Spectroscopy

L

LNCaP Lymph Node Carcinoma of the Prostate

M

µM micro-Molar

MCF-7 Michigan Cancer Foundation-7

MDA-MB-231 M.D Anderson-Metastasis Breast cancer

MDR Multi-drug resistance

MHz Mega hertz

MIA-Pa-Ca-2 Human pancreatic carcinoma

MIC_{9O} 90 % Minimum inhibitory concentration

mp melting point

MTT assay (3-(4,5-dimethylthiazol-2-yl)-2,5-diphenyltetrazoliumbromide) tetrazolium assay

N

NAD^+ Nicotinamide Adenine Dinucleotide

NBS N-Bromosuccinimide

NCI	National Cancer Institute
$NF_{K\beta}$	Nuclear factor kappa enhancer of activated B cells
NMR	Nuclear magnetic resonance

P

PARP-1	Poly (ADP-ribose) polymerase-1
PC-3	human prostate cancer cell line
PDE-4	Phosphodiesterase-4
PEGA resin	Acrylamide-PEG Co-polymer resin
Per-6-ABCD	Per-6-amino-β-cyclodextrin
PPA	polyphosphoric acid
ppm	part per million
p-TSA	p-Toluenesulfonic acid

R

RuAAC	Ruthenium-Catalysed Azide Alkyne Cycloaddition reaction

S

SAR	Structure-activity relationship
SET	Single electron transfer

T

T47-D	Human Breast cancer cell line
TBTA	Tris(1-benzyl-4-triazolyl) methyl) amine
TFA	Trifluoroacetic acid
THF	Tetrahydrofuran
TLC	Thin-Layer Chromatography
TMC-207	Bedaquiline

TMSA	Trimethylsilyl acetylene
TRAP-assay	Telomerase Repeated Amplification Protocol
TTN	Thallium (III) nitrate
TTS	Thallium (III) p-tosylate

U

UV	Ultra-violet

Abstract

The aim of the project was to synthesize quinoline-1,2,3-triazole Schiff base hybrids as promising anti-cancer agents. A laboratory prepared 2-Amino-3,5-dibromoactophenone was subjected to Claisen-Schmidt aldol-condensation with benzaldehyde derivatives to form 2-aminochalones. The step was followed by an acid mediated-cyclization reaction to form 2-substituted 2,3-dihydro-quinolin-4(*1H*)-ones, which in turn underwent dehydrogenation and oxidative aromatization to afford 2-substituted quinolin-4(*1H*)-ones derivatives. The nucleophilic substitution of the latter with sodium azide yielded the 2-substituted 4-azidoquinolines, which underwent Huisgen cycloaddition reaction to form the 4-triazolo-quinoline derivatives in high yields and further confirmed using X-ray diffraction analysis. The 4-triazolo quinoline derivatives formed from propargyl alcohol, served as precursors for oxidation reaction to afford carbaldehyde triazolyl-quinoline derivatives, which in turn were reacted with 2-picolylamine to produce a quinoline-triazolyl Schiff base ligand derivatives in low yields through condensation reaction. The 3-fluoro-phenyl triazole derivatives were subjected to metal coordination with Ruthenium (II) p-cymene *bis*-chloride to form ruthenium arene coordinated complexes, showing a CIS in the range of δ (-0.003-0.047) ppm for ^{1}H NMR and δ (-0.058-0.010 ppm) for ^{13}C NMR. All the synthesised compounds were confirmed using a combination of ^{1}H-NMR, ^{13}C-NMR, FT-IR, and mass spectrometry. The triazolyl quinoline derivative compounds were tested against MDA-MB-231 cell line (breast cancer) here (6,8-dibromo-4-(4-(3-fluorophenyl)1H-1,2,3-triazol-1-yl)-2-(4-methoxyphenyl) quinoline **153 h** showed a good cytotoxicity effect compared to other compounds with an IC_{50} of 40.7 µM. The quinoline triazolyl compound molecular docking revealed that(6,8-dibromo-4-(4-(3-fluorophenyl)1H-1,2,3-triazol-1-yl)-2-(4-methylphenyl) quinoline **153 g** displays good binding energy of -10.9 k calmol and an inhibitory concentration of 0.80 µM against VEGFR-2 tyrosine kinase referenced to Sorafenib (standard).

Chapter 1

Introduction

1.1 Importance of heterocyclic compounds in the treatment of cancer

Cancer is one of the lethal diseases, caused by abnormal cell growths which spread across the body caused by angiogenesis, a physiological growth of blood vessels from other blood vessels [1-2]. Different strategies to treat cancer are available, such as surgical resection [3], combination-drug therapies [4], chemotherapy [5], radiotherapy [6] and the use of *in-vitro* models to understand the progression of cancer by using variation assays, for example, migration, invasion, trans-endothelial migration assays [7]. The strategies are reported to be effective whilst some are either risky or toxic i.e. affects the immune system causing the susceptibility to host other diseases [8] or expose cancer patients to experience side effects, such as memory loss/fatigue and pneumonia [6]. As a results of the rise in number of cancer deaths, scientists have been studying different heterocyclic compounds among others to develop a potential anti-cancer drug. Heterocycles are among the most studied organic compounds in chemistry, represented by joined rings (five/six membered) which may contain elements such as nitrogen (N), sulphur (S) and oxygen (O) [9], for example pyrrole [10], furan [11] and thiophene [12].

Heterocyclic compounds are prominent in medicinal chemistry and are regarded as important given the widespread reference, in literature for their biological activity against cancer [13], inflammation and many bacterial diseases [14]. There are many medicinal compounds containing heterocyclic rings that have been approved as anti-cancer agents by the FDA [15], for example 147 pyrimidine fused heterocycles are either used in clinics or are under clinical assessments, [13] such as those found in the lead compounds for the development of many methods to produce anti-cancerous drugs to date. It is against this background, that the *N*-heterocycles receive attention because of their reported biological activity [16]. 2,3-*O*-Cyclophenylidene-1,2,4-triazolyl has been reported to have anti-proliferative properties against lymphoma cell line [17]. The benzimidazole and pyrazolines derivatives, also showed an activity against 60-tumor cell lines with a good inhibitory activity, [18] such as MCF-7, T47D and HeLa cancer cell line [19].

Cancer continues to evolve, as such, causing the cancerous cell lines to be drug-resistant [20]. The drug resistivity may be due to the weight of the tumour, its heterogeneity or undruggable cancer driver outcomes due to therapeutic strategies [21]. Researchers have come up with some strategies to overcome resistance of drugs and to destroy target cells causing the proliferation of present diseases through the synthesis of multi-target drugs [22-23]. One of the strategies is through combination therapy (cocktail - drugs) where drugs that have different mechanisms target cancerous cell to reduce drug-resistance [23]. Another strategy is the synthesis of hybrid molecules through multi-scaffold, where two different moieties are combined to form a new moiety through a chemical reaction [24]. Hybrid molecules formed between two compounds are usually formed, via a linker (in a form of a chemical group) through a specific reaction mechanism[25]. In this project, we aim to form molecular hybrids of N-heterocyclic compounds that are composed of the quinoline and triazole-Schiff base moieties.

1.2 An overview of quinolines and quinoline-appended molecular hybrids with biological importance

Quinolines were first discovered in the 1960s, as a by-product of the famous chloroquine **1,** shown (**Figure 1**) below, known as 7-chloro-1-ethyl-1,4-dihydro-4-oxoquinoline-3-carboxylic acid (by product) which was later modified to a nalidixic acid **2** [26]. Quinolines are used and studied in the world because of the pharmacological qualities they bear, for example, they are reported to exhibit good anti-bacterial [27], anti-cancerous [27], cardiovascular [28] and anti-tubercular activities [29].

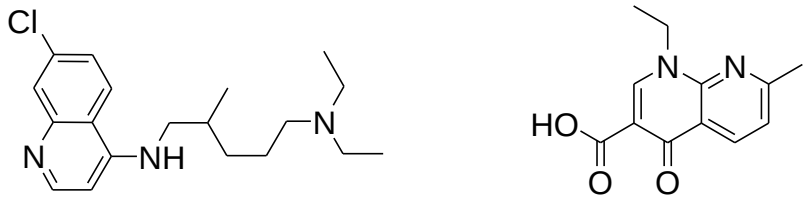

1 **2**

Figure 1. Examples of biologically active quinoline and quinolone derivatives

Quinolines with pharmacological properties are either chemically synthesised or naturally produced. Naturally produced quinolines were isolated from plant material and characterised. For example, quinine **3** was extracted from a tree bark called

Cichona and was found to treat malaria though no longer used due to resistance caused by *P. falciparum* [30]. Chloroquine was later developed as a breakthrough in the treatment of malaria [26]. The 8-hydroxyquinoline derivatives **4**, (**Figure 2**) below, were reported to be produced in the form of extracts from a plant timber called *Broussonetta zylarica* [31]. Wat *et al.* [32], isolated the Camptotheicin **5,** a quinoline extracts from a tree stem called a Happy Tree (*Camptotheca acuminata*) and reported to be a good inhibitor of leukaemia and alkaloid tumour.

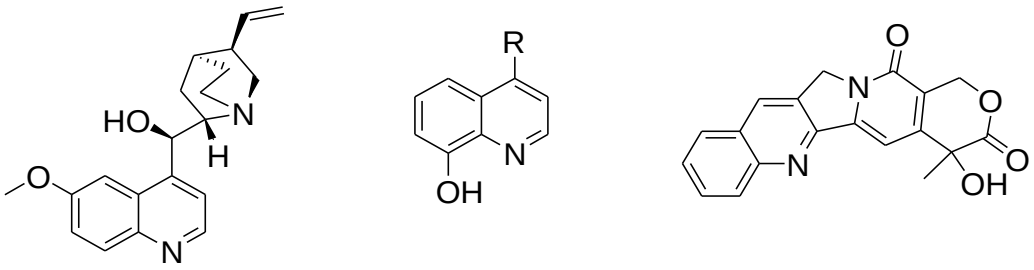

3 **4** **5**

Figure 2. Example of quinolines alkaloids with biological importance

More examples of naturally occurring quinoline alkaloids are compound **6** and **7** (**Figure 3**), substituted at the second position, were isolated from a medicinal plant called G. *longiflora* and are used for the treatment of ulcers. Compound **6,** named Chimanine D was reported to have a 50 % inhibitory concentration (IC_{50}) of 25 µg/ml against *L. amazonesis*, a parasite responsible for the disease Leishmaniasis [33].

6 **7**

Figure 3. Examples of 2-subtitutes quinoline alkaloids with biological importance.

Many quinolines are chemically synthesised and studied further for their biological activity. In medicinal chemistry, selected quinolines are reported to show inhibitory activities against tyrose kinase [33], NF-K_β transcripitory activities [34], to induce cell apoptosis (interferes with the bacterial DNA replication) and exhibit good cytotocixity [35]. The *N*^{l}-6-methoxyquinolin-4-yl derivative **8** bearing an oxothiazolidine in (**Figure 4**), was reported to be a multi-tyrosine kinase inhibitor, for example a C-Met (a member of the tyrosine kinase receptor family). Compound **8** exhibited a good

cytotoxicity with an inhibition percentage of 83.8 % against C-Met and was further reported to show a good IC_{50} of 0.073 µM against the HT-29 cancer cell line [36].

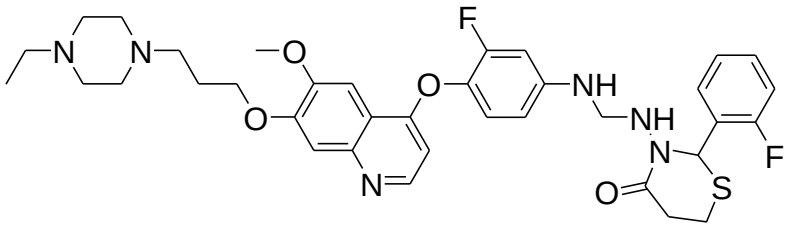

8

Figure 4. Example of a quinoline bearing an oxothiazolidine as a tyrosine kinase inhibitor

Furthermore, different derivatives of quinolines fused with other heterocycles were reported to have anti-cancer activity by targeting topoisomerase I, telomerase, farmasyl transferase, protein kinase Ck-11 [37]. Caprio *et al.* [38] synthesised an inhibitor of telomerase based on an alkaloid quinoline **9 (Figure 5**), called bis-methylamino ethyl quinoline derivative **10**, which was subjected to a TRAP assay to check its inhibitory activity against telomerase enzyme (extracted from ovarian carcinoma A2780 cell) and it was reported to have an inhibitory concentration of 16 µM. Mikata *et al.* [39] reported 2-phenyl quinolines with 2-(aminoethyl)-aminoethyl at the 7th, 6^{th,} and 4th position **11**, which are an example of quinoline tested against the HeLa cell (cancer cell line). The 2-phenylquinoline with the 2-(aminoethyl)-aminoethyl at the 8th position is reported to show a good activity and cytotoxicity against HeLa cells.

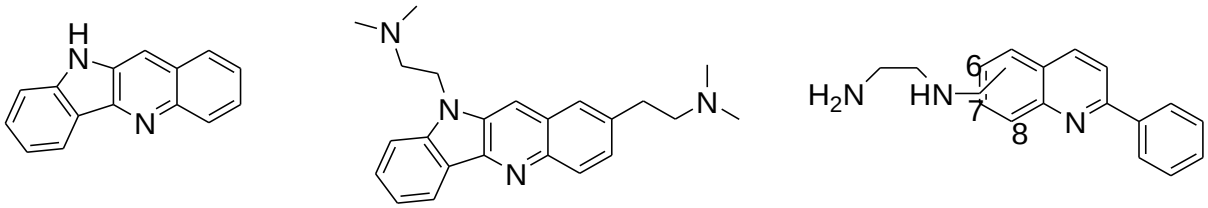

9 **10** **11**

Figure 5. Examples of quinoline-amino derivatives with different biological activities

The proliferation of unwanted cells is one of the causes of excessive organ failures according to literature [40]. The 5-chloro-2-(pyridine-2ylamino) quinoline-8-ol **12** (**Figure 6**), was reported to possess anti-proliferative activities which is liaised by inducing apoptosis and a potential cell cycle arrest against PC-3 cell line (prostate cancer) with IC_{50} of 1.29 µM and to inhibit Pim-1 kinase (a regulator that plays an important role in signalling tumour emigration and invasion) with a good IC_{50} of 0.75 µM [41]. The phosphorus substituted quinoline derivatives **13** and **14** also show inhibitory activity against Top-1 (topoisomerase 1) and an anti-proliferative activity of 0.2 µM and 0.6 µM against lung carcinoma (A549 cell line) respectively [42]. The (4-imidzazolyl methyl)-2-aryl-quinoline derivatives **15** and **16**, were found to exhibit inhibitory activity against aromatase enzyme which is found in the breast tissue and its function is to release estrogen which is responsible for the growth of breast cancer cells [43]. Compounds **15** and **16** were found to show an inhibitory concentration IC_{50} of less than 0.5 µM against breast cancer MCF-7 cell line (with a 2% and 3.8% cell survival after a 72-hour exposure) and IC_{50} of less than 10 µM against T47D cell line (with both the 0.7% cell survival after a 72-hour exposure), by using (3-[4,5-dimethylthiazol-2-yl]-2,5-diphenyltetrazolium bromide MTT assay [44].

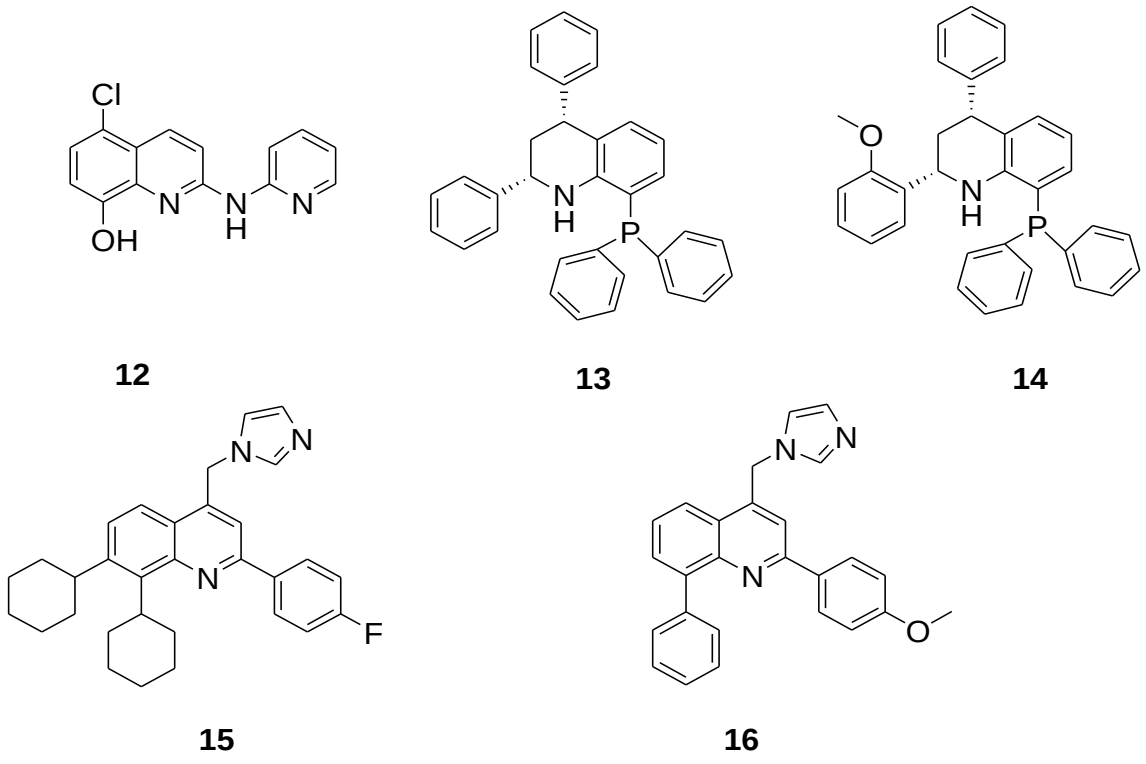

12 **13** **14**

15 **16**

Figure 6. Examples of quinoline derivatives with antiproliferative activities as inhibitory characteristics

Quinolines in medicine are reported to have a potential to be anti-cancerous drugs by inducing oxidative stress-mediated DNA damage [45]. The benzo(*h*) quinolines (**17**, **18** ,**19**) (**Figure 7**) were tested on cultured skin cancer (G_{361}), lung cancer (H_{460}) and breast cancer (MCF-7) and were found to induce DNA oxidation and apoptosis. These compounds were reported to dock perfectly to the target receptor protein aromatase through the hydrophobic pocket and CDk-2 (cyclin kinases-2), thus inducing stress mediated DNA damage [46]. Some quinoline drugs have been tested by the National cancer cell institute (NCI) against different 60 cancer cell lines [47]. He *et al*.[48] reported 11-*H*-indolo quinoline derivatives **20** and **21** with an ethoxy-side chain which were evaluated against the NCI 60 cell line group and reported to show an impressive activity.

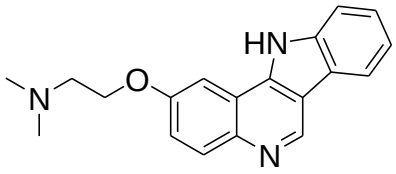

20

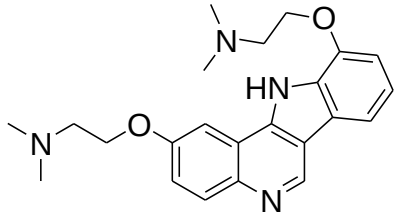

21

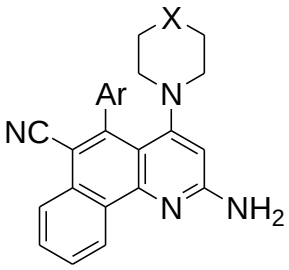

	Ar	X
17	C_6H_5	CH_2
18	4-Cl-C_6H_5	CH_2
19	3-Br-C_6H_5	CH_2

Figure 7. Different quinoline compounds known to induce DNA oxidation and apoptosis

Furthermore, quinolines are reported in literature to show anti-bacterial and anti-fungal activities, for example, 4-amino-7-chloroquinoline derivative **22** was synthesised and tested against *M. tuberculosis* ($H_{37}Rv$ strain), which exhibits an IC_{50} of 125 µg/ml and after metal coordination of platinum to compound **22** forming compound **23**, the activity reportedly increased significantly to 15.2 µg/ml [49]. The United States food and drug administration accepted quinoline derivatives as drugs for the treatment of multi-drug resistant *mycobacterium* (bacterium responsible for the disease tuberculosis-MDR-TB) [50]. In 2012, diarylquinoline (1-(6-bromo2-methoxy-quinolin-3-yl)-4-dimethyamino-2-naphthalen-1-yl-1-phenyl-butanol) **24** also known as TMC207, has been reported to inhibit resistant MDR-TB, showing a good activity both *in-vitro* and *in-vivo* with an excellent anti-mycobacterial spectrum showing an IC_{50} of 0.6 µg/ml through the proton pump interaction of ATP-synthase [51]. Fluorinated compounds have been shown in literature to exhibit an increased potential for a good activity against some selected diseases, this is because fluorine increases the lipophilicity of a compound (ability to cross the membrane of the targeted cell site) [52]. The thiourea-fluorinated quinoline derivative **25** (**Figure 8**) exhibited an activity against the gram-positive *S. aures* (*Staphylococcal aures*) and the gram-negative *E. coli* (*Escherichia coli*), where compound **25** showed a MIC_{90} of < 6.25 µM against *S. aures.* [53]

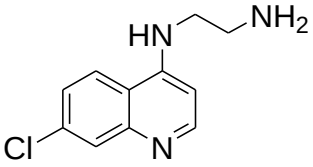

22

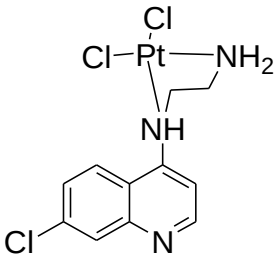

23

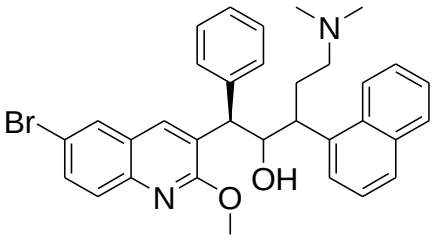

24

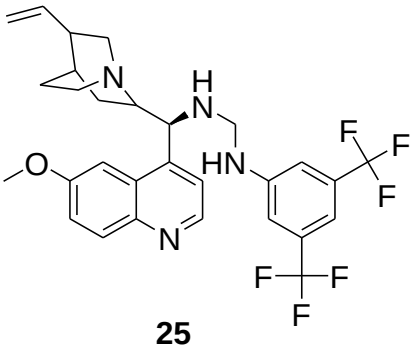

25

Figure 8. Examples of quinolines with anti-bacterial properties

1.3 An overview of triazoles and triazole appended molecular hybrids with biological importance

Triazoles receive much attention in medicinal chemistry and possess broad biological applications [54], such as, antibacterial [54-55], anti-cancer [55], anti-inflammatory [56], anti-convulsant [56] and antirheumatic properties [57]. The 2-*H*-1,2,3-triazole hybrid **26** (**Figure 9**), was reported to show potent cytotoxic activity against prostate cancer (PC-3 cell line), where the triazole ring acts as a pharmacophore interacting with colchicine and combretastatin A-4 site (potent inhibitors of cancer [58, 59]) [60]. The 1,2,3-triazoles are identified to be enzyme inhibitors [59]. For example, compound **27** has been reported to be an inhibitor of tubulin polymerization [62], histone deacetylase, PDE4 and alkaline phosphate [63] enzyme inhibitors.

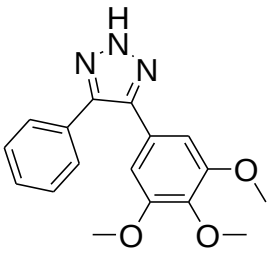

26

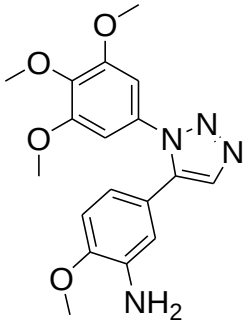

27

Figure 9. Examples of 1,2,3-triazole-hybrids as potential inhibitors

Triazoles are used mainly as linkers through molecular hybridization, where triazole-containing compounds are used as a foundation to study their structure activity relationship (SAR) [64]. Compound **28** (**Figure 10**) for example, was reported to have an inhibitory concentration (IC_{50}) of 0.56 µM against breast cancer (MCF-7 cell line), which led to the discovery of compound **29**, which exhibited an IC_{50} of 0.046 µM [65]. The 1,2,3-triazole-chalcone hybrids **30**, **31** and **32**, were reported to possess high cytotoxicity and show an activity against different cancer cell lines, such as cervical cancer (HeLa) and breast cancer (MCF-7 and MDA-MB 231). Compound **32** showed IC_{50} of 0.78 µM against the MDA-MB 231 cell line, which is unfortunately lower than the standard cisplatin drug [66]. The chalcone-triazole hybrid **33** was reported to be synthesised under green synthesis via cellulose catalysed copper nanoparticle's

reaction and tested against pancreatic cancer (MIA-Pa-Ca-2) cell line. It has exhibited some characteristics such as inducing apoptosis, showing a G_2IR arrest in MIA-Pa-Ca-2 cell line with an IC_{50} of 4.0 µM [67]. Compound **34**, a chalcone-triazole derivative was also reported to exhibit a good anti-cancerous activity against leukaemia cancer cell line [67].

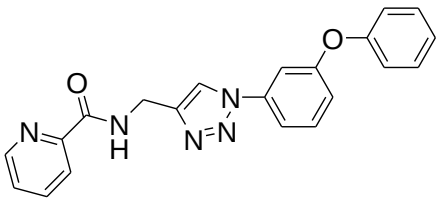

28

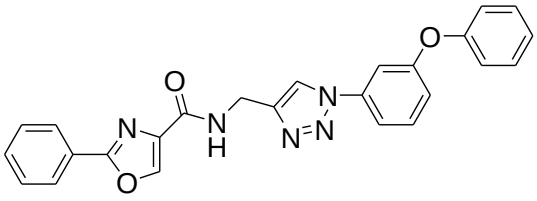

29

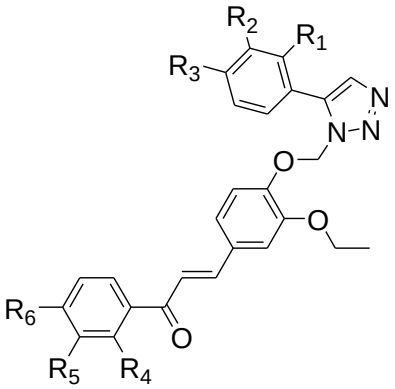

	R_1	R_2	R_3	R_4	R_5	R_6
30	OH	H	H	H	OMe	OMe
31	OH	H	H	H	H	Br
32	OH	H	Me	H	OMe	OMe

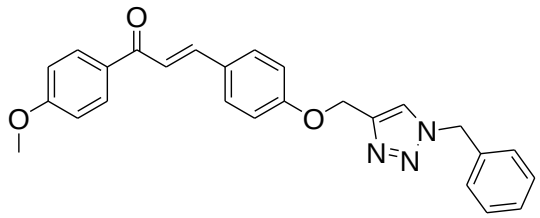

33

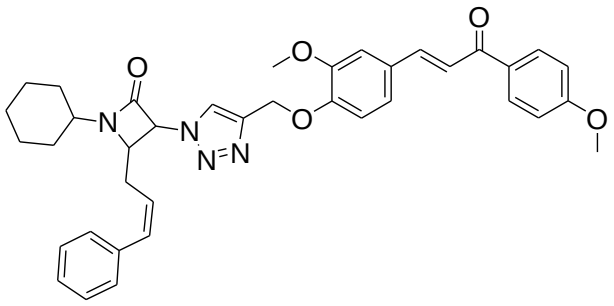

34

Figure 10. Examples of 1,2,3-triazoles and 1,2,3-triazole-chalcone derivatives as anti-cancer agents

The polysubstituted pyrrolidine-1,2,3-triazole derivative **35** (**Figure 11**) has been reported to possess some activity against the proliferation of cancer cell lines such as PC_3-cell (human prostate cancer) by using a MTT assay [68]. The amide-1,4-disubstituted 1,2,3-triazoles **36**, **37** and **38** were tested against different cancer cell

lines and reported to be antioxidants by using a 1,1-diphenyl-2-picryhydrazy (DPPH) radical. The compound **38** showed an IC_{50} value of 95.2 µM against Fr2 (Breast epithelial) cell line and presented good antioxidant properties, as it displayed a scavenging effect on the DPPH radical with an IC_{50} of 1.61 µg/ml [69]. As mentioned above, the 1,2,3-triazoles also exhibit anti-inflammatory activities [56]. The novel 2-mercapto linked with 1,2,3-triazoles **39** and **40** were reported to show an anti-inflammatory activity by inhibiting COX-2 using biochemical cyclooxygenase (COX) activity assays (a type of assay for inhibitory activities) [70].

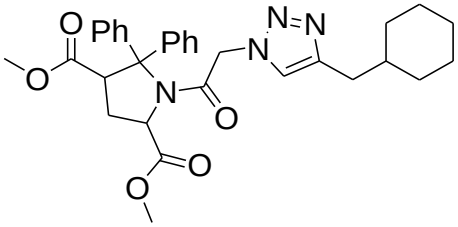

35

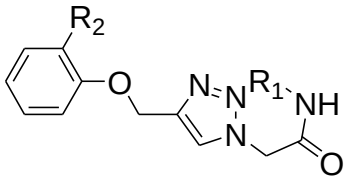

	R_1	R_2
36	$\alpha C_{10}H_7$	2-CH_2OH
37	4-$NO_2C_6H_4$	3-CH_2OH
38	C_6H_5	2-CH_2OH

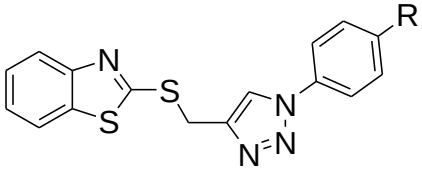

	R
39	p-F
40	p-Br

Figure 11. Examples of 1,2,3-triazole derivatives as anti-cancer and anti-inflammatory agents

Human cancers are known to have Polya(ADP-ribose)polymerase-1 (PARP-1), an infinitely expressed NAD^+ dependent nuclear enzyme that has a huge value for the abundance of the disease [71]. The erythrina-1,2,3 triazole derivative **41** (**Figure 12**), for example, was reported to be a PARP- 1 inhibitor and found to show anti-proliferative activity with an IC_{50} value of 14.42 µM and 0.23 µM respectively, which is higher compared to Rucaparib (standard) with inhibitory activity with an IC_{50} of 23 µM [72].

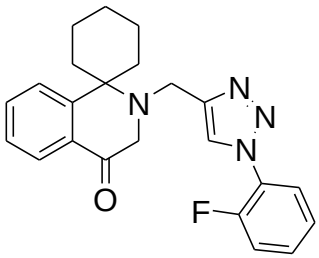

41

Figure 12. Erythrina-1,2,3 triazole derivative 41 as a PARP-1 inhibitor and an anti-proliferation agent

The eugenol-triazole derivative **42** was screened and reported to show an activity against leishmaniasis (parasite disease) with an IC_{50} of 7.4 µmol/ml and conveniently used for drug development [73]. The 7-chloroquinolino-triazole (**43**) [74] and mefloquine-triazole (**44**) [75] have reportedly been tested against plasmodium falciparum (*P. falciparum,* NF54 strain) which is responsible for the malaria disease and were found exhibit an inhibitory concentration of 9.6 µM and 1.0 µM respectively.

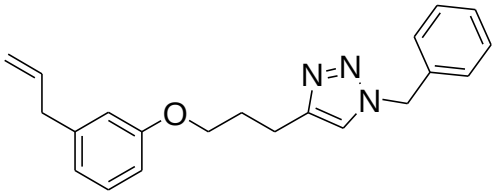

42

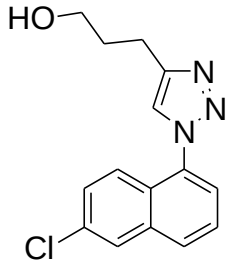

43

Figure 13. Examples of 1,2,3-triazole compounds with some biological activities.

The 1,2,3-triazoles in literature have been found to show some activity against bacterial strains where, triazole containing derivatives **45** and **46** were reported to show an activity against *Monilia albicans* (*M. albicans*) and *Escherichia Ecoli* (*E. coli*) at a concentration of 0.01 mg/ml with an inhibitory concentration ratio of 80.1 % and 79.9 % compared to the standards triclosan and flucorazole with ratio of 51.9 % and 41.0 % respectively [76]. The triazole indole-(piperazin-1-yl) benzo[*d*]-isoxazole derivative **47** was found to exhibit anti-tuberculosis activities and reported to show an activity of about ±6.16 µM against H_{37}RV, Spec 210, and Spec 192 TB strains [77]. The triazole-linked compound **48** (**Figure 14**) was tested against both the bacterial and fungal strains such as the gram positive bacteria (*B. subtilis, S. aureus*), and the

gram negative bacteria (*E. coli, P. vulgaris* and *C. albicans*) respectively. It exhibited a minimum inhibitory concentration of 3.125 µg/ml against both the gram positive and negative bacteria and an anti-fungal inhibitory activity of 6.25 µg/ml against the fungal strains mentioned above [78].

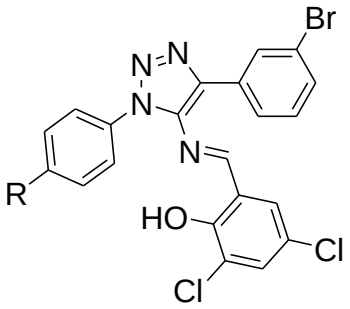

	R
45	H
46	Br

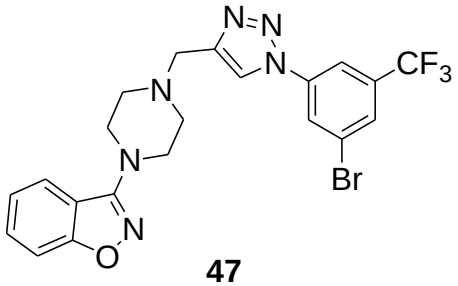

47

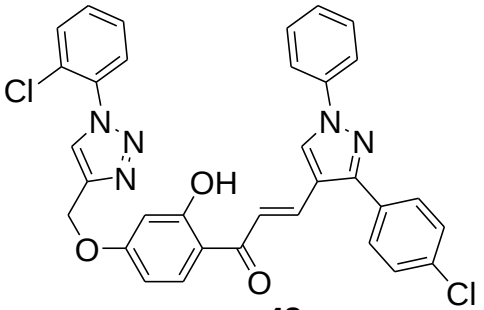

48

Figure 14. Examples of 1,2,3-triazole derivatives that have potential to act as anti-bacterial and anti-fungal drugs

1.4 Methods for the synthesis of chalcones

Chalcones are known to be synthesised through a classical method called the Claisen Schmidt condensation, a reaction between an acetophenone and a benzaldehyde and are characterised by an alpha-beta unsaturated ketone [79]. Chalcones in most procedures serve as intermediates for biological compounds because they contain conjugated bonds and three electrophilic carbon system [80] for the formation of iso-flavonoids/ flavonones [81]. Base catalysed-condensation reaction has been employed to produce chalcones in literature [79]. Tanemura *et al*.[82] (**Scheme 1**) reported the synthesis of a chalcone **51** in water by reacting an aminoacetophenone **49** and benzaldehyde **50** in the presence of NaOH (a base). Another strategy for the synthesis of chalcones that has been reported incorporates acetophenones and 1-(furan/thiophen-2-yl) ethenone through Claisen-Schmidt aldol condensation also using sodium hydroxide [83]. Wang *et al.* [84] discovered a procedure to synthesize chalcones accidentally, which involves a mixture of a metal catalyst Ag_2CO_3, a terminal alkyne, pyridine, and a benzaldehyde under solvent free conditions.

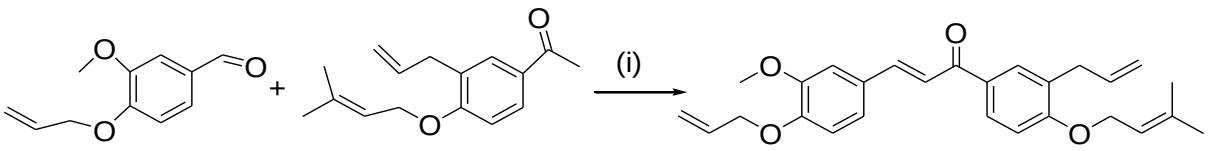

49 **50** **51**

Reaction conditions (i) 50% mmol KOH in ethanol

Scheme 1. Base catalysed reaction for the formation of chalcones

The formation of chalcones involve metal mediated coupling [85], such as Suzuki coupling, which involves the dehydrogenation of methoxystyrene through borylation using pinalcolborane and $RuCl(cod)_2$ (ruthenium complex) followed by oxidative cleavage reaction by sodium periodate ($NaIO_4$) to form a boronic-phenyl ethyl compounds. The boronic compounds produced serve as precursors for Suzuki-coupling with benzyl chlorides catalysed by kis-(triphenylphosphine) palladium(0) under basic condition to produce a chalcone [85].Another coupling method is called

Stille coupling, a reaction between chloro-carbon compound and organo-stannanes [86]. In **Scheme 2**, 2-α-sulfonyl-β-chloro arylamides **52** was reacted with arylstannanes **53** to produce a chalcone derivative **54** [87].

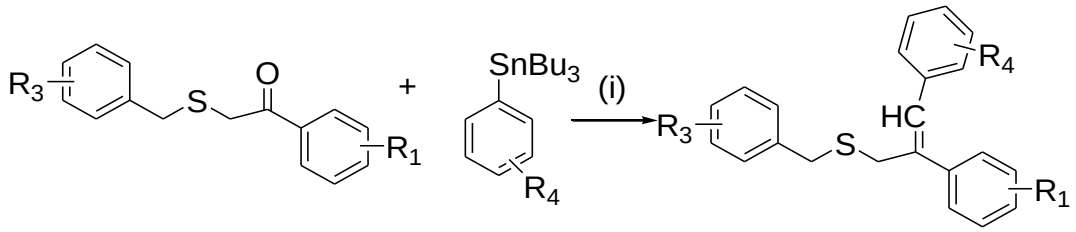

52 **53** **54**

R_1= 4-OMe, Me, F R_3= H, Cl, 4-OMe R_4= 4-OMe, 4-F, 4-Me, 4-NO_2

Reaction conditions (i) Pd catalyst (5 %mmol) in acetonitrile at RT, inert condition for 2 h

Scheme 2. Palladium catalysed - Stille coupling reaction for the reaction of a chalcone derivative.

1.5 Methods for the synthesis of triazoles

Methods for the synthesis of triazoles are developed using the reaction called “click chemistry”. It is one of the most studied and developed reaction defined as a Huisgen cycloaddition (1,3-dipolar cycloaddition) and a water tolerant reaction between azides and acetylides to produce 1,2,3-triazoles [88]. In the literature, 1,2,3-triazoles compounds are differentiated by the position of each substituent, for example, 1,5-disubstituted, 1,4,5-trisubstituted and 1,5-disibstituted 1,2,3-triazoles [88]. The 1,2,3-triazole derivative **57** (**Scheme 3**) was formed by the reaction of **55** and **56** and are reported to be assisted by ligands in the presence of metals (as catalysts) [89], tris(benzyltriazolylmethyl)-amine (TBTA) ligand or p-ethynylanisole [90]. Fokindia and co-workers [91] reported the synthesis of 1,5-disubstituted-1,2,3-triazole derivative through a one-step metal mediated cycloaddition reaction in the presence of 2 mol % ruthenium catalyst ($Cp^*RuCl(PPh_3)_2$ in dioxane under reflux. This type of reaction is called Ruthenium catalysed azide alkyne cycloaddition (RuAAC). The 1,5-disubstituted-1,2,3-triazole zinc-mediated reaction has been reported in literature and produced through an excess zinc catalyst ($ZnEt_2$) and the alkyne at room temperature using dioxane as a solvent [92]. The solid aid/support of silica-based reaction has also been developed to produce 1,4-disubstituted-1,2,3-triazoles, in the

presence of 20 mg silica-zinc catalyst, an organic halide as a base, sodium azide, an alkyne in water and t-BuOH at 55ºC [93].

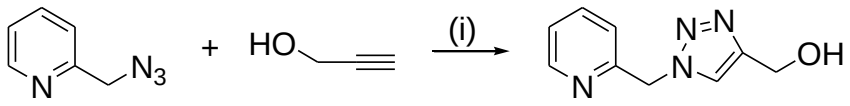

55 **56** **57**

Reaction conditions (i) t-BuOH: H_2O (1:1) (v/v), tris(benzyltriazolylmethyl)-amine (20 µmol) and $Cu(OAc)_2$ (10 µmol)

Scheme 3. Copper catalysed Click chemistry reaction.

Metal free methods are currently used and are described as eco-friendly methods. For example, the [3+2] cycloaddition of azides and alkynes through a bio-orthogonal reaction (chemical reaction performed in living systems) [94]. Wan *et al.* [95] reported a metal free and an azide-iodinated synthesis of 1,5-disubstituted 1,2,3-triazole **60** through a C-N, N-N bond formation and acylation migration, which involved a three-component reaction of enaminone **58** based with both tosylhydrazine **59** (mainly substituting the metal catalyst) and a primary amine (**Scheme 4**),

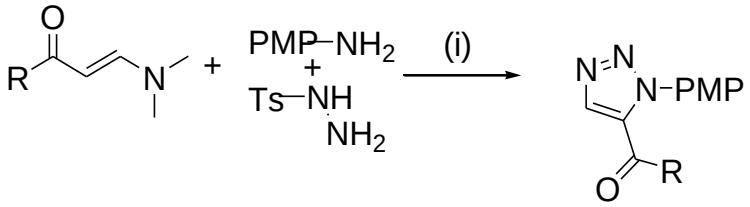

58 **59** **60**

R	Yields %
-Ph	71
-PMP	58
-Ph-4CH_3	67
-Ph-3NO2	53

Reaction conditions (i) iodine (1 equiv.) for 12 h at 110 ºC

Scheme 4. Three component-metal free 1,2,3-triazole reaction.

Kwok and co-workers [96], reported the synthesis of triazoles under base-mediated metal-free conditions, where bases such as anhydrous sodium, potassium, cesium and trimethyl hydroxides act as catalysts to activate the acetylides. Reasonable "click chemistry" that has been reported as the first eco-friendly reaction is called green click synthesis [97]. Mohamed *et al.*[98] developed a method for the preparation of new fluorinated 1,2,3-triazoles **63** through Huisgen 1,3-dipolar cycloaddition reaction between dimethylacetylene dicarboxylate (DMADC) **61** and fluorophenyl azide **62** under solvent free conditions in a sealed tube (in hot water bath) to form the desired 1-(Fluorophenyl)-1,2,3-triazoles with a 96 % yield (**Scheme 5**).

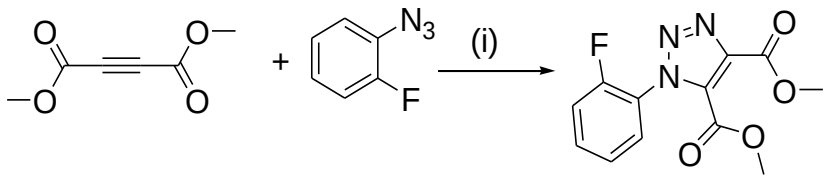

61 **62** **63**

Reaction conditions (i) heated (in water bath) 2-3 min

Scheme 5. Green click chemistry to form 1,2,3-triazole derivatives

The formation of 1,2,3-triazole derivatives methods are still being developed. Microwave mediated method, for example, is characterised by a shorter reaction time compared to other methods [99]. Bouasla *et al.*[100] developed a method for synthesizing 1,4,5-trisubstituted 1,2,3-trazoles, where products were formed in high yields, with low regio-isomeric mixtures. The 1,2,3-triazole is formed via cycloaddition reaction between 2-phenyl azides and dimetheylacetylene dicarboxylate (DMADC) in CH_2Cl_2 under 300 W microwave heating for 14 minutes. Li *et al.*[101] also reported a microwave assisted new 1,2,3-triazole derivatives **66** (**Scheme 6**) bearing an isoxazole ring in the presence of copper acetate as a catalyst, an azide containing compound **64** and some different isoxazole alkynes **65**. The derivatives **66** were then synthesised with 83-95 % yield after a 10-minute reaction time.

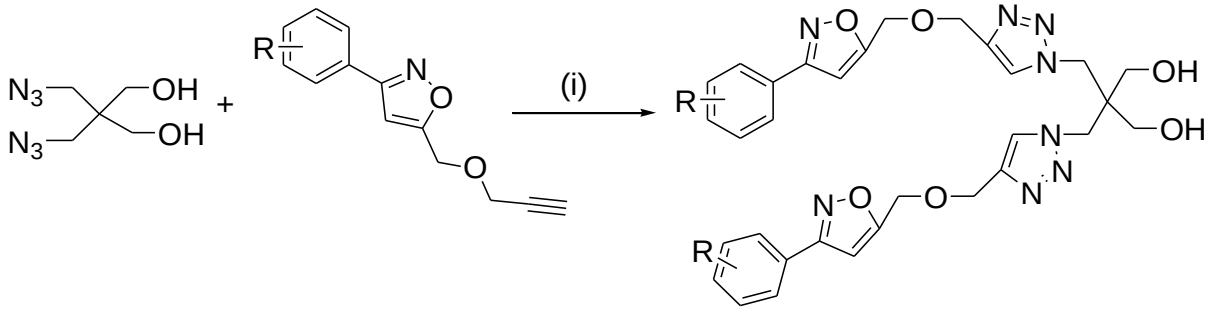

64 **65** **66**

R	Yields %
-4-Cl	85
-2-OCH_3	93
-4CH_3	91
-4-F	80

Reaction conditions (i) t-BuOH: THF 1:3 v/v and Cu salt (0.1 equiv.) and sodium ascorbate in 2 ml H_2O, 250 W, 10 min

Scheme 6. Microwave assisted reaction of 1,2,3-triazole-isoxazole ring derivative

Other efficient methodologies to produce 1,2,3-triazole are available, for example, “click chemistry” on polymer support [102]. An example of polymer support reported in literature are Merrifield polysterene resin, Jandajel resin and PEGA resin [103]. These types of support begin by linking the polymer and the azide derivative, followed by the cycloaddition reaction between polymer-azide and an alkyne derivative, lastly by a cleavage from the polymer support through oxidative elimination with a solid phase organic synthesis which has been listed to be advantageous, odourless and involves no by-products [104]. The polysterene - supported lithium selenide **68** (**Scheme 7**) was reacted with 3/2-azida-1-iodoethane/propane **69** to form a resin-polysterine supported 2-azidoethyl/propyl phenyl selenide **70**. Compound **70** was then reacted with different terminal alkynes **71**, where phenyl acetate was used for the template reaction with **70**. At the end of the reaction, the resin was washed after filtration with pyridine and dried to form 1-vinyl/1-allyl-1,2,3-triazole derivatives **72** [104].

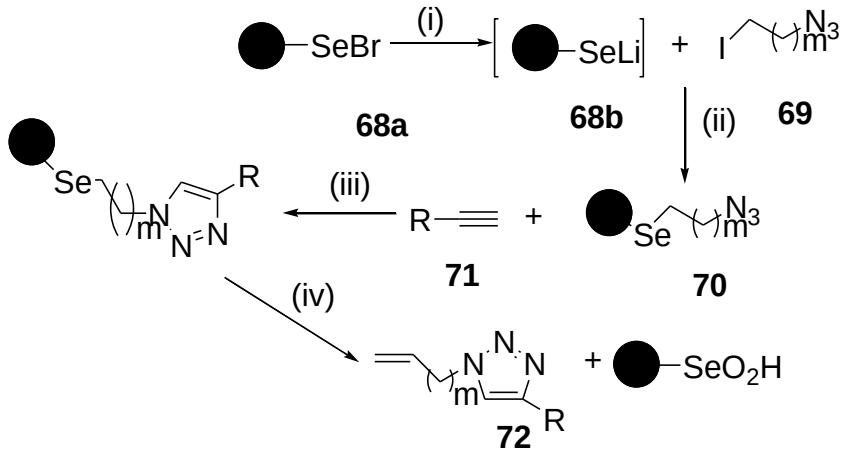

R	Yields %
-Ph	98
-n-C_3H_7	86
-CH_2OH	83
-$CO_2C_2H_5$	94

Reaction conditions (i) $LiBH_4$, under N_2 atm in 10 ml THF for 30 min, (ii) THF 2 ml added for 10 h, (iii) CuI and DIPEA, DMF: THF (2:1), (iv) Add in 1 ml of 30 % H_2O_2 and 10 ml THF

Scheme 7. Solid phase polymer-click chemistry organic synthesis

1.6 Methods for the synthesis of quinolines and their quinoline derivatives

The quinoline structure design has been reported in literature through classical routes (**Scheme 8**), such as Friedlander annulation (i) to form *ortho*-aminoacetophenones **A** [105], Skraup (ii) [106], Doebner-Miller (iii) [107], Condrad-Limpach (iv) [108], Combes's reaction (v) [109] from anilines **D** and, pfitzinger (vi) [110] from isatin **I**. The Friedlander annulation is a straightforward reaction to produce quinolines under different conditions, such as, the use of basic or acidic catalysts [111]under microwave-radiation [112] or a polymer mediated reaction [113]. The disadvantages of the above-mentioned classical methods are that they require the use of highly acidic or oxidising agents, high temperatures and thus donate environmental poisoning due to the excess usage of reagents causing high amount of toxic waste [105].

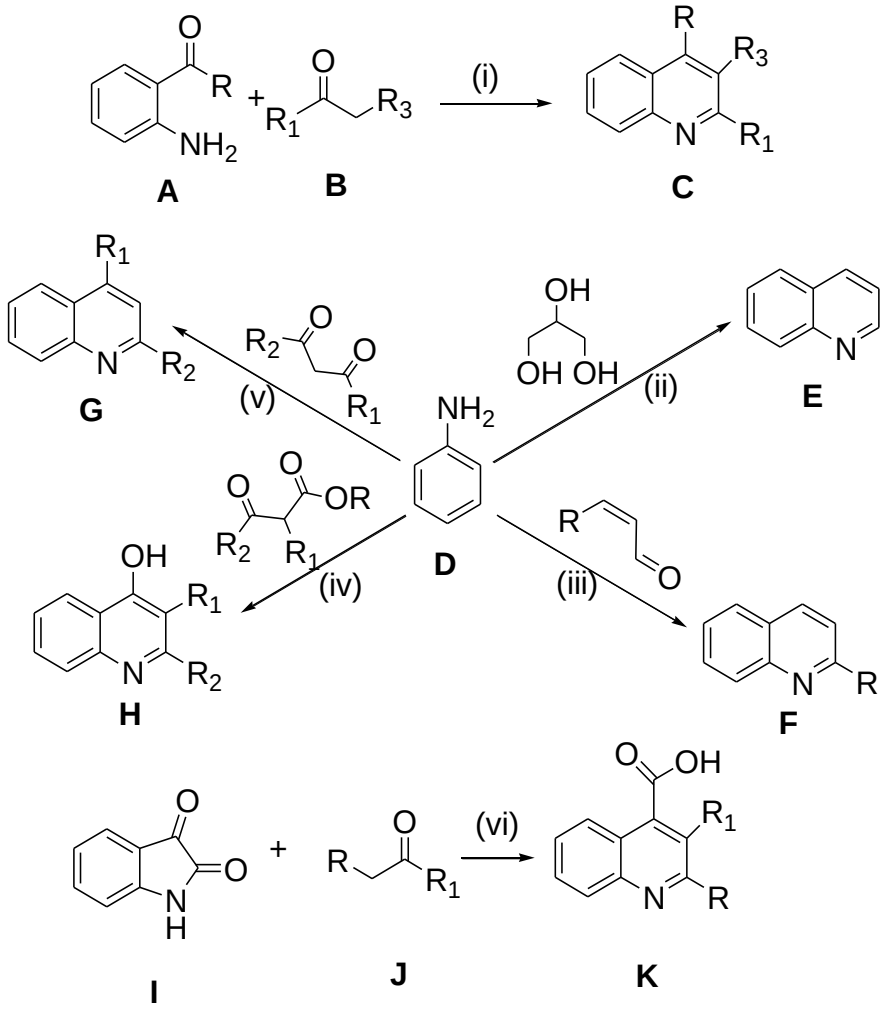

Scheme 8. Classical reaction methods of quinolines

1.6.1 Synthesis of 2-aryl-2,3- dihydroquinolin-4(1*H*)-ones

The synthesis of quinolines continues to be developed by researchers through intramolecular aza-Michael addition reaction which plays an important role in the cyclization of a compound through the formation of a C-N bond [114]. The 2-aryl-2,3-dihydroquinolin-4(*1H*)-one **74** has been reported in literature to be synthesised in high yields, where 2-aminochalcone **73** serves as a precursor in the presence of 10% mmol of antimony chloride ($SbCl_3$) in acetonitrile [115] or 1-octyl-aza-1-azoniabicyclo [2.2.2] octane bromide (C_8dabco] Br), a recyclable catalyst under heat and solvent free conditions [116]. Donnelly and Farrell [117] in 1989, reported the use of orthophosphoric acid in acetic acid through an acid -catalysed reaction to form **74** by using 2-aminochalcones **73** (because of the nucleophilicity of the -NH2, and the presence of the alpha-beta unsaturated carbonyl resulting in Michael addition reaction[118]), (**Scheme 9**). Dhiman *et al*.[119] showed a different acid catalysed

reaction, which involves cyclization reaction under an acid promoted deprotection reaction by using an acetylated-chalcone and 5 % HCl in ethanol under heat to form **74**.

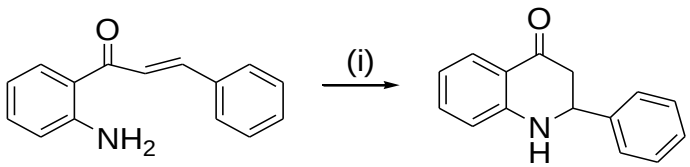

73 **74**

Reaction conditions (i) acetic acid (30 ml) and orthophosphoric acid 90 % (30 ml), reflux for 2 h

Scheme 9. Acid-catalysed cyclization reaction

The 2-subtituted-2,3-dihydroquinolon-4(*1H*)-ones continue to be produced, for example, through the use of montmorillonite K10 clay at a 110-104 ºC for 2 min and extracted with dichloromethane [120] or synthesised in the presence of indium chloride ($InCl_3$) supported by silica gel (SiO_2) with the yield of 72-90 % [121]. Lu *et al*.[122] reported a bifunctional thiourea cyclization mediated method for the preparation of 2-aryl-2,3-dihydroquinolon-4(*1H*)-ones **77**, where the bifunctional thiourea acts as a catalyst to react with an alkaline β-ketoester's nitrogen **75** in the presence of a sulphonamide group **76** and later treated with p-toluene sulfonic acid to afford **77** in

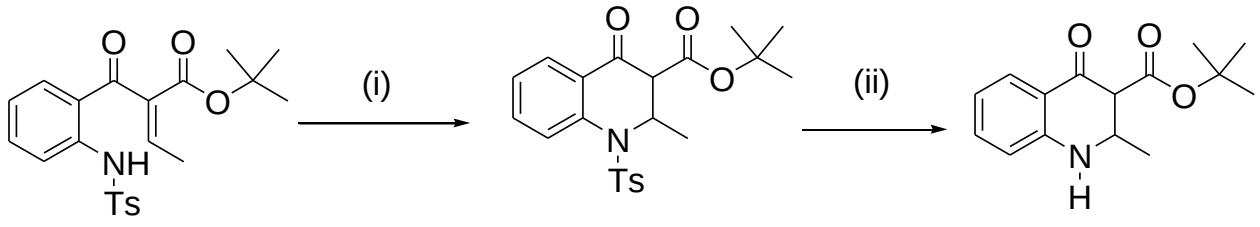

75 **76** **77**

Scheme 10 below.

Reaction conditions (i) Bifunctional thiourea 10 mol% in toluene at 0 ºC. (ii) TsOH in toluene at 80 ºC, Mg in MeOH

Scheme 10. Bifunctional thiourea cyclization mediated method

The 2-aryl-2,3-dihydroquinolin-4(*1H*)-one has been also reported in literature to be synthesised in the presence of both a 2-aminoacetophenone and a benzaldehyde by using catalysts namely per-6-amino-β-cyclodextrin (Per-6-ABCD) [123] or N-2,4,6-tris-(methylbenzene) sulphonyl-L-proline-amide [124]. Polintanskaya *et al*.[125] also reported the synthesis of 2-aryl-2,3-dihydroquinolin-4(*1H*)-one **80** using a fluorinated 2-aminoacetophenone **78**, a benzaldehyde **79**, 1-equivalence of *p*-toluene-sulfonic acid and anhydrous $MgSO_4$ as presented in **Scheme 11** below,

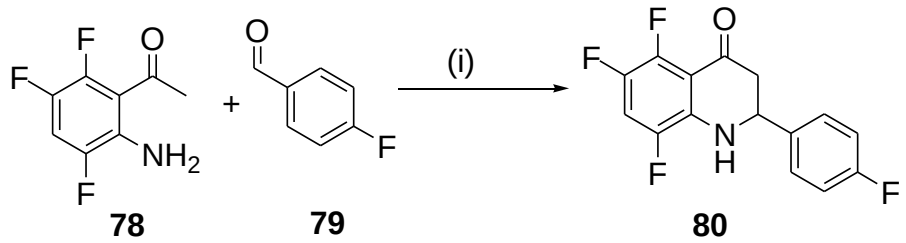

78 **79** **80**

Reaction conditions (i) *P*-TSA monohydrate and anhydrous $MgSO_4$ in toluene, under reflux, 6-7 h

Scheme 11. *P*-Toluene sulfonic acid mediated reaction of a fluorinated 2-aminochlacone and a benzaldehyde

1.6.2 Synthesis of 2- substituted-quinolin-4*(1H)*-ones

Some methods for the synthesis of 2- substituted-quinolin-4*(1H)*-ones are metal mediated. For example, 2-substituted-quinolin-4*(1H)*-one derivatives **82** were reported to be synthesised from 2-nitro-chalcones **81** in the presence of ruthenium ($Ru_3(CO)_{12}$) and DIAN(Me) as a co-catalyst for the reduction of NO_2 to NH_2 followed by a cyclization reaction with 2-substituted-dihydro quinolin-4*(1H)-one* as a by-product (**Scheme 12**)[126]. Tois *et al*.[127] also reported a Leimgrumber-Batch method which involved dimethyl acetal to form an enaminone group, which in presence of metal catalyst, the -NO_2 **81** undergoes a reduction reaction through a catalytic transfer hydrogen condition initiating a Michael addition reaction resulting in the removal of the dimethylamine through elimination reaction to form **82**.

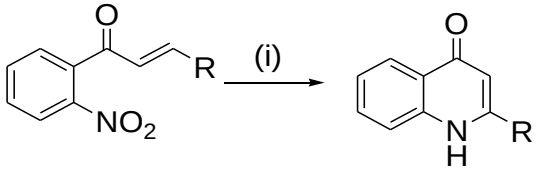

81 **82**

Reaction conditions (i) DIAN-Me (3 equiv.) in EtOH: H_2O (23.5 ml: 1.5 ml), R= H, Ph-4-OCH_3

Scheme 12. Ruthenium catalysed 2-substituted quinoline-4*(1H)* one method

Jones *et al*.[128] reported another metal mediated procedure for the formation of 2-substituted-quinolin-4*(1H)-one*s with a 72-97 % yield (**Scheme 13**). The reaction involves a two-step camps cyclization with a copper catalysed and a base mediated halogenated acetophenones **83** as precursors. Compound **83** was reacted with a halogenated amide group **84**, a diamine ligand and copper iodide to afford **85**. To form, 2-substituted-quinolin-4*(1H)-one*s **86**, **85** was subjected under a base catalysed cyclization reaction in 1,4-dioxane.

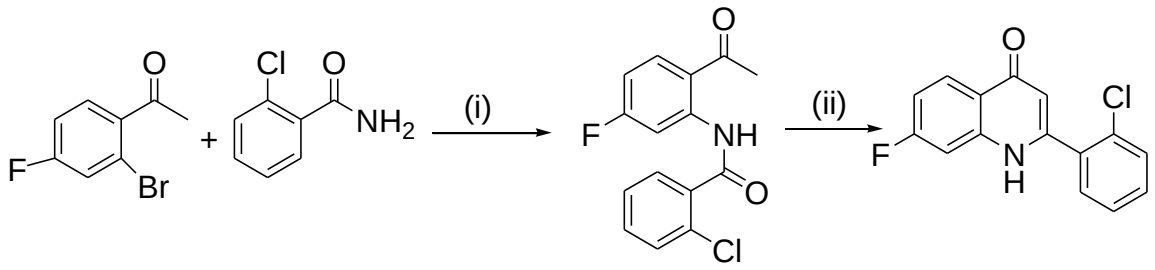

83 **84** **85** **86**

Reaction conditions (i) K_2CO_3, 200 mg molecular sieves in 1 ml toluene. (ii) NaOH, toluene (3.9 ml) 1 h, reflux

Scheme 13. Cyclization reaction to form 2-substituted-quinolin-4*(1H)-one* derivatives

Methods for producing 2-substituted-quinolin-4*(1H)*-ones are reported in literature to follow from alkynyl containing groups which are activated by a metal catalyst and amine-benzene groups [129]. Seppanen and co-workers developed an asymmetric transfer hydrogenation procedure through gold catalysed methods forming 2-substituted-quinolin-4*(1H)-one*s **89**. Gold is characterised as being a good activator of C-C unsaturated compounds to bond with nucleophiles (e.g. amines) [130]. Many metal mediated methods have been reported, for example an interesting iron catalysed procedure, which involves treatment of 2-amino phenyl ketone with alcohols, $Fe(OTf)_3$ (metal catalyst) and an oxidant called di-tert-butyl peroxide (DTBP). In this procedure, the alcohol undergoes oxidation to afford aldehydes as

intermediates and in the presence of the iron catalyst, the aldehyde reacts with the 2-amino phenyl to afford 2-substituted-quinolin-4*(1H)-one*s [130]. The copper catalysed method (**Scheme 14**) was reported to form **89** through an intramolecular cyclization reaction between phenyl alkynyl ester **87** and benzyl-amine **88** in the presence of HOTf as an additive (to improve the outcome of the reaction) and $Cu(OTf)_2$ as the metal catalyst (to activate the alkynyl) [131].

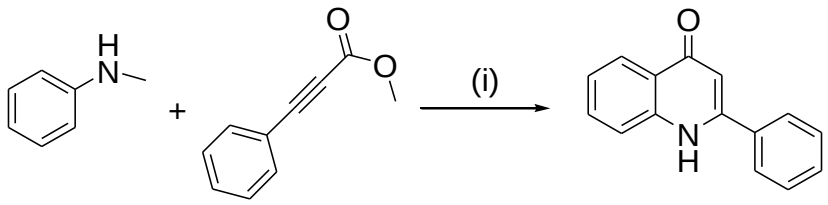

87 **88** **89**

Reaction condition (i) $Cu(OTf)_2$ (5 mol%) and HOTf (5 mol%) in DCM reflux under inert atmosphere

Scheme 14. Copper catalysed intramolecular cyclization to form 2-substituted-quinolin-4*(1H)-one*

According to literature, a substrate in an aromatic system do not react normally with nucleophiles through substitution reaction but in the presence of electron withdrawing groups situated at the ortho or para positions, thus allowing substitution reaction happen [132]. Laroshenko *et al.*[133] reported a base mediated intramolecular cyclized Michael addition (**Scheme 15**) of 2-fluorophenyl alkynyl group **90**. Compound **91** was reacted with Li_2CO_3 (a base) to enable a good substitution at the 2-position by forming a F-Li^+ group **90a** as an intermediate, which later undergoes amination reaction and forms a stable 2-substituted quinolin-4*(1H)* one **91** at high yield through intramolecular cyclization. Another base catalysed method of annulation reaction was reported (**Scheme 15**). The method involves a one-pot metal free synthesis, with 3-oxo-3-aryl propanoates **92** and amides **93** as pre-required reagents in the presence of base. Thereafter, under reflux 2-substituted-3-carboxy-quinolon-4*(1H)-one* **94** was formed through an addition-elimination tandem reaction in the presence of an imine-enamine compound which serves as an intermediate [134].

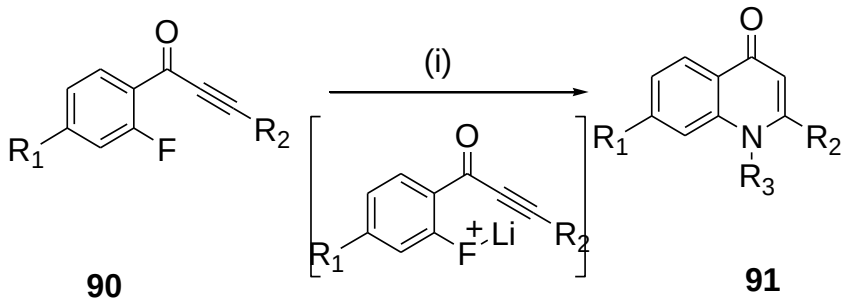

90 **90a** **91**

Reaction conditions (i) Li_2CO_3 (2 equiv.) in DMA-anhydrous, argon air R_1= F, H, R_2= Ph, 4-t-BuC_6H_4, R_3= 4-ClC_6H_4, $(CH_2)_2$Ph

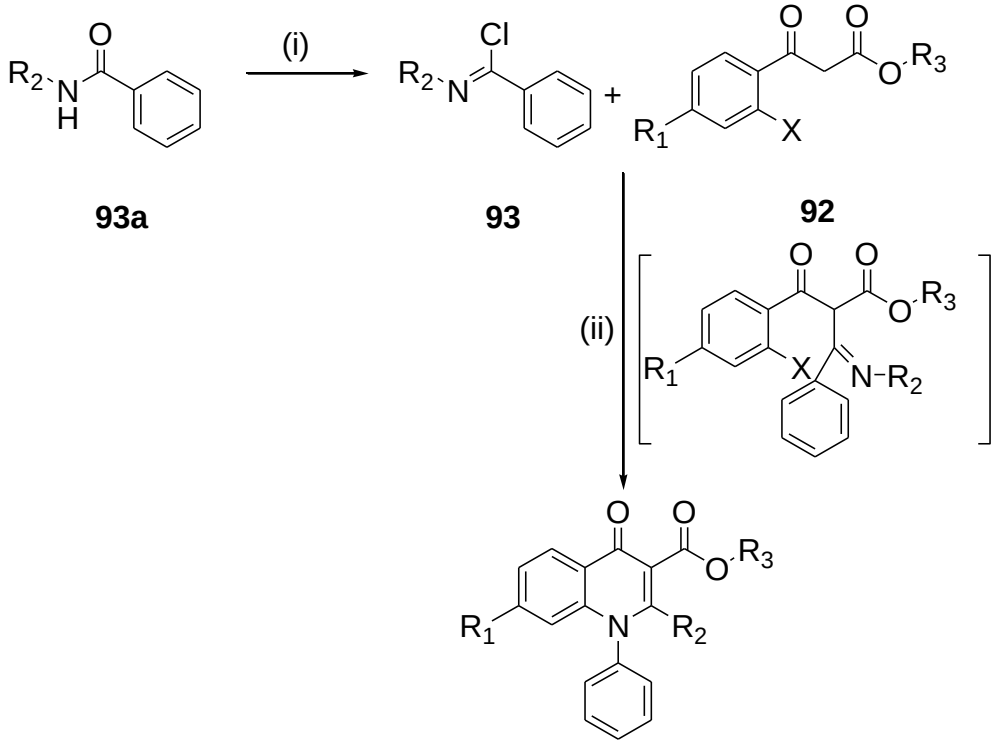

93a **93** **92** **94**

Reaction conditions (i) $SOCl_2$ (ii) K_2CO_3 (3 equiv.) and DIPEA (2 equiv.) in 10 ml DMF R_1= 6,7,8-trifluoro, R_2= CH_3, R_3= O-CH_2CH_3 and X= F

Scheme 15. Base catalysed procedures for 2-ubstituted quinolon-4*(1H)-one*

1.6.3 Synthesis of the 2-aryl-2,3-dihydroquin-4*(1H)-one* via dehydrogenation of the 2-substituted-2,3-dihydro- quinolon-4*(1H)-one*

Mphahlele *et al*.[135] reported an interesting method for the synthesis of 2-substituted quinolon-4*(1H)-one* **96** from 2-substituted-2,3-dihydro- quinolon-4*(1H)-one* **95**

through dehydrogenation reaction by using thallium(III) *p*-toluene sulfonate as on oxidative aryl rearranging agent (**Scheme 16**). Sigh *et al*.[136, 137] also developed a reaction which involves the use of thallium(III) salts for oxidative rearrangement of 2,3-dihydro-flavanones and another available procedure to synthesize **96**, is in the presence of diacetoxyiodo benzene, potassium hydroxide, **95** and methanol [137].

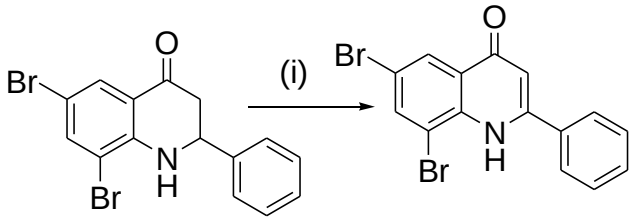

95 **96**

Reaction conditions (i) TTS in DMF reflux, 30 min

Scheme 16. Dehydrogenation using thallium (III) salts

Huagh *et al.* [138] reported a procedure to form quinolon-4*(1H)*-one **99** (**Scheme 17**), by using a Merrified resin as a starting material in a solid organic phase. The resin was synthetically made from a Meldrums acid, through the reaction of sodium ethyl acetate, followed by decarboxylation reaction and the introduction of malonic acid respectively to form an ester functionalized resin compound. The ester compound resin **97** was then reacted with anilines to give an aryl amino-cyclic malonic resin derivative **98**. The quinolon-4*(1H)*-one **99** formed through thermal cyclization of **98** using ethanol to wash, which results in the cleavage of the resin.

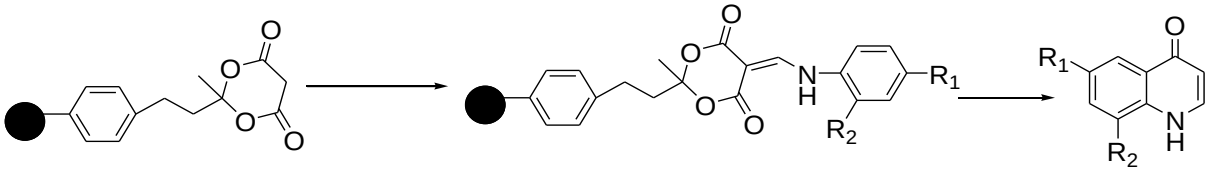

97 **98** **99**

Reaction condition (i) Triethyl-orthoformate 5 ml for 6 h, reflux. (ii) arylamine 20 h, reflux.

Scheme 17. Solid organic reaction condition phase method to form quinolon-4*(1H)*-*one* derivatives

1.7 Methods for the synthesis of halogenated quinolines

Halogens play an important role in the organic skeletal structure to enhance the activity towards certain diseases [139, 140]. Gothard and co-workers [141] performed a chlorination reaction of 2,4-dihydroxyquinoline to form 2,4-dichloroquinoline. To show the variety, Maluleka *et al*. [142] reported the synthesis of 5-bromo-4-chloro-8-iodo-4-oxoquinoline-3-carboxyaldehyde which underwent Sonogashira coupling via iodine at the 8th position (because of its reactivity compared to other halogens). The 2-aryl-6,8-dibromo-quinol-4*(1H)* one **101** and 2-aryl-6-bromo-quinol-4*(1H)-one* **102**, in (**Scheme 18**), were synthesised through bromination reaction of 2-aryl-quinol-4*(1H)-one* **100** in excess NBS [143] and 1 equivalence NBS respectively [144].

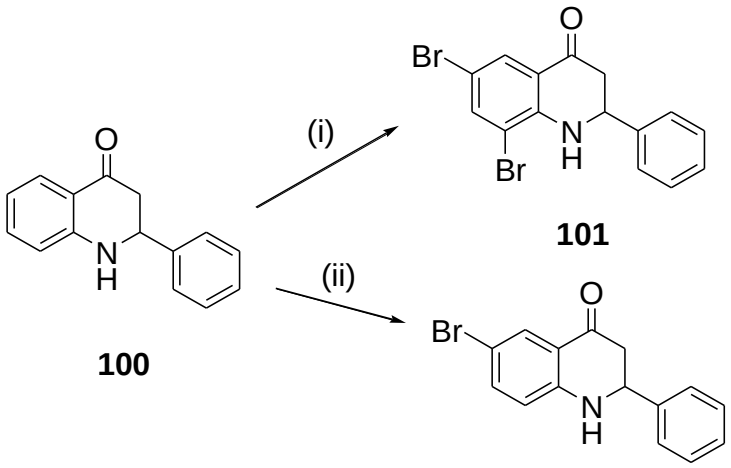

Reaction Conditions (i) Chloroform (3/2 v/v), NBS (2.5 equiv.) 3 h. (ii) $CHCl_3$ 30 ml, Br_2 (1 equiv.)

Scheme 18. Bromination of 2-aryl-quinol-4*(1H)-one*

Sharma *et al*.[145] reported two different reaction conditions for chlorination. The first one is the reaction of di(chloro-iodo) benzene and 2-substituted-2,3-dihyro-quinol-4*(1H)*-one **103** to form 2-substituted 6-chloro-2,3-dihydro-quinol-4*(1H)-one* **104** which was confirmed by the ^{1}H-NMR (J-coupling) and the mass analysis with the yield of 53-76%. Lastly, chlorination was achieved by using chlorine gas which afforded 5,6,7,8-tetrachloro-quinol-4*(1H)*-one **105**.

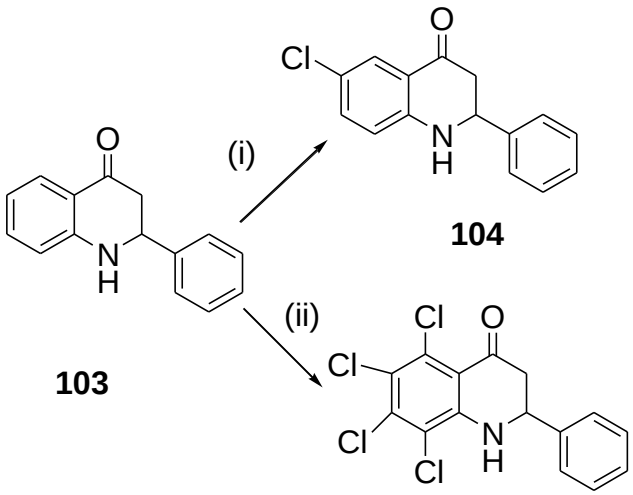

Reaction Conditions (i) $PhICl_2$ (1.5 equiv.), DCM 20 ml, 2 h RT

(ii) Cl_2 gas in 40 ml DCM, the gas inlet and outlet

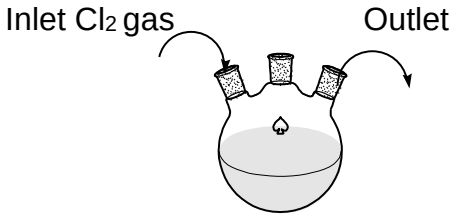

Scheme 19. Single/poly-chlorination of 2-aryl-quinol-4*(1H)* one

Vandekerckhove *et al*.[146] reported the halogenation of 4-quinoline at the 3rd position with >95 % (NMR results) and 89-99 % yield, by using 1,5 equivalence of NBS and CH_2Cl_2 at room temperature for 24 hours. Some halogens can be introduced in the presence of a metal through single electron transfer SET mechanism (**Scheme 21)** under acidic conditions for dehydrogenation oxidative chlorination reaction. An 8-substituted quinoline **106** was reacted with copper metal through a C-H oxidative chlorination reaction to form 8-substituted-5-chloro quinoline **107** (**Scheme 20**)[147].

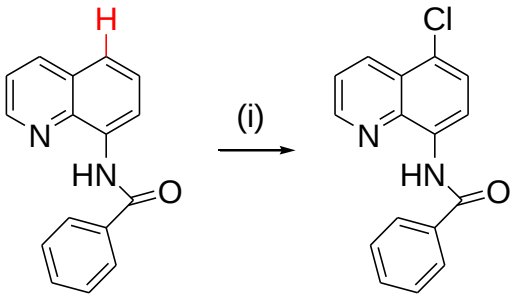

106 **107**

Reaction conditions (i) 1 atm O_2, LiCl, in AcOH at 100 ºC for 17 h

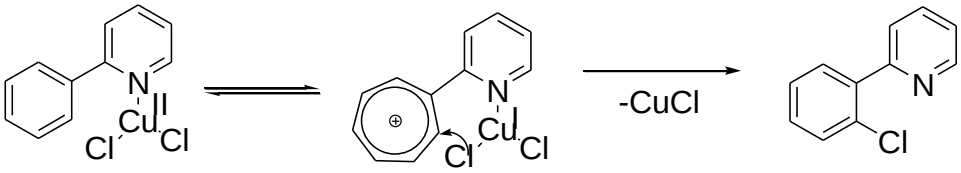

109 **110**

Scheme 20. Proposed SET Mechanism for oxidative chlorination

Scheme 21. Oxidative chlorination reaction through SET mechanism

In the literature, several methods are used to form 4-chloroquinoline **112** derivative, i.e., through oxidative aromatization [148] and substitution reaction in the presence of a ketone and hydroxy group at the 4th position [141] using $POCl_3$ as a chlorinating agent.

Reaction conditions (i) $POCl_3$ at 110-120ºC with 1 h with 95 % yield

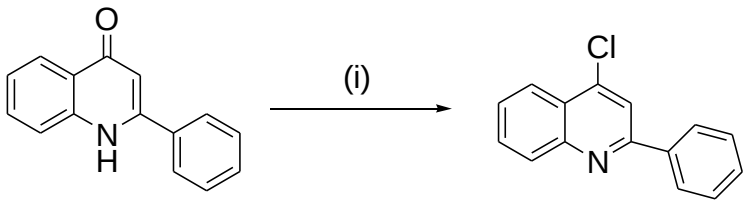

111 **112**

Scheme 22. Oxidative aromatization reaction

1.8 Quinoline Schiff base ligands and their coordinated complexes

1.8.1 An overview of Schiff base ligands and Schiff base complexes molecular hybrids with biological importance

The Schiff bases (imine) are compounds name after Hugo Schiff [149] and are characterised by the presence of an azomethine group (-C=N-) and have been mostly acquired by the condensation of aldehydes/ketones and amines [150]. Schiff bases as ligands are widely used as catalysts, for example in the Suzuki-Miyuara reaction [151] play a role in dye technique [152]. In medicinal chemistry, Schiff bases have been reported to show a wide range of biological properties such as anti-microbial, antioxidant [153], anti-bacterial, anti-fungal [154] and anti-cancerous activities [155]. The *N*-(salicylidene)-2-hydroxy-aniline **113** in **Figure 15** below, is an example of a Schiff base ligand which act as anti-bacterial agent [156]. In literature Schiff base ligands **114** [157] and **115** [158] were found to possess pharmacological activities, in which compound **114** showed antioxidant activity with an IC_{50} 0.44 µM and compound **115** an anti-cancerous drug with a good cytotoxicity with an IC_{50} 7.75 µM and 3.01 µM when tested against breast cancer (MCF-7) cell line after a 24 h and 48 h incubation time respectively. Gaballa *et al.* [159] produced Schiff base ligands **116** and **117** with antimicrobial activities by studying their diameter of inhibitory zones (mm) against bacterial, fungal and yeast cell lines. Compounds **116** and **117** exhibited a diameter of inhibitory zones against bacterial cells of a range 11.6-27.0 mm, 9.6-27.0 mm against fungal cell lines and 0-11.0 mm against yeast cell lines, with Tetraceycline (bacterial positive control) and Fluconazol (fungal and yeast positive control) showing a diameter of inhibitory zones of a range 29.6-32.3 mm and 25.6-27.6 mm respectively. (NB: Diameter of inhibitory zones refers to the study of the sensitivity of the cell line to the Schiff base)

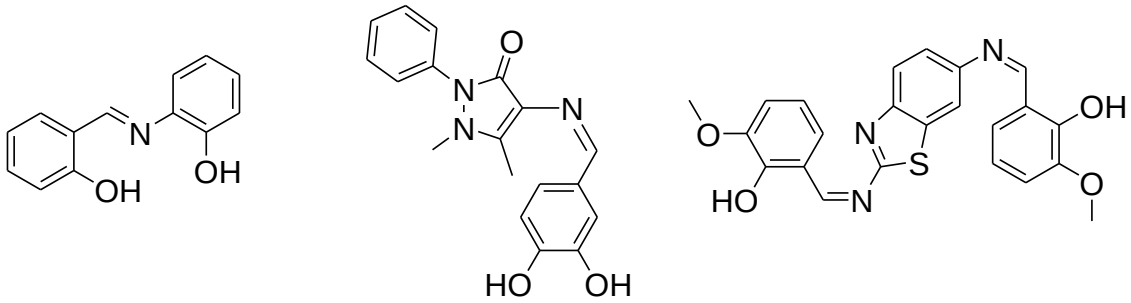

113 **114** **115**

116 **117**

Figure 15. Examples of Schiff base ligands as antimicrobial agents

Schiff base derivatives are studied mostly because of their readiness to form complexes [160] and as good chelating ligands through the nitrogen (N), oxygen (O) and sulphur (S) atoms [161]. Schiff base complexes are synthesised through metal coordination reaction of transition metals and Schiff base ligands [162], as S/O, N donor ligands [163], i.e. compound **118** (bidentate ligand [164]), O^N^O/ N^N^O donor ligands, compound **119** (tridentate ligand) [165] and N^N^O^O ligands, compound **120** (tetradentate ligand) [166,167]

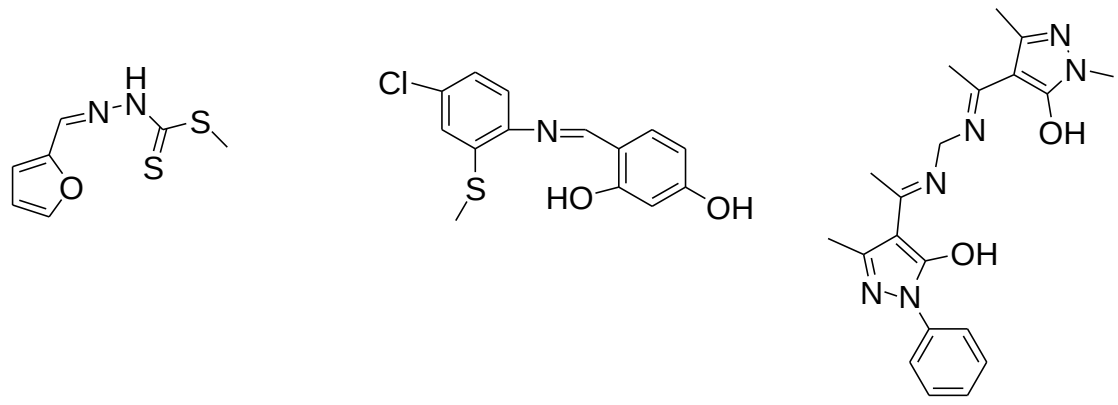

118 **119** **120**

Figure 16. Examples of Schiff base compounds as chelating ligands

The Schiff base complexes are known to be good catalysts for both Heck [168] and Suzuki [169] coupling reactions and equally possess some biological properties such as anti-bacterial [170], anti-microbial [171], anti-cancerous and anti-proliferation [172]. Neelaktan *et al.*[173] reported Schiff base complexes **121** and **122**, which were found to possess a good biological activity against bacteria and fungi compared to the standard used. The Schiff base complex **123** (**Figure 17**), displayed activity against bacterial cell cultures such as *Escherichia coli* (*E. coli*), *Bacillus subtilis* (*B. subtilis*), *Staphylococcus aureus* (*S. aureus*), showing an antimicrobial screening (mm) of 22-42 mm against the cell cultures whilst amikacin (standard) showe a range of 23-50 mm [174]. Al-Aghbari *et al.*[175] produced Pt (II) Schiff base complex **124** confirmed by the NMR, IR and UV-vis-light characterisation and evaluated it against cancer cell lines (HeLa-cervical and PC_3-prostate cancer cell lines) showing an IC_{50} 22.4 µg/ml and 32.5 µg/ml against PC_3 and HeLa cell lines respectively.

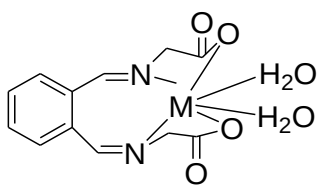

121,122

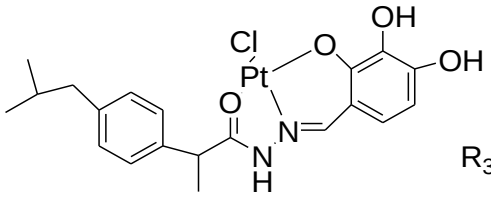

123

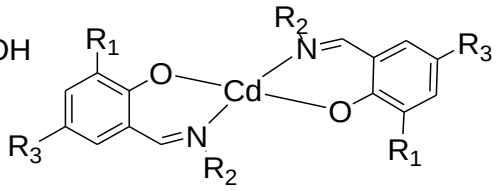

124

M(II)= Ni, Mn

R_1=H, $R_{2=}$ $C_{10}H_{12}$, R_3= NEt_2

Figure 17. Schiff base complexes with some biological activities

In the literature, Schiff base complexes exhibits a good biological activity compared to its Schiff base ligand from which they were synthesised from [176]. Naureen *et al.* [177] reported a comparison iron (Fe) and zinc (Zn) monodentate Schiff base complexes relative to their Schiff base ligands as anti-microbial agents and to reduce drug resistance problems. Schiff base ligand **125** and complex **126** were tested against fungal species *Candida albican* and *Candida glabrata*, in which **126** showed an exceptional antifungal activity with a zone of inhibition of 24 mm and **125** with a zone of inhibition of 12 mm, thus showing that the complex has twice the activity as of the

ligand. A bidentate Schiff base ligand **127** and its Schiff base complex **128** (**Figure 18**), were developed and exhibited an activity against cancer using the MCF-7 breast cancer cell line which displayed an average percentage growth of -16.3 % and 25.7 % when tested against **128** and **127** respectively. This also provided compelling evidence of improved activity in the presence of a metal towards cancer cell line [178].

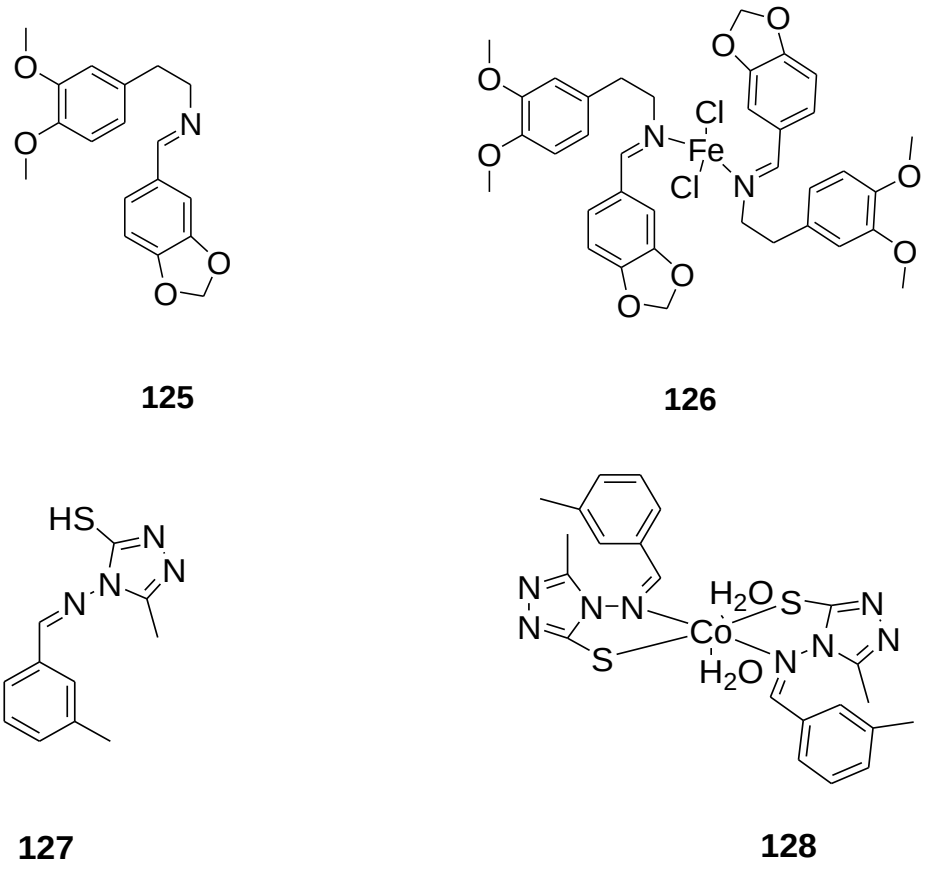

125 **126**

127 **128**

Figure 18. Schiff base ligands and their complexes

1.8.2 Methods of synthesis of Schiff base ligands

The Schiff base ligands are synthesised following different methods, such as microwave, reflux method, normal room temperature reaction [179], sonication [180] and using molecular sieves (as good catalysts and dehydrogenating agents because the formation of Schiff bases involves H_2O as a by-product) [181]. Other methods involve the use of tetraethyl-orthosilicate in the presence of an acid [182] and Lewis acids such as HBr, $ZnCl_2$, LiH [183], $NaHCO_3$ or $MgSO_4$ to attack the carbonyl group and cause the amine (nucleophile) to come in to form a (-C=N-) group [148]. Many procedures

have been discovered but exhibit disadvantages, such as the use of harsh conditions, consume time and have low yields [184]. For example, Schiff base ligand **131** (**Scheme 23**), was formed from the reaction between 2-amino-benzthiazole **129** and a benzaldehyde derivative **130** in good 66-97 % yield but relatively harsher conditions [185].

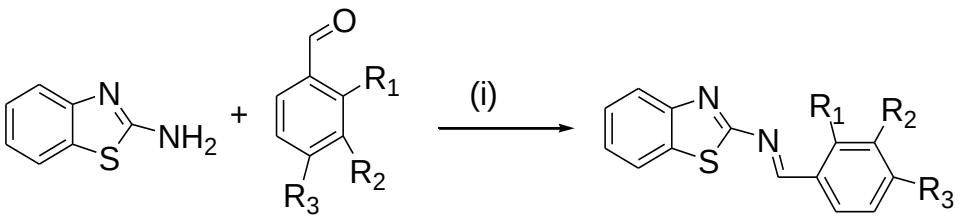

129 **130** **131**

Reaction condition: (i) Ethanol 25 ml, under reflux 2 h

Scheme 23. Synthesis of a Schiff base ligand through condensation reaction

The greener environmental methodologies have also been reported for the synthesis of Schiff base ligands, such as water mediated, less-solvent microwave irradiation and stone -grinder solvent free reaction where these procedures are developed to reduce energy-wastage and generate fewer toxic wastes [186]. Naqui *et al.* [187] synthesised a Schiff base ligand **134** (**Scheme 24**) through condensation reaction by reacting a benzaldehyde **132** and amine-derivative **133** in a water-based reaction where temperature was monitored (meaning the temperature must not exceed 20ºC + room temperature), in the microwave irradiation where DMSO was used a solvent and the reaction took about 3-6 minutes and, in a grind-stone reaction, (no solvent), and the reagents were grinded in a mortar for 5-10 minutes to afford **134**. Above all, the water-based reaction produced high yields of **134** and therefore regarded as good method, because water is available and cheaper.

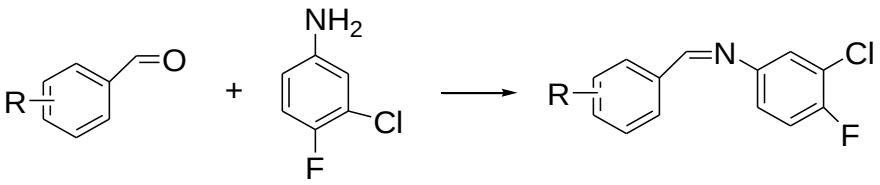

132 **133** **134**

R= 3,4-di-OCH_3, 2-Cl, 4-Cl, 2-OH

Scheme 24. Synthesis of Schiff base ligands using different methodologies

A comparison between conventional method and microwave irradiation has been reported in the production of Schiff base ligands. For example, in the presence of methanol as a solvent, in a conventional method the reaction takes about 3 hours but in a microwave irradiation method the reaction takes about 1.5-3 minutes [188]. A polymer mediated method is also reported, where PEG-400 is used (PEG-400 is an eco-friendly, inexpensive reaction medium and it's used in organic mediums [189]) to produce sulphonated Schiff base ligands **138**, where benzoic acid ethyl ester derivative **135** and a hydrazine **136** are firstly reacted in the presence of PEG-40 through amination reaction and the lastly an aldehyde **137** is added to form **138** through condensation reaction [190].

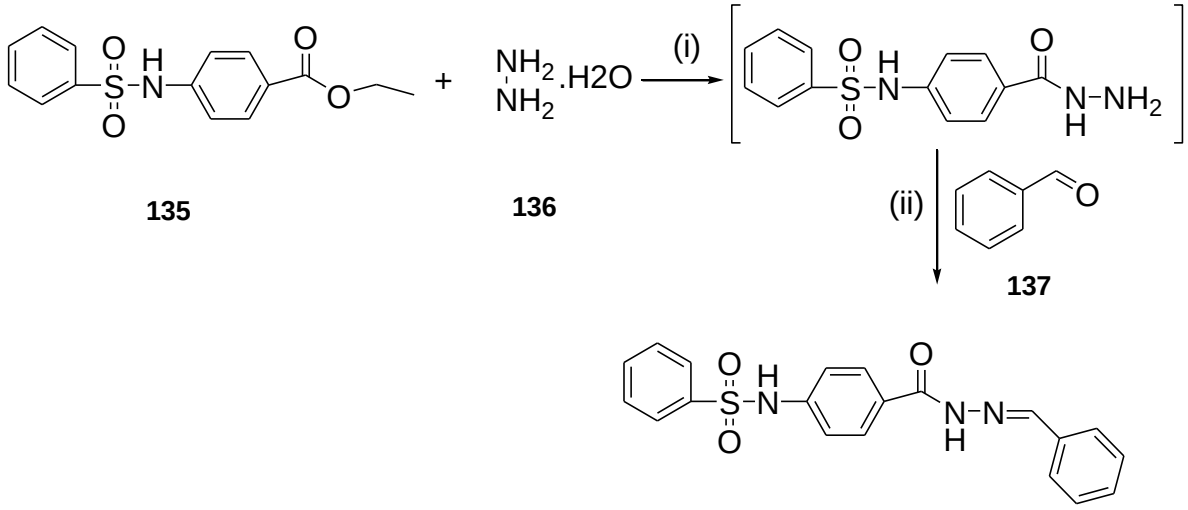

Reaction conditions: (i) PEG-40 15 ml, 6 h. (ii) Aldehyde (**137**), 4 h

Scheme 25. PEG-400 catalysed condensation reaction

1.8.3 Methods of synthesis of Schiff base complexes

Different methods for synthesis of Schiff base complexes have been reported, such as microwave irradiation [191] and conventional methods [192], solvent-free, egg white catalysed synthesis of a Schiff base complex i.e., Cp method using a nano-silver as a present metal [193]. Saritha and Metilda [194] synthesised a Schiff base complex **141** (**Scheme 26**) from N^N^O tridentate Schiff base ligand **143** to form transition metal complexes **140** through coordination reaction in a ratio of 1:2.

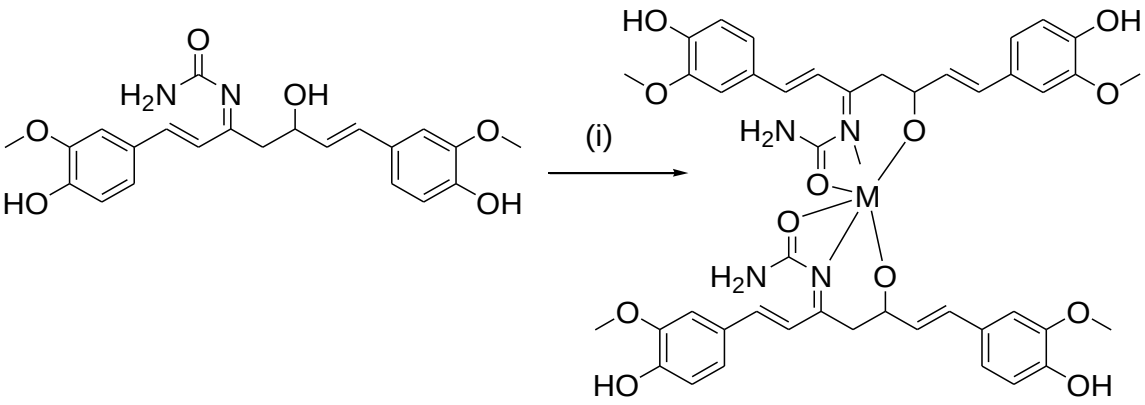

139 **140**

Reaction condition (i) Methanol 50 ml, reflux for 4 h M(II)= Zn, Co, Ni, Cu

Scheme 26. Metal coordination reaction

1.8.4 An overview of Quinoline-Schiff base ligands and quinoline-Schiff base complexes molecular hybrids with biological importance

Quinoline Schiff base ligands are mostly synthesised from quinoline-formyl derivative and an amine/ a quinoline-amine and a formyl derivative vice versa [195]. Quinoline Schiff base complexes are reported to be catalysts in ethylene polymerization [196] and show some biological activity against some cancer [195, 197], bacterial and fungal [198] cell cultures. MiLacic *et al.*[199] reported in literature, a copper metal quinoline-Schiff base complex **142** as an anticancer agent which was tested against the MDA-MB 231 culture breast cancer cell line, and exhibited 90.93 % inhibition at the concentration of 25 µM but showed less effect on proteasomal inhibition by using wig Western blog analysis. A quinoline-2-carboxaformyl derivative **143** (**Figure 22**), has been found to show an activity against prostate cancer (using PC-3 and LNCaP cancer cell line) with a good inhibition concentration (IC_{50}) of 5 µM and 7 µM, comparing it to its ligand with an IC_{50} 16 and 21 µM against PC-3 and LNCaP cancer cell line respectively [200]. Althabiti *et al.* [201] reported compound **144** and **145** which were discovered to show anti-bacterial and anti-fungal activities by using gram negative and positive bacterial and fungal strains. According to the reported results, the zone of inhibition of compound **144** (quinoline - Schiff base complex) showed 31 mm and 32 mm (which are said to be highly active) against the gram positive bacteria *S. aures and E. faecalis* and 12 mm against the gram negative bacteria *E. coli*.

However, complex **145** showed a zone of inhibition of 25 and 28 mm against the above-mentioned gram positive and negative bacteria respectively.

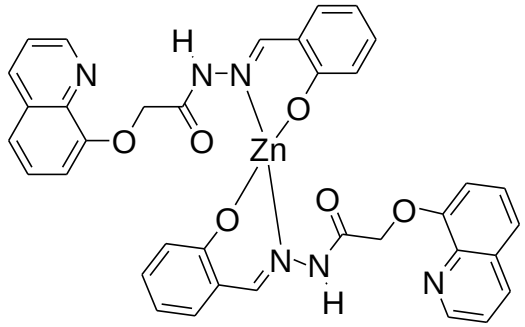

142

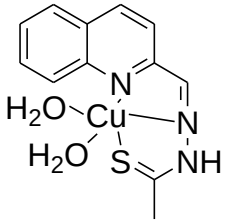

143

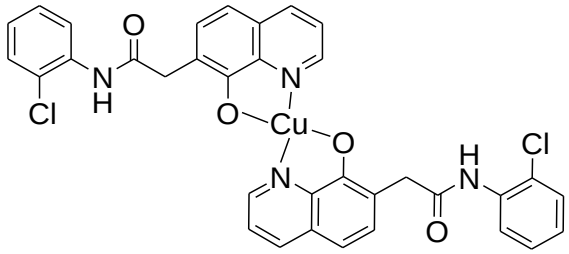

144

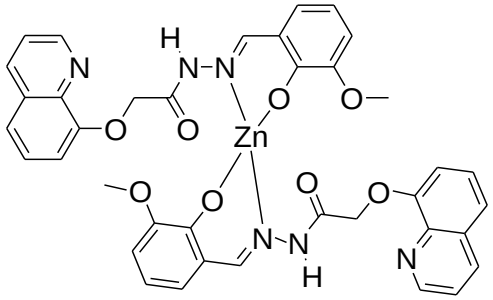

145

Figure 19. Examples of Quinoline Schiff base complexes showing some biological activities

1.9 Project design

Based on the results of the literature in the previous sections, the quinoline moiety has been shown to be an important scaffolding in the design and synthesis of bioactive molecules with the ability to treat a wide range of diseases, which include human disorders such as cancer [27]. This scaffold has been linked to several pharmacophores for the synthesis of quinoline-based molecular hybrids with increased biological activities as discussed in the respective previous sections. However, there have been no examples in the literature in which the quinoline

scaffold binds to the basic part of the triazole derivative to form molecular hybrids for the coordination of transition metals. It is expected that the binding of quinoline scaffold with pharmacophoric moieties such as triazole and the Schiff base would allow the addition of molecular hybrids to quinoline with possible anticancer activities.

1.9.1 Aim of the study

The aim of this project is to synthesise quinoline-4-triazolyl Schiff base complexes as anticancer agents. Our approach was to first halogenate 2-aminoacetophenone **146** at the 3rd and 5th position, which would serve as precursors for the synthesis of 3,5-dibromo α-β unsaturated chalcones **148** to further undergo intramolecular condensation forming 6,8-dibromo-2,3-dihydro quinoline-4(*1H*)-ones **149**. Due to the presence of some electrophilic/nucleophilic factors on 6,8-dibromo-2,3-dihydro quinoline-4(*1H*)-one **149**, dehydrogenation reaction could occur to produce a ketone α-β unsaturated compounds called 6,8-dibromo quinoline-4(*1H*)-ones **150**, which in its tautomeric form (a hydroxy at the 4th position) and by the introduction of a chlorinating agent, a nucleophilic reaction occurs to form compounds **151**. A substitution reaction would probably occur at the 4th position in the presence of a nucleophile (an azide group-N_3), to form a 6,8-dibromo-4-azido quinoline derivatives **152** and further be reacted with different alkynyl derivatives to form a 6,8-dibromo-4-triazolyl phenyl quinoline derivatives **153-155** and 6,8-dibromo-4-triazolyl methanol quinoline derivatives **156** through “click chemistry” reaction. The quinoline triazolyl methanol derivatives would undergo oxidation reaction to form quinoline-triazole-4-carbaldehydes **157** which will be condensed with an amine to form Schiff base ligand for coordination with transition metals to form 6,8-dibromo-4-triazolyl quinoline Schiff base ligands **158** and 6,8-dibromo-4-triazolyl quinoline Schiff base complexes **159** respectively.

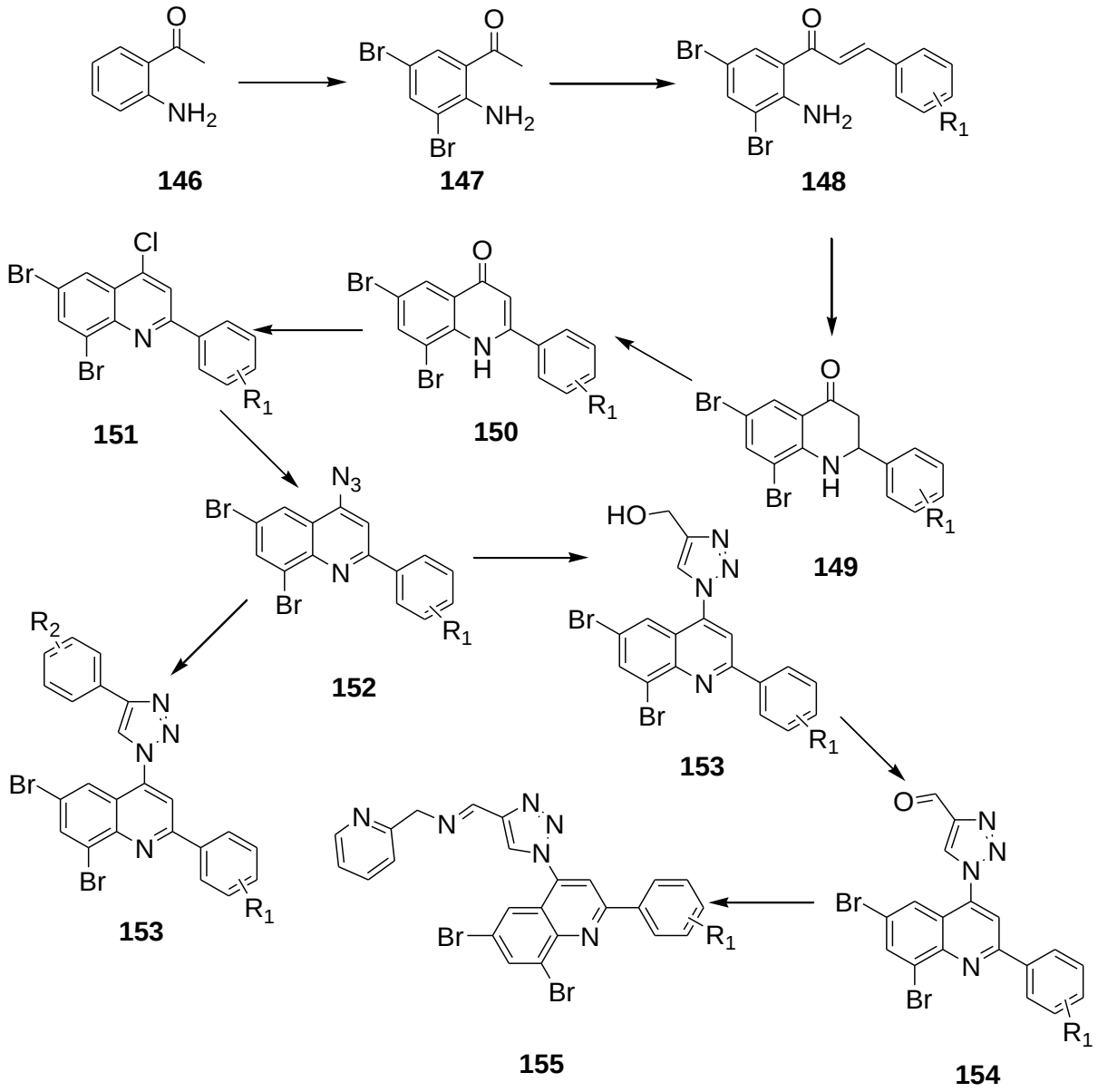

Figure 20. Designed scheme showing pathways to synthesise compounds desired for this study

1.9.2 Specific objectives for this study are to:

i. synthesise halogenated-2-Aminoacetophenone **147** derivatives and to form 3,5-dibromo α-β unsaturated chalcones **148,** Aldol-condensation reaction with benzaldehyde derivatives
ii. prepare 2,3-dihydroquinolin-4(*1H*)-ones **149**, through an acid-mediated cyclization of the 3,5-dibromo α-β unsaturated chalcones **148**
iii. to dehydrogenate the latter to form the quinoline-4(*1H*) ones **150**
iv. synthesize 4-chloro-quinoline **151**, through the chlorination of **150** derivatives
v. subject the 4-chloroquinolines to nucleophilic substitution using sodium azide to afford the 4-azido-quinolines **152**,
vi. introduce acetylene derivatives to form quinoline 2-(4-(4-phenyl-*1H*-1,2,3-triazol-1-yl) derivatives **153** through click chemistry,
vii. synthesize quinoline 2-(4-(*1H*-1,2,3-triazol-1-yl) carbaldehyde **154**, through oxidation reaction,
viii. couple the quinoline derivatives **154** with an amine to form Schiff-Base quinazoline compounds **155**,
ix. coordinate the Schiff-Base quinoline molecular hybrids with a library of transition-metals,
x. characterise all the synthesised compounds using Nuclear Magnetic Resonance (NMR), Fourier Transform Infrared Spectroscopy (FTIR), Mass Spectroscopy (MS), Ultraviolet-visible Spectroscopy (UV-vis spectroscopy) and Single crystal X-ray diffraction,
xi. perform the *in-vitro* and *in-silico* studies.

1.10 References

1. Birgül, K., Yıldırım, Y., Karasulu, H.Y., Karasulu, E., Uba, A.I., Yelekçi, K., Bekçi, H., Cumaoğlu, A., Kabasakal, L., Yılmaz, Ö. and Küçükgüzel, Ş.G., 2020. Synthesis, molecular modeling, in vivo study and anticancer activity against prostate cancer of (+)(S)-naproxen derivatives. *European Journal of Medicinal Chemistry*, *208*, 112841.
2. Garrabrant, T., Tuman, R., Ludovici, D., Tominovich, R., Simoneaux, R. and Galemmo, R., 2004. Small molecule inhibitors of methionine aminopeptidase type 2 (MetAP-2) fail to inhibit endothelial cell proliferation or formation of microvessels from rat aortic rings in vitro. *Angiogenesis*, *7*(2), 91-96.
3. Ducreux, M., Cuhna, A.S., Caramella, C., Hollebecque, A., Burtin, P., Goéré, D., Seufferlein, T., Haustermans, K., Van Laethem, J.L., Conroy, T. and Arnold, D., 2015. Cancer of the pancreas: ESMO Clinical Practice Guidelines for diagnosis, treatment and follow-up. *Annals of Oncology*, *26*, v56-v68.
4. Folprecht, G., Martinelli, E., Mazard, T., Modest, D.P., Tsuji, A., Esser, R., Cremolini, C. and Falcone, A., 2022. Triplet chemotherapy in combination with anti-EGFR agents for the treatment of metastatic colorectal cancer: Current evidence, advances, and future perspectives. *Cancer treatment reviews*, *102*, p.102301.
5. Li, L., Han, J., Mo, H. and Ma, F., 2021. Expert consensus on diagnosis, treatment and fertility management of young breast cancer patients. *Journal of the National Cancer Center, 1*, 23-30.
6. Barazzuol, L., Coppes, R.P. and van Luijk, P., 2020. Prevention and treatment of radiotherapy-induced side effects. *Molecular Oncology*, *14*(7), 1538-1554.
7. Katt, M.E., Placone, A.L., Wong, A.D., Xu, Z.S. and Searson, P.C., 2016. In vitro tumor models: advantages, disadvantages, variables, and selecting the right platform. *Frontiers in Bioengineering and Biotechnology*, *4*, p.12.
8. Mokhtari, R.B., Homayouni, T.S., Baluch, N., Morgatskaya, E., Kumar, S., Das, B. and Yeger, H., 2017. Combination therapy in combating cancer. *Oncotarget*, *8*(23), p.38022.

9. Arora, P., Arora, V., Lamba, H.S. and Wadhwa, D., 2012. Importance of heterocyclic chemistry: a review. *International Journal of Pharmaceutical Sciences and Research*, *3*(9), p.2947.
10. Aljamali, N.M. and Jwad, S.M., 2015. Survey in pyrrole compounds and biological activity. *ITIRJ*, *1*, 1-8.
11. Avan, I., 2011. *Synthesis and Biological Activity of Novel Furan and 1h-pyrrole-containing Heterocyclic Compounds as HIV-1 Fusion Inhibitors* (Doctoral dissertation, University of Florida).
12. Mishra, R., Jha, K.K., Kumar, S. and Tomer, I., 2011. Synthesis, properties, and biological activity of thiophene: A review. *Der Pharma Chemica*, *3*(4), 38-54.
13. Wang, S., Yuan, X.H., Wang, S.Q., Zhao, W., Chen, X.B. and Yu, B., 2021. FDA-approved pyrimidine-fused bicyclic heterocycles for cancer therapy: Synthesis and clinical application. *European Journal of Medicinal Chemistry*, *214*, p.113218.
14. Jaiswal, S., 2019. Five and Six Membered Heterocyclic Compound with Antimicrobial Activity. *Journal for Modern Trends in Science and Technology*, *5*(06), 36-39.
15. Pearce, S., 2017. The importance of heterocyclic compounds in anti-cancer drug design. *Drug Discovery*, p.67.
16. Mermer, A., Keles, T. and Sirin, Y., 2021. Recent Studies of Nitrogen Containing Heterocyclic Compounds as Novel Antiviral Agents: A Review. *Bioorganic Chemistry*, p.105076.
17. Avanzo, R.E., Anesini, C., Fascio, M.L., Errea, M.I. and D'Accorso, N.B., 2012. 1, 2, 4-Triazole D-ribose derivatives: design, synthesis and antitumoral evaluation. *European Journal of Medicinal Chemistry*, *47*, 104-110.
18. Paul, K., Bindal, S. and Luxami, V., 2013. Synthesis of new conjugated coumarin–benzimidazole hybrids and their anticancer activity. *Bioorganic & Medicinal Chemistry Letters*, *23*(12), 3667-3672.
19. Wahyuningsih, T.D., Suma, A.A.T. and Astuti, E., 2019. Synthesis, anticancer activity, and docking study of N-acetyl pyrazolines from veratraldehyde. *J Appl Pharm Sci*, *9*(3), 14-20.
20. Vasan, N., Baselga, J. and Hyman, D.M., 2019. A view on drug resistance in cancer. *Nature*, *575*(7782), 299-309.

21. Wang, X., Zhang, H. and Chen, X., 2019. Drug resistance and combating drug resistance in cancer. *Cancer Drug Resistance (Alhambra, Calif.)*, *2*, p.141.
22. Nepali, K., Sharma, S., Sharma, M., Bedi, P.M.S. and Dhar, K.L., 2014. Rational approaches, design strategies, structure activity relationship and mechanistic insights for anticancer hybrids. *European Journal of Medicinal chemistry*, *77*, 422-487.
23. Gediya, L.K. and Njar, V.C., 2009. Promise and challenges in drug discovery and development of hybrid anticancer drugs. *Expert Opinion on Drug Discovery*, *4*(11), 1099-1111.
24. Viegas-Junior, C., Danuello, A., da Silva Bolzani, V., Barreiro, E.J. and Fraga, C.A.M., 2007. Molecular hybridization: a useful tool in the design of new drug prototypes. *Current Medicinal Chemistry*, *14*(17), 1829-1852.
25. Kolb, H.C. and Sharpless, K.B., 2003. The growing impact of click chemistry on drug discovery. *Drug Discovery Today*, *8*(24), 1128-1137.
26. Witte, W., 2003. Fluoroquinolone Antibiotics. Milestones in Drug Therapy. *International Journal of Medical Microbiology*, *293*(5), p.383.
27. Jin, G., Li, Z., Xiao, F., Qi, X. and Sun, X., 2020. Optimization of activity localization of quinoline derivatives: Design, synthesis, and dual evaluation of biological activity for potential antitumor and antibacterial agents. *Bioorganic Chemistry*, *99*, p.103837.
28. Henriquez, F.L. and d Roderick, A.M., 2020. Knowing one's enemy: the Plasmodium parasite. In *Antimalarial Agents* (49-64). Elsevier.
29. Egan, T.J., 2006. Chloroquine and primaquine: combining old drugs as a new weapon against falciparum malaria?. *Trends in Parasitology*, *22*(6), 235-237.
30. Gunatilaka, A.L., 1998. Alkaloids from Sri Lankan flora. *Chemistry and Biology*.
31. Oliveri, V. and Vecchio, G., 2016. 8-Hydroxyquinolines in medicinal chemistry: A structural perspective. *European Journal of Medicinal Chemistry*, *120*, 252-274.
32. Wall, M.E., Wani, M.C., Cook, C.E., Palmer, K.H., McPhail, A.A. and Sim, G.A., 1966. Plant antitumor agents. I. The isolation and structure of camptothecin, a novel alkaloidal leukemia and tumor inhibitor from

camptotheca acuminata1, 2. *Journal of the American Chemical Society*, *88*(16), 3888-3890.

33. A Reynolds, K., A Loughlin, W. and J Young, D., 2013. Quinolines as chemotherapeutic agents for leishmaniasis. *Mini Reviews in Medicinal Chemistry*, *13*(5), 730-743.
34. Kalac, M., Mangone, M., Rinderspacher, A., Deng, S.X., Scotto, L., Markson, M., Bansal, M., Califano, A., Landry, D.W. and O'Connor, O.A., 2020. N-quinoline-benzenesulfonamide derivatives exert potent anti-lymphoma effect by targeting NF-κB. *Iscience*, *23*(12), p.101884.
35. Yadav, P. and Shah, K., 2021. Quinolines, a perpetual, multipurpose scaffold in medicinal chemistry. *Bioorganic Chemistry*, p.104639.
36. Qi, B., Yang, Y., Gong, G., He, H., Yue, X., Xu, X., Hu, Y., Li, J., Chen, T., Wan, X. and Zhang, A., 2019. Discovery of N1-(4-((7-(3-(4-ethylpiperazin-1-yl) propoxy)-6-methoxyquinolin-4-yl) oxy)-3, 5-difluorophenyl)-N3-(2-(2, 6-difluorophenyl)-4-oxothiazolidin-3-yl) urea as a multi-tyrosine kinase inhibitor for drug-sensitive and drug-resistant cancers treatment. *European Journal of Medicinal Chemistry*, *163*, 10-27.
37. Kumar, S., Bawa, S. and Gupta, H., 2009. Biological activities of quinoline derivatives. *Mini Reviews in Medicinal Chemistry*, *9*(14), 1648-1654.
38. Caprio, V., Guyen, B., Opoku-Boahen, Y., Mann, J., Gowan, S.M., Kelland, L.M., Read, M.A. and Neidle, S., 2000. A novel inhibitor of human telomerase derived from 10H-indolo [3, 2-b] quinoline. *Bioorganic & Medicinal Chemistry Letters*, *10*(18), 2063-2066.
39. Mikata, Y., Yokoyama, M., Ogura, S.I., Okura, I., Kawasaki, M., Maeda, M. and Yano, S., 1998. Effect of side chain location in (2-aminoethyl) aminomethyl-2-phenylquinolines as antitumor agents. *Bioorganic & Medicinal Chemistry Letters*, *8*(10), 1243-1248.
40. Monis, B. and Eynard, A.R., 1981. Abnormal cell proliferation and differentiation and urothelial tumorigenesis in essential fatty acid deficient (EFAD) rats. *Progress in Lipid Research*, *20*, 691-703.
41. Li, K., Li, Y., Zhou, D., Fan, Y., Guo, H., Ma, T., Wen, J., Liu, D. and Zhao, L., 2016. Synthesis and biological evaluation of quinoline derivatives as potential anti-prostate cancer agents and Pim-1 kinase inhibitors. *Bioorganic & Medicinal Chemistry*, *24*(8), 1889-1897.

42. Alonso, C., Fuertes, M., Martín-Encinas, E., Selas, A., Rubiales, G., Tesauro, C., Knudssen, B.K. and Palacios, F., 2018. Novel topoisomerase I inhibitors. Syntheses and biological evaluation of phosphorus substituted quinoline derivates with antiproliferative activity. *European Journal of Medicinal Chemistry*, *149*, 225-237.
43. Chen, H., Yu, C., Shen, L., Wu, Y., Wu, D., Wang, Z., Song, G., Chen, L. and Hong, Y., 2020. NFIB functions as an oncogene in estrogen receptor-positive breast cancer and is regulated by miR-205-5p. *Pathology-Research and Practice*, *216*(12), p.153236.
44. Ghodsi, R., Azizi, E., Grazia Ferlin, M., Pezzi, V. and Zarghi, A., 2016. Design, synthesis and biological evaluation of 4-(imidazolylmethyl)-2-aryl-quinoline derivatives as aromatase inhibitors and anti-breast cancer agents. *Letters in Drug Design & Discovery*, *13*(1), 89-97.
45. Li, D., Li, Z., Qiu, C., Peng, B., Zhang, Y., Sun, H. and Wang, S., 2021. 2-Amino-3-methylimidazo [4, 5-f] quinoline induced oxidative stress and inflammation via TLR4/MAPK and TLR4/NF-κB signaling pathway in zebrafish (Danio rerio) livers. *Food and Chemical Toxicology*, *157*, p.112583.
46. Yadav, D.K., Rai, R., Kumar, N., Singh, S., Misra, S., Sharma, P., Shaw, P., Pérez-Sánchez, H., Mancera, R.L., Choi, E.H. and Kim, M.H., 2016. New arylated benzo [h] quinolines induce anti-cancer activity by oxidative stress-mediated DNA damage. *Scientific Reports*, *6*(1), 1-13.
47. Chen, Y.L., Chen, I.L., Wang, T.C., Han, C.H. and Tzeng, C.C., 2005. Synthesis and anticancer evaluation of certain 4-anilinofuro [2, 3-b] quinoline and 4-anilinofuro [3, 2-c] quinoline derivatives. *European Journal of Medicinal Chemistry*, *40*(9), 928-934.
48. He, L., Chang, H.X., Chou, T.C., Savaraj, N. and Cheng, C.C., 2003. Design of antineoplastic agents based on the '2-phenylnaphthalene-type'structural pattern—synthesis and biological activity studies of 11H-indolo [3.2-c] quinoline derivatives. *European Journal of Medicinal Chemistry*, *38*(1), 101-107.
49. Liu, X. and Lu, Y., 2010. Asymmetric synthesis of 2-aryl-2, 3-dihydro-4-quinolones via bifunctional thiourea-mediated intramolecular cyclization. *Organic Letters*, *12*(23), 5592-5595.

50. Bhattacharya, R.N., Kundu, P. and Maiti, G., 2010. Antimony Trichloride: An Efficient and Mild Catalyst for Cyclization of 2-Aminochalcones to the Corresponding 2-Aryl-2, 3-Dihydroquinolin-4 (1 H)-Ones. *Synthetic Communications*®, *40*(4), 476-481.
51. Varma, R.S. and Saini, R.K., 1997. Microwave-assisted isomerization of 2'-aminochalcones on clay: an easy route to 2-aryl-1, 2, 3, 4-tetrahydro-4-quinolones. *Synlett*, *1997*(07), 857-858.
52. Jeffries, B., Wang, Z., Troup, R.I., Goupille, A., Le Questel, J.Y., Fallan, C., Scott, J.S., Chiarparin, E., Graton, J. and Linclau, B., 2020. Lipophilicity trends upon fluorination of isopropyl, cyclopropyl and 3-oxetanyl groups. *Beilstein Journal of Organic Chemistry*, *16*(1), 2141-2150.
53. Kumar, K.H., Muralidharan, D. and Perumal, P.T., 2004. Indium (III) chloride/silica gel-promoted facile and rapid cyclization of 2-aminochalcones to 2-aryl-2, 3-dihydroquinolin-4 (1H)-ones under solvent-free conditions. *Synthesis*, *2004*(01), 63-68.
54. Reddy, K.R., Rao, P.S., Dev, G.J., Poornachandra, Y., Kumar, C.G., Rao, P.S. and Narsaiah, B., 2014. Synthesis of novel 1, 2, 3-triazole/isoxazole functionalized 2H-Chromene derivatives and their cytotoxic activity. *Bioorganic & Medicinal Chemistry Letters*, *24*(7), 1661-1663.
55. Choudhury, P. and Basu, B., 2020. Graphene oxide nanosheets as sustainable carbocatalysts: Synthesis of medicinally important heterocycles. In *Green Approaches in Medicinal Chemistry for Sustainable Drug Design* (47-74). Elsevier.
56. Moussa, G., Alaaeddine, R., Alaeddine, L.M., Nassra, R., Belal, A.S., Ismail, A., El-Yazbi, A.F., Abdel-Ghany, Y.S. and Hazzaa, A., 2018. Novel click modifiable thioquinazolinones as anti-inflammatory agents: Design, synthesis, biological evaluation and docking study. *European Journal of Medicinal chemistry*, *144*, 635-650.
57. Pinheiro, S., Pessôa, J.C., Pinheiro, E.M., Muri, E.M., Venturini Filho, E., Loureiro, L.B., Freitas, M.C.R., Junior, C.M.S., Fiorot, R.G., Carneiro, J.W.M. and Rotamiro, K.M., 2020. 2H-1, 2, 3-Triazole-chalcones as novel cytotoxic agents against prostate cancer. *Bioorganic & Medicinal Chemistry Letters*, *30*(19), p.127454.

58. Lai, Q., Wang, Y., Wang, R., Lai, W., Tang, L., Tao, Y., Liu, Y., Zhang, R., Huang, L., Xiang, H. and Zeng, S., 2018. Design, synthesis and biological evaluation of a novel tubulin inhibitor 7a3 targeting the colchicine binding site. *European Journal of Medicinal Chemistry*, *156*, 162-179.
59. Ducki, S., Mackenzie, G., Greedy, B., Armitage, S., Chabert, J.F.D., Bennett, E., Nettles, J., Snyder, J.P. and Lawrence, N.J., 2009. Combretastatin-like chalcones as inhibitors of microtubule polymerisation. Part 2: Structure-based discovery of alpha-aryl chalcones. *Bioorganic & Medicinal Chemistry*, *17*(22), 7711-7722.
60. Pinheiro, S., Pessôa, J.C., Pinheiro, E.M., Muri, E.M., Venturini Filho, E., Loureiro, L.B., Freitas, M.C.R., Junior, C.M.S., Fiorot, R.G., Carneiro, J.W.M. and Rotamiro, K.M., 2020. 2H-1, 2, 3-Triazole-chalcones as novel cytotoxic agents against prostate cancer. *Bioorganic & Medicinal Chemistry Letters*, *30*(19), p.127454.
61. Odlo, K., Hentzen, J., dit Chabert, J.F., Ducki, S., Gani, O.A., Sylte, I., Skrede, M., Flørenes, V.A. and Hansen, T.V., 2008. 1, 5-Disubstituted 1, 2, 3-triazoles as cis-restricted analogues of combretastatin A-4: synthesis, molecular modeling and evaluation as cytotoxic agents and inhibitors of tubulin. *Bioorganic & Medicinal Chemistry*, *16*(9), 4829-4838.
62. Dheer, D., Singh, V. and Shankar, R., 2017. Medicinal attributes of 1, 2, 3-triazoles: Current developments. *Bioorganic Chemistry*, *71*, 30-54.
63. Agard, N.J., Prescher, J.A. and Bertozzi, C.R., 2004. A strain-promoted [3+ 2] azide− alkyne cycloaddition for covalent modification of biomolecules in living systems. *Journal of the American Chemical Society*, *126*(46), 15046-15047.
64. Reddy, T.R., Li, C., Guo, X., Fischer, P.M. and Dekker, L.V., 2014. Design, synthesis, and SAR exploration of tri-substituted 1, 2, 4-triazoles as inhibitors of the annexin A2–S100A10 protein interaction. *Bioorganic & Medicinal Chemistry*, *22*(19), 5378-5391.
65. Stefely, J.A., Palchaudhuri, R., Miller, P.A., Peterson, R.J., Moraski, G.C., Hergenrother, P.J. and Miller, M.J., 2010. N-((1-Benzyl-1 H-1, 2, 3-triazol-4-yl) methyl) arylamide as a new scaffold that provides rapid access to antimicrotubule agents: synthesis and evaluation of antiproliferative activity against select cancer cell lines. *Journal of Medicinal Chemistry*, *53*(8), 3389-3395.

66. Gurrapu, N., Kumar, E.P., Kolluri, P.K., Putta, S., Sivan, S.K. and Subhashini, N.J.P., 2020. Synthesis, biological evaluation and molecular docking studies of novel 1, 2, 3-triazole tethered chalcone hybrids as potential anticancer agents. *Journal of Molecular Structure*, *1217*, p.128356.
67. Yadav, P., Lal, K., Kumar, A., Guru, S.K., Jaglan, S. and Bhushan, S., 2017. Green synthesis and anticancer potential of chalcone linked-1, 2, 3-triazoles. *European Journal of Medicinal Chemistry*, *126*, 944-953.
68. Ince, T., Serttas, R., Demir, B., Atabey, H., Seferoglu, N., Erdogan, S., Sahin, E., Erat, S. and Nural, Y., 2020. Polysubstituted pyrrolidines linked to 1, 2, 3-triazoles: Synthesis, crystal structure, DFT studies, acid dissociation constant, drug-likeness, and anti-proliferative activity. *Journal of Molecular Structure*, *1217*, p.128400.
69. Kaushik, C.P., Sangwan, J., Luxmi, R., Kumar, D., Kumar, D., Das, A., Kumar, A. and Singh, D., 2021. Design, synthesis, anticancer and antioxidant activities of amide linked 1, 4-disubstituted 1, 2, 3-triazoles. *Journal of Molecular Structure*, *1226*, p.129255.
70. Shafi, S., Alam, M.M., Mulakayala, N., Mulakayala, C., Vanaja, G., Kalle, A.M., Pallu, R. and Alam, M.S., 2012. Synthesis of novel 2-mercapto benzothiazole and 1, 2, 3-triazole based bis-heterocycles: their anti-inflammatory and anti-nociceptive activities. *European Journal of Medicinal Chemistry*, *49*, 324-333.
71. Schiewer, M.J. and Knudsen, K.E., 2014. Transcriptional roles of PARP1 in cancer. *Molecular Cancer Research*, *12*(8), 1069-1080.
72. Li, S., Li, X.Y., Zhang, T.J., Zhu, J., Xue, W.H., Qian, X.H. and Meng, F.H., 2020. Design, synthesis, and biological evaluation of erythrina derivatives bearing a 1, 2, 3-triazole moiety as PARP-1 inhibitors. *Bioorganic Chemistry*, *96*, p.103575.
73. Teixeira, R.R., Gazolla, P.A.R., da Silva, A.M., Borsodi, M.P.G., Bergmann, B.R., Ferreira, R.S., Vaz, B.G., Vasconcelos, G.A. and Lima, W.P., 2018. Synthesis and leishmanicidal activity of eugenol derivatives bearing 1, 2, 3-triazole functionalities. *European Journal of Medicinal Chemistry*, *146*, 274-286.
74. Pereira, G.R., Brandao, G.C., Arantes, L.M., de Oliveira Jr, H.A., de Paula, R.C., do Nascimento, M.F.A., dos Santos, F.M., da Rocha, R.K., Lopes,

J.C.D. and de Oliveira, A.B., 2014. 7-Chloroquinolinotriazoles: Synthesis by the azide–alkyne cycloaddition click chemistry, antimalarial activity, cytotoxicity and SAR studies. *European Journal of Medicinal Chemistry*, *73*, 295-309.

75. Zhang, J., Chen, W., Wang, B., Zhao, Z., Wang, X. and Hu, Y., 2015. One-pot three-component synthesis of 1, 4, 5-trisubstituted 5-iodo-1, 2, 3-triazoles from 1-copper (I) alkyne, azide and molecular iodine. *RSC Advances*, *5*(19), 14561-14566.
76. Zhao, X., Lu, B.W., Lu, J.R., Xin, C.W., Li, J.F. and Liu, Y., 2012. Design, synthesis and antimicrobial activities of 1, 2, 3-triazole derivatives. *Chinese Chemical Letters*, *23*(8), 933-935.
77. Naidu, K.M., Srinivasarao, S., Agnieszka, N., Ewa, A.K., Kumar, M.M.K. and Sekhar, K.V.G.C., 2016. Seeking potent anti-tubercular agents: Design, synthesis, anti-tubercular activity and docking study of various ((triazoles/indole)-piperazin-1-yl/1, 4-diazepan-1-yl) benzo [d] isoxazole derivatives. *Bioorganic & Medicinal Chemistry Letters*, *26*(9), 2245-2250.
78. Ashok, D., Kavitha, R., Gundu, S. and Hanumantha, R.V., 2017. Microwave-assisted synthesis of new pyrazole derivatives bearing 1, 2, 3-triazole scaffold as potential antimicrobial agents. *Journal of the Serbian Chemical Society*, *82*(4), 357-366.
79. Sharma, B., Agrawal, S.C. and Gupta, K.C., 2008. Colour reactions of chalcones and their mechanism (a review). *Oriental Journal of Chemistry*, *24*(1), p.289.
80. Yerragunta, V., Kumaraswamy, T., Suman, D., Anusha, V., Patil, P. and Samhitha, T., 2013. A review on Chalcones and its importance. *PharmaTutor*, *1*(2), 54-59.
81. Ngameni, B., Cedric, K., Mbaveng, A.T., Erdoğan, M., Simo, I., Kuete, V. and Daştan, A., 2021. Design, synthesis, characterization, and anticancer activity of a novel series of O-substituted chalcone derivatives. *Bioorganic & Medicinal Chemistry Letters*, *35*, p.127827.
82. Tanemura, K. and Rohand, T., 2020. Activated charcoal as an effective additive for alkaline and acidic hydrolysis of esters in water. *Tetrahedron Letters*, *61*(44), p.152467.

83. Da Silva, P.T., da Cunha Xavier, J., Freitas, T.S., Oliveira, M.M., Coutinho, H.D.M., Leal, A.L.A.B., Barreto, H.M., Bandeira, P.N., Nogueira, C.E.S., Sena Jr, D.M. and Almeida-Neto, F.W.Q., 2021. Synthesis, spectroscopic characterization and antibacterial evaluation by chalcones derived of acetophenone isolated from Croton anisodontus Müll. Arg. *Journal of Molecular Structure*, *1226*, p.129403.
84. Li, N., Xu, S., Wang, X., Xu, L., Qiao, J., Liang, Z. and Xu, X., 2021. Ag2CO3-catalyzed efficient synthesis of internal or terminal propargylicamines and chalcones via A3-coupling under solvent-free condition. *Chinese Chemical Letters*.
85. Eddarir, S., Cotelle, N., Bakkour, Y. and Rolando, C., 2003. An efficient synthesis of chalcones based on the Suzuki reaction. *Tetrahedron Letters*, *44*(28), 5359-5363.
86. Aguilar-Aguilar, A. and Peña-Cabrera, E., 2007. Selective Cross-Couplings. Sequential Stille− Liebeskind/Srogl Reactions of 3-Chloro-4-arylthiocyclobutene-1, 2-dione. *Organic Letters*, *9*(21), 4163-4166.
87. Kearney, A.M., Murphy, L., Murphy, C.C., Eccles, K.S., Lawrence, S.E., Collins, S.G. and Maguire, A.R., 2021. Synthesis and reactivity of α-sulfenyl-β-chloroenones, including oxidation and Stille cross-coupling to form chalcone derivatives. *Tetrahedron*, *88*, p.132091.
88. Kolb, H.C., Finn, M.G. and Sharpless, K.B., 2001. Click chemistry: diverse chemical function from a few good reactions. *Angewandte Chemie International Edition*, *40*(11), 2004-2021.
89. Michaels, H.A. and Zhu, L., 2011. Ligand-Assisted, Copper (II) Acetate-Accelerated Azide–Alkyne Cycloaddition. *Chemistry–An Asian Journal*, *6*(10), 2825-2834.
90. Kuang, G.C., Michaels, H.A., Simmons, J.T., Clark, R.J. and Zhu, L., 2010. Chelation-assisted, copper (II)-acetate-accelerated azide− alkyne cycloaddition. *The Journal of Organic Chemistry*, *75*(19), 6540-6548.
91. Brotherton, W.S., 2012. Development of Copper (II)-Mediated Azide-Alkyne Cycloaddition Reactions Using Chelating Azides.
92. Smith, C.D. and Greaney, M.F., 2013. Zinc mediated azide–alkyne ligation to 1, 5-and 1, 4, 5-substituted 1, 2, 3-triazoles. *Organic Letters*, *15*(18), 4826-4829.

93. Sharma, R.K., Mishra, M., Sharma, S. and Dutta, S., 2016. Zinc (II) complex immobilized on amine functionalized silica gel: a novel, highly efficient and recyclable catalyst for multicomponent click synthesis of 1, 4-disubstituted 1, 2, 3-triazoles. *Journal of Coordination Chemistry*, *69*(7), 1152-1165.
94. Agard, N.J., Prescher, J.A. and Bertozzi, C.R., 2004. A strain-promoted [3+ 2] azide− alkyne cycloaddition for covalent modification of biomolecules in living systems. *Journal of the American Chemical Society*, *126*(46), 15046-15047.
95. Wan, J.P., Cao, S. and Liu, Y., 2015. A metal-and azide-free multicomponent assembly toward regioselective construction of 1, 5-disubstituted 1, 2, 3-triazoles. *The Journal of Organic Chemistry*, *80*(18), 9028-9033.
96. Kwok, S.W., Fotsing, J.R., Fraser, R.J., Rodionov, V.O. and Fokin, V.V., 2010. Transition-metal-free catalytic synthesis of 1, 5-diaryl-1, 2, 3-triazoles. *Organic Letters*, *12*(19), 4217-4219.
97. Palumbo Piccionello, A., Pibiri, I., Buscemi, S. and Pace, A., 2019. Recent development in fluorinated antibiotics.
98. Aouad, M.R., 2015. Efficient eco-friendly solvent-free click synthesis and antimicrobial evaluation of new fluorinated 1, 2, 3-triazoles and their conversion into Schiff Bases. *Journal of the Brazilian Chemical Society*, *26*, 2105-2115.
99. Kuhnert, N., 2002. Microwave-assisted reactions in organic synthesis—are there any nonthermal microwave effects?. *Angewandte Chemie International Edition*, *41*(11), 1863-1866.
100. Bouasla, S., Fatmi, C.E. and Teguiche, M., 2012. Synthesis of some 1, 2, 3-triazoles derivatives. *Rev. Roum. Chim*, *57*(12), 1037-1040.
101. Li, J., Liu, H., Meng, F., Yan, L., Shi, Y., Zhang, Y. and Gu, Q., 2018. Microwave-assisted synthesis of new 1, 2, 3-triazoles bearing an isoxazole ring by the azide-alkyne cycloaddition click chemistry. *Chemical Research in Chinese Universities*, *34*(2), 197-202.
102. Lligadas, G., Ronda, J.C., Galià, M. and Cádiz, V., 2013. Monomers and polymers from plant oils via click chemistry reactions. *Journal of Polymer Science Part A: Polymer Chemistry*, *51*(10), 2111-2124.
103. Collot, M., Eller, S., Weishaupt, M. and Seeberger, P.H., 2013. Glycosylation efficiencies on different solid supports using a hydrogenolysis-labile linker. *Beilstein Journal of Organic Chemistry*, *9*(1), 97-105.

104. Wang, Q.Y., Sheng, W.S., Sheng, S.R., Li, Y., and Cai, M.Z., 2014. Click chemistry on polymer support: Synthesis of 1-vinyl-and 1-allyl-1, 2, 3-triazoles via selenium linker. *Synthetic Communications*, *44*(1), 59-67.

105. Dutt, S. and Tyagi, V., 2021. Biocatalytic synthesis of quinoline derivatives via α-amylase catalysed one-pot domino aza-Michael/Aldol/aromatization reactions. *Tetrahedron Letters*, *87*, p.153527.

106. Manske, R.H. and Kulka, M., 2004. The S kraup Synthesis of Quinolines. *Organic Reactions*, *7*, 59-98.

107. Li, J.J., 2014. Doebner–von Miller reaction. *Name Reactions: A Collection of Detailed Mechanisms and Synthetic Applications Fifth Edition*, p.221.

108. Li, J.J., 2009. Conrad–Limpach reaction. In *Name Reactions* (133-134). Springer, Berlin, Heidelberg.

109. Born, J.L., 1972. Mechanism of formation of benzo [g] quinolones via the Combes reaction. *The Journal of Organic Chemistry*, *37*(24), 3952-3953.

110. N Sangshetti, J., S Zambare, A., Gonjari, I. and B Shinde, D., 2014. Pfitzinger reaction in the synthesis of bioactive compounds-a review. *Mini-Reviews in Organic Chemistry*, *11*(2), 225-250.

111. Das, B., Damodar, K., Chowdhury, N. and Kumar, R.A., 2007. Application of heterogeneous solid acid catalysts for Friedlander synthesis of quinolines. *Journal of Molecular Catalysis A: Chemical*, *274*(1-2), 148-152.

112. Muscia, G.C., Bollini, M., Carnevale, J.P., Bruno, A.M. and Asis, S.E., 2006. Microwave-assisted Friedländer synthesis of quinolines derivatives as potential antiparasitic agents. *Tetrahedron Letters*, *47*(50), 8811-8815.

113. Maleki, B., Seresht, E.R. and Ebrahimi, Z., 2015. Friedlander synthesis of quinolines promoted by polymer-bound sulfonic acid. *Organic Preparations and Procedures International*, *47*(2), 149-160.

114. De, S.K. and Gibbs, R.A., 2005. A mild and efficient one-step synthesis of quinolines. *Tetrahedron Letters*, *46*(10), 1647-1649.

115. Bhattacharya, R., Kundu, P., and Maiti, G., 2010. Antimony Trichloride: An Efficient and Mild Catalyst for Cyclization of 2-Aminochalcones to the corresponding 2-Aryl-2,3-Dihydroquinolin-(1H)-ones. *Synthetic Communications,* 40, 476-481.

116. Derabli, C., Mahdjoub, S., Boulcina, R. 2016. [C_8dabco]Br: a mild and convenient catalyst for intramolecular cyclization of 2-aminochalcones to the corresponding 2-aryl-2,3-dihydroquinolin-4(1*H*)-ones. *Chemistry Heterocyclic Compounds,* 52, 99–103.

117. Donnelly, J, A., and Farrell, D, F., 1990. The chemistry of 2-Amino Analogues of 2-Hydroxychalcone and its derivatives. *ChemInform*, 21.

118. Wei, X., Chen, G. and Peng, Y., 2020. Tandem nucleophilic addition/oxa-Michael reaction of ortho-formyl chalcones with dimethyl (diazomethyl) phosphonate for the synthesis of phosphine-containing 1, 3-disubstituted phthalans. *Tetrahedron Letters*, *61*(33), p.152174.

119. Dhiman, R., Sharma, S., Singh, G., Nepali, K. and Singh Bedi, P.M., 2013. Design and synthesis of aza-flavones as a new class of xanthine oxidase inhibitors. *Archiv der Pharmazie*, *346*(1), 7-16.

120. Varma, R.S. and Saini, R.K., 1997. Microwave-assisted isomerization of 2'-aminochalcones on clay: an easy route to 2-aryl-1, 2, 3, 4-tetrahydro-4-quinolones. *Synlett*, *1997*(07), 857-858.

121. Kumar, K.H., Muralidharan, D. and Perumal, P.T., 2004. Indium (III) chloride/silica gel-promoted facile and rapid cyclization of 2-aminochalcones to 2-aryl-2, 3-dihydroquinolin-4 (1H)-ones under solvent-free conditions. *Synthesis*, *2004*(01), 63-68.

122. Liu, X. and Lu, Y., 2010. Asymmetric synthesis of 2-aryl-2, 3-dihydro-4-quinolones via bifunctional thiourea-mediated intramolecular cyclization. *Organic Letters*, *12*(23), 5592-5595.

123. Kanagaraj, K. and Pitchumani, K., 2013. Per-6-amino-β-cyclodextrin as a chiral base catalyst promoting one-pot asymmetric synthesis of 2-aryl-2, 3-dihydro-4-quinolones. *The Journal of Organic Chemistry*, *78*(2), 744-751.

124. Zheng, H., Liu, Q., Wen, S., Yang, H. and Luo, Y., 2013. One-pot asymmetric synthesis of 2-aryl-2, 3-dihydro-4-quinolones catalyzed by amino acid-derived sulfonamides. *Tetrahedron: Asymmetry*, *24*(15-16), 875-882.

125. Politanskaya, L., Rybalova, T., Zakharova, O., Nevinsky, G. and Tretyakov, E., 2018. p-Toluenesulfonic acid mediated one-pot cascade synthesis and cytotoxicity evaluation of polyfluorinated 2-aryl-2, 3-dihydroquinolin-4-ones and their derivatives. *Journal of Fluorine Chemistry*, *211*, 129-140.

126. Tollari, S., Cenini, S., Ragaini, F. and Cassar, L., 1994. Intramolecular amination of olefins. Synthesis of 2-substituted-4-quinolones from 2-nitrochalcones catalysed by ruthenium. *Journal of the Chemical Society, Chemical Communications*, (15), 1741-1742.

127. Tois, J., Vahermo, M. and Koskinen, A., 2005. Novel and convenient synthesis of 4 (1H) quinolones. *Tetrahedron Letters*, *46*(5), 735-737.

128. Jones, C.P., Anderson, K.W. and Buchwald, S.L., 2007. Sequential Cu-catalyzed amidation-base-mediated camps cyclization: a two-step synthesis of 2-aryl-4-quinolones from o-halophenones. *The Journal of Organic Chemistry*, *72*(21), 7968-7973.

129. Xu, X., Sun, R., Zhang, S., Zhang, X. and Yi, W., 2018. Divergent Synthesis of Quinolones and Dihydroepindolidiones via Cu (I)-Catalyzed Cyclization of Anilines with Alkynes. *Organic Letters*, *20*(7), 1893-1897.

130. Lee, S.B., Jang, Y., Ahn, J., Chun, S., Oh, D.C. and Hong, S., 2020. One-Pot Synthesis of 4-Quinolone via Iron-Catalyzed Oxidative Coupling of Alcohol and Methyl Arene. *Organic Letters*, *22*(21), 8382-8386.

131. Xu, Xuefeng, and Xu Zhang. "Direct synthesis of 4-quinolones via copper-catalyzed anilines and alkynes." *Organic Letters* 19, no. 18 (2017): 4984-4987.

132. Tjosaas, F. and Fiksdahl, A., 2006. A simple synthetic route to methyl 3-fluoropyridine-4-carboxylate by nucleophilic aromatic substitution. *Molecules*, *11*(2), 130-133.

133. Iaroshenko, V.O., Mkrtchyan, S. and Villinger, A., 2013. Efficient [5+ 1] Synthesis of 4-Quinolones by Domino Amination and Conjugate Addition Reactions of 1-(2-Fluorophenyl) prop-2-yn-1-ones with Amines. *Synthesis*, *45*(02), 205-218.

134. Lin, J.P. and Long, Y.Q., 2013. Transition metal-free one-pot synthesis of 2-substituted 3-carboxy-4-quinolone and chromone derivatives. *Chemical communications*, *49*(46), 5313-5315.

135. Mphahlele, M.J. and Oyeyiola, F.A., 2011. Suzuki–Miyaura cross-coupling of 2-aryl-6, 8-dibromo-1, 2, 3, 4-tetrahydroquinolin-4-ones and subsequent dehydrogenation and oxidative aromatization of the resulting 2, 6, 8-triaryl-1, 2, 3, 4-tetrahydroquinolin-4-ones. *Tetrahedron*, *67*(36), 6819-6825.

136. Singh, O.V., Muthukrishnan, M. and Sundaravadivelu, M., 2001. Thallium (III) salts in heterocyclic synthesis: Synthesis of 3-aryl-9-methyl-1, 2, 4-triazolo [4, 3-a] quinolines.

137. Singh, O.V. and Kapil, R.S., 1993. A general method for the synthesis of isoflavones by oxidative rearrangement of flavanones using thallium (III) perchlorate. *Indian Journal of Chemistry Section B*, *32*, 911-911.

138. Huang, X. and Liu, Z., 2001. Preparation of a resin-bound cyclic malonic ester and a facile solid-phase synthesis of 4 (1H) quinolones. *Tetrahedron Letters*, *42*(43), 7655-7657.

139. Basak, A., Abouelhassan, Y., Kim, Y.S., Norwood IV, V.M., Jin, S. and Huigens III, R.W., 2018. Halogenated quinolines bearing polar functionality at the 2-position: identification of new antibacterial agents with enhanced activity against Staphylococcus epidermidis. *European Journal of Medicinal Chemistry*, *155*, 705-713.

140. Huigens III, R.W., 2018. The path to new halogenated Quinolines with enhanced activities against Staphylococcus epidermidis. *Microbiology Insights*, *11*, p.1178636118808532.

141. Gothard, C.M., Soh, S., Gothard, N.A., Kowalczyk, B., Wei, Y., Baytekin, B. and Grzybowski, B.A., 2012. Rewiring chemistry: algorithmic discovery and experimental validation of one-pot reactions in the network of organic chemistry. *Angewandte Chemie International Edition*, *51*(32), 7922-7927.

142. Maluleka, M.M., Mphahlele, M.J. and Onwu, E.E., 2019. Crystal structure of 8-bromo-6-oxo-2-phenyl-6H-pyrrolo [3, 2, 1-ij] quinoline-5-carbaldehyde, C18H11BrNO2. *Zeitschrift für Kristallographie-New Crystal Structures*, *234*(5), 1063-1065.

143. Mphahlele, M.J. and Oyeyiola, F.A., 2011. Suzuki–Miyaura cross-coupling of 2-aryl-6, 8-dibromo-1, 2, 3, 4-tetrahydroquinolin-4-ones and subsequent dehydrogenation and oxidative aromatization of the resulting 2, 6, 8-triaryl-1, 2, 3, 4-tetrahydroquinolin-4-ones. *Tetrahedron*, *67*(36), 6819-6825. (ref. 116)

144. Tókés, A.L. and Forró, I., 1991. Bromo-derivatives of 2′-NHR-3, 4-Methylenedioxychalcone and its 4-Quinolone Isomer. *Synthetic Communications*, *21*(10-11), 1201-1211.

145. Sharma, D., Ranjan, P. and Prakash, O., 2009. Facile Iodine (III)-Mediated Approach for the Regioselective Chlorination of 2-Aryl-2, 3-dihydro-4 (1 H)-quinolones. *Synthetic Communications*®, *39*(4), 596-603

146. Vandekerckhove, S., Desmet, T., Tran, H.G., de Kock, C., Smith, P.J., Chibale, K. and D'hooghe, M., 2014. Synthesis of halogenated 4-quinolones and evaluation of their antiplasmodial activity. *Bioorganic & Medicinal Chemistry Letters*, *24*(4), 1214-1217.

147. Suess, A.M., Ertem, M.Z., Cramer, C.J. and Stahl, S.S., 2013. Divergence between organometallic and single-electron-transfer mechanisms in copper (II)-mediated aerobic C–H oxidation. *Journal of the American Chemical Society*, *135*(26), 9797-9804.

148. Tsai, J.Y., Chang, C.S., Huang, Y.F., Chen, H.S., Lin, S.K., Wong, F.F., Huang, L.J. and Kuo, S.C., 2008. Investigation of amination in 4-chloro-2-phenylquinoline derivatives with amide solvents. *Tetrahedron*, *64*(51), 11751-11755.

149. Al Zoubi, W., 2013. Solvent extraction of metal ions by use of Schiff bases. *Journal of Coordination Chemistry*, *66*(13), 2264-2289.

150. Al Zoubi, W. and Ko, Y.G., 2016. Organometallic complexes of Schiff bases: Recent progress in oxidation catalysis. *Journal of Organometallic Chemistry*, *822*, 173-188.

151. Das, P. and Linert, W., 2016. Schiff base-derived homogeneous and heterogeneous palladium catalysts for the Suzuki–Miyaura reaction. *Coordination Chemistry Reviews*, *311*, 1-23.

152. Abuamer, K.M., Maihub, A.A., El-Ajaily, M.M., Etorki, A.M., Abou-Krisha, M.M. and Almagani, M.A., 2014. The role of aromatic Schiff bases in the dyes techniques. *International Journal of Organic Chemistry*, *2014*.

153. Awantu, A.F., Fongang, Y.S.F., Ayimele, G.A., Nantia, E.A., Fokou, P.V., Boyom, F.F., Ngwang, C.K., Lenta, B.N. and Ngouela, S.A., 2020. Novel Hydralazine Schiff Base Derivatives and Their Antimicrobial, Antioxidant and Antiplasmodial Properties. *International Journal of Organic Chemistry*, *10*(01), p.1.

154. Jaman, Z., Karim, M.R., Dumenyo, K. and Mirza, A.H., 2014. Antibacterial Activities of New Schiff Bases and Intermediate Silyl Compounds

Synthesised from 5-Substituted-1, 10-phenanthroline-2, 9-dialdehyde. *Advances in Microbiology*, *4*(15), p.1140.

155. Elshaarawy, R.F., Refaee, A.A. and El-Sawi, E.A., 2016. Pharmacological performance of novel poly-(ionic liquid)-grafted chitosan-N-salicylidene Schiff bases and their complexes. *Carbohydrate Polymers*, *146*, 376-387.

156. Da Silva, C.M., da Silva, D.L., Modolo, L.V., Alves, R.B., de Resende, M.A., Martins, C.V. and de Fátima, Â., 2011. Schiff bases: A short review of their antimicrobial activities. *Journal of Advanced research*, *2*(1), 1-8.

157. Alam, M.S., Choi, J.H. and Lee, D.U., 2012. Synthesis of novel Schiff base analogues of 4-amino-1, 5-dimethyl-2-phenylpyrazol-3-one and their evaluation for antioxidant and anti-inflammatory activity. *Bioorganic & Medicinal Chemistry*, *20*(13), 4103-4108.

158. Shokrollahi, S., Amiri, A., Fadaei-Tirani, F. and Schenk-Joß, K., 2020. Promising anti-cancer potency of 4, 5, 6, 7-tetrahydrobenzo [d] thiazole-based Schiff-bases. *Journal of Molecular Liquids*, *300*, p.112262.

159. Gaballa, A.S., Asker, M.S., Barakat, A.S. and Teleb, S.M., 2007. Synthesis, characterization and biological activity of some platinum (II) complexes with Schiff bases derived from salicylaldehyde, 2-furaldehyde and phenylenediamine. *Spectrochimica Acta Part A: Molecular and Biomolecular Spectroscopy*, *67*(1), 114-121.

160. Olalekan, T.E., Ogunlaja, A.S., VanBrecht, B. and Watkins, G.M., 2016. Spectroscopic, structural and theoretical studies of copper (II) complexes of tridentate NOS Schiff bases. *Journal of Molecular Structure*, *1122*, 72-79.

161. Garnovskii, A.D. and Vasil'chenko, I.S., 2002. Rational design of metal coordination compounds with azomethine ligands. *Russian Chemical Reviews*, *71*(11), 943-968.

162. Abu-Dief, A.M. and Mohamed, I.M., 2015. A review on versatile applications of transition metal complexes incorporating Schiff bases. *Beni-suef University Journal of Basic and Applied Sciences*, *4*(2), 119-133.

163. Tarafder, M.T.H., Chew, K.B., Crouse, K.A., Ali, A.M., Yamin, B.M. and Fun, H.K., 2002. Synthesis and characterization of Cu (II), Ni (II) and Zn (II) metal complexes of bidentate NS isomeric Schiff bases derived from S-

methyldithiocarbazate (SMDTC): Bioactivity of the bidentate NS isomeric Schiff bases, some of their Cu (II), Ni (II) and Zn (II) complexes and the X-ray structure of the bis [S-methyl-β-N-(2-furyl-methyl) methylenedithiocarbazato] zinc (II) complex. *Polyhedron*, *21*(27-28), 2683-2690.

164. Khera, B., Sharma, A.K. and Kaushik, N.K., 1983. Bis (indenyl) titanium (IV) and zirconium (IV) complexes of monofunctional bidentate salicylidimines. *Polyhedron*, *2*(11), 1177-1180.

165. Kuchtanin, V., Kleščíková, L., Šoral, M., Fischer, R., Růžičková, Z., Rakovský, E., Moncoľ, J. and Segľa, P., 2016. Nickel (II) Schiff base complexes: Synthesis, characterization and catalytic activity in Kumada–Corriu cross-coupling reactions. *Polyhedron*, *117*, 90-96.

166. Marchetti, F., Pettinari, C., Pettinari, R., Cingolani, A., Leonesi, D. and Lorenzotti, A., 1999. Group 12 metal complexes of tetradentate N2O2–Schiff-base ligands incorporating pyrazole: synthesis, characterisation and reactivity toward S-donors, N-donors, copper and tin acceptors. *Polyhedron*, *18*(23), 3041-3050.

167. Pang, X., Du, H., Chen, X., Wang, X. and Jing, X., 2008. Enolic Schiff base aluminum complexes and their catalytic stereoselective polymerization of racemic lactide. *Chemistry–A European Journal*, *14*(10), 3126-3136.

168. Elantabli, F.M., Radebe, M.P., Motswainyana, W.M., Owaga, B.O., El-Medani, S.M., Ekengard, E., Haukka, M., Nordlander, E. and Onani, M.O., 2017. Thiophene based imino-pyridyl palladium (II) complexes: Synthesis, molecular structures and Heck coupling reactions. *Journal of Organometallic Chemistry*, *843*, 40-47.

169. Tajuddin, A.M., Bahron, H., Kassim, K., Nazihah, W., Ibrahim, W. and Yamin, B.M., 2012. Synthesis and characterisation of palladium (II) Schiff base complexes and their catalytic activities for Suzuki coupling reaction. *Malaysian Journal of Analytical Sciences*, *16*(1), 79-87.

170. Low, M.L., Maigre, L., Tahir, M.I.M., Tiekink, E.R., Dorlet, P., Guillot, R., Ravoof, T.B., Rosli, R., Pagès, J.M., Policar, C. and Delsuc, N., 2016. New insight into the structural, electrochemical, and biological aspects of macroacyclic Cu (II) complexes derived from S-substituted dithiocarbazate schiff bases. *European Journal of Medicinal Chemistry*, *120*, 1-12.

171. Vlad, A., Zaltariov, M.F., Shova, S., Cazacu, M., Avadanei, M., Soroceanu, A. and Samoila, P., 2016. New Zn (II) and Cu (II) complexes with in situ generated N2O2 siloxane Schiff base ligands. *Polyhedron*, *115*, 76-85.

172. Tyagi, P., Tyagi, M., Agrawal, S., Chandra, S., Ojha, H. and Pathak, M., 2017. Synthesis, characterization of 1, 2, 4-triazole Schiff base derived 3d-metal complexes: Induces cytotoxicity in HepG2, MCF-7 cell line, BSA binding fluorescence and DFT study. *Spectrochimica Acta Part A: Molecular and Biomolecular Spectroscopy*, *171*, 246-257.

173. Neelakantan, M.A., Rusalraj, F., Dharmaraja, J., Johnsonraja, S., Jeyakumar, T. and Pillai, M.S., 2008. Spectral characterization, cyclic voltammetry, morphology, biological activities and DNA cleaving studies of amino acid Schiff base metal (II) complexes. *Spectrochimica Acta Part A: Molecular and Biomolecular Spectroscopy*, *71*(4), 1599-1609.

174. Irfan, R.M., Shaheen, M.A., Saleem, M., Tahir, M.N., Munawar, K.S., Ahmad, S., Rubab, S.L., Tahir, T., Kotwica-Mojzych, K. and Mojzych, M., 2021. Synthesis of new cadmium (II) complexes of Schiff bases as alkaline phosphatase inhibitors and their antimicrobial activity. *Arabian Journal of Chemistry*, *14*(10), p.103308.

175. Al-Aghbari, S.A., Al-Shuja'a, O.M., Al-Badani, R. and Japir, A.A.W.M., 2019. Synthesis, characterization and anticancer activity studies of new Schiff base Pt (II) complex. *Journal of Materials Science and Chemical Engineering*, *7*(08), p.1.

176. Mishra, A.P., Sharma, N. and Jain, R.K., 2013. Microwave synthesis, spectral, thermal, and antimicrobial studies of some Ni (II) and Cu (II) Schiff base complexes.

177. Naureen, B., Miana, G.A., Shahid, K., Asghar, M., Tanveer, S. and Sarwar, A., 2021. Iron (III) and zinc (II) monodentate Schiff base metal complexes: Synthesis, characterisation and biological activities. *Journal of Molecular Structure*, *1231*, p.129946.

178. Deodware, S.A., Barache, U.B., Chanshetti, U.B., Sathe, D.J., Ashok, U.P., Gaikwad, S.H. and Kollur, S.P., 2021. Newly synthesised triazole-based Schiff base ligands and their Co (II) complexes as antimicrobial and anticancer agents: Chemical synthesis, structure and biological investigations. *Results in Chemistry*, *3*, p.100162.

179. Yang, Z. and Sun, P., 2006. Compare of three ways of synthesis of simple Schiff base. *Molbank*, *2006*(6), p.M514.

180. Kargar, H., Fallah-Mehrjardi, M., Behjatmanesh-Ardakani, R., Torabi, V., Munawar, K.S., Ashfaq, M. and Tahir, M.N., 2021. Sonication-assisted synthesis of new Schiff bases derived from 3-ethoxysalicylaldehyde: Crystal structure determination, Hirshfeld surface analysis, theoretical calculations and spectroscopic studies. *Journal of Molecular Structure*, *1243*, p.130782.

181. Westheimer, F.H. and Taguchi, K., 1971. Catalysis by molecular sieves in the preparation of ketimines and enamines. *The Journal of Organic Chemistry*, *36*(11), 1570-1572.

182. Love, B.E. and Ren, J., 1993. Synthesis of sterically hindered imines. *The Journal of Organic Chemistry*, *58*(20), 5556-5557.

183. BILLMAN, J.H. and Tai, K.M., 1958. Reduction of schiff bases. II. Benzhydrylamines and structurally related compounds1a, b. *The Journal of Organic Chemistry*, *23*(4), 535-539.

184. Ghaffari, A., Behzad, M., Dutkiewicz, G., Kubicki, M. and Salehi, M., 2012. Crystal structure, electrochemistry, and catalytic studies of a series of new oxidovanadium (IV) Schiff-base complexes derived from 1, 2-diphenyl-1, 2-ethylenediamine. *Journal of Coordination Chemistry*, *65*(5), 840-855.

185. Ashraf, M.A., Mahmood, K., Wajid, A., Maah, M.J. and Yusoff, I., 2011. Synthesis, characterization, and biological activity of Schiff bases. *IPCBEE*, *10*(1), p.185.

186. Khadsan, R.E., Tambatkar, G.D. and Meshram, Y.K., 2010. Synthesis of Schiff Bases Via Eco-Friendly and Energy Efficient Greener Methodologies Synthesis of Schiff Bases Via Eco-Friendly and Energy Efficient Greener Methodologies. *Oriental Journal of Chemistry*, *26*(2), p.681.

187. Naqui, A., Shahnawaaz, M., Rao, A.V., Seth, D.S. and Sharma, N.K., 2009. Synthesis of schiff bases via environmentally benign and energy-efficient greener methodologies. *E-Journal of Chemistry*, *6*(S1), S75-S78.

188. Mermer, A., Demirbas, N., Uslu, H., Demirbas, A., Ceylan, S. and Sirin, Y., 2019. Synthesis of novel Schiff bases using green chemistry techniques; antimicrobial, antioxidant, antiurease activity screening and molecular docking studies. *Journal of Molecular Structure*, *1181*, 412-422.

189. Das, B., Reddy, V.S. and Krishnaiah, M., 2006. An efficient catalyst-free synthesis of thiiranes from oxiranes using polyethylene glycol as the reaction medium. *Tetrahedron Letters*, *47*(48), 8471-8473.

190. Jagrut, V.B., Netankar, P.D., Mane, R.A. and Jadhav, W.N., 2012. Efficient and eco-friendly synthesis of Schiff bases under catalyst free condition. *International Journal of Chemical Sciences*, *10*(3), 1705-1711.

191. Otani, N., Furuya, T., Katsuumi, N., Haraguchi, T. and Akitsu, T., 2021. Synthesis of amino acid derivative Schiff base copper (II) complexes by microwave and wet mechanochemical methods. *Journal of the Indian Chemical Society*, *98*(1), p.100004.

192. Manjunath, M., Kulkarni, A.D., Bagihalli, G.B., Malladi, S. and Patil, S.A., 2017. Bio-important antipyrine derived Schiff bases and their transition metal complexes: Synthesis, spectroscopic characterization, antimicrobial, anthelmintic and DNA cleavage investigation. *Journal of Molecular Structure*, *1127*, 314-321.

193. Kannaiyan, S., Kannan, K. and Andal, V., 2021. Green synthesis of Phenothiazinium Schiff base and its nano silver complex using egg white as a catalyst under solvent free condition. *Materials Today: Proceedings*.

194. Saritha, T.J. and Metilda, P., 2021. Synthesis, spectroscopic characterization and biological applications of some novel Schiff base transition metal (II) complexes derived from curcumin moiety. *Journal of Saudi Chemical Society*, *25*(6), p.101245.

195. Patil, S.K. and Vibhute, B.T., 2021. Synthesis, characterization, anticancer and DNA photocleavage study of novel quinoline Schiff base and its metal complexes. *Arabian Journal of Chemistry*, *14*(8), p.103285.

196. Paolucci, G., Zanella, A., Sperni, L., Bertolasi, V., Mazzeo, M. and Pellecchia, C., 2006. Tridentate [N, N, O] Schiff-base group 4 metal complexes: Synthesis, structural characterization and reactivity in olefin polymerization. *Journal of Molecular Catalysis A: Chemical*, *258*(1-2), 275-283.

197. Li, B., Yao, J., He, F., Liu, J., Lin, Z., Liu, S., Wang, W., Wu, T., Huang, J., Chen, K. and Fang, M., 2021. Synthesis, SAR study, and bioactivity evaluation of a series of Quinoline-Indole-Schiff base derivatives: Compound

10E as a new Nur77 exporter and autophagic death inducer. *Bioorganic Chemistry*, *113*, p.105008.

198. Jabbi, A.M., Aliyu, H.N., Isyaku, S. and Kabir, A.M., 2020. Preparation, Characterization and Antimicrobial Studies of Mn (II) and Fe (II) Complexes with Schiff Base Ligand Derived from 2-aminophenol and 3-formyl-2-hydroxy-6-methoxyquinoline. *Open Journal of Inorganic Chemistry*, *10*(2), 15-24.

199. Milacic, V., Jiao, P., Zhang, B., Yan, B. and Dou, Q.P., 2009. Novel 8-hydroxylquinoline analogs induce copper-dependent proteasome inhibition and cell death in human breast cancer cells. *International Journal of Oncology*, *35*(6), 1481-1491.

200. Adsule, S., Barve, V., Chen, D., Ahmed, F., Dou, Q.P., Padhye, S. and Sarkar, F.H., 2006. Novel Schiff base copper complexes of quinoline-2 carboxaldehyde as proteasome inhibitors in human prostate cancer cells. *Journal of Medicinal Chemistry*, *49*(24), 7242-7246.

201. Althobiti, H.A. and Zabin, S.A., 2020. New Schiff bases of 2-(quinolin-8-yloxy) acetohydrazide and their Cu (II), and Zn (II) metal complexes: *in vitro* antimicrobial potentials and in silico physicochemical and pharmacokinetics properties. *Open Chemistry*, *18*(1), 591-607.

Chapter 2

Results and discussion

The target compounds presented below were successfully synthesised in different yields and are generally characterized by a light yellow or deep orange colour. The compounds were synthesised following established literature procedures and also novel, modified methods. They are all relatively stable in an open-air environment in solid form.

2.1 Preparation of substrates

To achieve different derivatives of quinoline triazole-Schiff base ligands, it was crucial to firstly study their general structures, functional groups (study the functional group interchange (FGI) and functional group removal (FGR) and apply retrosynthetic analysis technique. As such, this lead us to the functionalisation of 2-aminoacetophenone **146** as a staring material, as explained in the next section.

2.1.1 Synthesis of 3,5-dibromo-2-amino-acetophenone (147)

According to literature compound **147** has been synthesised before by Bheemanapalli *et al.* **147** (as a major product), using 2-aminoacetophenone, bromine and dichloromethane at lower temperatures for 7 hours with an 80 % yield [1]. Baker *et al.* under similar conditions, brominated 2-aminoacetophenone in acetic acid to afford compound **147** after purification under silica-chromatography [2]. On the other hand, the use of oxone to activate the arenes and acetonitrile can also yield product **147** [3]. The bromination of 2-aminoacetophenone begins by inductive effects through electrophilic attack of the pi-bond of the aromatic system, leading a resonance stabilized carbocation. In the presence of bromine, electrophilic aromatic substitution (halogenation) occurs at the 5th position, because of the meta and para directing effect of $COCH_3$ and NH_2 groups respectively and in the presence of an excess bromine, halogenation continues at the 3rd position because NH_2 is a strong activator and also an ortho director [4,5,6]. In this study we opted for the halogenation reaction of 2-aminoacetophenone and excess *N*-bromosuccinimide (NBS) in acetonitrile at 0 ºC for 3 hours, which was later crystallized to produce **147** with a 73 % yield.

The prepared 3,5-dibromoacetophenone **147** was synthesised to serve as a starting material for the synthesis of chalcones and the procedure for this transformation is described below.

2.1.2 Synthesis of 3,5-dibromo chalcone derivatives (148 a–e)

Chalcones are synthesised through many methods namely Claisen Schmidt condensation [7], aldol condensation [8], grinding method [9], ultrasound irradiation [10], Koclenski-Julia olefination [11] and coupling reactions [12]. The base catalysed condensation is frequently used as it produces desirable products in good yields [13]. The base catalysed reaction usually occurs when the hydroxide salts form alkoxide alkene from the 2-aminoacetophenone, which later acts as nucleophile to form a carbon-carbon bond with each benzaldehyde derivative eventually forming water as a by-product and α-β unsaturated 2-aminochalcone [14]. Hence, in this study we chose the Claisen Schmidt condensation reaction of 2-amino-3,5-dibromoacetophenone **147** with benzaldehyde derivatives using potassium hydroxide (KOH) at room temperature in ethanol for 7 h to afford 2-aminochalcone derivatives **148a–e** (**Scheme 28**) with yields of 89-98 %. The ^{1}H NMR spectrum of each chalcone derivative confirms the disappearance of acetyl, COC$\underline{H}_3$ as a singlet (representing the starting material **147**) accompanied by the addition of peaks in the aromatic region from the benzaldehyde derivatives at δ 7-7.6 ppm. The vinylic *α-β* unsaturated protons appeared downfield due to some resonance effects [15] at δ 7.5 (*α*-H) and 7.7 (*β*-H) ppm (both as doublets (d), with a coupling constants of *J* = 15 Hz). The ^{1}H-NMR spectrum displayed the presence of a broad signal integrating for two protons at δ 6.9 ppm representing the -N$\underline{H}_2$ group and an additional peak in the aromatic region, for 6-H and 4-H from the 3,5-dibromoacetophenone **147** shifted downfield at around δ 7.71 and 7.90 ppm respectively (both as d, *J* = 2 Hz) and peaks between δ 7.0-7.6 ppm from the benzaldehyde, depending on the substituent attached (**Figure 21**). The FTIR spectra for compounds **148a–e** showed two weak peaks at *ν* 3418 and 3301 (cm^{-1}), representing an amine group (-NH_2) and a strong carbonyl -C=O signal at *ν* 1654 (cm^{-1}) (**Figure 23**). **Table 1** shows so discrepancy of the melting points obtained and compared to the one on literature, which may be due to some impurities.

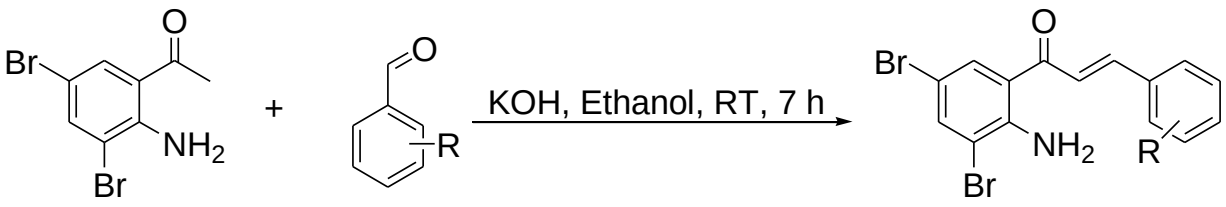

147 **148 a-e**

Scheme 28. Condensation reaction of **147** with benzaldehyde derivatives

Table 1. Substitution pattern, percentage yield and melting point values of **148 a–e**

Compound	R	% Yield	Mp ºC	
148a	H	98	107-110	(120-123) [16]
148b	4-CH_3	89	97-100	
148c	4-OCH_3	96	110-116	(139-141) [16]
148d	3-OCH_3	90	122-126	
148e	4-F	93	149-153	(149-150) [16]

The ^{1}H NMR spectra of **148 e** conveniently displays the presence of a para-substituted fluorine, where it shows the presence of a set of multiplet-like signals indicating the spin-spin interaction where fluorine couples with two *ortho* (2^{1}, 6^{1}-H) and two meta protons (3^{1}, 5^{1}-H) at δ 7.65 and 7.11 ppm. The ^{13}C NMR shows signals as doublets with their coupling constants at δ 116.27 (*J* = 23 Hz, 3^{1}, 5^{1}-C), 121.57 (*J* = 3 Hz 1^{1}-C), 130.41 (J = 9 Hz, 2^{1}, 6^{1}-C), 165.33 (J = 251 Hz, 4^{1}-C) ppm.

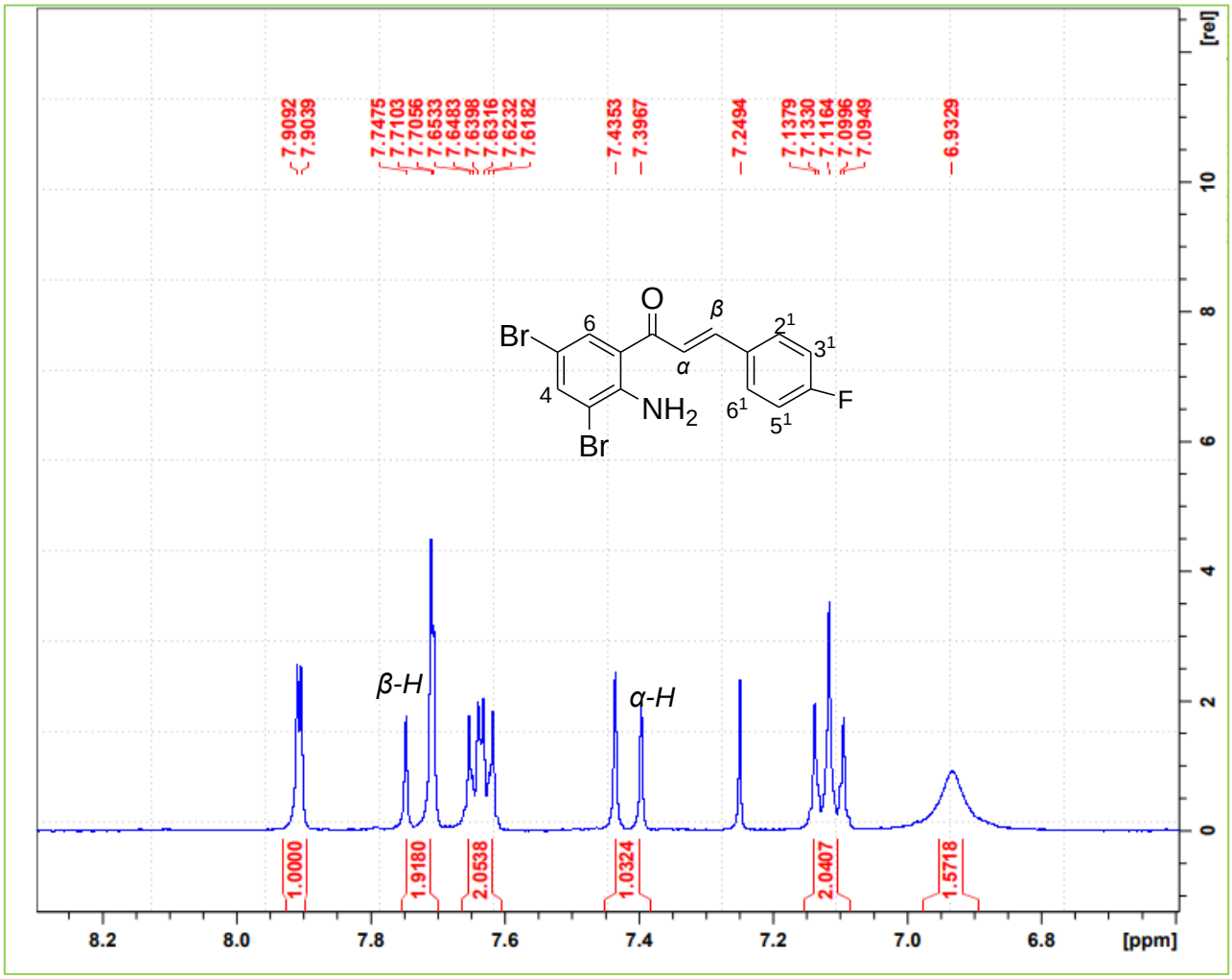

Figure 21. ^{1}H NMR spectrum of a chalcone compound **148 e**

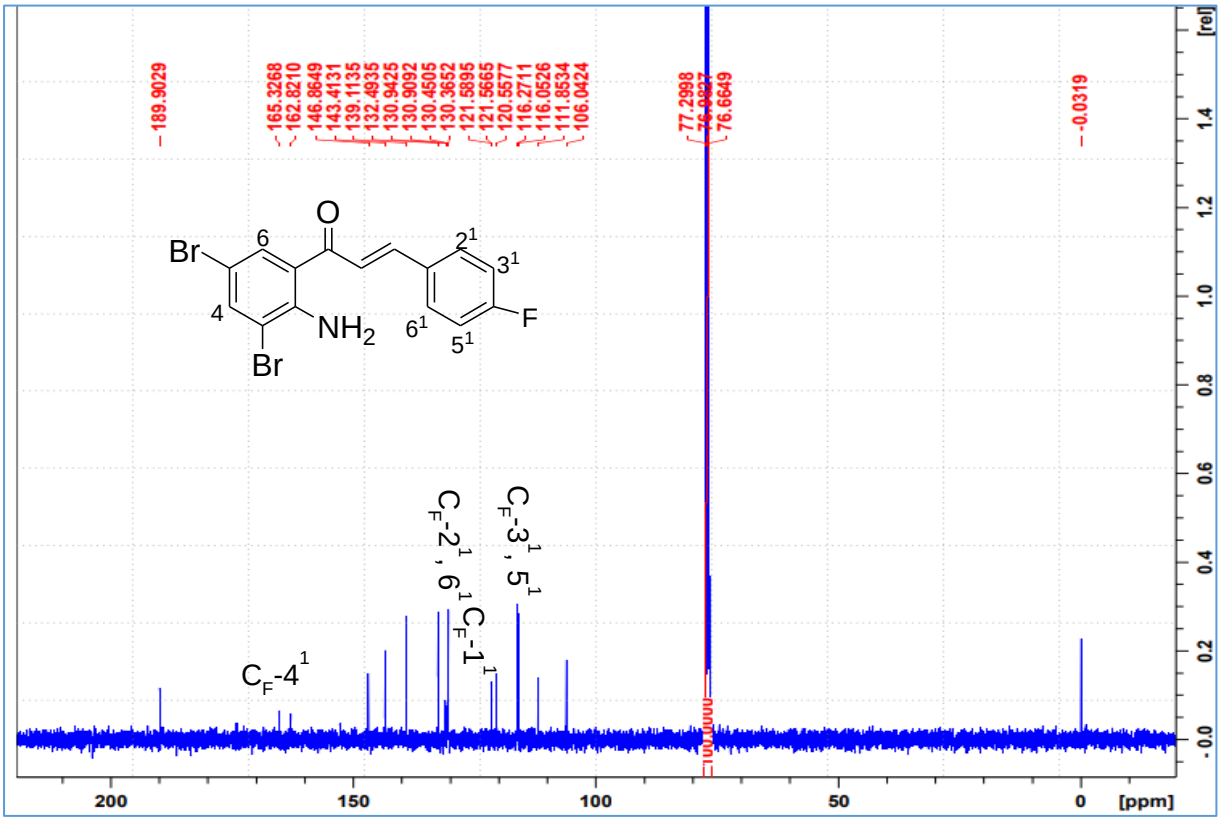

Figure 22. The ^{13}C NMR spectrum of a chalcone compound **148 e**

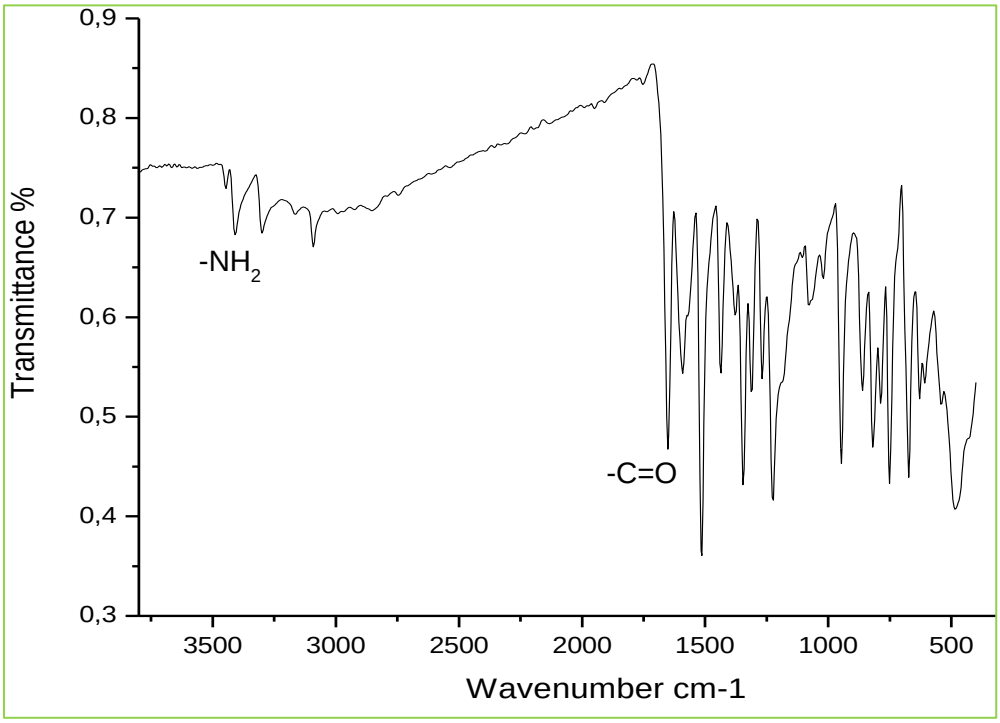

Figure 23. The IR spectrum of compound **148 e**

The 3,5-dibromo-2-aminochalcones further serve as precursors for the intramolecular cyclization reaction as described in the next section

2.2 Synthesis of 2-substituted-2,3-dihydroquinolones (149 a–e)

Khoza and co-workers [16,17] have previously synthesised 2-substituted-2,3-dihydro quinolones based on acid mediated cyclization from the 2-aminochalcone derivatives. Tokes *et al.* [18] on the other hand, produced 2,3-dihyroquinolones, by following acid prompted cyclization of 2-aminochalcones using; trifluoroacetic acid (TFA) with trimethyl silylacetylene (TMSA). The polyphosphoric acid (PPA) is reported to be a good protonating and cyclizing agent in the presence of vinyl ketones [19]. The presence of the electro-positivity (δ^+) at the beta-carbon (3-C), leads to the electrophile (δ^-) $\underline{N}H_2$ to attack the beta-carbon which in the presence of H^+ protonation occurs at the alpha carbon forming a cyclized 2-substituted-2,3-dihydro quinolone [20]. We opted for the use of the acid-mediated cyclization reaction of 2-aminochalcones **148 a–e** and orthophosphoric in acetic acid to afford 2,3-dihydroquinolones **149 a–e** (**Scheme 29**). The ^{1}H NMR spectra of **149 a–e** showed the absence of *α-β* unsaturated protons (with *J* = 15 Hz value), and the primary amine protons signal. The ^{1}H NMR revealed the presence of additional signals at the saturated allylic region, at δ 1.0-2.9 ppm representing the 3-H protons whereas the 2-H is identified at δ ~4.7 ppm (dd, *J* = 4 Hz) appear downfield due to the deshielding effect of the electronegative nitrogen at secondary amine (-N<u>H</u>-) exhibiting a broad signal at δ 5.0 ppm (**Figure 24**). The ^{13}C NMR spectra of **149 a–e** displayed carbon peaks at the up-field region, which represent carbon 2 and 3 at δ 57.1 and 45.3 ppm respectively and shows the presence of the carbonyl carbon at approximately 190 ppm (**Figure 25**). The FTIR spectrum of **149a–b** exhibited a strong signal of carbonyl group, and a sharp weak peak representing the secondary amine group absorption peak at *ν* 1670 and 3375 (cm^{-1}) respectively (**Figure 26**).

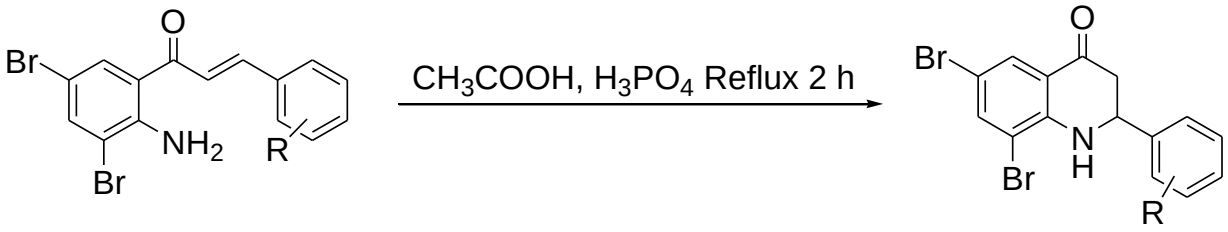

148 a-e **149 a-e**

Scheme 30. Acid promoted cyclization reaction

Table 2. Showing benzaldehyde derivatives, percentage yield and melting point values

Compound	R	% Yield	Mp ºC	
149a	H	77	99-106	(135-136) [16]
149b	4-CH_3	68	152-156	
149c	4-OCH_3	63	148-152	(143-145) [16]
149d	3-OCH_3	93	87-90	
149e	4-F	77	122-125	(127-129) [16]

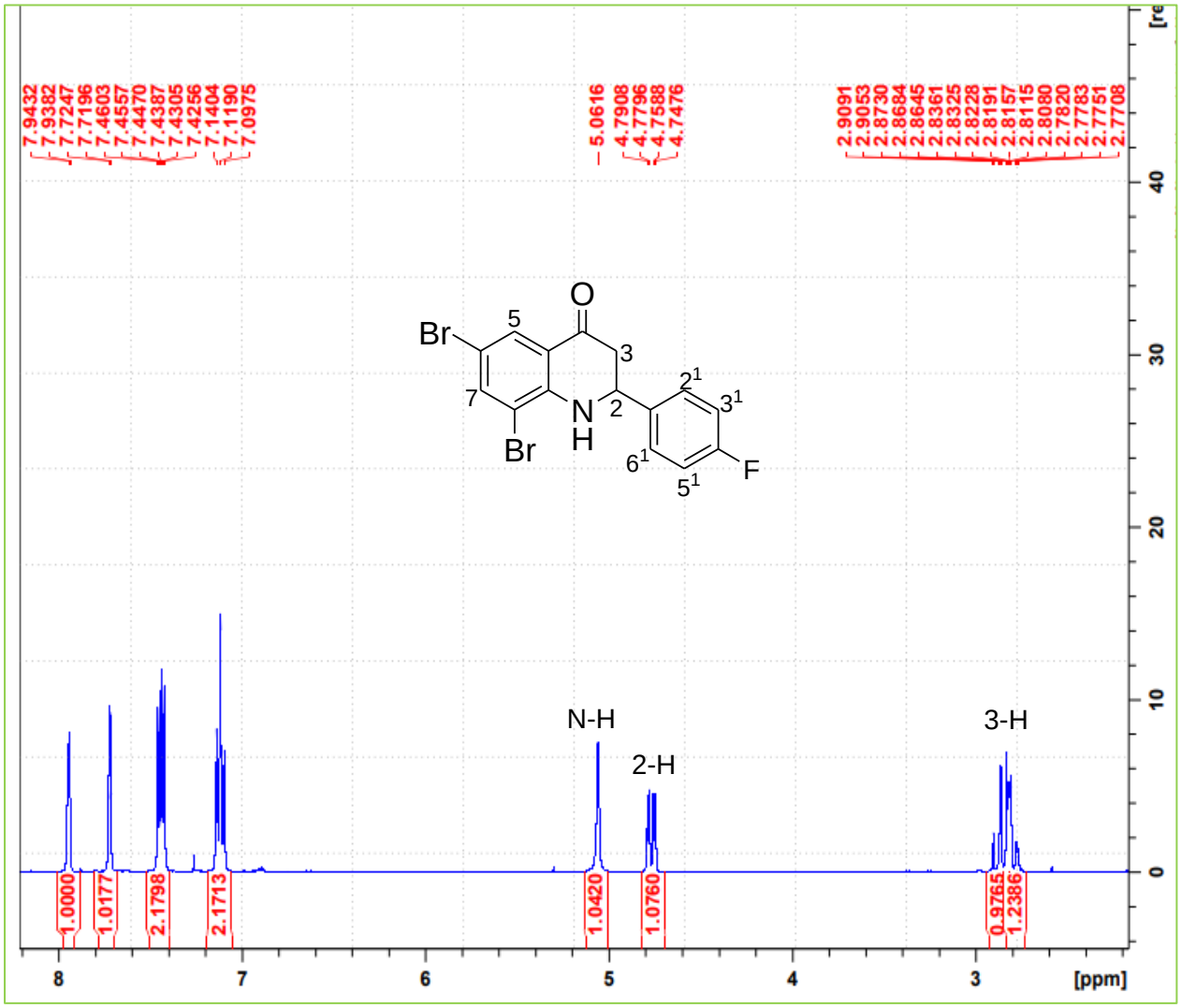

Figure 24. The ^{1}H NMR spectrum of a cyclized compound **149 e**

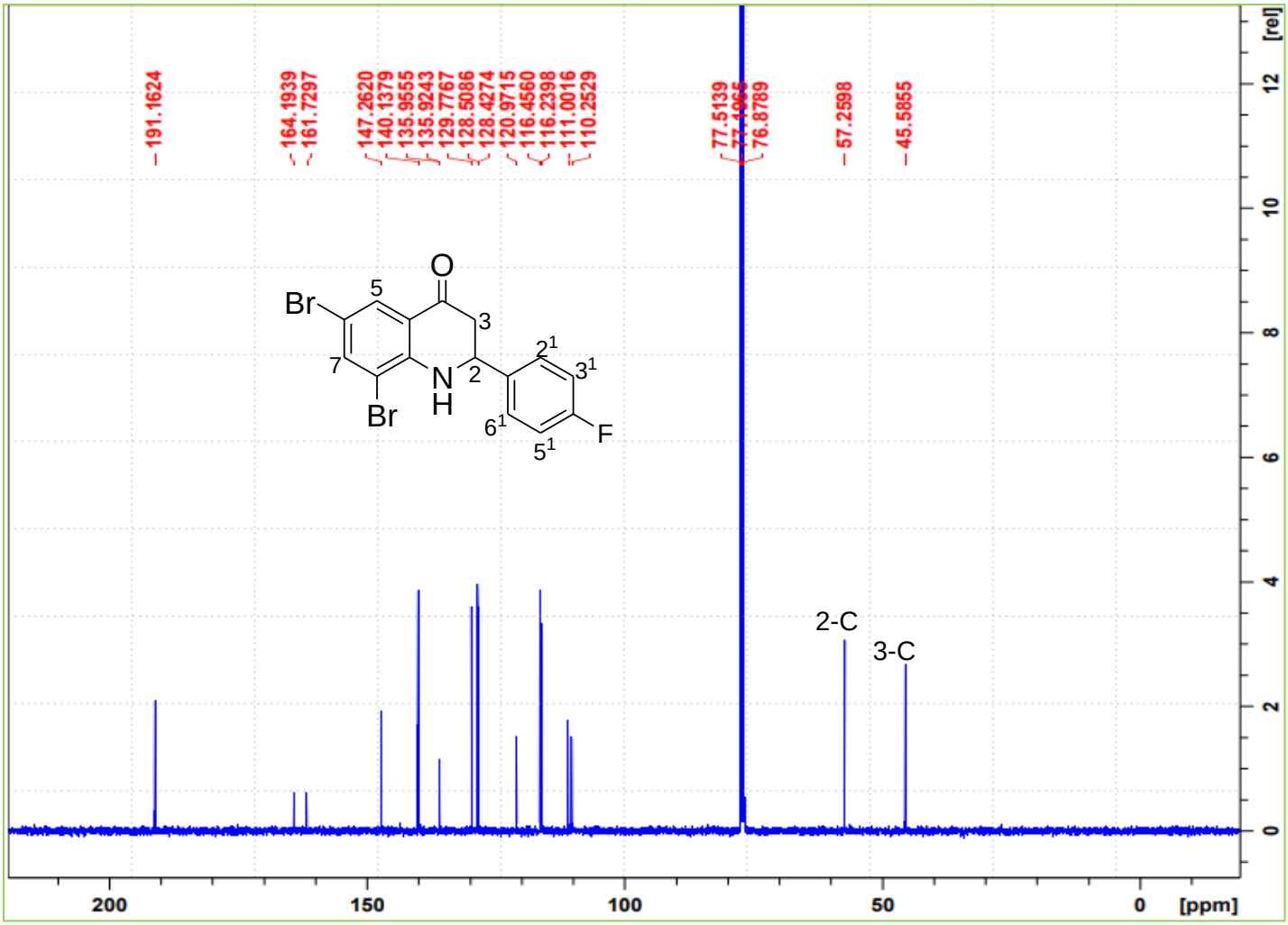

Figure 25. The ^{13}C NMR spectrum of a cyclized compound **149 e**

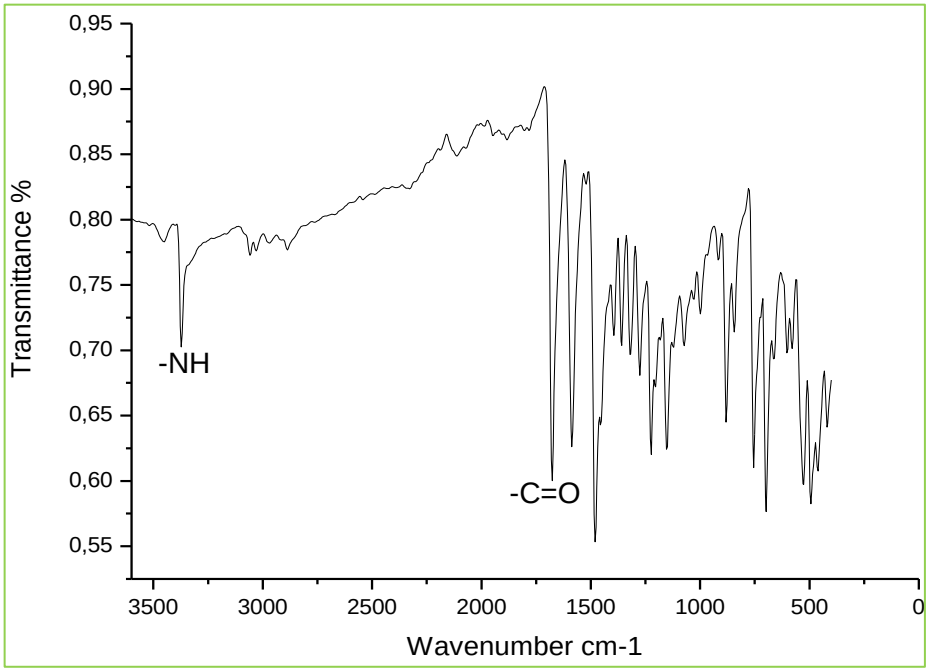

Figure 26. The IR spectrum of compound **149 e**

The successful synthesis of cyclized products **149 a–e** prompted us to further study dehydrogenation reaction in the next section.

2.3 Synthesis of 2-subtituted-quinolin-4(*1H*)-one derivative 150 a–e

Methods for the synthesis of 2-subtituted-quinolin-4(*1H*)-ones **150 a–e,** usually proceeds via dehydrogenation reaction of the 2-subtituted-2,3-dihydroquinolin-4(*1H*)-ones usually using oxidants such us KMnO4 [21], DDQ [22] and TTS [23]. Mphahlele *et al.* [24] synthesised 2-aryl-quinolin-4(*1H*)-ones using TTS under reflux conditions for 30 minutes in DME with yields of 55-90 %. In this study we opted for the use 1.5 equivalence of TTN as an oxidising agent to dehydrogenate compounds **149 a–e** in acetonitrile under heat for 2 h (**Scheme 31**) and the reaction was monitored by TLC. The mechanism of dehydrogenation of **149 a–e** derivatives by TTN, takes place via enolization of **149 a–e** compounds (2-substituted-2,3-dihydroquinolones), followed by electrophilic attack on TTN and subsequent dethallation prompted by the loss of trans-protons (2,3-H) forming an azaflavanone [25]. The ^{1}H NMR spectra of **150 a–e** was confirmed by the absence of the saturated allylic protons in the up-field region. The ^{1}H NMR spectra of **150 b**, for example, revealed the presence of 3-H singlet at δ 6.5 ppm for the newly formed *α-β* unsaturated cyclic carbonyl, with secondary amine (-NH-) peak resonating downfield at δ 8.6 ppm (**Figure 27**). The ^{13}C NMR spectra of **150 b** exhibited the absence of signals of $C_{2,3}$ up-field at the olefinic region and the presence of a carbonyl carbon at δ 162.0 ppm (**Figure 28**). The FTIR spectra of compounds **150 a–e** confirms the presence of the secondary amine group and carbonyl group signals at ν 3375 and 1662 (cm^{-1}) respectively (**Figure 29**). The compounds **150 b** and **150 e** were obtained at low yields, which may be due to the electronegativity of the substituents (-R group) or the work up of each derivative.

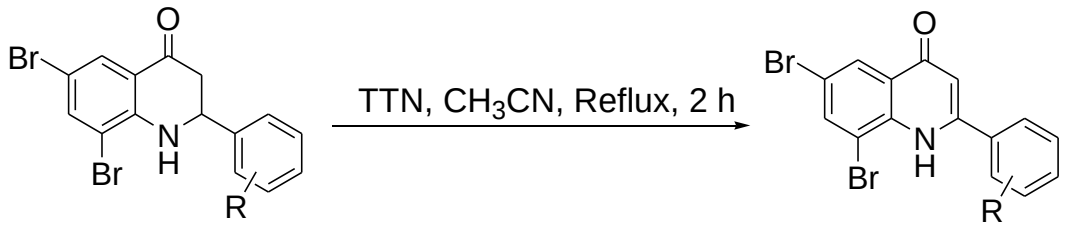

149 a-e **150 a-e**

Scheme 31. Dehydrogenation of compound **149 a–e**

Table 4. Showing percentage yields and melting point values of compound **150 a–e**

Compound	R	% Yield	Mp ºC	
150a	H	71	158-163	(212-214) [16]
150b	4-CH_3	55	157-160	
150c	4-OCH_3	77	189-193	(200-201) [16]
150d	3-OCH_3	85	180-184	
150e	4-F	48	143-147	(222-224) [24]

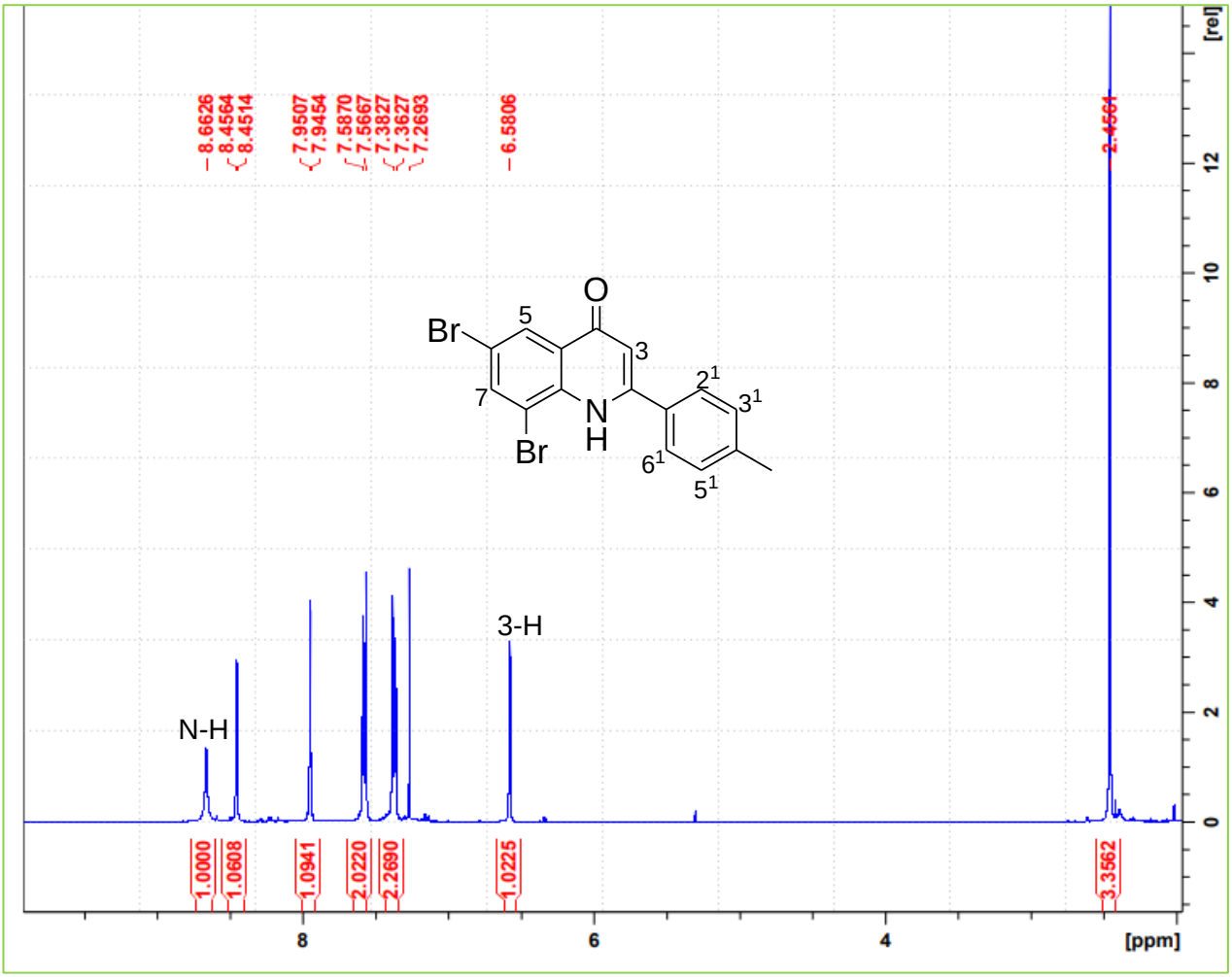

Figure 27. The ^{1}H NMR spectrum of a dehydrogenated compound **150 b**

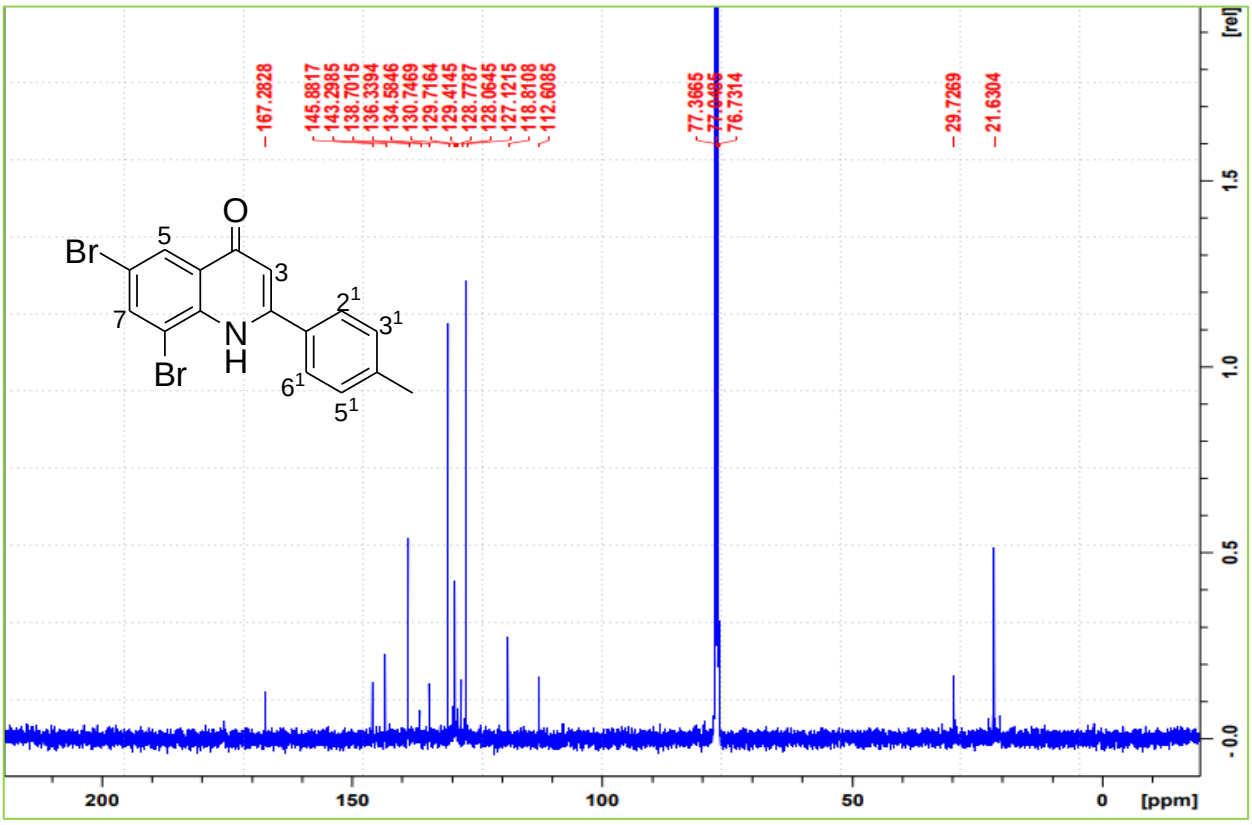

Figure 28. The ^{13}C NMR spectrum of a dehydrogenated compound **150 b**

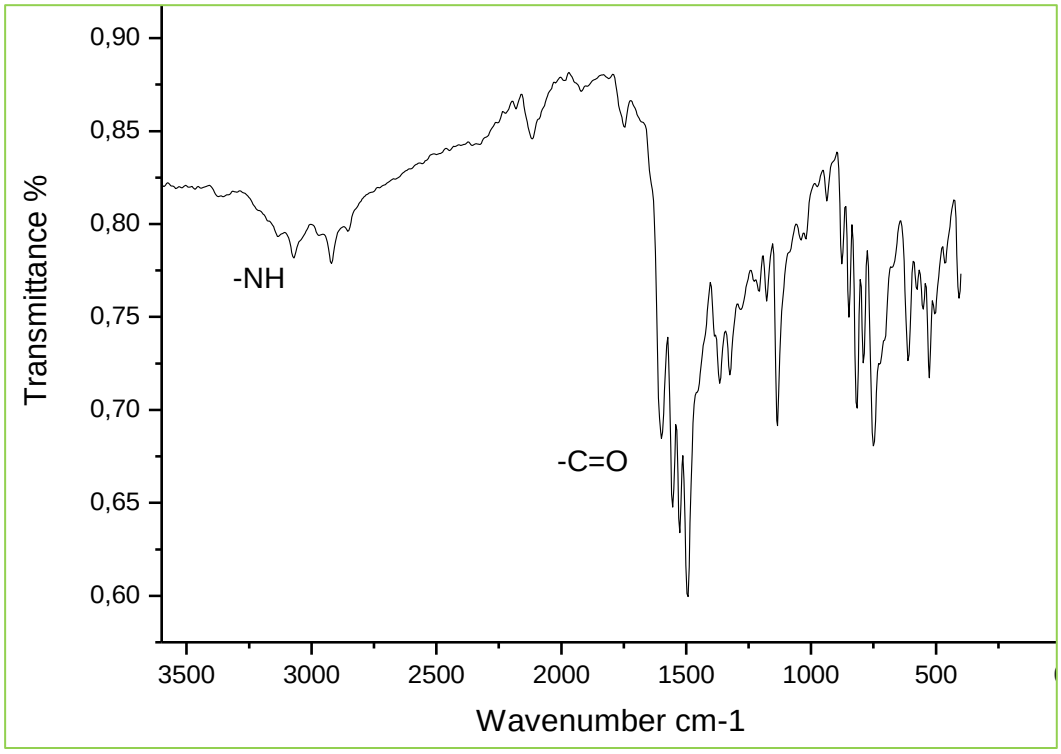

Figure 29. The IR spectrum of a dehydrogenated compound **150 b**

Having achieved compounds **150 a–e**, we further aimed to investigate their reactivity through oxidative aromatization reaction.

2.4 The synthesis of 2-aryl-4-chloro-quinolines (151 a–e)

There are literature methods reported to promote cyclization to form 4-quinolines, which incorporate the use of reagents such as iodine [26] and phosphorus oxy-chloride [27] or thionyl chloride [28] through oxidative aromatization reaction and through known classical methods, such as, Combes, Skraup, and Dobner-Miller reactions [29a]. However, the application of these classical methods to produce 2-aryl-4-chloro-quinolines was shown to be inefficient, as they have a disadvantage of the substituents that are introduced [24]. The mechanism is such that the 4-quinolone forms its tautomeric equilibrium 4-quinolinol, this has been proved through an investigation using X-ray and spectroscopic crystallography, thus making halogenation reaction at the 4th position easy [16]. In this study, we opted for the use of oxidative aromatization reaction of **150 a–e** and phosphorus oxy-chloride to form an electrophilic carbon (4-C) by introducing a partially electronegative halogen (**Scheme 32**). The initial attempt to aromatise using of thionyl chloride which later resulted in the mixture of two products according to the ^{1}H NMR, was later replaced by $POCl_3$ reacting 2-aryl-quinolin-4(*1H*)-one (**150 a–e**) in DMF. According to the ^{1}H NMR (**Figure 30**), compounds **151 a–e** was successfully formed without any further purification with the yield of 61- 86 %. The ^{1}H NMR spectrum of compounds **151 a–e** indicates the absence of NH signal and the chemical shift of 3-H from around δ 6.5 to 8.0 ppm (downfield showing the electronegativity effect of the chlorine) and the presence of all aromatic protons. The ^{13}C NMR spectrum reveals a shift of 3-C downfield at δ 121-126 ppm and 2-C at 157-160 ppm because of the formation of ((δ+) C=N (δ-)) bond (**Figure 31**). The FTIR spectrum shows an absorption at *v* 1595-1657 (cm^{-1}) representing the C=N group and the absence of the N-H weak peak (**Figure 32**).

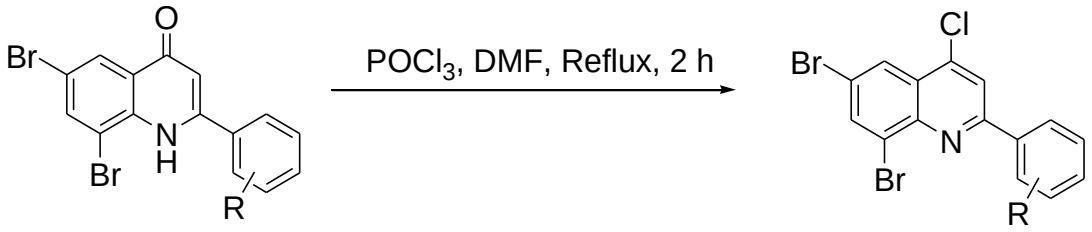

150 a-e **151 a-e**

Scheme 32. Oxidative aromatization reaction of compound **150 a–e**

Table 5. Showing compound 151 a–e derivatives, percentage yields and melting point values

Compound	R	% Yield	Mp ºC
151a	H	80	159-161
151b	4-CH_3	66	181-184
151c	4-OCH_3	74	150-154
151d	3-OCH_3	75	106-110
151e	4-F	87	195-198

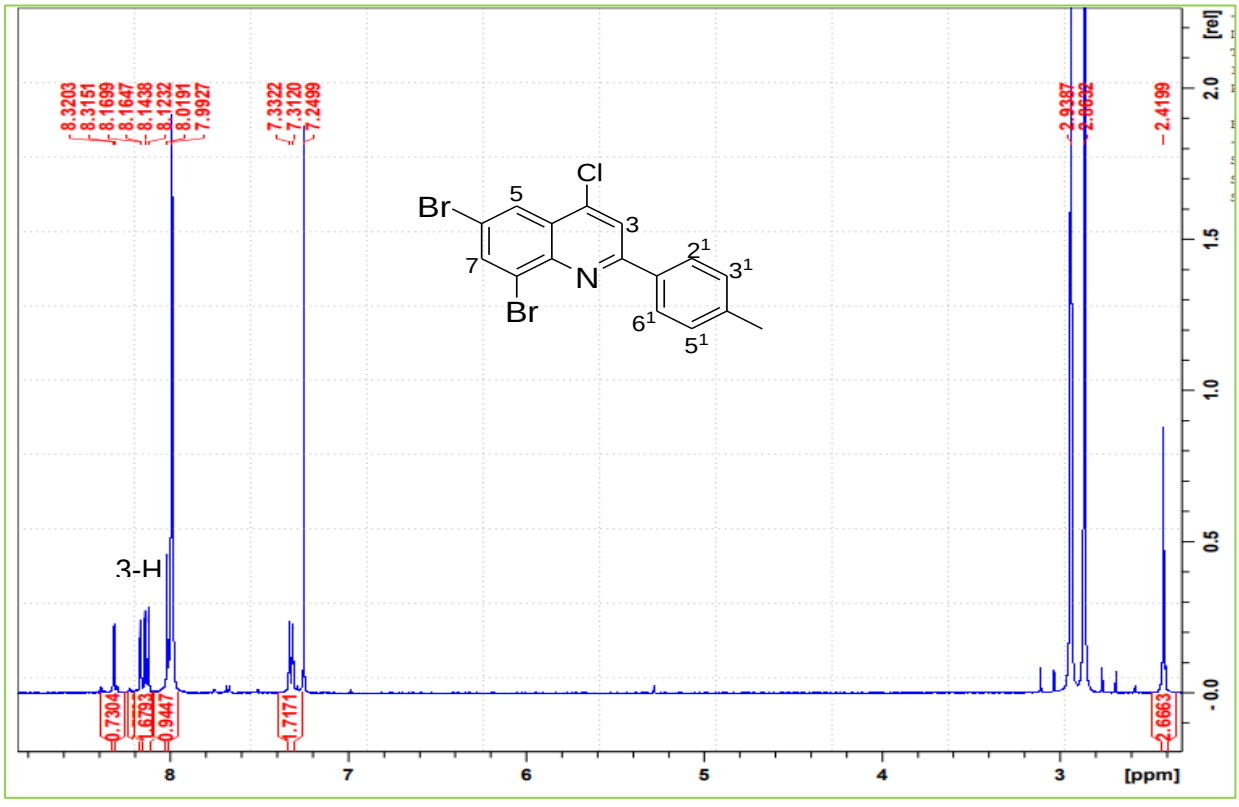

Figure 30. The ^{1}H NMR spectrum of a chlorinated compound **151 b**

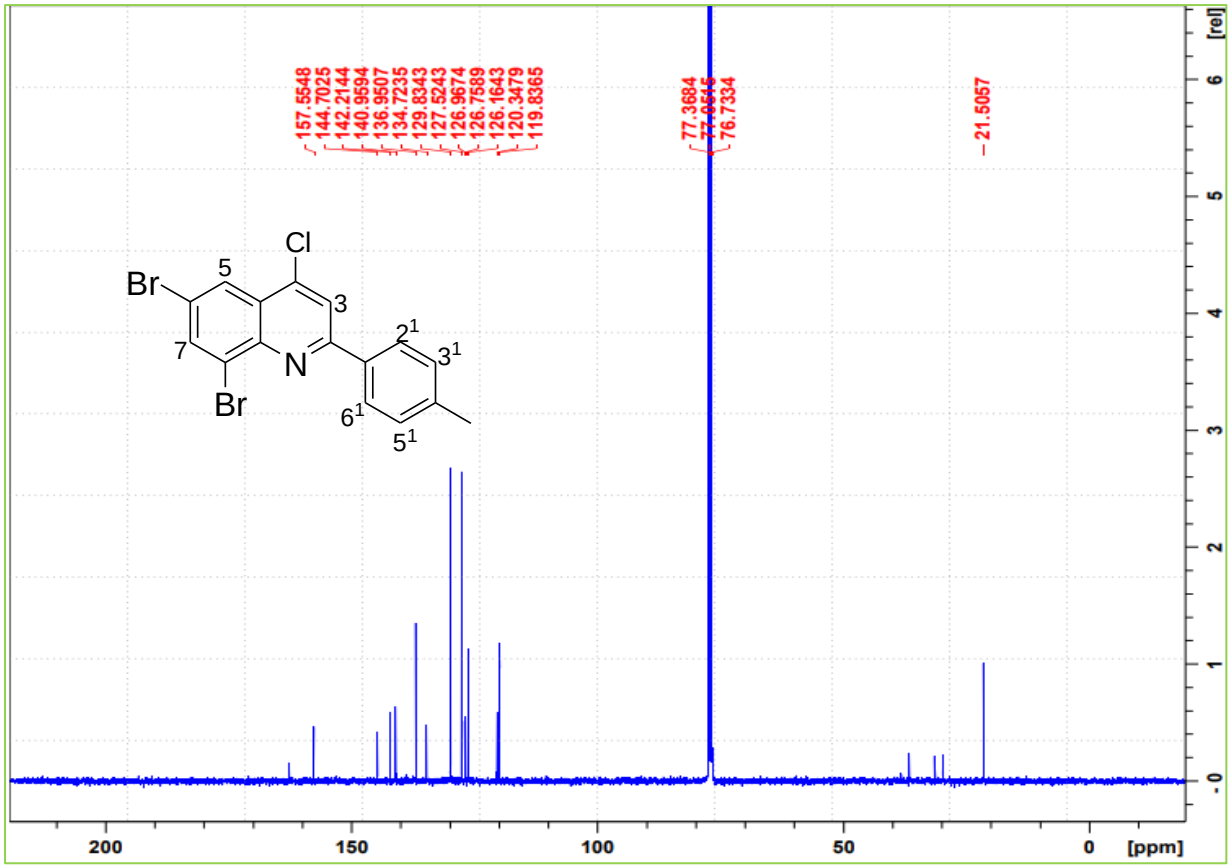

Figure 31. The ^{13}C NMR spectrum of a chlorinated compound **151 b**

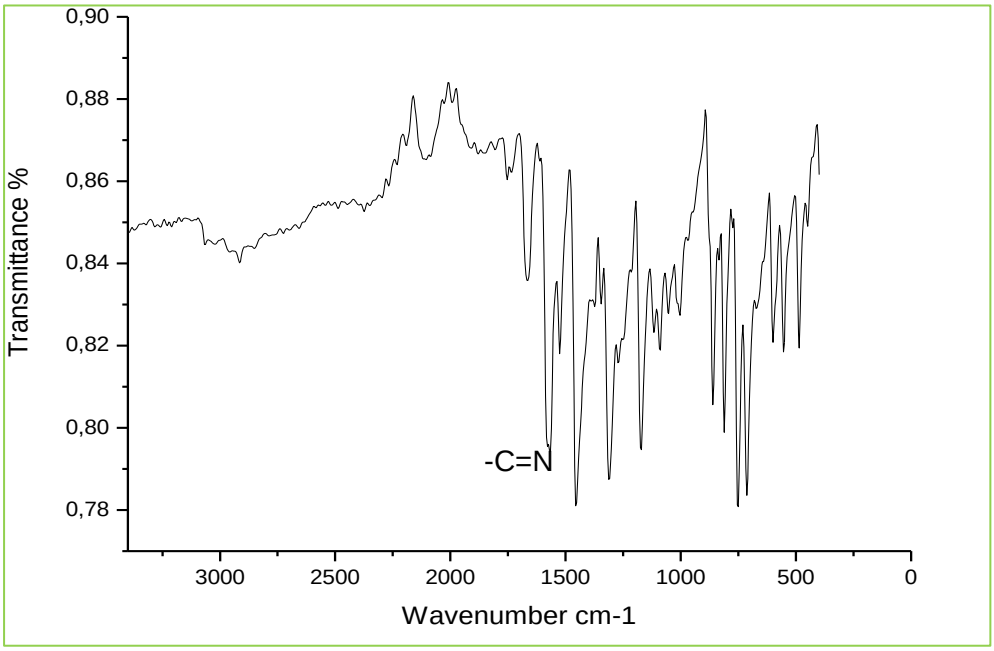

Figure 32. The IR spectrum of the chlorinated compound **151 b**

The presence of chlorine at the 4th position of compounds **151 a–e,** comprises a carbon 4 (electropositive C^{+}-Cl^{-}) to be exposed to nucleophilic substitution. We then decided to investigate nucleophilic substitution reaction as described in the next section

2.5 The synthesis of 2-substituted-4-azido-quinoline (152 a–e)

The 2-substituted-4-azido-quinoline (**152 a–e)** has been synthesised mainly from nucleophilic substitution using sodium azide [30]. Wolf *et al.* [30] subjected the 4-chloro quinoline under substitution reaction to form 4-iodo-quinoline, using NaI (sodium iodide) in acetonitrile as a solvent under reflux for 24 h. Sodium azide and dimethyl formamide are also reported to afford 4-azido-quinoline under reflux [31,32]. We however adopted the literature method [31,32] to achieve compounds **152 a–e** following a nucleophilic attack at 4-C position of compound **151 a–e** and 1.2 equivalent of sodium azide and in THF for 12 h under reflux (**Scheme 33**). The effect of the new substituent is confirmed by the ^{1}H NMR spectrum of **152 a–e** which showed the same number of protons as compounds **151 a–e**, except 3-H which shifted upfield to δ 7.6 ppm (**Figure 33**) for compound **152 a**. The FTIR confirmed (**Figure 35**) the presence of an azide group by showing a strong absorption peak at *v* 2100 (cm^{-1}) as reported in literature [33].

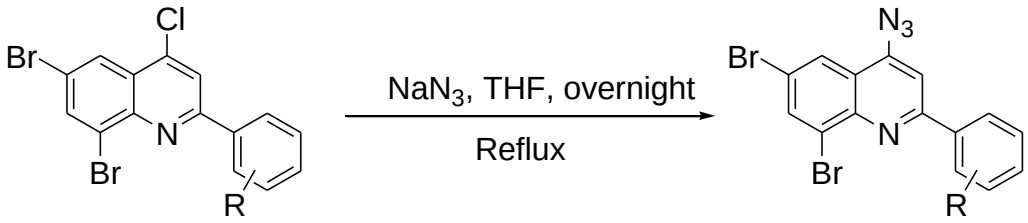

151 a-e **152 a-e**

Scheme 33. Nucleophilic substitution reaction of compound **151 a–e** using sodium azide

Table 6. Substitution pattern, percentage yield and melting point values of 4-azido quinoline derivatives **152 a–e**

Compound	R	% Yield	Mp ºC
152a	H	81	98-103
152b	4-CH_3	63	157-161

152c	4-OCH_3	62	164-167
152d	3-OCH_3	66	129-136
152e	4-F	87	182-186

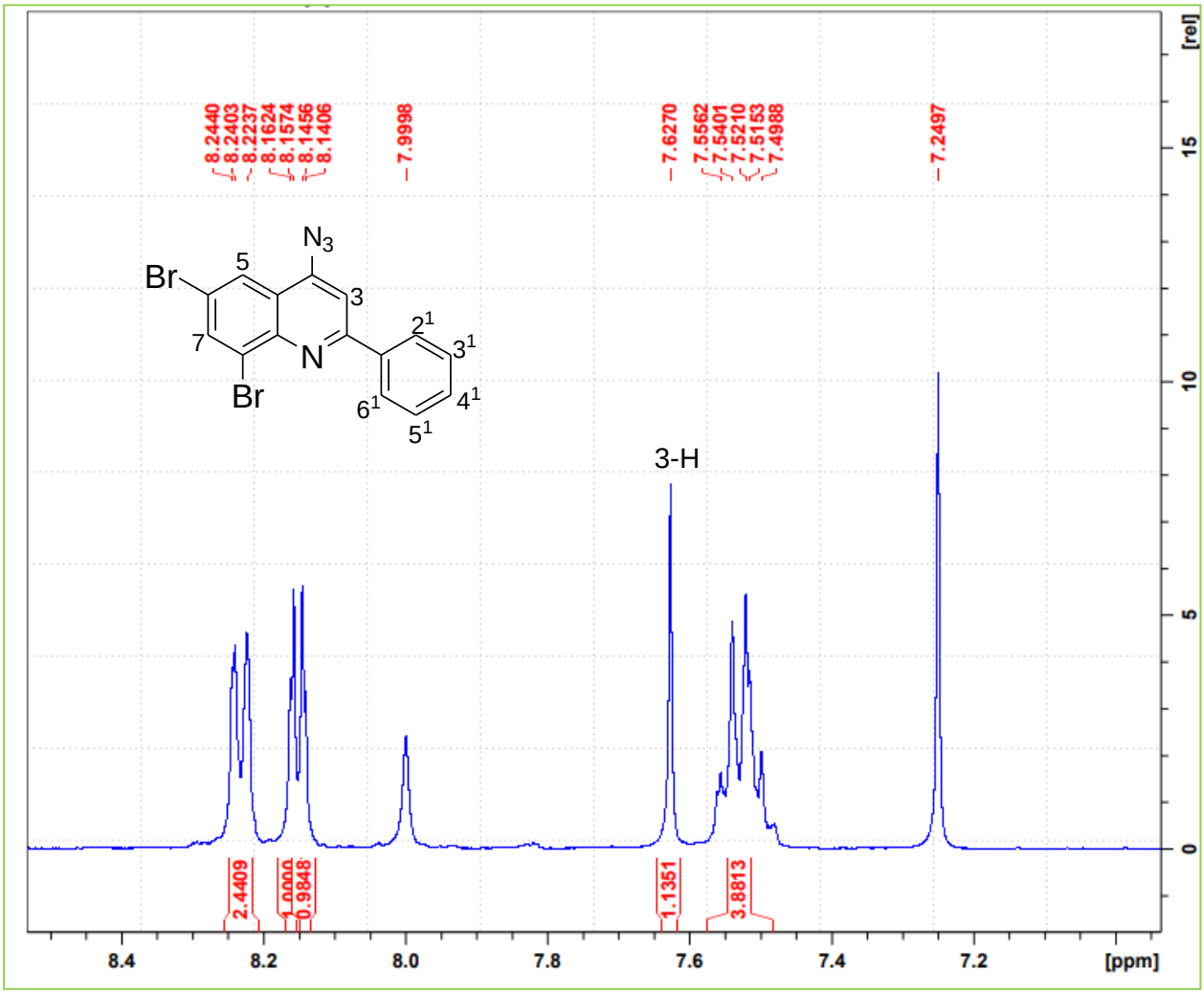

Figure 33. The ^1H NMR spectrum of compound **152 a**

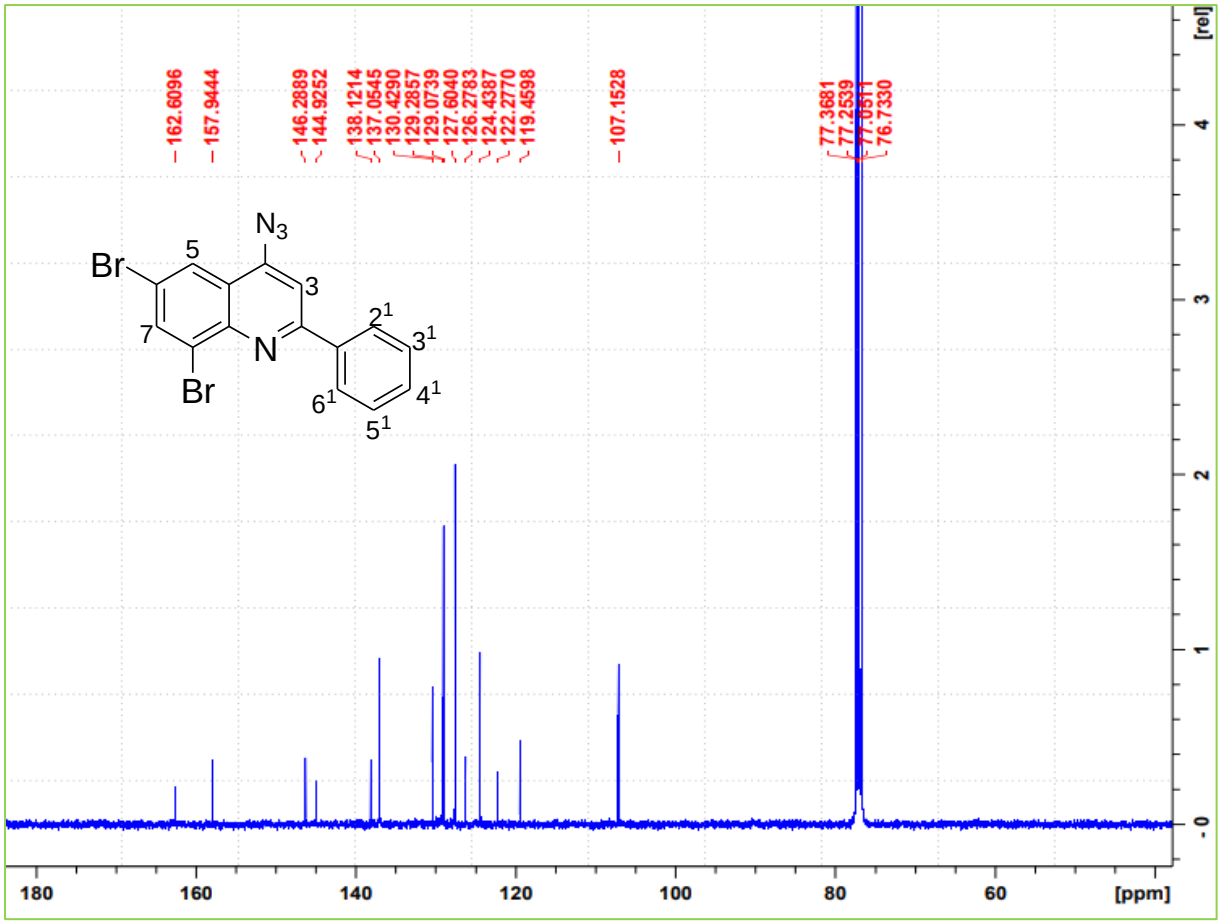

Figure 34. The ^{13}C NMR spectrum of compound **152 a**

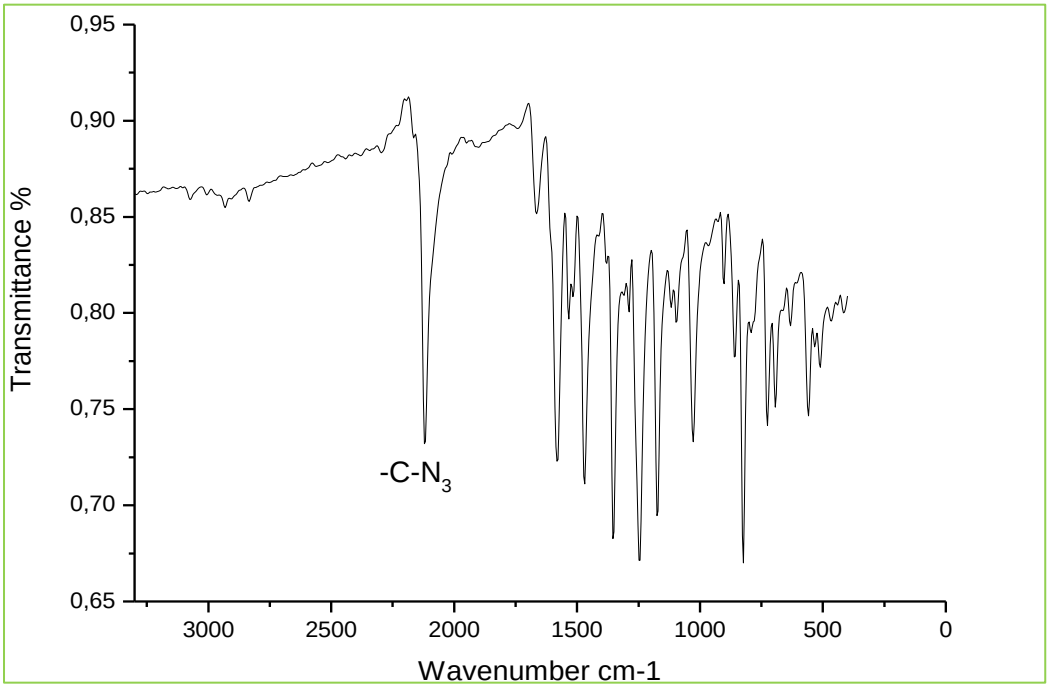

Figure 35. The IR spectrum of compound **152 c**

The 4-quinolines are applicable to molecular hybridization which is an exceptional approach concerning new-drug development. Therefore, in the presence of an azide group at the 4th position, we decided to investigate the pericyclic reaction, as described in the next section

2.5 The synthesis of triazolyl quinoline derivatives 153 a–q

The 6,8-dibromo-4-azido-quinoline derivatives **152 a–e** were subjected to click chemistry or 1,4-cycloaddition reaction conditions [34]. In this study we used copper sulphate pentahydrate ($CuSO_4.5H_2O$) as catalyst and, sodium ascorbate as a base to react the 4-azidoquinolines **152 a–e** with alkyne derivatives to produce triazolylquinolines **153 a–q** (**Scheme 34**). The copper sulphate in this reaction is reported to have an oxidation state of +1, which is achieved *in-situ* with a reducing agent, sodium ascorbate (as a ligand) [34]. Therefore, Cu^1Ln continues to form a complex with the azido on-route to synthesise triazole derivatives [35]. The 4-azido quinolines **152 a–e** were reacted with substituted phenyl acetylenes and propargyl alcohol in the presence of sodium ascorbate and copper sulphate pentahydrate under reflux for 2-4 hours. We decided to optimize the reaction, by using 1.2 equivalence of propargyl alcohol reacted with **152 a–e**, 40 % of the base and 10 % the copper catalyst under reflux to form compounds **153 a–e,** we discovered that the phenyl-triazole derivatives **153 f–q**, 40 % of copper catalyst and 2 equivalence for the substituted phenyl acetylenes and base gave better yields.

2.5.1 The synthesis of (1-(6,8-dibromo-2-(phenyl) quinoline-4-yl)-1*H*-(1,2,3-triazo-4-yl) derivatives 153 a–q

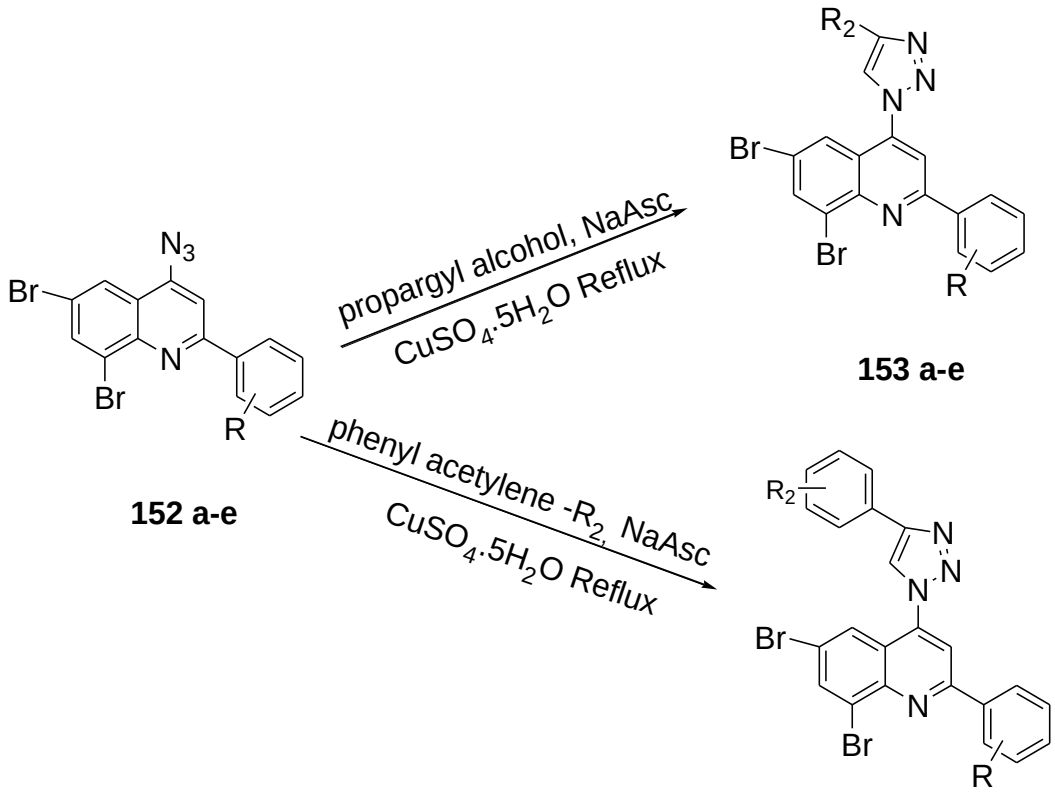

Scheme 34. The click chemistry reaction of compound **152 a–q** with acetylene derivatives (R_2 = 3F, 3Cl, H)

Table 7. Substitution pattern, percentage yield and melting point values of 4-triazolyl quinoline derivatives **153 a–q**

Compound	R	R_2	% Yield	Mp ºC	Triazole proton (ppm
153a	H	CH_2OH	81	207-210	8.07
153b	4-CH_3	CH_2OH	69	209-212	8.06
153c	4-OCH_3	CH_2OH	85	219-221	7.98
153d	3-OCH_3	CH_2OH	50	220-222	7.91
153e	4-F	CH_2OH	75	234-239	7.99
153f	H	3-F	66	229-232	8.19
153g	4-CH_3	3-F	76	225-228	8.16

153h	4-OCH_3	3-F	68	231-234	8.04
153i	3-OCH_3	3-F	71	183-187	8.16
153j	4-F	3-F	99	223-226	8.22
153k	H	4-H	65	206-211	8.19
153l	4-CH_3	4-H	73	241-245	8.29
153m	4-OCH_3	4-H	44	219-222	8.15
153n	3-OCH_3	4-H	84	210-214	8.18
153o	4-F	4-H	68	237-240	8.28
153p	4-OCH_3	3-Cl	80	260-264	8.16
153q	3-OCH_3	3-Cl	25	127-131	8.15

Compounds **153 a–q** were easily distinguished from their precursor through characterization using the ^{1}H and ^{13}C NMR. The ^{1}H NMR of compounds **153 a–e** showed an additional two singlet signals at approximately δ 5.0 and 8.0 ppm indicating the presence of the triazole proton on the triazole (a-H) and the methylene protons (-C$\underline{H_2}$OH, c-H) (**Figure 36**). The ^{13}C NMR indicates addition of the -$\underline{C}H_2OH$ carbon signal at around δ 56 ppm (**Figure 38**). The 2D NMR spectrum "HSQC" (**Figure 40**) (homonuclear single quantum coherence) for compound **153 d**, shows the presence of a negatively phased (coded red) peak at ^{1}H NMR (δ 4.90 ppm) and ^{13}C NMR (δ 56.6 ppm), indicating the presence of a -CH_2 (c-H) group. The 2D NMR heteronuclear multiple bond correlation (HMBC) (**Figure 39**) shows the correlation of the 7-H proton and the c-H protons to a quaternary 4th-carbon (4-C) of the quinoline skeletal structure at 127.1 ppm through a ^{5}J coupling as shown in figure (circled in red). The FTIR of compound **153 e** (**Figure 37**), show the presence the OH group showing a weak broad absorption peak at ν 3347 (cm^{-1}).

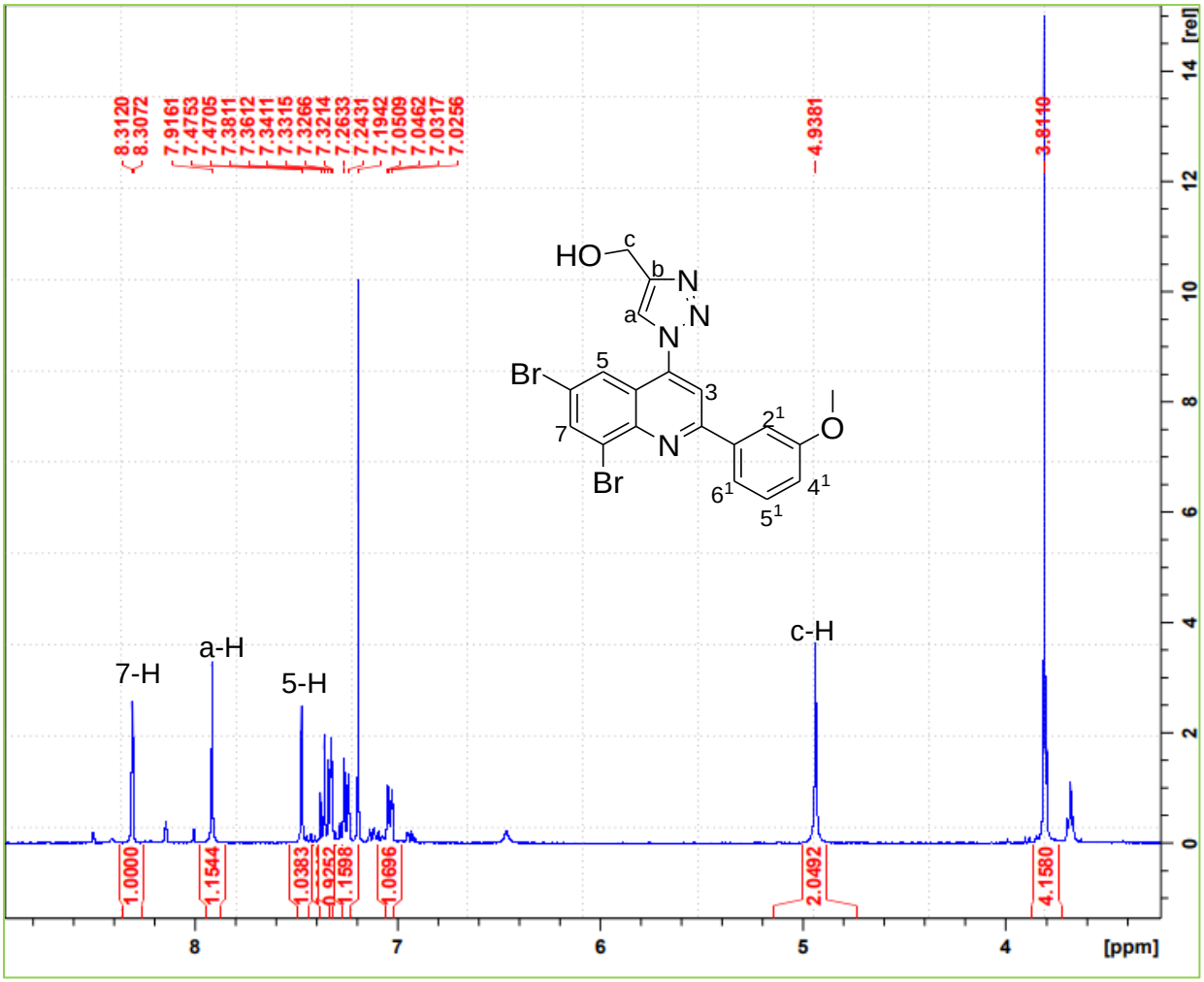

Figure 36. The ^{1}H NMR spectrum of compound **153 d**

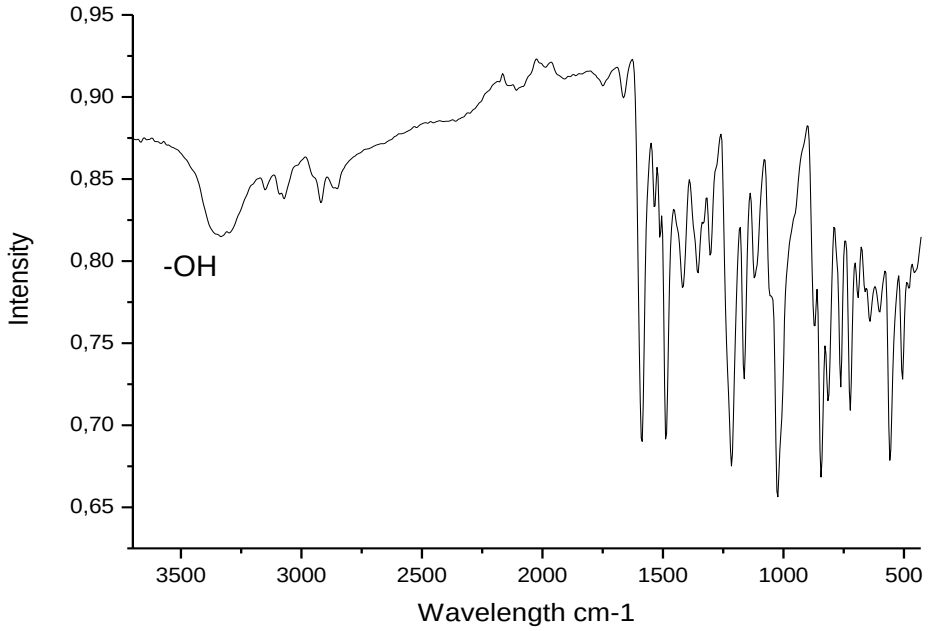

Figure 37. The IR spectrum of compound **153 e**

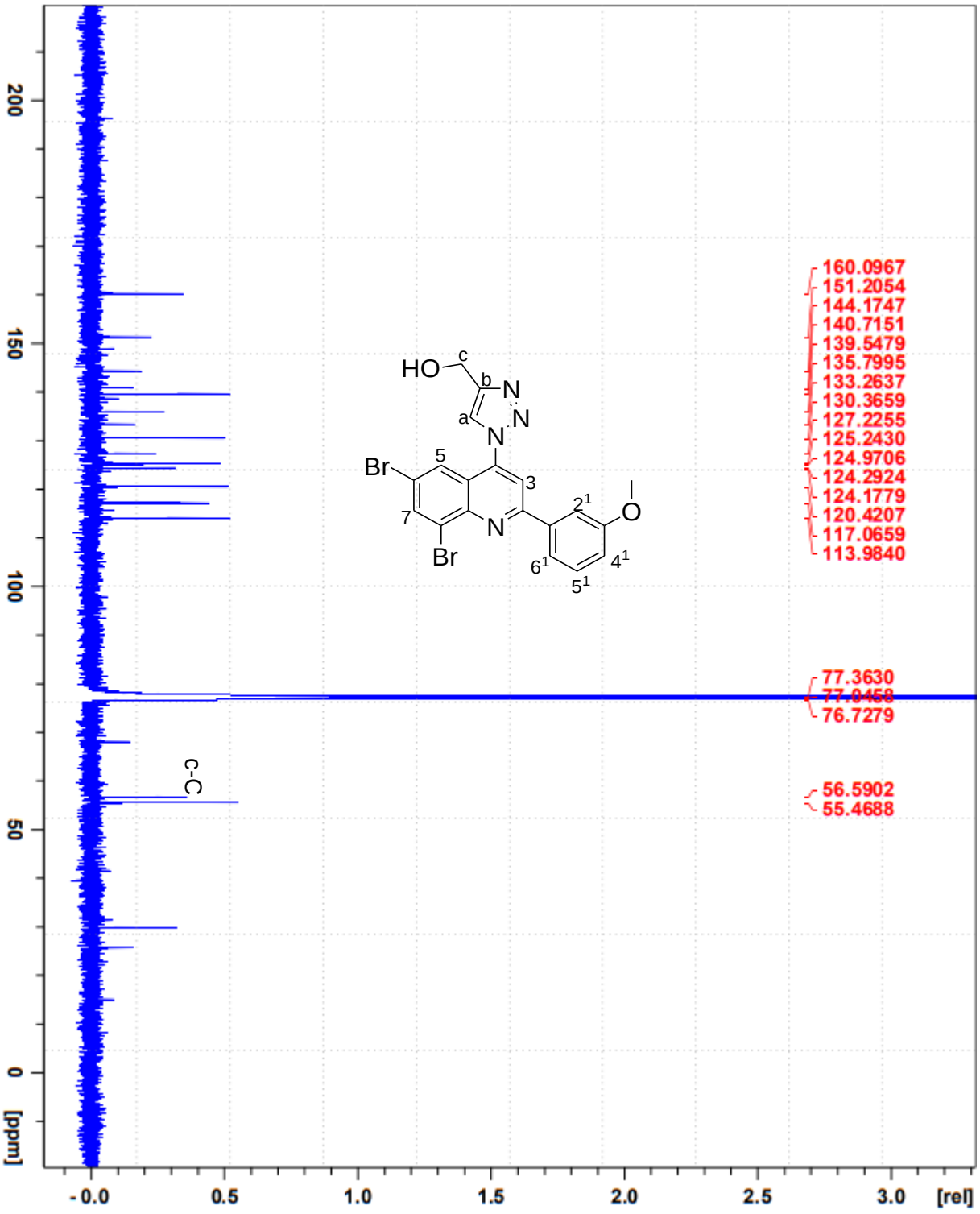

Figure 38. The ^{13}C NMR spectrum of compound **153 d**

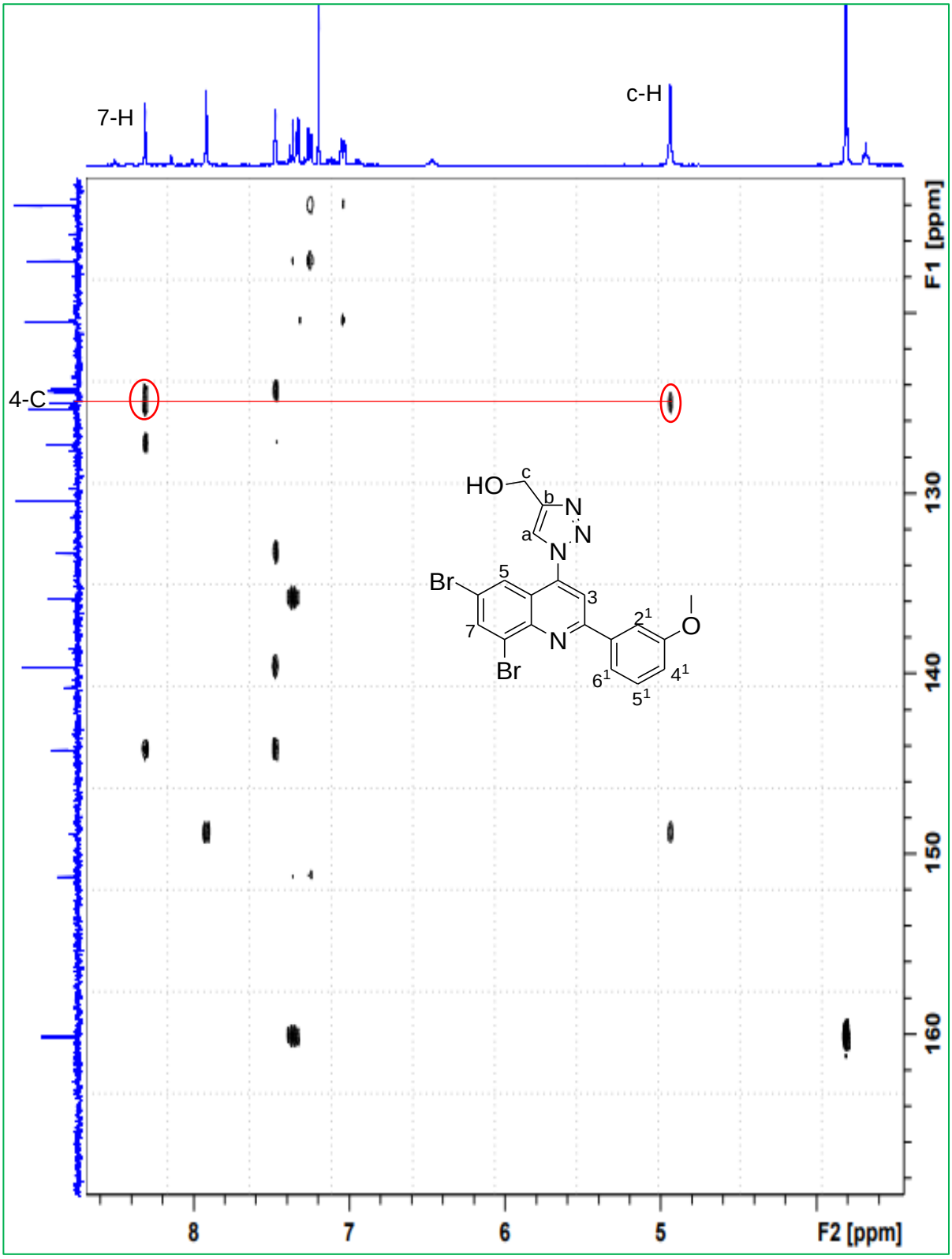

Figure 39. The 2D HMBC NMR spectrum of compound **153 d**

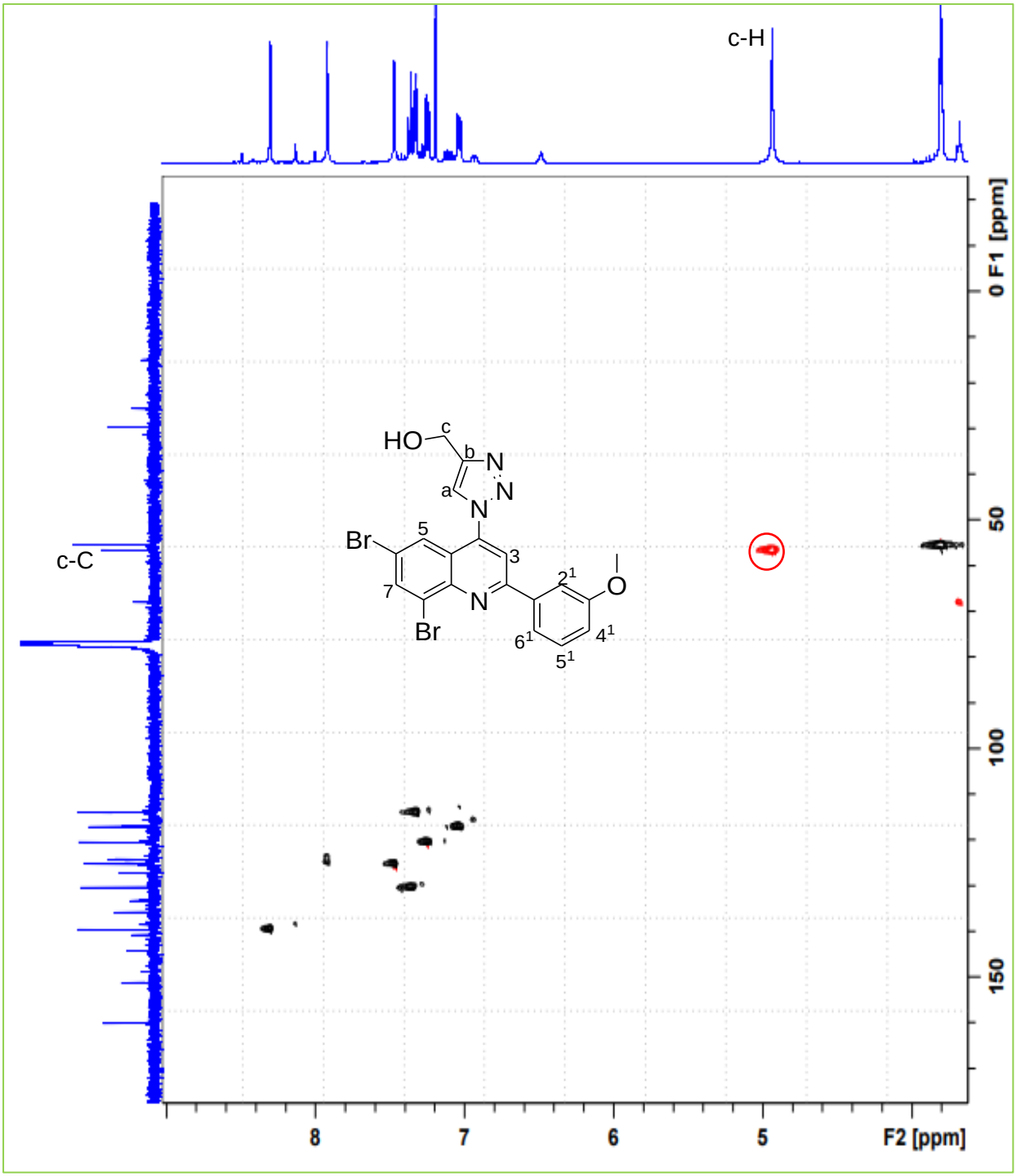

Figure 40. The 2D HSQC NMR spectrum of compound **153 d**

The ^{1}H NMR spectra of the substituted phenyl acetylenes showed some additional signals at the aromatic region at approximately δ 7.1-7.8 ppm indicating the presence of a singlet representing the triazole proton signal at δ 8.15 ppm the chemical shift of the 5-H proton from the quinoline skeletal structure to relatively higher field. The ^{1}H NMR spectrum of 6,8-dibromo-4(3-fluorophenyl)-1*H*-1,2,3-triazol-1-yl)-2-(phenyl) quinoline derivative **153 h**, synthesised from compound **152 c** and 1-ethynyl-3-fluorobenzene, shows proton signals at the aromatic region from the 3-fluorophenyl which are clearly identified like triplets at δ 7.4 and 7.3 ppm because fluorine has ½ spin nuclei similar to a hydrogen, and as such it couples with the hydrogens on the phenyl ring (**Figure 41**). The ^{13}C of NMR spectrum of **153 h**, shows additional signals where the effect of the carbon-fluorine (½ spin) interaction in the form of doublets resonating at δ 163.2, 112.0, 115.8, 131.6, 130.7 and 121.6 ppm corresponding to coupling constants $^{e}J_{C\text{-}F}$ 244 Hz, $^{d}J_{C\text{-}F}$ 23 Hz, $^{f}J_{C\text{-}F}$ 21 Hz, $^{g}J_{C\text{-}F}$ 9 Hz, $^{h}J_{C\text{-}F}$ 9 Hz and $^{c}J_{C\text{-}F}$ 2 Hz respectively (**Figure 42**). The 2D COSY NMR spectrum of compound **153 h** (**Figure 43**) , shows the correlation of 7-H proton at δ 8.22 ppm (d, *J* = 2 Hz) and H-5 proton at δ 7.7 ppm (d, *J* = 2 Hz), which proves the shift of the 5-H proton slightly up-field, which is further confirmed by the 2D HMBC NMR spectrum which shows the correlation of the 7-H proton with the 5-C carbon (circled **green**) (at δ 125.7 ppm) and the 5-H proton with the 7-C (circled **red**) (δ 137.5 ppm) through at $^{3}J_{C\text{-}H}$ coupling as (**Figure 44**).

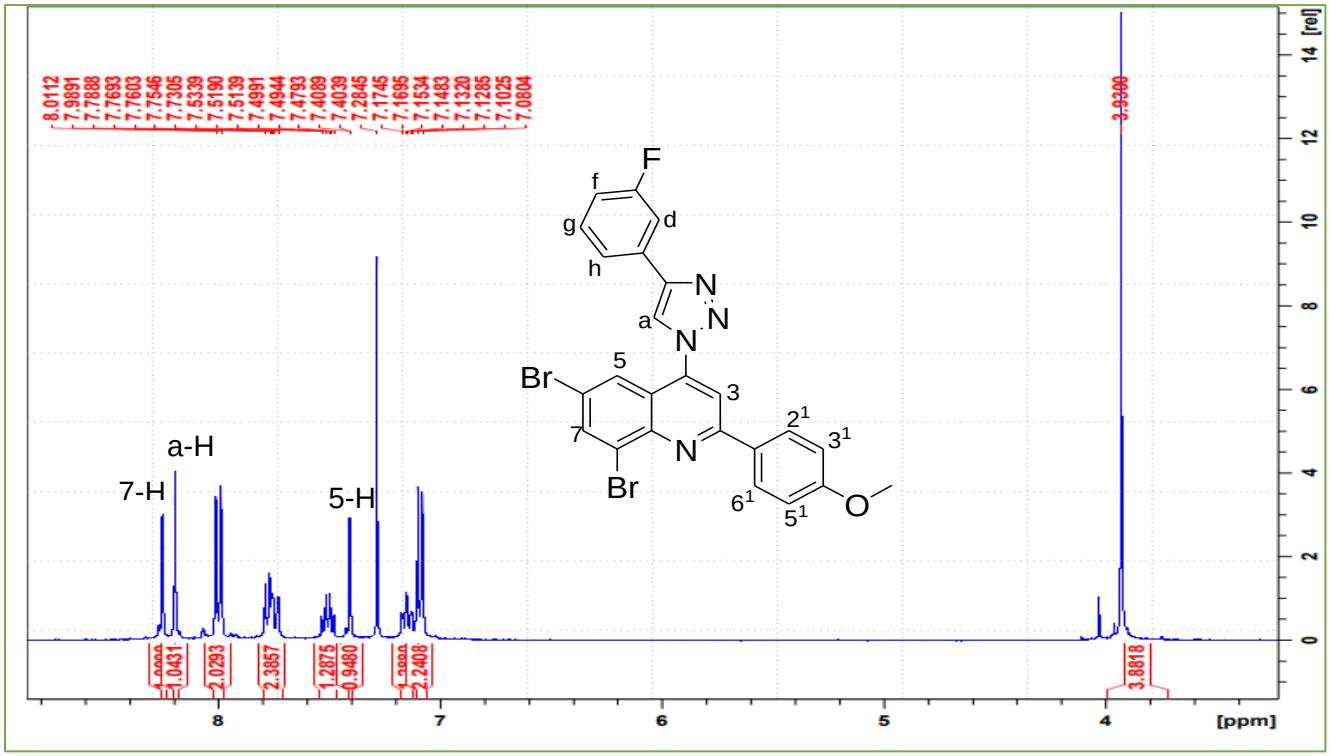

Figure 41. The ^{1}H NMR spectrum of compound **153 h**

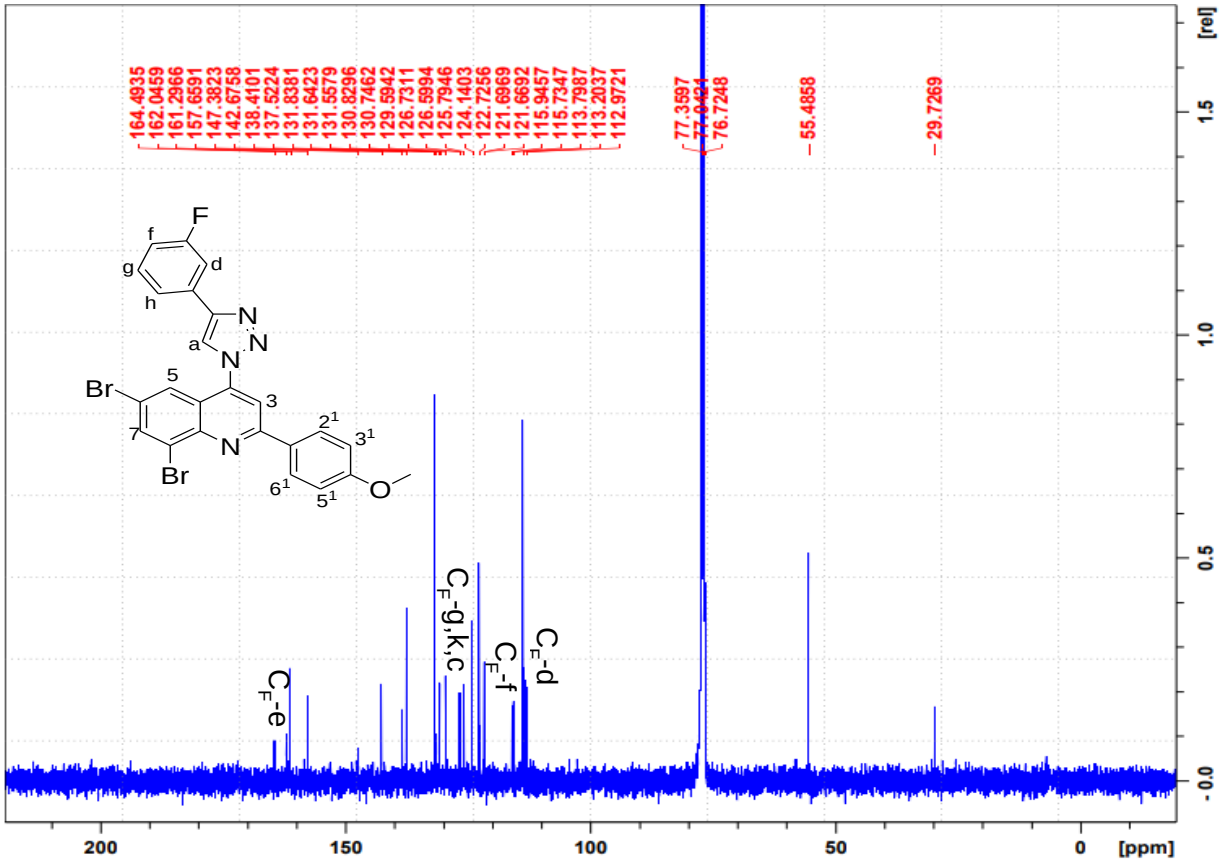

Figure 42. The ^{13}C NMR spectrum of compound **153 h**

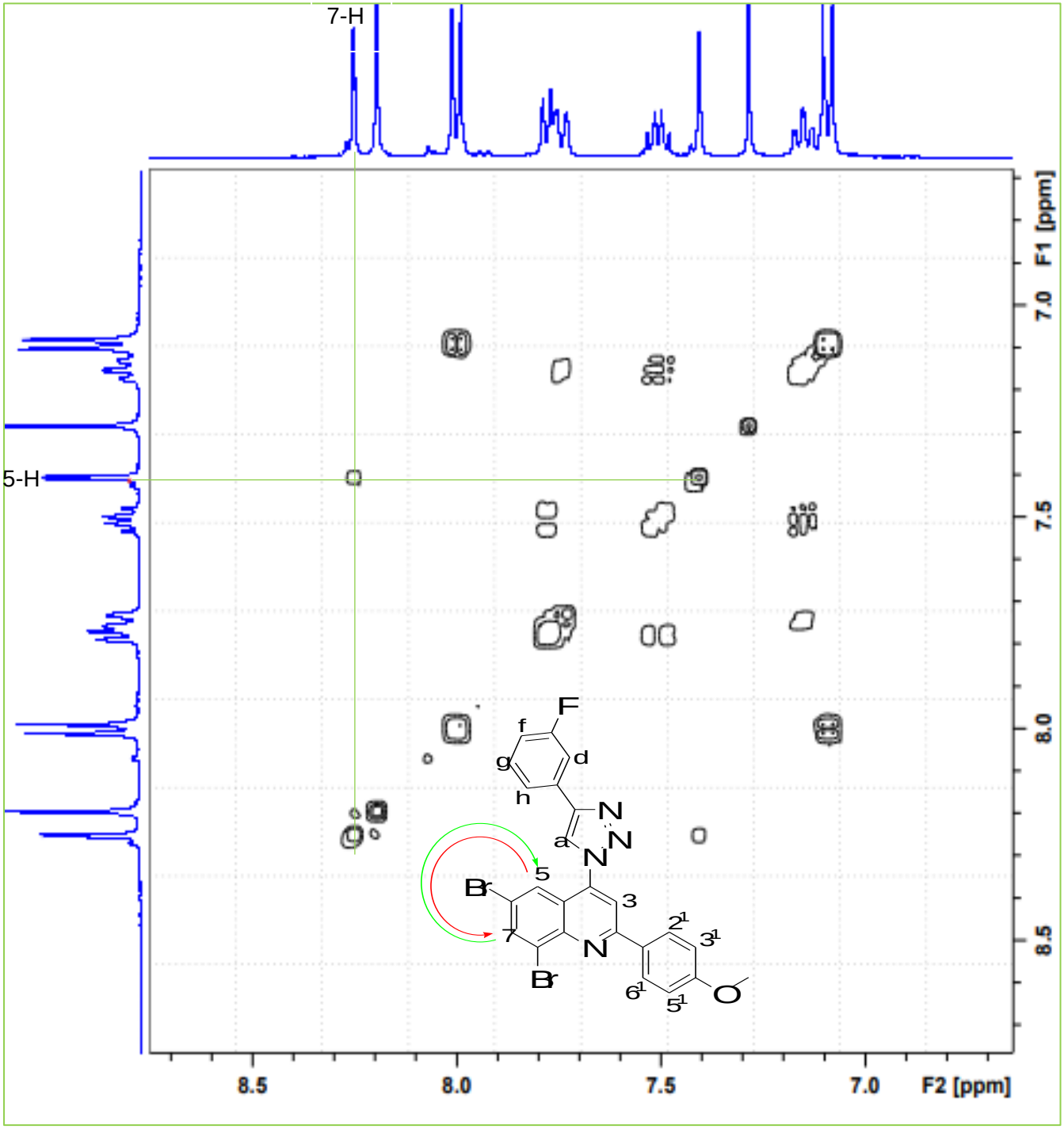

Figure 43. The COSY NMR spectrum of compound **153 h**

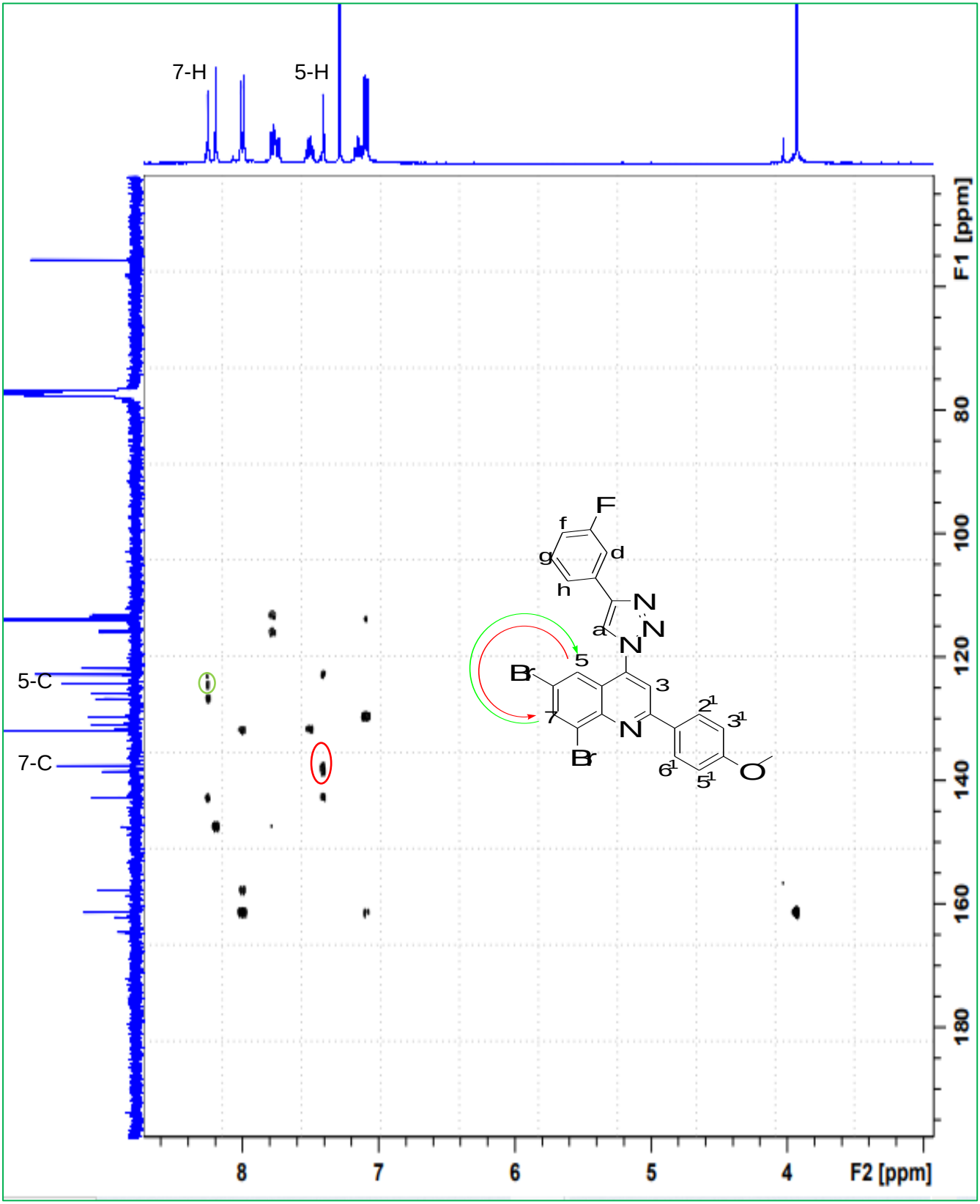

Figure 44. The 2D HMBC NMR spectrum of compound **153 h**

The structure of compounds **153** and their configuration were clearly confirmed by a single crystal X-ray diffraction (XRD) analysis (**Figure 45**). Compound **153 j** crystalizes in the P-1 spatial group, with four molecules in each asymmetric unit, with the following unit cell parameters *a* = 10.8328(13) Å, *b* = 12.5301(17) Å, *c* = 16.016(2) Å, *α* = 73.091(5) °, *β* = 74.512(4)°, *γ* = 87.355(5)°, thus resolving into the triclinic crystal system. The torsion angles between C(16)-N(1)-N(2)-N(3), C(7)-N(1)-N(2)-N(3) and N(1)-N(2)-N(3)-C(17) are 0.3 (3) Å, 180.0 (2) Å and 0.1 (3) Å respectively as summarized in **Table 8**, indicating that the substituted aromatic quinoline system and the triazole moiety are not planar. (**Figure 45**). The molecule is stabilized by intermolecular π- π stacking, C-H···F, C-H···Br and C-H···π interactions (**Figure 46**). The crystallographic data of compound **153 j** is summarized in **Table 9.**

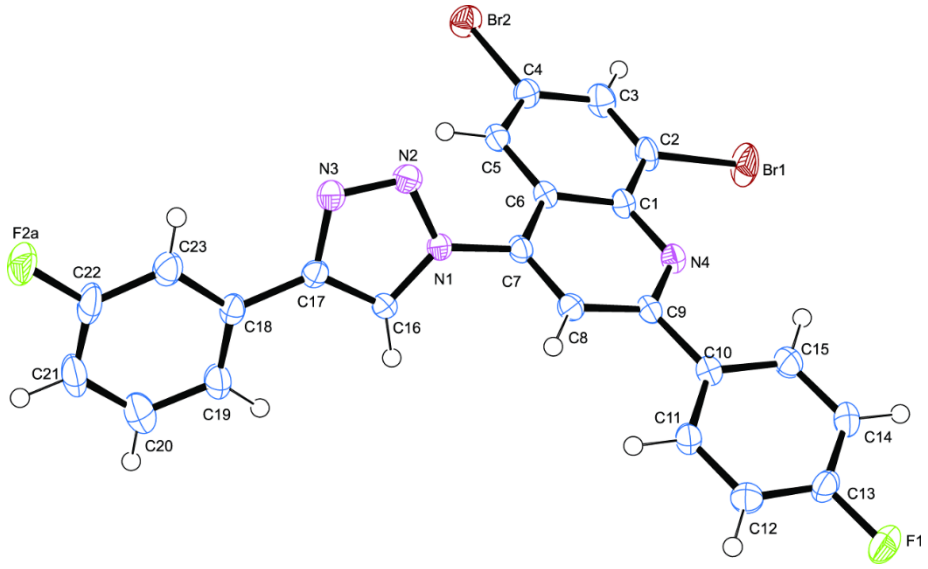

Figure 45. Oak Ridge Thermal Ellipsoid Plot (ORTEP) diagram of **153 j**. Displacement ellipsoids is drawn at the 50% probability level and H atoms are shown as small spheres of arbitrary radii

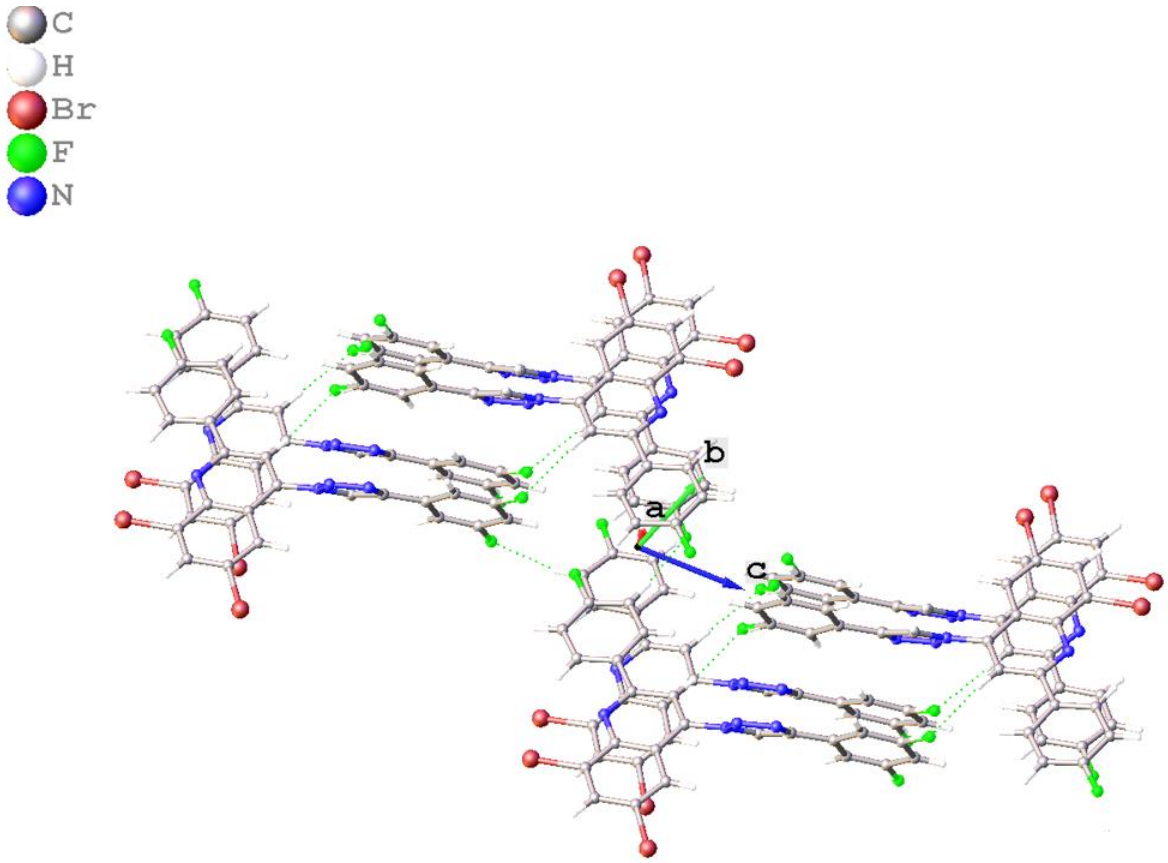

Figure 46. Packing diagram of **153 j** showing the C–H···F and π···π along the a-axis.

Table 8. Bond lengths [Å], angles and torsion angles [°] for crystal compound **153 j**

C(2)-Br(1)	1.889(3)
C(4)-Br(2)	1.896(3)
C(7)-N(1)	1.425(3)
C(16)-N(1)	1.347(4)
C(17)-N(3)	1.362(4)
N(1)-N(2)	1.361(3)
N(2)-N(3)	1.301(3
C(3)-C(2)-Br(1)	118.8(2)
C(1)-C(2)-Br(1)	118.4(2)
C(8)-C(7)-N(1)	119.1(3)
C(6)-C(7)-N(1)	119.8(3)
C(16)-N(1)-N(2)	110.6(2)
C(16)-N(1)-C(7)	128.2(2)
N(4)-C(9)-C(8)	121.8(3)

N(4)-C(9)-C(10)	116.7(2)
N(2)-N(1)-C(7)	121.2(2)
N(3)-N(2)-N(1)	106.6(2)
N(2)-N(3)-C(17)	109.8(2)
C(17)-C(16)-N(1)-N(2)	0.3(3)
C(17)-C(16)-N(1)-C(7)	-180.0(3)
C(8)-C(7)-N(1)-C(16)	-55.6(4)
C(6)-C(7)-N(1)-C(16)	122.3(3)
C(8)-C(7)-N(1)-N(2)	124.1(3)
C(6)-C(7)-N(1)-N(2)	-57.9(4)
C(16)-N(1)-N(2)-N(3)	-0.3(3)
C(7)-N(1)-N(2)-N(3)	180.0(2)
N(1)-N(2)-N(3)-C(17)	0.1(3)
C(1)-C(6)-C(7)-N(1)	-178.4(3)
N(1)-C(7)-C(8)-C(9)	179.1(3)
N(1)-C(16)-C(17)-N(3)	-0.2(3)
N(1)-C(16)-C(17)-C(18)	176.4(3)
N(3)-C(17)-C(18)-C(19)	168.4(3)
C(16)-C(17)-C(18)-C(19)	-7.8(5)
N(3)-C(17)-C(18)-C(23)	-10.3(4)

Table 9. Crystal structure refinement for compound **153 j**

Empirical formula	$C_{23}H_{12}N_4F_2Br_2$
Formula weight	542.19
Temperature/K	173(2)
Crystal system	Triclinic
Space group	P-1
a/Å	10.8328(13)
b/Å	12.5301(17)
c/Å	16.016(2)
α/°	73.091(5)

β/°	74.512(4)
γ/°	87.355(5)
Volume/Å^3	2003.2(5)
Z	4
ρ_{calc}g/cm^3	1.798
μ/mm^{-1}	4.084
F(000)	1064.0
Crystal size/mm^3	0.529 × 0.046 × 0.038
Radiation	MoKα (λ = 0.71073)
2Θ range for data collection/°	5.088 to 51
Index ranges	-13 ≤ h ≤ 13, -15 ≤ k ≤ 15, -19 ≤ l ≤ 19
Reflections collected	114164
Independent reflections	7441 [R_{int} = 0.0673, R_{sigma} = 0.0237]
Data/restraints/parameters	7441/0/578
Goodness-of-fit on F^2	1.077
Final R indexes [I>=2σ (I)]	R_1 = 0.0291, wR_2 = 0.0586
Final R indexes [all data]	R_1 = 0.0475, wR_2 = 0.0675
Largest diff. peak/hole / e Å^{-3}	0.68/-0.72

In the presence of the primary alcohol, compound **153 a–e,** were then investigated for the oxidation reaction to form aldehydes, as explained in the next section

2.6 The synthesis of quinoline-1,2,3-triazole carbaldehyde derivatives 154 a–b

The (1-(6,8-dibromo-2-(phenyl)quinoline-4-yl)-1*H*-(1,2,3-triazo-4-yl) methanol derivatives **153 a** and **d** were subjected to oxidation reaction conditions. Collins *et al*. [37] reported that Dipyridine-Chromium (vi) oxide in dichloromethane (DCM) can be used for the oxidation of primary and secondary alcohols. Corey *et al.*[38] prepared aldehydes through oxidation of primary alcohols using pyridinium chlorochromate (PCC), pyridine and hydrochloric acid. From the literature other oxidising agents such as Jones reagent [40] and the use of *y*-alumina supported by silver (Ag/Al_2O_3) [39] were also found effective. In this study, we opted for the use of Jones reagent (in

terms of availability), compound **153 a** and **d** in acetone at 0º for 1 h to afford compound **154 a–b** (**Scheme 35**).

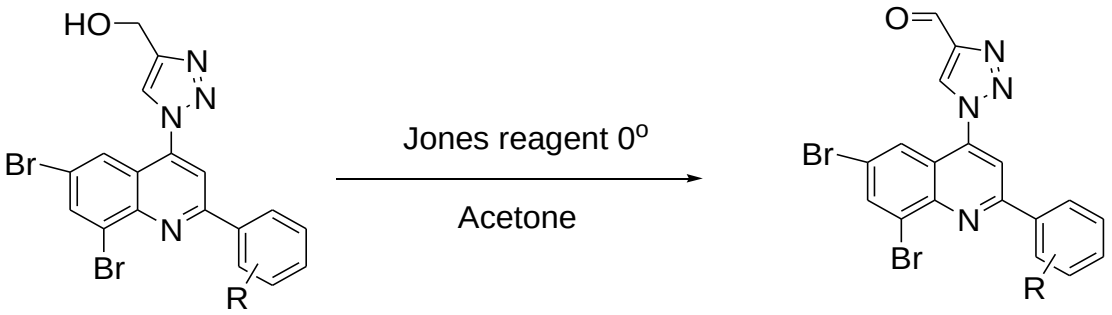

153 a,d **154 a-b**

Scheme 35. Oxidation reaction of a primary alcohol to an aldehyde using Jones reagent

Table 10. Substitution pattern, percentage yield and melting point values of carbaldehyde triazolyl quinoline derivatives **154 a–b**

Compound	R	Mp ºC	% Yield	Carbaldehyde proton
154 a	H	162-168	98	10.3
154 b	3-OMe	126-131	45	10.2

According to the ^{1}H NMR spectra of compounds **154 a–b** we noted the disappearance of the -C$\underline{H_2}$OH (c-H) signal from the previous ^{1}H NMR spectrum of compound **153 a–e** and an additional singlet (c-H) downfield at δ 10.3 ppm representing the presence of an aldehyde group (**Figure 47**). The ^{13}C NMR spectrum exhibits the chemical shift of the c-C from a higher field to a lower field at δ 207.2 ppm indicating the introduction of a carbonyl group (**Figure 48**). The 2D HMBC NMR spectrum (**Figure 50**) of compound **154 b** shows the correlation of the aldehyde (c-H) signal at δ 10.3 ppm and a-C at δ 147.9 ppm through a $^{3}J_{C\text{-}H}$ coupling (circled red). The FTIR of compound **154 a** (**Figure 49**), show the presence the carbonyl group showing a weak absorption peak at ν 1696 (cm^{-1}).

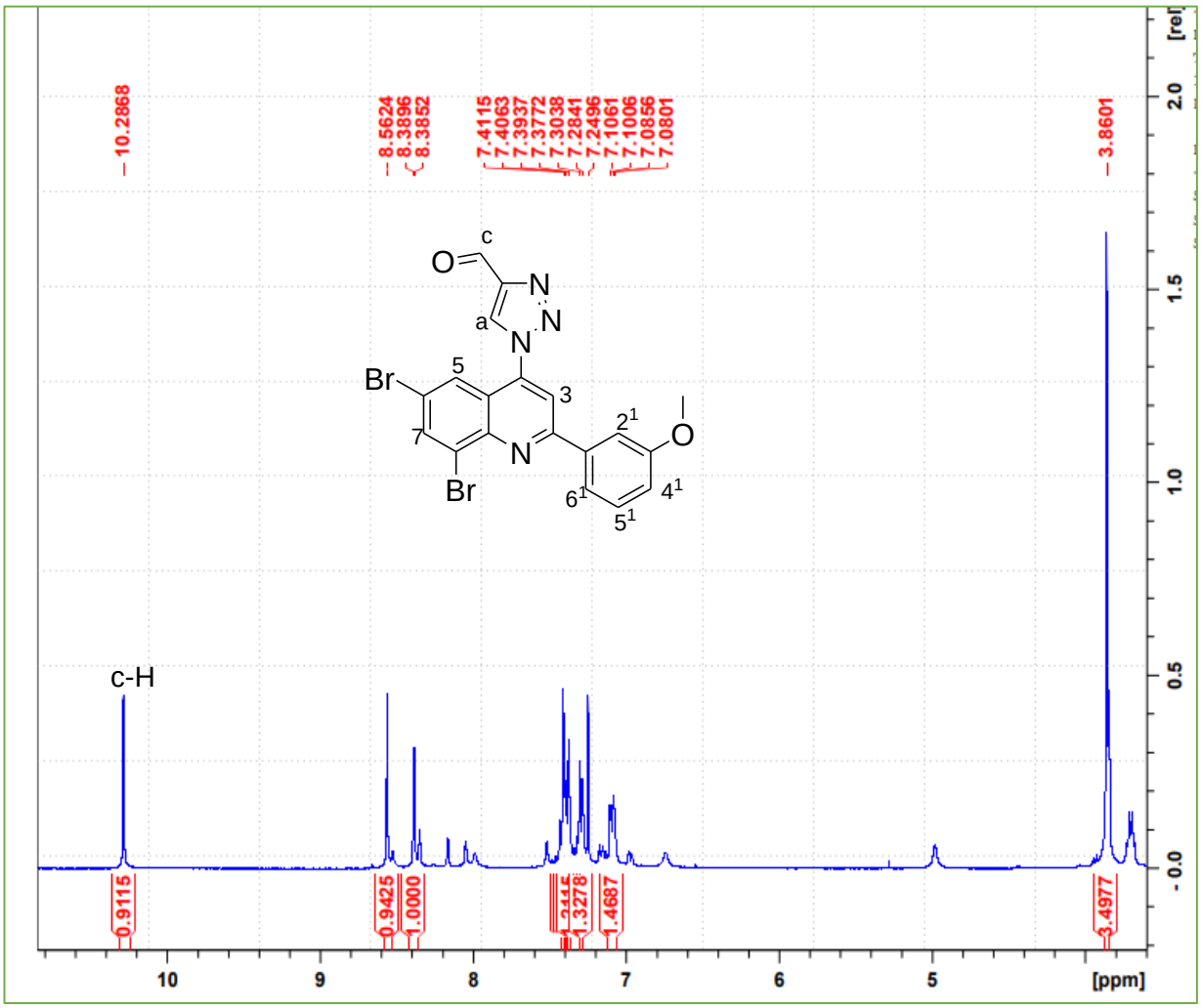

Figure 47. The ^{1}H NMR spectrum of compound **154 b**

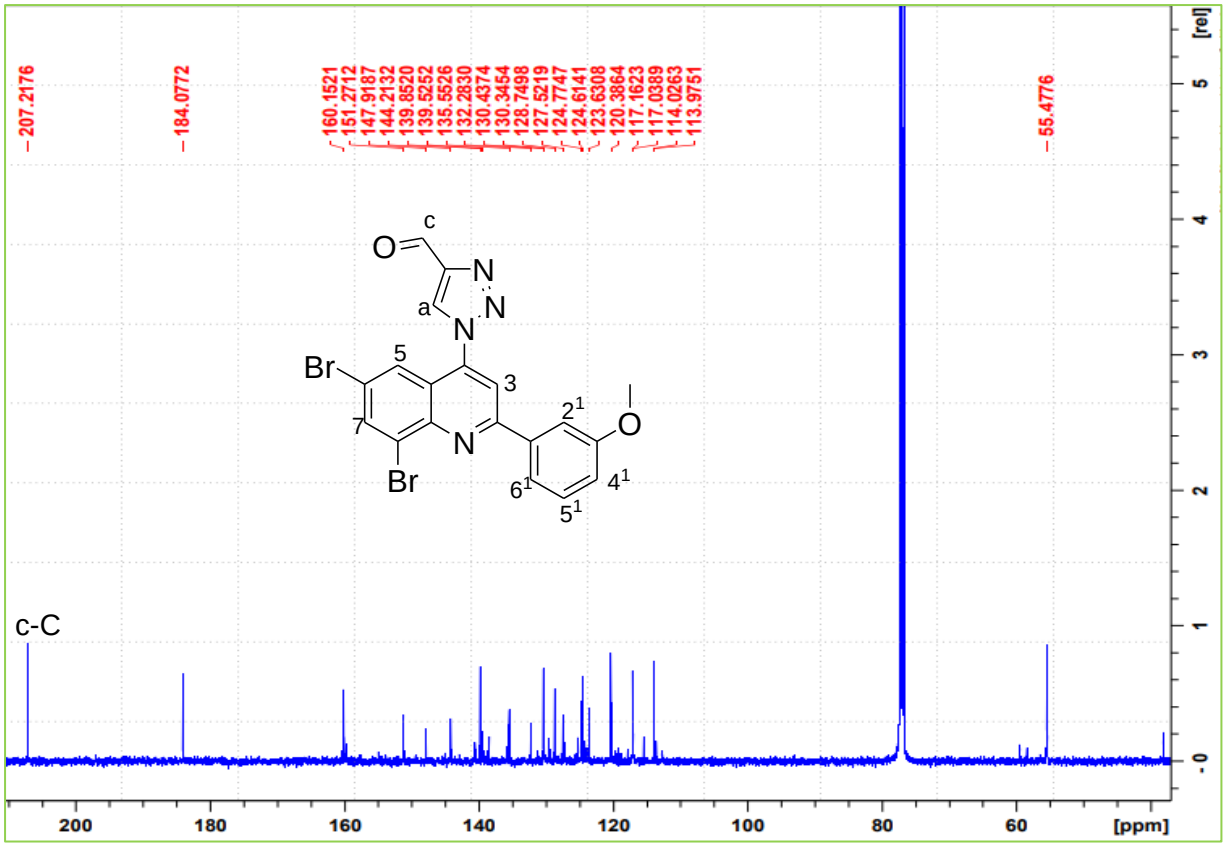

Figure 48. The ^{13}C NMR spectrum of compound **154 b**

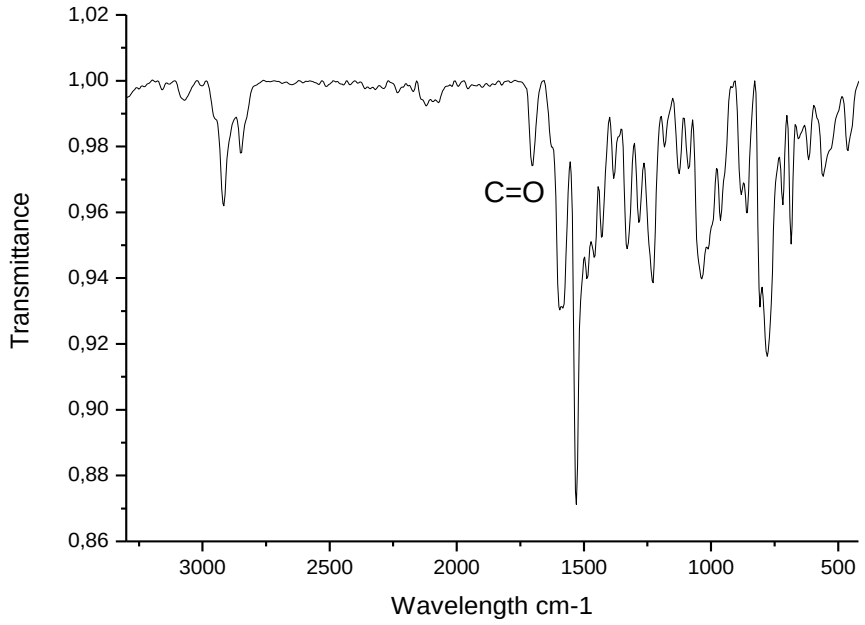

Figure 49. The IR spectrum of compound **154 a**

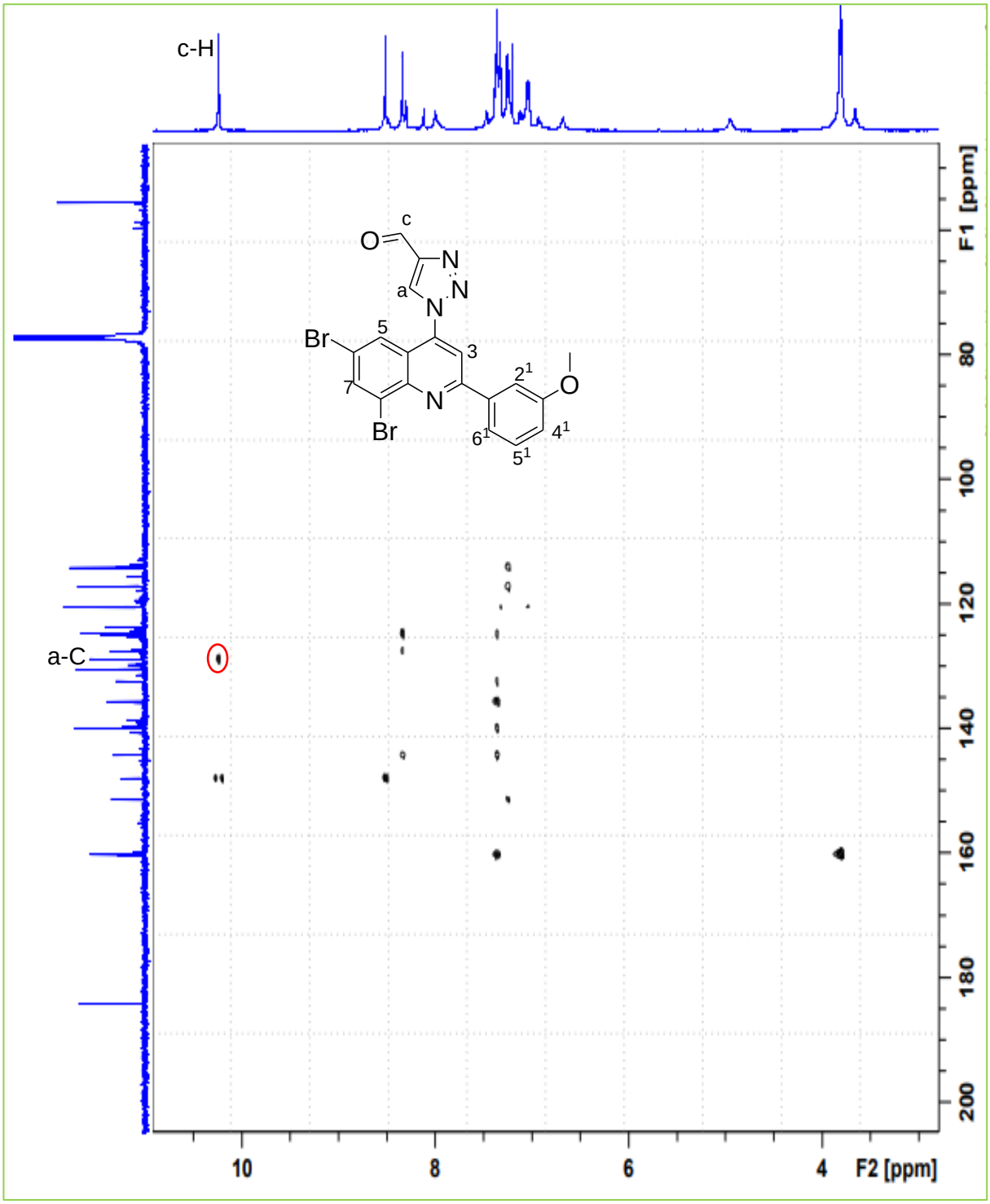

Figure 50. The 2D HMBC NMR spectrum of compound **154 b**

In the presence of the aldehyde derivatives **154 a–b**, we decided to investigate the condensation reaction in the presence of a nucleophile, as explained in the next section

2.7 Synthesis of Schiff base ligands 156 a-c

The Schiff bases compounds are reported to be synthesised in the presence of an aldehyde group and an amine group to produce H_2O as a by-product, as such the method is called condensation reaction [41]. The mechanism to form Schiff bases, is that the amine acts as a nucleophile which reacts with the aldehyde to form an intermediate in reaction called carbinol amine (an alcohol) and at the end of the reaction it undergoes dehydration to form (R_1-C=N-R_2) Schiff base ligand [42]. In this study we reacted compounds **155 a–b** and an amine in ethanol in the presence of a drying agent called $NaHCO_3$ (**Scheme 36**).

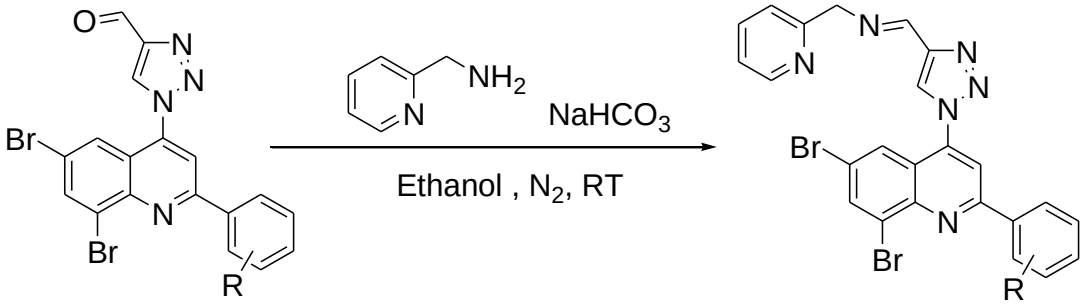

154 a-b **155 a-b**

Scheme 36. Synthesis of Schiff base ligands through condensation reaction

Table 11. Substitution pattern, percentage yield and melting point values of Schiff base-triazolyl quinoline derivatives **155 a-b**

Compound	R	Mp ºC	% Yield	Schiff base ligand proton
155 a	H	147-151	18	8.17
155 b	3-OMe	151-155	22	8.16

The ^{1}H NMR spectrum of **155 a–b** compounds are confirmed by the addition of signals at the aromatic region at δ 7.1-8.6 ppm compared to the precursor, including the Schiff base proton (c-H) at δ 8.2 ppm, the presence of the benzylic -C$\underline{H_2}$ (d-H) at δ 4.7 ppm and the disappearance of the aldehyde signal (**Figure 51**). The ^{13}C NMR

spectrums shows the disappearance of the carbonyl signal downfield, with the introduction of a carbon signal representing the -$\underline{C}H_2$ at around δ 47.7 ppm and additional signals in the aromatic region representing the carbons from the pyridine (**Figure 52**).

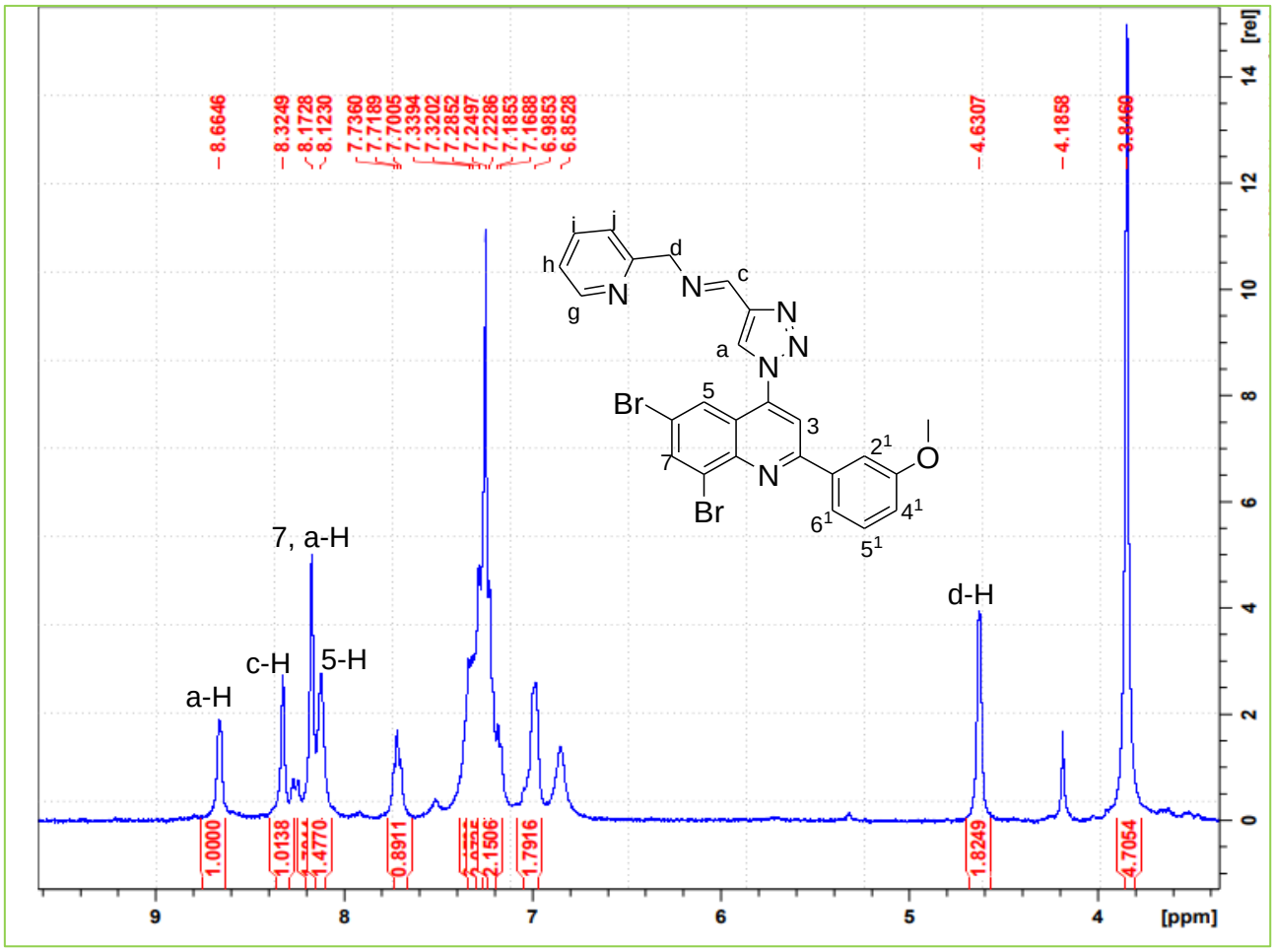

Figure 51. The ^{1}H NMR spectrum of compound **155 b**

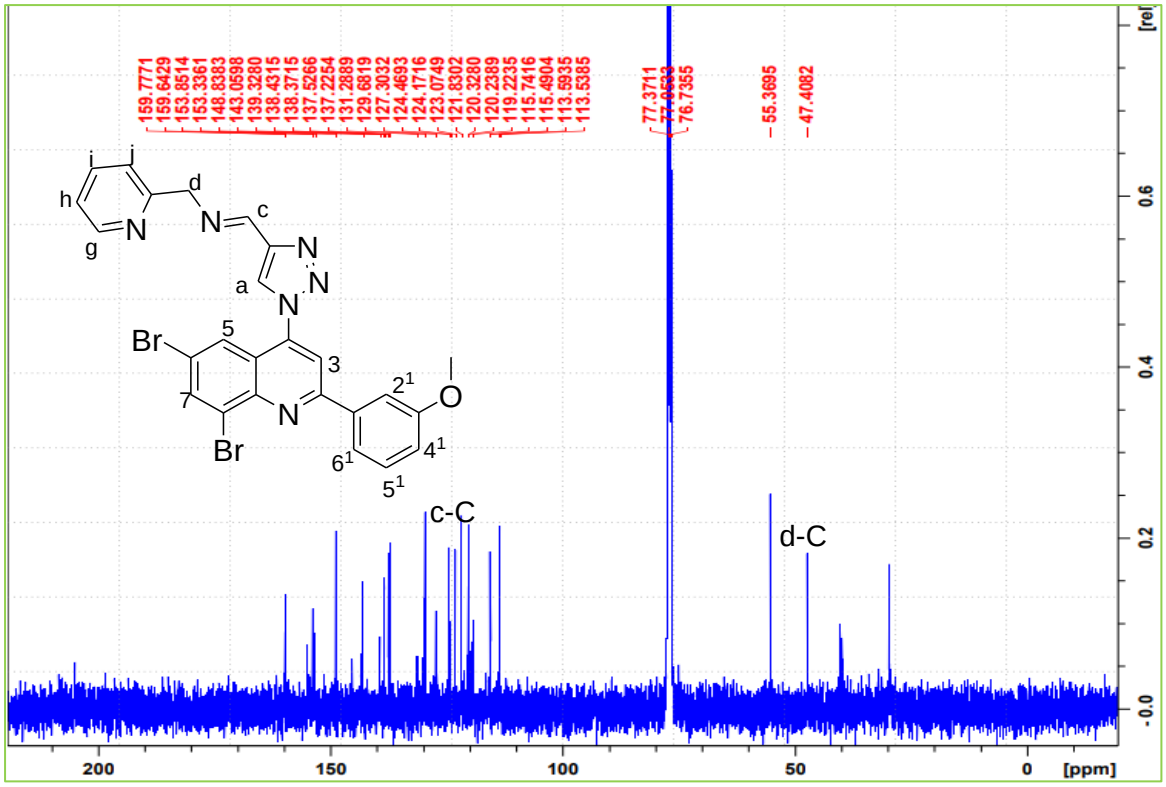

Figure 52. The ^{13}C NMR spectrum of compound **155 b**

The 2D HSQC-edited NMR spectrum (**Figure 53**) of compound **155 b** proves the presence of a -C$\underline{H_2}$ group in a form of a red peak (circled **red)** at ^{1}H NMR spectrum (δ 4.6 ppm) and ^{13}C NMR spectrum (δ 47.4 ppm). The 2D HMBC NMR spectrum (**Figure 54**) of compound **155 a** show the correlation of proton 7-H at δ 8.1 ppm and carbon 5-C at δ 123.8 ppm (circled **red**). It also shows the correlation of 5-H proton at δ 8.0 ppm with carbon 7-C δ 138.36 ppm (circled **green**) both through a $^{3}J_{C\text{-}H}$ coupling. The Schiff base proton at δ 8.33 ppm correlates with carbon a (a-C) at δ 137.5 ppm through a $^{3}J_{C\text{-}H}$ coupling. The Schiff base proton (c-H) at δ 8.33 ppm, the a-H proton at δ 8.2 ppm, the 5-H proton and the -CH_2 (d-H) signal correlate with quartet (carbon) at 143.2 ppm which is carbon b-C through a $^{2}J_{C\text{-}H}$, $^{2}J_{C\text{-}H}$, $^{6}J_{C\text{-}H}$, and $^{4}J_{C\text{-}H}$ coupling (all circled **blue**), respectively. The Schiff base proton (c-H), the a-H proton, the 5-H proton also correlates with a quartet at 119.1 ppm which is carbon 4-C located at the quinoline skeletal structure through a $^{5}J_{C\text{-}H}$, $^{3}J_{C\text{-}H}$, and $^{3}J_{C\text{-}H}$ (all circled **yellow**) coupling respectively.

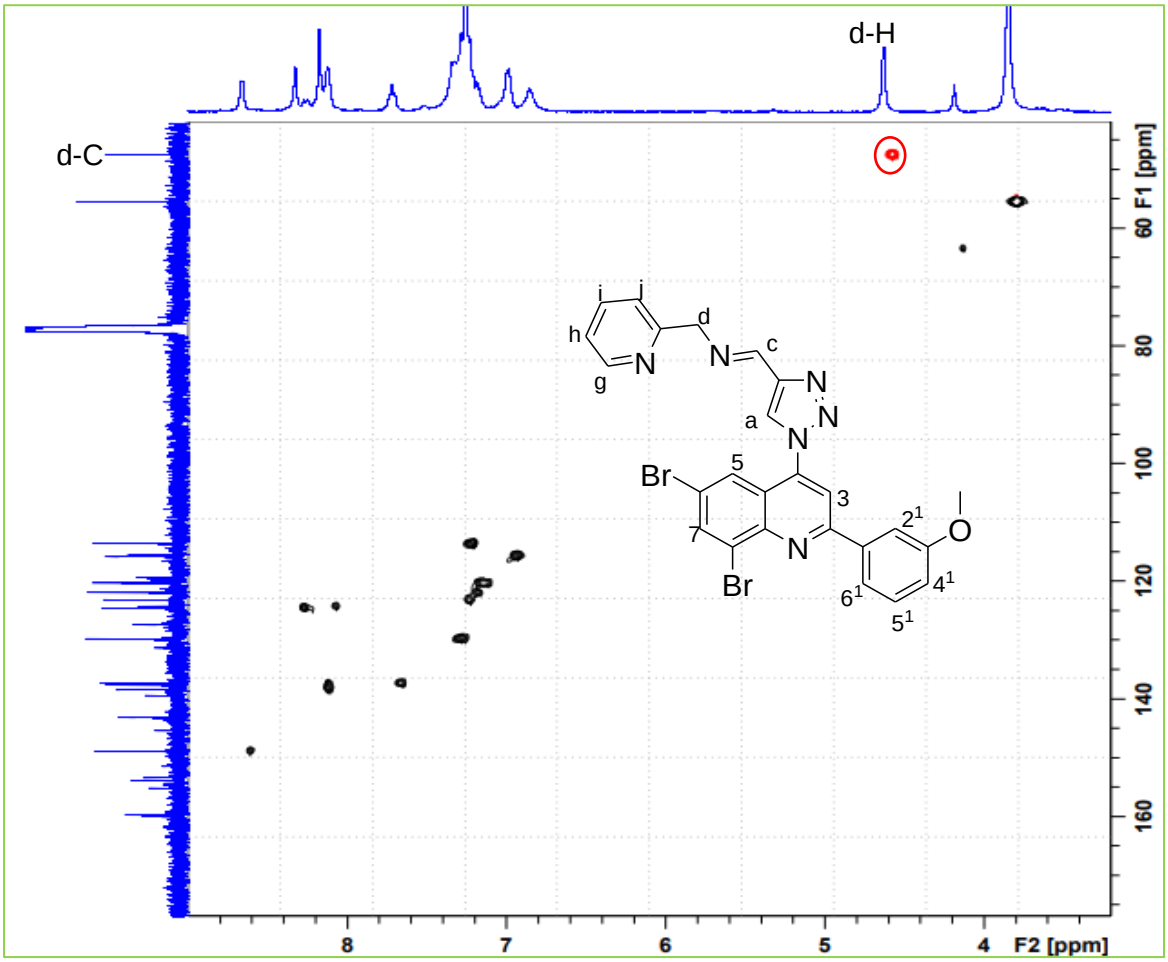

Figure 53. The 2D HSQC NMR spectrum of compound **155 b**

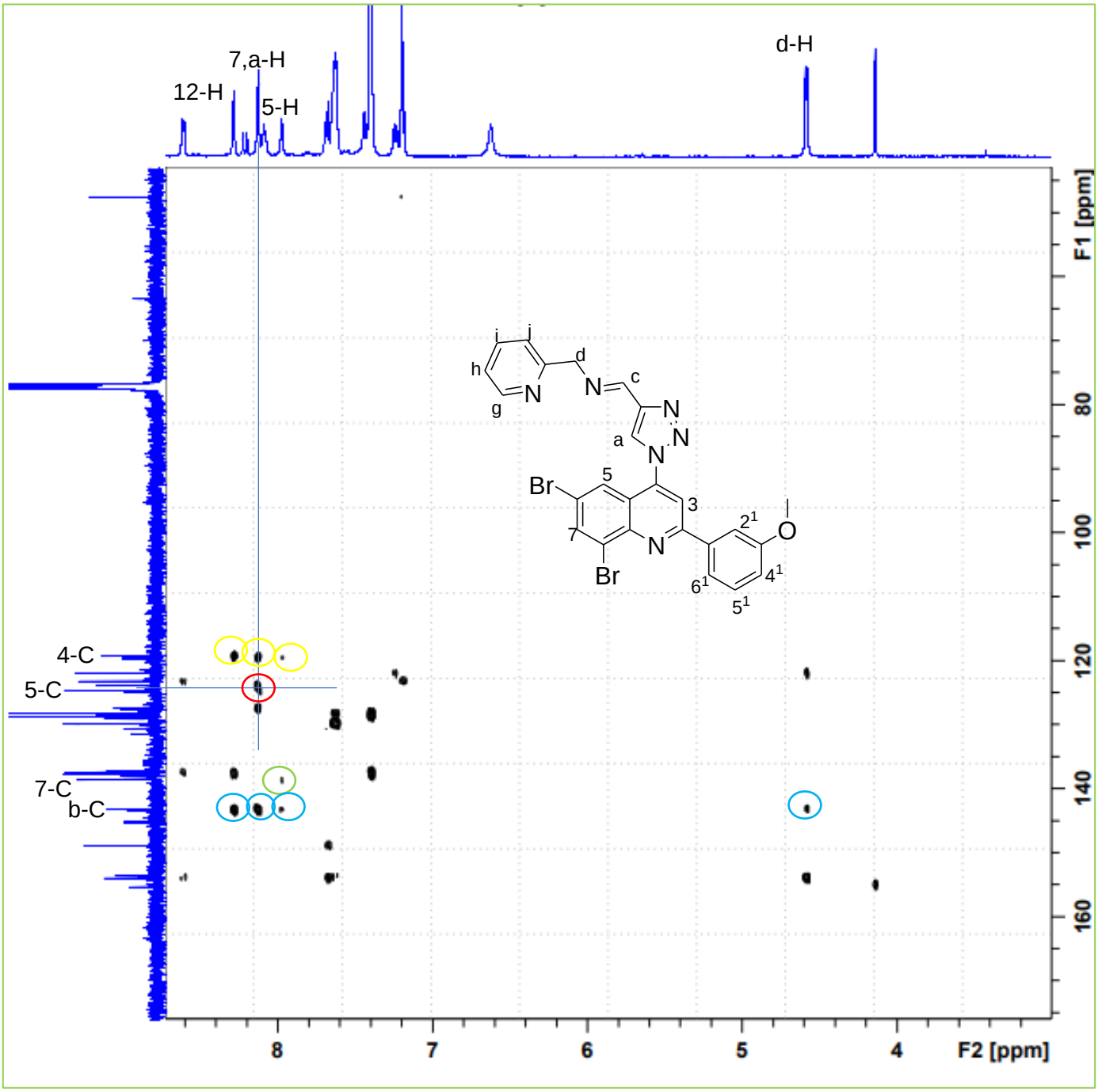

Figure 54. The 2D HMBC NMR spectrum of compound **155 a**

2.8 Metal coordination of Quinoline-3-fluorophenyl-triazolyl derivatives

The 3-fluorophenyl-triazolyl quinoline were subjected to metal coordination reaction. In this study we investigated metal introduction by using only ruthenium(II)*p*-cymene di-chloride dimer. Ruthenium containing complexes are identified to be substitutes for platinum complexes as promising anti-cancer drugs with reduced side effects [43]. On the ruthenium *p*-cymene *bis*-chloride, the arene is reported to enhance the uptake of the compound in the cell [43]. In this investigation we used two derivatives of 3-fluorophenyl triazolyl derivatives. To produce compounds **156 a–b** 1.0 equivalence ruthenium *p*-cymene di-chloride dimer was used in DCM, under argon atmosphere for 24 hours at room temperature.

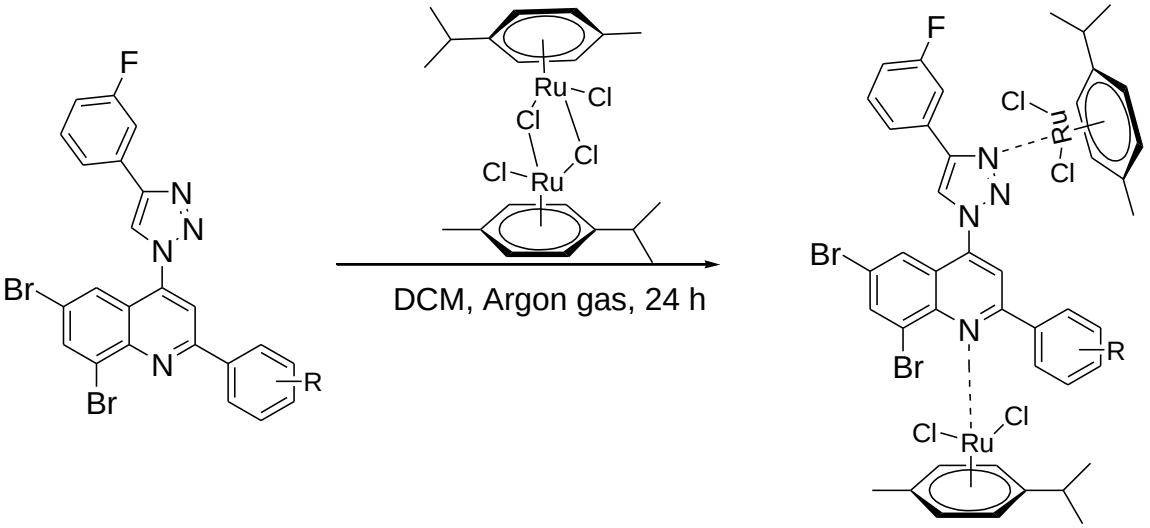

153 b, d **156 a-b**

Scheme 37. Synthesis of quinoline-triazolyl complexes through metal-coordination reaction

Table 12. Substitution pattern, percentage yield and melting point values of **156 a–b**

Compound	R	% Yield	Mp ºC
156a	4-CH_3	56	214-221
156b	3-OCH_3	73	165-170

The ^{1}H NMR spectrum (**Figure 55**) of the complexes (**156**) revealed additional signals at δ 1.25-2.91 ppm, which are proton signals indicating the presence of the methyl and isopropyl group, which are in para position to each other on the *p*-cymene. The signal at the up-field region at δ 1.25 ppm, δ 2.90 ppm and at δ 2.14 ppm indicate the methyl groups s-H, since they appear on the same environment (on the isopropyl group) emerging as a doublet (*J* = 6.4 Hz), proton signal r-H (as a multiplet) and the methyl group (as a singlet). The symmetrical proton signals p, n-H and k, m-H appear as doublets (*J* = 5.6 Hz) at δ 5.31 ppm and δ 5.45 ppm respectively. The ^{13}C NMR spectrum (**Figure 56**) of the complexes (**156**) also show additional signals at δ 17.93, 21.13, 29.59, 79.48 and 80.28 ppm indicating carbons located on the p-cymene, which are q-C, s-C, r-C, k, m-C and p, n-C respectively, this were identified by using the HSQC spectrum (**Figure 57**). The presence of a metal was further confirmed by using Coordination Induced Shifts (CIS) defined as an assignment of the changes occurring upon metal coordination based on NMR chemical shifts, obtained by subtracting chemical shift of the ligand from that of a complex (CIS = δcomplex-δligand) [44], where δ of protons and carbon correlating to those protons were used, as shown in **Table 13** and **14** below. The CIS data for complex **156 a** (**Table 13**) showed moderate result, for ^{1}H NMR CIS reveal that protons 7-H and -C$\underline{H_3}$ on the quinoline moiety showed a shift compared to the other protons slightly downfield with CIS values of δ 0.017 and 0.011 ppm respectively, thus concluding that the coordination occurred at the nitrogen on the quinoline moiety. The CIS data for the di-substituted complex **156 b** (**Table 14**) for ^{1}H NMR CIS show that protons of the 3-fluorophenyl were obscurely deshielded with CIS values of δ 0.006, 0.017 and 0.015 ppm for protons d-H, g, h-H, and a-H and also proton 4^{1}-H shifted slightly downfield with a CIS value of 0.047 ppm, thus concluding that the coordination occurred at both at the nitrogen on the quinoline moiety and at third nitrogen on the triazole moiety.

The ^{13}C CIS data is almost similar for all carbons with a CIS value of approximately -1.000 ppm

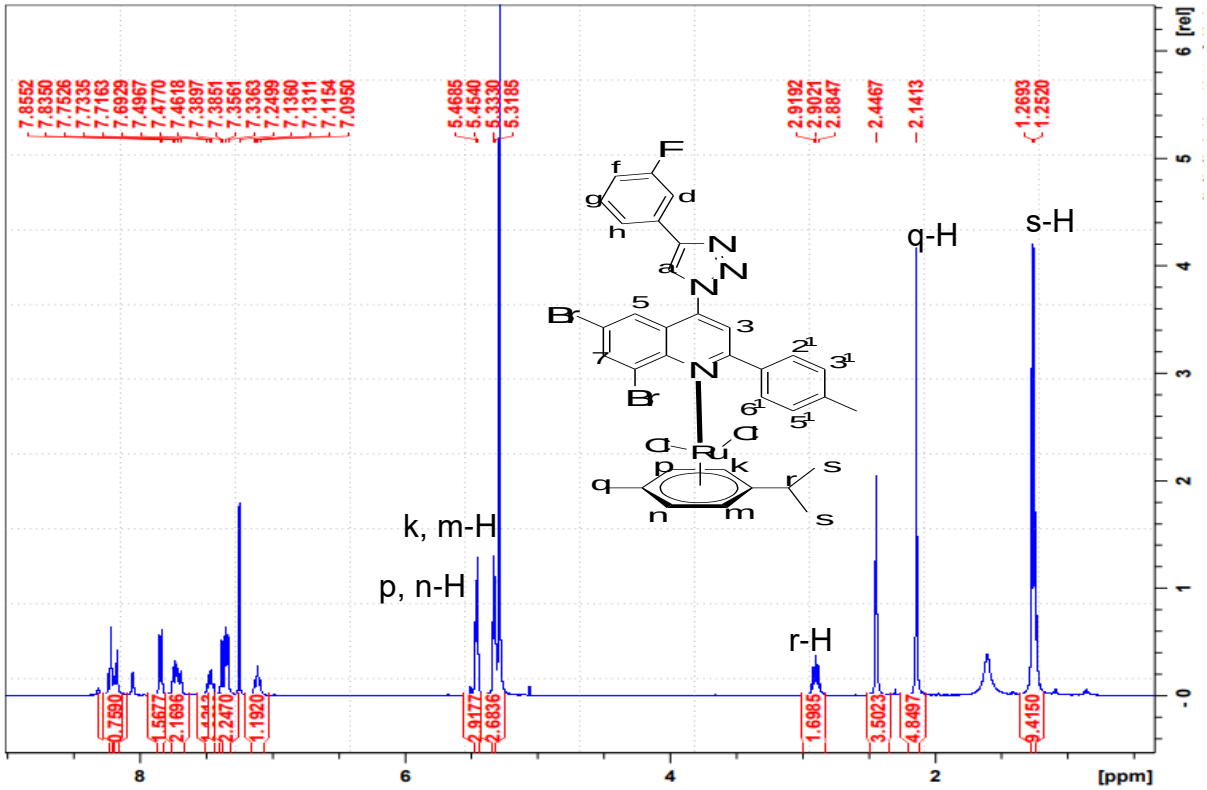

Figure 55. The ^{1}H NMR spectrum of compound **156 a**

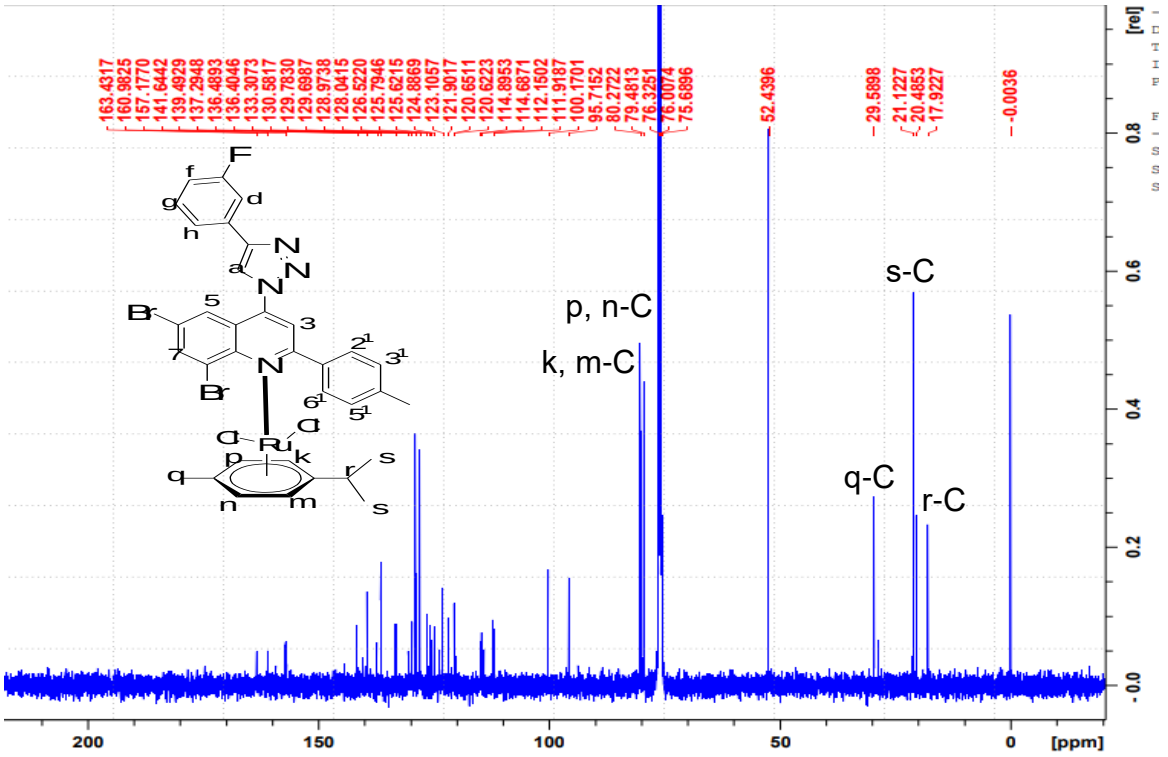

Figure 56. The ^{13}C NMR spectrum of compound **156 a**

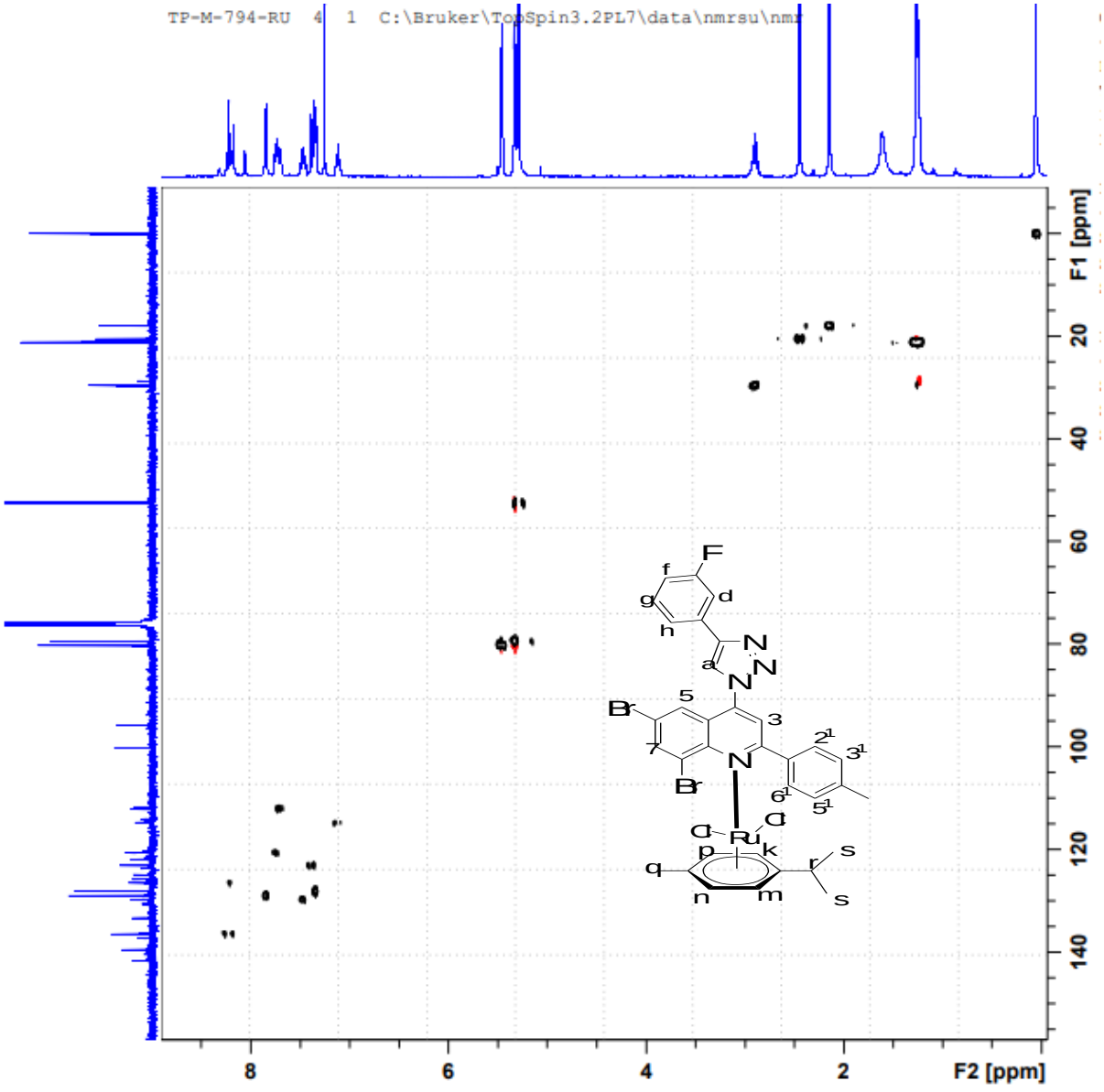

Figure 57. The 2D HSQC spectrum of compound **156 a**

Table 13. The proton-carbon coordination induced shifts (CIS) of compound **156 a**

	CIS = $\delta_{complexed}$ - δ_{free} for δ_H				**CIS = $\delta_{complexed}$ - δ_{free} for δ_C**		
#	Complexed	Free ligand	^{1}H CIS (ppm)	#	Complexed	Free ligand	^{13}C CIS (ppm)
-C<u>H</u>$_3$	2.466	2.449	0.017	-C<u>H</u>$_3$	20.49	21.49	-1.000
f-H	7.115	7.118	-0.003	f-C	114.79	115.79	-1.000
3^1,5^1-H	7.346	7.348	-0.002	3^1,5^1-C	128.04	129.05	-1.010
5-H	7.387	7.389	-0.002	5-C	123.11	124.11	-1.000
d-H	7.469	7.470	-0.001	d-C	129.74	130.74	-1.000
g, h-H	7.725	7.720	0.005	g, h-C	112.03 120.63	113.04 121.63	-1.010
2^1, 6^1-H	8.377	8.330	-0.002	2^1, 6^1-C	128.97	129.05	-0.080
7-H	8.175	8.164	0.011	7-C	136.29	137.49	-0.800
a-H	8.217	8.211	0.006	a-C	126.52	127.50	-0.980

Table 14. The proton-carbon coordination induced shifts (CIS) of compound **157 b**

	CIS = $\delta_{complexed}$ - δ_{free} for δ_H				**CIS = $\delta_{complexed}$ - δ_{free} for δ_C**		
#	Complexed	Free ligand	^{1}H CIS (ppm)	#	Complexed	Free ligand	^{13}C CIS (ppm)
-OC<u>H</u>$_3$	3.870	3.871	0.001	-OC<u>H</u>$_3$	54.44	54.43	0.010
4^1, f-H	7.105	7.058	0.047	4^1, f-C	115.02	116.12	-1.100
5^1, 2^1-H	7.325	7.323	0.002	5^1, 2^1-C	120.83 129.35	121.80 130.34	-0.970 -0.990
6^1-H	7.399	7.400	0.001	6^1-C	112.45	113.31	-0.860
d-H	7.448	7.442	0.006	d-C	129.80	130.81	-1.010
5-H	7.588	7.587	0.001	5-C	129.76	130.34	-0.580
g, h-H	7.702	7.685	0.017	g, h-C	112.33 126.22	113.18 127.22	-0.850 -1.000
a-H	8.213	8.198	0.015	a-C	123.34	124.34	-1.000
7-H	8.377	8.372	0.005	7-C	138.54	139.54	-1.000

2.9 The evaluation of quinoline-triazolyl derivatives for anti-cancer properties

Quinoline-triazole containing compounds have been reported to show biological activity against various cancer cell lines [45]. The selected synthesised triazole derivatives **153 f–j** and **153 m**, **o**, were tested against breast cancer using the MDA-MB-231 cell line. Curcumin which is known as a turmeric derivative, and an anti-breast cancer drug [46], is used as a positive control. The cells were treated with 25, 50 and 100 µM of each compound and were incubated for 24 hours to determine % cell viability and cytotoxicity, in comparison to curcumin. **Figure 58**, shows a dose-dependent effect of all the compounds on cell viability of MDA-MB cell line, especially compounds with the highest concentration. Compound **153 h** (3-fluoro-phenyl triazolyl quinoline derivative) shows a significant cytotoxicity effect with an IC_{50} of 40.7 µM compared to **153 m** (phenyl triazolyl quinoline derivative) with an IC_{50} of 48.8 µM in which both possess a methoxy group at *para*-position, as such this shows the inhibitory effect of the halogen on compound **153 h** has on the cells **(Table 15)**

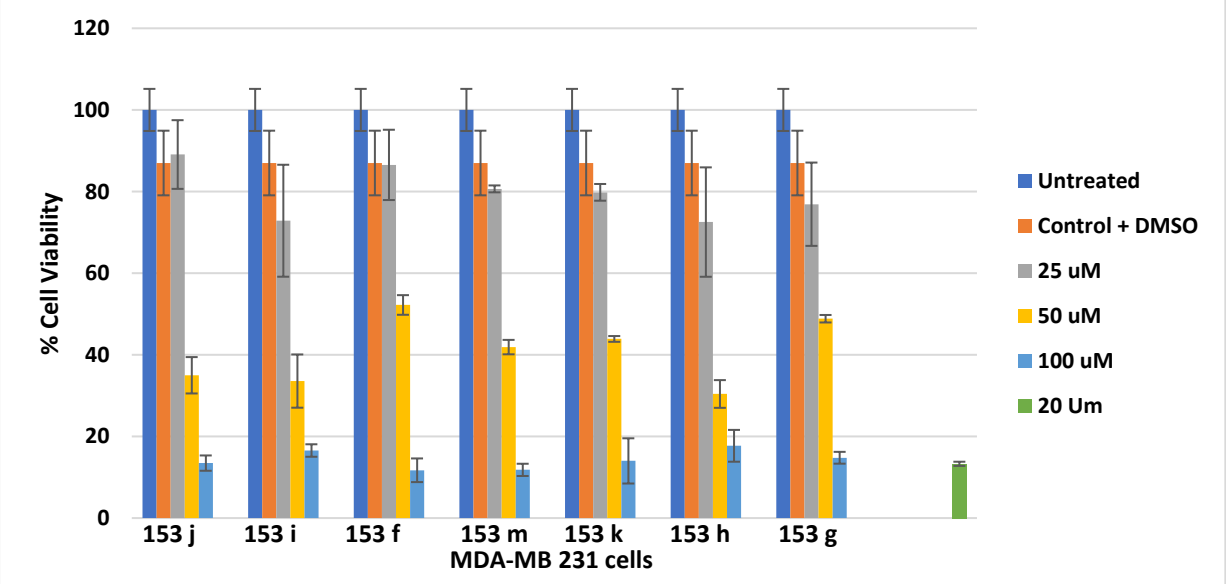

Figure 58. Cell viability analysis using the MTT cytotoxicity assay. Representative graph showing dose-dependent effect of compounds **153 f–j** and **153 m**, **o** on cell viability in MDA-MB 231 cells. Data points on graphs are mean values of triplicates.

Table 15. Cytotoxicity activity of synthesised compounds as IC_{50} (ug/ml) in MDA-MB 231

Compounds	IC_{50} values ± SD
153 j	46.79 ± 22.99
153 l	42.74 ± 15.73
153 f	50.79 ± 4.36
153 m	48.87 ± 6.13
153 k	49.14 ± 4.25
153 h	40.71 ± 20.77
153 g	50.91 ± 4.24

Molecular docking (*in silico*) was performed on the quinoline-triazoles against VEGFR-2 protein to determine plausible protein-drug interactions on a molecular level.

2.10 Inhibition of the VEGFR-2 against compounds 153 through molecular docking

VEGFR-2 is a vascular endothelial growth factor receptor, found in the family of receptor tyrosine kinase family and known to induce endothelial cell proliferation/ angiogenesis [46]. The VEGFR-2 is activated by the interaction with VEGFs which initiates phosphorylation that causes migration of cells [47]. Therefore, VEGFR-2 has become a great target to the drug development programme. As such, VEGFR-2 inhibitors are available to block the binding of growth factors to the receptors and stop the phosphorylation process [48]. For example, Sorafenib is reported to be a kinase inhibitor that attacks vascular endothelial growth factor receptors [49]. The triazolyl-quinoline derivatives **153 h**, **153 m**, **153 o**, **153 g**, **153 j**, **153 i** and **153 f** were biologically tested against the MDA-MB-231 cell line and were further studied computationally against VEFGR-2 tyrosine kinase through molecular docking using the PDB ID: 3EWH found from the protein data bank. The docking results of the compounds were compared to those of Sorafenib (as a positive control) against

VEFGR-2. The inhibitory and binding energy effects of the compounds and the standard against VEFGR-2 were revealed in **Table 16.** Compound **153 j** and **153 g** revealed significant inhibitory effects each having an inhibitory concentration of 0.10 µM and 0.80 µM, with -10.5 and -10.9 kcalmol binding energies respectively.

Table 16. Binding Energies with inhibitory concentration (Ki) value

Compound	ΔG (kcalmol)	Ki (µM)
153 f	-10.1	0.20
153 j	-10.5	0.10
153 g	-10.9	0.08
153 i	-9.8	0.52
153 h	-9.8	0.52
153 o	-9.4	1.15
153 m	-9.4	1.15
Sorafenib	-10.8	0.09

The docking results of compound **153 j** and **153 g**, **Figure 59 (A, B and C)**, showed binding modes of the compounds to the binding cavity of the ATP of the VEGFR-2 tyrosine kinase (using the PDB :3EWH). Compound **153 g** (**A**) revealed an alkyl interaction of the methyl group with LEU1019 and HIS 1026 residues. The VAL916 shows a π···δ, alkyl and π···alkyl interaction with the quinoline moiety and the bromine, where VAL916 serves as a gatekeeper [48]. The triazole moiety establishes a π···δ, π···π T-shaped and π···alkyl interactions with LEU 1035, PHE1047 and CYS1045, VAL889 residues respectively. Molecule **153 j** (**B**) also reveals π···δ, π···sulphur, π···π T-shaped, π···alkyl and halogen interactions with LEU 1035, PHE1047, CYS1045, VAL889 and ALA866 protein residues. The compounds have similar docking interactions to the standards interactions (**C**). All compounds showed an increase in the interaction with the ATP-active sites, with compound **153 g** exhibiting significant results.

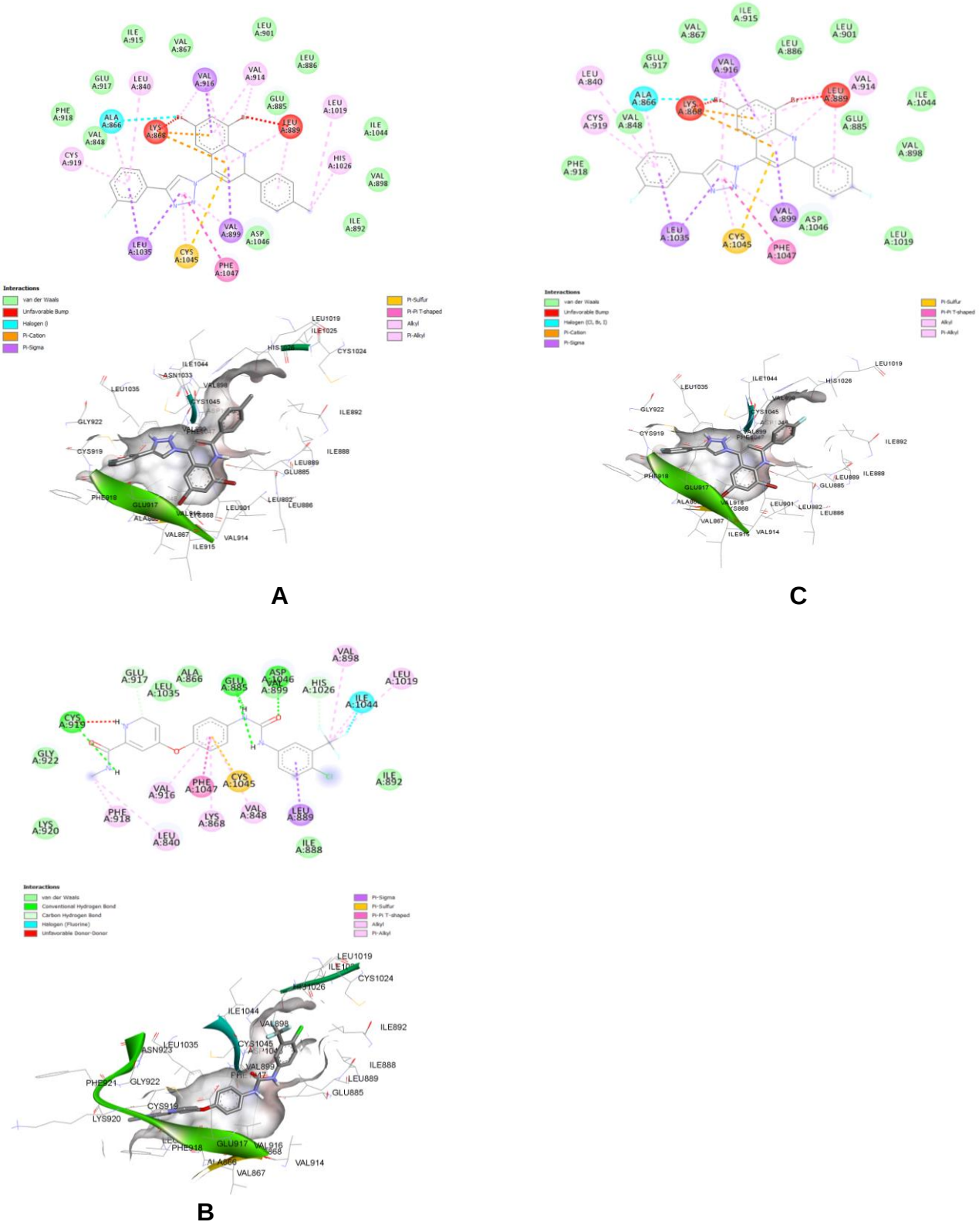

Figure 59. 2D interaction diagrams for the binding of VEGFR-2 with sorafenib (**C**), **153 g** (**A**) and **153 j** (**A**). Residues are annotated with their three-letter amino acid code

2.11 References

1. Bheemanapalli, L.N., Kaur, A., Arora, R., Akkinepally, R.R. and Javali, N.M., 2012. Synthesis, evaluation of 6, 8-dibromo-2-aryl-2, 3-dihydroquinolin-4 (1H)-ones in MCF-7 (breast cancer) cell lines and their docking studies. *Medicinal Chemistry Research*, *21*(8), 1741-1750.
2. Baker, L.J., Copp, B.R. and Rickard, C.E., 2001. 2′-Amino-3′, 5′-dibromoacetophenone. *Acta Crystallographica Section E: Structure Reports Online*, *57*(6), 538-o539
3. Lee, K.J., Cho, H.K. and Song, C.E., 2002. Bromination of activated arenes by Oxone® and sodium bromide. *Bulletin of the Korean Chemical Society*, *23*(5), 773-775.
4. Jalali, E., 2017. Regiospecific P-Bromination of Activated Aromatic Systems–Greener Approach.
5. Galabov, B., Nalbantova, D., Schleyer, P.V.R. and Schaefer III, H.F., 2016. Electrophilic aromatic substitution: New insights into an old class of reactions. *Accounts of Chemical Research*, *49*(6), 1191-1199.
6. Bevan, C.W.L., Hughes, E.D. and Ingold, C.K., 1953. Effects of Alkyl Groups in Nucleophilic Substitution. *Nature*, *171*(4346), 301-302.
7. Yerragunta, V., Kumaraswamy, T., Suman, D., Anusha, V., Patil, P. and Samhitha, T., 2013. A review on Chalcones and its importance. *PharmaTutor*, *1*(2), 54-59.
8. Chavan, B.B., Gadekar, A.S., Mehta, P.P., Vawhal, P.K., Kolsure, A.K. and Chabukswar, A.R., 2016. Synthesis & Medicinal Significance of Chalcones-A Review. *Asian Journal of Biomedical and Pharmaceutical Sciences*, *6*(56), p.01.
9. Rateb, N.M. and Zohdi, H.F., 2009. Atom-efficient, solvent-free, green synthesis of chalcones by grinding. *Synthetic Communications®*, *39*(15), 2789-2794.
10. Chtourou, M., Abdelhédi, R., Frikha, M.H. and Trabelsi, M., 2010. Solvent free synthesis of 1, 3-diaryl-2-propenones catalyzed by commercial acid-clays under ultrasound irradiation. *Ultrasonics Sonochemistry*, *17*(1), 246-249.

11. Kumar, A., Sharma, S., Tripathi, V.D. and Srivastava, S., 2010. Synthesis of chalcones and flavanones using Julia–Kocienski olefination. *Tetrahedron*, *66*(48), 9445-9449.
12. Rammohan, A., Reddy, J.S., Sravya, G., Rao, C.N. and Zyryanov, G.V., 2020. Chalcone synthesis, properties and medicinal applications: a review. *Environmental Chemistry Letters*, *18*(2), 433-458.
13. Zhuang, C., Zhang, W., Sheng, C., Zhang, W., Xing, C. and Miao, Z., 2017. Chalcone: a privileged structure in medicinal chemistry. *Chemical Reviews*, *117*(12), 7762-7810.
14. Burger, B., An Aldol Condensation to synthesize Chalcones, Penn State, https://sites.psu.edu.
15. Thungatha, L., Alapour, S. and Koorbanally, N.A., 2020. Synthesis, structural elucidation, intramolecular hydrogen bonding and DFT studies of quinoline-chalcone-chromene hybrids. *Organic Chemistry*, (part iii), 74-89.
16. Khoza, T.A., Maluleka, M.M., Mama, N. and Mphahlele, M.J., 2012. Synthesis and photophysical properties of 2-aryl-6, 8-bis (arylethenyl)-4-methoxyquinolines. *Molecules*, *17*(12), 14186-14204.
17. Donnelly, J.A. and Farrell, D.F., 1990. The chemistry of 2'-amino analogs of 2'-hydroxychalcone and its derivatives. *The Journal of Organic Chemistry*, *55*(6), 1757-1761.
18. Tökés, A.L. and Litkei, G., 1993. Schmidt Reaction on 2-Aryl-1, 2, 3, 4-tetrahydro-4-quinolone. *Synthetic communications*, *23*(7), 895-902.
19. Allen, J.M., Johnston, K.M., Jones, J.F. and Shotter, R.G., 1977. Friedel-crafts cyclisation—VI: Polyphosphoric acid-catalysed reactions of crotonophenones and chalcones. *Tetrahedron*, *33*(16), 2083-2087.
20. McMurry, J.E., 2014. *Organic chemistry*. Cengage Learning.
21. Fatiadi, A.J., 1986. The oxidation of organic compounds by active manganese dioxide. In *Organic syntheses by oxidation with metal compounds* (119-260). Springer, Boston, MA.
22. Zhai, L., Shukla, R. and Rathore, R., 2009. Oxidative C− C bond formation (Scholl reaction) with DDQ as an efficient and easily recyclable oxidant. *Organic Letters*, *11*(15), 3474-3477.

23. Singh, O.V. and Kapil, R.S., 1993. A new route to 2-aryl-4-quonolones via thallium (III) p-tolylsulphonate mediated oxidation of 2-aryl-1, 2, 3, 4-tetrahydro-4-quinolones. *Synthetic Communications*, *23*(3), 277-283.
24. Mphahlele, M.J. and Oyeyiola, F.A., 2011. Suzuki–Miyaura cross-coupling of 2-aryl-6, 8-dibromo-1, 2, 3, 4-tetrahydroquinolin-4-ones and subsequent dehydrogenation and oxidative aromatization of the resulting 2, 6, 8-triaryl-1, 2, 3, 4-tetrahydroquinolin-4-ones. *Tetrahedron*, *67*(36), 6819-6825.
25. Khanna, M.S., Singh, O.V., Garg, C.P. and Kapoor, R.P., 1992. Oxidation of flavanones using thallium (III) salts: a new route for the synthesis of flavones and isoflavones. *Journal of the Chemical Society, Perkin Transactions 1*, (19), 2565-2568.
26. Mphahlele, M.J., 2009. Molecular iodine—an expedient reagent for oxidative aromatization reactions of α, β-unsaturated cyclic compounds. *Molecules*, *14*(12), 5308-5322.
27. Luo, W., Lv, J.W., Wang, T., Zhang, Z.Y., Guo, H.Y., Song, Z.Y., Wang, C.J., Ma, J. and Chen, Y.P., 2020. Synthesis, in vitro and in vivo biological evaluation of novel graveolinine derivatives as potential anti-Alzheimer agents. *Bioorganic & Medicinal Chemistry*, *28*(1), p.115190.
28. Tsai, J.Y., Chang, C.S., Huang, Y.F., Chen, H.S., Lin, S.K., Wong, F.F., Huang, L.J. and Kuo, S.C., 2008. Investigation of amination in 4-chloro-2-phenylquinoline derivatives with amide solvents. *Tetrahedron*, *64*(51), 11751-11755.
29. (a) Mphahlele, M.J., 2010. Synthesis of 2-arylquinolin-4 (1H)-ones and their transformation to N-alkylated and O-alkylated derivatives. *Journal of Heterocyclic Chemistry*, *47*(1), 1-14.
30. Wolf, C., Tumambac, G.E. and Villalobos, C.N., 2003. Acid-mediated halogen exchange in heterocyclic arenes: A highly effective iodination method. *Synlett*, *2003*(12), 1801-1804.
31. Natarajan, S., Rajesh, K., Vijayakumar, V., Suresh, J. and Lakshman, P.N., 2009. 4-Azido-2-chloro-6-methylquinoline. *Acta Crystallographica Section E: Structure Reports Online*, *65*(4), o671-o671.
32. Malle, E., Stadlbauer, W., Ostermann, G., Hofmann, B., Leis, H.J. and Kostner, G.M., 1990. Synthesis of new 2-, 3-, and 4-substituted

azidoquinolines: Inhibitors of human blood platelet aggregation in vitro. *European Journal of Medicinal Chemistry*, *25*(2), 137-142.

33. Wang, Q.Y., Sheng, W.S., Sheng, S.R., Li, Y. and Cai, M.Z., 2014. Click chemistry on polymer support: Synthesis of 1-vinyl-and 1-allyl-1, 2, 3-triazoles via selenium linker. *Synthetic Communications*, *44*(1), 59-67.
34. Hong, V., Udit, A.K., Evans, R.A. and Finn, M.G., 2008. Electrochemically Protected Copper (I)-Catalyzed Azide–Alkyne Cycloaddition. *ChemBioChem*, *9*(9), 1481-1486.
35. Kuang, G.C., Michaels, H.A., Simmons, J.T., Clark, R.J. and Zhu, L., 2010. Chelation-assisted, copper (II)-acetate-accelerated azide− alkyne cycloaddition. *The Journal of Organic Chemistry*, *75*(19), 6540-6548.
36. Odlo, K., Hentzen, J., dit Chabert, J.F., Ducki, S., Gani, O.A., Sylte, I., Skrede, M., Flørenes, V.A. and Hansen, T.V., 2008. 1, 5-Disubstituted 1, 2, 3-triazoles as cis-restricted analogues of combretastatin A-4: Synthesis, molecular modeling and evaluation as cytotoxic agents and inhibitors of tubulin. *Bioorganic & Medicinal Chemistry*, *16*(9), 4829-4838.
37. Collins, J.C., Hess, W.W. and Frank, F.J., 1968. Dipyridine-chromium (VI) oxide oxidation of alcohols in dichloromethane. *Tetrahedron Letters*, *9*(30), 3363-3366.
38. Corey, E.J. and Suggs, J.W., 1975. Pyridinium chlorochromate. An efficient reagent for oxidation of primary and secondary alcohols to carbonyl compounds. *Tetrahedron Letters*, *16*(31), 2647-2650.
39. Shimizu, K.I., Sugino, K., Sawabe, K. and Satsuma, A., 2009. Oxidant-Free Dehydrogenation of Alcohols Heterogeneously Catalyzed by Cooperation of Silver Clusters and Acid–Base Sites on Alumina. *Chemistry–A European Journal*, *15*(10), 2341-2351.
40. Lou, J.D., Ma, Y.C., Gao, C.L. and Li, L., 2006. A new efficient oxidation of alcohols with Jones reagent supported on kieselguhr. *Synthesis and Reactivity in Inorganic, Metal-Organic and Nano-Metal Chemistry*, *36*(5), 381-383.
41. Alam, M.S., Choi, J.H. and Lee, D.U., 2012. Synthesis of novel Schiff base analogues of 4-amino-1, 5-dimethyl-2-phenylpyrazol-3-one and their evaluation for antioxidant and anti-inflammatory activity. *Bioorganic & Medicinal Chemistry*, *20*(13), 4103-4108.

42. Xavier, A. and Srividhya, N., 2014. Synthesis and study of Schiff base ligands. *IOSR Journal of Applied Chemistry*, *7*(11), 06-15.
43. Zhao, J.W., Wu, Z.H., Guo, J.W., Huang, M.J., You, Y.Z., Liu, H.M. and Huang, L.H., 2019. Synthesis and anti-gastric cancer activity evaluation of novel triazole nucleobase analogues containing steroidal/coumarin/quinoline moieties. *European Journal of Medicinal Chemistry*, *181*, 111520.
44. Orellana, G., Alvarez Ibarra, C. and Santoro, J., 1988. Hydrogen-1 and carbon-13 NMR coordination-induced shifts in a series of tris (. alpha.-diimine) ruthenium (II) complexes containing pyridine, pyrazine, and thiazole moieties. *Inorganic Chemistry*, *27*(6), 1025-1030.
45. Wang, Y., Yu, J., Cui, R., Lin, J. and Ding, X., 2016. Curcumin in treating breast cancer: A review. *Journal of Laboratory Automation*, *21*(6), 723-731.
46. Roth, G.S. and Decaens, T., 2017. Liver immunotolerance and hepatocellular carcinoma: Patho-physiological mechanisms and therapeutic perspectives. *European Journal of Cancer*, *87*, 101-112.
47. Jackson, R.C., 1997, April. Contributions of protein structure-based drug design to cancer chemotherapy. In *Seminars in Oncology* (Vol. 24, No. 2164-172).
48. Modi, S.J. and Kulkarni, V.M., 2019. Vascular endothelial growth factor receptor (VEGFR-2)/KDR inhibitors: medicinal chemistry perspective. *Medicine in Drug Discovery*, *2*, p100009.
49. Dao, T.V., Tran, T.V., Lebœuf, C., El-Bouchtaoui, M., Verine, J., Janin, A. and Bousquet, G., 2016. Sorafenib Acts through VEGFR-2 Inhibition in a Metastatic Clear-Cell Sarcoma of the Kidney. *Journal of Cancer Therapy*, *7*(7), 487-493.

CHAPTER 3

Conclusion

The reactivity of 2-amino chalcones were investigated and were found to be applicable to annulation reaction to construct a six-membered ring through an acid catalysed reaction to afford a 2-substituted 2,3-dihydroquinolone. The substituted 2,3-dihydroquinolones underwent an oxidative rearrangement using TTN to form 2-subtituted- quinolones (α, β carbonyl derivatives) without any traces of its tautomeric structure 2-substituted quinolinol. The ketone *α, β* unsaturated derivatives experienced a nucleophilic attack at the carbonyl with $POCl_3$, to produce a 4-chloro-quinoline through an *α*-conjugative system and a N-H proton cleavage. The 4-chloro-quinolines were identified to carry an electropositive carbon at the 4^{th} position to give its bond to the chlorine, making it vulnerable to nucleophilic substitution with sodium azide to form a stable 4-azido-quinoline derivatives, later the $N=N^+=N^-$ facilitated cycloaddition reaction with acetylene derivatives to form 4-triazolyl-quinolines, which were confirmed further by X-ray diffraction analysis. The triazolyl derivative formed from an acetylene derivative (propargyl alcohol) go through oxidative reaction (resulting in the loss of the OH) resulting in the production of a carbaldehyde-triazolyl quinoline, which in the presence of 2-picolyl amine (through condensation reaction) produced Schiff base ligands, in which due to the typre of work-up we chose low yields of up to 22 % were obtained . The 4-triazolyl-quinoline derivatives (as ligands) were then subjected to coordination in the presence of ruthenium(II) reagent to produce complexes. Our analysis suggest that coordination occurred on the nitrogen of the quinoline moiety and on the nitrogen of the triazole group, this is supported the CIS calculation in the range of δ (-0.003-0.047) ppm for ^1H NMR and δ (-0.058-0.010 ppm) for ^{13}C NMR, given 1:1 reaction ratio of the ruthenium p-cymene to the quinoline-triazolyl derivative. Molecular docking was studied on quinoline-triazole compounds against VEGFR-2 tyrosine kinase in which compounds **153 g** and **153 j** showed significant interaction results with a good binding energy of -10.9 and 10.5 k cal mol, whereas compound **153 h** showed good results compared to **153 g** on in-vitro study against a breast cancer line (MDA-MB 231) with MIC values of 40.71 ug/ml and 50.91 ug/ml**.** Therefore, this outcome can give good direction towards anticancer studies.

In future, the Schiff base ligands will be synthesised in higher yields by modifying the procedure which was used and produce more Schiff base derivatives by introducing amine derivatives. To further do a study on metal coordination of quinoline triazole containing compounds and Schiff base ligands. The binding energy of these compounds will be obtained through computational chemistry and the in-vitro studies will be done to compare the presence of a metal on complexes to their ligands. Lastly, to do an antimicrobial biological investigation against compounds that showed a good binding energy.

CHAPTER 4

Experimental

General

Chemical reagents were purchased from the Sigma Aldrich and Merck Company and were used without further purification. The melting point data was acquired from Stuart SMP10 Digital melting point (United Kingdoms) apparatus. The infrared (IR) spectra were recorded using the Bruker FTIR FT-IR spectrometer equipped with ATR (Bruker optics, USA). The ^{1}H and ^{13}C nuclear magnetic resonance were obtained using the 400 MHz Bruker spectrometer (Bruker optics, USA) and displaying chemical shifts in parts per million. The proton (^{1}H) and carbon (^{13}C) spectra were obtained as deuterated chloroform ($CDCl_3$) solutions, with chloroform resonating 7.25 and 77.0 ppm respectively. High Resolution mass spectrometry analysis was obtained on AB SCIEX X500 QTOF system (SCIEX, USA) in positive and negative ESI mode.

4.1 Halogenation of the 2-aminoacetophenone

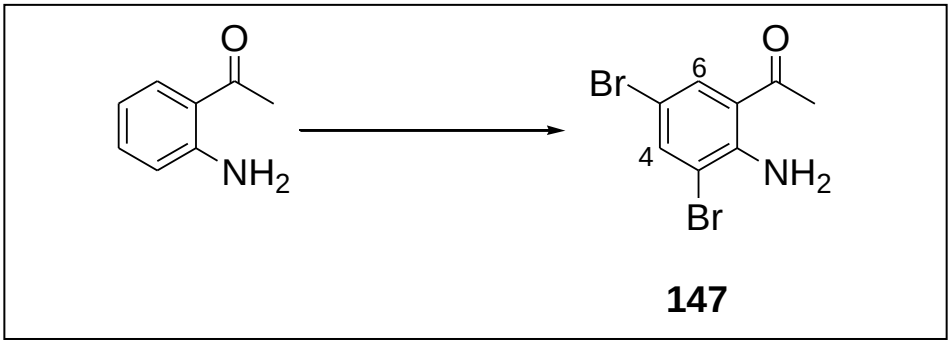

147

A stirred mixture of 2-aminoacetophenone (5 g, 36.99 mmol) and *N*-bromosuccinimide (13.17 g, 73.98 mmol) in acetonitrile 100 ml was stirred at 0 ^{0}C for 3h. The mixture was then filtered, and the precipitates were recrystallized by using hexane to afford (**147**) as a yellow solid (7.91 g, 73.07 %), mp (126-129) ^{0}C, ν_{max} 3401, 3295, 1647, 1602, 1561, 1513, 1443, 1435, 1349, 1231, 1068, 954, 868, 742, 672, 681, 628, 460, 3 δ_H (400 MHz, $CDCl_3$, ppm) 2.57 (3H, s, -COC<u>H</u>$_3$), 6.93 (2H, br s, -N<u>H</u>$_2$) 7.68 (1H, d, *J* = 2.4 Hz, 4-H), 7.79 (1H, d, *J* = 2.4 Hz, 6-H), δ_C (400 MHz,

$CDCl_3$, ppm) 27.96, 105.77, 111.74, 119.60, 133.66, 139.21, 146.26, 199.07 $C_7H_8{}^{81}Br{}^{81}BrNO^+$ requires 295.8853, found 295.1950

4.2 Synthesis of (E)-2-Amino-3,5-dibromochalcone derivatives

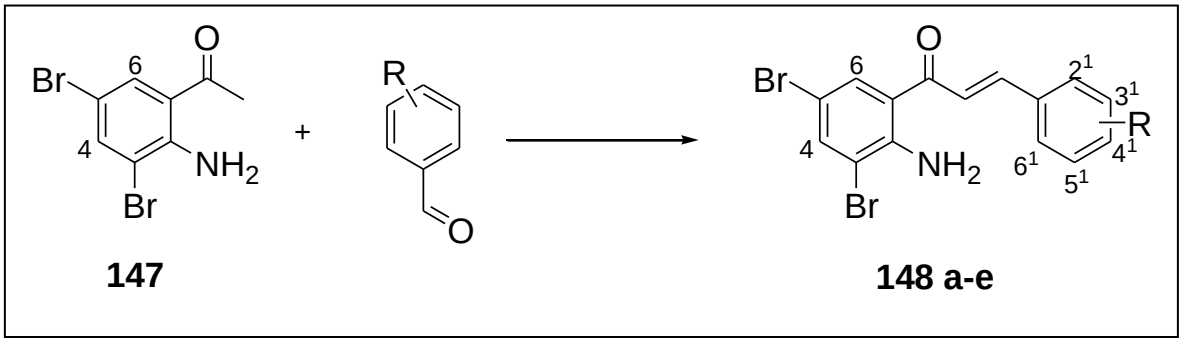

A stirred mixture of 2-amino-3,5-dibromoacetophenone (**147**) (1 mmol), benzaldehyde (1.2 equiv.) and potassium hydroxide (0.67 g) in 100 ml ethanol, was stirred overnight at room temperature. The mixture was stirred in ice and the resultant precipitate was filtered to (**148 a–e**)

4.2.1 *(E)*-1-(2-amino-3,5-dibromophenyl)-3-phenylprop-2-en-1-one (148 a)

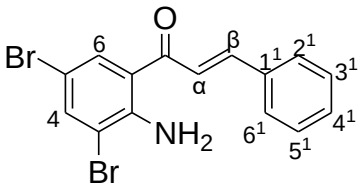

A stirred mixture of 2-amino-3,5-dibromoacetophenone (**147**) (4 g, 13.65 mmol), benzaldehyde (1.74 g, 16.39 mmol) and potassium hydroxide (0.67 g) in 100 ml ethanol, was stirred to afford **148 a** as a yellow solid (5.10 g, 98%), mp 107-110 ^{0}C (120-123 ^{0}C)[1]; ν_{max} 3415, 3309, 3252, 2171, 1982, 1686, 1604, 1572, 1540, 1498, 1416, 1359, 1269, 1187, 1121, 1072, 949, 867, 777, 728, 687, 581, 499, 441, δ_H (400 MHz, $CDCl_3$, ppm) 6.92 (2H, br s, -N$\underline{H_2}$), 7.42 (3H, d, *J* = 8.8 Hz, 3^1, 4^1 ,5^1-H), 7.47 (1H, d, *J* = 15.2 Hz, β-H), 7.63 (2H, d, *J* = 8.4 Hz, 2^1, 6^1-H), 7.72 (1H, d, *J* = 2.0 Hz, 4-H), 7.73 (1H, d, *J* = 15.2 Hz, α-H), 7.92 (1H, d, *J* = 2.0 Hz, 6-H), δ_C (100 MHz, $CDCl_3$, ppm) 106.67, 111.89, 120.48, 122.29, 129.27, 129.65, 132.51, 133.17,

136.54, 139.21, 143.23, 146.93, 189.80, HRMS $C_{15}H_{11}{}^{79}Br^{81}BrNO^{+}$ requires 383.9166, found, 383.2557

4.2.2 *(E)*-1-(2-amino-3,5-dibromophenyl)-3-p-tolylprop-2-en-1-one (148 b)

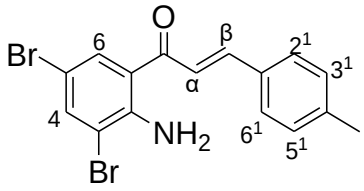

A stirred mixture of 2-amino-3,5-dibromoacetophenone (**147**) (4 g, 13.65 mmol), p-tolylbenzaldehyde (1.97 g, 16.39 mmol) and potassium hydroxide (0.67 g) in 100 ml ethanol, was stirred to afford **148 b** as a yellow solid (4.80 g, 89%), mp 97-100 ^{0}C; ν_{max} 3457, 3293, 3052, 1637, 1587, 1507, 1416, 1335, 1293, 1170, 1015, 982, 850, 761, 678, 532, 490, 449, δ_H (400 MHz, $CDCl_3$, ppm) 2.41 (3H, s, Ar- CH_3), 6. 93 (2H, br s, -N$\underline{H_2}$), 7.22 (2H, d, J = 8.0 Hz , 3^1, 5^1-H), 7.46 (1H, d, *J* = 15.2 Hz, β-H), 7.55 (2H, d, *J* = 8 Hz, 2^1, 6^1-H), 7.70 (1H, d, *J* = 2.4 Hz, 4-H), 7.76 (1H, d, *J* = 15.2 Hz, α-H), 7.92 (1H, d, *J* = 2.0 Hz, 6-H), δ_C (100 MHz, $CDCl_3$, ppm) 18.45, 58.51, 106.09, 111.84, 120.88, 120.89, 128.59, 129.77, 131.98, 132.58, 139.00, 141.31, 144.93, 146.83, 190.310 HRMS $C_{16}H_{13}{}^{81}Br^{81}BrNO^{+}$ requires 398.9364, found 398.2427

4.2.3 *(E)*-1-(2-amino-3,5-dibromophenyl)-3-(4-methoxyphenyl)prop-2-en-1-one (148 c)

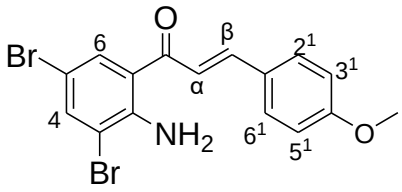

A stirred mixture of 2-amino-3,5-dibromoacetophenone (**147**) (4 g, 13.65 mmol), 4-methoxybenzaldehyde (2.23 g, 16.39 mmol) and potassium hydroxide (0.67 g) in 100 ml ethanol, was stirred to afford **148 c** as a yellow solid (5.41 g, 96%), mp 110-116 ^{0}C(139-141 ^{0}C)[1]; ν_{max} 3418, 3288, 3071 1637, 1597, 1507, 1425, 1351, 1293, 1260, 1195, 1163, 1121, 1015, 974, 876, 761, 687, 605, 523, δ_H (400 MHz, $CDCl_3$, ppm) 3.85 (3H, s, -OC$\underline{H_3}$), 6. 89 (2H, br s, -N$\underline{H_2}$), 6.94 (2H, d, *J* = 8.8 Hz, 3^1, 5^1-H), 7.38 (1H, d, *J* = 15.2 Hz, β-H), 7.61 (2H, d, *J* = 8.8 Hz, 2^1, 6^1-H), 7.69 (1H, d, *J* = 2 Hz, 4-H), 7.76 (1H, d, *J* = 15.2 Hz, α-H), 7.91 (1H, d, *J* = 2.0 Hz, 6-H), δ_C (100 MHz, $CDCl_3$, ppm) 55.43, 105.87, 111.76, 114.42, 119.50, 119.62, 121.00, 130.33, 132.46,

133.68, 139.24, 144.66, 146.28, 199.10 HRMS $C_{16}H_{13}{}^{81}Br^{81}BrNO_2^+$ requires 413.9313, found 413.3253

4.2.4 *(E)*-1-(2-amino-3,5-dibromophenyl)-3-(3-methoxyphenylprop-2-en-1-one (148 d)

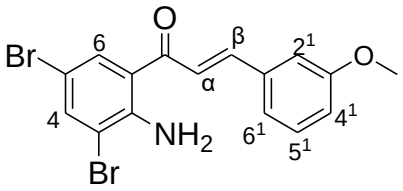

A stirred mixture of 2-amino-3,5-dibromoacetophenone (**147**) (4 g, 13.65 mmol), 4-chlorobenzaldehyde (2.23 g, 16.39 mmol) and potassium hydroxide (0.67 g) in 100 ml ethanol, was stirred to afford **148 d** as a yellow solid (5.21 g, 90 %), mp 180-184 ^{0}C, ν_{max} 3481, 3293, 2957, 1646, 1580, 1514, 1482, 1310, 1253, 1179, 1043, 991, 892, 843, 793, 687, 581, 523, 482, 449, δ_H (400 MHz, $CDCl_3$) 3.86 (3H, s, -OC<u>H</u>$_3$), 6.92 (2H, br s, -N<u>H</u>$_2$), 6.96 (1H, dd, *J* = 5.6 Hz, *J* = 8.0 Hz, 4^1-H), 7.13 (1H, m, 5^1-H), 7.23 (1H, d, *J* = 9.6 Hz, 2^1-H), 7.34 (1H, t, *J* = 8.0 Hz, 6^1-H), 7.48 (1H, d, *J* = 15.2 Hz, β-H), 7.73 (1H, d. *J* = 15.2 Hz, α-H), 7.90 (1H, d, *J* = 2.0 Hz, 4-H) 7.93 (1H, d, *J* = 2.0 Hz, 6-H), δ_C (100 MHz, $CDCl_3$, ppm) 55.45, 87.66, 106.91, 113.57, 116.31, 119.88, 121.18, 122.10, 130.03, 133.60, 136.11, 144.70, 145.56, 149.05, 159.94, 190.08 HRMS $C_{16}H_{13}{}^{81}Br^{81}BrNO_2^+$ requires 413.9313, found 413.3222

4.2.5 *(E)*-1-(2-amino-3,5-dibromophenyl)-3-(4-fluorophenylprop-2-en-1-one (148 e)

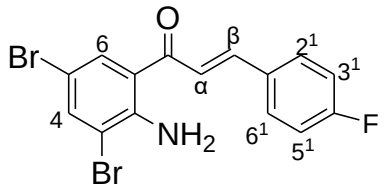

A stirred mixture of 2-amino-3,5-dibromoacetophenone (**147**) (4 g, 13.65 mmol), 4-fluorobenzaldehyde (2.30 g, 16.39 mmol) and potassium hydroxide (0.67 g) in 100 ml ethanol, was stirred to afford **148 e** as a yellow solid (5.04 g, 93%), mp 149-153 ^{0}C(149-150 ^{0}C)[1]; ν_{max} 3470, 3305, 1659, 1600, 1553, 1506, 1400, 1353, 1318, 1200, 1165, 1083, 953, 848, 777, 694, 589, 542, 506, 459, δ_H (400 MHz, $CDCl_3$, ppm) 6.93 (2H, br s, -N<u>H</u>$_2$), 7.11 (2H, m, 3^1, 5^1-H), 7.39 (1H, d, J= 15.2, β-H), 7.65 (2H, m, 2^1, 6^1-H), 7.70 (2H, m, 4, α-H), 7.90 (1H, d, J = 2Hz, 6-H), δ_C (400 MHz, $CDCl_3$, ppm)

111.85, 116.27 (J = 23 Hz), 120.58, 121.57 (J = 3 Hz), 130.41 (J = 9 Hz), 140.93 (J = 3 Hz), 132.49, 139.11, 143.41, 146.86, 165.33 (J = 251 Hz), 189.90 HRMS $C_{15}H_7{}^{79}Br^{81}BrNO^+$ requires 399.9113, found 399.3080

4.3 Synthesis of 6,8-dibromo-2,3-dihydroquinolin-4(1H)-one

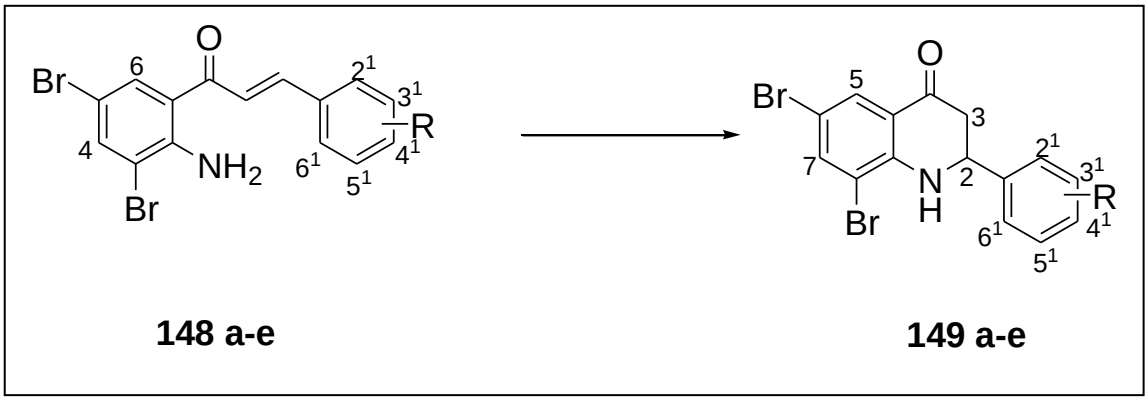

A stirred reaction of **148 a–e** (1 mmol) and orthophosphoric acid (40 ml) in glacial acetic acid (80 ml) was refluxed for 2h. The mixture was then cooled down to room temperature, the quenched with ice. Dichloromethane was then added to extract the product, and the combined organic phases were washed with a saturated solution of sodium carbonate and dried over with $MgSO_4$ anhydrous. The solvent was removed under reduced pressure and the resultant residue was recrystallized using ethanol, to afford **149 a–e**

4.3.1 6,8-Dibromo-2,3-dihydro-2-phenylquinolin-4(1H)-one (149 a)

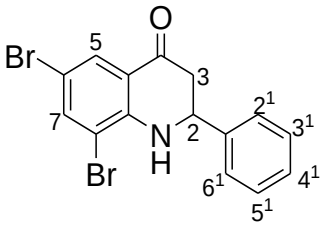

A stirred reaction of **148 a** (5.23 g, 13.73 mmol) and orthophosphoric acid (40 ml) in glacial acetic acid (80 ml) to afford **149 a** as a yellow solid (3.6 g, 77%), mp 99-106 ^{0}C (135-136)[1]; ν_{max} 3375, 3064, 2892, 2113, 1957, 1679, 1580, 1482, 1392, 1351, 1277, 1220, 1137, 1072, 876, 753, 605, 581, 532, 482, 466, 417, δ_H (400 MHz, $CDCl_3$) 2.93 (2H, m, 3a,b-H), 4.79 (1H, dd, *J* = 4.4 Hz, *J* = 12.8 Hz, 2-H), 5.09 (1H, br

s, -NH), 7.46 (5H, m, 2^1,3^1,4^1,5^1,6^1-H), 7.71 (1H, d, *J* = 2.4 Hz, 7-H), 7.94 (1H, d, *J* = 2.0 Hz, 5-H), δ_C (100 MHz, $CDCl_3$, ppm) 45.30, 57.67, 109.80, 110.79, 120.67, 126.51, 128.79, 129.20, 129.55, 139.90, 139.92, 147.24, 191.35 HRMS $C_{15}H_{11}{}^{79}Br^{81}BrNO^+$ requires 380.9207, found 380.3295

4.3.2 6,8-Dibromo-2,3-dihydro-2-p-tolylquinolin-4(1H)-one (149 b)

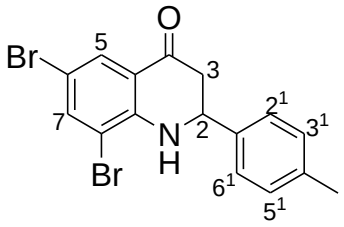

A stirred reaction of **148 b** (5.23 g, 13.73 mmol) and orthophosphoric acid (40 ml) in glacial acetic acid (80 ml) to afford (**149 b**) as a yellow solid (3.6 g, 68%), mp 152-156 ^{0}C; ν_{max} 3375, 3022, 2916, 1670, 1597, 1482, 1335, 1277, 1163, 1113, 1080, 925, 876, 818, 786, 671, 572, 499, 449, 433, δ_H (400 MHz, $CDCl_3$) 2.39 (3H, s, -CH$_3$), 2.92 (2H, m, 3a,b-H), 4.74 (1H, dd, *J* = 4.4 Hz, *J* = 13.6 Hz, 2-H), 5.06 (1H, br s, -NH), 7.25 (2H, d, *J* = 8.0 Hz, 3^1, 5^1-H), 7.34 (2H, d, *J* = 8 Hz, 2^1, 6^1-H), 7.71 (1H, d, *J* = 2.4 Hz, 7-H), 7.95 (1H, d, *J* = 2.0 Hz, 5-H), δ_C (100 MHz, $CDCl_3$, ppm) 21.16, 45.34, 57.43, 109.71, 110.76, 120.66, 126.46, 129.56, 136.93, 138.71, 139.89, 147.30, 194.30 HRMS $C_{16}H_{13}{}^{79}Br^{81}BrNO^+$ requires 394.9364, found 394.3473

4.3.3 6,8-Dibromo-2,3-dihydro-2-(4-methoxyphenyl)quinolin-4(1H)-one (149 c)

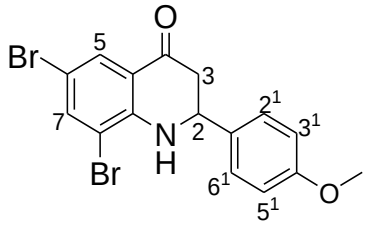

A stirred reaction of **148 c** (5.23 g, 13.73 mmol) and orthophosphoric acid (40 ml) in glacial acetic acid (80 ml) to afford (**149 c**) as a yellow solid (3.6 g, 63%), mp 148-152 ^{0}C (143-145 ^{0}C)[1]; ν_{max} 3318, 3064, 2892, 2834, 1654, 1589, 1498, 1400, 1335, 1236, 1170, 1146, 1022, 958, 916, 876, 818, 777, 720, 597, 548, 490, 466, δ_H (400 MHz, $CDCl_3$) 2.87 (2H, m, 3a,b-H), 3.82 (3H, s, -OCH$_3$) 4.72 (1H, dd, *J* = 4.0 Hz *J* = 13.2 Hz, 2-H), 5.03 (1H, br s, -NH), 6.94 (2H, d, *J* = 8 Hz, 3^1, 5^1-H), 7.37 (2H, d, *J* = 8 Hz, 2^1, 6^1-H), -7.71 (1H, d, *J* = 2.4 Hz, 7-H), 7.94 (1H, d, *J* = 2.0 Hz, 5-H), δ_C (100

MHz, $CDCl_3$, ppm) 45.39, 55.38, 57.14, 109.72, 110.76, 114.46, 120.67, 127.80, 129.56, 131.88, 139.87, 147.29, 159.83, 191.64 HRMS $C_{16}H_{13}{}^{79}Br^{81}BrNO_2{}^+$ requires 411.9370, found 411.9368, $C_{16}H_{13}{}^{81}Br^{81}BrNO_2{}^+$ requires 412.9370, found 412.3093

4.3.4 6,8-Dibromo-2-(3-methoxyphenyl)-2,3-dihydroquinolin-4(1H)-one (149 d)

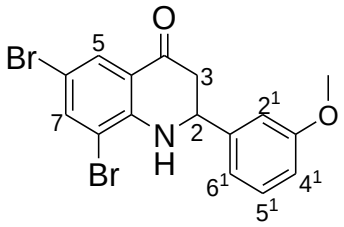

A stirred reaction of **148 d** (5.00 g, 13.12 mmol) and orthophosphoric acid (40 ml) in glacial acetic acid (80 ml) to afford (**149 d**) as a yellow solid (3.85 g, 77.0 %), mp 87-90 ^{0}C; ν_{max} 3381, 3051, 2921, 1677, 1587, 1467, 1346, 1316, 1256, 1226, 1136, 1045, 884, 785, 694, 654, 584, 504, 484, δ_H (400 MHz, $CDCl_3$) 2.86 (2H, m, 3a,b-H), 3.77 (3H, s, -OC<u>H</u>$_3$), 4.71 (1H, dd, J = 4.4 Hz J = 13.6 Hz, 2-H), 5.04 (1H, br s, -N<u>H</u>), 6.86 (1-H, m, 4^1-H), 6.96 (2-H, m, 5^1,2^1-H), 7.29 (1-H, t, J = 8.0 Hz ,7.6 Hz, 6^1-H), 7.66 (1H, d, J = 2.0 Hz, 7-H), 7.84-7.89 (1H, d, J = 2.0 Hz, 5-H), δ_C (100 MHz, $CDCl_3$) 45.36, 55.38, 57.69, 109.87, 110.84, 112.33, 113.88, 120.75, 118.73,120.75, 129.59, 130.35, 139.94, 141.60, 147.23, 160.18, 191.29 HRMS $C_{16}H_{13}{}^{79}Br^{81}BrNO_2{}^+$ requires 411.9370, found 411.2817

4.3.5 6,8-dibromo-2-(4-fluorophenyl)-2,3-dihydroquinolin-4(1H)-one (149 e)

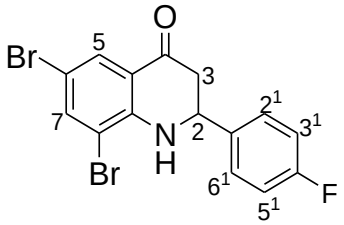

A stirred reaction of **148 e** (4 g, 9.97 mmol) and orthophosphoric acid (40 ml) in glacial acetic acid (80 ml) to afford (**149 e**) as a yellow solid (2.74 g, 50.8%) mp 122-125 ^{0}C (127-129 ^{0}C)[1]; ν_{max} 3352, 1677, 1577, 1486, 1317, 1276, 1226, 1146, 1085, 996, 895, 835, 716, 705, 594, 534, 514, 464, δ_H (400 MHz, $CDCl_3$) 2.89 (2H, m, 3a,b-H), 4.73-4.78 (1H, dd, *J* = 4.0 Hz, *J* = 13.6 Hz, 2-H), 5.03 (1H, br s, -N<u>H</u>), 7.13 (2H, t, *J*= 8.8 Hz, 3^1, 5^1-H), 7.44 (2H, m, 2^1, 6^1-H), 7.72 (1H, d, *J* = 2.4 Hz, 7-H), 7.95 (1H, d, *J* = 2.4 Hz, 5-H), δ_C (100 MHz, $CDCl_3$, ppm) 45.43, 57.10, 110.07, 110.86, 116.30 (*J*

= 23 Hz), 120.76, 128.38 (*J* = 3 Hz), 129.60, 135.79 (*J* = 3 Hz), 139.99, 147.13, 164.10 (*J* = 251 Hz), 191.09 HRMS $C_{15}H_{10}{}^{79}Br^{81}BrNOF^{+}$ requires 398.9113, found 398.3091

4.4 Synthesis of 6,8-dibromo-quinolin-4(*1H*)-one 150 a-e

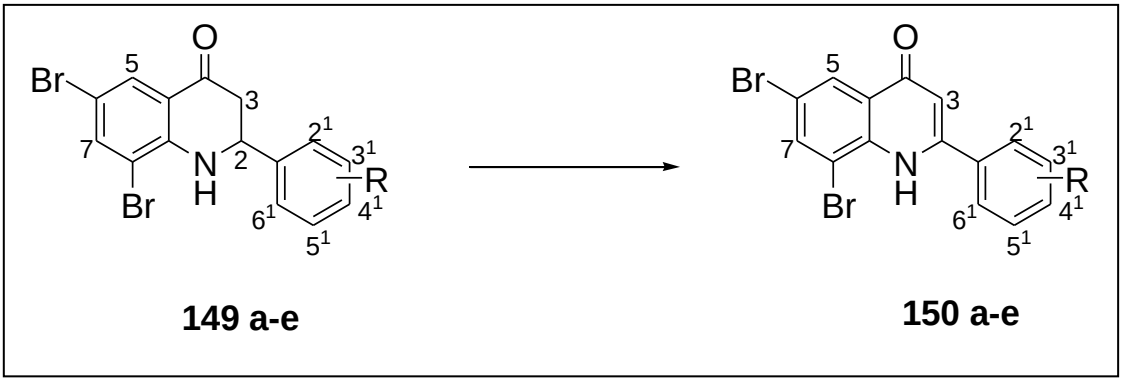

A stirred reaction of **149 a–e** (1 mmol) and Thallium (III) nitrate hydrate (TTN) (1.5 equiv.) in 30 ml of acetonitrile was refluxed for 4h. The mixture was then cooled down to room temperature, filtered and the filtrate was quenched with ice. Dichloromethane was then added to extract the product, and the combined organic phases were washed with a saturated solution of sodium carbonate and dried over with $MgSO_4$ anhydrous. The solvent was removed under reduced pressure and the resultant residue was afforded as **150 a–e**

4.4.1 6,8-Dibromo-2-phenylquinolin-4(*1H*)-one (150 a)

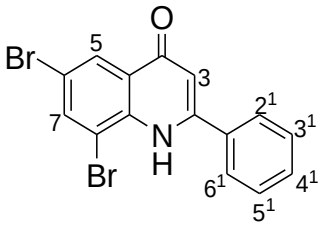

A stirred reaction of **149 a** (2.00 g, 5.25 mmol) and TTN (3.50 g, 7.88 mmol) in 30 ml of acetonitrile to afford **150 a** as a brown solid (1.43 g, 71.5%), mp 158-163 ^{0}C; ν_{max} 3375, 3064, 2908, 1621, 1540, 1490, 1375, 1365, 1211, 1113, 1072, 916, 826, 769, 728, 678, 572, 523, 482, δ_H (400 MHz, $CDCl_3$) 6.58 (1H, s, 3-H), 7.58 (3H, m, 3^1, 4^1, 5^1-H), 7.69 (2-H, m, 2^1, 6^1-H), 7.96 (1H, d, *J* = 2.4 Hz, 7-H), 8.45-8.46 (1H, d, *J* = 2.0 Hz, 5-H), 8.66 (1H, s, -N<u>H</u>) δ_C (100 MHz, $CDCl_3$, ppm) 109.08, 112.32, 116.96,

126.37, 127.31, 128.79,131.37, 133.85, 136.11, 137.37, 149.58, 177.09 HRMS $C_{15}H_9{}^{79}Br^{81}BrNO^+$ requires 379.9030, found 379.2208

4.4.2 6,8-Dibromo-2-p-tolyl quinolin-4(*1H*)-one (150 b)

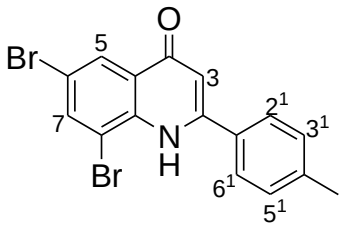

A stirred reaction of **149 b** (2.00 g, 5.06 mmol) and TTN (3.37 g ,7.59 mmol) in 30 ml of acetonitrile to afford **150 b** as a yellow solid (1.10 g, 55.27%), mp 157-160 ^{0}C; ν_{max} 3064, 2916, 2105, 1744, 1589, 1556, 1514, 1498, 1368, 1318, 1203, 1137, 1039, 933, 876, 818, 786, 744, 613, 523, 466, 400, δ_H (400 MHz, $CDCl_3$) 2.39 (3H, s, -C$\underline{H_3}$), 6.53 (1H, s, 3-H), 7.32 (2H, d, *J* = 8 Hz, 3^1,5^1-H), 7.51 (2H, d, *J* = 8.4 Hz, 2^1,6^1-H), 7.89 (1H, d, *J* = 2 Hz, 7-H), 8.41 (1H, d, *J* = 2 Hz, 5-H), 8.59 (1H, s, -N$\underline{H}$), δ_C (100 MHz, $CDCl_3$, ppm) 21.63, 112.61, 118.81, 127.12, 128.06, 129.41, 129.72, 130.75, 134.58, 136.34, 138.70, 143.30, 145.88, 167.28 HRMS $C_{16}H_{11}{}^{79}Br^{81}BrNO^+$ requires 392.9187, found 393.9266

4.4.3 6,8-Dibromo-2-(4-methoxyphenyl) quinolin-4(*1H*)-one (150 c)

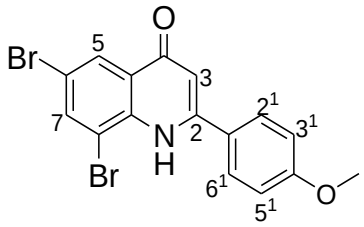

A stirred reaction of **149 c** (2.20 g, 5.35 mmol) and TTN (3.57 g, 8.03 mmol) in 30 ml of acetonitrile to afford **150 c** as a yellow solid (1.70 g, 77.62 %), mp 189-193 ^{0}C (200-201 ^{0}C)[1]; ν_{max} 3064, 2932, 2834, 1597, 1556, 1498, 1441, 1335, 1293, 1244, 1170, 1105, 925, 843, 810, 769, 564, 539, 499, 482, δ_H (400 MHz, $CDCl_3$) 3.89 (3H, s, -OC$\underline{H_3}$), 6.57 (1H, s, *J* = 3-H), 7.08 (2H, d, *J* = 8.8 Hz, 3^1,5^1-H), 7.65 (2H, d, *J* = 8.8 Hz, 2^1,6^1-H), 7.95 (1H, d, *J* = 2 Hz, 7-H), 8.47 (1H, d, *J* = 2 Hz, 5-H), 8.63 (1H, s, -N$\underline{H}$), δ_C (100 MHz, $CDCl_3$, ppm) 55.68, 112.59, 114.50, 115.53, 118.70, 121.85, 127.98, 128.93, 129.37, 130.20, 130.41, 130.85, 134.60, 138.64, 145.52, 162.81, HRMS $C_{16}H_{11}{}^{79}Br^{81}BrNO_2^+$ requires 409.9152, found 409.9212

4.4.4 6,8-dibromo-2-(3-methoxyphenyl) quinolin-4(*1H*)-one (150 d)

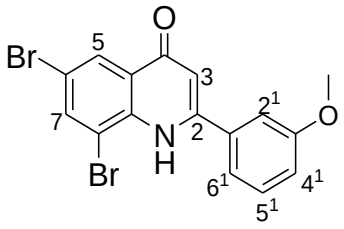

A stirred reaction of **149 d** (3.00 g, 7.30 mmol) and TTN (4.87 g, 10.95 mmol) in 30 ml of acetonitrile to afford **150 d** as a yellow solid (2.56 g, 85.6%), mp 180-184 ^{0}C; ν_{max} 3064, 2916, 1728, 1557, 1482, 1425, 1351, 1277, 1220, 1130, 1031, 949, 867, 793, 720, 671, 621, 532, 457, δ_H (400 MHz, $CDCl_3$) 3.82 (3H, s, -OC$\underline{H_3}$), 7.09 (1H, m , 4^1-H), 7.17 (2-H, m 2^1, 5^1-H), 7.50 (1H, t, J= 8 Hz, 6^1-H), 8.07 (1H, d, J= 2 Hz, 7-H), 8.49 (1H, s, -N$\underline{H)}$, 8.55 (1H, d, J= 1.6 Hz, 5-H), δ_C (100 MHz, $CDCl_3$, ppm) 55.65, 112.69, 112.82, 117.91, 118.91, 119.28, 128.12, 129.39, 131.14, 131.31, 134.56, 138.79, 145.55, 160.47, 167.25 HRMS $C_{16}H_{11}{}^{79}Br^{81}BrNO^+$ requires 409.9152, found 409.9226

4.4.5 6,8-Dibromo-2-(4-flourophenyl) quinolin-4(*1H*)-one (150 e)

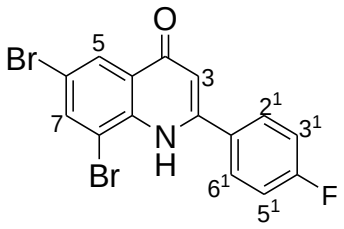

A stirred reaction of **149 e** (2.00 g, 5.01 mmol) and 1.5 equivalence of TTN (3.34 g, 7.51 mmol) in 30 ml of acetonitrile to afford **150 e** as a yellow solid (0.95 g, 47.7%), mp 143-147 ^{0}C (222-224 ^{0}C)[2]; ν_{max} 3383, 3080, 2965, 2908, 1662, 1597, 1556, 1498, 1351, 1318, 1277, 1146, 1064, 859, 810, 711, 621, 572, 532, 490, 409, δ_H (400 MHz, $CDCl_3$) 6.54 (1H, s, 3-H), 7.29 (2H, d, *J* = 8 Hz, 3^1,5^1-H), 7.70 (2H, m, 2^1, 6^1-H), 7.98 (1H, d, *J* = 2.0 Hz, 7-H), 8.47 (1H, d, *J* = 2.0 Hz, 5-H), 8.56 (1H, s, -N$\underline{H)}$ δ_C (100 MHz, $CDCl_3$, ppm) 112.64, 117.51 (*J* = 23 Hz), 119.07, 126.02 (*J* = 3 Hz),128.14, 129.48 ,129.79 (*J* = 9 Hz), 134.52, 138.87, 144.69, 164.96 (*J*= 254 Hz),167.18 HRMS $C_{15}H_8{}^{79}Br^{81}BrNOF^+$ requires 398.8912, found 398.2415

4.5 Synthesis of 6,8-dibromo-4-chloro-quinoline 151 a-e

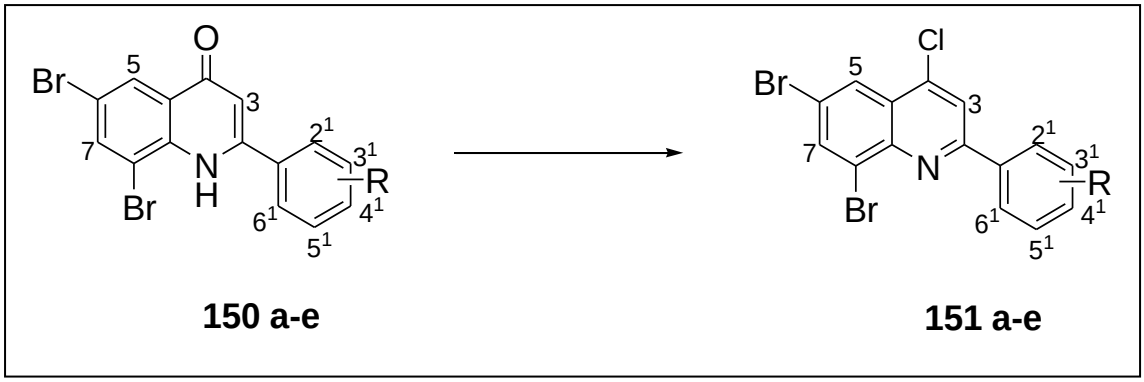

150 a-e **151 a-e**

A stirred reaction of **150 a–e** (1 mmol) and 10 ml of phosphorous chloride in 20 ml of DMF was refluxed for 2h. The mixture was then cooled down to room temperature, was quenched in a mixture of 1 ml of ammonium solution and ice. Dichloromethane was then added to extract the product, and the combined organic phases were washed with a saturated solution of sodium carbonate and dried over with $MgSO_4$ anhydrous. The solvent was removed under reduced pressure and the resultant residue was afforded (**151 a–e**)

4.5.1 6,8-Dibromo-4-chloro-2-phenylquinoline (151 a)

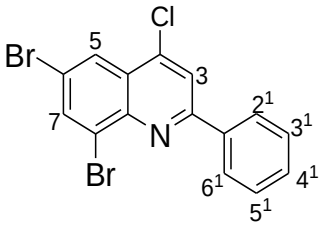

A stirred reaction of **150 a** (1.20 g, 3.16 mmol) and 10 ml of phosphorous chloride in 20 ml of DMF to afford **151 a** as a yellow solid (1.05 g, 74.08 %), mp 159-161 ^{0}C; ν_{max} 2916, 2840, 1627, 1520, 1443, 1305, 1044, 1059, 829, 753, 676, 615, 553, δ_H (400 MHz, $CDCl_3$) δ_C (100 MHz, $CDCl_3$, ppm) 7.51 (3H, m, 3^1, 4^1, 5^1-H), 7.72 (2H, m, 2^1, 6^1-H), 8.27 (1H, d, *J* = 2.0 Hz, 7-H), 8.39 (1H, d, *J* = 2.0 Hz, 5-H), δ_C (100 MHz, $CDCl_3$, ppm) 121.92, 122.69, 125.26, 126.73, 128.20, 129.06, 130.62, 135.36, 135.54, 138.86, 143.54, 152.05 HRMS $C_{15}H_8{}^{81}Br^{81}BrClN^+$ requires 398.8671, found 398.2411

4.5.2 6,8-Dibromo-4-chloro-2-p-tolylquinoline (151 b)

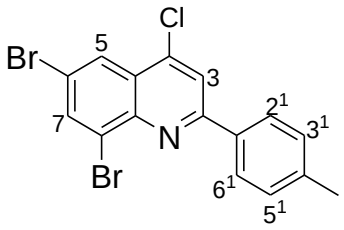

A stirred reaction of **150 b** (1.20 g, 3.05 mmol) and 10 ml of phosphorous chloride in 20 ml of DMF to afford **151 b** as a yellow solid (0.83 g, 66.13 %), mp 181-184 ^{0}C; ν_{max} 2930, 1657, 1549, 1457, 1304, 1274, 1165, 1089, 989, 859, 813, 737, 691, 582, 536, 475, 445, δ_H (400 MHz, $CDCl_3$) 2.42 (3H, s, -C$\underline{H}_3$), 7.33 (2H, d, *J* = 8.0 Hz, 3^1, 5^1-H), 8.14 (2H, d, *J* = 8.0 Hz, 2^1,6^1-H), 8.17 (1H, d, *J* = 2.0 Hz, 7-H), 8.31 (1H, d, *J* = 2.0 Hz, 5-H) δ_C (100 MHz, $CDCl_3$, ppm) 21.51, 119.84, 125.35, 126.16, 126.76, 126.97, 127.52, 129.83, 134.72, 136.95, 140.96, 142.21, 144.70, 157.55 HRMS $C_{16}H_{10}{}^{81}Br^{81}BrClN^+$ requires 413.8869, found 413.3233

4.5.3 6,8-Dibromo-4-chloro-2-(4-methoxyphenyl) quinoline (151 c)

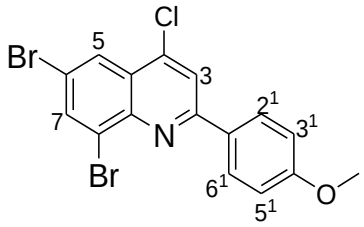

A stirred reaction of **150 c** (1.00 g, 2.44 mmol) and 10 ml of phosphorous chloride in 20 ml of DMF to afford **151 c** as a yellow solid (0.77 g, 73.80 %), mp 150-154 ^{0}C; $\nu_{max\ 3068,}$ 2868, 1595, 1519, 1427, 1335, 1258, 1165, 1135, 1089, 1028, 951, 844, 752, 721, 613, 552, 521, 429, δ_H (400 MHz, $CDCl_3$) 3.86 (3H, s, -OC$\underline{H}_3$), 7.02 (2H, d, *J* = 8.8 Hz, 3^1, 5^1-H), 7.76 (2H, d, *J* = 8.8 Hz, 2^1,6^1-H), 8.29 (1H, d, *J* = 2.0 Hz, 7-H), 8.38 (1H, d, *J* = 2.0 Hz, 5-H) δ_C (100 MHz, $CDCl_3$, ppm) 55.44, 113.55, 121.55, 126.47, 126.64, 127.49, 130.46, 131.72, 136.79, 140.04, 142.05, 157.45, 160.95 HRMS $C_{15}H_{11}{}^{79}Br^{81}BrNO^+$ requires 425.8818, found 425.1515

4.5.4 6,8-Dibromo-4-chloro-2-(3-methoxyphenyl) quinoline (151 d)

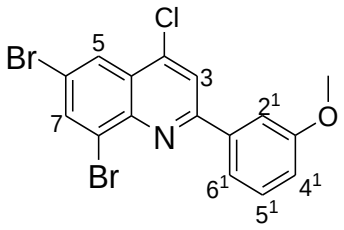

A stirred reaction of **150 d** (1.30 g, 3.18 mmol) and 10 ml of phosphorous chloride in 20 ml of DMF to afford **151 d** as a yellow solid (1.02 g, 75.11 %), mp 106-110 ^{0}C; ν_{max} , δ_H (400 MHz, $CDCl_3$) 3.86 (3H, s, -OC$\underline{H_3}$), 7.08 (1H, m, 4^1-H), 7.33 (1H, d, *J* = 7.6 Hz, 5^1-H), 7.42 (2H, m, 2^1, 6^1-H), 8.01 (1H, s, 3-H), 8.34 (1H, d, *J* = 2.0 Hz, 7-H), 8.42 (1H, d, *J* = 2.0 Hz, 5-H), δ_C (100 MHz, $CDCl_3$, ppm) 55.44, 113.83, 116.92, 120.44, 123.24, 126.26, 126.93, 127.13, 130.24, 133.79, 136.12, 138.95, 143.24, 150.88, 159.99 HRMS $C_{16}H_{10}{}^{79}Br^{81}BrNO^+$ requires 425.8818, found 425.1515

4.5.5 6,8-Dibromo-4-chloro-2-(4-fluorophenyl) quinoline (151 e)

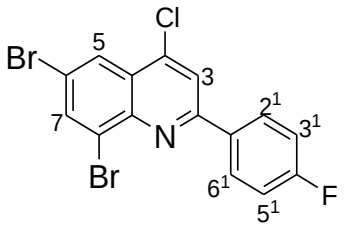

A stirred reaction of **150 e** (1.30 g, 3.27 mmol) and 10 ml of phosphorous chloride in 20 ml of DMF to afford **151 e** as a yellow solid (1.24 g, 91.31 %), mp 195-198 ^{0}C; ν_{max} , δ_H (400 MHz, $CDCl_3$) 7.20 (2H, t, *J* = 8.8 Hz J = 8.4 Hz, 3^1,5^1-H), 7.79 (2H, m, 2^1, 6^1-H), 8.00 (1H, s, 3-H), 8.33 (1H, d, *J* = 2 Hz, 7-H), 8.42 (1H, d, *J* = 2 Hz, 5-H), δ_C (100 MHz, $CDCl_3$, ppm) 116.41 (*J* = 23 Hz), 119.66, 123.30, 126.18, 126.97 (*J* = 9 Hz), 130.54 (*J* = 3 Hz), 133.96, 137.16, 139.05, 143.22, 149.86, 164.47 (*J* = 250 Hz) HRMS $C_{15}H_7{}^{79}Br^{81}BrClNF^+$ requires 415.8618, found 415.2694

4.6 Synthesis of 6,8-dibromo-4-azido-quinoline 152 a-c

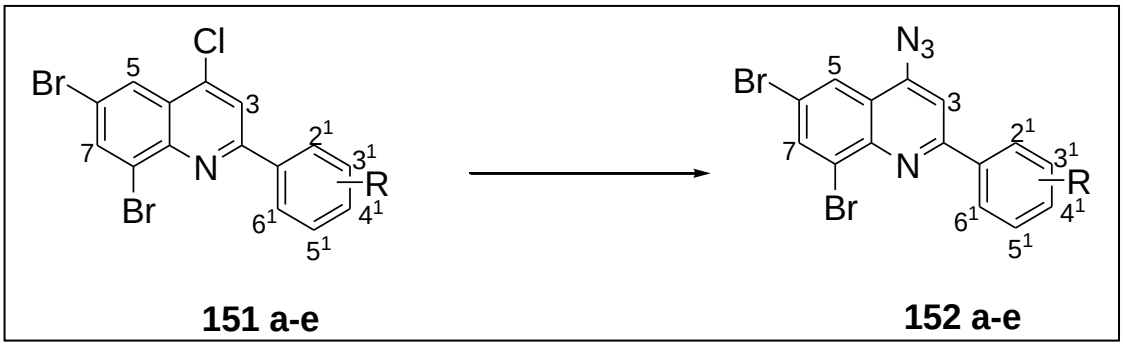

151 a-e **152 a-e**

A stirred reaction of **151 a–e** (1 mmol) and sodium azide (1.2 equiv.) in 30 ml tetrahydrofuran (THF) was refluxed at 70 ºC overnight. The mixture was then quenched with ice and filtered, and the resultant residue afforded compound **152 a–e**)

4.6.1 4-Azido-6,8-dibromo-2-phenyl quinoline (152 a)

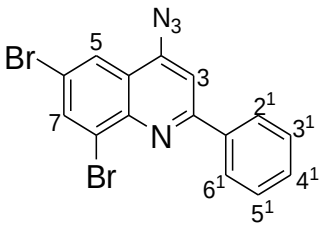

A stirred reaction of **151 a** (0.54 g, 1.35 mmol) and sodium azide (0.11 g, 1.62 mmol) in tetrahydrofuran (THF) to afford a yellow solid (**152 a**) (0.44 g, 80.73 %), mp 98-103 ºC; ν_{max} 3064, 2932, 2359, 2113, 1572, 1531, 1465, 1342, 1253, 1080, 1039, 867, 769, 728, 687, 548, 532, 482, δ_H (400 MHz) 7.52 (3H, m, 5^1, 4^1, 3^1-H), 7.73 (2H, m, 2^1, 6^1-H), 8.28 (1H, d, *J* = 2.0 Hz, 5-H), 8.39 (1H, d, *J* = 2.0 Hz, 7-H) δ_C (100 MHz, $CDCl_3$, ppm) 107.15, 119.46, 122.28, 124.44, 126.28, 127.60, 129.07, 129.29, 130.43, 137.05, 138.12, 146.29, 157.94, HRMS $C_{15}H_8{}^{79}Br^{81}BrN_4{}^+$ requires 403.8095, found 403.2921

4.6.2 4-Azido-6,8-dibromo-2-(p-tolylphenyl) quinoline (152 b)

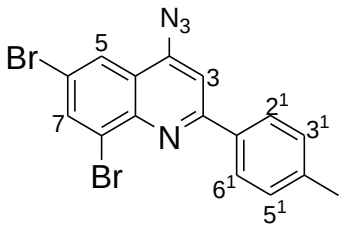

A stirred reaction of **151 b** (1.20 g, 2.91 mmol) and sodium azide (0.23 g, 3.49 mmol) in tetrahydrofuran (THF) to afford a yellow solid (**152 b**) (0.76 g, 62.50 %), mp 157-161 ºC; ν_{max} 3022, 2916, 2113, 1580, 1540, 1474, 1351, 1253, 1179, 1097, 1031, 850, 818, 728, 695, 548, 490, δ_H (400 MHz) 2.47 (3H, s, -C$\underline{H_3}$), 7.38 (2H, d, *J* = 8.0 Hz, 3^1, 5^1-H), 7.66 (1H, s, 3-H), 8.20 (4H, m, 2^1,6^1, 7, 5-H) δ_C (100 MHz, $CDCl_3$, ppm) 21.49, 106.91, 119.17, 122.18, 124.40, 126.18, 127.46, 129.78, 135.32, 136.94, 140.75, 144.90, 146.10, 157.88, HRMS $C_{16}H_{10}{}^{81}Br^{81}BrN_4{}^+$ requires 419.9231, found 419.2738

4.6.3 4-Azido-6,8-dibromo-2-(4-methoxyphenyl) quinoline (152 c)

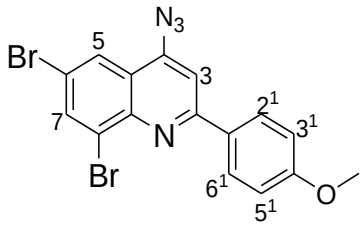

A stirred reaction of **151 c** (0.57 g, 1.38 mmol) and sodium azide (0.12 g, 1.65 mmol) in tetrahydrofuran (THF) to afford a yellow solid (**152 c**) (0.76 g, 62.50 %), mp 164-167 ºC; ν_{max} 3080, 2932, 2121, 1580, 1531, 1465, 1362, 1236, 1170, 1022, 859, 818, 720, 687, 556, 506, 457, δ_H (400 MHz) 3.86 (3H, s, -OC$\underline{H_3}$), 7.02 (2H, d, *J* = 8.8 Hz, 3^1, 5^1-H), 7.79 (2H, d, *J* = 8.8 Hz, 2^1,6^1-H), 8.30 (1H, d, *J* = 2.0 Hz, 7-H), 8.38 (1H, d, *J* = 2.0 Hz, 5-H) δ_C (100 MHz, $CDCl_3$, ppm) 55.48, 106.53, 114.38, 118.89, 121.97, 124.40, 125.99, 129.04, 130.63, 136.90, 144.87, 146.03, 157.43, 161.63, HRMS $C_{16}H_{10}{}^{79}Br^{81}BrN_4O^+$ requires 432.9221, found 432.2939

4.6.4 4-Azido-6,8-dibromo-2-(3-methoxyphenyl) quinoline (152 d)

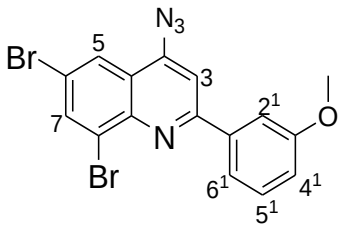

A stirred reaction of **151 d** (0.75 g, 1.82 mmol) and sodium azide (0.14 g, 2.18 mmol) in tetrahydrofuran (THF) afford a yellow solid (**152 d**) (0.52 g, 65.82 %), mp 129-136 ºC ν_{max} 3080, 2941, 2121, 1580, 1531, 1449, 1359, 1244, 1203, 1121, 1048, 974, 867, 802, 777, 720, 678, 556, 515, 457, δ_H (400 MHz) 3.85 (3H, s, -OC$\underline{H_3}$), 7.07 (1H, dd, *J* = 2.0 Hz, *J* = 8.4 Hz 4^1-H), 7.26 (2H, m, $3,5^1$-H), 7.30 (1H, m, 2^1-H), 7.37 (1H, t, *J* = 8 Hz, 6^1-H), 8.28 (1H, d, *J* = 2.0 Hz, 5-H), 8.39 (1H, d, *J* = 2.0 Hz, 7-H) δ_C (100 MHz, $CDCl_3$, ppm) 55.43, 113.75, 116.56, 120.29, 121.96, 122.74, 125.25, 126.74, 130.13, 135.47, 136.53, 128.86, 151.85, 159.93, HRMS $C_{16}H_{10}{}^{79}Br^{81}BrN_4O^+$ requires 433.9221, found 433.2420

4.6.5 4-Azido-6,8-dibromo-2-(4-flourophenyl) quinollne (152 e)

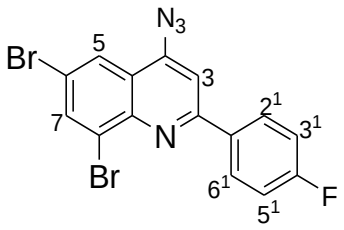

A stirred reaction of **151 e** (1.0 g, 2.44 mmol) and sodium azide (0.19 g, 2.98 mmol) in tetrahydrofuran (THF) to afford a yellow solid (**152 e**) (0.88 g, 86.95 %), mp 182-186 ºC; ν_{max} 3064, 2916, 2105, 1564, 1531, 1514, 1474, 1351, 1227, 1154, 1097, 1055, 900, 876, 834, 720, 687, 629, 548, 499, 417, δ_H (400 MHz) 7.24 (2H, t, *J* = 8.8 Hz, *J* = 8.4 Hz, $3^1,5^1$-H), 7.58 (1H, s, 3-H), 8.15 (1H, d, *J* = 2.0 Hz, 5-H), 8.17 (1H, d, *J* = 2.0 Hz, 7-H), 8.23 (2H, dd, *J* = 5.2 Hz, *J* = 8.8 Hz, 2^1, 6^1-H), δ_C (100 MHz, $CDCl_3$, ppm) 106.73, 116.08 (*J* = 21 H), 119.52, 122.14, 124.44, 126.16, 129.57 (*J* = 8 Hz), 134.27 (*J* = 3 Hz), 137.16, 144.84, 146.41, 156.75, 164.40 (*J* = 250 Hz) HRMS $C_{15}H_7{}^{79}Br^{81}BrFN_4{}^+$ requires 422.9001, found 422.3790

4.7.1 Synthesis of (1-(6,8-dibromo-quinolin-4-yl)-1H-1,2,3-triazol-4-yl) methanol 153 a-e

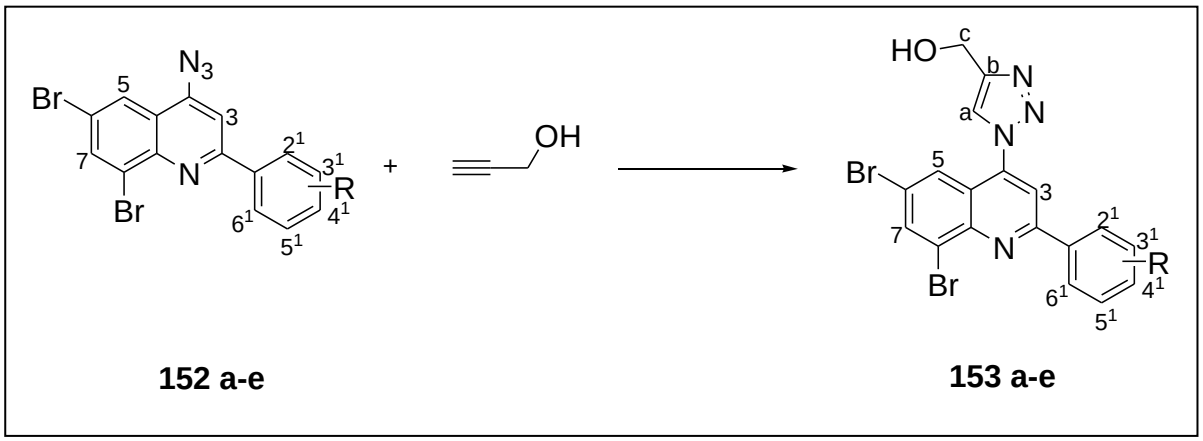

152 a-e **153 a-e**

A stirred reaction of **152 a–e** (1 mmol) in EtOH: H_2O: THF (1:1:2) and propargyl alcohol (1.2 equiv.), sodium ascorbate (40 % mmol) and $CuSO_4$. $5H_2O$ (10 % mmol) were added and refluxed for 4 hours. The mixture was then cooled down to room temperature and quenched with ice. The precipitate was then filtered and air dried to afford **153 a–e**

4.7.1.1 (1-(6,8-Dibromo-2-phenylquinolin-4-yl)-1*H*-1,2,3-triazol-4-yl)methanol (153 a)

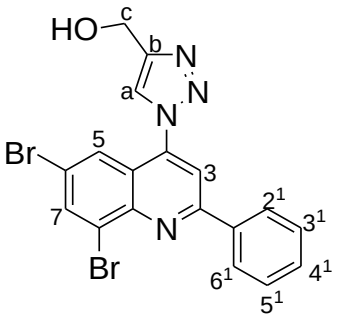

A stirred reaction of **152 a** (0.29 g, 0.72 mmol) in EtOH: H_2O: THF (1:1:2) and 1.2 equiv. propargyl alcohol (0.05 g ,0.86 mmol), sodium ascorbate (0.06 g, 0.288 mmol) and $CuSO_4$. $5H_2O$ (0.02 g, 0.072 mmol) were added to afford a yellow solid **153 a** (0.29 g, 88.78 %), mp 207-210 ºC, ν_{max} 3342, 2973, 2908, 2359, 2121, 1572, 1474, 1351, 1260, 1031, 859, 720, 678 δ_H (400 MHz) 5.01 (2H, s, -C$\underline{H_2}$OH), 7.54 (3H, m, 5^1, 4^1, 3^1-H), 8.06 (2H, m, 2^1, 6^1-H), 8.25 (1H, d, J = 2.0 Hz, 5^1-H), 8.28 (1H, s, a-H),

8.30 (1H, d, *J* = 2.0 Hz, 7-H), δ_C (100 MHz) 56.65, 115.25, 121.58, 123.05, 124,68, 121.21 HRMS $C_{18}H_{12}{}^{79}Br^{81}BrN_4O^+$ requires 460.9357, found 460.9480

4.7.1.2 (1-(6,8-Dibromo-2-p-tolylquinolin-4-yl)-1*H*-1,2,3-triazol-4-yl) methanol (153 b)

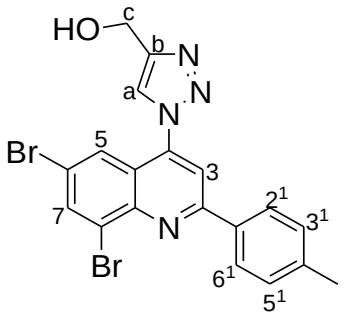

A stirred reaction of **152 b** (0.25 g, 0.59 mmol) in EtOH: H2O: THF (1:1:2) and 1.2 equiv. propargyl alcohol (0.04 g ,0.71 mmol), sodium ascorbate (0.05 g, 0.24 mmol) and $CuSO_4$. $5H_2O$ (0.01 g, 0.06 mmol) were added to afford a yellow solid **153 b** (0.19 g, 68.90 %), mp 209-212 ºC, ν_{max} δ_H (400 MHz) 2.4 (3H, s, -C<u>H</u>$_3$), 4.9 (2H, s, -C<u>H</u>$_2$OH), 7.24 (1H, s, 3-H), 7.28 (2H, d, *J* = 8.0 Hz, 3^1, 5^1-H), 7.45 (1H, d, *J* = 2.0 Hz, 5-H), 7.6 (2H, d, *J* = 8.4 Hz, 2^1, 6^1-H), 7.73 (1H, s, a-H), 8.30 (1H, d, *J* = 2.0 Hz, 7-H), 21.54, 56.62, 123.99, 124.94, 125.20, 127.16, 128.34, 129.47, 129.88, 130.06, 131.84, 133.25, 138.76, 139.46, 141.78, 144.23, 151.38 HRMS $C_{19}H_{14}{}^{81}Br^{81}BrN_4O^+$ requires 475.9493, found 475.3259

4.7.1.3 (1-(6,8-Dibromo-2-(4-methoxyphenyl) quinolin-4-yl)-1*H*-1,2,3-triazol-4-yl) methanol (153 c)

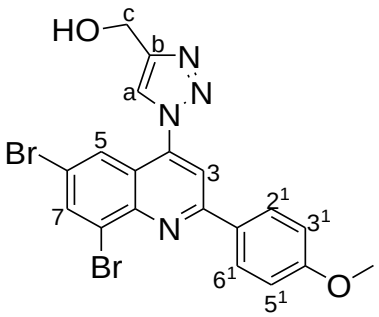

A stirred reaction of **152 c** (0.32 g, 0.74 mmol) in EtOH: H2O: THF (1:1:2) and 1.2 equiv. propargyl alcohol (0.05 g ,0.89 mmol), sodium ascorbate (0.06 g, 0.30 mmol) and $CuSO_4$. $5H_2O$ (0.02 g, 0.07 mmol) were added to afford a yellow solid **153 c** (0.35 g, 96.60 %), mp 219-221 ºC, ν_{max} 3326, 2908, 2826, 1572, 1507, 1307, 1260,

1170, 1113, 1022, 818, 761, 629, 564, 523, δ_H (400 MHz) 8.2 (1H, d, *J* = 2.0 Hz, 7-H), 7.9 (2H, d, *J* = 8.8 Hz, 2^1, 6^1-H), 7.9 (1H, s, a-H), 7.2 (1H, d, *J* = 2.0 Hz, 5-H), 7.1 (2H, d, *J* = 8.8 Hz), 5.0 (2H, s, -C$\underline{H_2}$OH), 3.8 (3H, s, -C$\underline{H_3}$), δ_C (100 MHz) 55.44, 56.71, 113.73, 114.86, 122.58, 124.08, 126.65, 129.56, 131, 50, 131.78, 134.52, 137.41, 140.07,142.59, 157.59, 161.22, 165.15 HRMS $C_{19}H_{14}{}^{79}Br^{81}BrNO_2^+$ requires 490.9484, found 490.9737

4.7.1.4 (1-(6,8-Dibromo-2-(3-methoxyphenyl)quinolin-4-yl)-1*H*-1,2,3-triazol-4-yl) methanol (153 d)

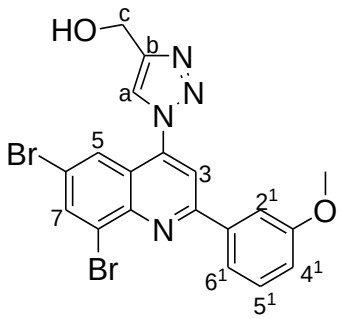

A stirred reaction of **152 d** (0.20 g, 0.46 mmol) in EtOH: H2O: THF (1:1:2) and 1.2 equiv. propargyl alcohol (0.03 g ,0.55 mmol), sodium ascorbate (0.04 g, 0.18 mmol) and $CuSO_4$. $5H_2O$ (0.02 g, 0.05 mmol) were added to afford a yellow solid **153 d** (0.11 g, 50 %), mp 220-222 ºC, ν_{max} 3260, 3055, 2916, 2834, 1580, 1531, 1465, 1432, 1318, 1244, 1031, 867, 777, 678, 556 δ_H (400 MHz) 3.81 (3H, s, -OC$\underline{H_3}$), 4.92 (2H, s, -C$\underline{H_2}$OH), 7.04 (1H, dd, J = 2.4 Hz, 4^1-H), 7.26 (1H, d, *J* = 7.6 Hz, 5^1-H), 7.32 (1H, s, 2^1-H), 7.36 (1H, t, *J* = 8.4 Hz 6^1-H), 7.48 (1H, d, *J* = 2.0 Hz, 5-H), 7.92 (1H, s, a-H), 8.31 (1H, d, *J* = 2.0 Hz, 7-H), δ_C (100 MHz) 55.47, 56.59, 113.98, 117.05, 120.42, 124.17, 124.97, 125.24, 127.22, 130.36, 133.26, 135.79, 139.54, 140.71, 144.17, 151.20, 160.09 HRMS $C_{19}H_{14}{}^{79}Br^{81}BrN_4O_2^+$ requires 490.9484, found 490.4447

4.7.1.5 (1-(6,8-Dibromo-2-(4-fluorophenyl)quinoline-4-yl)-1*H*-1,2,3-triazol-4-yl) methanol (153 e)

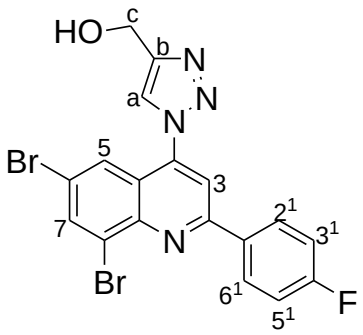

A stirred reaction of **152 e** (0.35 g, 0.83 mmol) in EtOH: H2O: THF (1:1:2) and 1.2 equiv. propargyl alcohol (0.05 g ,1.00 mmol), sodium ascorbate (0.07 g, 0.33 mmol) and $CuSO_4$. $5H_2O$ (0.02 g, 0.08 mmol) were added to afford a yellow solid **153 e** (0.30 g, 75.00 %), mp 207-210 ºC, ν_{max} 3323, 3066, 2902, 1592, 1486, 1393, 1206, 1170, 1030, 843, 796, 714, 656, 563, 504, δ_H (400 MHz) 5.01 (2H, s, -CH2OH), 7.26 (2H, m, 3^1, 5^1-H), 8.01 (1H, d, *J* = 2 Hz, 5-H), 8.06 (1H, s, a-H), 8.26 (1H, d, *J* = 2 Hz, 7-H) 8.31 (2H, dd, *J* = 5.2 Hz, J = 8.8 Hz, 2^1, 6^1-H), δ_C (100 MHz) 56.70, 115.01, 116.34 (J = 22 Hz), 122.88, 122.98, 123.53, 13.74, 124.70, 127.17, 129.71 (J = 9 Hz), 133.46, 137.63, 141.09, 142.32, 148.58, 157.23, 177.24 (J = 251 Hz) HRMS $C_{18}H_{11}{}^{81}Br^{81}BrN_4OF^+$ requires 479.9243, found 479.3351

4.7.2 Synthesis of 6,8-dibromo-4(3-fluorophenyl)-1H-1,2,3-triazol-1-yl)-2-(phenyl) quinoline derivatives 153 f-j

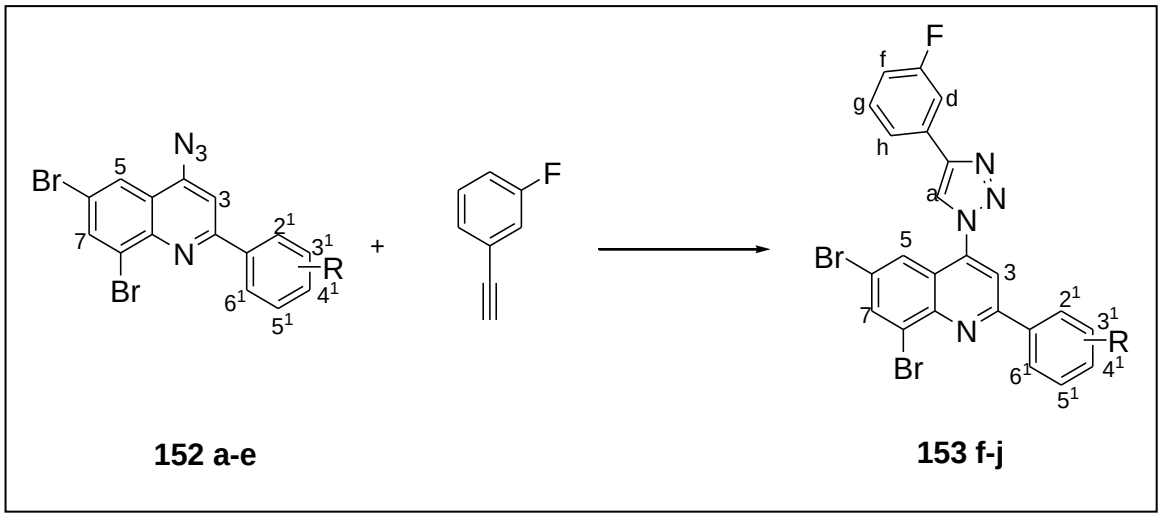

152 a-e **153 f-j**

A stirred reaction of phenyl acetylene (2 equiv.), sodium ascorbate (2 equiv.) and $CuSO_4$. $5H_2O$ (0.4 equiv.) were added in EtOH: H_2O: THF (1:1:2) and after 5 minutes, a mixture of 5 ml and **152 a–e** (1 mmol) were then added and refluxed for 4 hours. The mixture was then cooled down to room temperature and quenched with ice. The precipitate was then filtered and air dried to afford **153 f–j**

4.7.2.1 6,8-Dibromo--4-(4-(3-fluorophenyl-1*H*-1,2,3-triazol-1-yl)-2-phenylquinoline 153 f

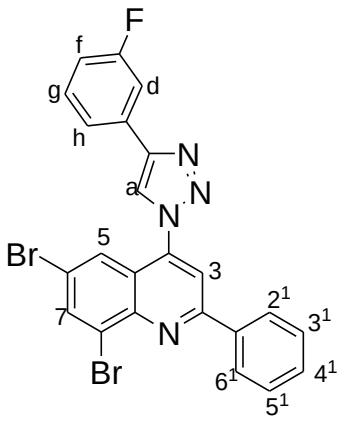

A stirred reaction of 1-ethynyl-3-fluoro-phenyl (0.09 g, 0.74 mmol), sodium ascorbate (0.15 g, 0.74 mmol) and $CuSO_4$. $5H_2O$ (0.05 g, 0.19 mmol) were added in EtOH: H_2O: THF (1:1:2) and **152 a** (0.14 g, 0.37 mmol) were then added to afford a yellow solid **153 f** (0.17 g, 65.0 %) mp 229-232 ºC, ν_{max} 3080, 1598, 1537, 1476, 1382, 1329, 1129, 1022, 859, 777, 720, 678, 613 δ_H (400 MHz, $CDCl_3$, ppm) 7.13 (1H, ddd, *J* = 1.6 Hz, *J* = 6.8 Hz, f-H), 7.44 (1H, dd, *J* = 14.0 Hz, *J* = 8.0 Hz, d-H), 7.58 (3H, m, 5^1, 4^1, 3^1-H), 7.60 (1H, d, *J* = 2.0 Hz, 5-H), 7.71 (2H, m, g, h-H), 7.81 (2H, m, 2^1, 6^1-H), 8.19 (1H, s, a-H), 8.38 (1H, d, *J* = 2.0 Hz, 7-H), δ_C (100 MHz, $CDCl_3$, ppm) 113.24 (*J* = 24 Hz), 116.13 (*J* = 21 Hz), 121.82 (*J* = 3 Hz), 122.91, 124.08, 124.32, 125.19, 127.25, 128.39, 129.29, 130.82 (*J* = 9 Hz), 130.94, 139.59,144.27, 151.40, 163.21 (*J* = 245 Hz) HRMS $C_{23}H_{13}{}^{79}Br^{81}BrN_4F^+$ requires 525.9491, found 525.3784

4.7.2.2 6,8-Dibromo-4-(4-(3-fluorophenyl-1*H*-1,2,3-triazol-1-yl)-2-p-tolyl quinoline (153 g)

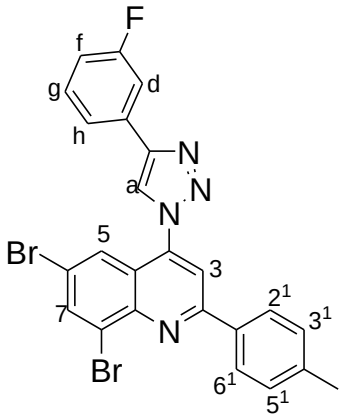

A stirred reaction of 1-ethynyl-3-fluoro-phenyl (0.14 g, 1.16 mmol), sodium ascorbate (0.23 g, 1.16 mmol) and $CuSO_4$. $5H_2O$ (0.07 g, 0.29 mmol) were added in EtOH: H_2O: THF (1:1:2) and **152 b** (0.26 g, 0.58 mmol) were then added to afford a yellow solid **153 g** (0.24 g, 76.2 %) mp 225-228 ºC, ν_{max} 2981, 2908, 2367, 1589, 1487, 1326, 1253, 1187, 1105, 1022, 859, 810, 786, 744, 678 δ_H (400 MHz, $CDCl_3$, ppm) 2.42 (3H, s, -C<u>H</u>$_3$), 7.13 (1H, t, *J* = 8.4 Hz, f-H), 7.33 (2H, d, J = 8.0 Hz, 5^1, 3^1-H), 7.38 (1H, d, *J* = 2.0 Hz, 5-H), 7.46 (1H, dd, *J* = 14.0 Hz, *J* = 8.0 Hz, d-H), 7.75 (2H, m, g, h-H), 7.84 (2H, d, J = 8.0 Hz, 2^1, 6^1-H), 8.16 (1H, s, a-H), 8.24 (1H, d, *J* = 2.0 Hz, 7-H), δ_C (100 MHz, $CDCl_3$, ppm) 29.61, 113.04 (*J* = 24 Hz), 115.79 (*J* = 21 Hz), 121.62 (*J* = 3Hz), 122.66, 122.91, 124.11, 125.88, 126.62, 126.80, 127.50, 129.05, 129.95, 130.74 (*J* = 9 Hz), 134.31, 137.50, 138.29, 140.50, 142.65, 147.26, 158.18, 163.4 (*J* = 244 Hz) HRMS $C_{24}H_{15}{}^{81}Br^{81}BrN_4F^+$ requires 539.9607, found 539.2089

4.7.2.3 6,8-Dibromo-4-(4-(3-fluorophenyl)-1*H*-1,2,3-triazol-1-yl)-2-(4-methoxyphenyl) quinoline (153 h)

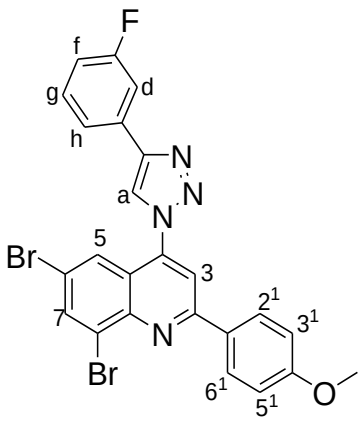

A stirred reaction of 1-ethynyl-3-fluoro-phenyl (0.13 g, 1.10 mmol), sodium ascorbate (0.22 g, 1.10 mmol) and $CuSO_4$. $5H_2O$ (0.07 g, 0.28 mmol) were added in EtOH: H_2O: THF (1:1:2) and **152 c** (0.24 g, 0.55 mmol) were then added to afford a yellow solid **153 h** (0.21 g, 67.9 %) mp 231-234 ºC, ν_{max} 2973, 2928, 1589, 1523, 1472, 1335, 1253, 1170, 1113, 991, 859, 778, 678, 564, 532, δ_H (400 MHz, $CDCl_3$, ppm) 3.89 (3H, s, -OC$\underline{H_3}$), 7.05 (2H, d, J = 8.0 Hz, 5^1, 3^1-H), 7.14(1H, t, *J* = 8.4 Hz, f-H), 7.37 (1H, d, *J* = 2.0 Hz, 5-H), 7.48 (1H, dd, *J* = 14.0 Hz, *J* = 8.0 Hz, d-H), 7.72 (2H, m, g, h-H), 7.92 (2H, d, J = 8.0 Hz, 2^1, 6^1-H), 8.16 (1H, s, a-H), 8.22 (1H, d, *J* = 2.0 Hz, 7-H), δ_C (100 MHz, $CDCl_3$, ppm) 55.49, 113.7 (*J* = 24 Hz), 115.80 (*J* = 21 Hz), 121.63 (*J* = 2 Hz), 122.66, 122.91, 124.11, 125.88, 126.62, 126.80, 127.50, 129.05, 129.95, 130.74 (*J* = 9 Hz), 134.31, 137.50, 138.29, 140.50, 142.65, 147.26, 158.18, 163.4 (*J* = 244 Hz) HRMS $C_{24}H_{15}{}^{79}Br^{81}BrN_4FO^+$ requires 555.9556, found 555.4212

4.7.2.4 6,8-Dibromo-4-(4-(3-fluorophenyl-1*H*-1,2,3-triazol-1-yl)-2-(3-methoxyphenyl)- quinoline (153 i)

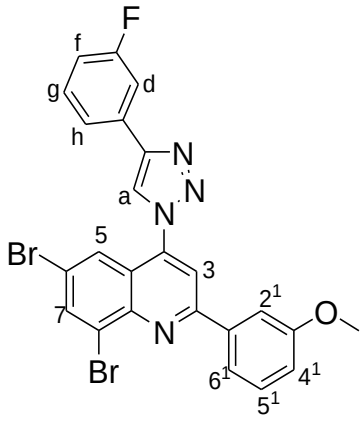

A stirred reaction of 1-ethynyl-3-fluoro-phenyl (0.12 g, 0.96 mmol), sodium ascorbate (0.19 g, 0.96 mmol) and $CuSO_4$. $5H_2O$ (0.06 g, 0.24 mmol) were added in EtOH: H_2O: THF (1:1:2) and **152 d** (0.21 g, 0.48 mmol) were then added to afford a yellow solid **153 i** (0.19 g, 70.9 %) mp 183-187 ºC, ν_{max} 2973, 2924, 2350, 2014, 1580, 1531, 1465, 1318, 1220, 1121, 965, 859, 786, 678, 515, 457δ_H (400 MHz, $CDCl_3$, ppm) 3.82 (3H, s, -CH_3), 7.07 (2H, m, 4^1, f-H), 7.26 (2H, m, 5^1, 2^1-H), 7.38 (2H, m, 6^1, d-H), 7.53 (1H, d, J = 2 Hz, 5-H), 7.61 (2H, m, g, h-H), 8.14 (1H, s, a-H), 8.32 (1H, d, J = 2 Hz, 7-H), δ_C (100 MHz, $CDCl_3$, ppm) 55.48, 113.38 (*J* = 23 Hz), 114.00, 116.30 (*J* = 21 Hz), 117.11, 120.44, 121.88, 122.98, 124.17, 124.40, 130.41, 130.81,

(J = 8 Hz), 133.10, 135.10, 135.79, 139.63, 151.24, 160.13, 161.8 (*J* = 242 Hz), HRMS $C_{24}H_{15}{}^{79}Br^{81}BrN_4FO^+$ requires 555.9556, found 555.3180

4.7.2.5 6,8-Dibromo-2-(4-fluoropheny)-4-(4-(3-fluorophenyl)-1*H*-1,2,3-triazol-1-yl) quinoline (153 j)

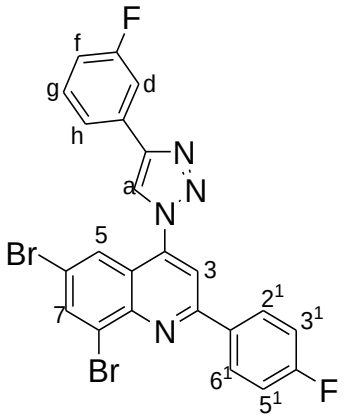

A stirred reaction of 1-ethynyl-3-fluoro-phenyl (0.06 g, 0.52 mmol), sodium ascorbate (0.10 g, 0.52 mmol) and $CuSO_4$. $5H_2O$ (0.03 g, 0.13 mmol) were added in EtOH: H_2O: THF (1:1:2) and after 5 minutes, a mixture of 5 ml and **152 e** (0.11 g, 0.26 mmol) were then added to afford a yellow solid **153 j** (0.14 g, 99.3 %), mp 223-226 ºC, ν_{max} 2965, 2916, 2359, 2096, 1589, 1490, 1441, 1326, 1220, 1146, 1036, 867, 834, 777 δ_H (400 MHz) 7.12 (1H, t, *J* = 8.4 Hz, f-H), 7.22 (2H, m, 5^1, 3^1-H), 7.48 (1H, dd, *J* = 14.0 Hz, *J* = 8.0 Hz, d-H), 7.72 (2H, m, g, h-H), 8.07 (1H, d, *J* = 2.0 Hz, 5-H), 8.27 (1H, d, *J* = 2.0 Hz, 7-H), 8.28 (1H, s, a-H), 8.32 (2H, dd, J = 5.2 Hz, J = 8.8 Hz, 2^1, 6^1-H), δ_C (100 MHz, $CDCl_3$, ppm) 113.10 (*J* = 23 Hz), 114.93, 115.96 (*J* = 21 Hz), 116.35 (*J* = 22 Hz), 121.68, 121.70, 122.37 (*J* = 3 Hz), 122.96, 124.75, 127.17, 129.72 (*J* = 9 Hz), 130.84 (*J* = 9 Hz), 131.50 (*J* = 9 Hz), 133.44 (*J* = 3 Hz), 137.69, 141.11, 145.39, 156.75, 162.05 (*J* = 245 Hz), 163.46 (*J* = 297 Hz) HRMS $C_{23}H_{12}{}^{81}Br^{81}BrN_4F_2^+$ requires 535.9397, found 535.4254

4.7.3 Synthesis of 6,8-dibromo-4-(4-phenyl-1H-1,2,3-triazol-1-yl) quinoline derivatives 153 k-o

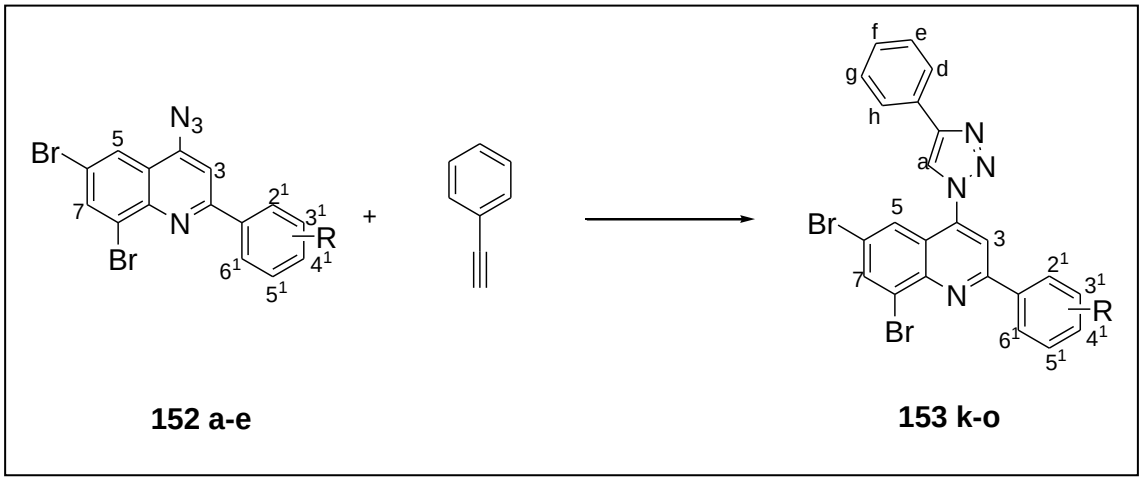

152 a-e **153 k-o**

A stirred reaction of phenyl acetylene (2 equiv.), sodium ascorbate (2 equiv.) and $CuSO_4$. $5H_2O$ (0.4 equiv.) were added in EtOH: H_2O: THF (1:1:2) and after 5 minutes, a mixture of 5 ml and **152 a–e** (1 mmol) were then added and refluxed for 4 hours. The mixture was then cooled down to room temperature and quenched with ice. The precipitate was then filtered and air dried to afford **153 k–o**

4.7.3.1 6,8-Dibromo-2-phenyl-4-(4-phenyl-1*H*-1,2,3-triazol-1-yl) quinoline (153 k)

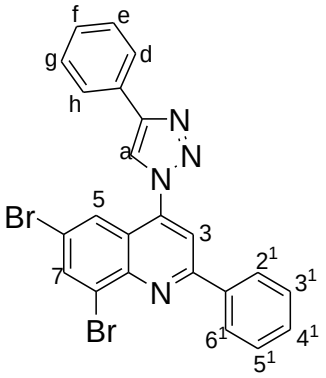

A stirred reaction of phenyl acetylene (0.11 g, 1.04 mmol), sodium ascorbate (0.20 g, 1.04mmol) and $CuSO_4$. $5H_2O$ (0.05 g, 0.21 mmol) in EtOH: H_2O: THF (1:1:2) and **152 a** (0.21 g, 0.52 mmol) was then added to afford a yellow solid **153 k** (0.17 g, 65.0 %) mp 206-211 ºC, ν_{max} 3080, 2973, 2162, 2030, 1604, 1540, 1474, 1384, 1381, 1227, 1022, 834, 769, 671, δ_H (400 MHz, $CDCl_3$, ppm) 7.48 (3H, m, e, f, j-H), 7.55 (3H, m, 5^1, 4^1, 3^1-H), 7.61 (1H, d, *J* = 2 Hz, 5-H), 7.81 (2H, d, *J* = 7.2 Hz, d, h-

H), 7.95 (2H, d, 8.4 Hz, 2^1, 6^1-H), 8.19 (1H, s, a-H), 8.37 (1H, d, *J* = 2 Hz, 7-H), δ_C (100 MHz, $CDCl_3$, ppm) 122.50, 124.17, 214.24, 125.33, 126.18, 127.19, 128.40, 128.79, 129.15, 128.28, 131.16, 133.29, 134.65, 139.54, 144.26, 148.28, 151.41 HRMS $C_{23}H_{14}{}^{79}Br^{81}BrN_4^+$ requires 507.9544, found 507.3303

4.7.3.2 6,8-Dibromo-4-(4-phenyl-1*H*-1,2,3-triazol-1-yl)-2-p-tolyl quinoline (153 l)

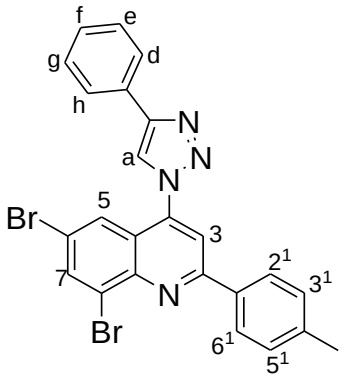

A stirred reaction of phenyl acetylene (0.13 g, 1.30 mmol), sodium ascorbate (0.26 g, 1.30 mmol) and $CuSO_4$. $5H_2O$ (0.08 g, 0.33 mmol) in EtOH: H_2O: THF (1:1:2) and **152 b** (0.27 g, 0.65 mmol) were then added to afford a yellow solid **153 l** (0.24 g, 72.7 %) mp 241-245ºC, ν_{max} δ_H (400 MHz, $CDCl_3$, ppm) 2.43 (3H, s, -CH_3), 7.32 (2H, d, J = 8.4 Hz, 5^1, 3^1-H), 7.51 (3H, m, e, f, g-H), 7.96 (2H, d, J = 7.2 Hz, d, h-H), 8.07 (1H, d, J = 2 Hz, 5-H), 8.18 (2H, d, J = 8.4 Hz, 2^1, 6^1-H), 8.22 (1H, d, J = 2 Hz, 7-H), 8.28 (1H, s, a-H), δ_C (100 MHz, $CDCl_3$, ppm) 21.49, 106.86, 114.89, 121.24, 121.38, 122.94, 124.83, 126.00, 126.99, 127.47, 129.09, 129.43 129.90, 134.40, 137.31, 141.35, 145.29, 148.58, 157.76 $C_{24}H_{16}{}^{81}Br^{81}BrN_4^+$ requires 522.9701 , found 522.3969

4.7.3.3 6,8-Dibromo-2-(4-methoxyphenyl)-4-(4-phenyl-1*H*-1,2,3-triazol-1-yl) quinoline (153 m)

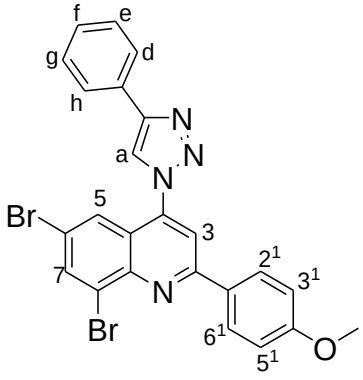

A stirred reaction of phenyl acetylene (0.11 g, 1.06 mmol), sodium ascorbate (0.21 g, 1.06 mmol) and $CuSO_4$. $5H_2O$ (0.07 g, 0.27 mmol in EtOH: H_2O: THF (1:1:2) and **152 c** (0.21 g, 0.53 mmol) were then added a yellow solid **153 m** (0.13 g, 43.9 %) mp 219-222 ºC, ν_{max} 2924, 2850, 2154, 1556, 1507, 1465, 1416, 1318, 1170, 1088, 1015, 834, 744, 687, 564δ_H (400 MHz, $CDCl_3$, ppm) 3.89 (3H, s, -OC$\underline{H_3}$), 7.06 (2H, d, J = 8.4 Hz, 5^1, 3^1-H), 7.38 (1H, d, J = 2 Hz, 5-H), 7.43 (1H, m, f-H), 7.50 (2H, m, f, g-H), 7.98 (4H, m, d, h, 2^1, 6^1-H), 8.15 (1H, s, a-H), 8.20 (1H, d, J = 2 Hz, 7-H), δ_C (100 MHz, $CDCl_3$, ppm) 55.43, 113.77, 114.91, 122.39, 122.65, 124.25, 125.87, 126.04, 126.66, 128.98, 129.15, 129.46, 129.64, 131.55, 131.84, 137.45, 138.59, 142.65, 157.64, 161.26 HRMS $C_{24}H_{16}{}^{79}Br^{81}BrN_4O^+$ requires 537.9650, found 537.4292

4.7.3.4 6,8-Dibromo-2-(3-methoxyphenyl)-4-(4-phenyl-1*H*-1,2,3-triazol-1-yl) quinoline (153 n)

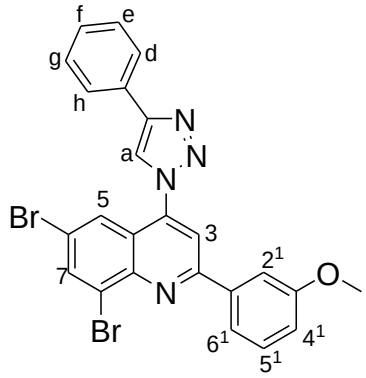

A stirred reaction of phenyl acetylene (0.94 g, 0.92 mmol), sodium ascorbate (0.18 g, 0.92 mmol) and $CuSO_4$. $5H_2O$ (0.06 g, 0.23 mmol) in EtOH: H_2O: THF (1:1:2) and **152 d** (0.20 g, 0.46 mmol) were then added to afford a yellow solid **153 n** (0.14 g, 57.0 %) mp 210-214 ºC, ν_{max} 2965, 2908, 1646, 1578, 1537, 1460, 1325, 1011, 864, 762, 522, 473 δ_H (400 MHz, CDCl3, ppm) 3.87 (3H, s, -OC$\underline{H_3}$), 7.11 (1H, dd, *J* = 2.4 Hz, *J* = 8.4 Hz, 4^1-H), 7.33 (3H, m, e, f, g-H), 7.39 (1H, m, 5^1-H), 7.43 (1H, m, 2^1-H), 7.50 (1H, m, 5^1-H), 7.61 (1H, d, *J* = 2.0 Hz, 5-H), 7.93 (2H, d, *J* = 8.8 Hz, d, h-H), 8.18 (1H, s, a-H), 8.37 (1H, d, *J* = 2.0 Hz, 7-H) δ_C (100 MHz, $CDCl_3$, ppm) 55.47, 113.98, 117.08, 120.45, 122.54, 124.26, 124.31, 125.36, 126.20, 126.94, 127.21, 128.81, 128.18, 129.30, 130.24, 130.38, 133.27, 135.84, 139.55, 139.55, 140.69, 144.22, 148.90, 151.24, 160.11 HRMS $C_{24}H_{15}{}^{79}Br^{81}BrN_4FO^+$ requires 555.9556, found 555.4212

4.7.3.5 6,8-Dibromo-2-(4-fluoropheny)-4-(4-phenyl-1*H*-1,2,3-triazol-1-yl) quinoline (153 o)

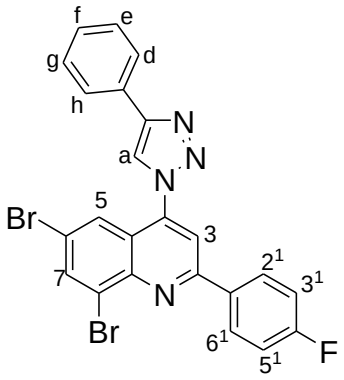

A stirred reaction of phenyl acetylene (0.11 g, 1.06 mmol), sodium ascorbate (0.21 g, 1.06 mmol) and $CuSO_4$. $5H_2O$ (0.07 g, 0.27 mmol) were added in EtOH: H_2O: THF (1:1:2) and **152 e** (0.22 g, 0.53 mmol) to afford a yellow solid **153 o** (0.19 g, 68.0 %) mp 237-240ºC, ν_{max} 2965, 2892, 2113, 1580, 1490, 1425, 1359, 1220, 1154, 1088, 1016, 826, 753, 687, 556, δ_H (400 MHz, $CDCl_3$, ppm) 7.22 (2H, m, 5^1, 3^1-H), 7.45 (1H, m, f-H), 7.51 (2H, m, e, g-H), 7.96 (2H, d, *J* = 7.6 Hz, d, h-H), 8.04 (1H, s, 3-H), 8.10 (1H, d, *J* = 2.0 Hz, 5-H), 8..26 (1H, d, *J* = 2.0 Hz, 7-H), 8.28 (1H, s, a-H), 8.32 (2H, m, 2^1, 6^1-H), δ_C (100 MHz, $CDCl_3$, ppm) 114.82, 116.28 (*J* = 22 Hz), 121.29, 121.64, 122.96, 124.41, 124.82, 126.02, 127.07, 129.03, 129.13, 129.33, 129.66 (*J* = 9 Hz), 133.42, 137.14, 137.57, 141.21, 145.32, 148.73, 156.69, 164.64 (*J* = 251 Hz) HRMS $C_{24}H_{15}{}^{79}Br^{81}BrN_4F^+$ requires 525.9450, found 525.3783

4.7.4 Synthesis of 6,8-dibromo-4(3-chlorophenyl)-1H-1,2,3-triazol-1-yl)-2-(phenyl) quinoline derivatives 153 p-q

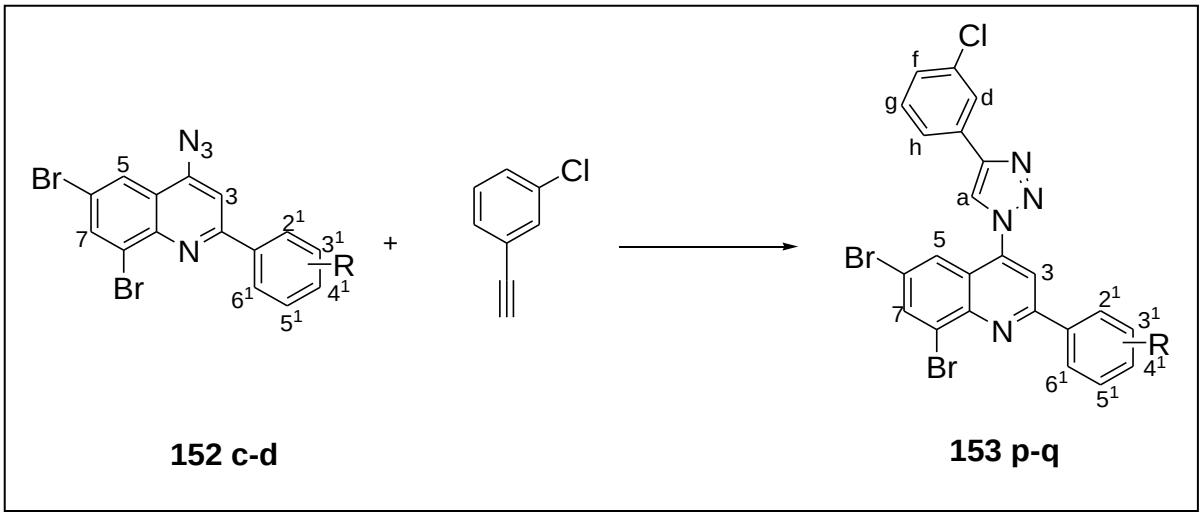

152 c-d **153 p-q**

A stirred reaction of phenyl acetylene (2 equiv.), sodium ascorbate (2 equiv.) and $CuSO_4$. $5H_2O$ (0.4 equiv.) were added in EtOH: H_2O: THF (1:1:2) and after 5 minutes, a mixture of 5 ml and **152 c–d** (1 mmol) were then added and refluxed for 4 hours. The mixture was then cooled down to room temperature and quenched with ice. The precipitate was then filtered and air dried to afford **153 p–q**

4.7.4.1 6,8-Dibromo-4-(4-(3-chlorophenyl)-1*H*-1,2,3-triazol-1-yl)-2-(4-methoxyphenyl) quinoline (153 p)

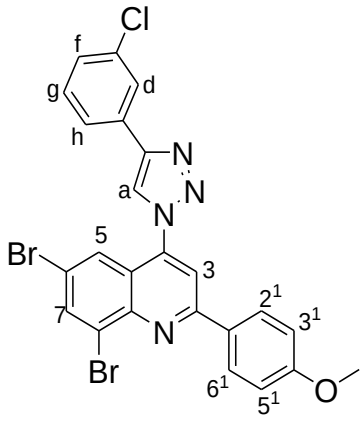

A stirred reaction of 1-chloro-3-ethynyl-phenyl (0.13 g, 1.01 mmol), sodium ascorbate (0.20 g, 1.01 mmol) and $CuSO_4$. $5H_2O$ (0.06 g, 0.25 mmol) were added in EtOH: H_2O: THF (1:1:2) and **152 c** (0.22 g, 0.50 mmol) were then added to afford a yellow solid **153 p** (0.23 g, 79.9 %) mp 260-264 ºC, ν_{max} 2973, 2030, 1613, 1507, 1465, 1335, 1244, 1163, 1006, 834, 777, 671, δ_H (400 MHz, $CDCl_3$, ppm) 3.89 (3H, s, -OC$\underline{H_3}$), 7.05 (2H, d, *J* = 8.4 Hz, 5^1, 3^1-H), 7.36 (1H, d, *J* = 2.0 Hz, 5-H), 7.40 (1H, s, f-H), 7.44 (1H, t, *J* = 8.0 Hz, h-H), 7.87 (1H, d, *J* = 8.0 Hz, d-H), 7.98 (3H, m, 2^1, 6^1, g-H), 8.16 (1H, s, a-H), 8.22 (1H, d, *J* = 2.0 Hz, 7-H), δ_C (100 MHz, $CDCl_3$, ppm) 55.48, 113.80, 122.74, 124.15, 125.79, 126.19, 126.75,128.98, 129.60, 130.44, 131.23, 131.83, 135.13, 137.54, 157.67, HRMS $C_{24}H_{15}{}^{79}Br^{81}BrN_4O^+$ requires 570.9281, found 570.9335

4.7.4.2 6,8-Dibromo-4-(4-(3-chlorophenyl-1*H*-1,2,3-triazol-1-yl)-2-(3-methoxyphenyl)- quinoline (153 q)

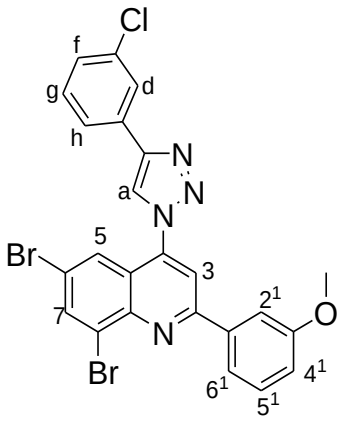

A stirred reaction of 1-chloro-3-ethynyl-phenyl (0.13 g, 0.92 mmol), sodium ascorbate (0.18 g, 0.92 mmol) and $CuSO_4$. $5H_2O$ (0.06 g, 0.23 mmol) were added in EtOH: H_2O: THF (1:1:2) and **152 d** (0.20 g, 0.46 mmol) were then added to afford a yellow solid **153 q** (0.07 g, 25.0 %) mp 127-131 ºC, ν_{max} 2993, 2901, 2333, 1581, 1520, 1458, 1321, 1229, 1029, 860, 753, 676, 660, δ_H (400 MHz, $CDCl_3$, ppm) 6.80 (1H, dd, *J* = 2.4 Hz, *J* = 8.4 Hz, 4^1-H), 7.11 (2H, m, f, h-H), 7.21 (1H, m, 6^1-H), 7.34 (2H, s, 2^1,5^1-H), 7.48 (1-H, t, *J* = 8.0 Hz, g-H), 7.85 (1H, d, *J* = 8.0 Hz, d-H), 7.93 (1H, d, *J* = 2.0 Hz, 5-H), 8.12 (1H, s, 3-H), 8.48 (1H, s, a-H), 8.50 (1H, d, *J* = 2.0 Hz, 7-H), δ_C (100 MHz, $CDCl_3$, ppm) 55.48, 113.84, 116.92, 120.43, 122.98, 124.14, 124.41, 125.22, 126.30, 126.94, 127.28, 129.17, 126.60, 130.24, 130.29, 130.48, 132.02, 133.08, 135.15, 138.97, 139.62, 144.22, 151.24, 160.12, $C_{24}H_{15}{}^{79}Br^{81}BrN_4O^+$ requires 570.9281, found 570.4742

4.8 Synthesis of quinoline-1,2,3-triazole carbaldehyde derivatives 154 a–b

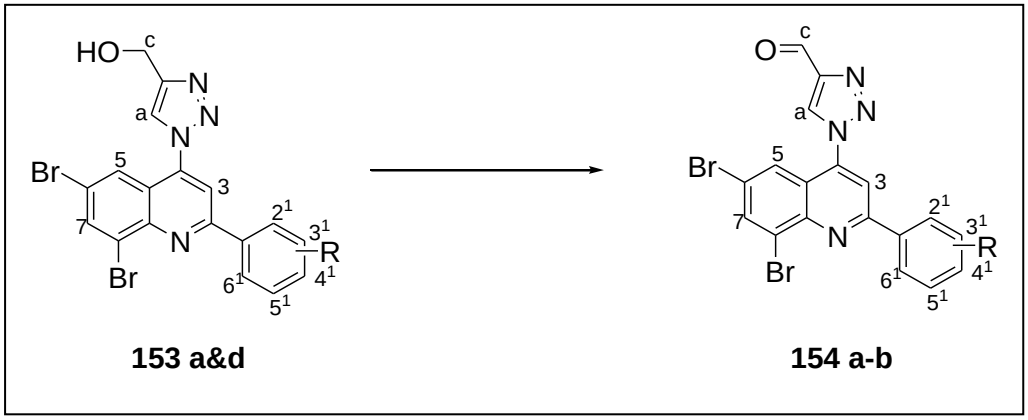

4.8.1 1-(6,8-Dibromo-2-phenylquinolin-4-yl)-1H-1,2,3-triazole-4-carbaldehyde (154 a)

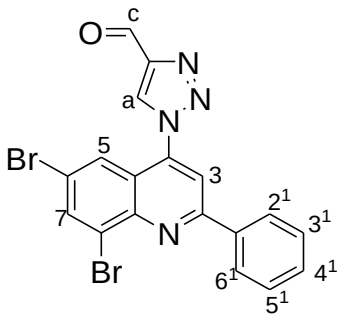

A stirred reaction of **153 a** (0.36 g, 0.77 mmol) and Jones Reagent (0.24 g, 0.93 mmol) in acetone were stirred at 0º and the completion of the reaction was monitored using TLC chromatography. The mixture was then quenched with ice cold water and the precipitates were filtered to afford a yellow solid **154 a** (0.34 g, 98.0 %), mp 162-168 ºC ν_{max} 2914, 2814, 1697, 1592, 1533, 1472, 1428, 1335, 1241, 1030, 960, 867, 773, 691, 563, 480, δ_H (400 MHz, $CDCl_3$, ppm) 7.45 (1H, d, *J* = 2.0 Hz), 7.48 (1H, s, 3-H), 7.58 (3H, m, 5^1, 4^1, 3^1-H), 7.84 (2H, d, *J* = 6.8 Hz, 2^1, 6^1-H), 8.43 (1H, d, *J* = 2.0 Hz, 7-H), 8.60 (1H, s, a-H), 10.33 (1H, s, -CO<u>H</u>), δ_C (100 MHz, $CDCl_3$, ppm) 123.58, 124.60, 124.78, 127.57, 128.13, 128.42, 128.68, 128.77, 129.31, 129.39, 129.77, 131.38, 132.33, 134.39, 139.38, 144.31, 151.55, 184.13 HRMS $C_{18}H_{10}{}^{81}Br^{81}BrN_4O^+$ requires 460.9180, found 460.4131

4.8.2 1-(6,8-Dibromo-2-(3-methoxyphenyl)quinolin-4-yl)-1H-1,2,3-triazole-4-carbaldehyde (154 b)

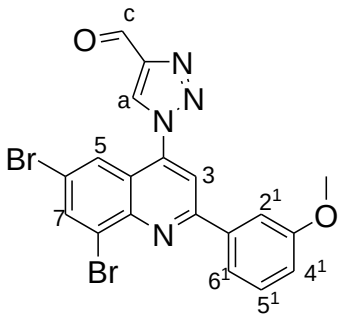

A stirred reaction of **153 d** (0.26 g, 0.53 mmol) and Jones Reagent (0.16 g, 0.64 mmol) in acetone were stirred at 0 º and the completion of the reaction was monitored using TLC chromatography. The mixture was then quenched with ice cold water and the precipitates were filtered to afford a yellow solid **154 b** (0.12 g, 45.0

%), mp 126-131 ºC ν_{max} 3018, 1697, 1601, 1592, 1533, 1381, 1335, 1276, 1241, 1112, 1030, 983, 761, 691, 645, 551, δ_H (400 MHz, $CDCl_3$, ppm) 3.86 (3H, s, -OC<u>H</u>$_3$), 7.10 (1H, dd, *J* = 2.4 Hz, *J* = 8.4 Hz), 4^1-H), 7.31 (1H, d, *J* = 7.6 Hz, 5^1-H), 7.41 (3H, m, 2^1, 6^1, 5-H), 8.40 (1H, d, *J* = 2 Hz, 7-H), 8.55 (1H, s, a-H), 10.29 (1H, s, -CO<u>H</u>), δ_C (100 MHz, $CDCl_3$, ppm) 55.48, 114.03, 117.19, 120.33, 120.40, 123.64, 124.60, 124.80, 128 .68, 130.45, 132.27, 138.55, 144.24, 147.99, 151.29, 160.17, 184.11, 207.27 HRMS $C_{19}H_{12}{}^{79}Br^{81}BrN_4O_2^+$ requires 488.9307, found 488.4302

4.9 Synthesis of Schiff base ligands 155 a-b

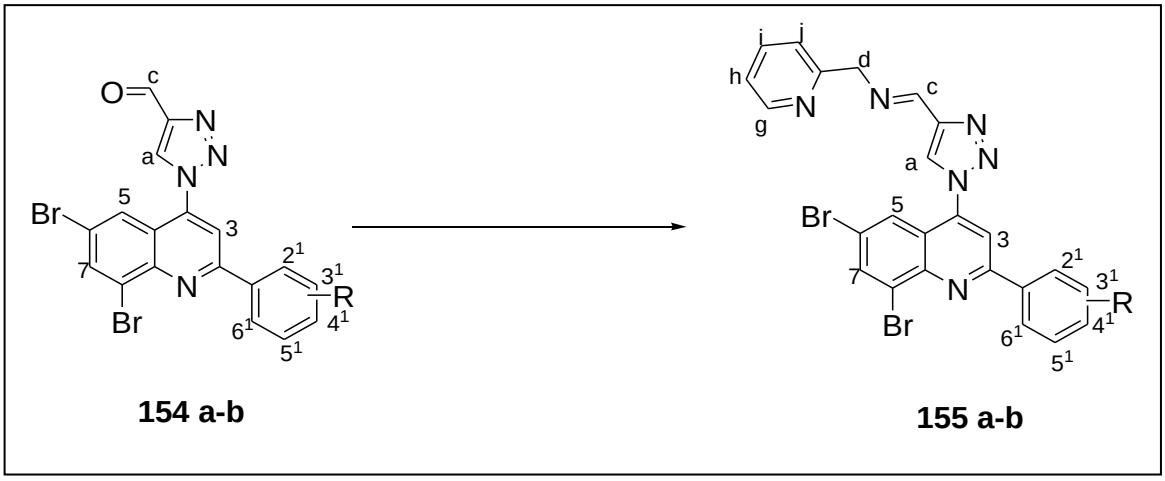

4.9.1 (*E*)-*N*-(1-(6,8-dibromo-2-phenylquinolin-4-yl)-1*H*-1,2,3-triazol-4-yl)methylene)(pyridine-2-yl)methanamine (155 a)

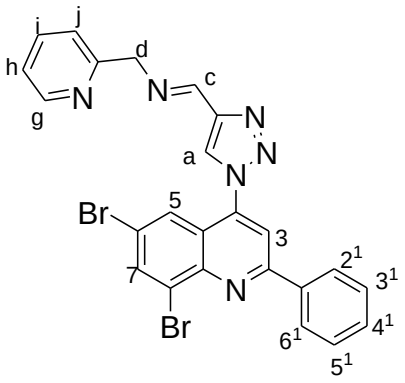

A stirred reaction of **154 a** (0.15 g, 0.33 mmol) in a Schlenk tube in methanol, $NaHCO_3$ (0.03 g, 0.33 mmol) and 2-picolylamine (0.04 g, 0.33 mmol) were added respectively, the mixture was under nitrogen gas for 24 h. the reaction was then added ice cold water and the precipitates were filtered to afford yellow solid **155 a**

(0.03 g, 18.0 %), mp 147-151 ºC, ν_{max} 3087, 2907, 1578, 1503, 1541, 1345, 1251, 962, 844, 762, 697, 546, 497, δ_H (400 MHz, $CDCl_3$, ppm) 4.62 (2H, d, *J* = 3.2 Hz, -C<u>H</u>$_2$N), 7.27 (2H, m, h, j-H), 7.45 (4H, m, 3^1,4^1, 5^1,3-H), 7.72 (3H, m, 2^1,6^1, i-H), 8.08 (2H, m, 5, 7-H), 8.17 (1H, s, a-H), 8.33 (1H, s, c-H), 8.66 (1H, d, J = 4.0 Hz, g-H), δ_C (100 MHz, $CDCl_3$, ppm) 47.48, 119.19, 121.76121.87, 123.10, 123.79, 124.51, 124.85, 128.07, 128.28, 128.69, 128.97, 129.74, 129.77, 130.50, 137.54, 138.50, 143.16, 148.79, 153.57, 153.86 HRMS $C_{24}H_{16}{}^{81}Br^{81}BrN_6^+$ requires 550.9762, found 550.6292

4.9.2 (*E*)-*N*-(1-(6,8-dibromo-2-(3-methoxyphenyl)quinolin-4-yl)-1*H*-1,2,3-triazol-4-yl)methylene)(pyridine-2-yl)methanamine (155 b)

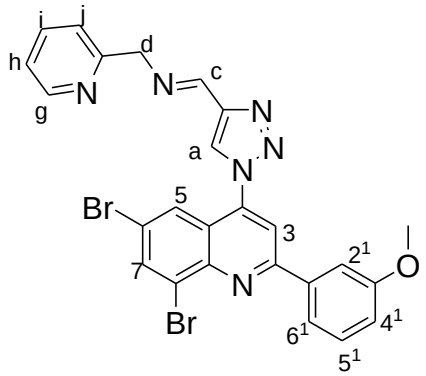

A stirred reaction of **154 b** (0.17 g, 0.35 mmol) in a Schlenk tube in methanol, $NaHCO_3$ (0.03 g, 0.35 mmol) and 2-picolylamine (0.04 g, 0.35 mmol) were added respectively, the mixture was under nitrogen gas for 24 h. the reaction was then added ice cold water and the precipitates were filtered to afford yellow solid **155 b** (0.04 g, 21.4 %), mp 151-155 ºC, ν_{max} 3089, 2902, 1568, 1533, 1499, 1428, 1346, 1241, 1136, 1030, 983, 878, 773, 691, 539, 445, δ_H (400 MHz, $CDCl_3$, ppm) 3.84 (3H, s, -OC<u>H</u>$_3$), 4.63 (2H, d, *J* = 3.2 Hz, -C<u>H</u>$_2$N), 6.98 (2H, m, 4^1, j-H), 7.16 (1H, m, 5^1-H), 7.29 (4H, m, 6^1,2^1, h, 3-H), 7.72 (1H, t, *J* = 7.2 Hz, *J* = 6.8 Hz, i-H), 8.16 (3H, m, a, 5, 7-H), 8.32 (1H, s, c-H), 8.66 (1H, d, *J* = 4.0 Hz, g-H), δ_C (100 MHz, $CDCl_3$, ppm) 47.41, 55.37, 113.54, 113.59, 115.49, 115.74, 119.22, 120.24, 120.33 121.83, 123.07, 124.17, 124.47, 127.30, 131.29, 137.23, 137.53, 138.37, 138.43, 139.33, 143, 06, 148.84, 153.34, 153.85, 159.64 $C_{25}H_{18}{}^{79}Br^{79}BrN_6O^+$ requires 575.9909, found 575.4133

4.10 Synthesis of 6.8-dibromoquinoline-3-fluorophenyl-triazolyl ruthenium dichloride p-cymene complexes 156 a–b

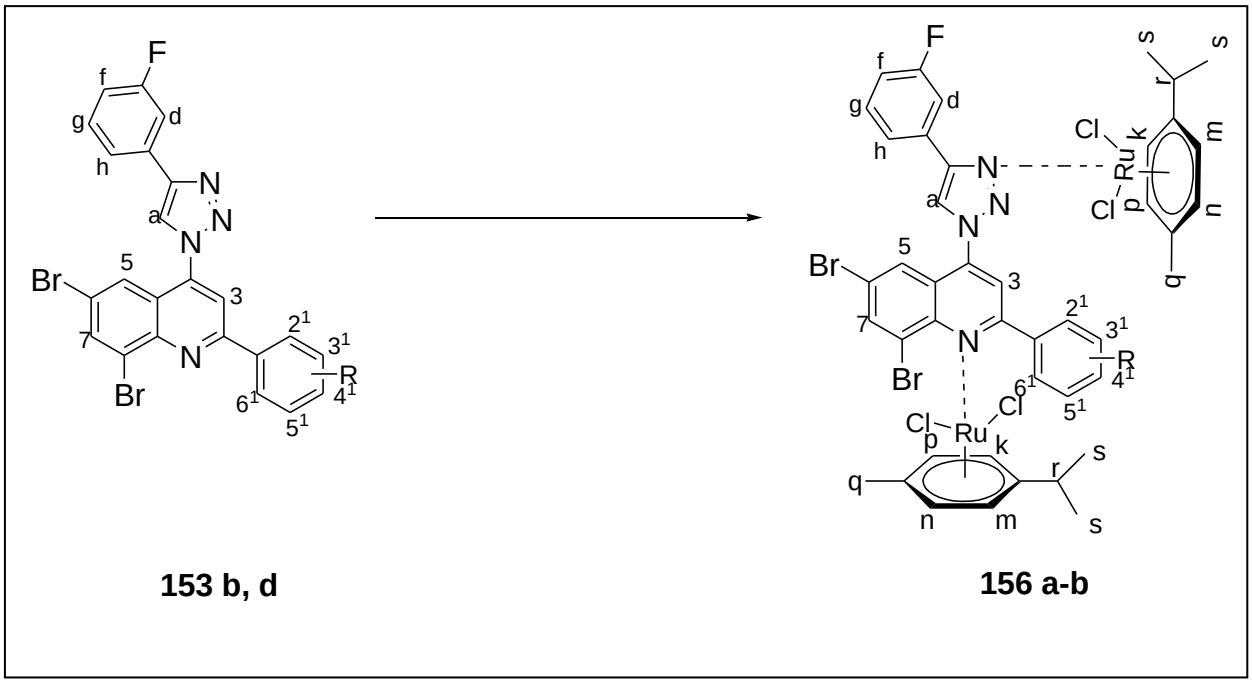

4.10.1 6,8-Dibromo-4-(4-(3-fluorophenyl-1*H*-1,2,3-triazol-1-yl)-2-p-tolyl quinoline ruthenium dichloro p-cymene complex (156 a)

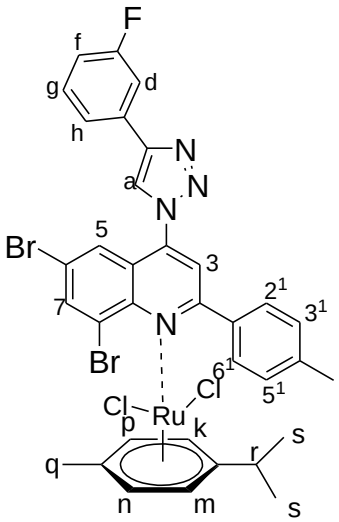

A stirred mixture of **153 b** (0.10 g, 0.18 mmol) in Dichloromethane and ruthenium p-cymene dichloride dimer (0.11 g, 0.18 mmol) was added to afford a brown solid **156 a** (0.09 g, 56.2%), mp 214-221 ºC, ν_{max} 3050, 3030, 2960, 2919, 2867, 1585, 1531, 1472, 1383, 1334, 1257, 1054, 1017, 871, 783, 746, 673, 558, 501, 451 δ_H (400

MHz, $CDCl_3$, ppm) 1.26 (6H, d, *J* = 6.4 Hz, s-H), 2.14 (3H, s, q-H), 2.46 (3H, s, -$C\underline{H_3}$), 2.90 (1H, t, *J* = 6.0 Hz, r-H), 5.33 (2H, d, *J* = 5.6 Hz, m, k-H), 5.45 (2H, d, *J* = 5.6 Hz, n, p-H), 7.12 (1H, t , *J* = 7.6 Hz, f-H), 7.35 (2H, d, *J* = 8 Hz, 5^1, 3^1-H), 7.39 (1H, d, *J* = 2 Hz, 5-H), 7.47 (1H, m, g-H), 7.73 (2H, m, g, h-H), 7.84 (2H, d, *J* = 8.4 Hz, 2^1, 6^1-H), 8.18 (1H, s, a-H), 8.22 (1H, d, *J* = 2 Hz, 7-H), δ_C (100 MHz, $CDCl_3$) 17.92, 20.49, 21.12, 29.59, 79.48, 80.27, 95.72, 1100.17, 112.02 (*J* = 23 Hz), 114.04, 114.79 (*J* = 21 Hz), 120.63 (*J* = 3 Hz), 121.90, 123.11, 123.72, 124.89, 125.62, 125.79, 126.52, 128.04, 128.97, 129.74, (*J* = 8 Hz), 130.58, 133.31, 136.44 (*J* = 9 Hz), 137.29, 139.49, 141.64, 157.18, 162.20 (*J* = 245 Hz)

4.10.2 6,8-Dibromo-4-(4-(3-fluorophenyl-1*H*-1,2,3-triazol-1-yl)-2-(3-methoxyphenyl)- quinoline ruthenium dichloro p-cymene (156 b)

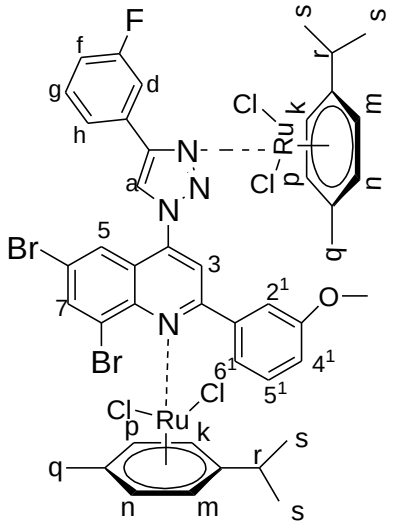

A stirred mixture of **153 d** (0.1 g, 0.19 mmol) in Dichloromethane and ruthenium p-cymene dichloride dimer (0.12 g, 0.19 mmol) was added to afford a brown solid **156 b** (0.11 g, 73 %), mp 165-170 ºC, ν_{max} 3051, 2960, 2923, 2868, 1584, 1537, 1463, 1382, 1324, 1258, 1087, 1016, 863, 791, 683, 617, 525, 451 δ_H (400 MHz, $CDCl_3$, ppm) 1.26 (12H, d, *J* = 6.9 Hz, s-H), 2.14 (6H, s, q-H), 2.90 (2H, t, *J* = 6.0 Hz, r-H),3.87 (3H, s, -CH_3), 5.33 (2H, d, *J* = 5.6 Hz, m, k-H), 5.45 (2H, d, *J* = 5.6 Hz, n, p-H), 7.11 (2H, m, 4^1, f-H), 7.32 (1H, d, *J* = 7.6 Hz, 2^1-H), 7.39 (1H, m, 5^1-H), 7.44 (2H, m, 6^1, d-H), 7.58 (1H, d, *J* = 2 Hz, 5-H), 7.70 (2H, m, g, h-H), 8.21 (1H, s, a-H), 8.37 (1H, d, *J* = 2 Hz, 7-H), δ_C (100 MHz, $CDCl_3$) 17.93, 21.13, 29.59, 54.44, 79.48, 80.28, 95.72, 100.17, 112.21 (*J* = 23 Hz), 112.95, 115.14 (*J* = 24 Hz), 116.04, 119.39,

120.83 (*J* = 3 Hz), 123.12, 123.34, 124.20, 126.22, 129.35, 129.80 (*J* = 8 Hz), 132.06, 134.74, 138.56, 138.64, 143.17, 150.19, 159.06, 162.16 (*J* = 246 Hz)

4.11 Single crystal X-ray diffraction

Intensity data was determined on a Bruker Venture D8 Photon CMOS diffractometer with graphite-monochromated $MoKa_1$ (l = 0.71073 Å) radiation at 173 K using an Oxford Cryostream 600 cooler. Data reduction was carried out using the program SAINT+, version 6.02 [3] and empirical absorption corrections were made using SADABS [3] Space group assignments was made using *XPRE* [3]. The structure was solved in the *WinGX* [4] Suite of programs, using intrinsic phasing through *SHELXT* [5] and refined using full-matrix least-squares/difference Fourier techniques on F^2 using *SHELXL-2017* [5] All C bound hydrogen atoms were placed at idealized positions and refined as riding atoms with isotropic parameters 1.2 times those of their parent atoms. The asymmetric unit consist of two symmetry independent molecules. The positional disorder of the F atoms was resolved by finding alternate positions in the difference map and then refining their site occupancies to final values of 0.641(4) and 0.359(4) for both symmetry independent molecules. Diagrams and publication material were generated using *ORTEP-3* [4] and *PLATON* [6].

4.12 Biological evaluation MTT assay method

The MTT assay was used to assess the cytotoxicity of synthetic compounds on MDA-MB 231 cells. Cells (1×10 4 cells/well) were seeded overnight for attachment, followed by treatment. After 24 hours of treatment, 5 mg/mL of MTT solution was added into the wells and further incubated for 2 hours. Following incubation, 100 µL DMSO was added to dissolve formazan crystals, and absorbance was measured at 560 nm using BioRad microplate reader. The concentration lethal to 50% of the cells (IC 50) was calculated using the AAT Bioquest online calculator.

4.13 Molecular Docking Method

The rationale behind this study is to throw the light on the binding propensities of ligands (Sorafenib standard and 7 ligands(**153 h**, **153 m**, **153 o**, **153 g**, **153 j**, **153 i** and **153 f**)) and (PDB IDs: 3WZE). Prior to the docking study with ligands, the protein files were drawn in ChemDraw 3 and protein data bank, respectively. Before performing molecular interaction studies, VEGFR-2 protein was further curated for

missing side-chain residues using openMM simulation tool (https://openmm.org/). Molecular docking studies were performed using Autodock v 4.2.6. Binding cavity for the ligands in VEGFR-2 protein was determined from the predefined co-crystallized X-ray structure from RCSB PDB. The residue positions were calculated within 3 Å space from the co-crystallized ligand. After the cavity selection in each case, the co-crystallized ligands were removed using Chimera tool (https://www.cgl.ucsf.edu/chimera/) and subsequently energy was minimized using steepest descent and conjugate gradient algorithm. Then finally, merging the nonpolar hydrogens, both receptor and target compounds were saved in pdbqt format. Grid boxes were created with specific dimensions in 0.3 Å spacing. Following the Lamarckian Genetic Algorithm (LGA), docking studies of the protein-ligand complex were performed to achieve the lowest free energy of binding (ΔG). During molecular docking studies, three replicates were performed having the total number of solutions computed 50 in each case, with population size 500, number of evaluations 2500000, maximum number of generations 27000 and rest the default parameters were allowed. After docking, the RMSD clustering maps were obtained by re-clustering with a clustering tolerance 0.25 Å, 0.5 Å and 1 Å, respectively, to obtain the best cluster having lowest energy score with high number of populations.

4.14 References

1. Khoza, T.A., Maluleka, M.M., Mama, N. and Mphahlele, M.J., 2012. Synthesis and photophysical properties of 2-aryl-6,8-bis(arylethenyl)-4-methoxyquinolines. *Molecules*, *17*(12), pp.14186-14204.

2. Mphahlele, M.J. and Oyeyiola, F.A., 2014. One-pot site-selective Sonogashira cross-coupling–heteroannulation of the 2-aryl-6,8-dibromoquinolin-4(1H)-ones: synthesis of novel 6-H-pyrrolo[3,2,1-ij]quinolin-6-ones. *Journal of Chemical Research*, *38*(9), pp.535-538.

3. Bruker, S.A.I.N.T., 1999. Version 6.02 (includes XPREP and SADABS). *Bruker AXS Inc., Madison, Wisconsin, USA*.

4. Farrugia, L.J., 2012. WinGX and ORTEP for Windows: an update. *Journal of Applied Crystallography*, *45*(4), pp.849-854.

5. Sheldrick, G.M., 2015. Crystal structure refinement with SHELXL. *Acta Crystallographica Section C: Structural Chemistry*, *71*(1), pp.3-8.

6. Spek, A.L., 2009. Structure validation in chemical crystallography. *Acta Crystallographica Section D: Biological Crystallography*, *65*(2), pp.148-155.

SUPPLEMENTARY DATA

^{1}H ^{13}C NMR, IR and HRMS spectra **148 a–e**

^{1}H ^{13}C NMR, IR and HRMS spectra **149 a–e**

^{1}H ^{13}C NMR, IR and HRMS spectra **150 a–e**

^{1}H ^{13}C NMR, IR and HRMS spectra **151 a–e**

^{1}H ^{13}C NMR, IR and HRMS spectra **152 a–e**

^{1}H ^{13}C NMR, IR and HRMS spectra **153 a–q**

^{1}H ^{13}C NMR, IR and HRMS spectra **154 a–e**

^{1}H ^{13}C NMR, IR and HRMS spectra **155 a–b**

^{1}H ^{13}C NMR spectra **156 a–b**

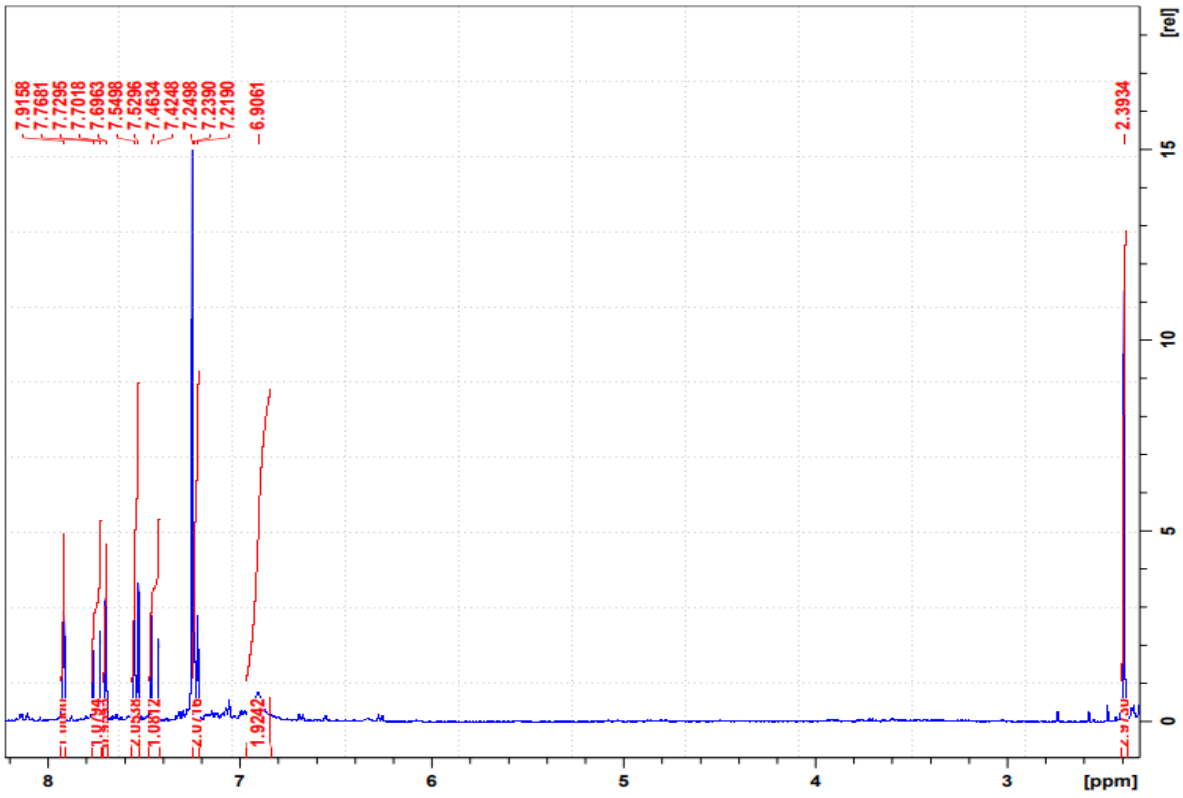

Figure 1. The ^{1}H NMR of compound **148 b**

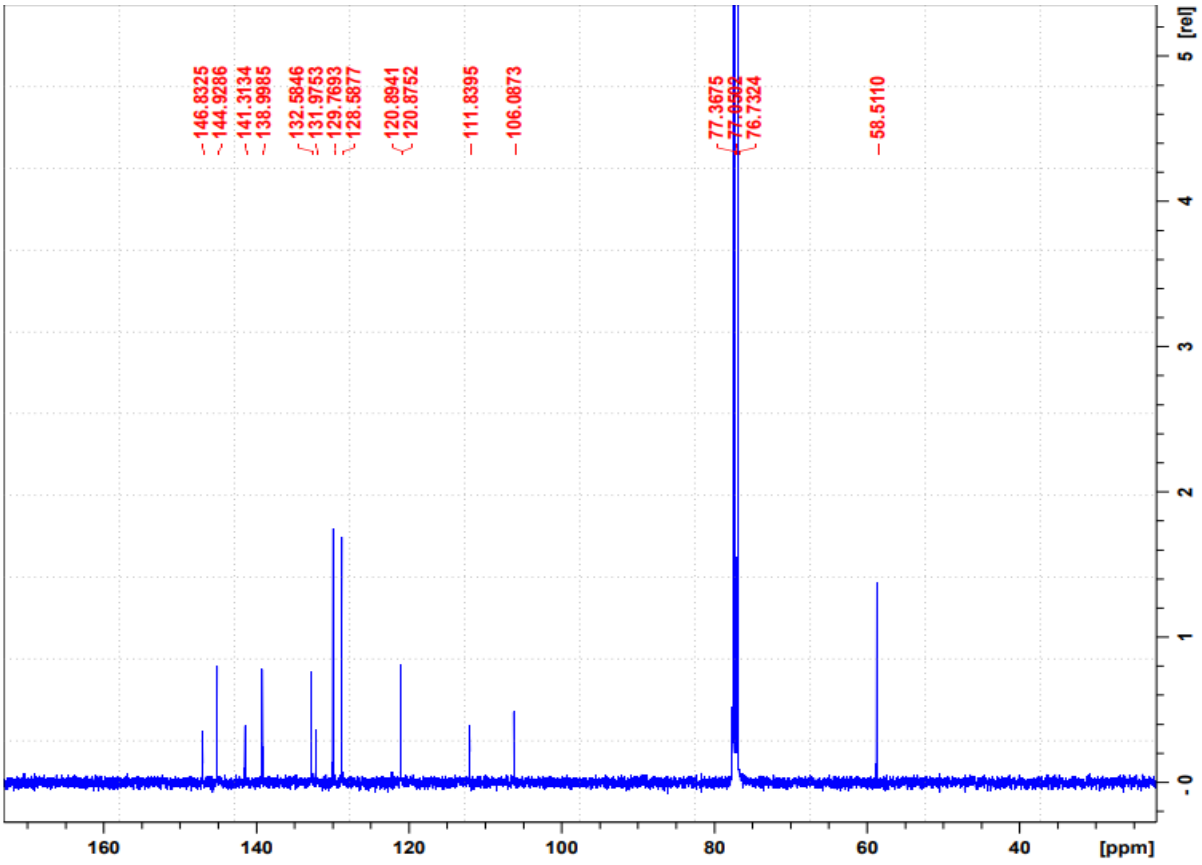

Figure 2. The ^{13}C NMR spectrum of compound **148 b**

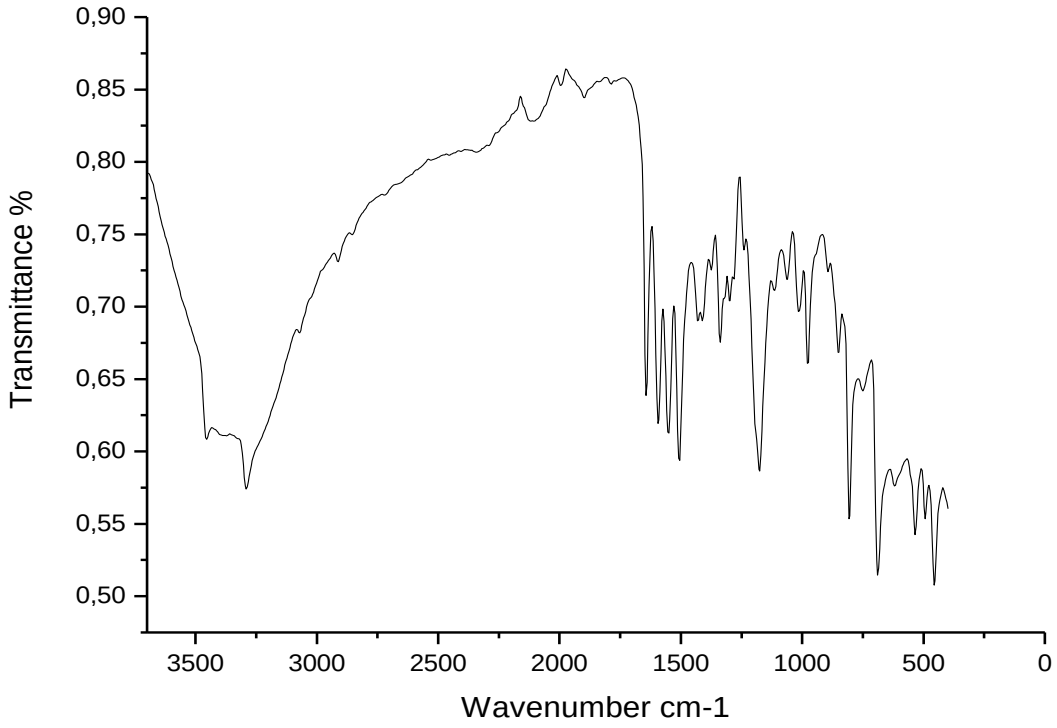

Figure 3. The FTIR spectrum of compound **148 b**

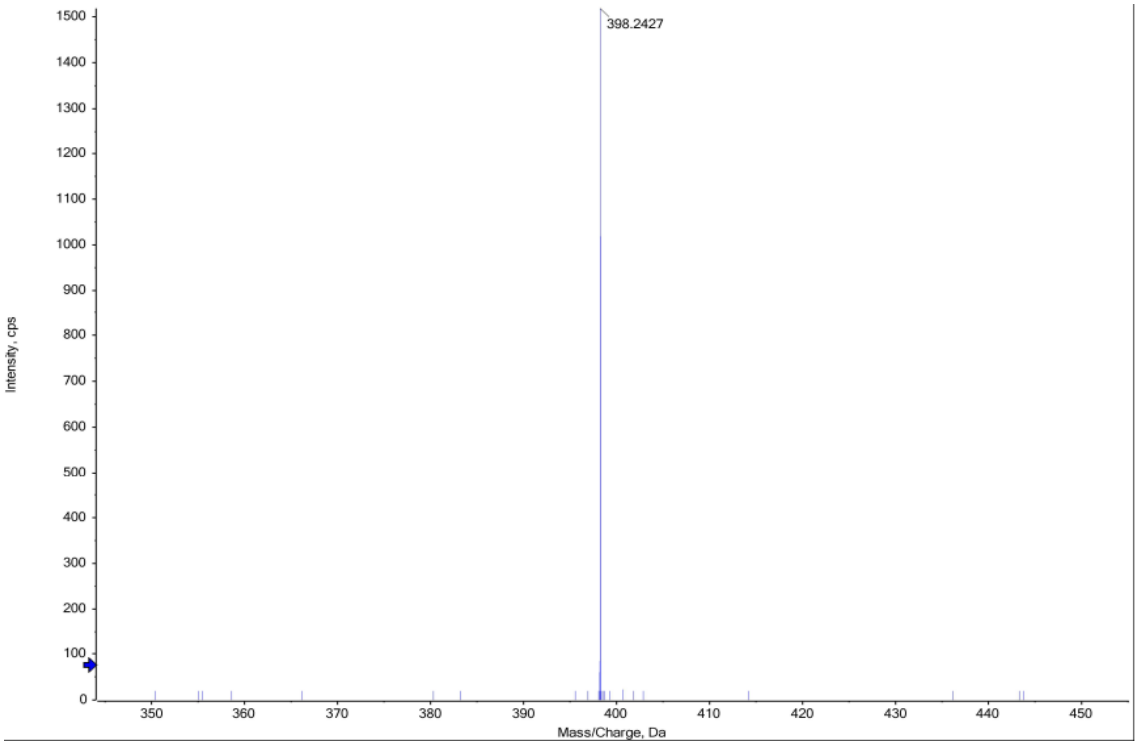

Figure 4. The HRMS spectrum of compound **148 b**

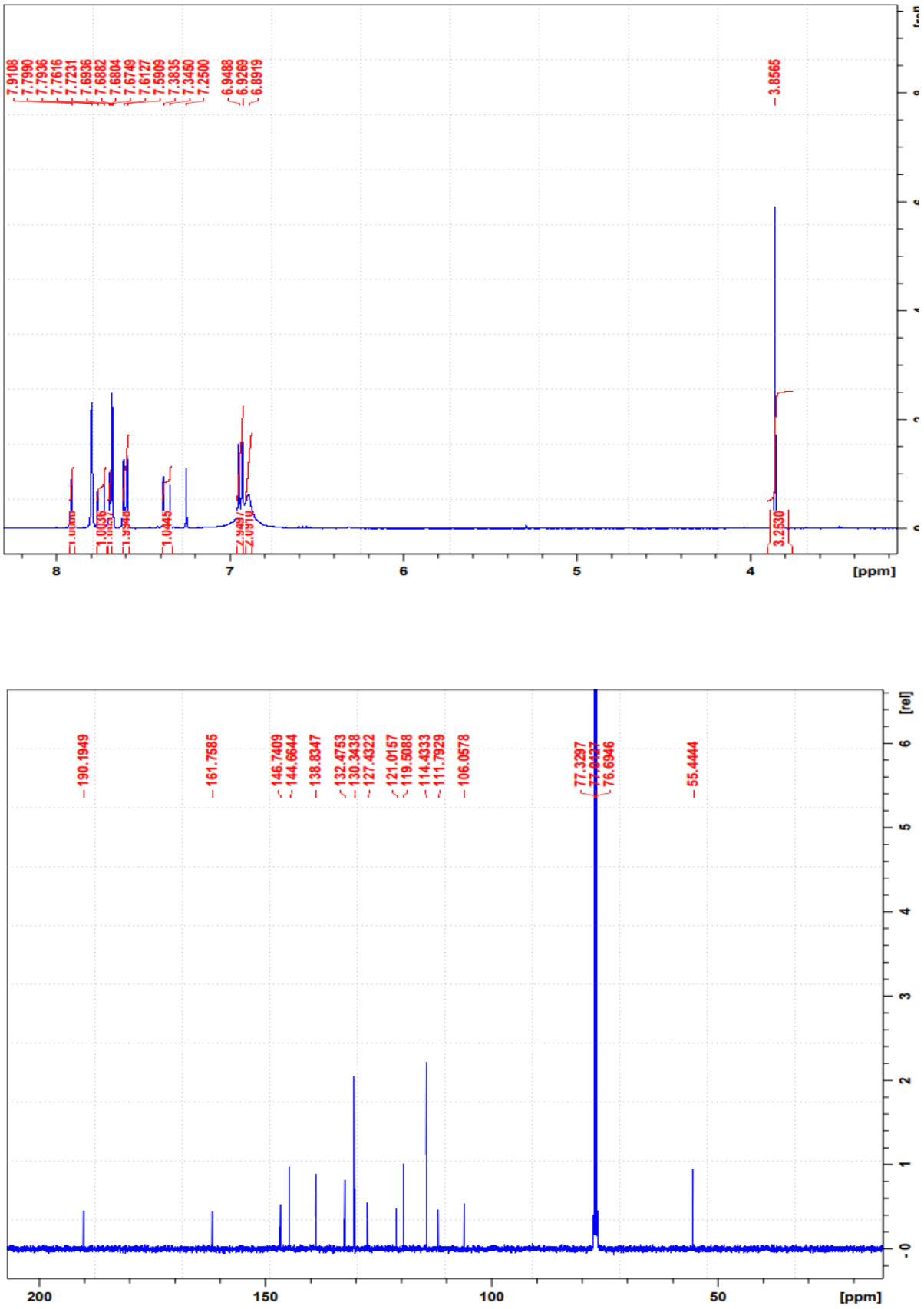

Figure 5. The ^{1}H NMR spectrum of compound **148 c**

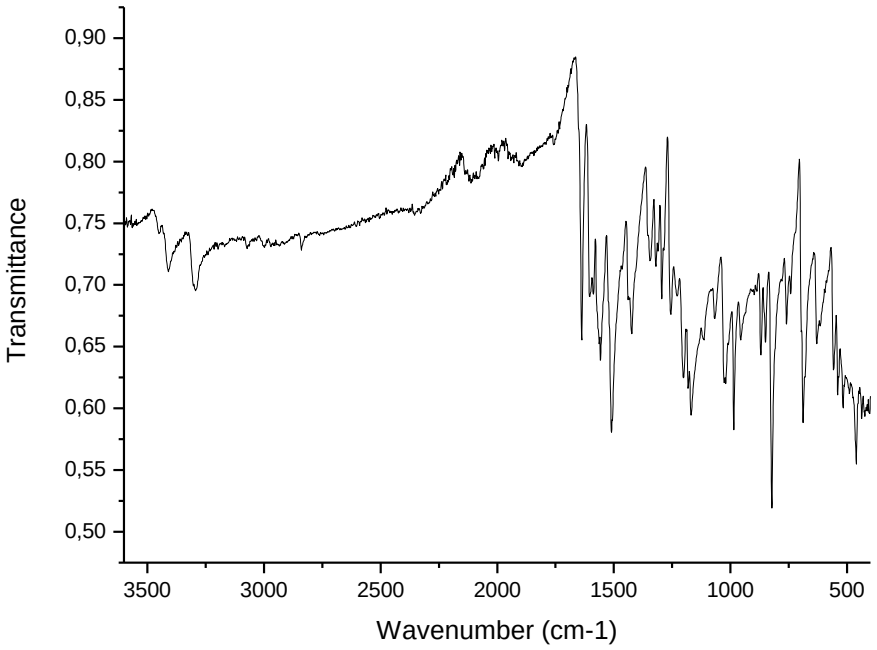

Figure 6. The ^{13}C NMR spectrum of compound **148 c**

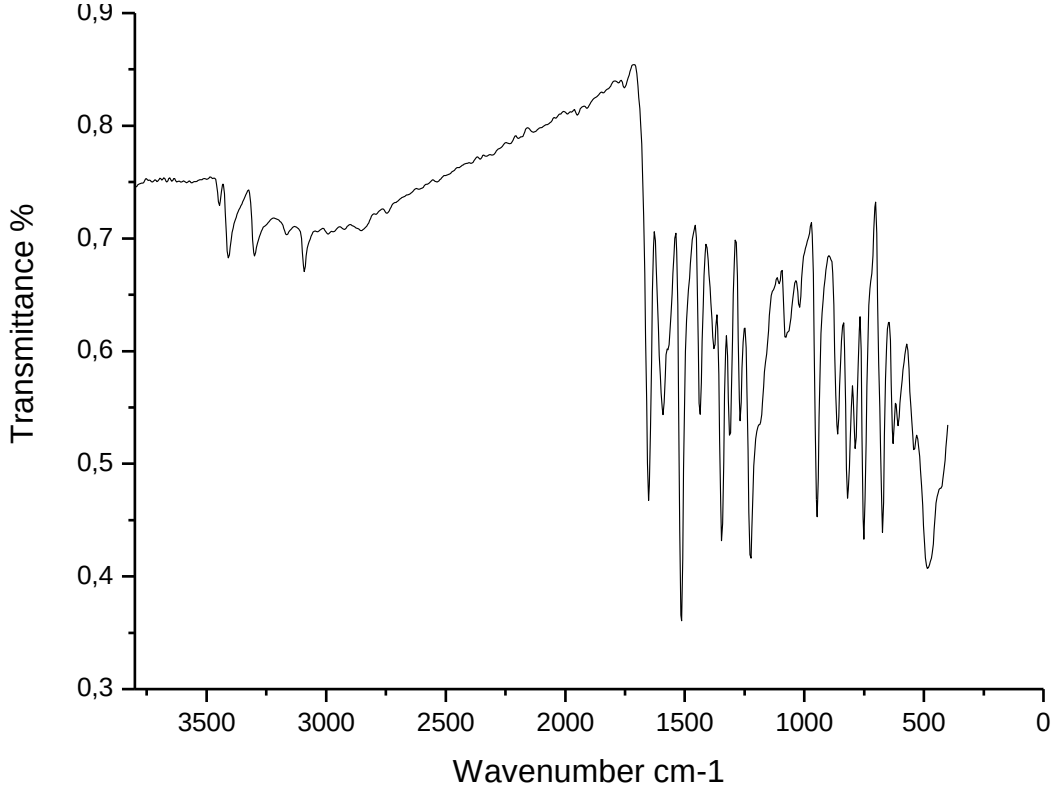

Figure 7. The FTIR spectrum of compound **148 c**

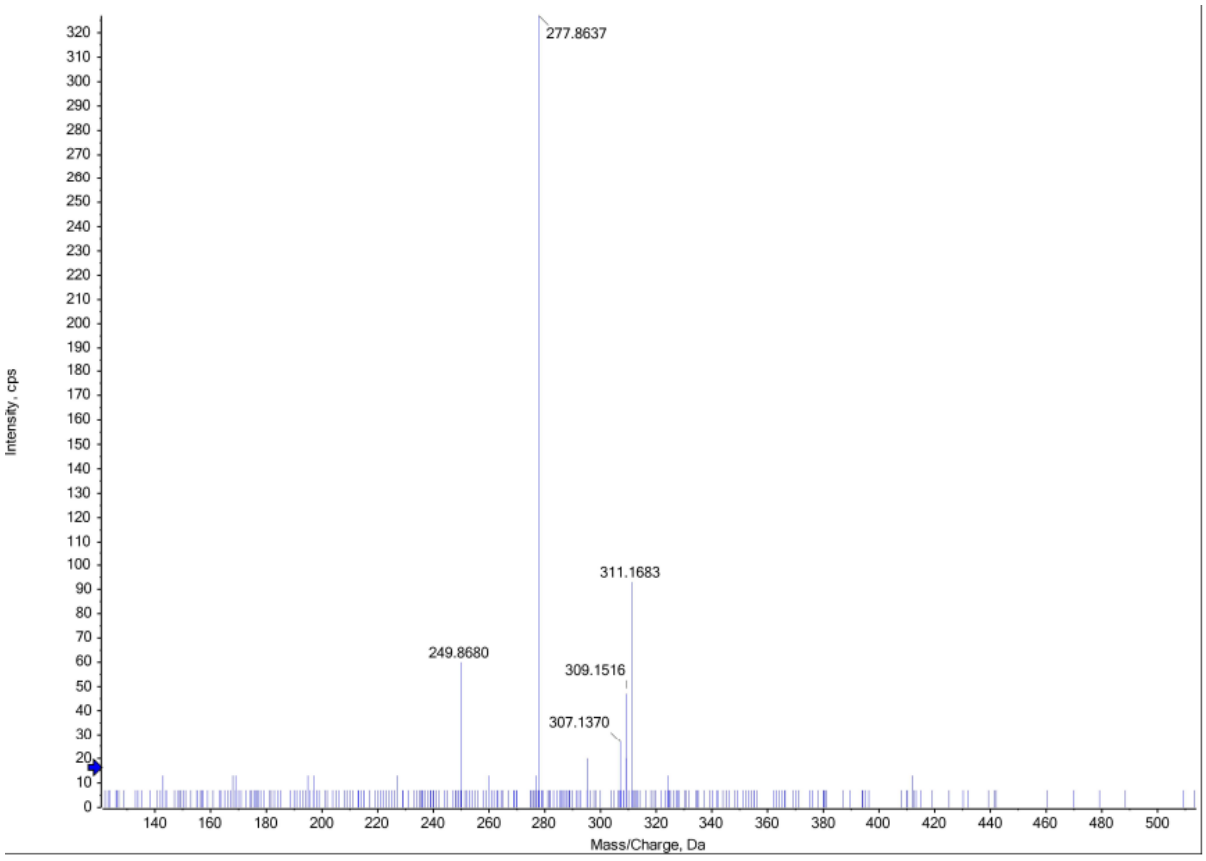

Figure 8. The HRMS spectrum of compound **148 c**

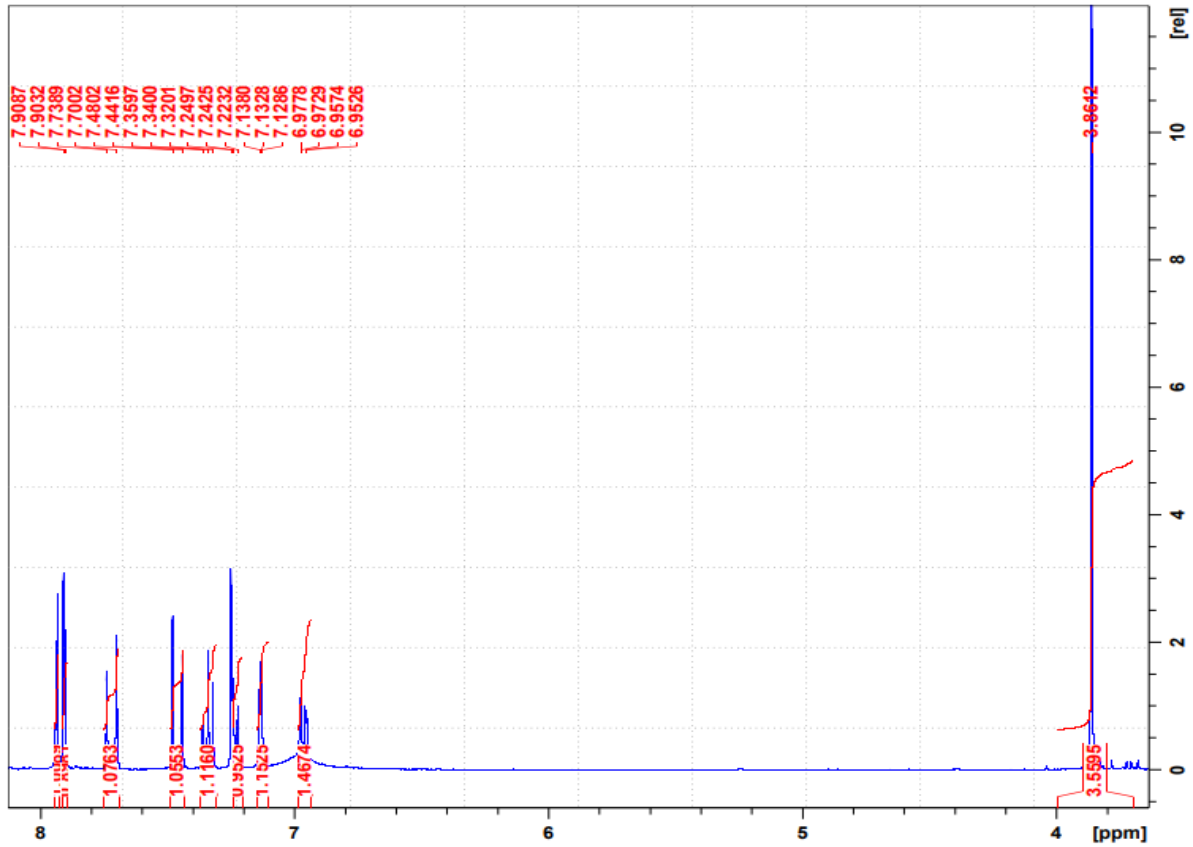

Figure 9. The ^{1}H NMR spectrum of compound **148 d**

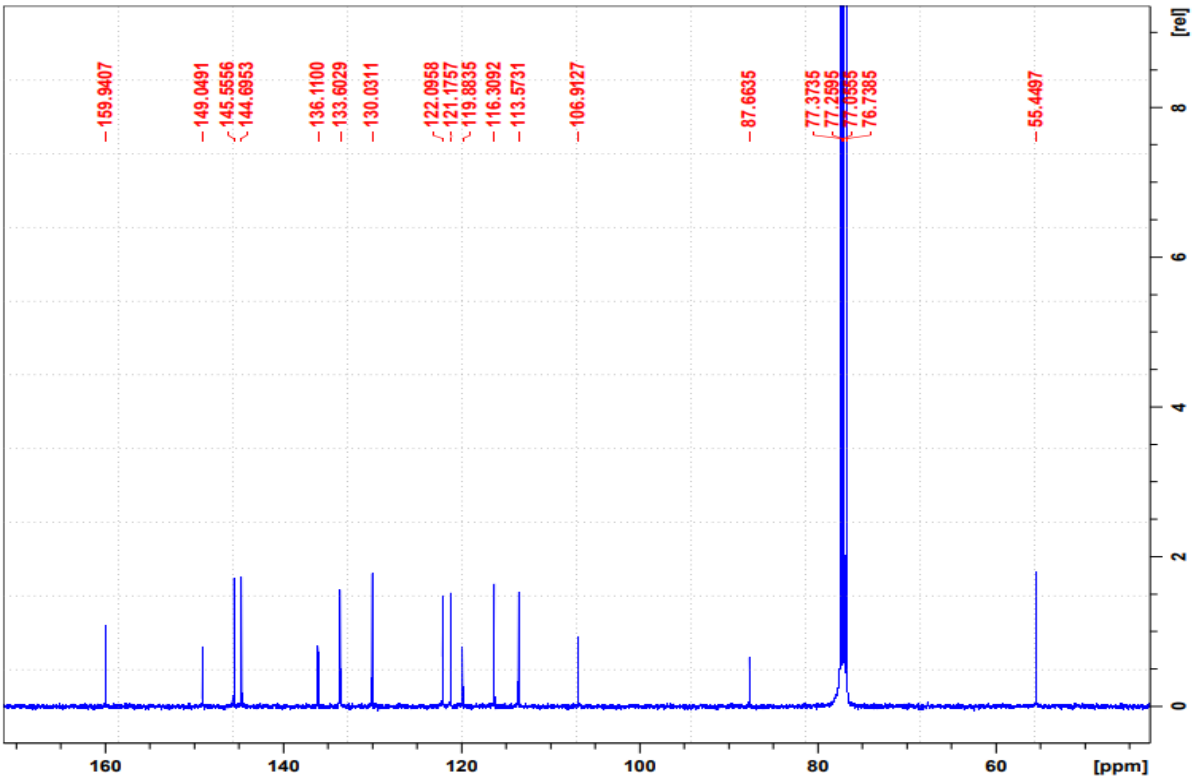

Figure 10. The ^{13}C NMR spectrum of compound **148 d**

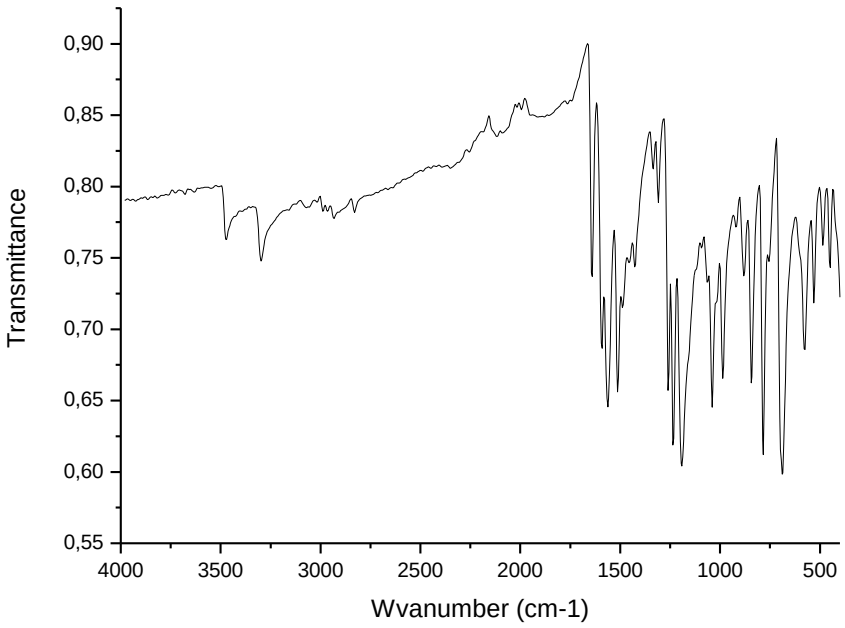

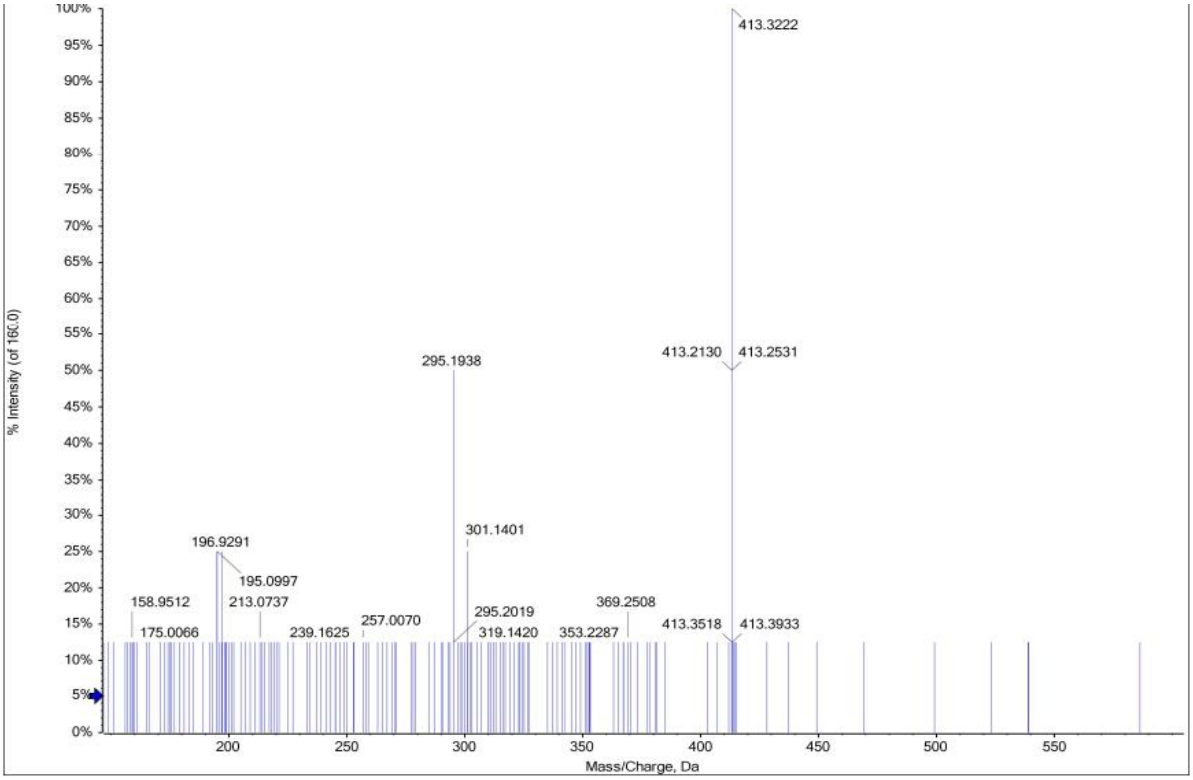

Figure 11. The FTIR spectrum of compound **148 d**

Figure 12. The HRMS spectrum of compound **148 d**

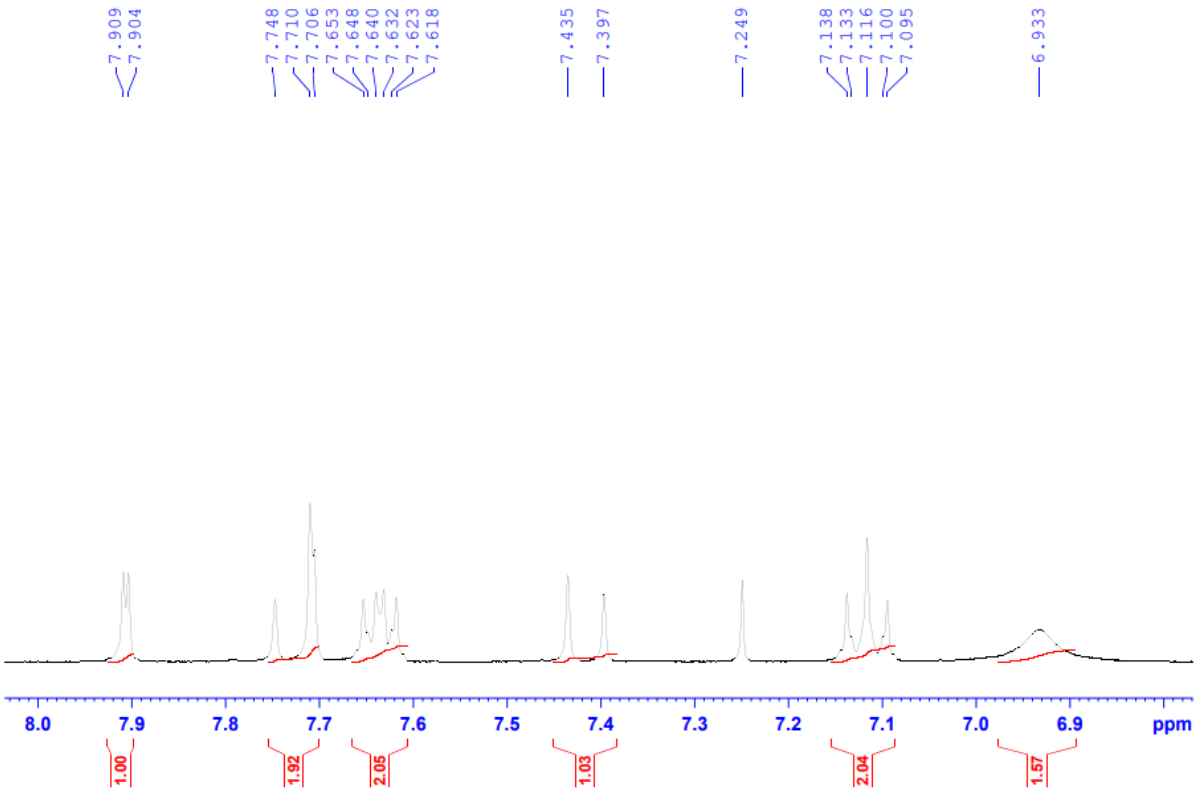

Figure 13. The ^{1}H NMR spectrum of compound **148 e**

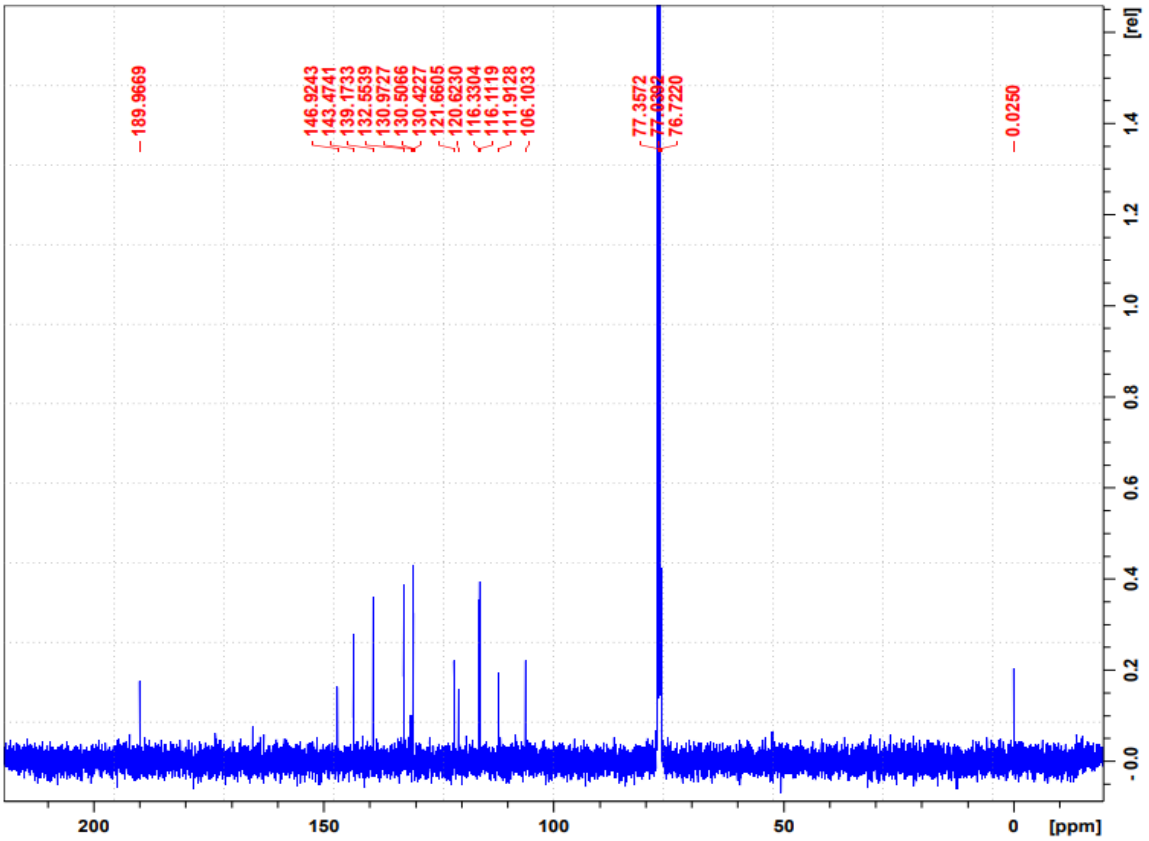

Figure 14. The ^{13}C NMR spectrum of compound **148 e**

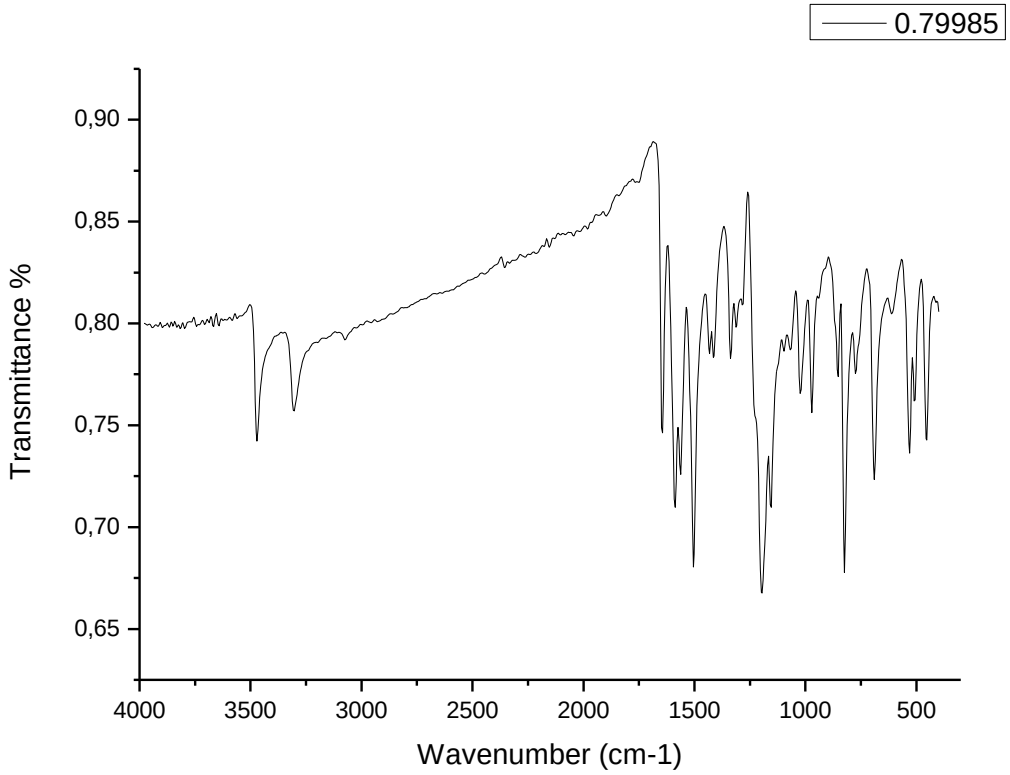

Figure 15. The FTIR spectrum of compound **148 e**

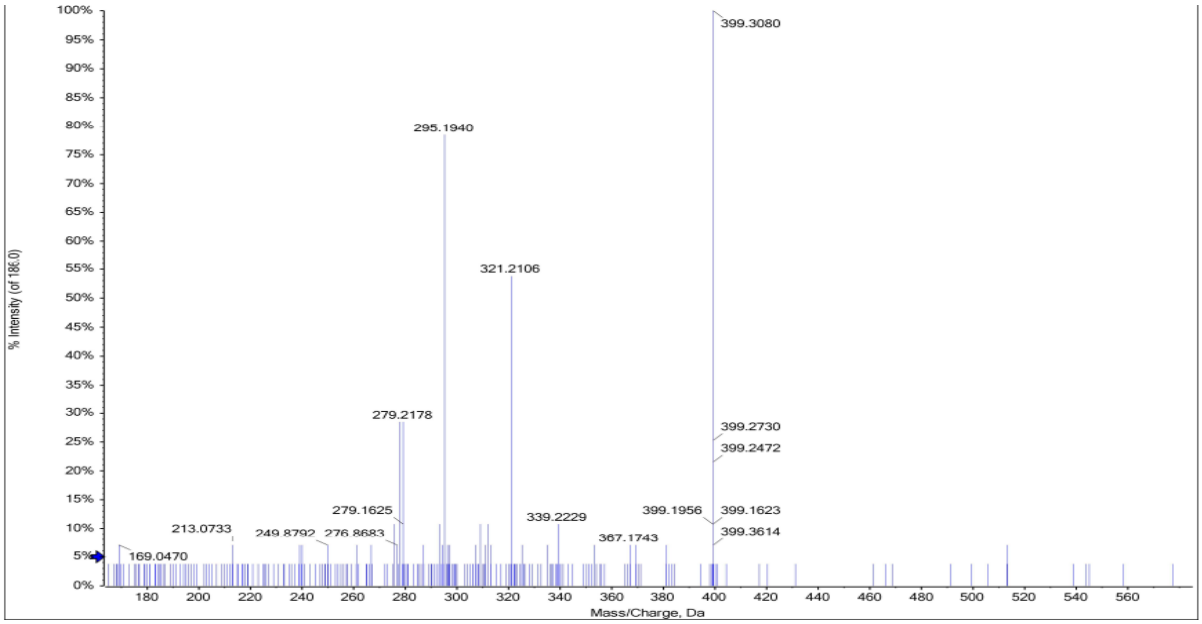

Figure 16. The FTIR spectrum of compound **148 e**

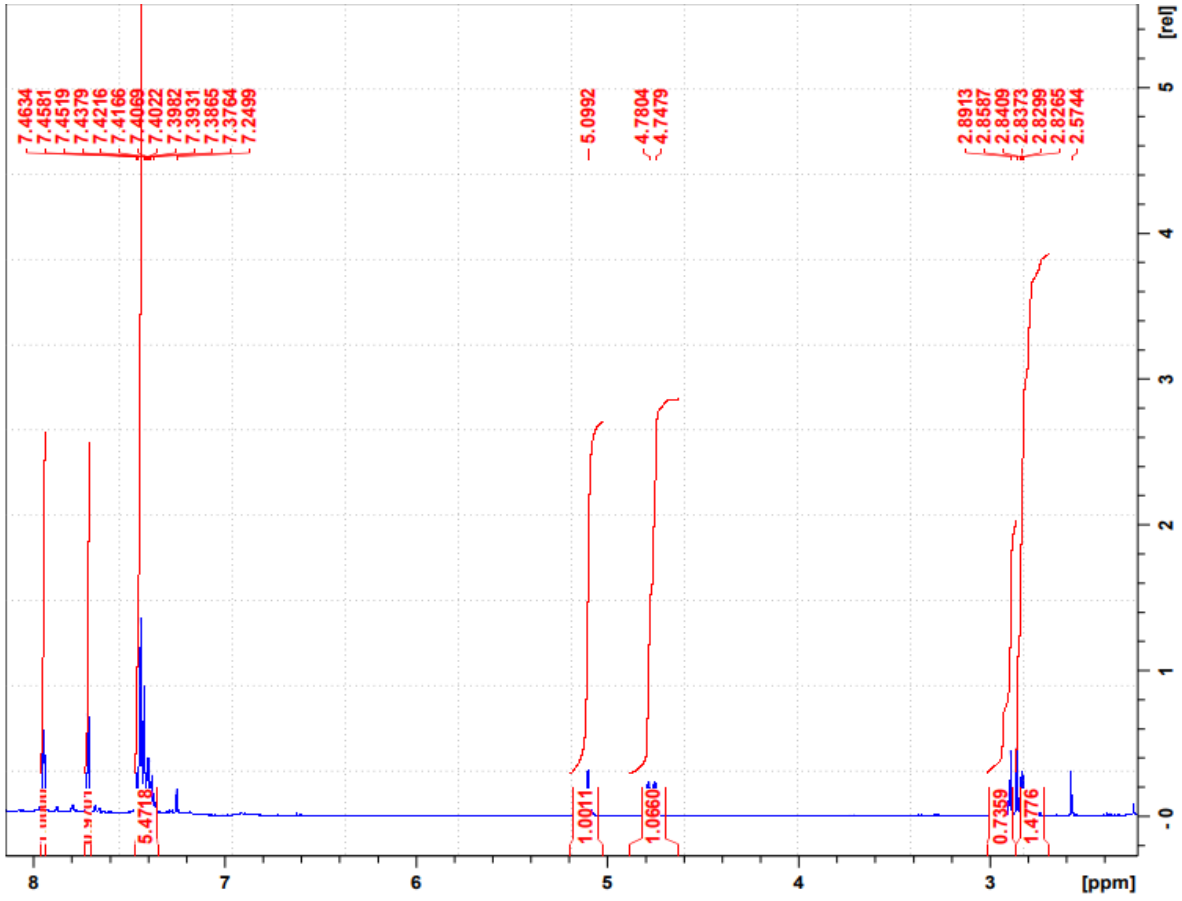
7.4634
7.4581
7.4519
7.4379
7.4216
7.4166
7.4069
7.4022
7.3982
7.3931
7.3865
7.3764
7.2499
5.0992
4.7804
4.7479
2.8913
2.8587
2.8409
2.8373
2.8299
2.8265
2.5744
5.4718
1.0011
1.0660
0.7359
1.4776
8
7
6
5
4
3
[ppm]
[rel]
5
4
3
2
1
-0

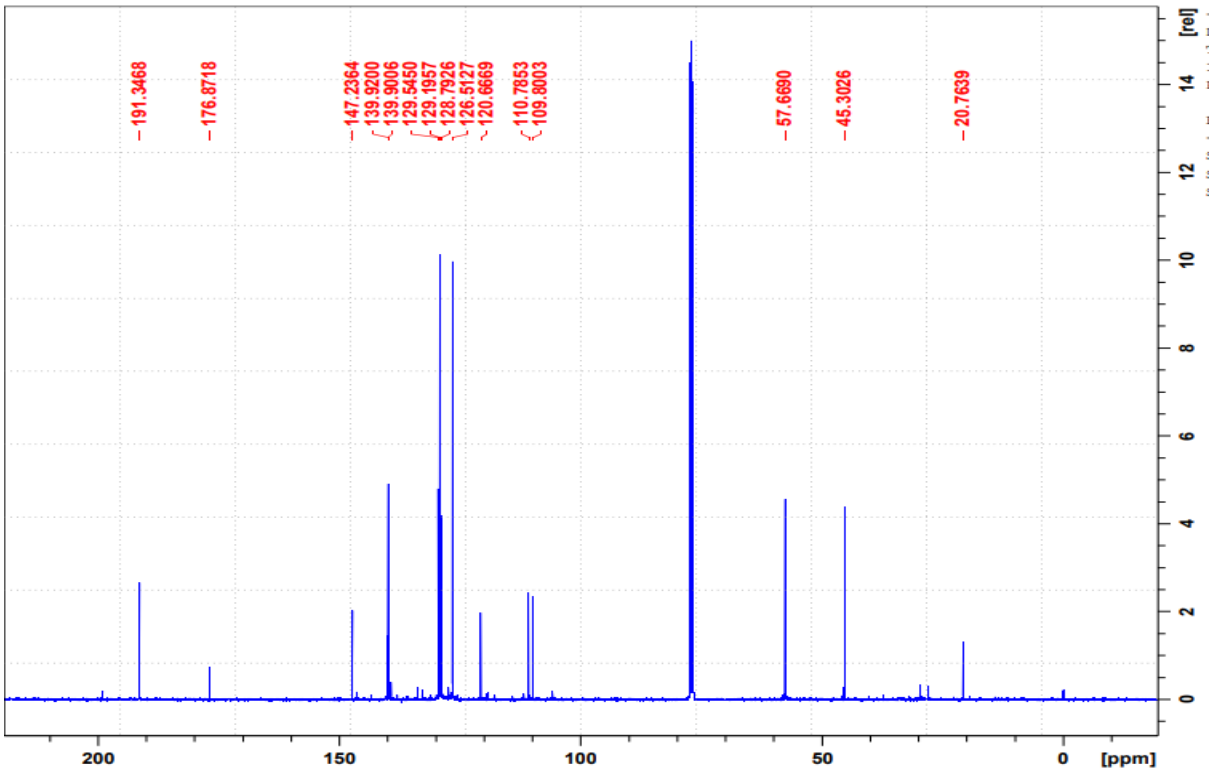

Figure 17. The ^{1}H NMR spectrum of compound **149 a**

Figure 18. The ^{13}C NMR spectrum of compound **149 a**

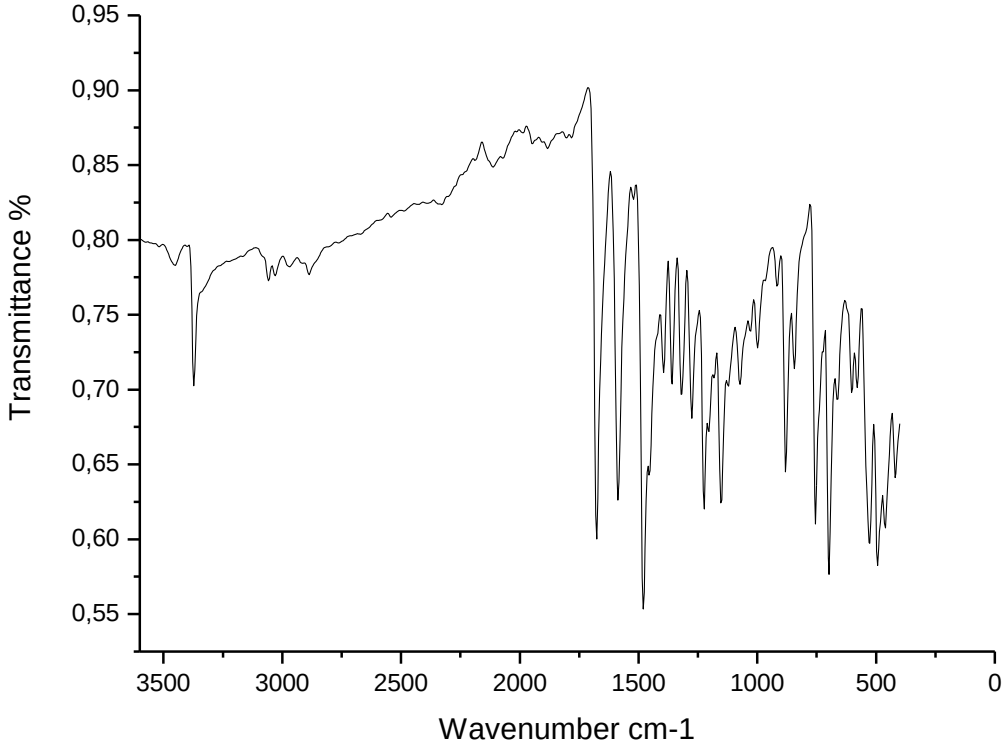

Figure 19. The FTIR spectrum of compound **149 a**

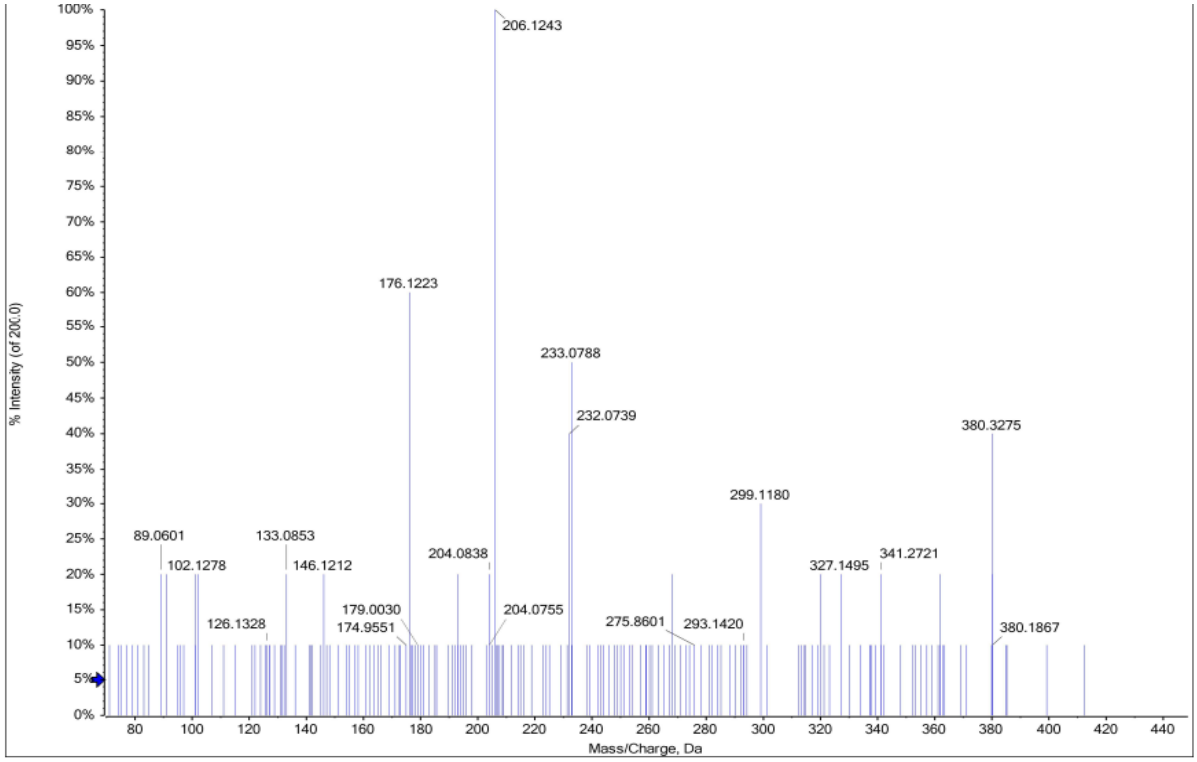

Figure 20. The HRMS spectrum of compound **149 a**

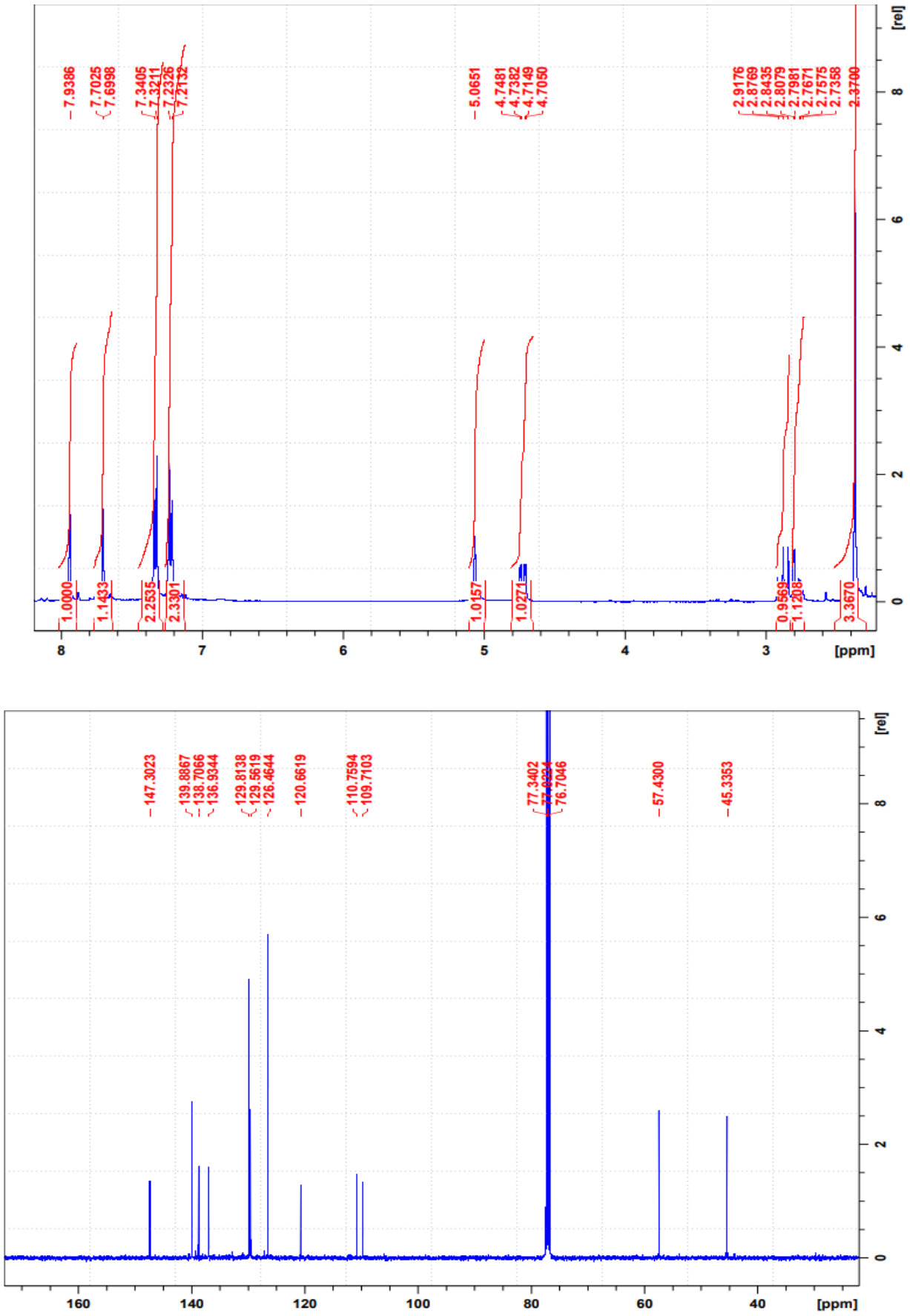

Figure 21. The ^{1}H NMR spectrum of compound **149 b**

Figure 22. The ^{13}C NMR spectrum of compound **149 b**

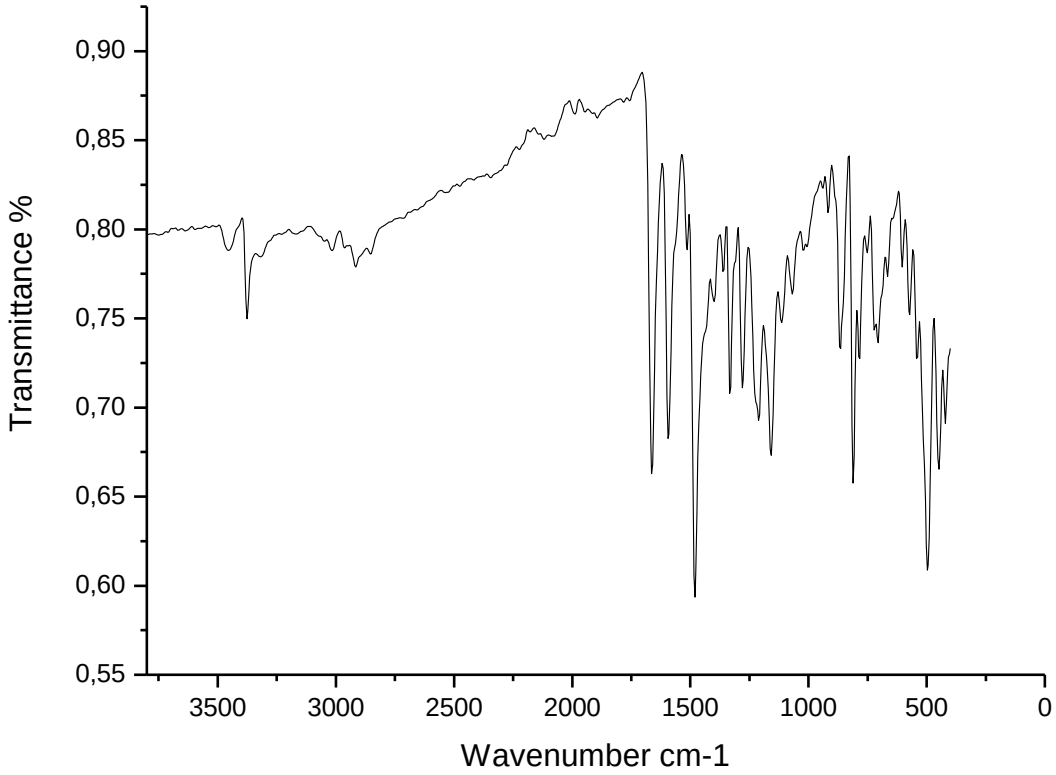

Figure 23. The FTIR spectrum of compound **149 b**

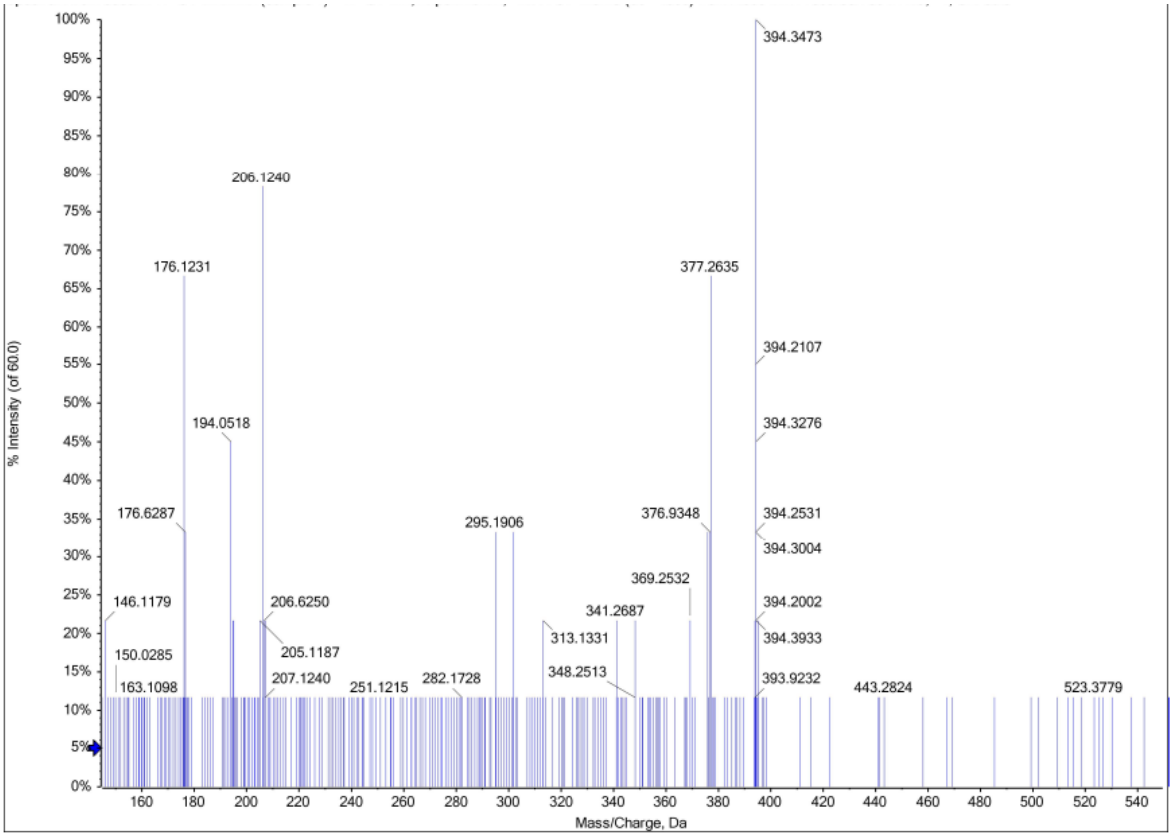

Figure 24. The HRMS spectrum of compound **149 b**

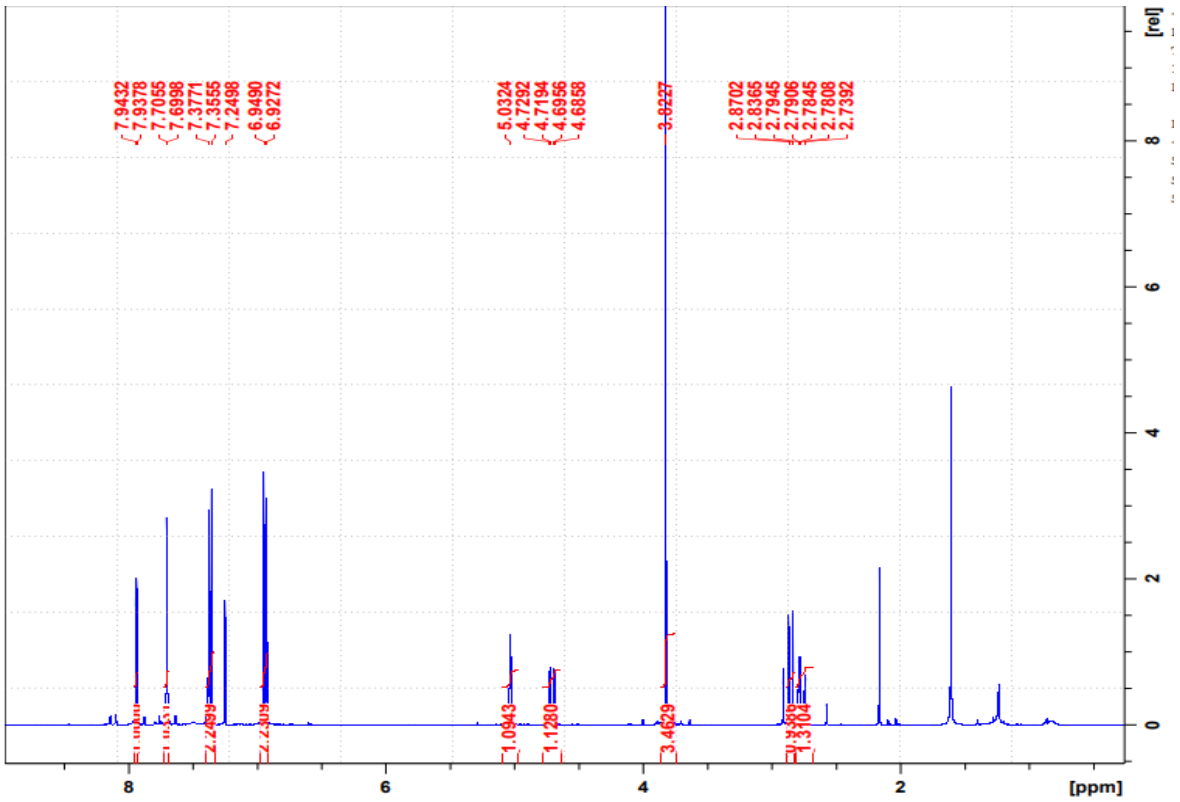

Figure 25. The ^{1}H NMR spectrum of compound **149 c**

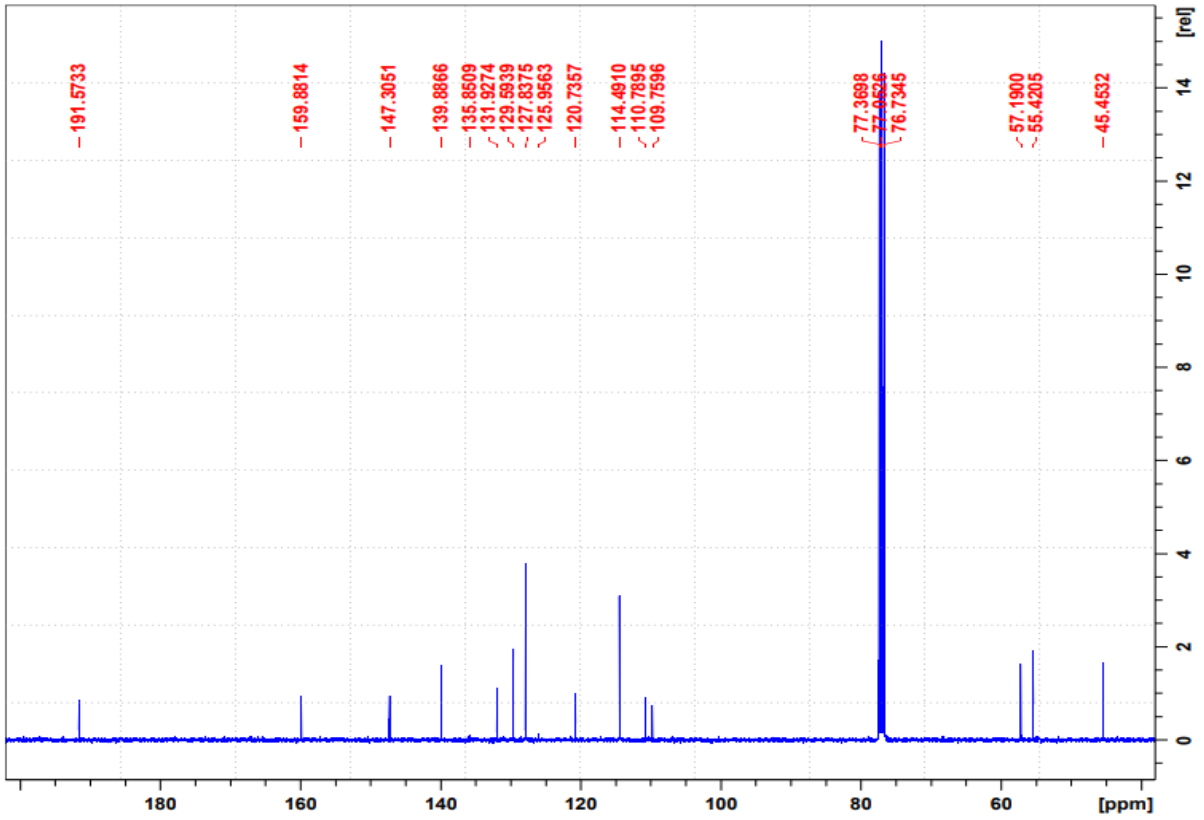

Figure 26. The ^{13}C NMR spectrum of compound **149 c**

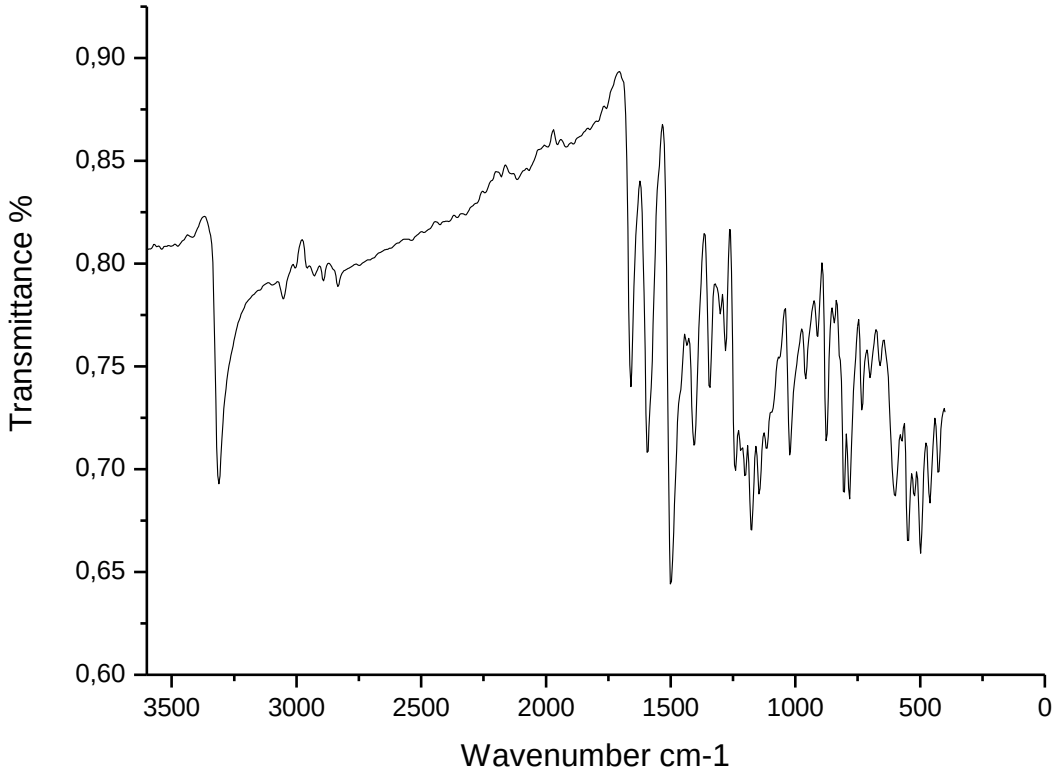

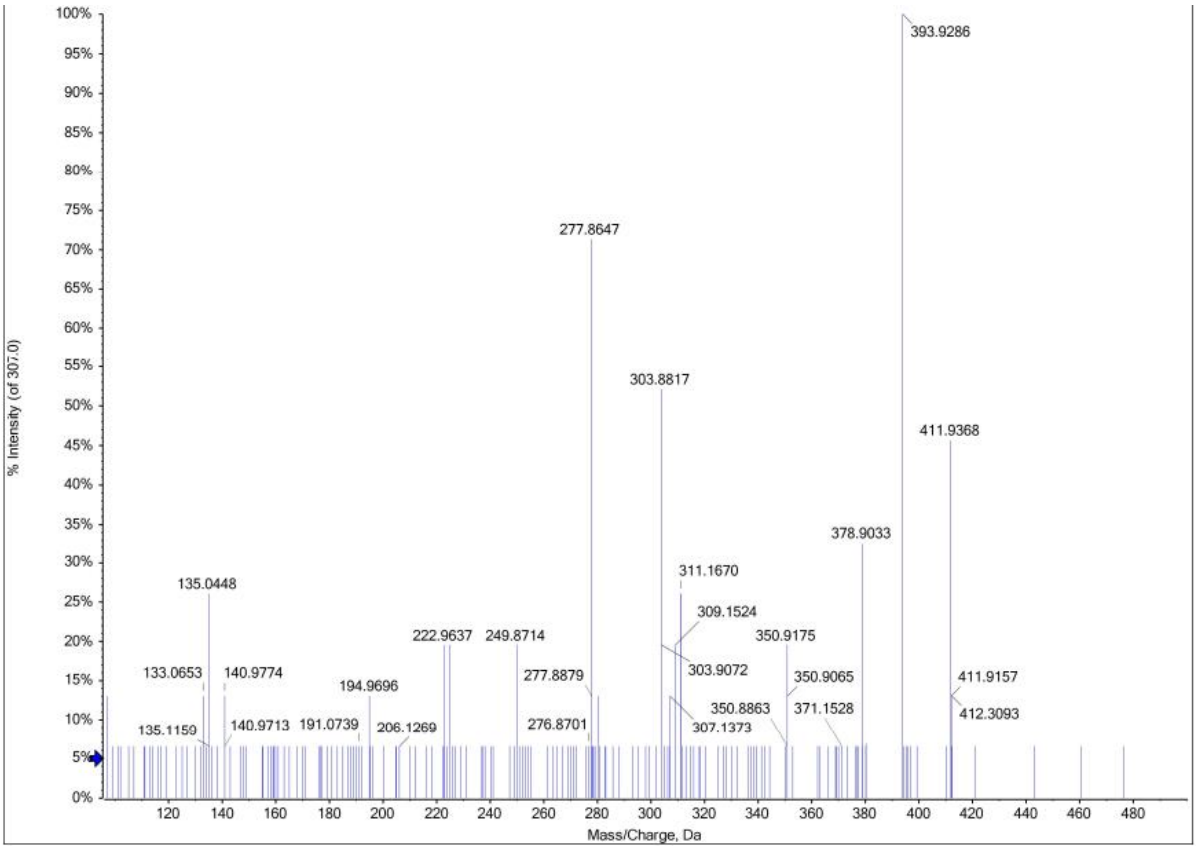

Figure 27. The FTIR spectrum of compound **149 c**

Figure 28. The HRMS spectrum of compound **149 c**

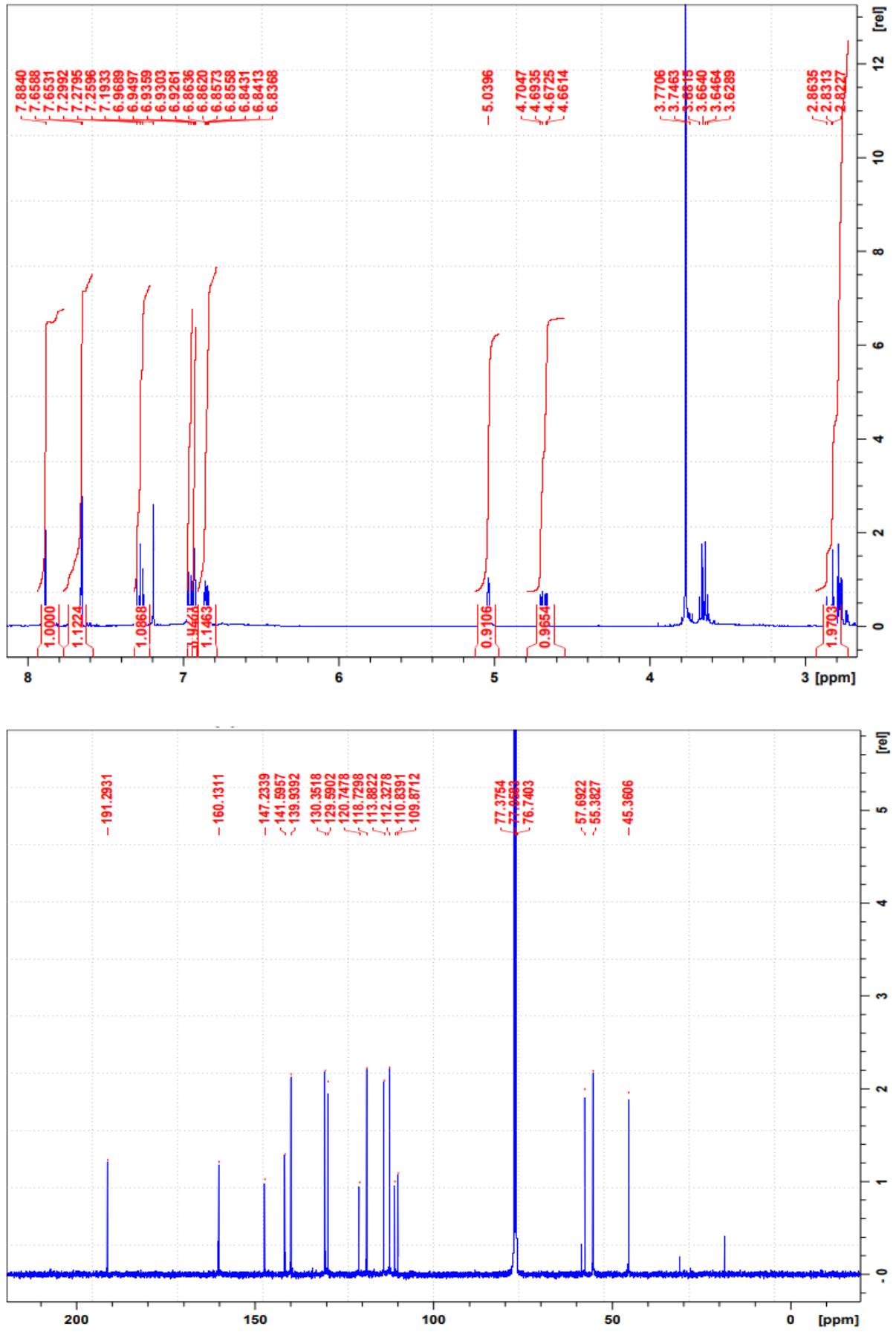

Figure 29. The ^{1}H NMR spectrum of compound **149 d**

Figure 30. The ^{13}C NMR spectrum of compound **149 d**

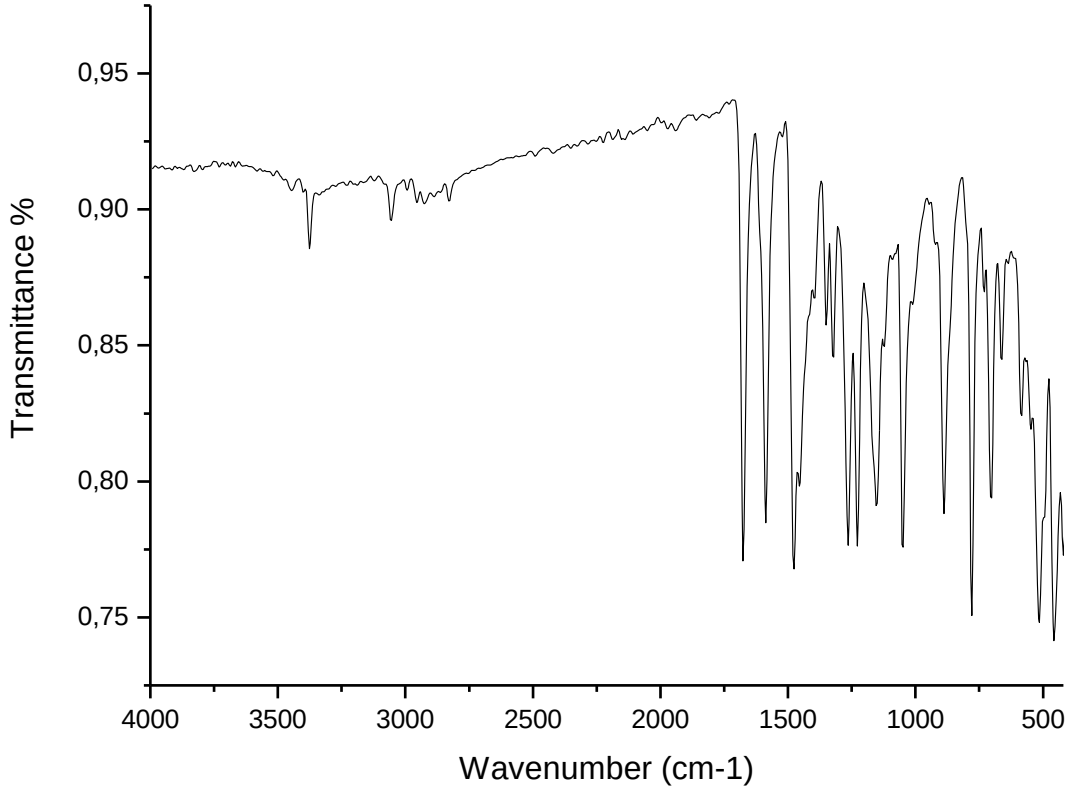

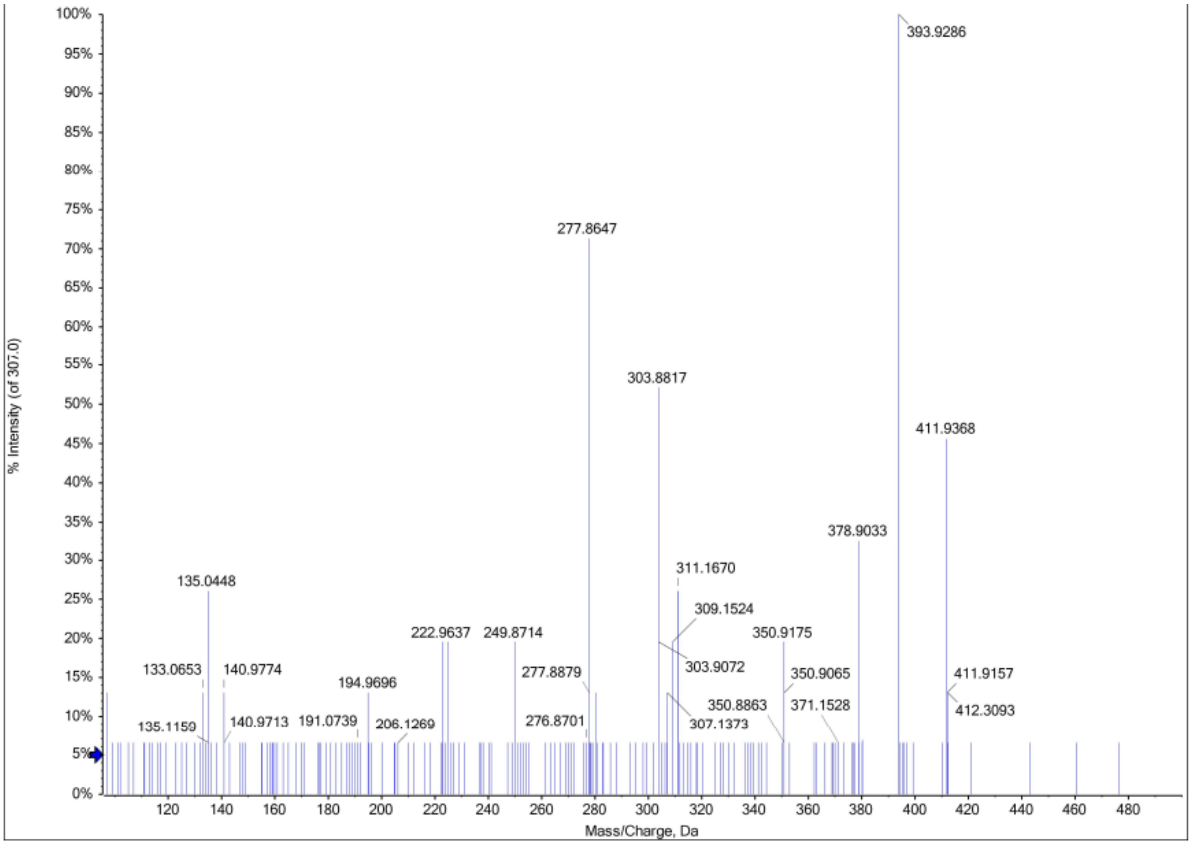

Figure 31. The FTIR spectrum of compound **149 d**

Figure 32. The HRMS spectrum of compound **149 d**

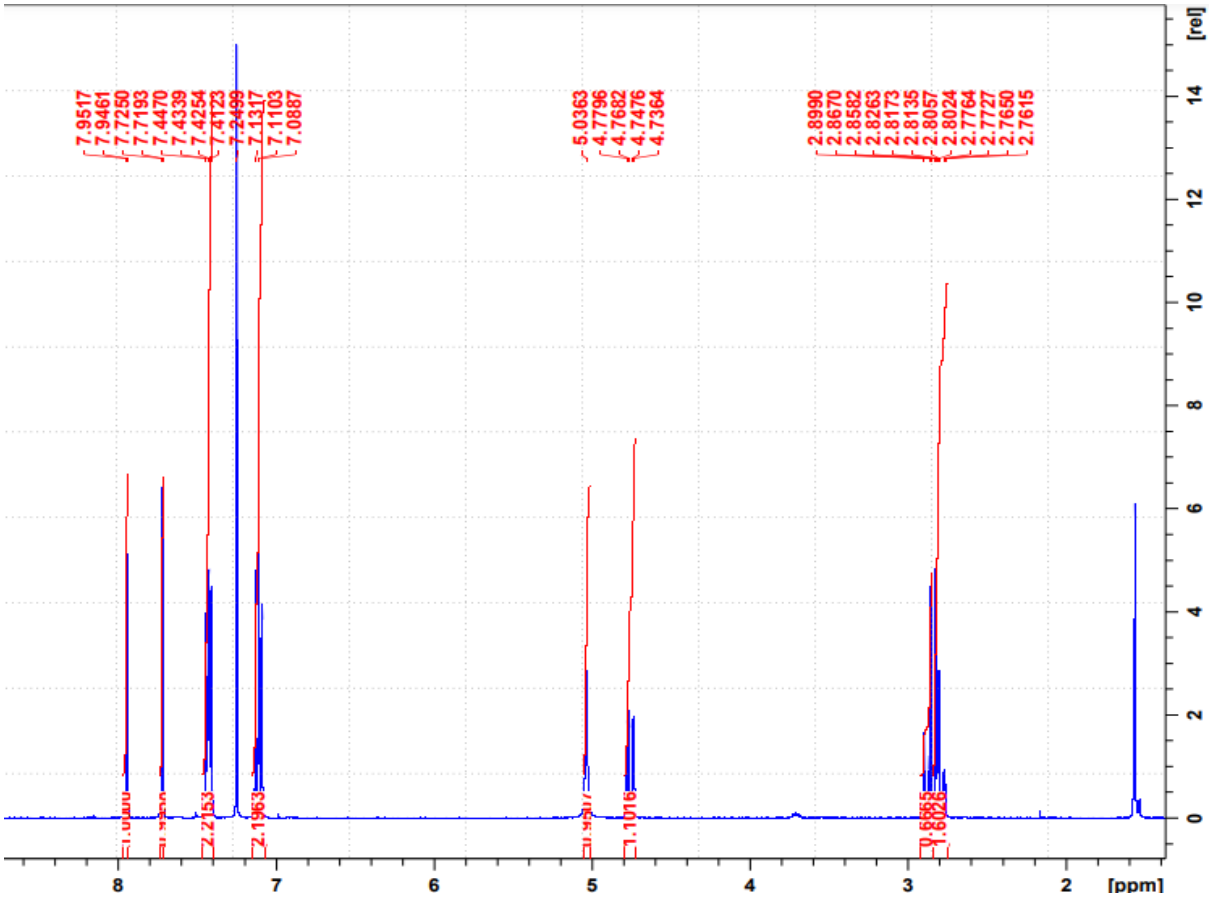

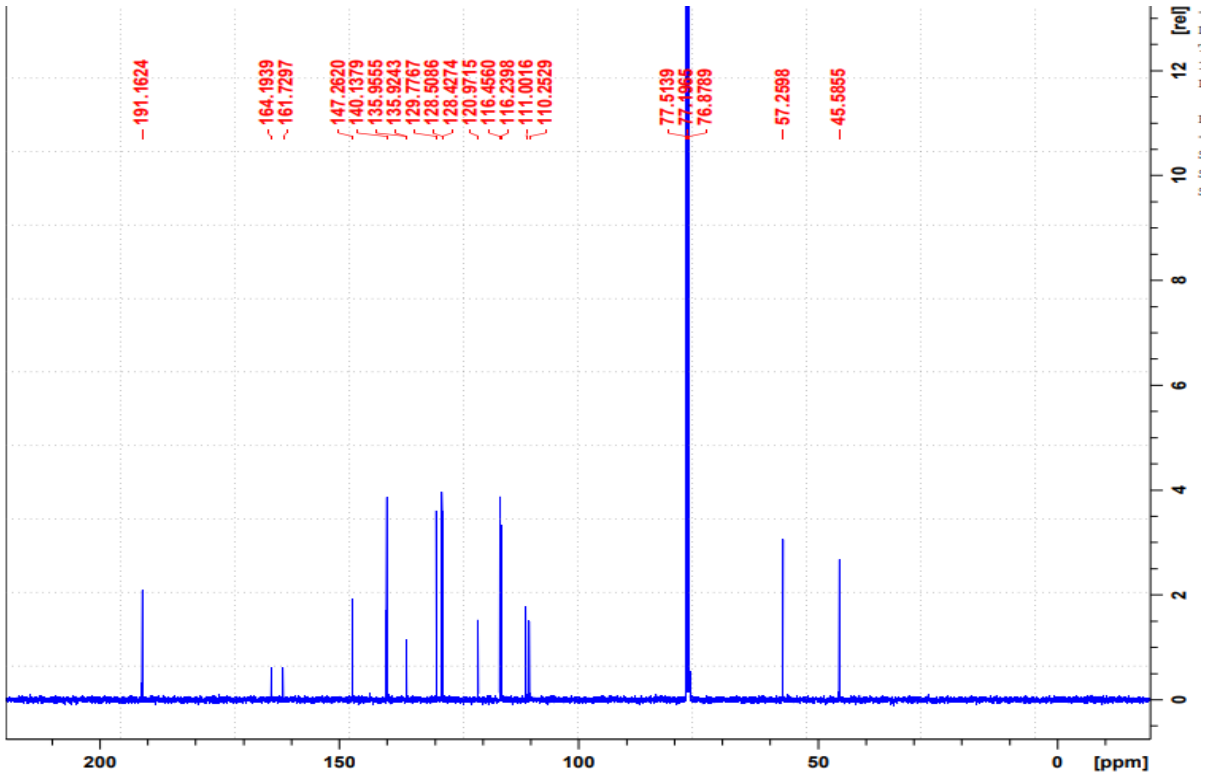

Figure 33. The ^{1}H NMR spectrum of compound **149 e**

Figure 34. The ^{13}C NMR spectrum of compound **149 e**

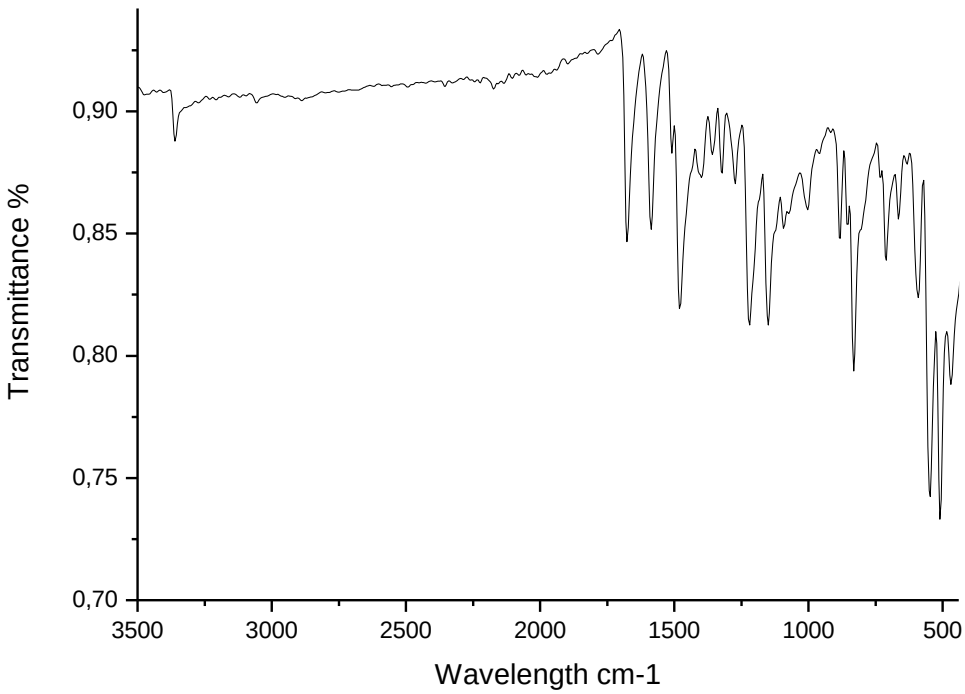

Figure 35. The FTIR spectrum of compound **149 e**

Figure 36. The HRMS spectrum of compound **149 e**

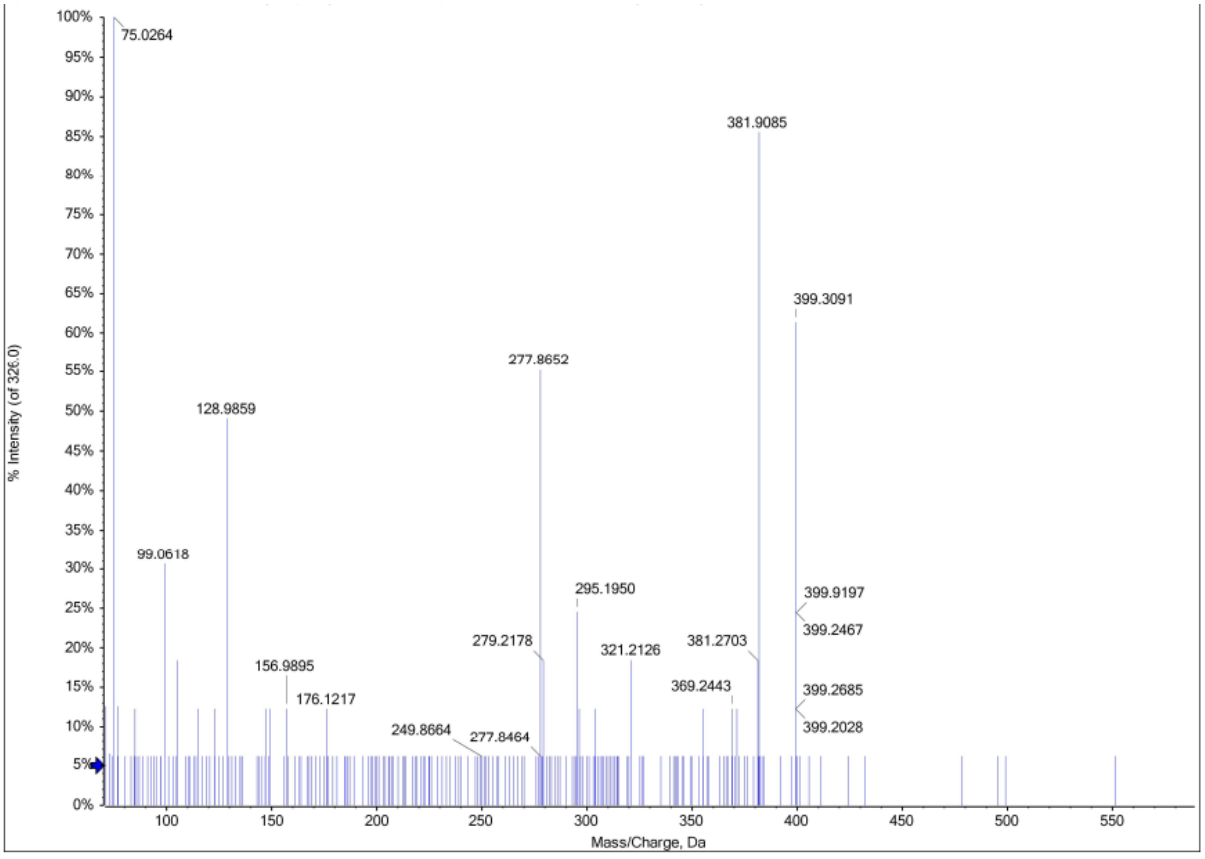

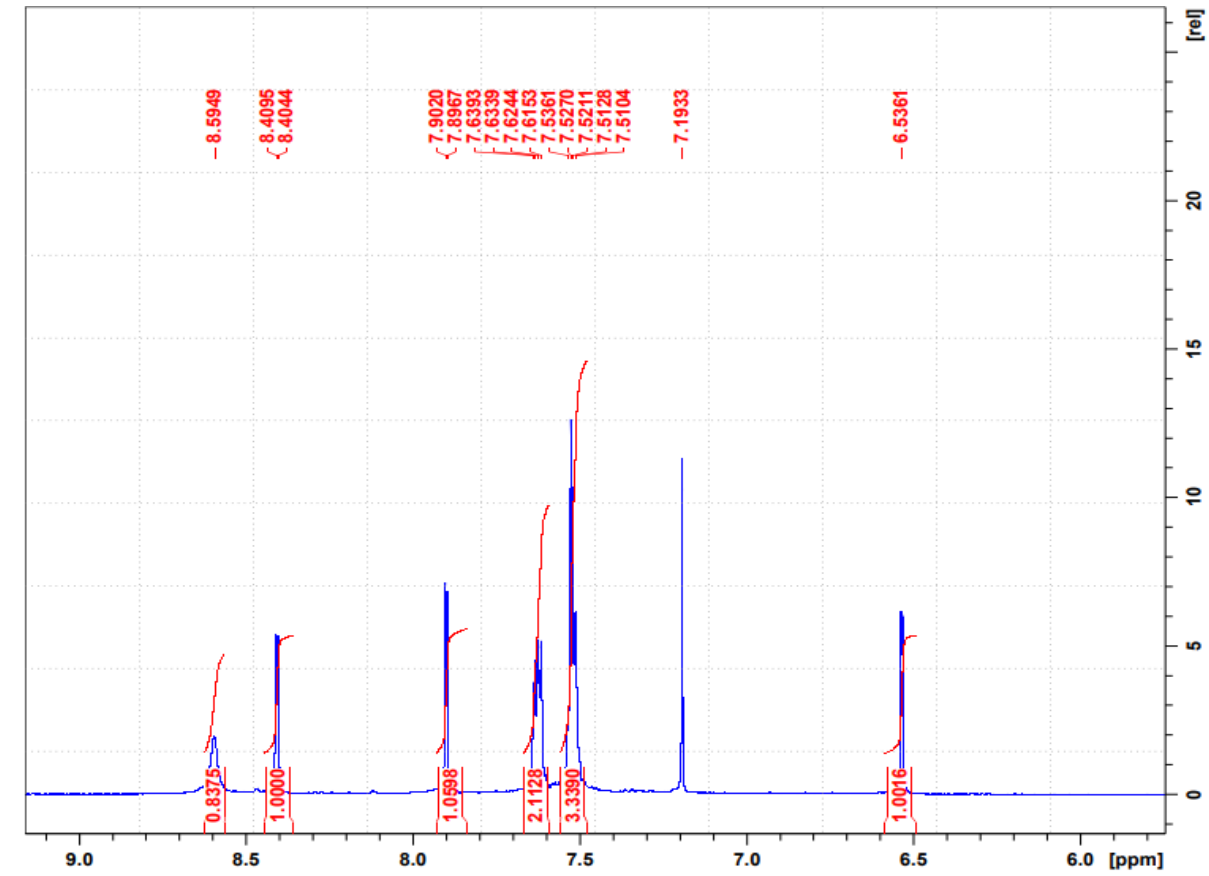

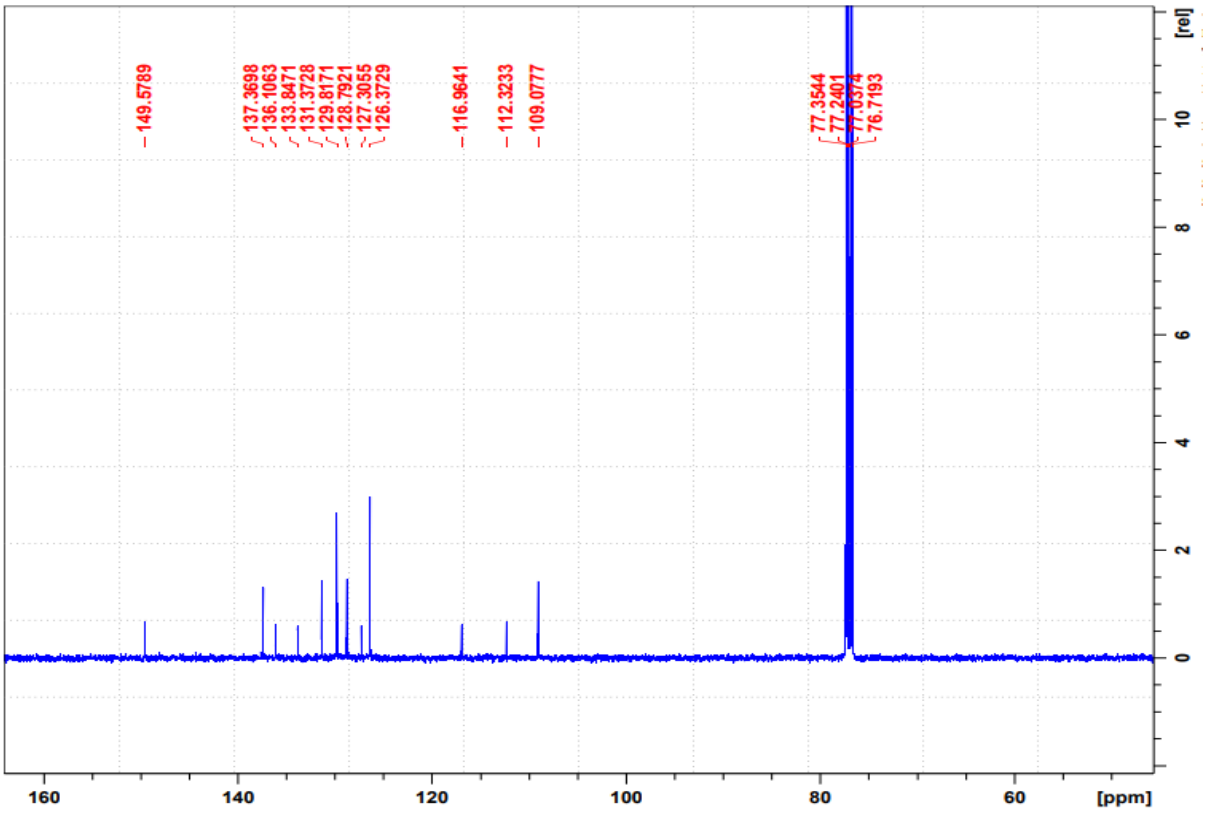

Figure 37. The ^{1}H NMR spectrum of compound **150 a**

Figure 38. The ^{13}C NMR spectrum of compound **150 a**

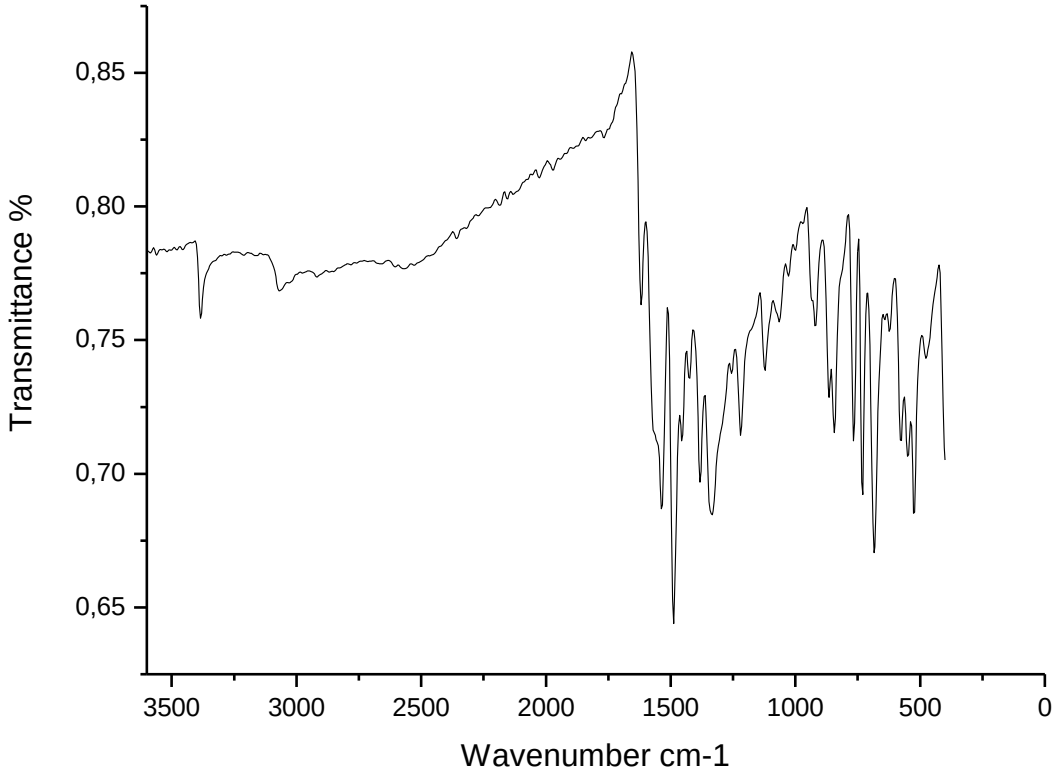

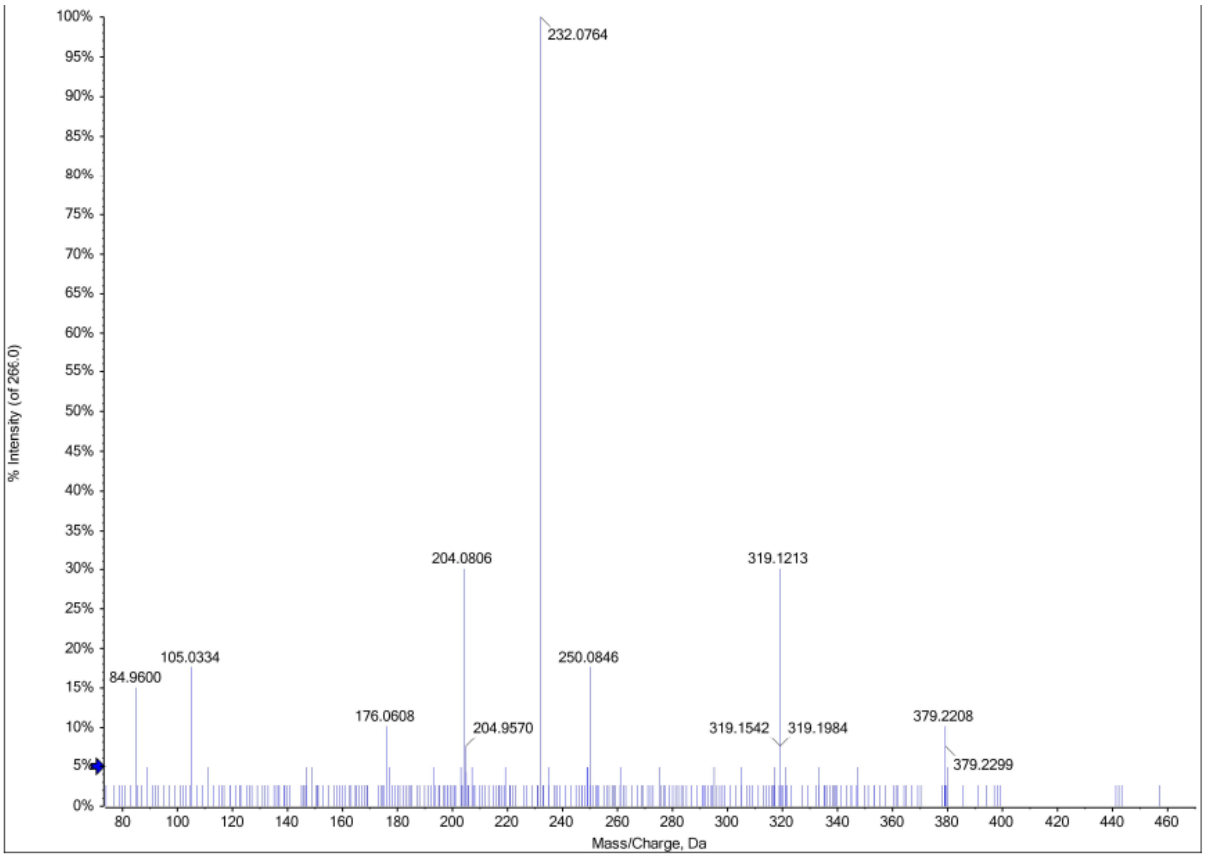

Figure 39. The FTIR spectrum of compound **150 a**

Figure 40. The HRMS spectrum of compound **150 a**

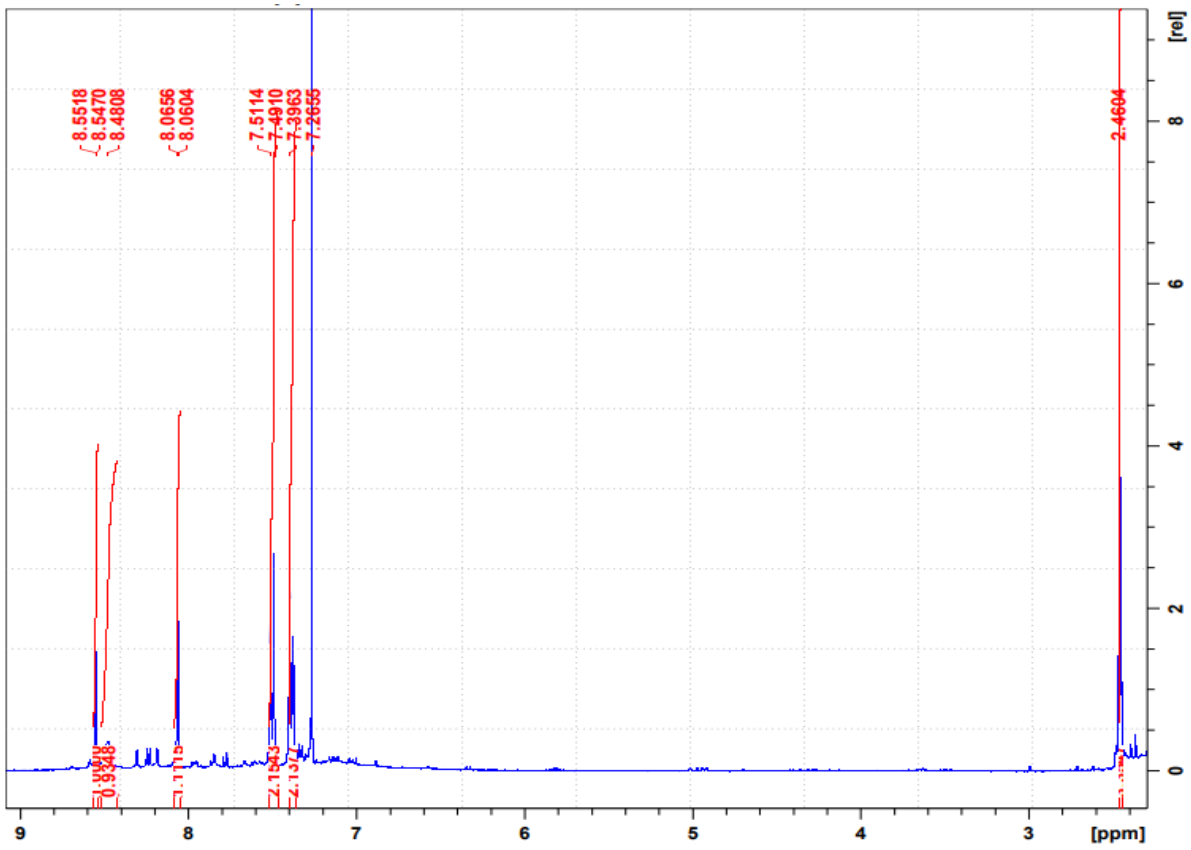

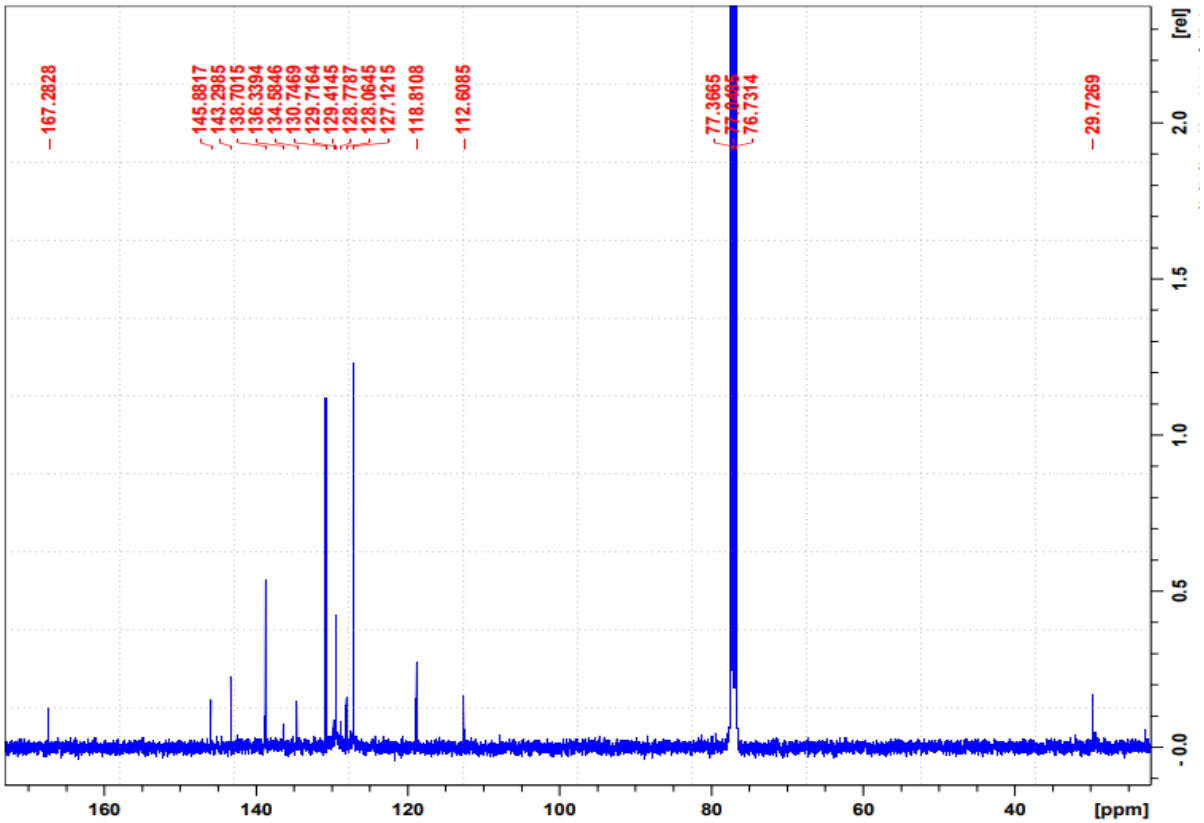

Figure 41. The ^{1}H NMR spectrum of compound **150 b**

Figure 42. The ^{13}C NMR spectrum of compound **150 b**

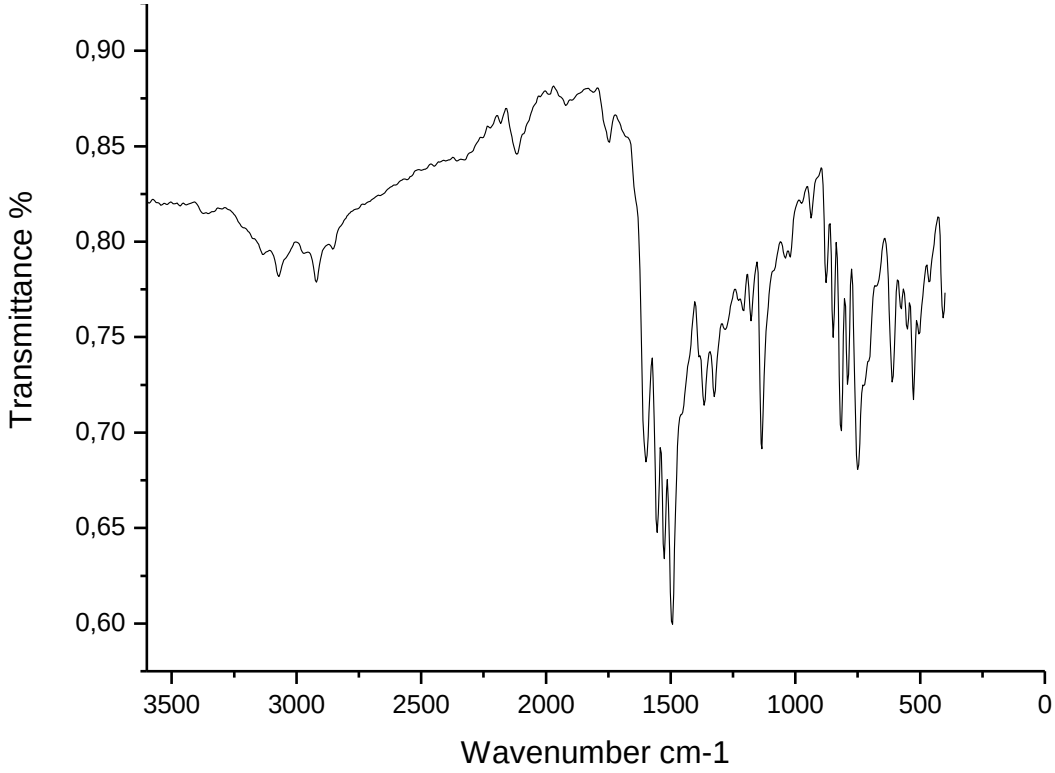

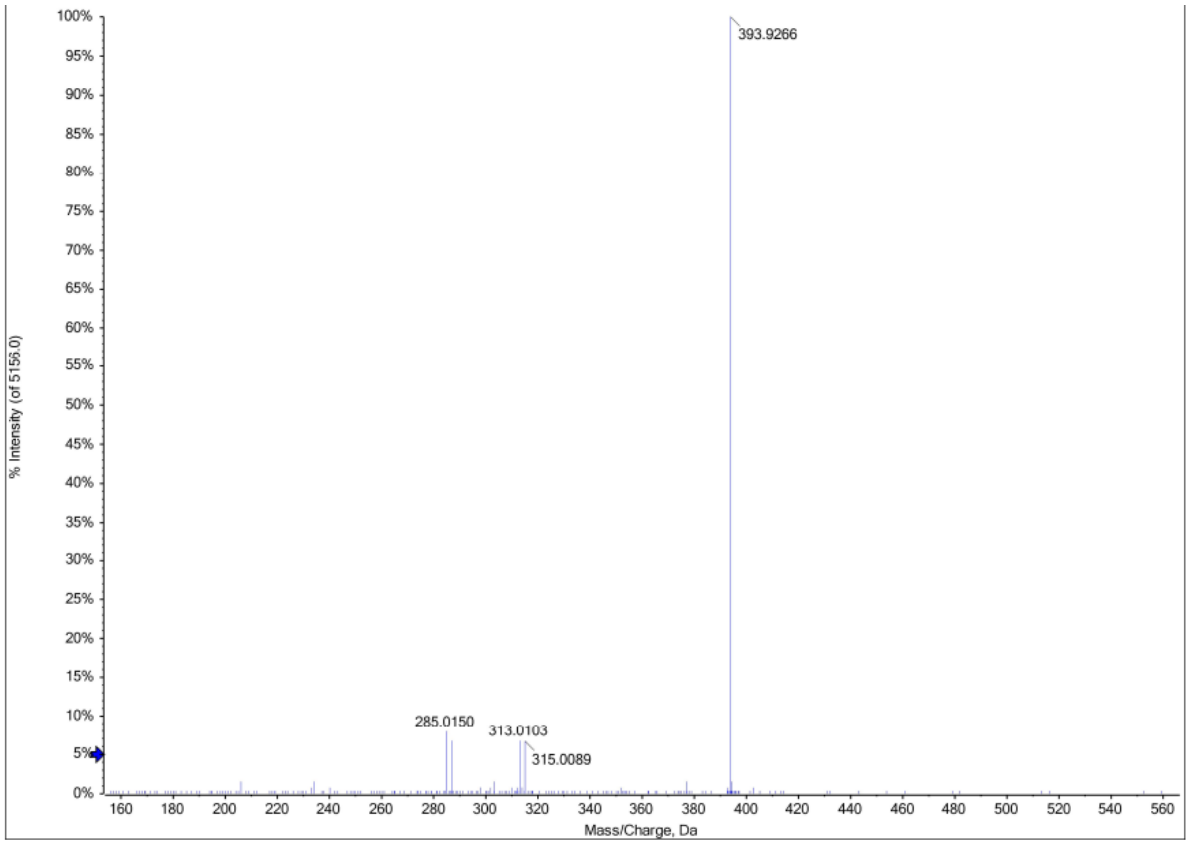

Figure 43. The FTIR spectrum of compound **150 b**

Figure 44. The HRMS spectrum of compound **150 b**

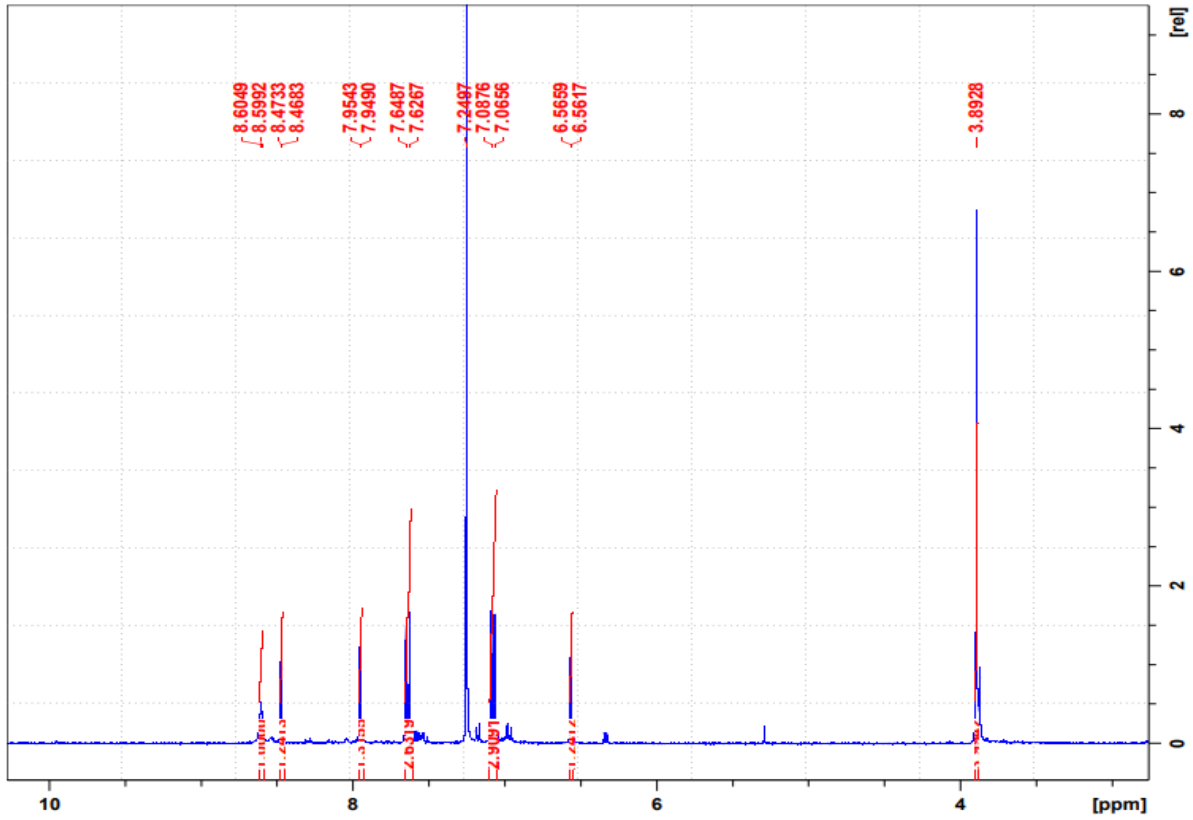

Figure 45. The ^{1}H NMR spectrum of compound **150 c**

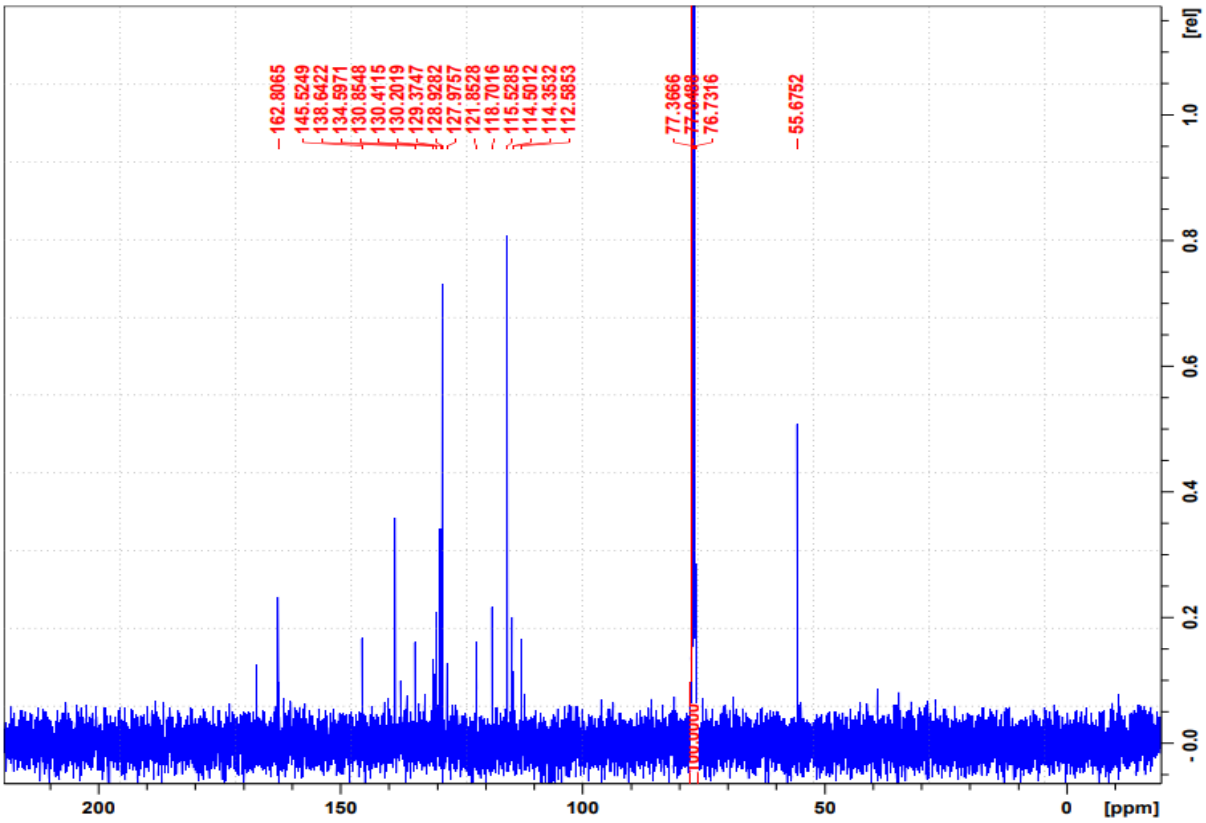

Figure 46. The ^{13}C NMR spectrum of compound **150 c**

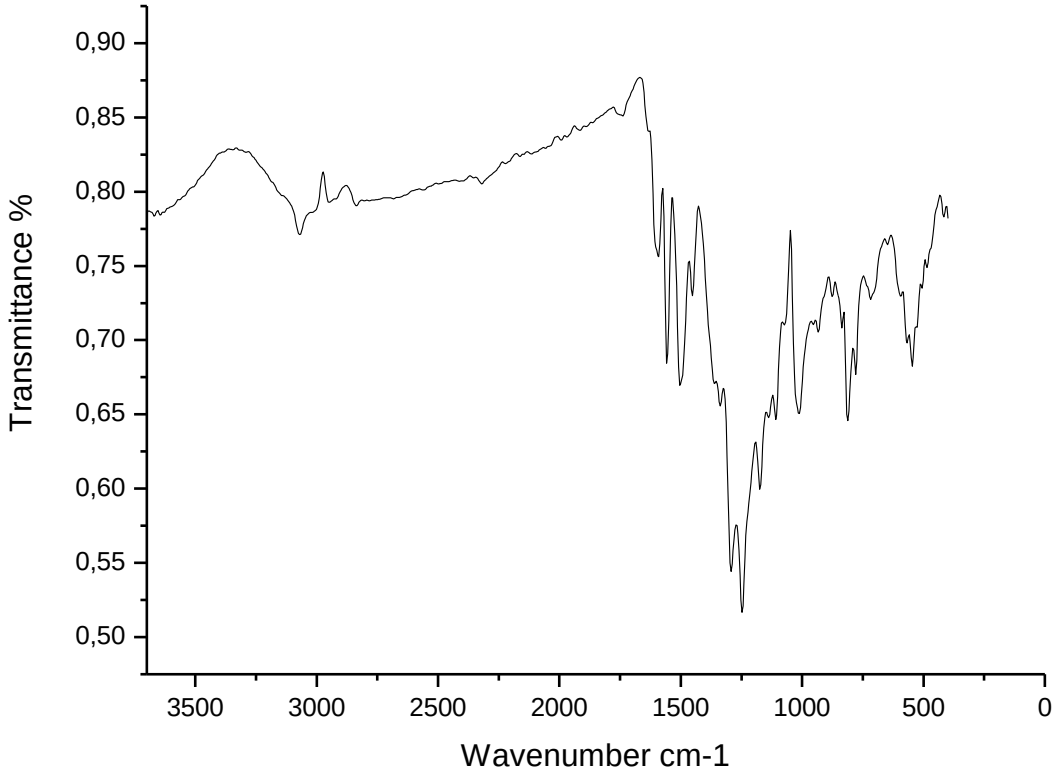

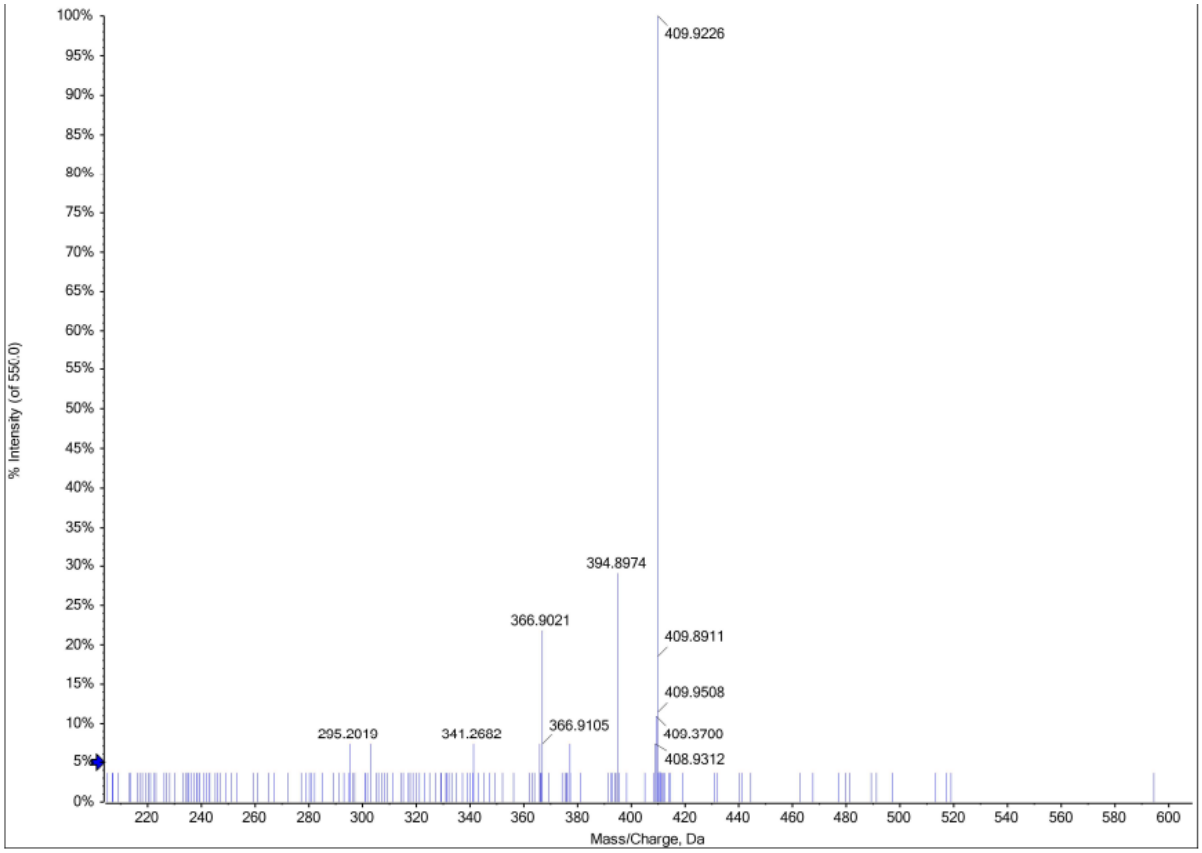

Figure 47. The FTIR spectrum of compound **150 c**

Figure 48. The HRMS spectrum of compound **150 c**

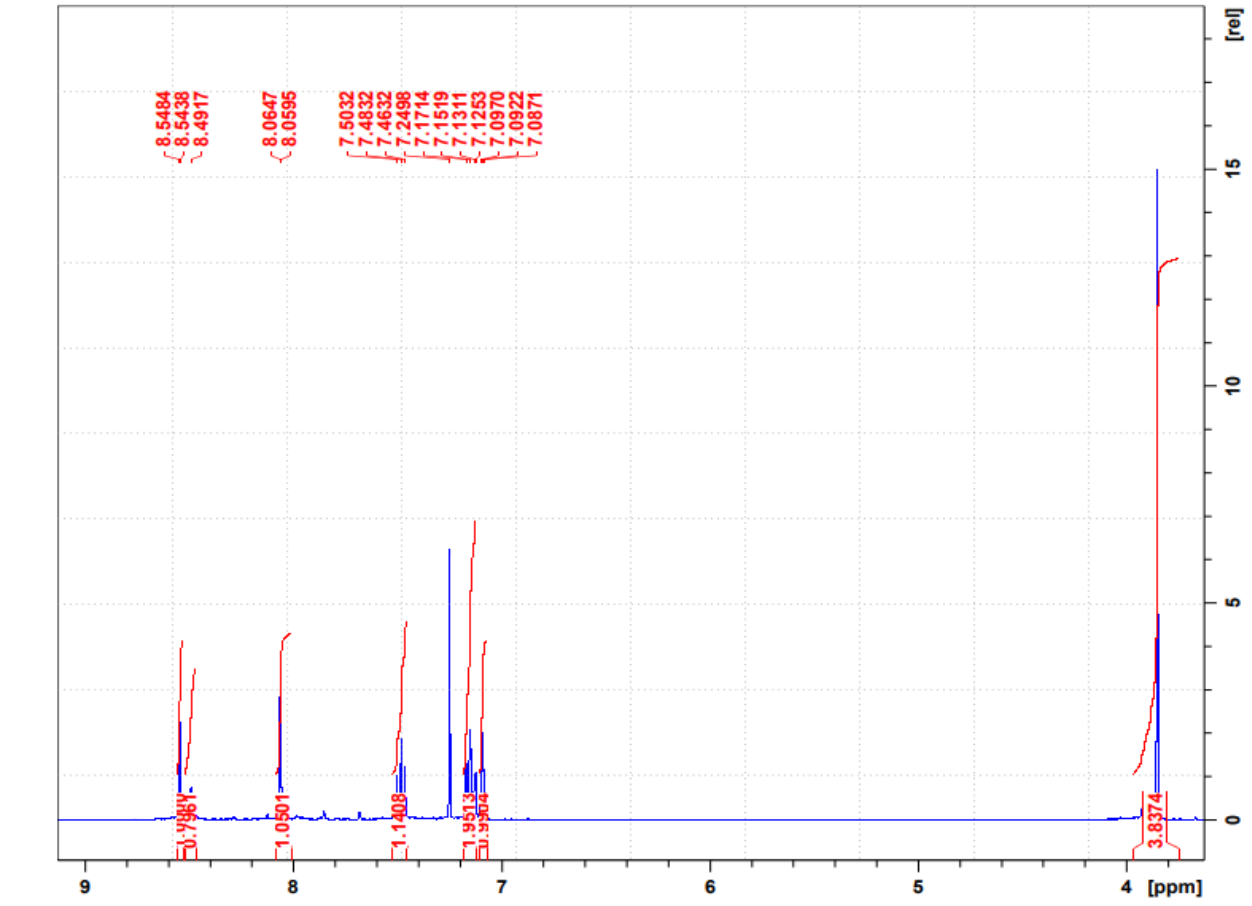

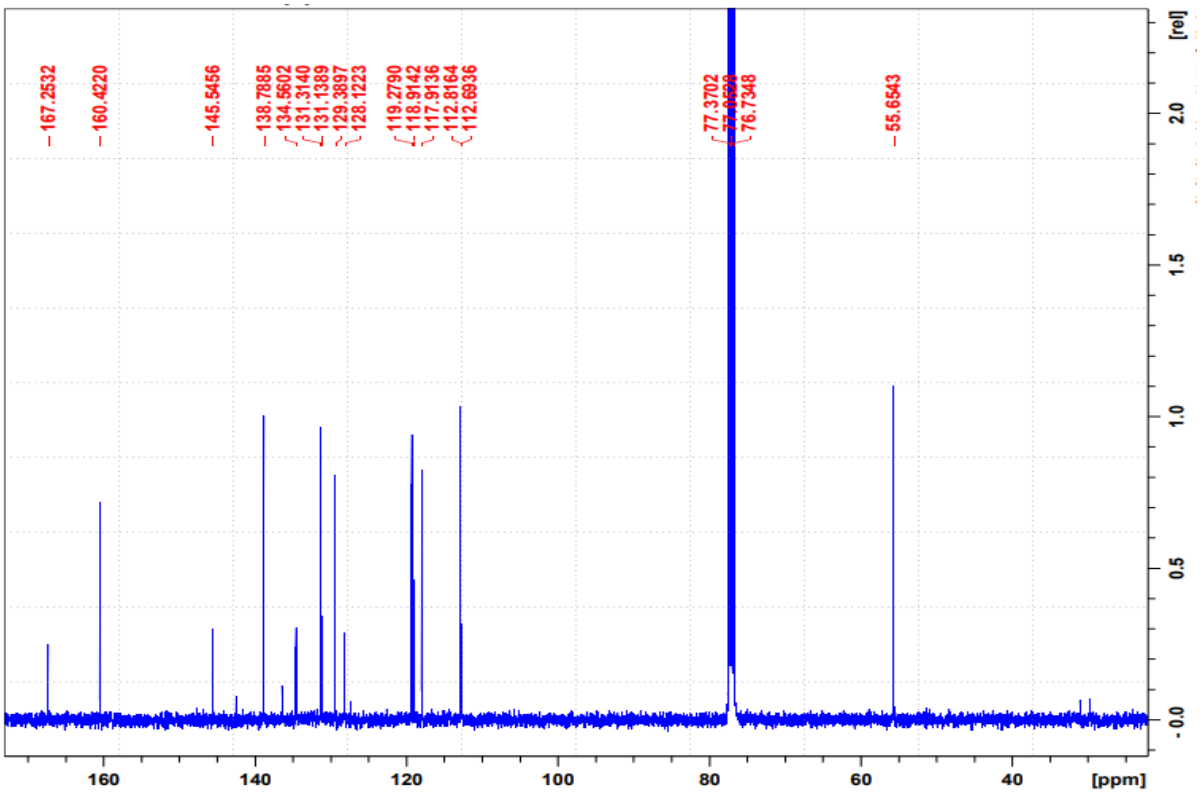

Figure 49. The ^{1}H NMR spectrum of compound **150 d**

Figure 50. The ^{13}C NMR spectrum of compound **150 d**

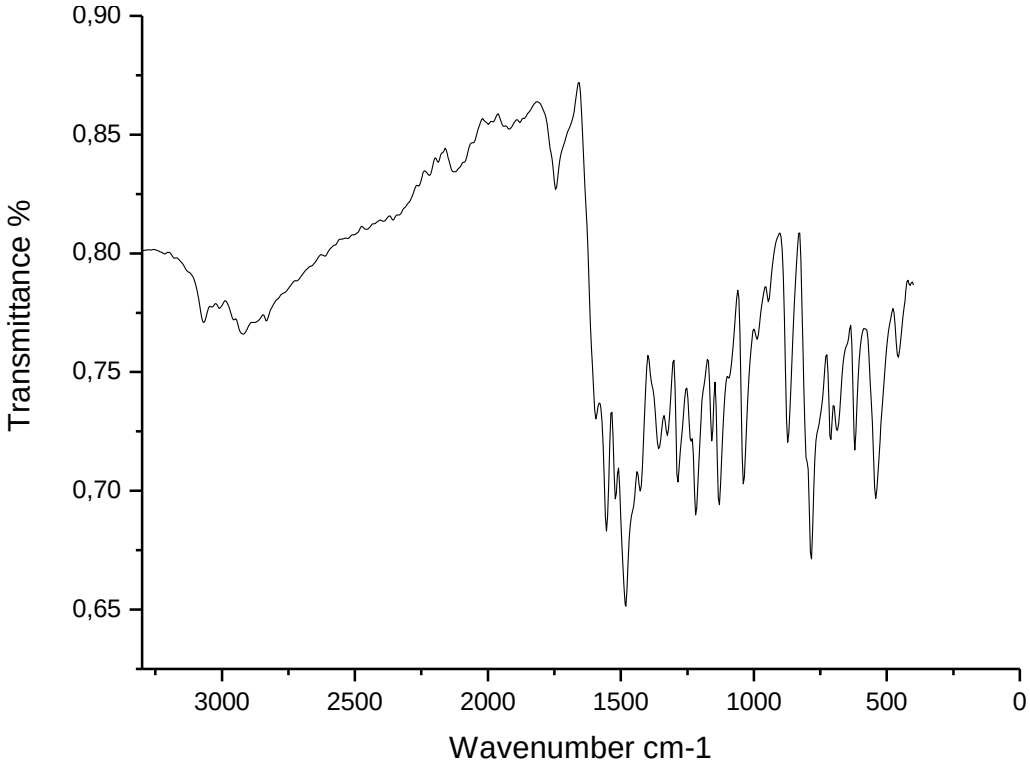

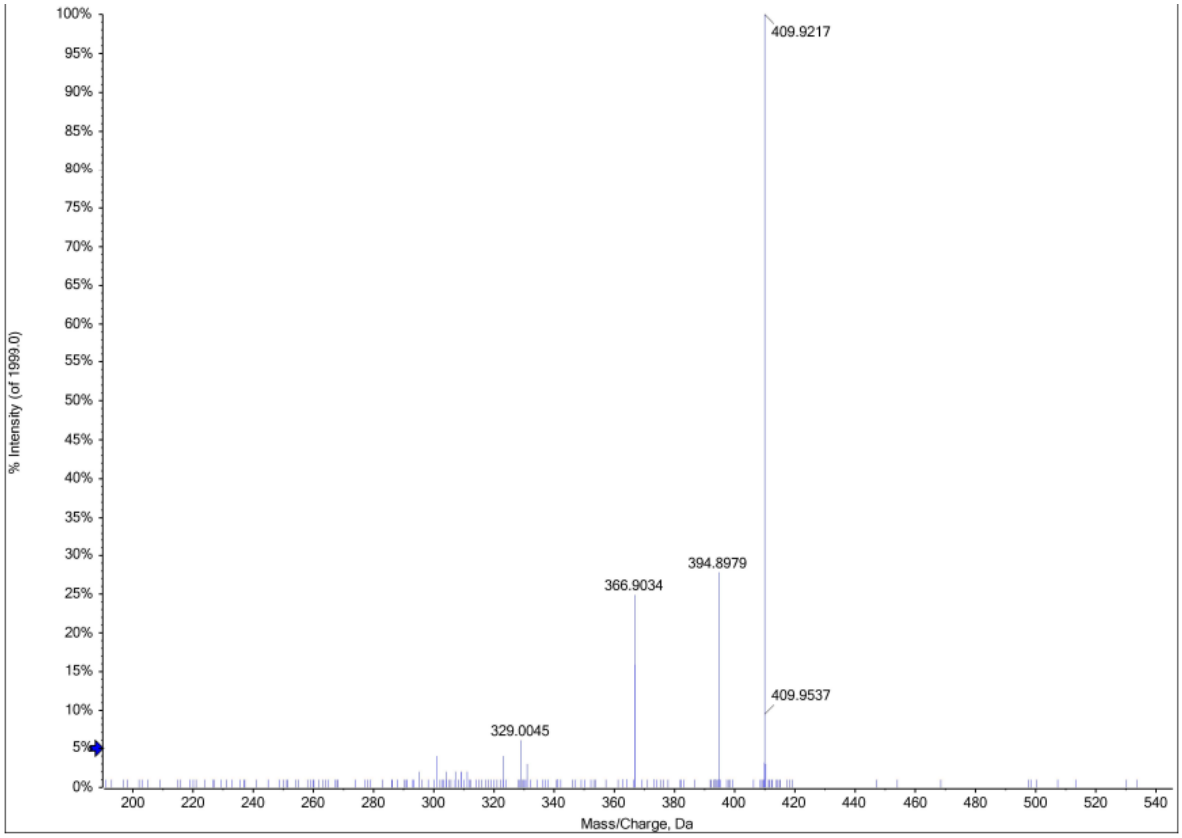

Figure 51. The FTIR spectrum of compound **150 d**

Figure 52. HRMS spectrum of compound **150 d**

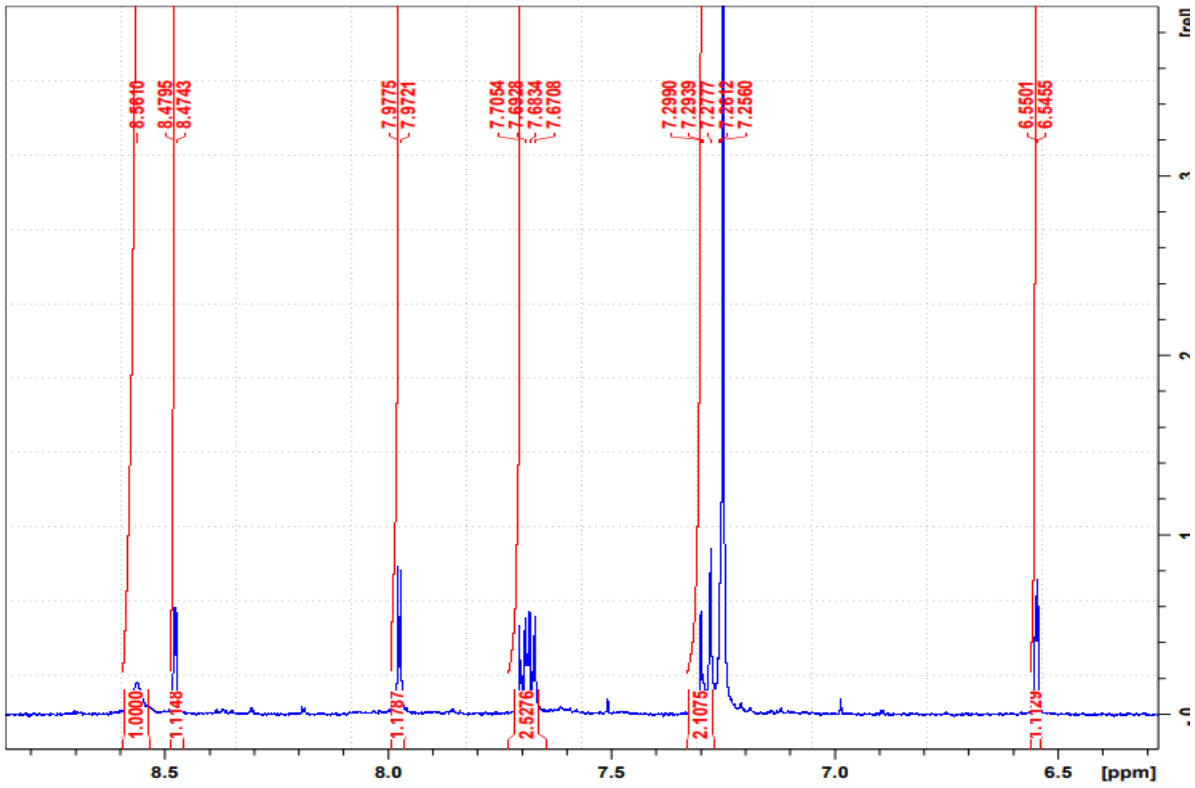

Figure 53. The ^{1}H NMR spectrum of compound **150 e**

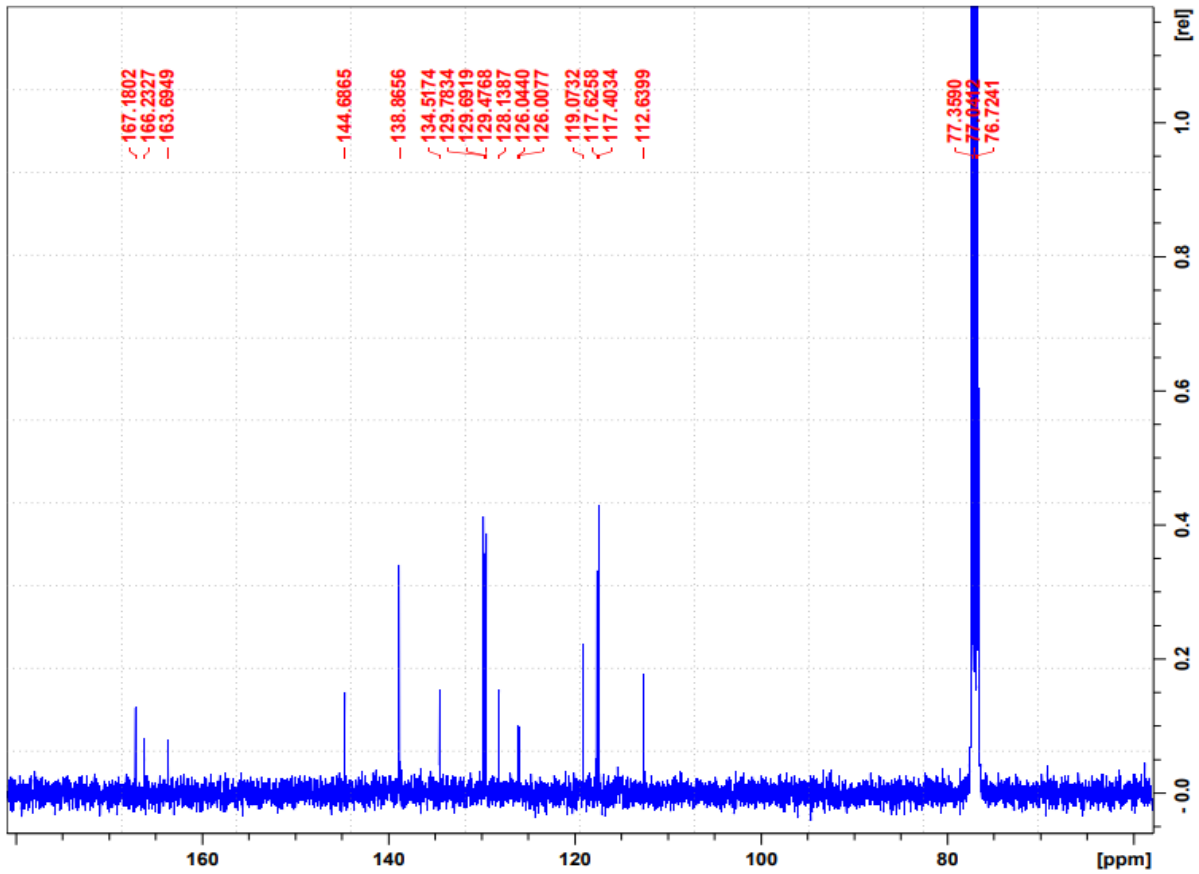

Figure 54. The ^{13}C NMR spectrum of compound **150 e**

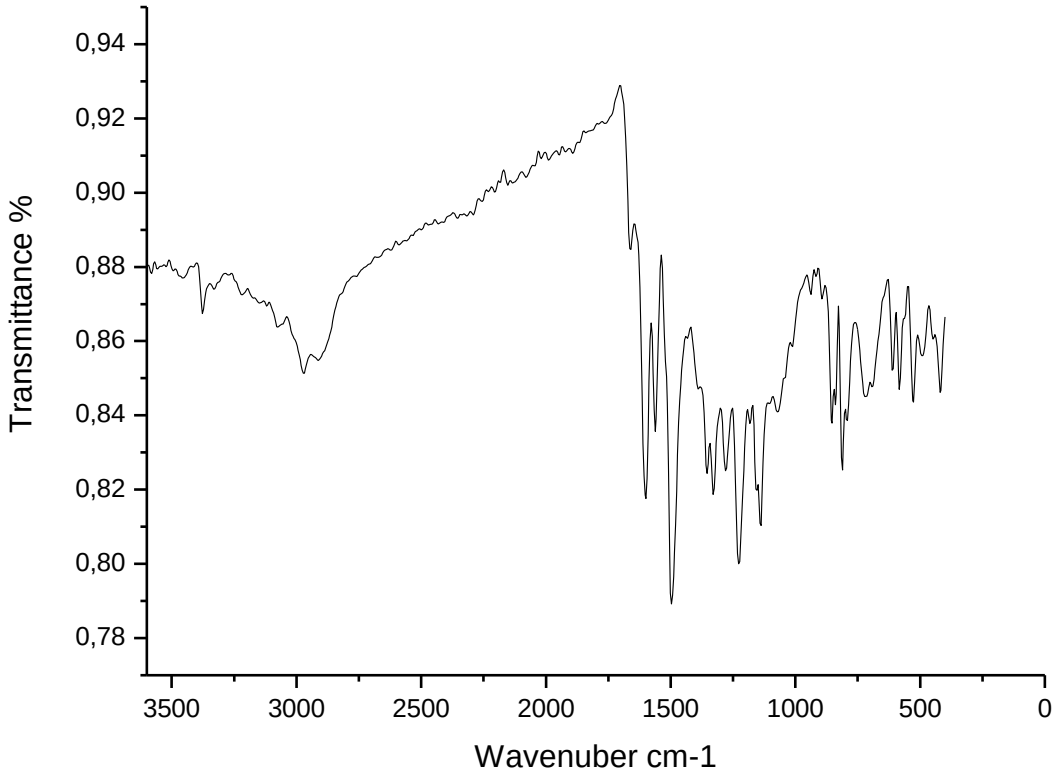

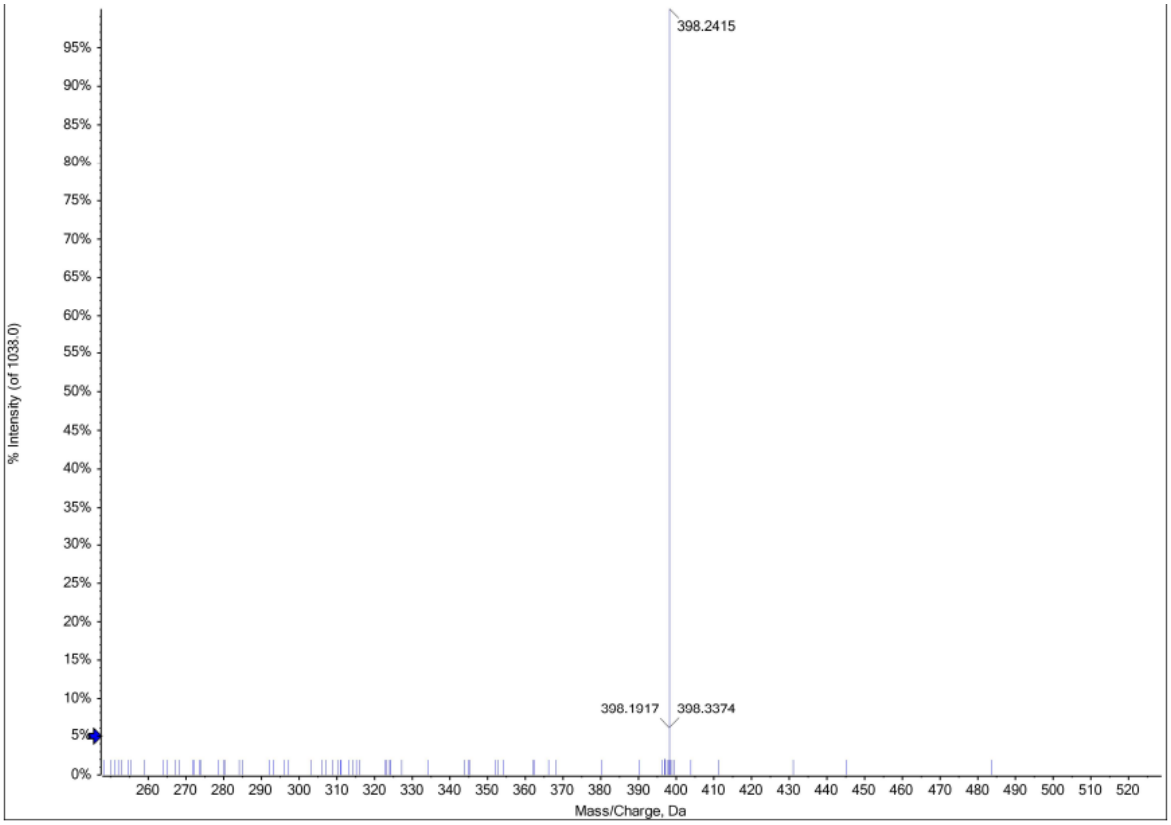

Figure 55. The FTIR spectrum of compound **150 e**

Figure 56. The HRMS spectrum of compound **150 e**

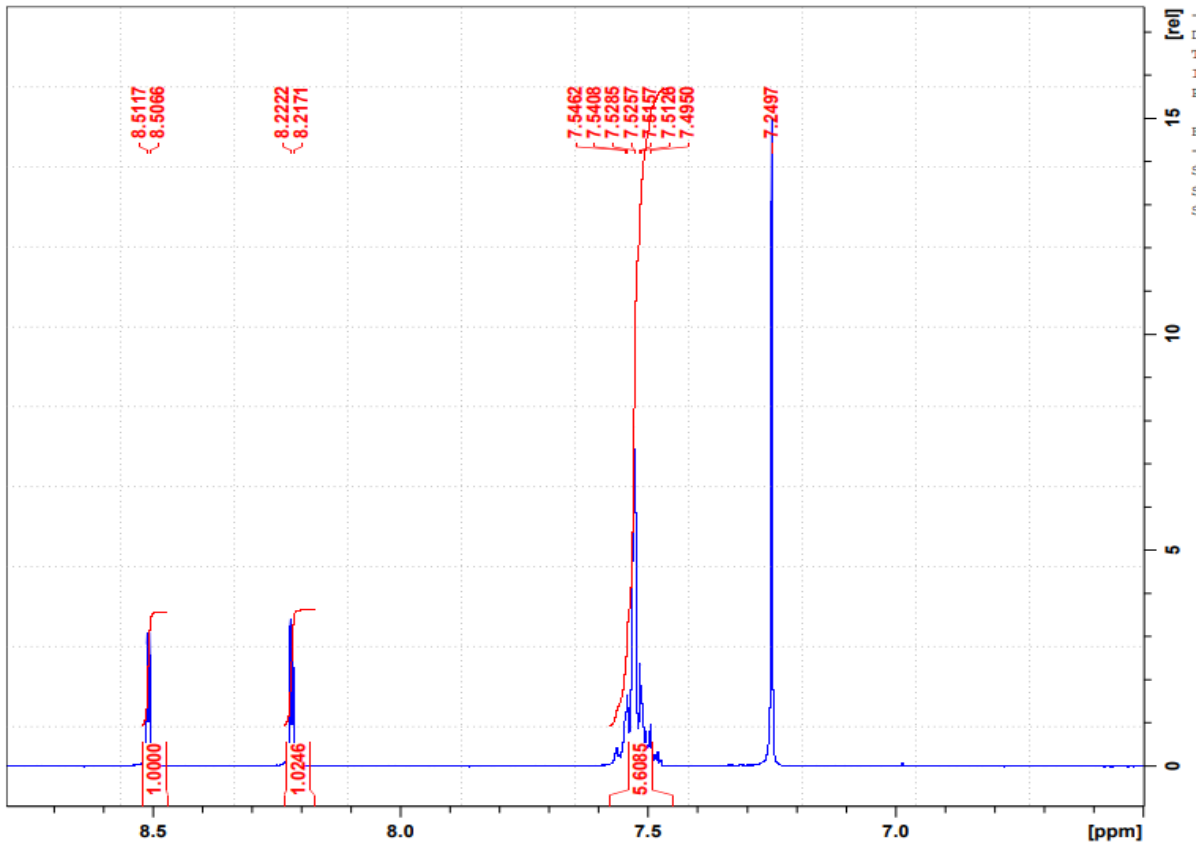

Figure 57. The ^{1}H NMR spectrum of compound **151 a**

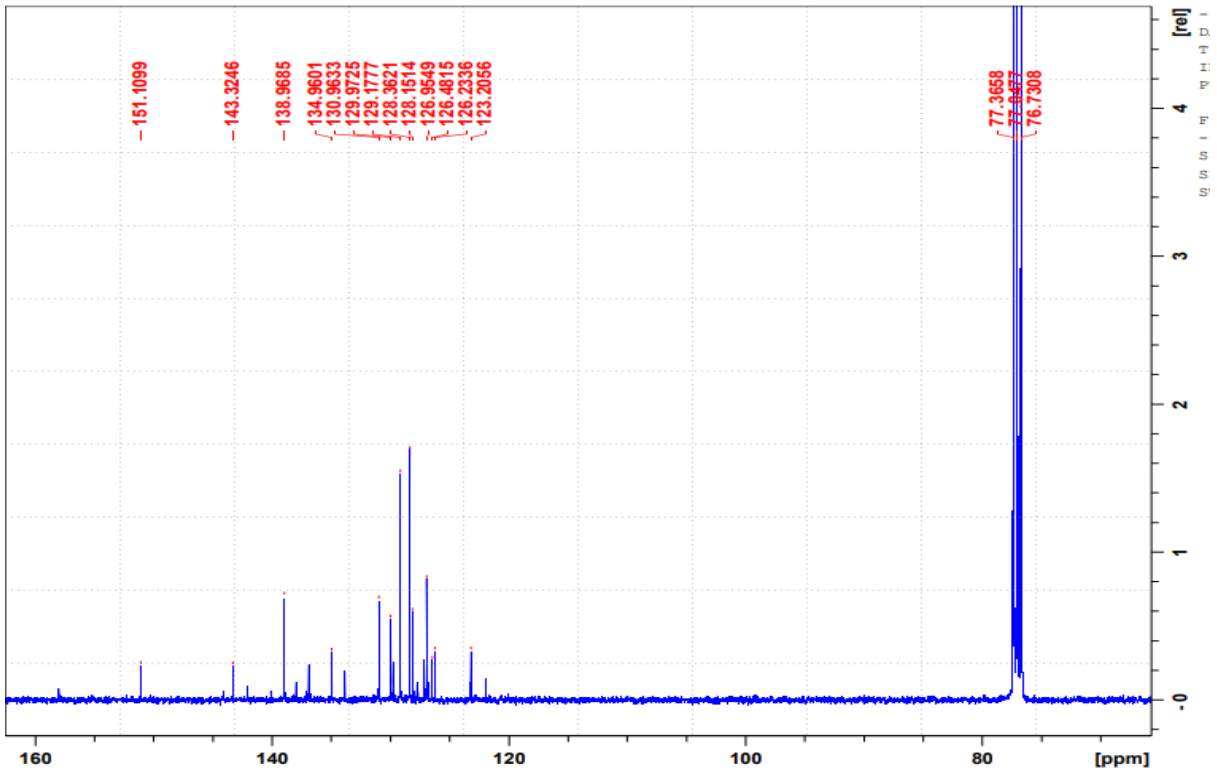

Figure 58. The ^{13}C NMR spectrum of compound **151 a**

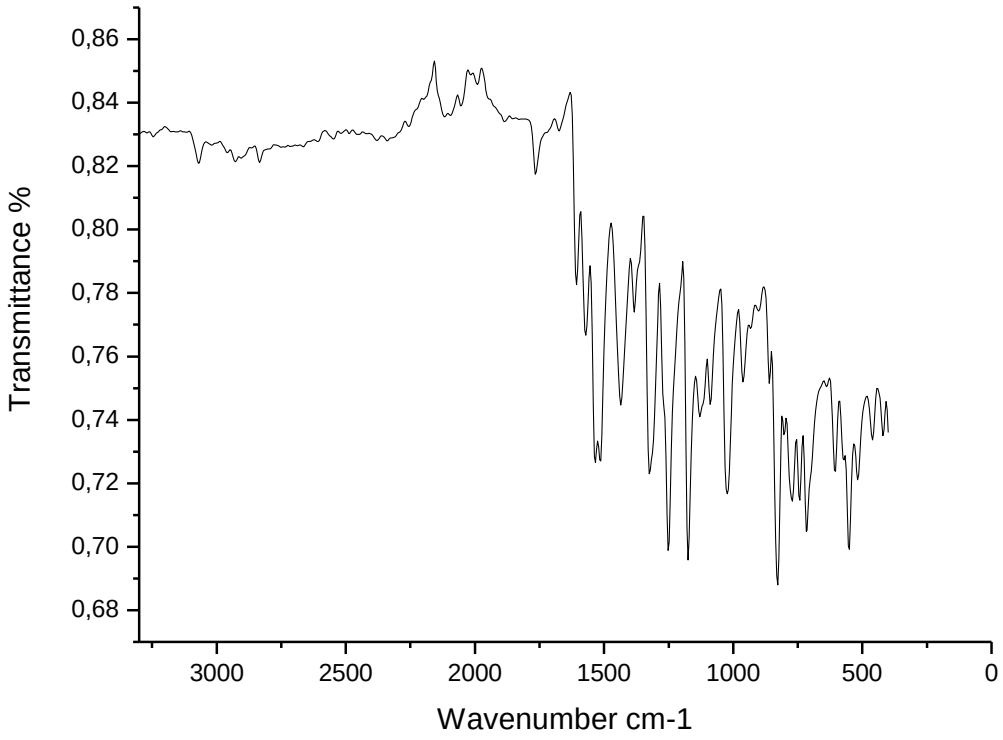

Figure 59. The FTIR spectrum of compound **151 a**

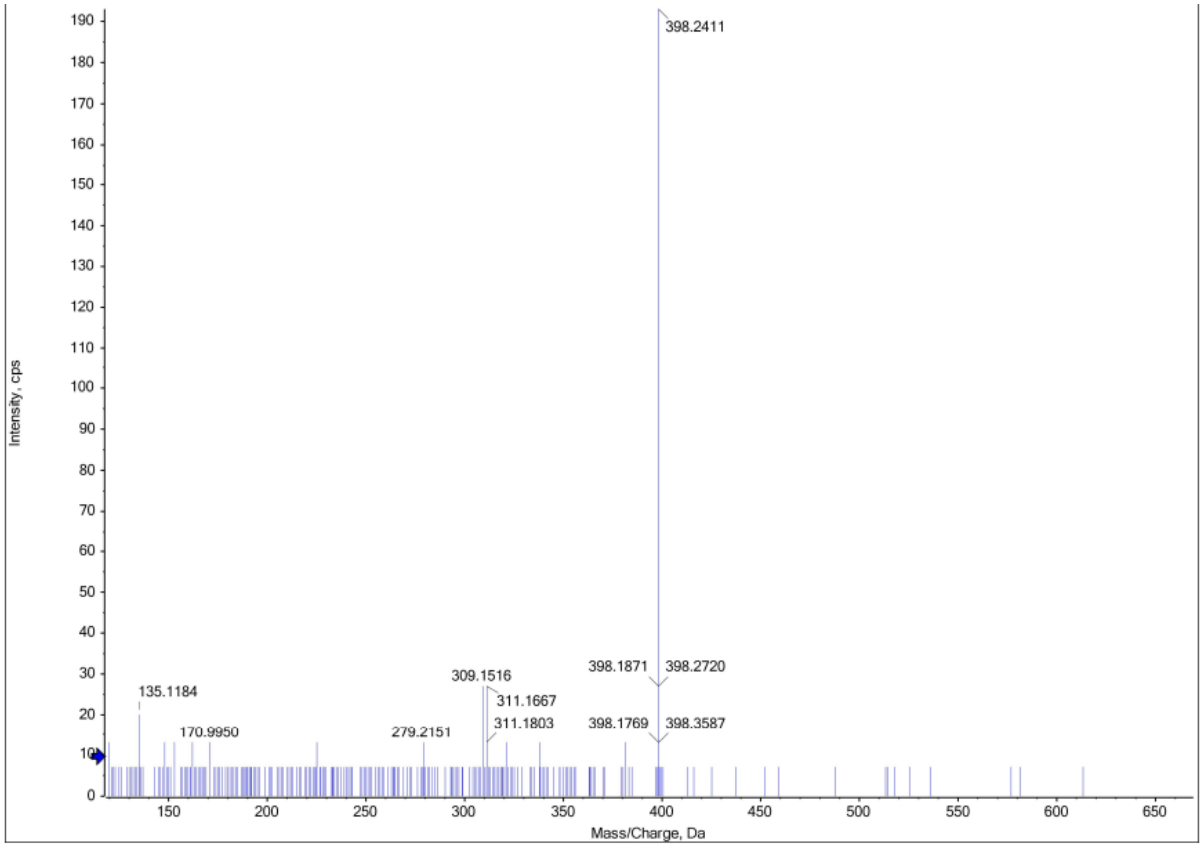

Figure 60. The HRMS spectrum of compound **151 a**

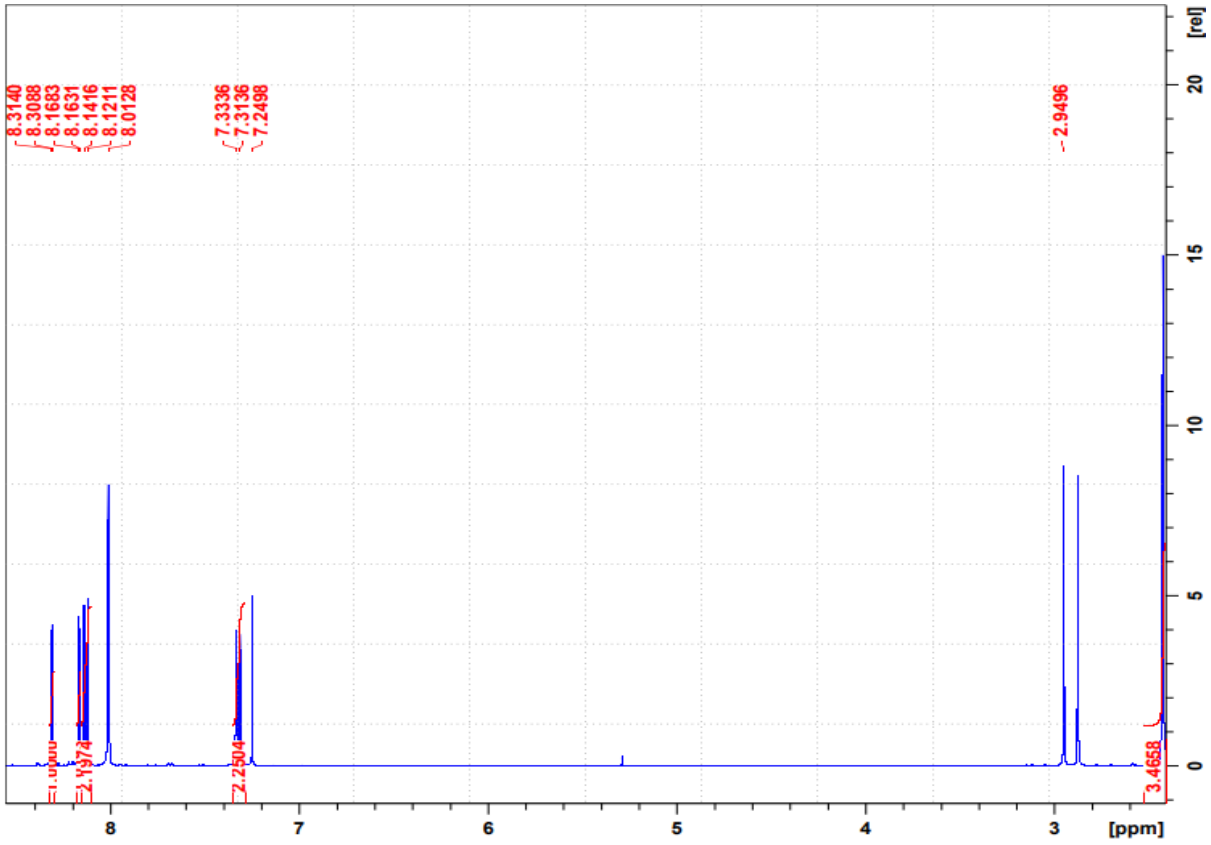

Figure 61. The ^{1}H NMR spectrum of compound **151 b**

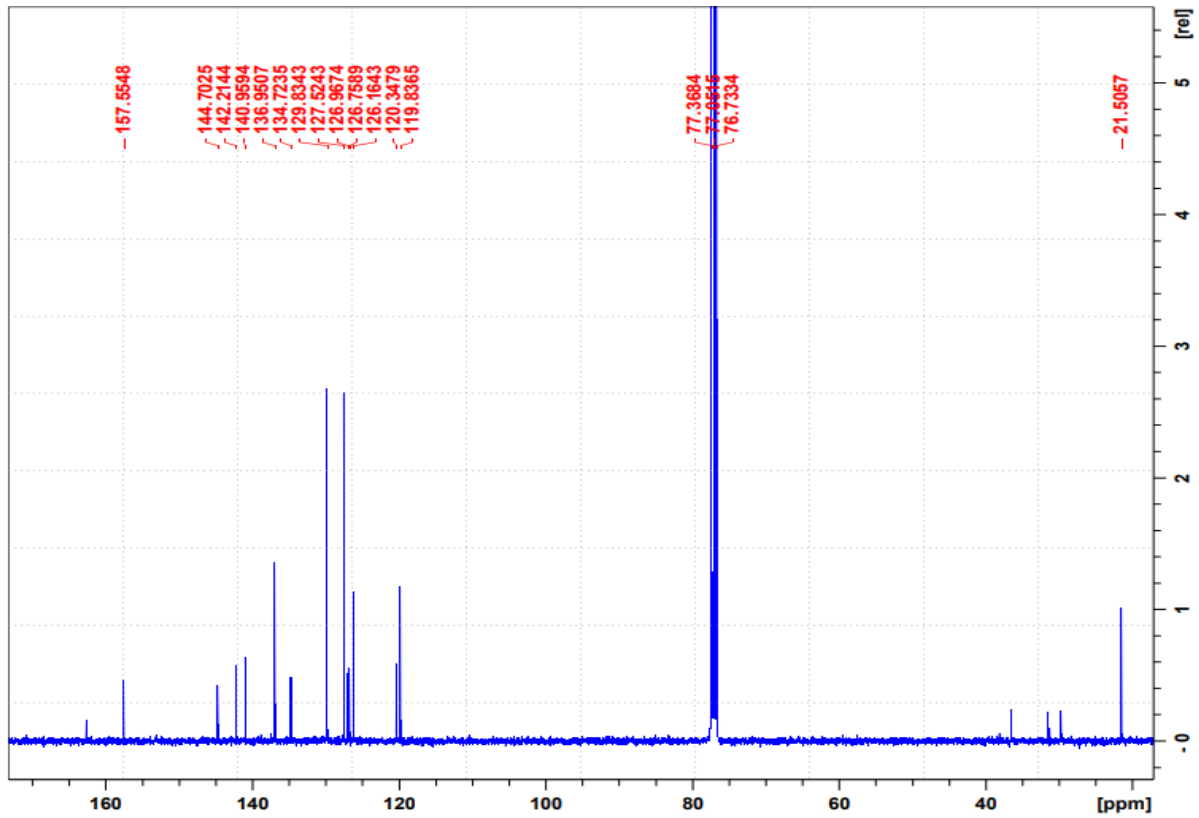

Figure 62. The ^{13}C NMR spectrum of compound **151 b**

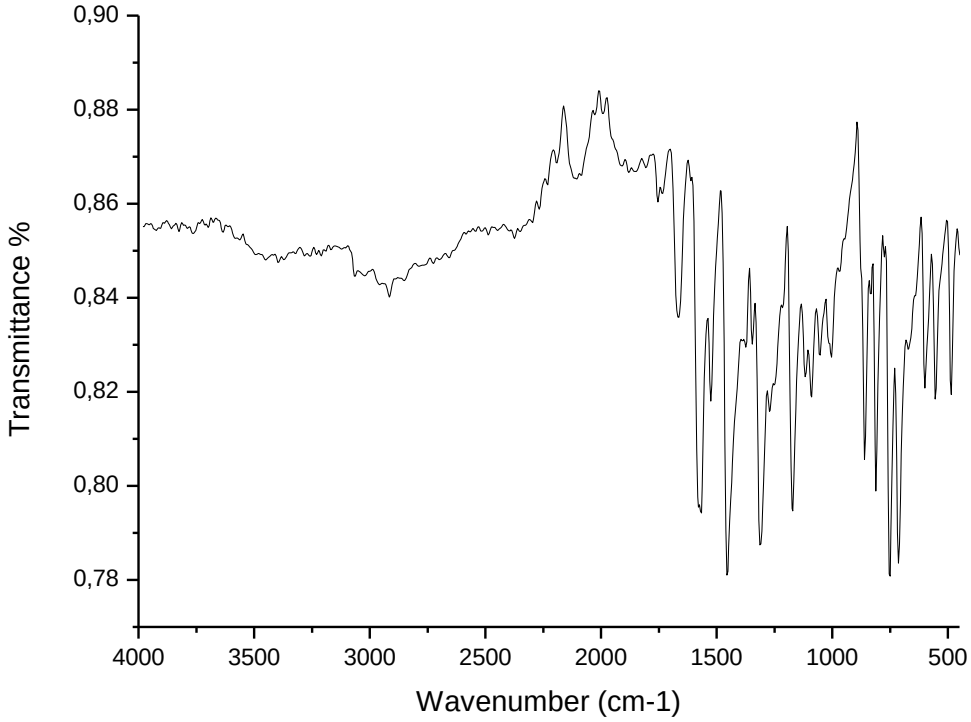

Figure 63. The FTIR spectrum of compound **151 b**

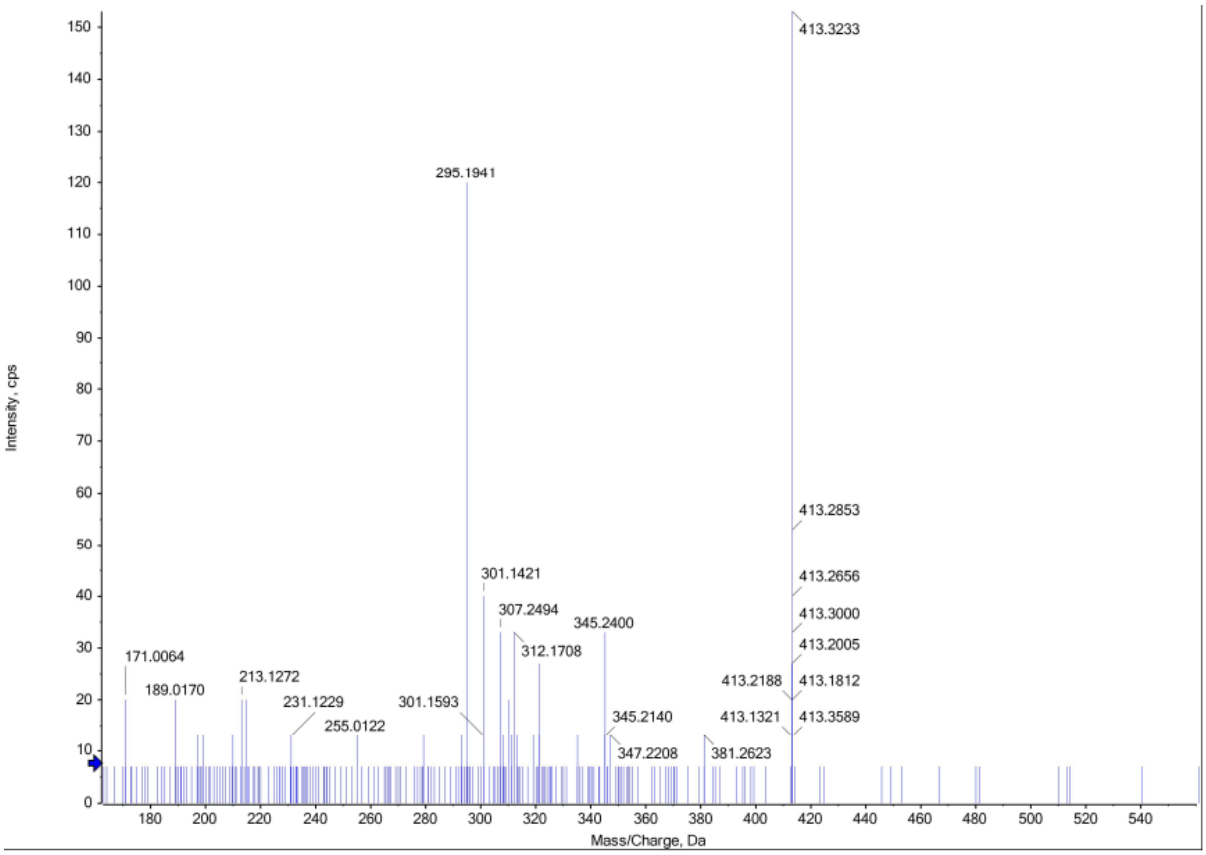

Figure 64. The HRMS spectrum of compound **151 b**

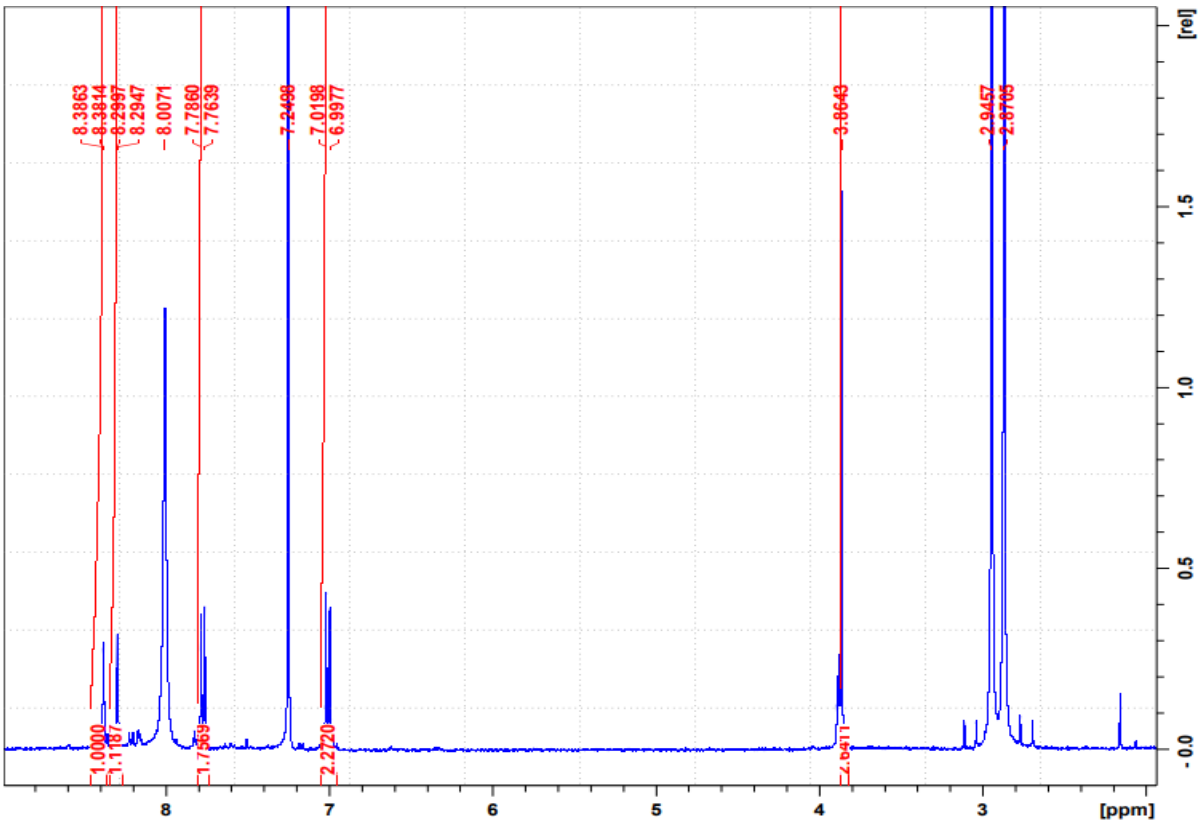
8.3863
8.3814
8.2997
8.2947
8.0071
7.7860
7.7639
7.2498
7.0198
6.9977
3.8643
2.9457
2.8705
1.0000
1.1187
2.2720
8
7
6
5
4
3
[ppm]
[rel]
1.5
1.0
0.5
-0.0

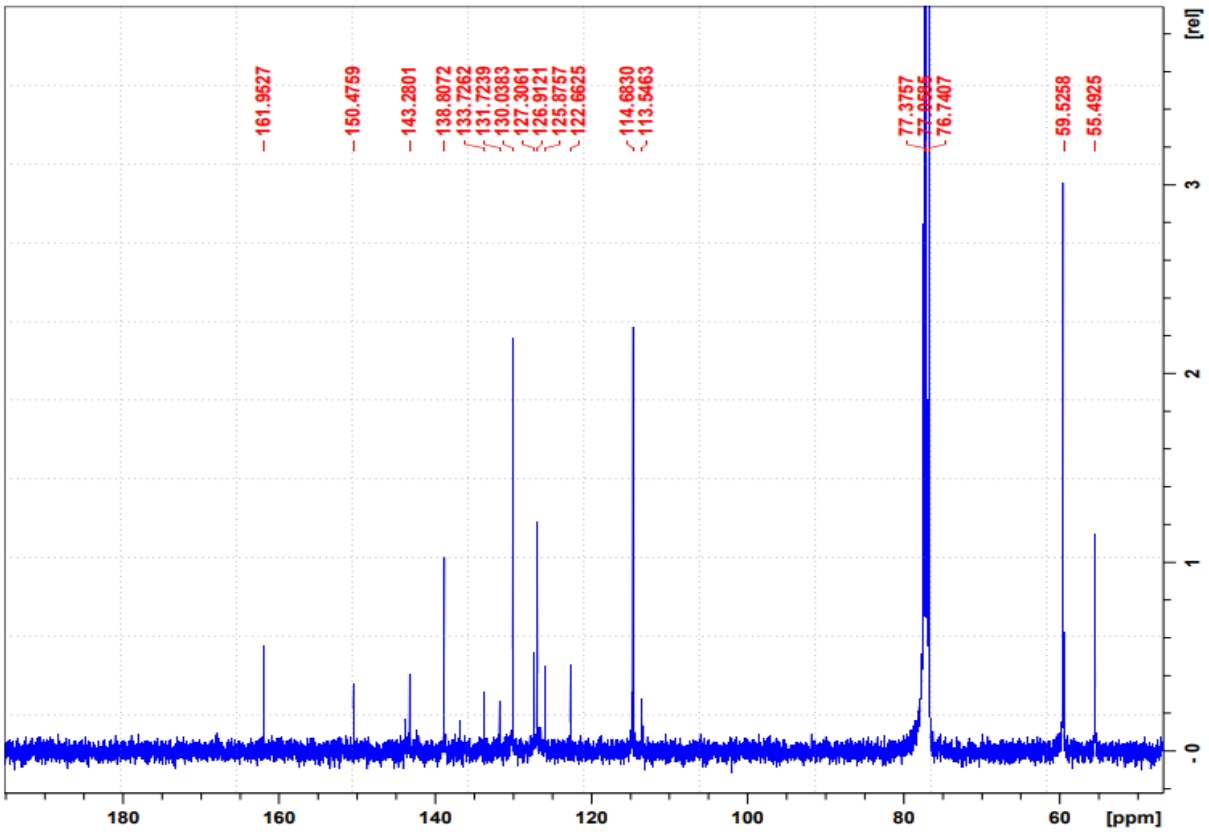

Figure 65. The 1H NMR spectrum of compound **151 c**

Figure 66. The ^{13}C NMR spectrum of compound **151 c**

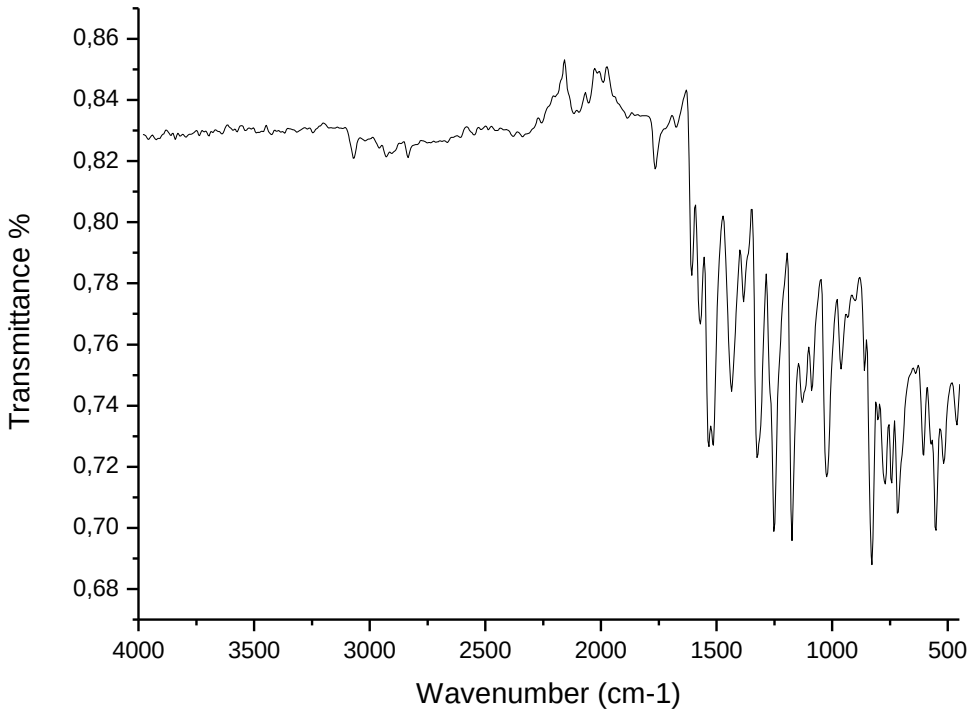

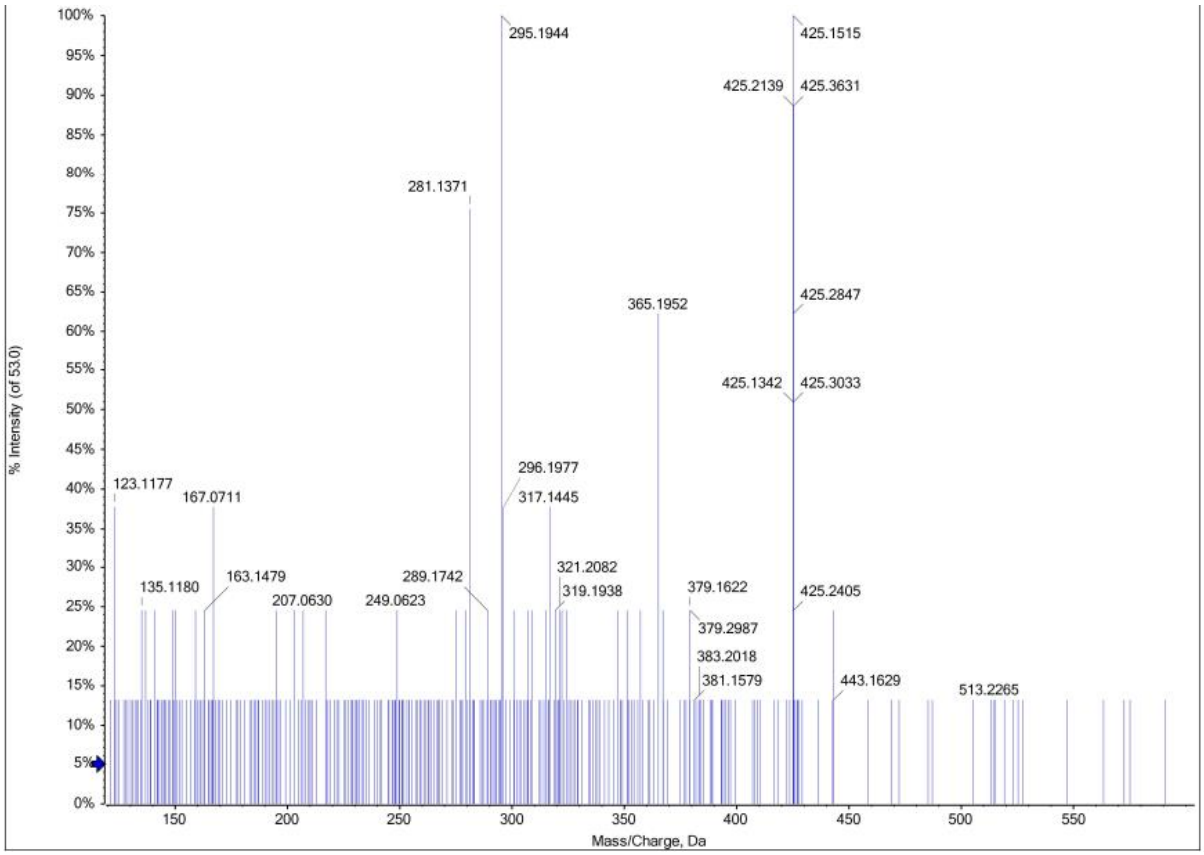

Figure 67. The FTIR spectrum of compound **151 c**

Figure 68. The HRMS spectrum of compound **151 c**

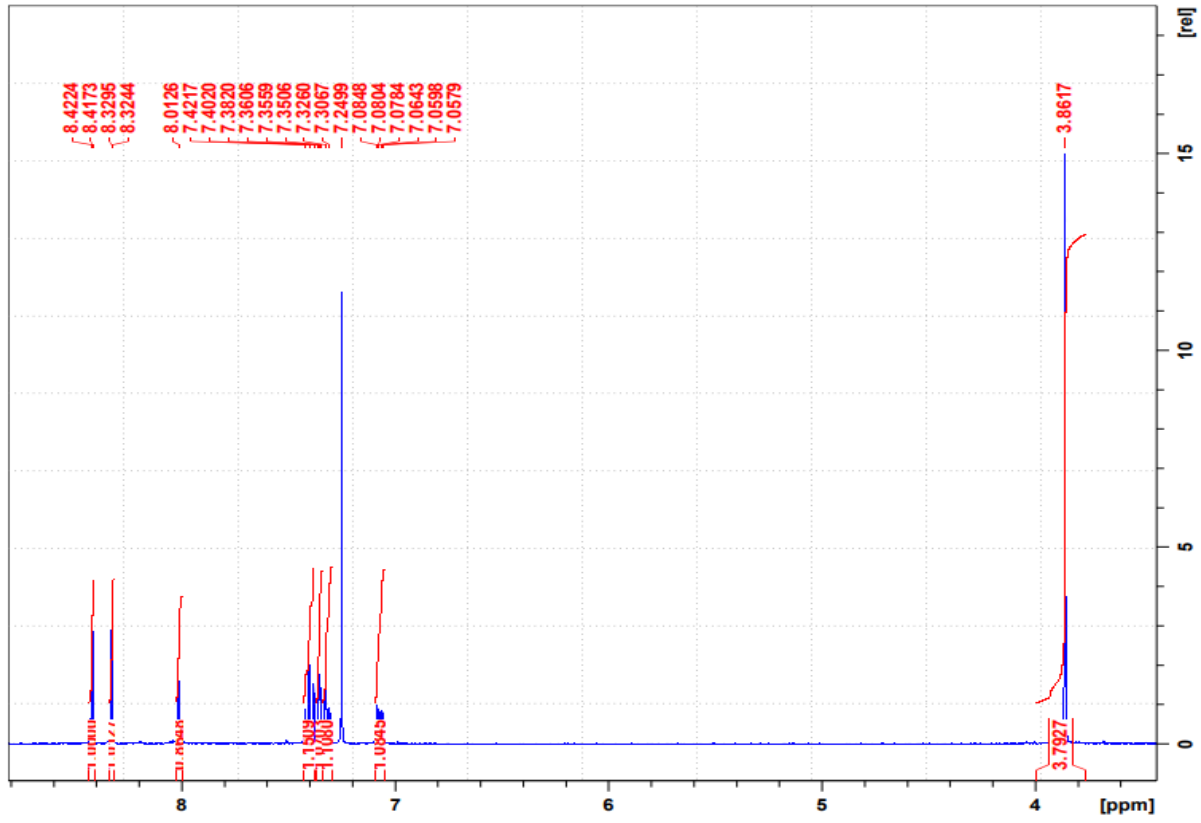

Figure 69. The ^{1}H NMR spectrum of compound **151 d**

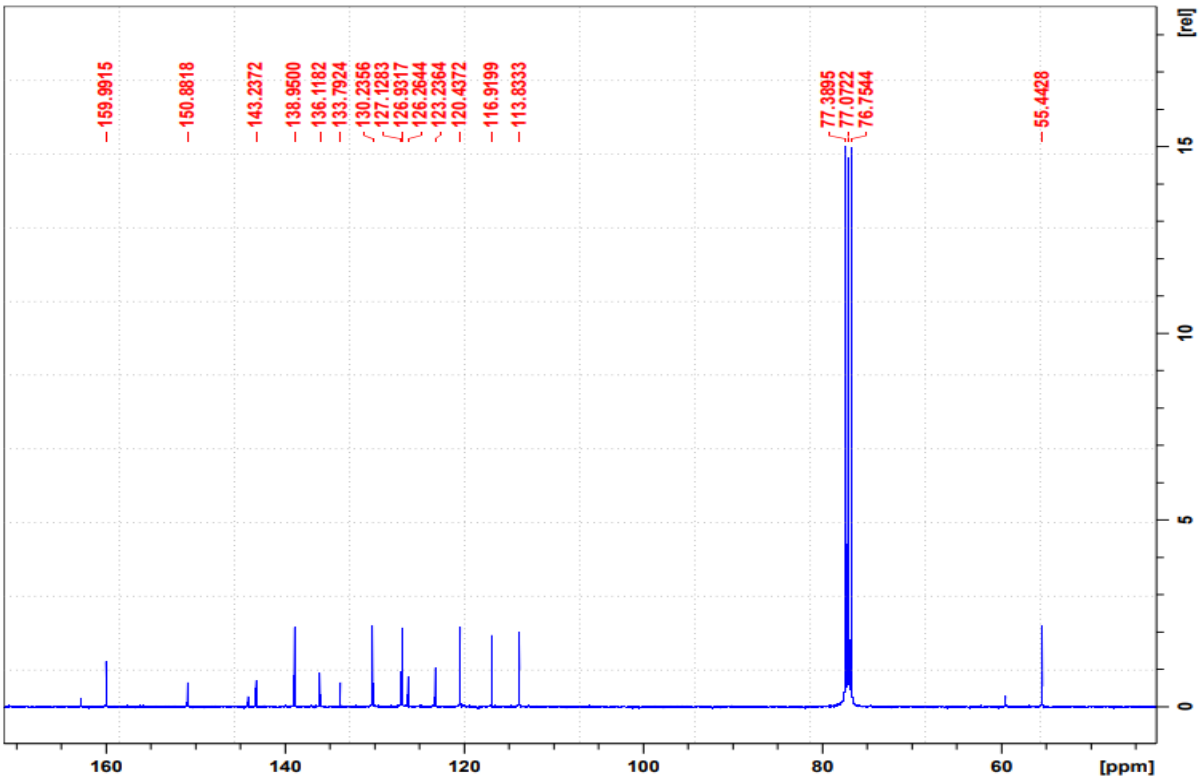

Figure 70. The ^{13}C NMR spectrum of compound **151 d**

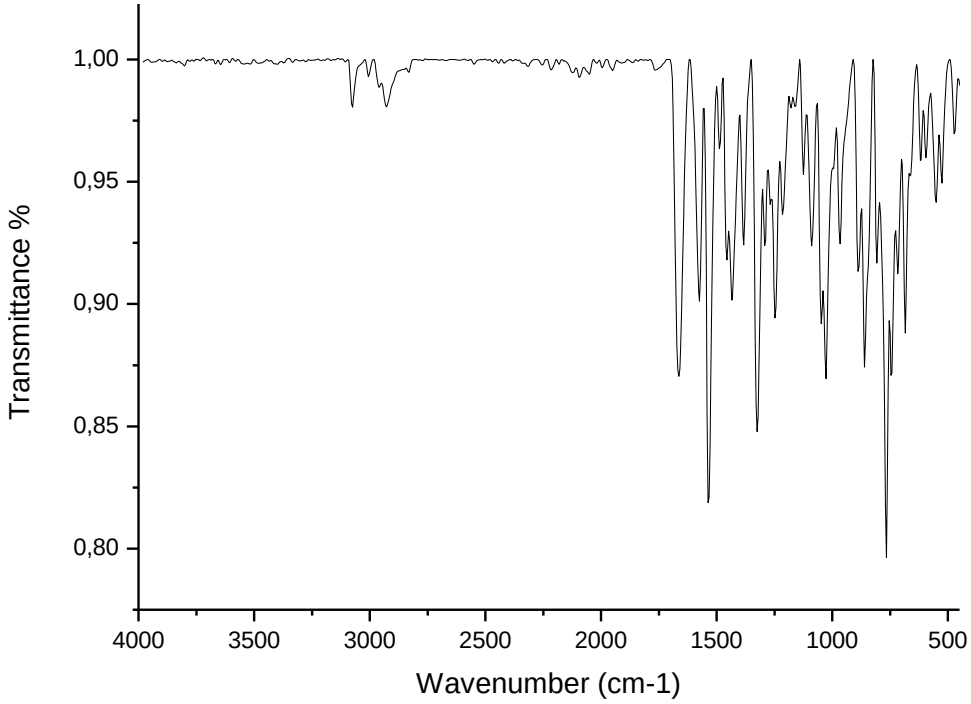

Figure 71. The FTIR spectrum of compound **151 d**

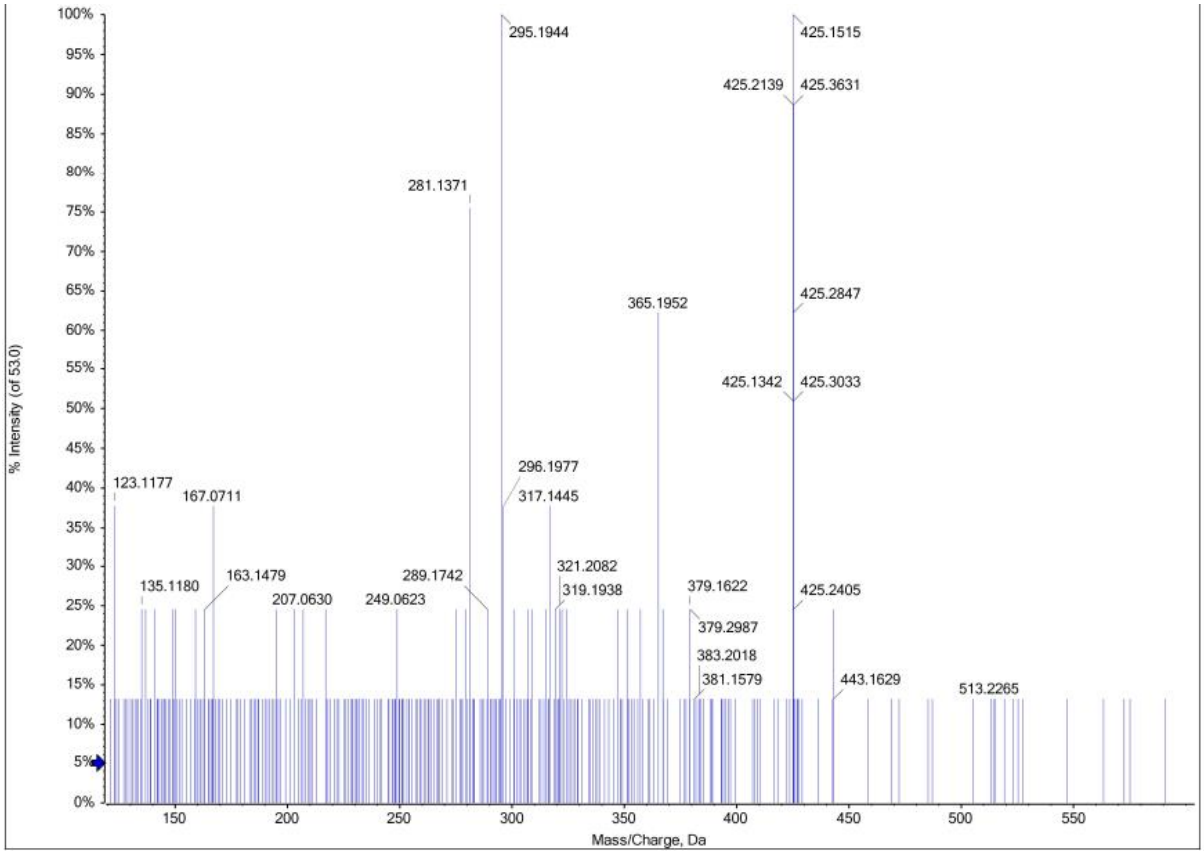

Figure 72. The HRMS spectrum of compound **151 d**

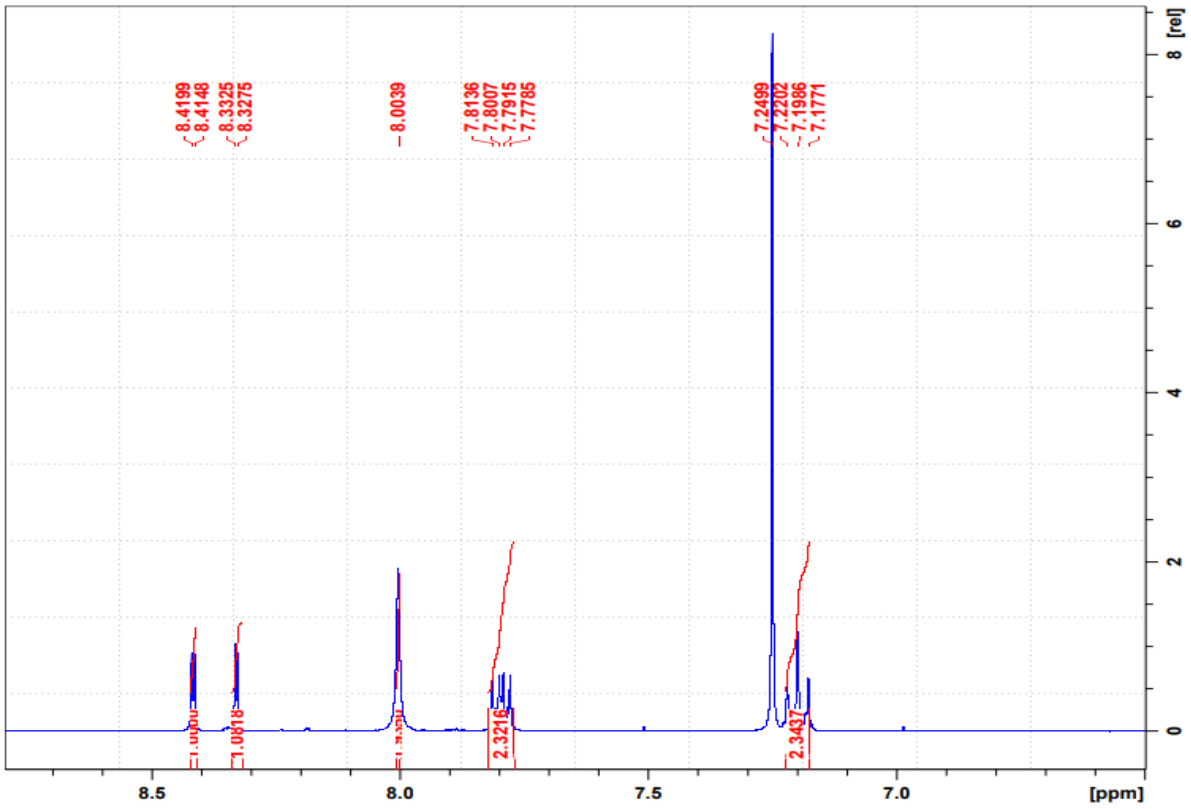

Figure 73. The ^{1}H NMR spectrum of compound **151 e**

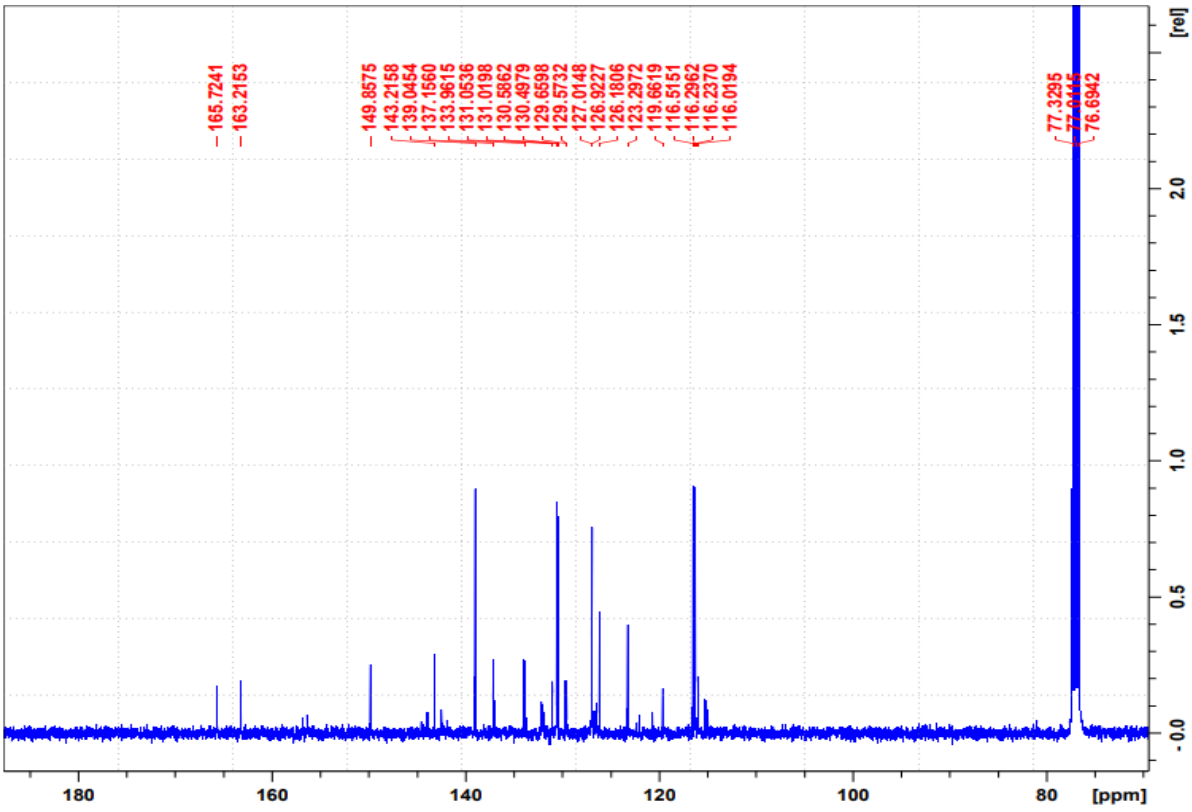

Figure 74. The ^{13}C NMR spectrum of compound **151 e**

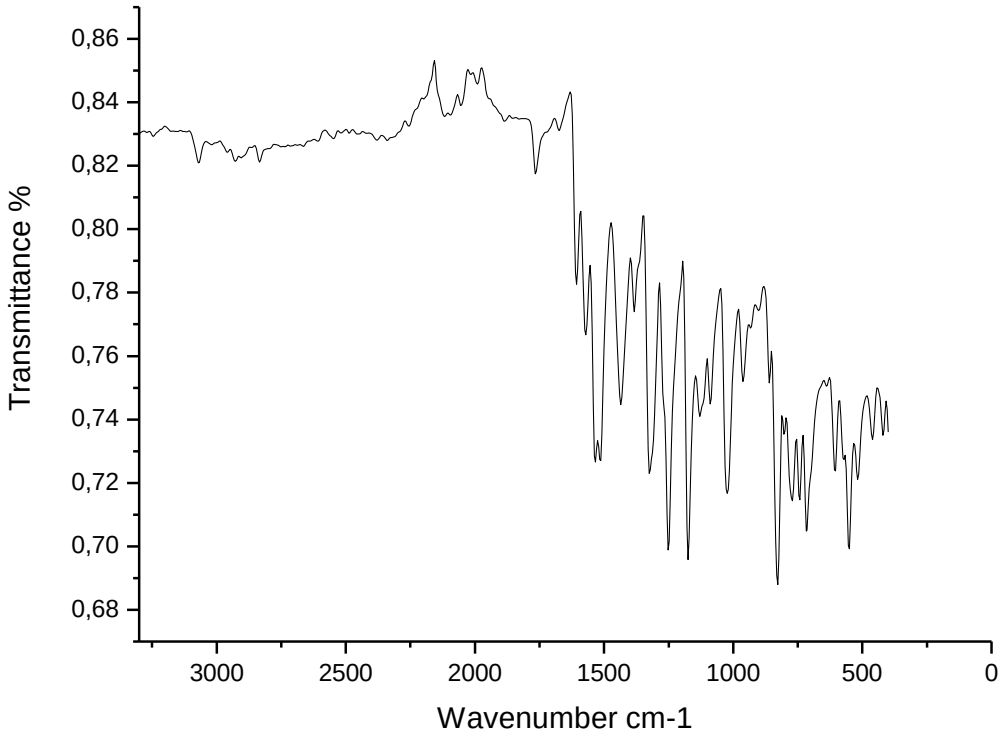

Figure 75. The FTIR spectrum of compound **151 e**

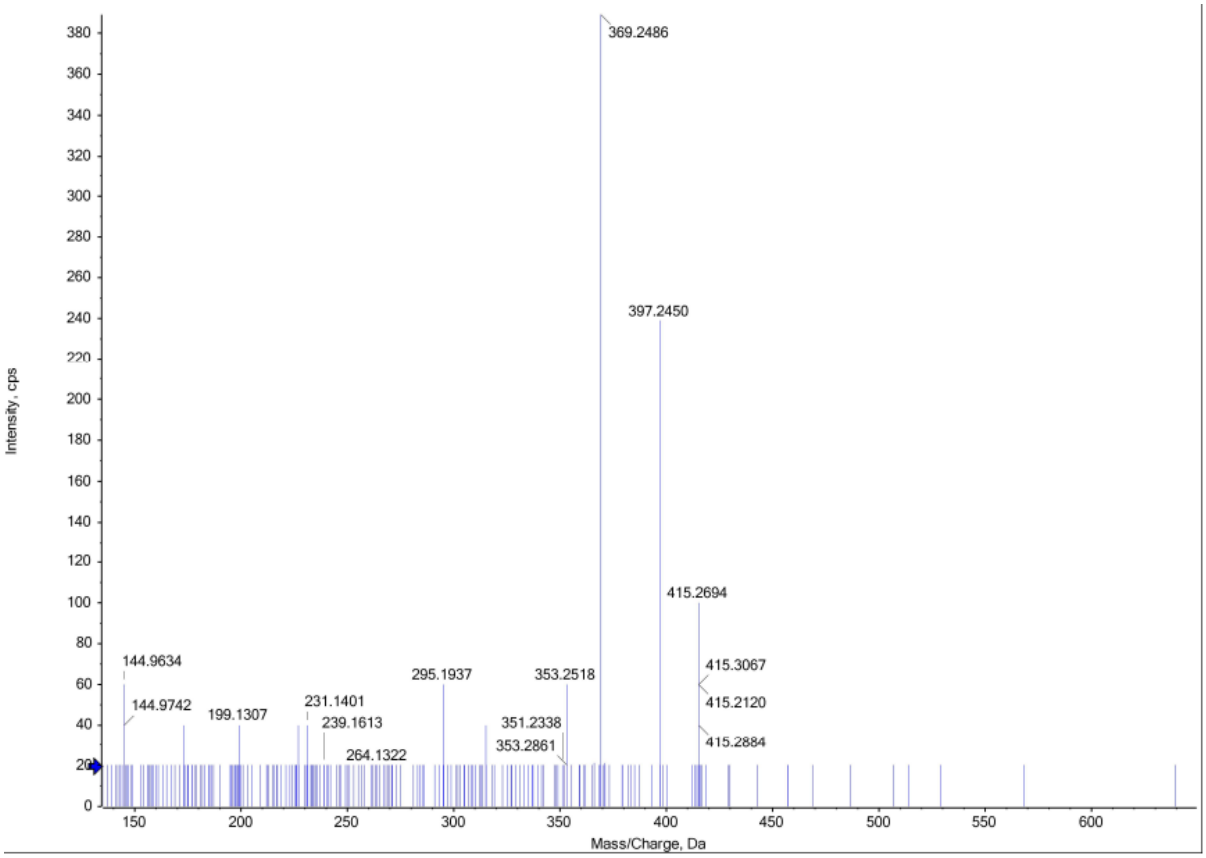

Figure 76. The HRMS spectrum of compound **151 e**

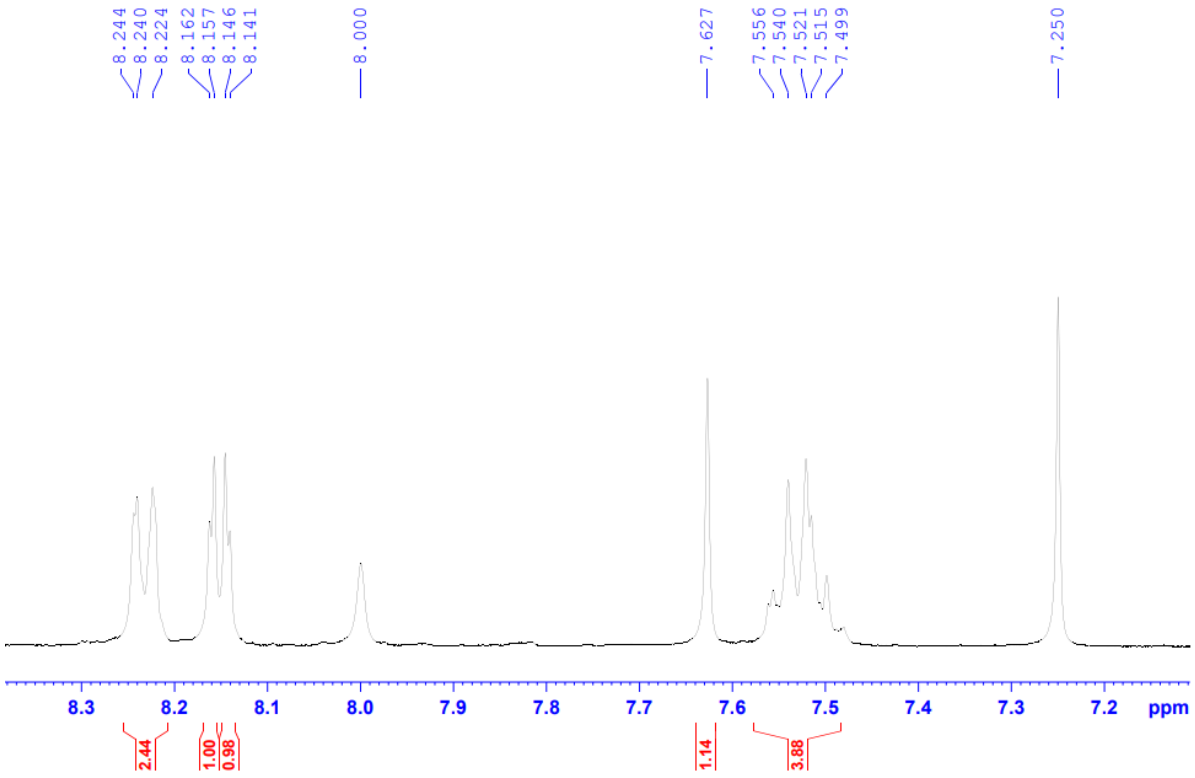

Figure 77. The ^{1}H NMR spectrum of compound **152 a**

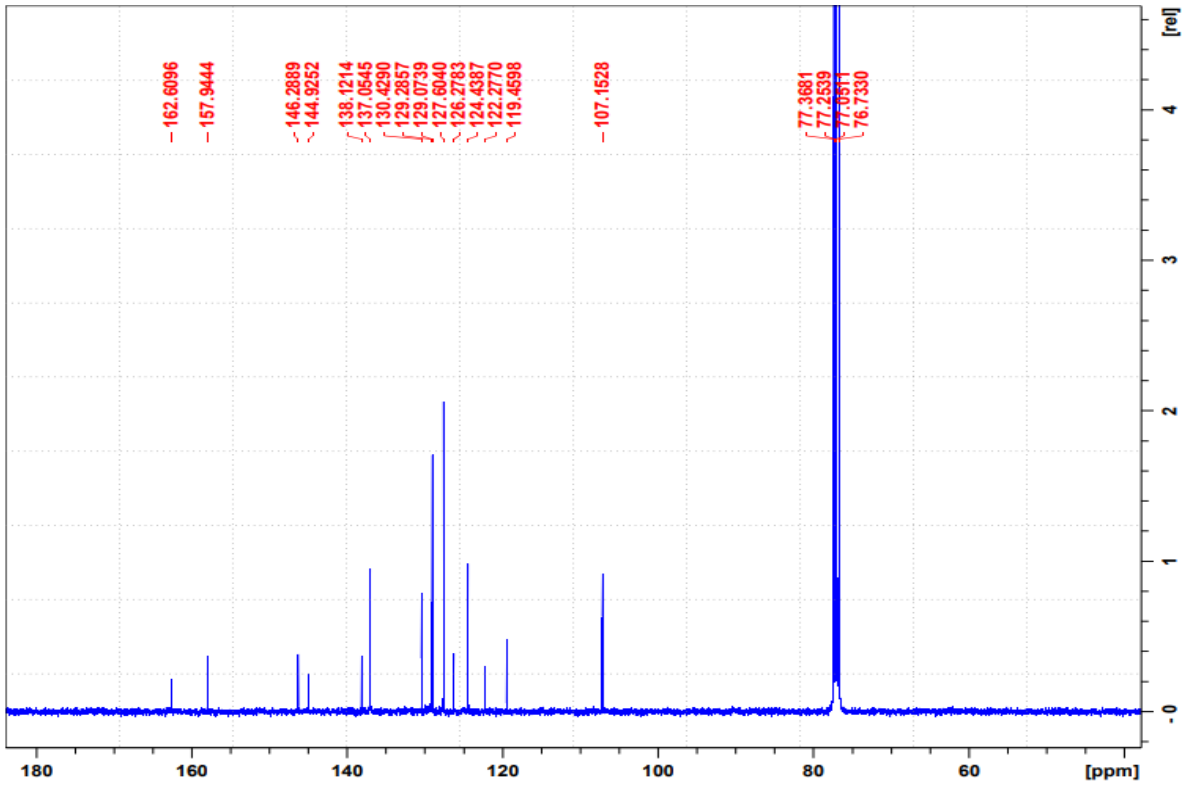

Figure 78. The ^{13}C NMR spectrum of compound **152 a**

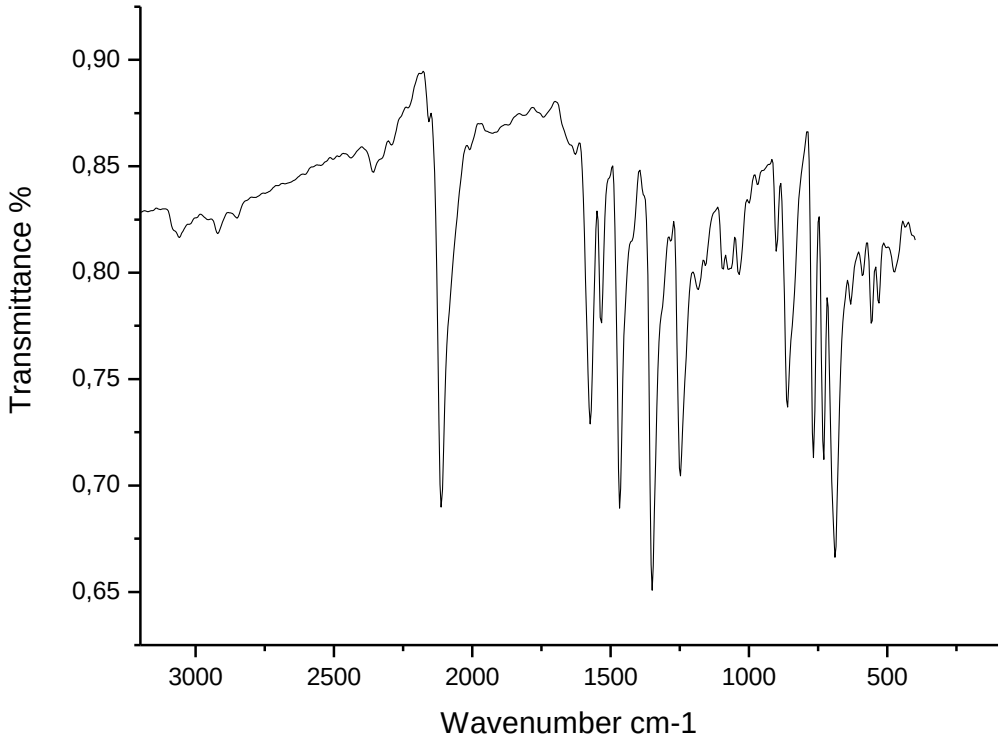

Figure 79. The FTIR spectrum of compound **152 a**

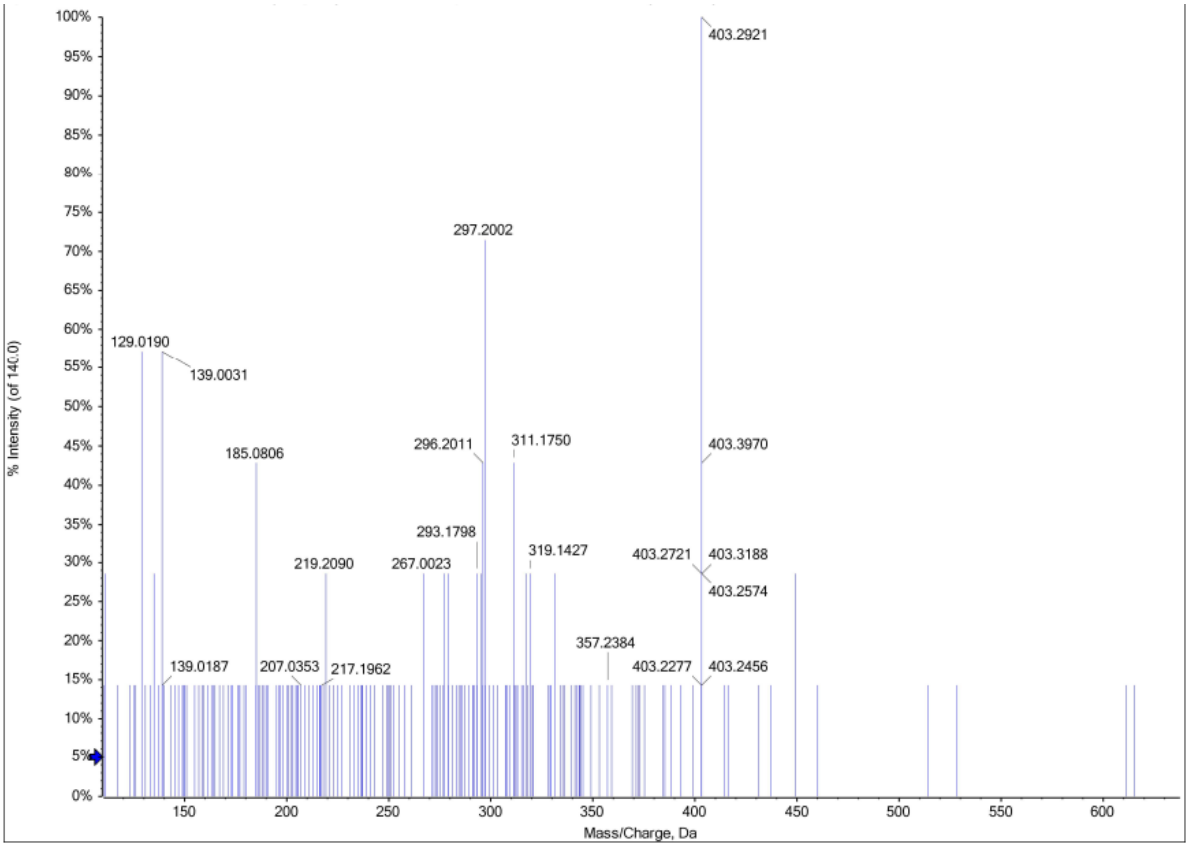

Figure 80. The HRMS spectrum of compound **152 a**

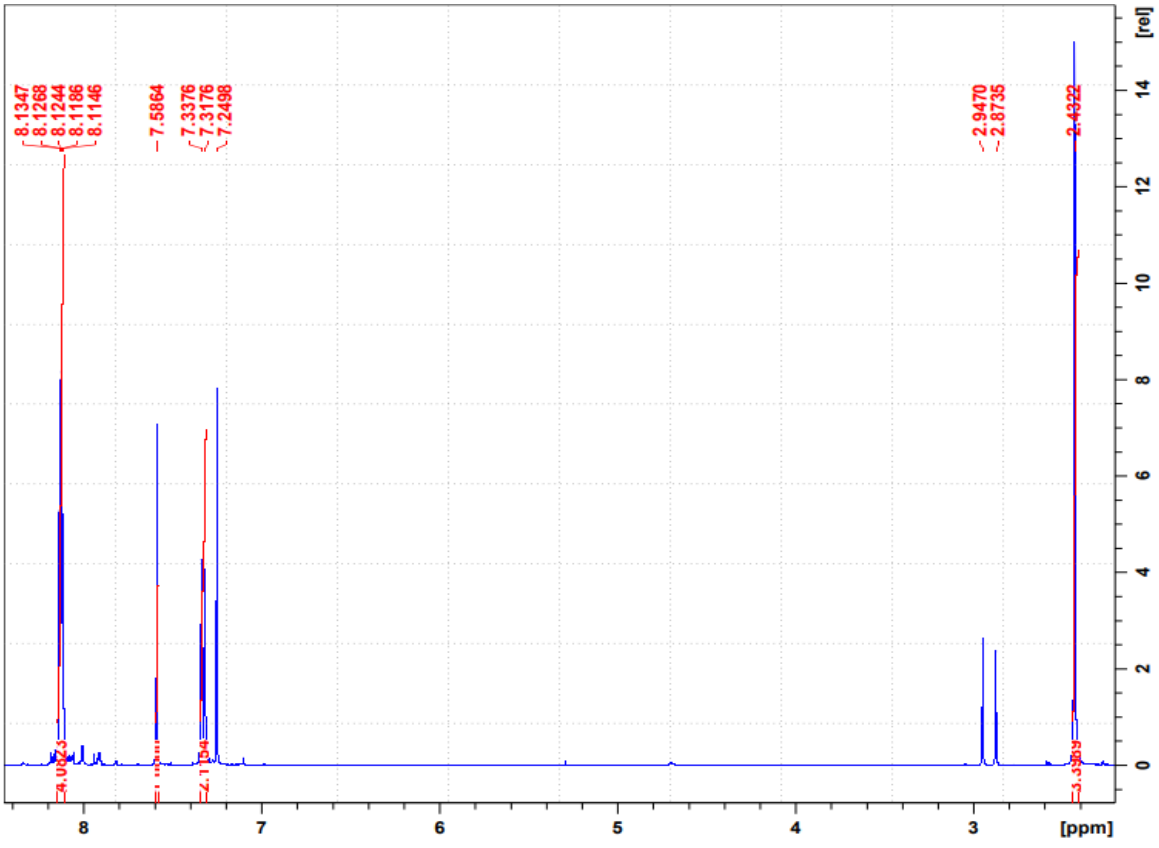

Figure 81. The ^{1}H NMR spectrum of compound **152 b**

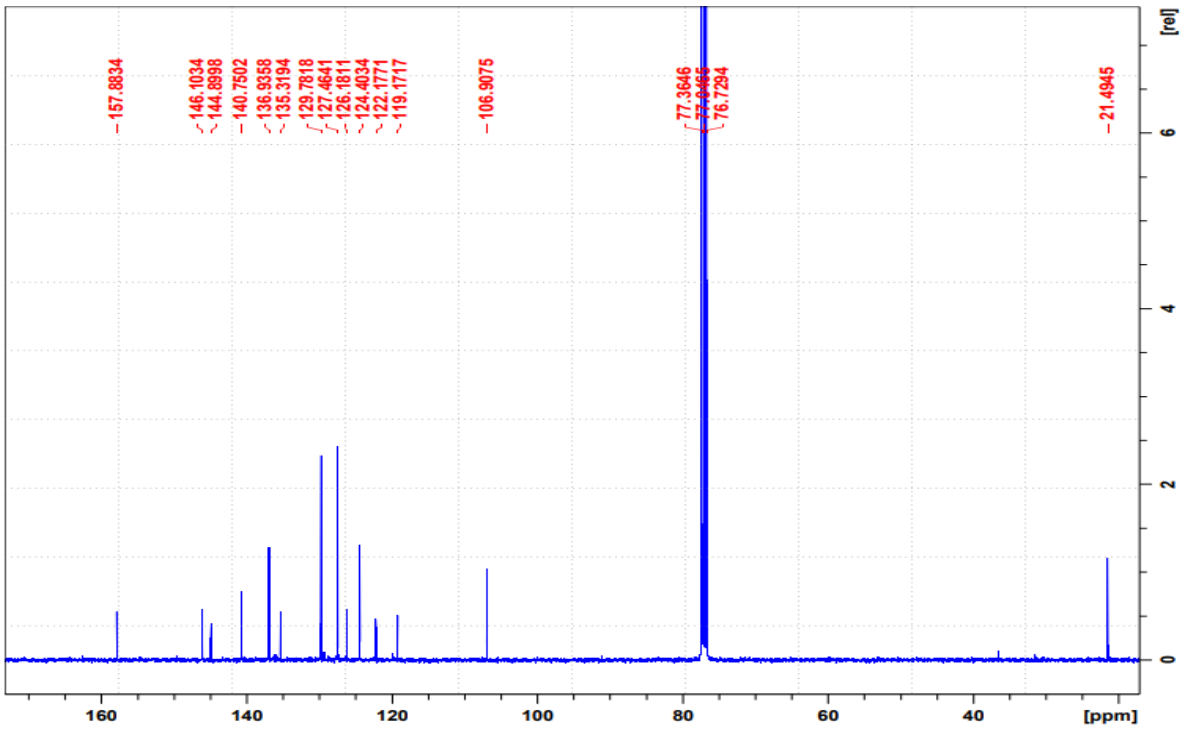

Figure 82. The ^{13}C NMR spectrum of compound **152 b**

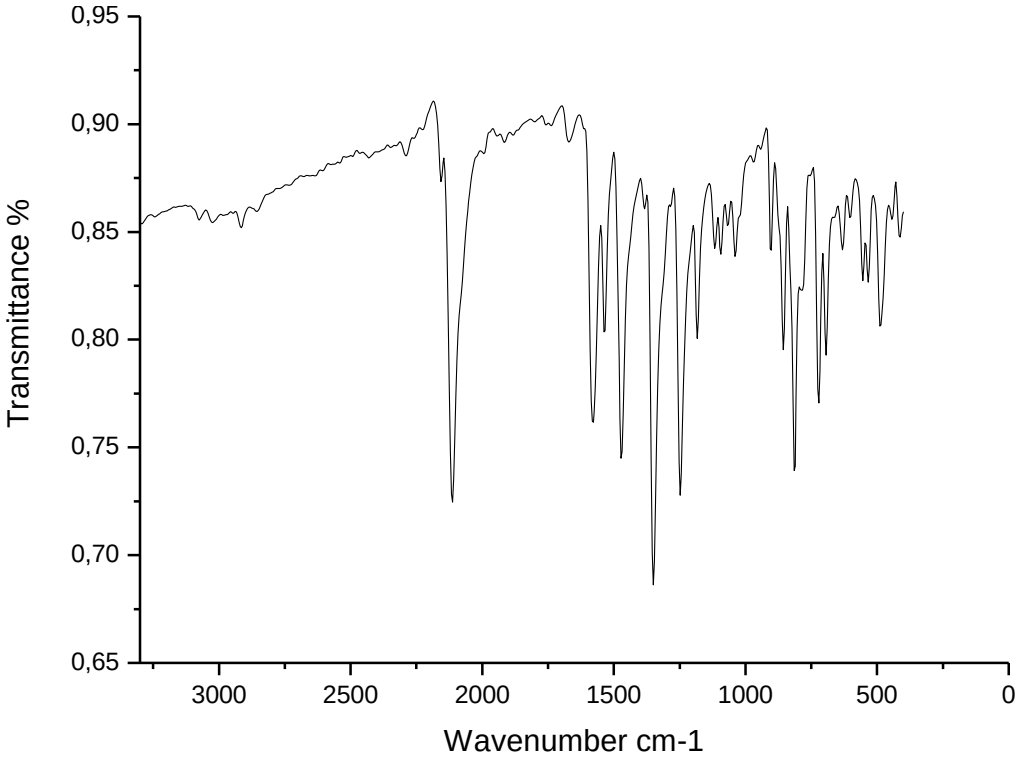

Figure 83. The FTIR spectrum of compound **152 b**

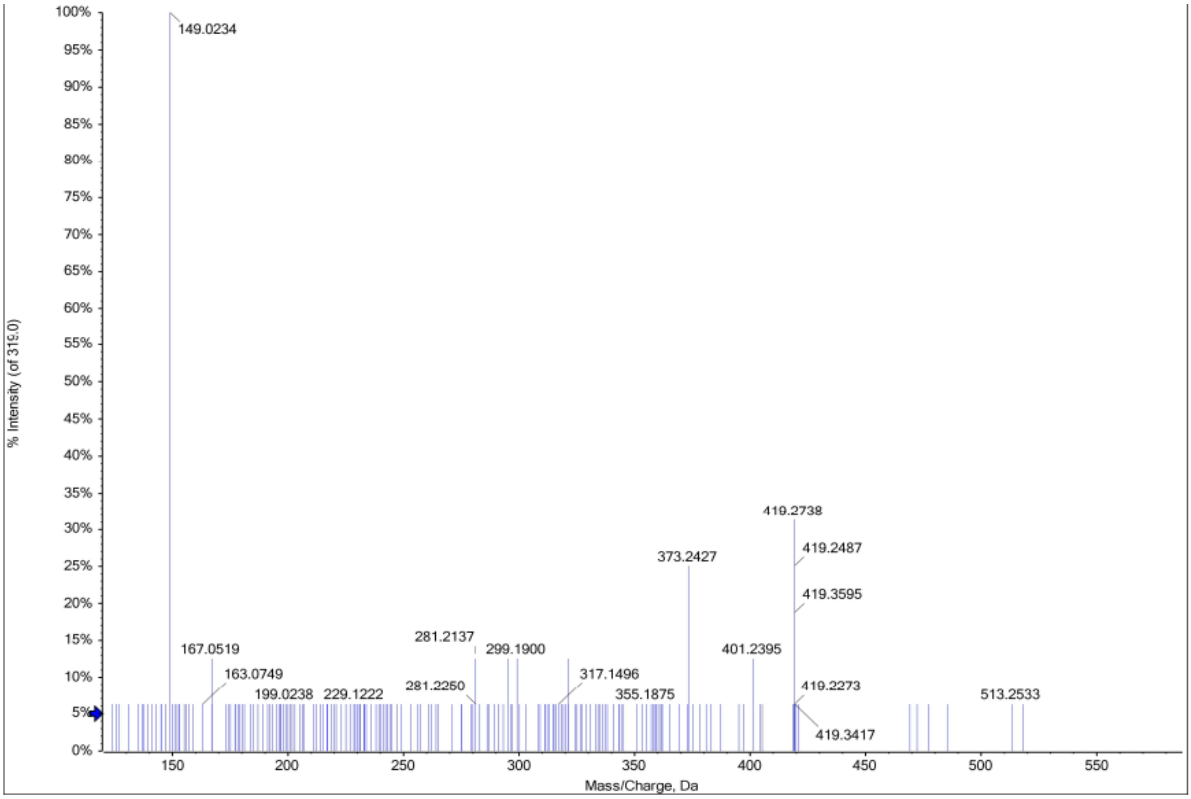

Figure 84. The HRMS spectrum of compound **152 b**

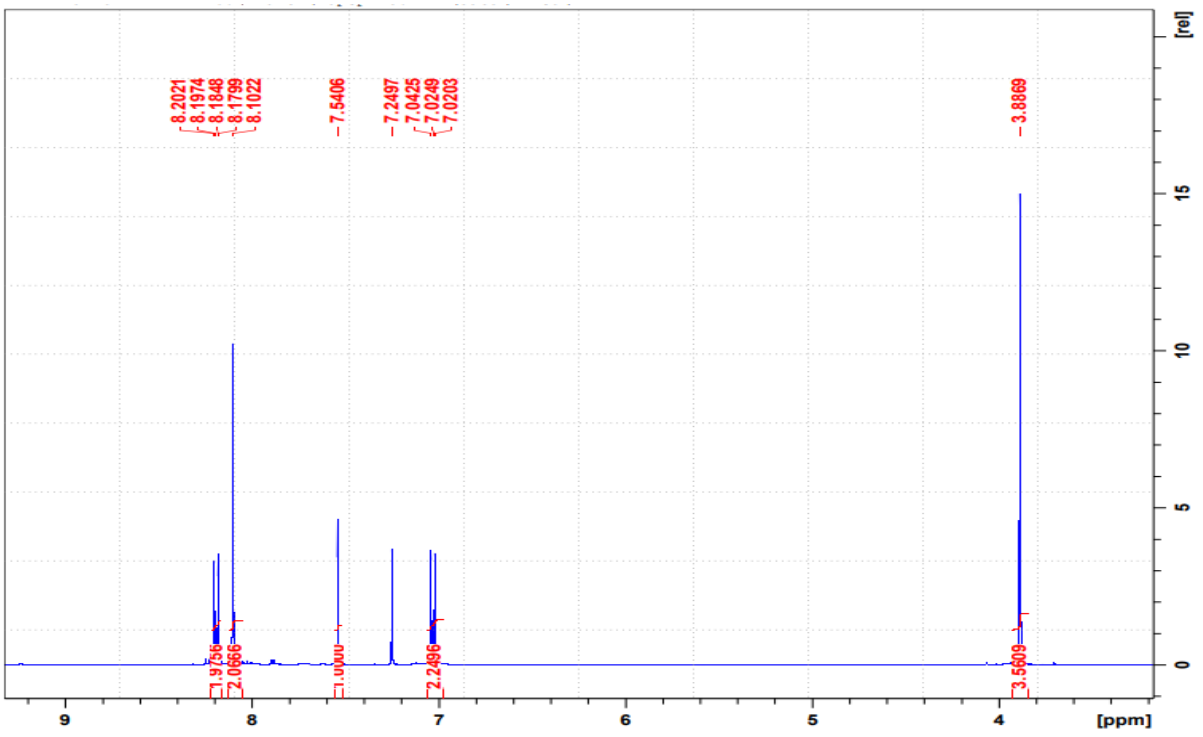

Figure 85. The ^{1}H NMR spectrum of compound **152 c**

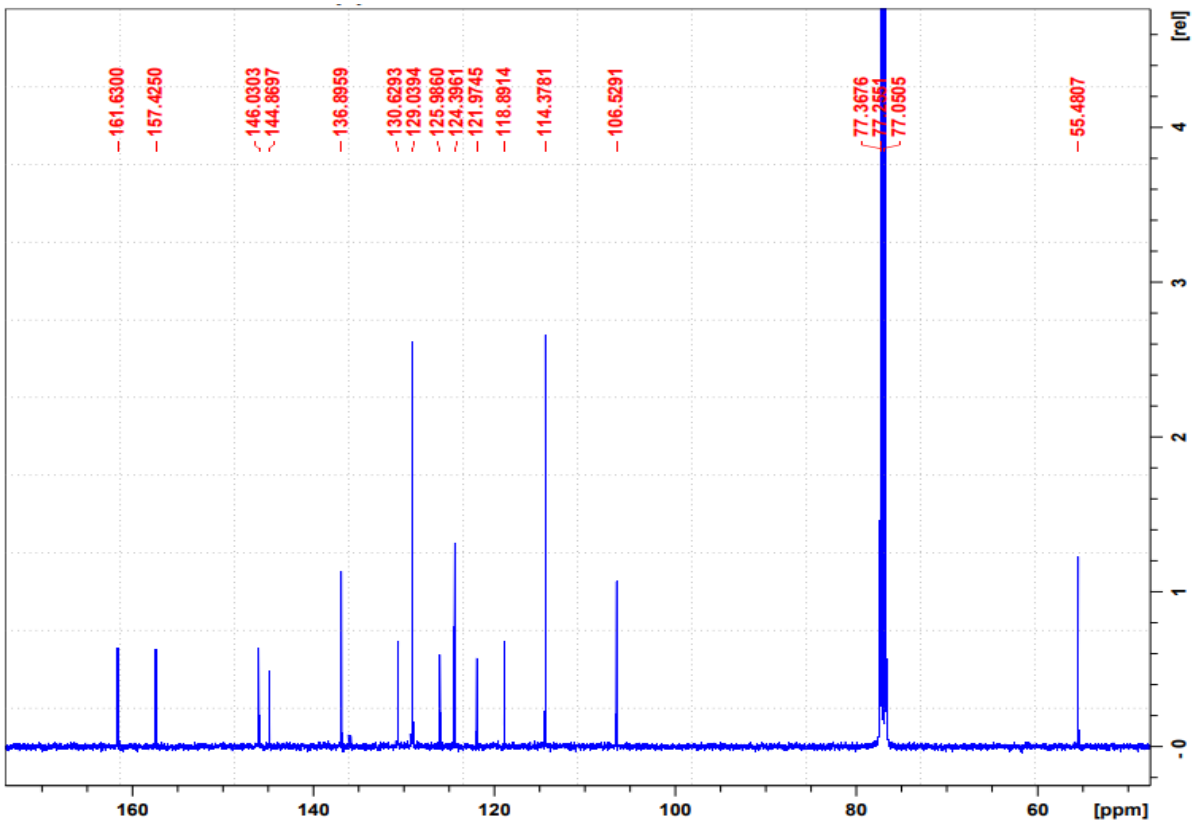

Figure 86. The ^{13}C NMR spectrum of compound **152 c**

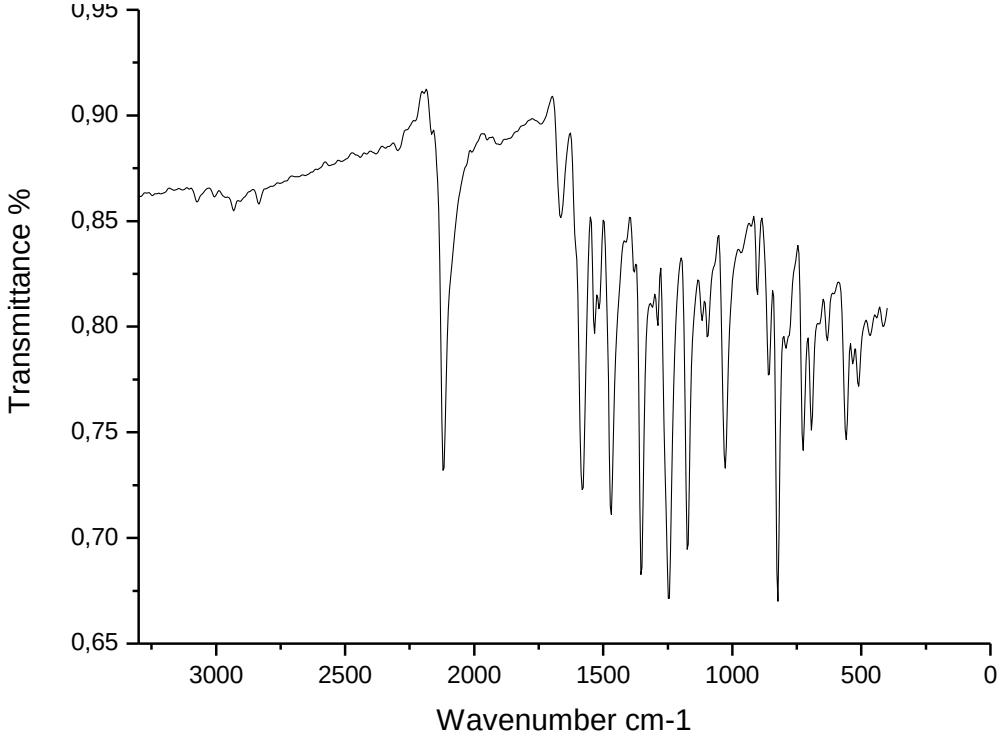

Figure 87. The FTIR spectrum of compound **152 c**

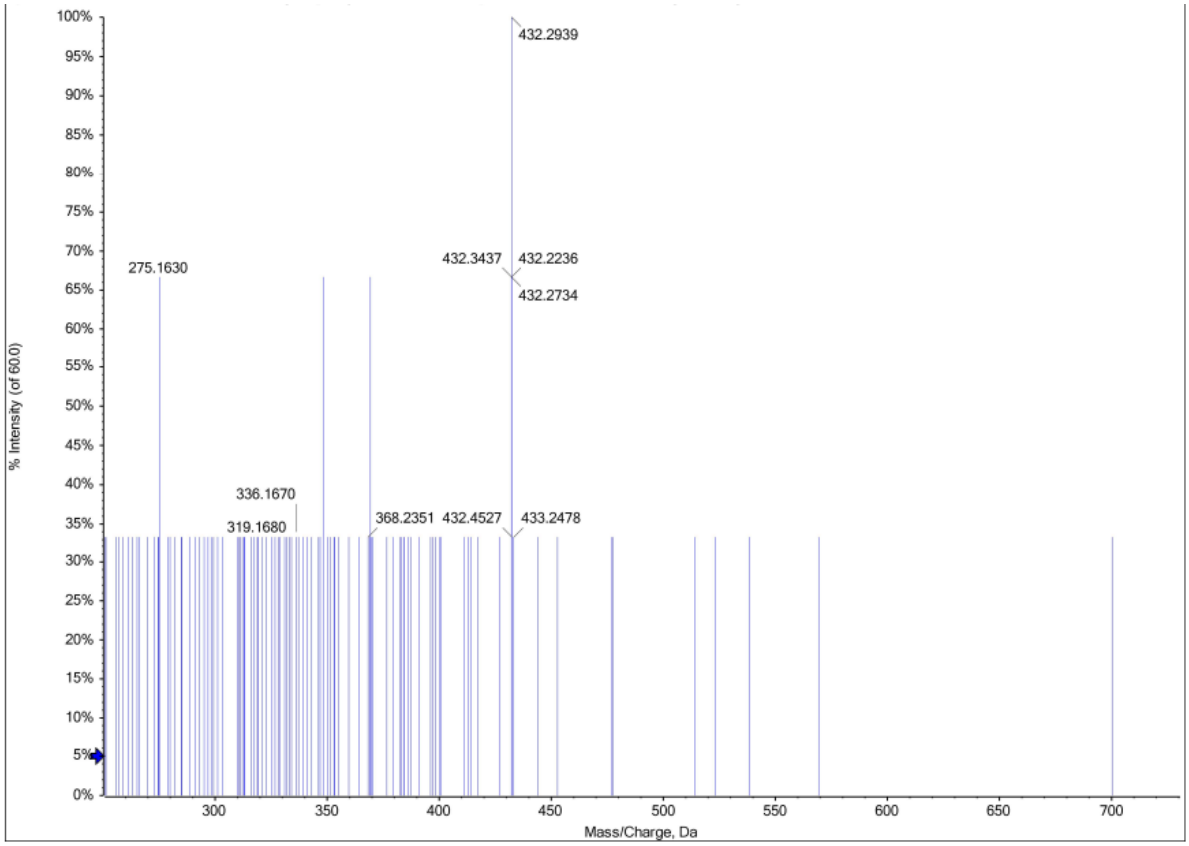

Figure 88. The HRMS spectrum of compound **152 c**

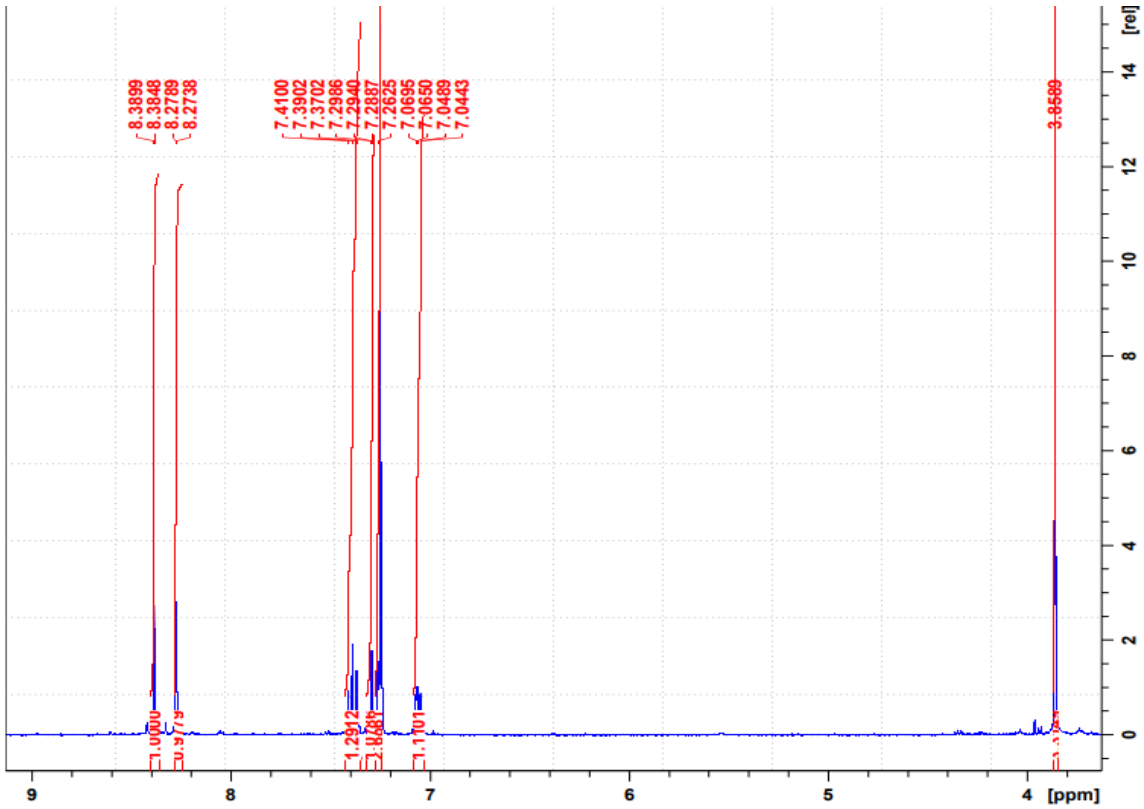

Figure 89. The ^{1}H NMR spectrum of compound **152 d**

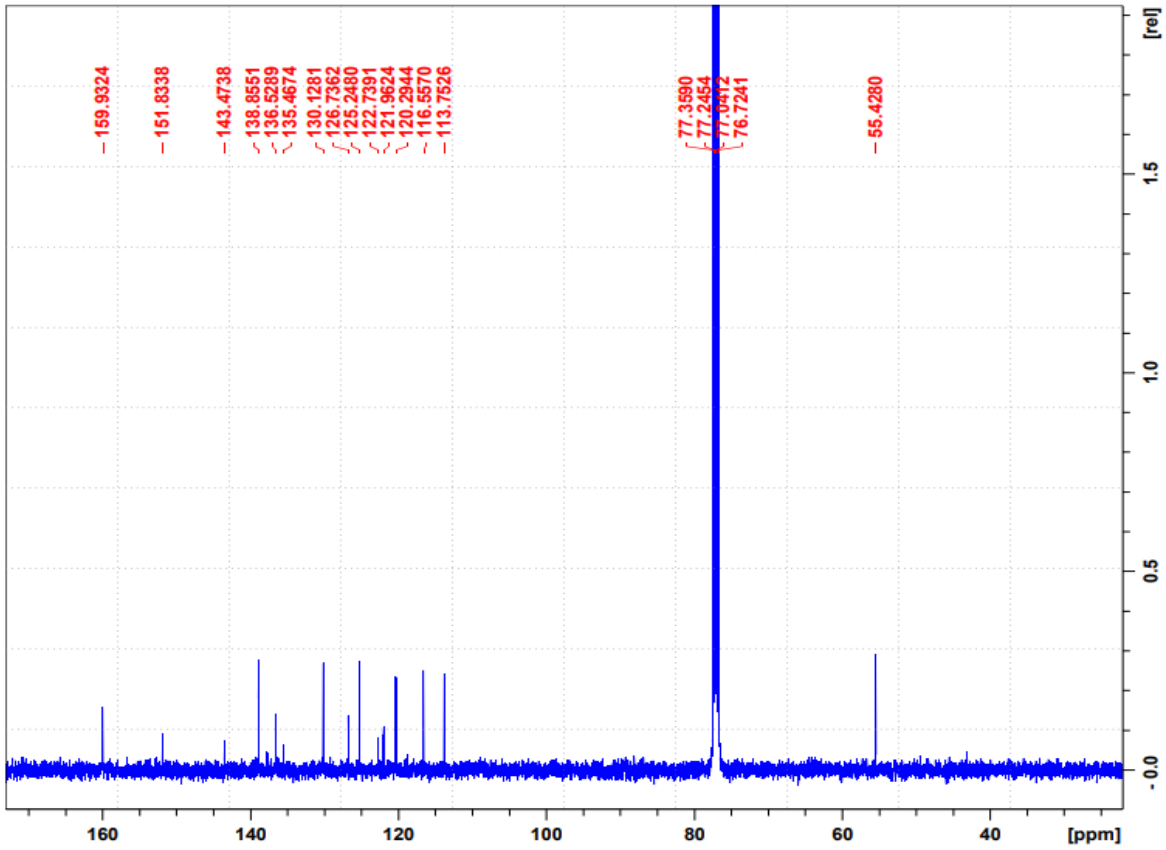

Figure 90. The ^{13}C NMR spectrum of compound **152 d**

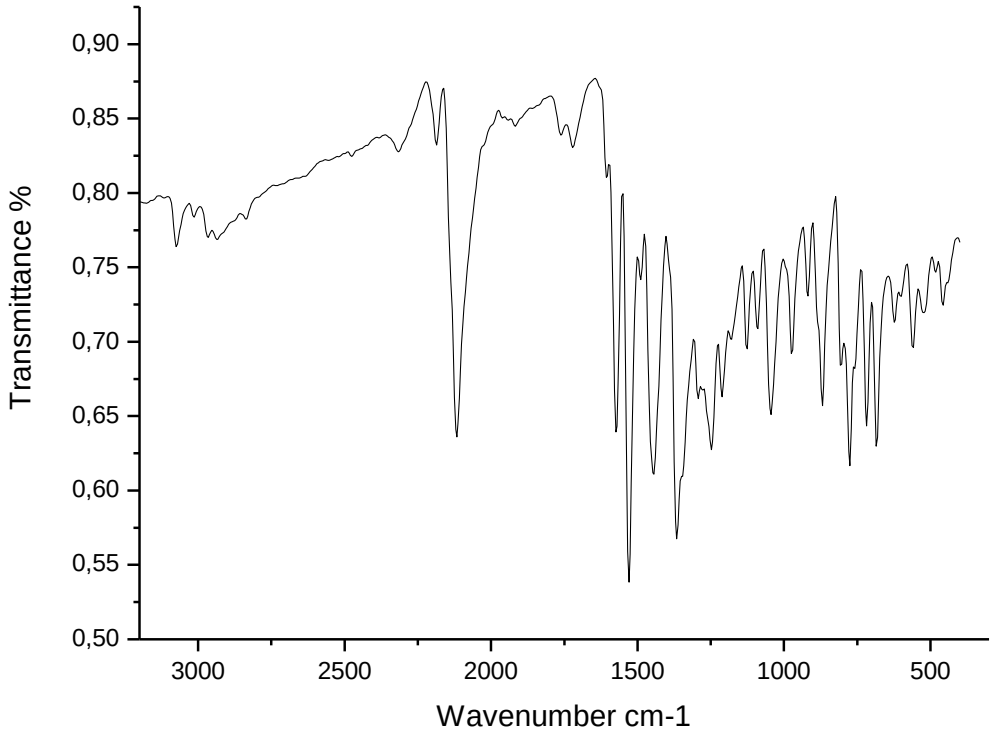

Figure 91. The FTIR spectrum of compound **152 d**

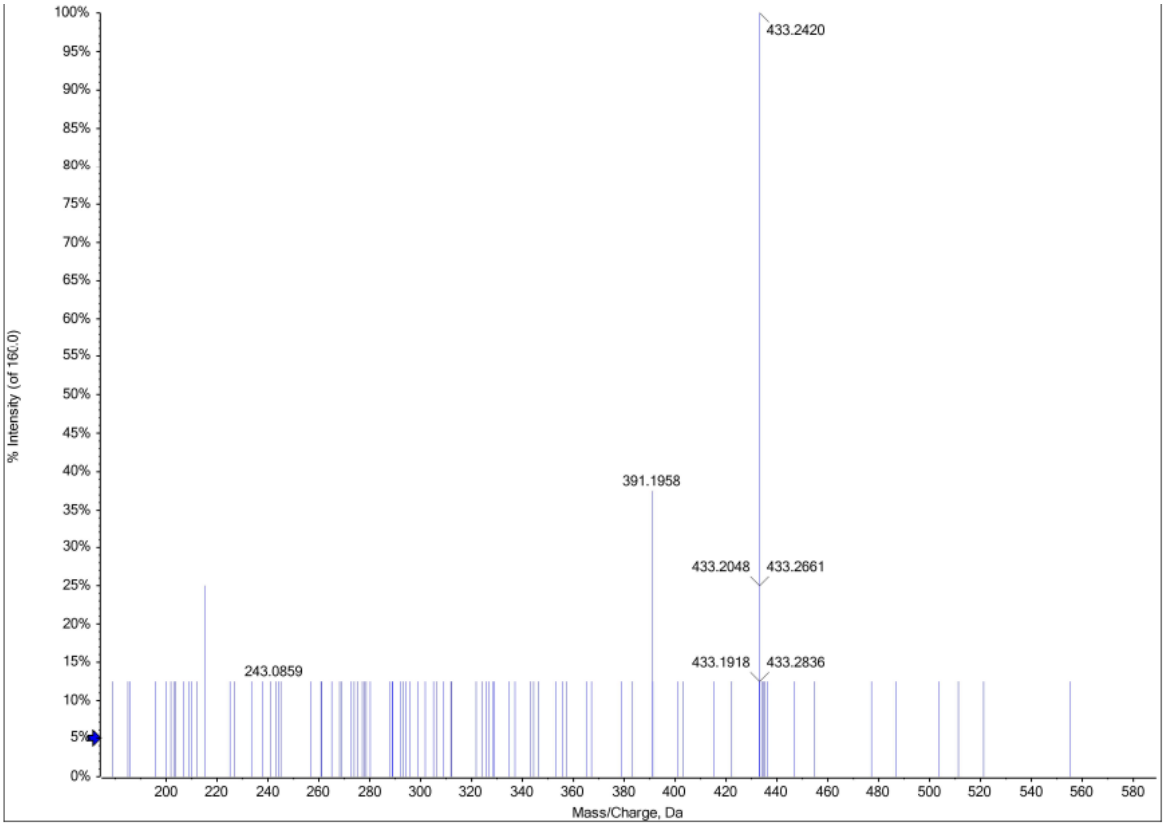

Figure 92. The HRMS spectrum of compound **152 d**

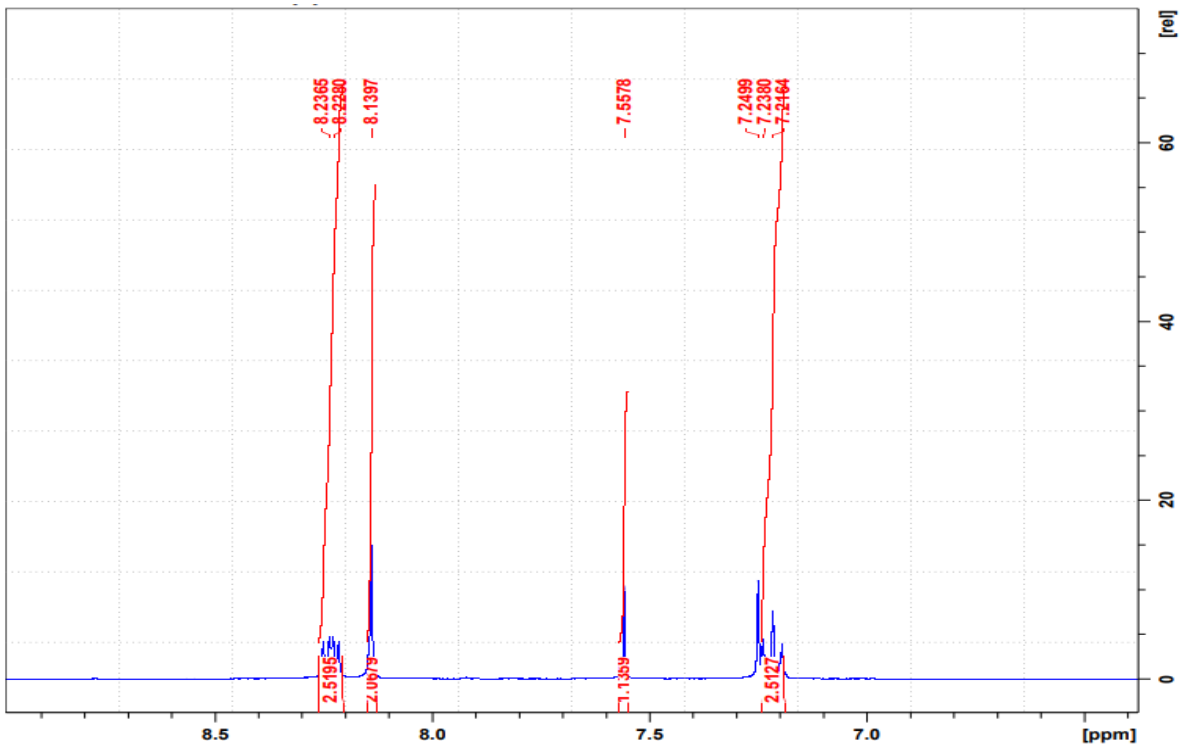

Figure 93. The ^{1}H NMR spectrum of compound **152 e**

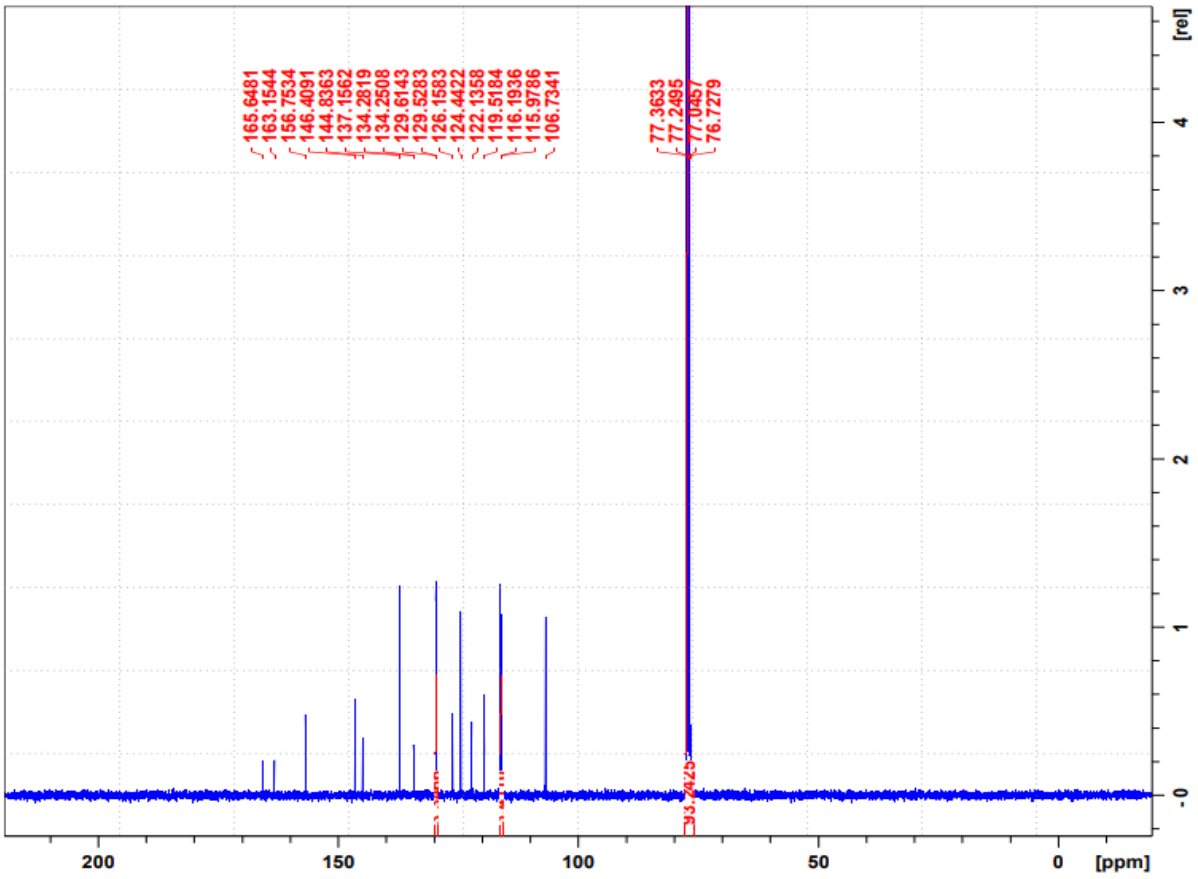

Figure 94. 13C NMR spectrum of compound **152 e**

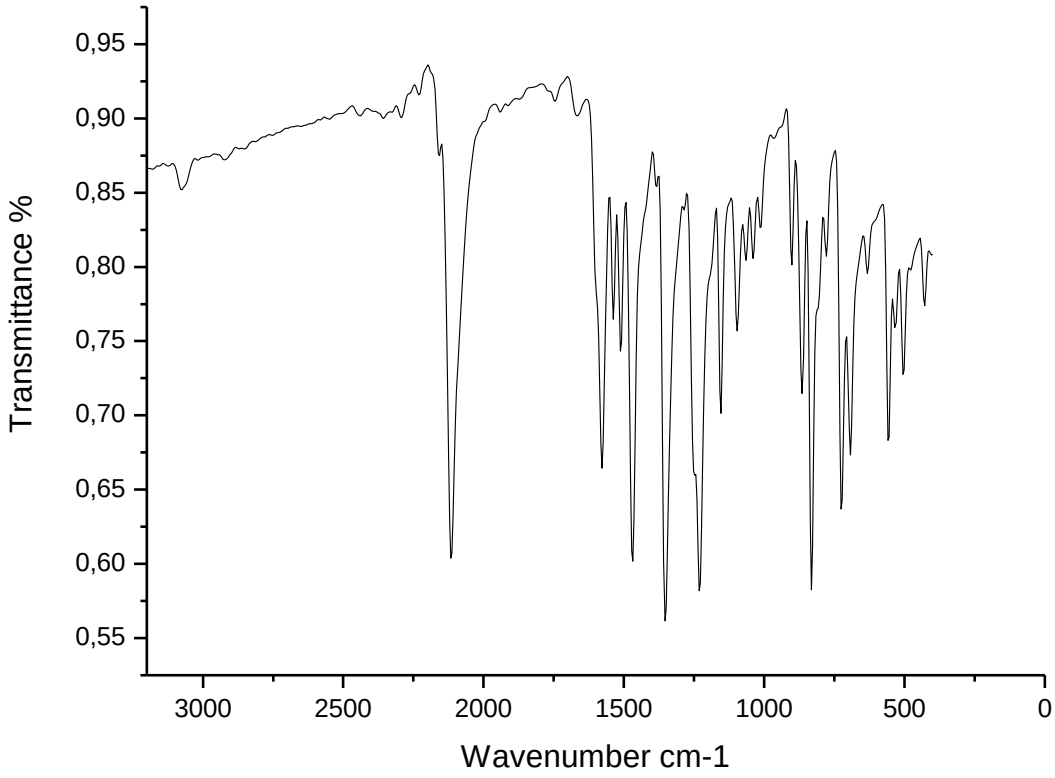

Figure 95. The FTIR spectrum of compound **152 e**

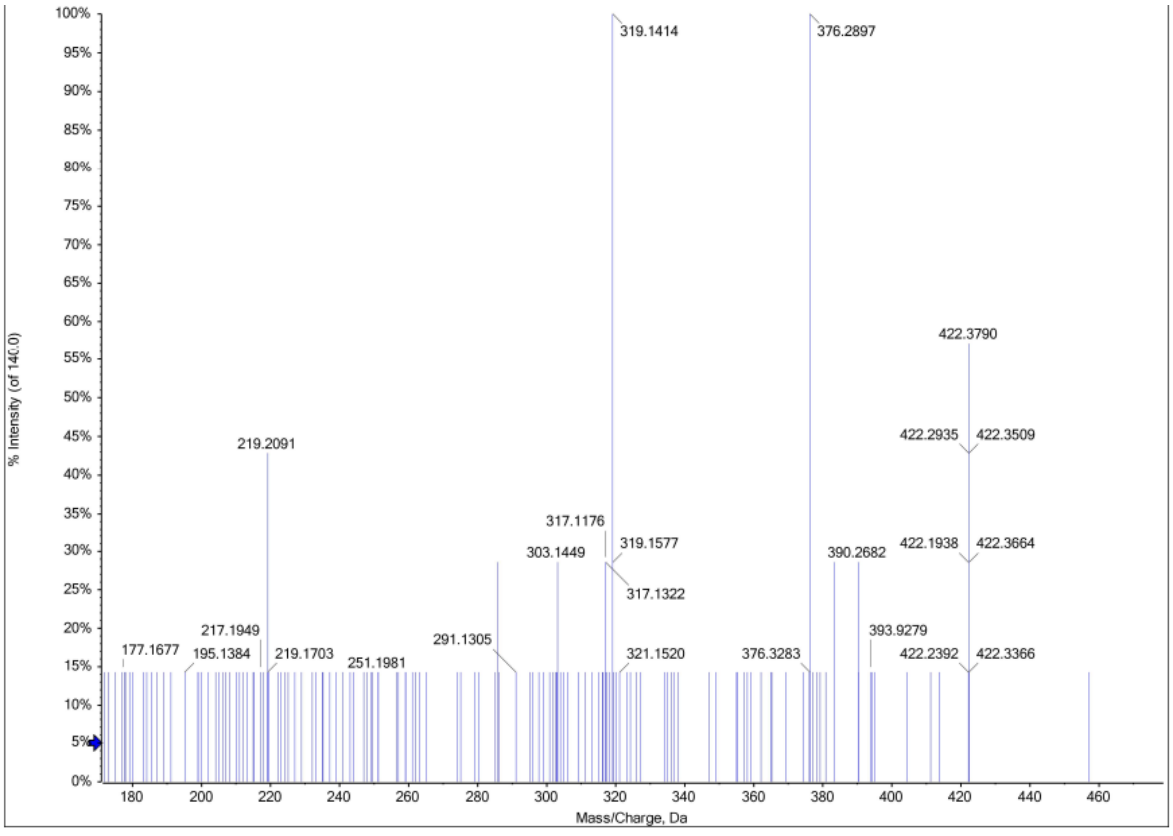

Figure 96. The HRMS spectrum of compound **152 e**

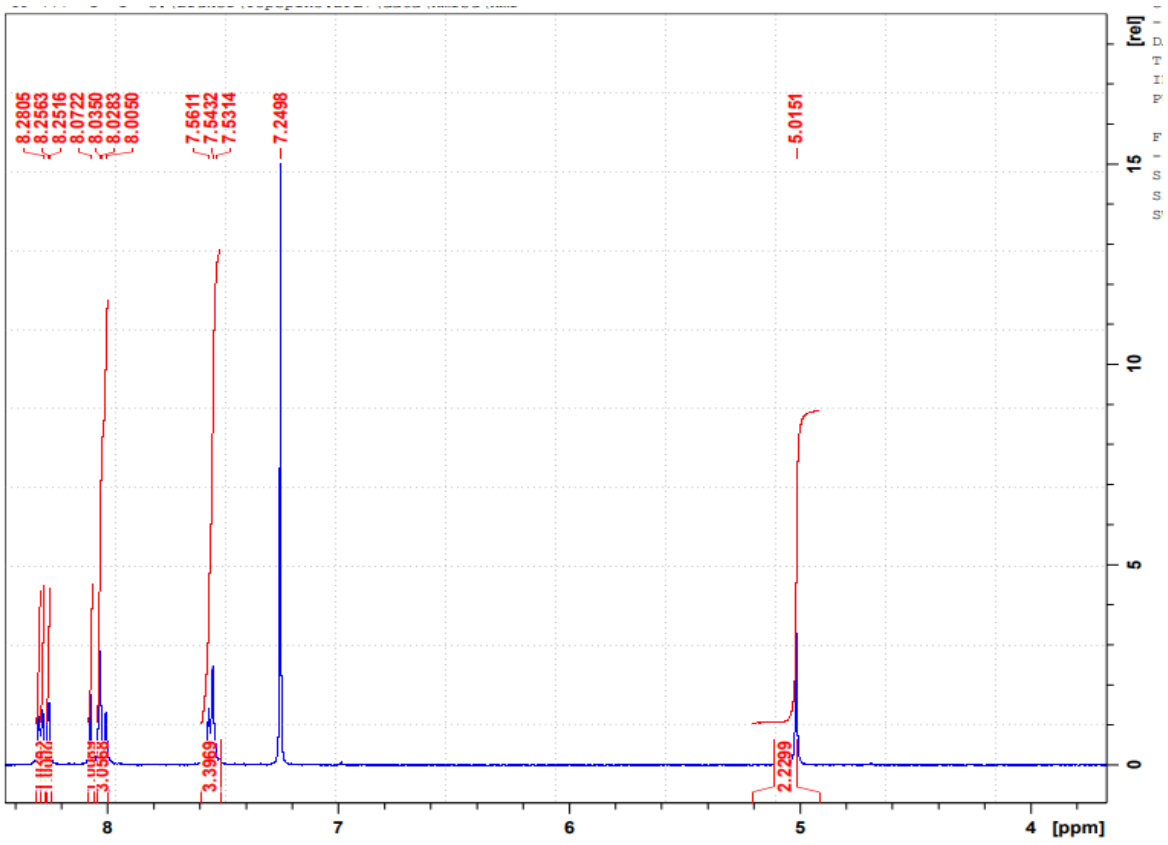

Figure 97. The ^{1}H NMR spectrum of compound **153 a**

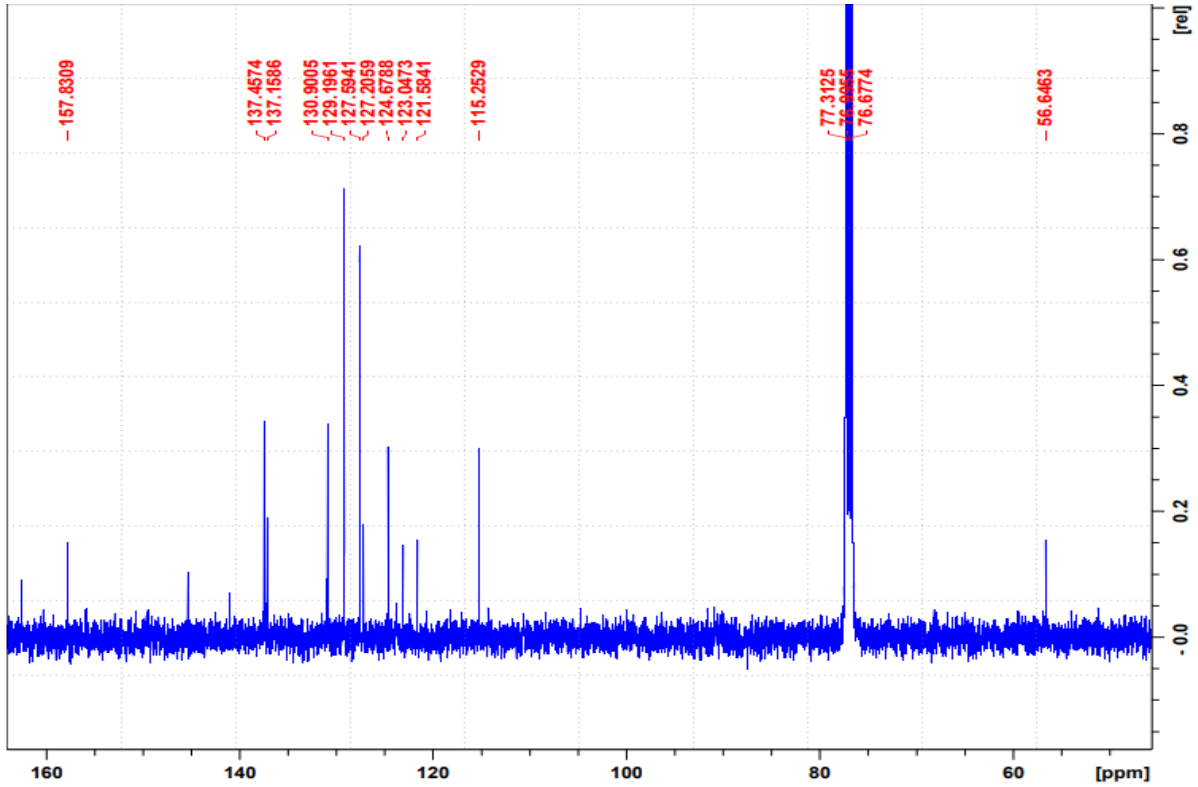

Figure 98. The ^{13}C NMR spectrum of compound **153 a**

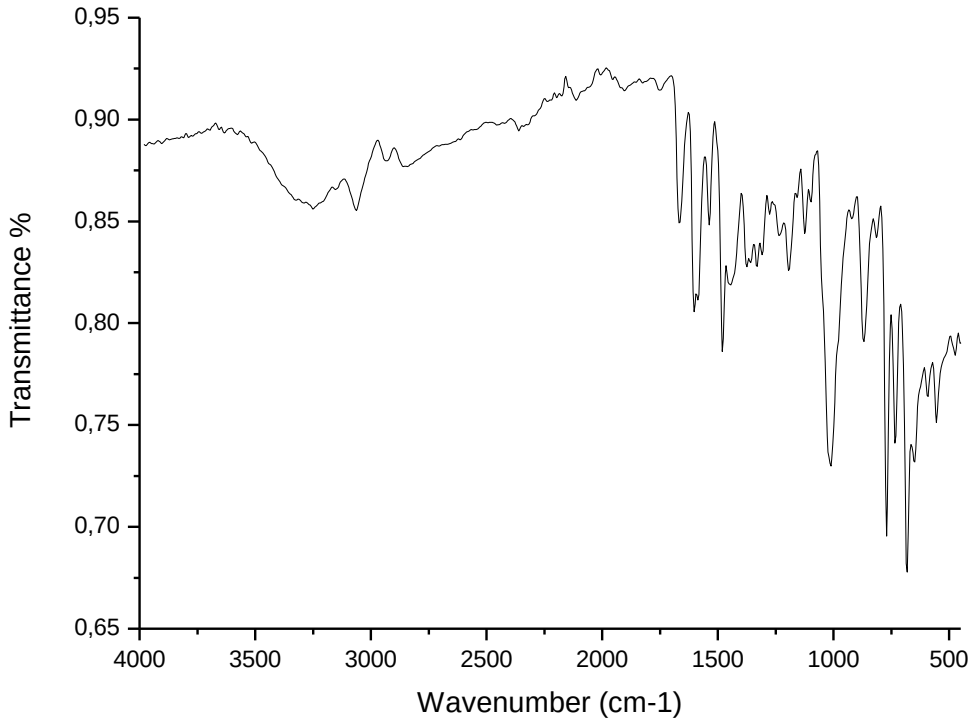

Figure 99. The FTIR spectrum of compound **153 a**

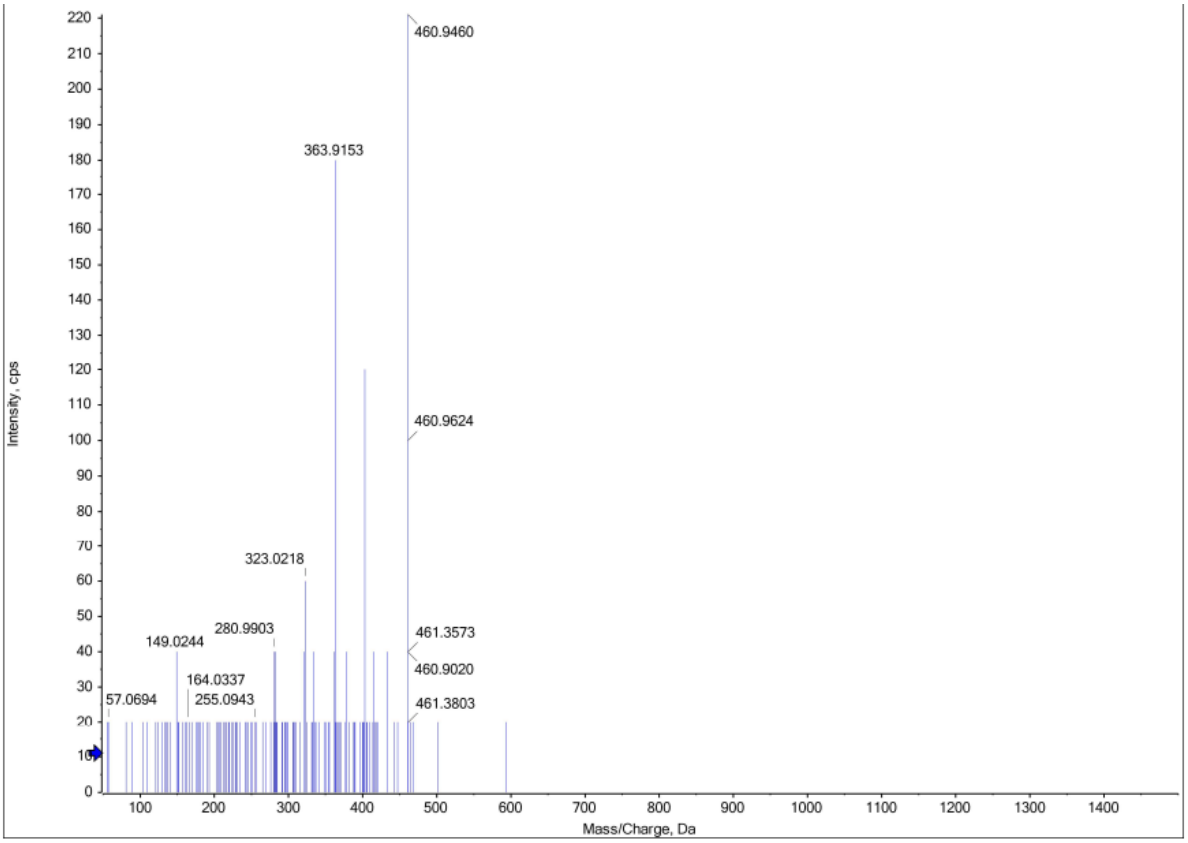

Figure 100. The HRMS spectrum of compound **153 a**

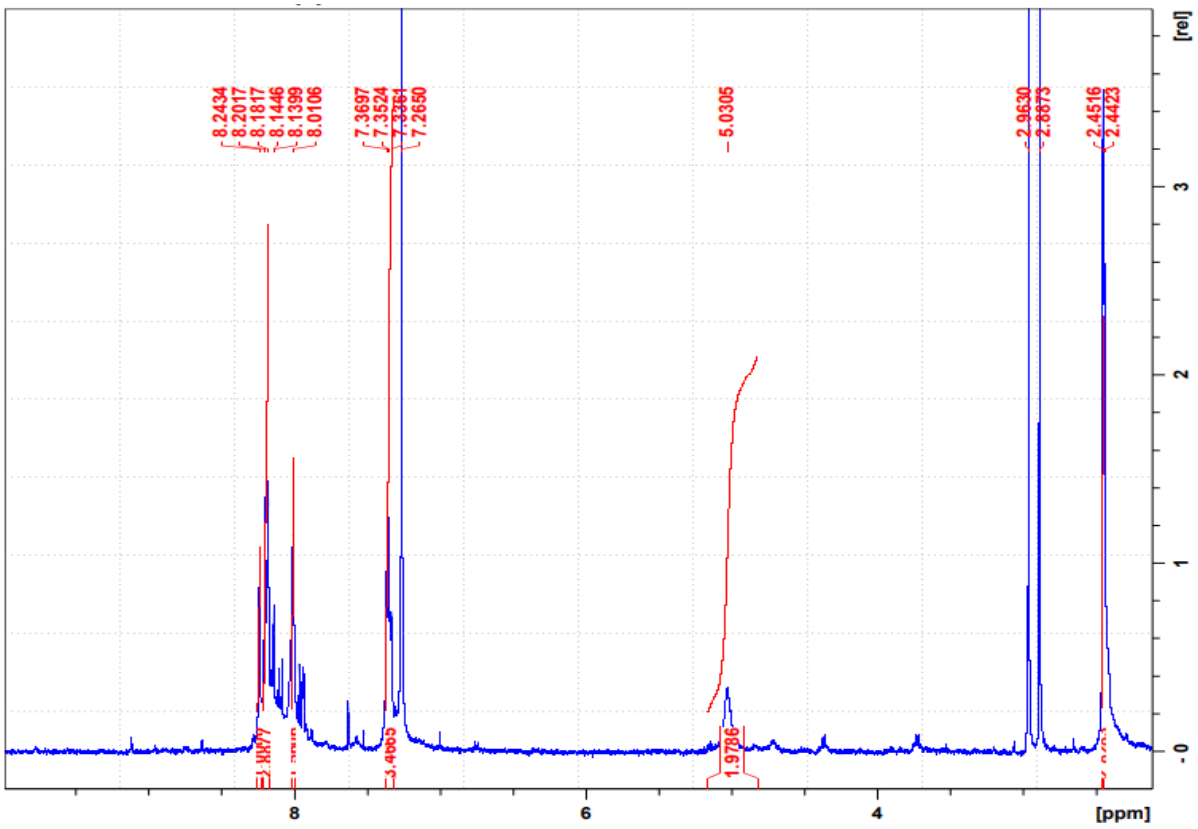
8.2434
8.2017
8.1817
8.1446
8.1399
8.0106
7.3697
7.3524
7.3361
7.2650
5.0305
2.9630
2.8873
2.4516
2.4423
1.9786
8
6
4
[ppm]
[rel]
3
2
1
0

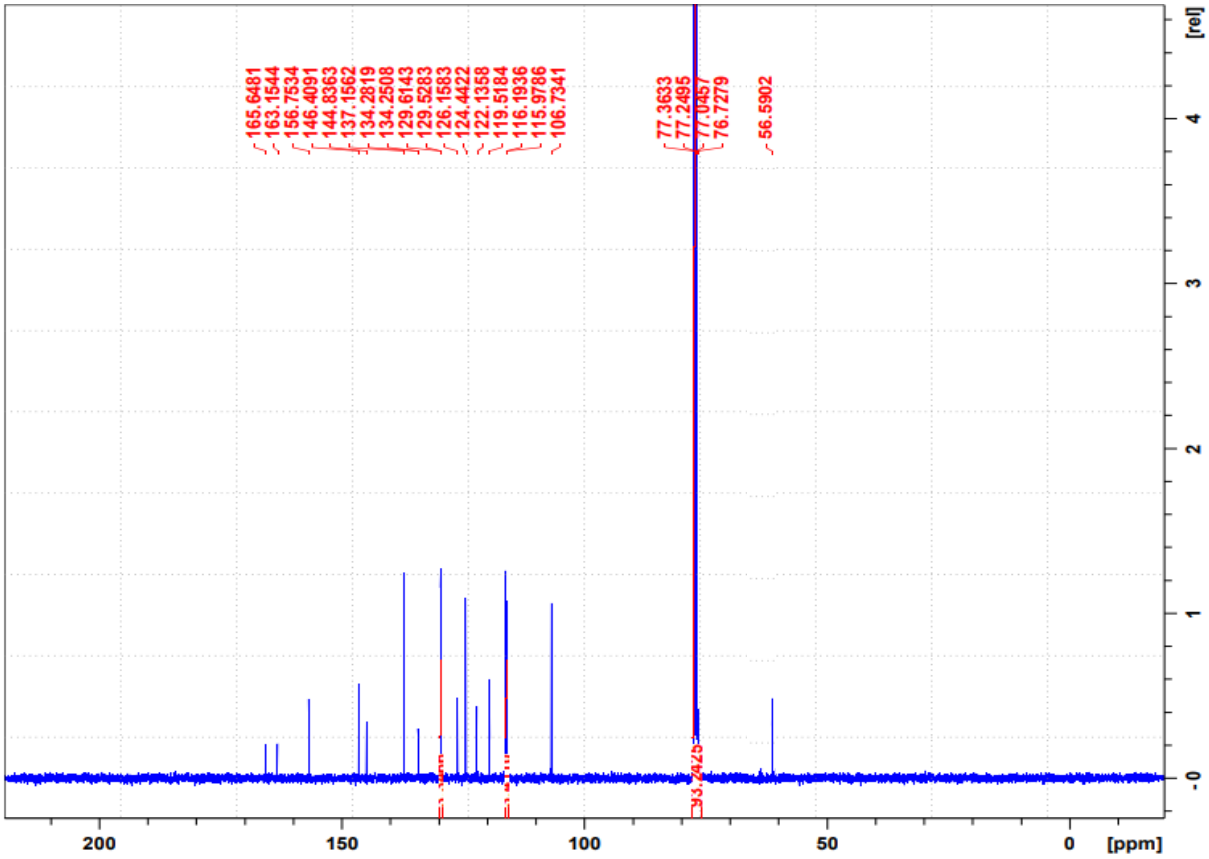

Figure 101. The ^{1}H NMR spectrum of compound **153 b**

Figure 102. The ^{13}C NMR spectrum of compound **153 b**

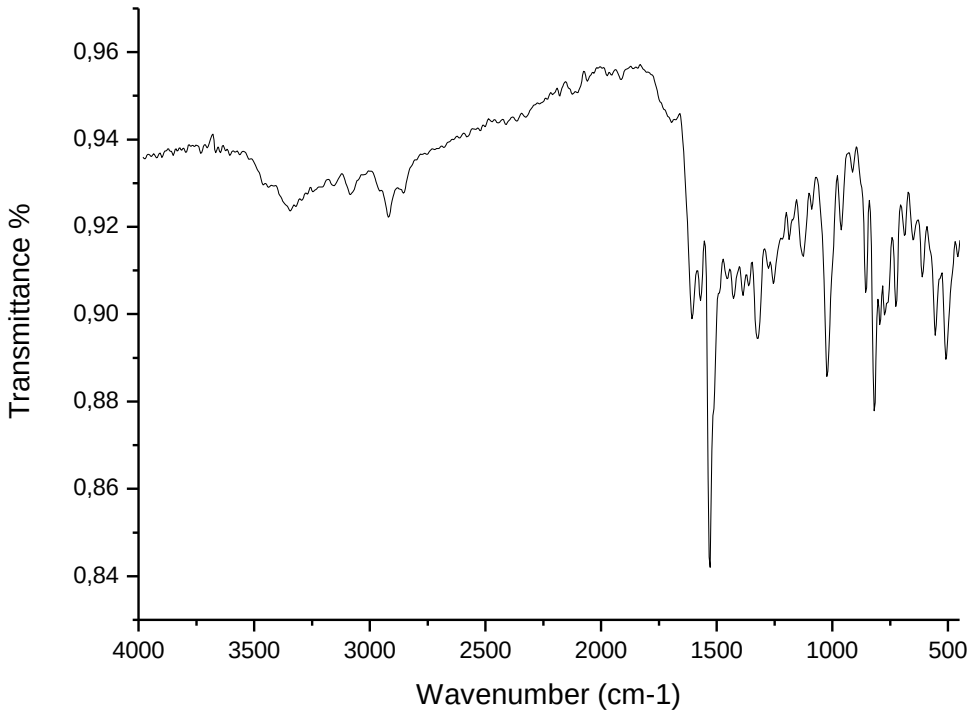

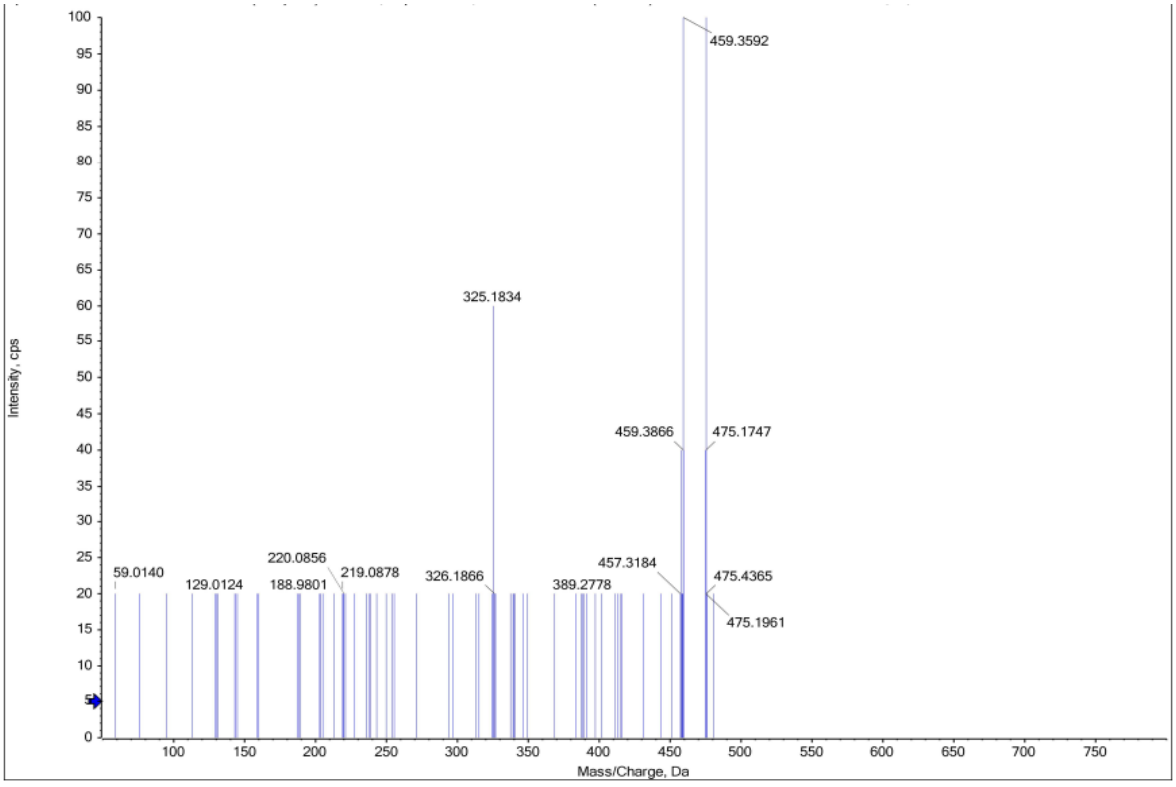

Figure 103. The FTIR spectrum of compound **153 b**

Figure 104. The HRMS spectrum of compound **153 b**

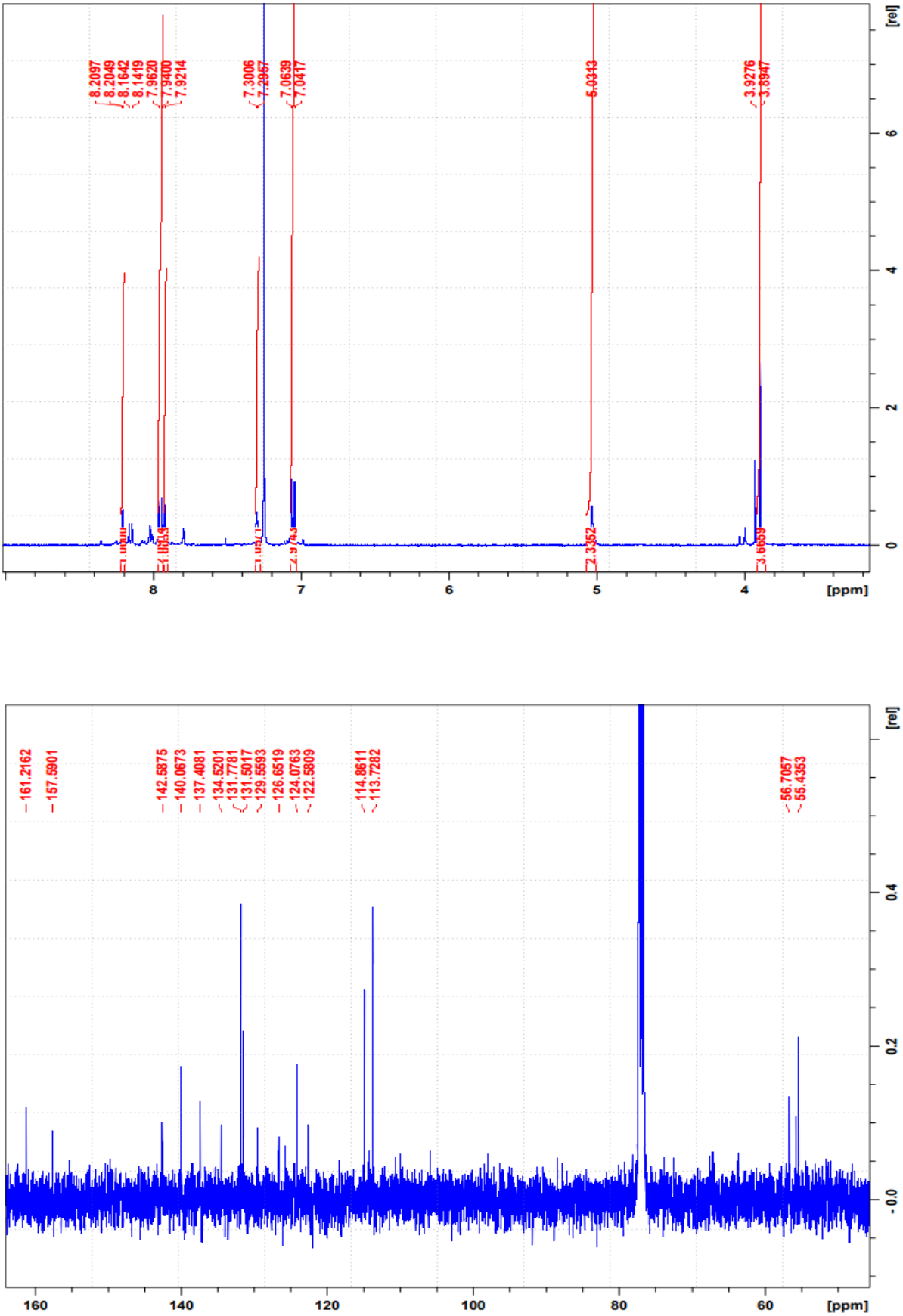

Figure 105. The ^{1}H NMR spectrum of compound **153 c**

Figure 106. The ^{13}C NMR spectrum of compound **153 c**

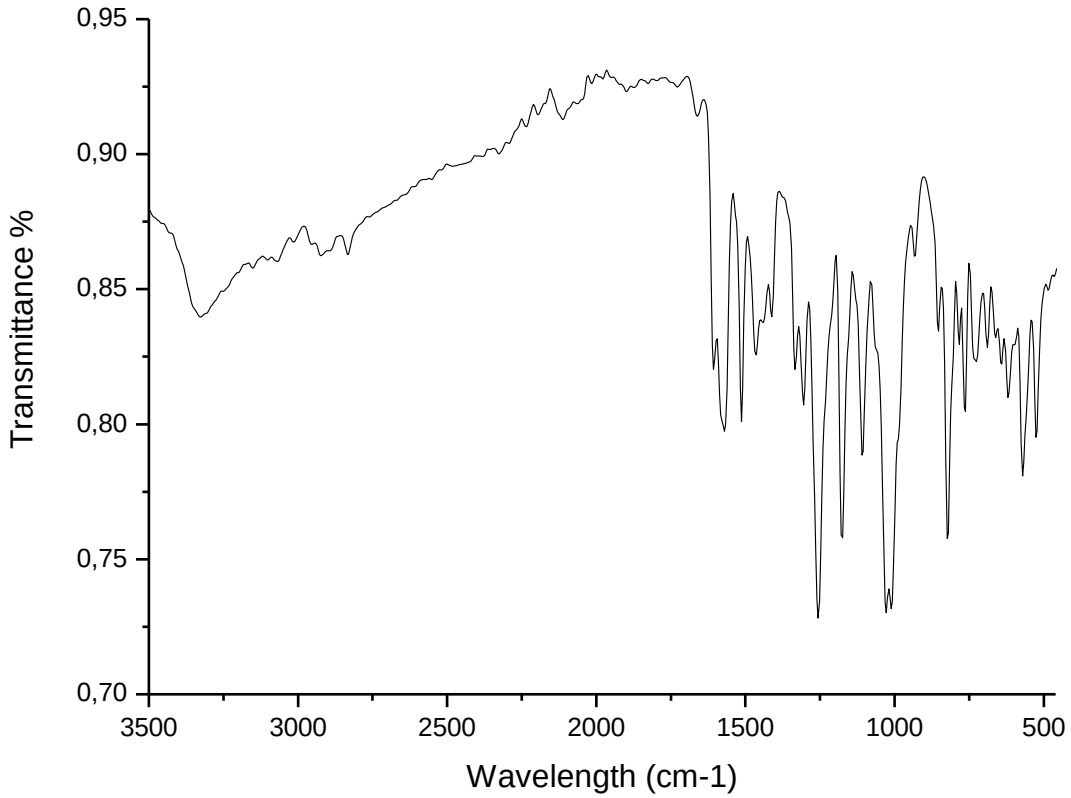

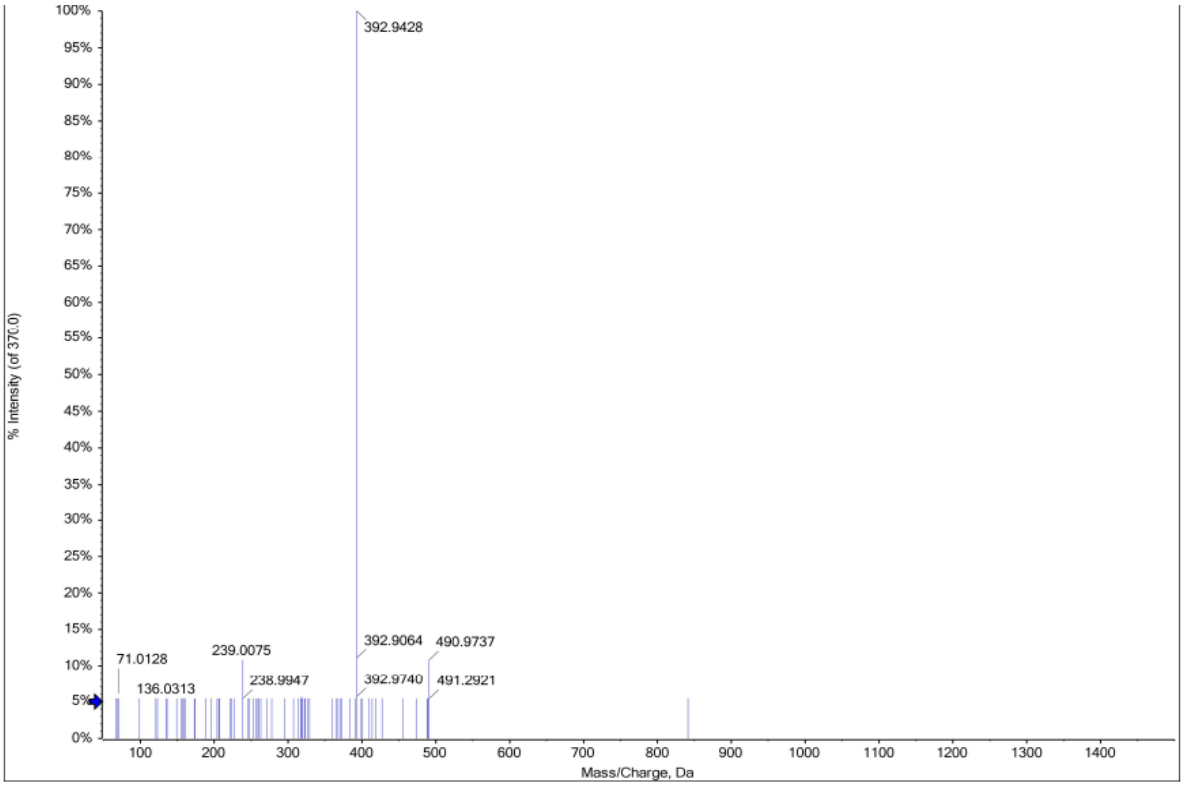

Figure 107. The FTIR spectrum of compound **153 c**

Figure 108. The HRMS spectrum of compound **153 c**

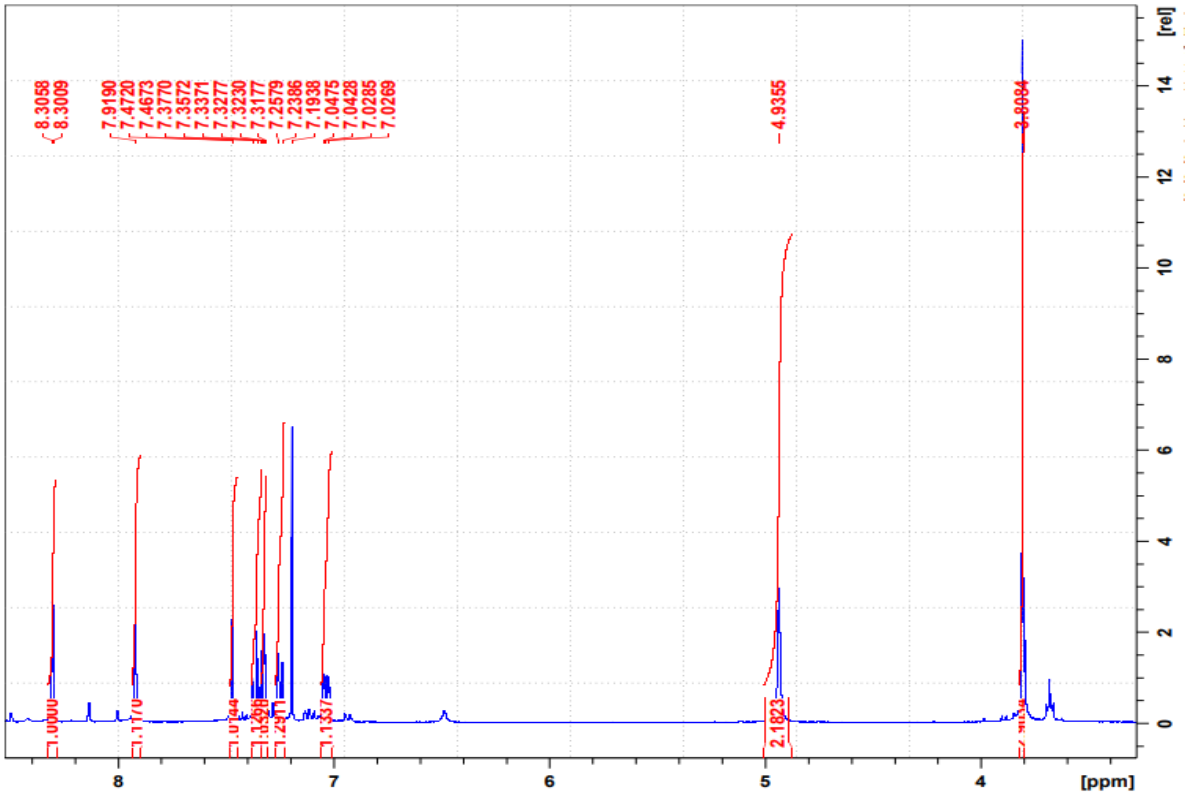

Figure 109. The ^{1}H NMR spectrum of compound **153 d**

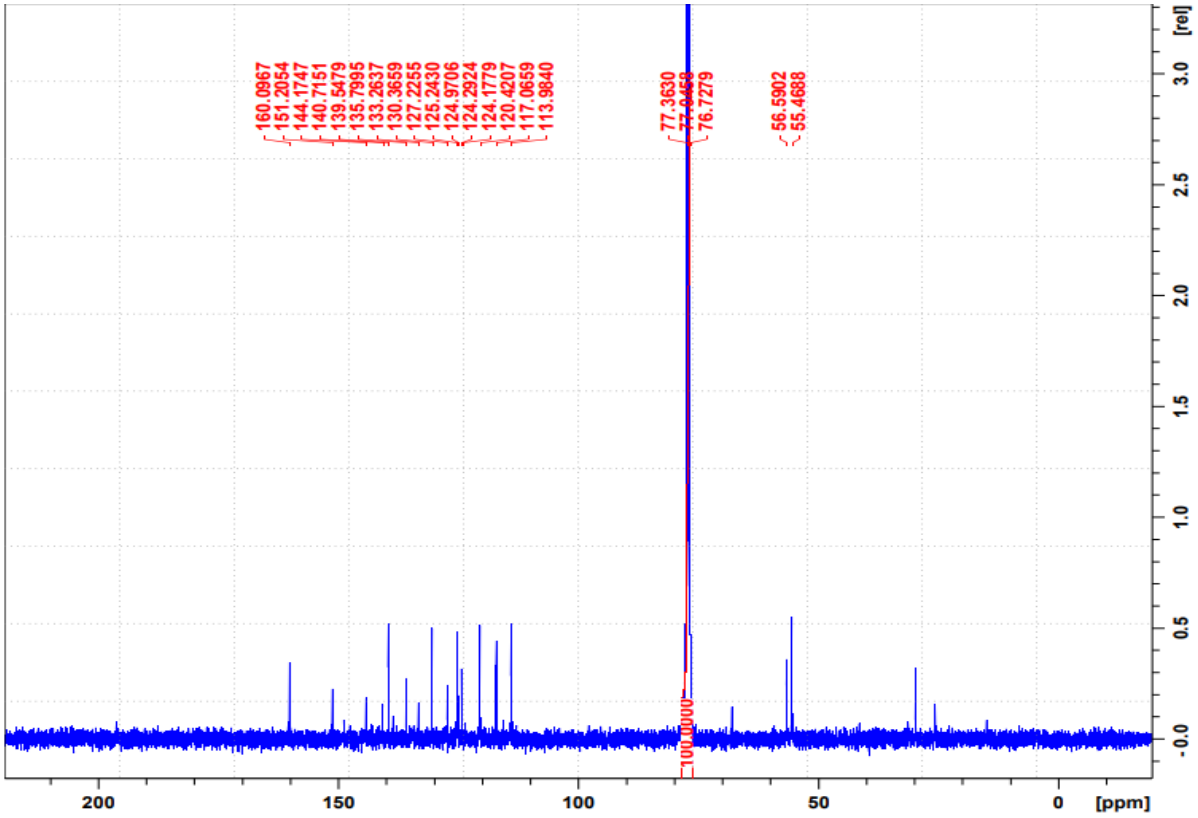

Figure 110. The ^{13}C NMR spectrum of compound **153 d**

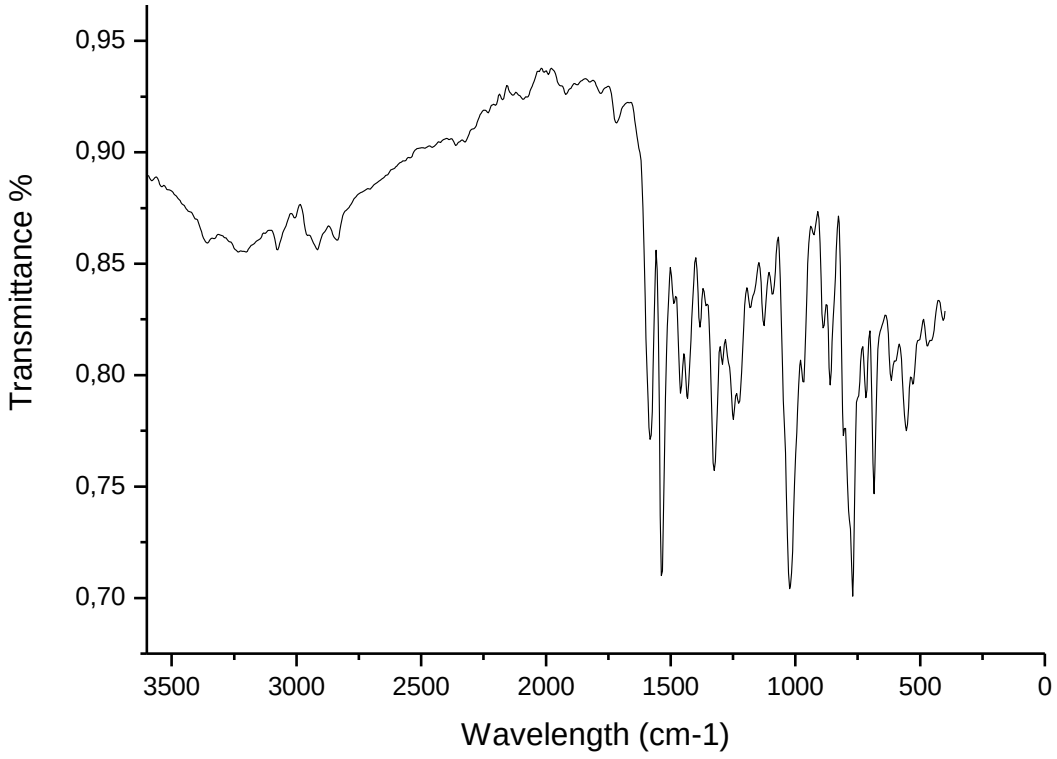

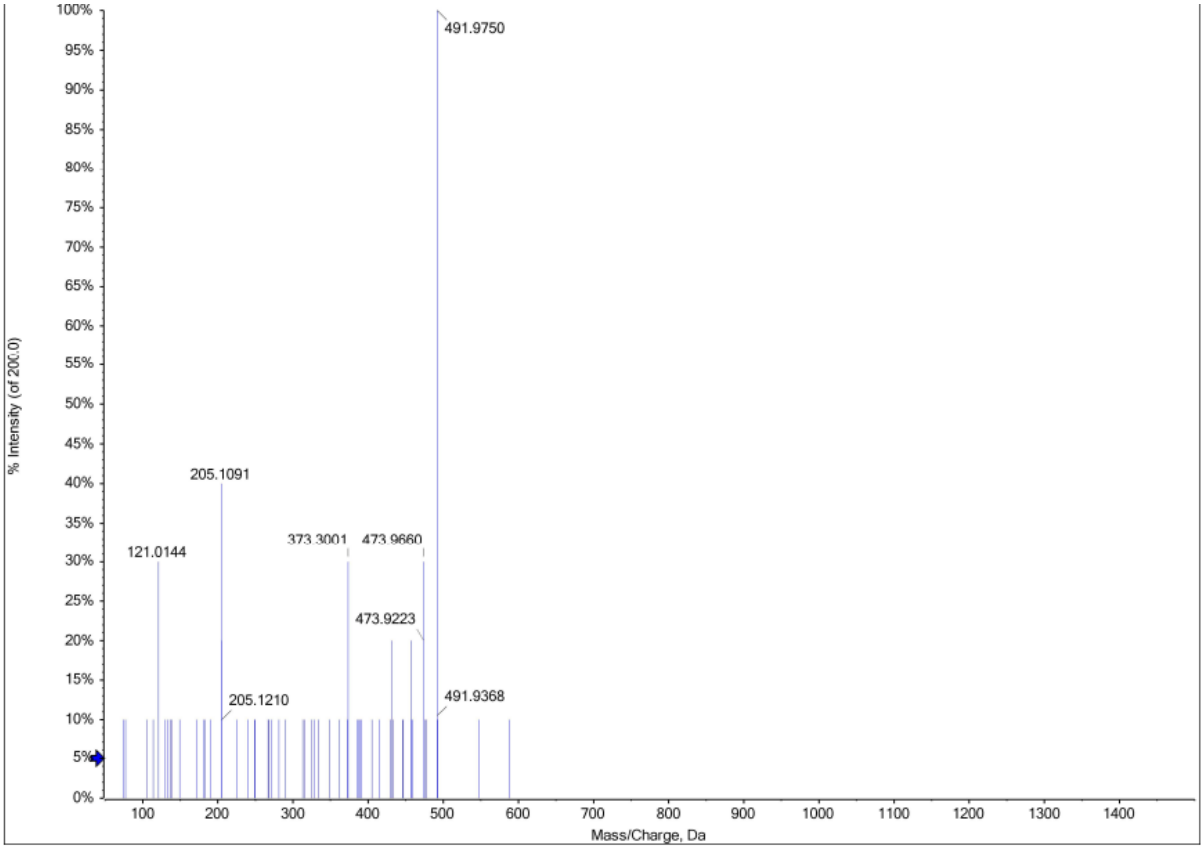

Figure 111. The FTIR spectrum of compound **153 d**

Figure 112. The HRMS spectrum of compound **153 d**

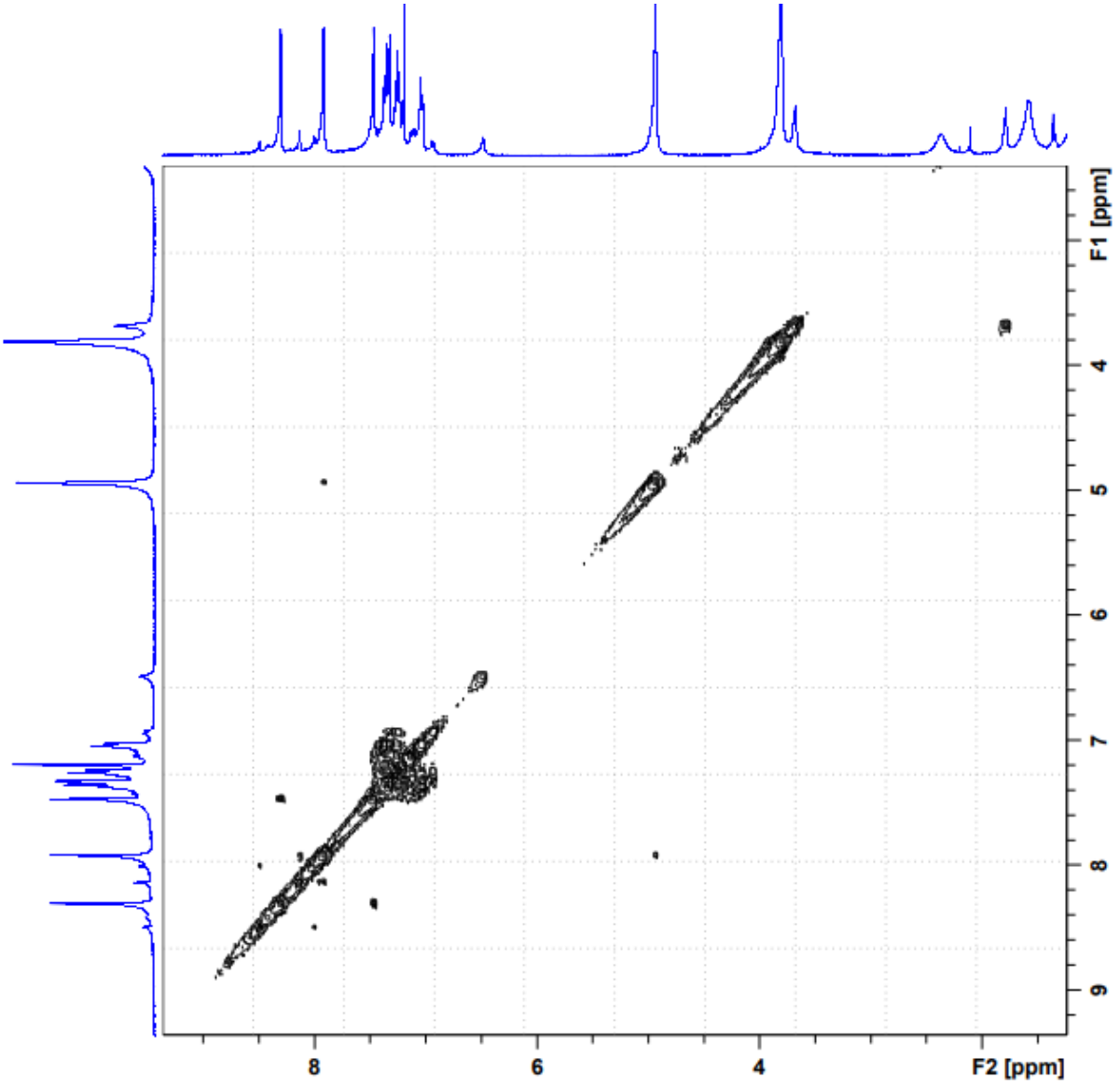

Figure 113. The COSY spectrum of compound **153 d**

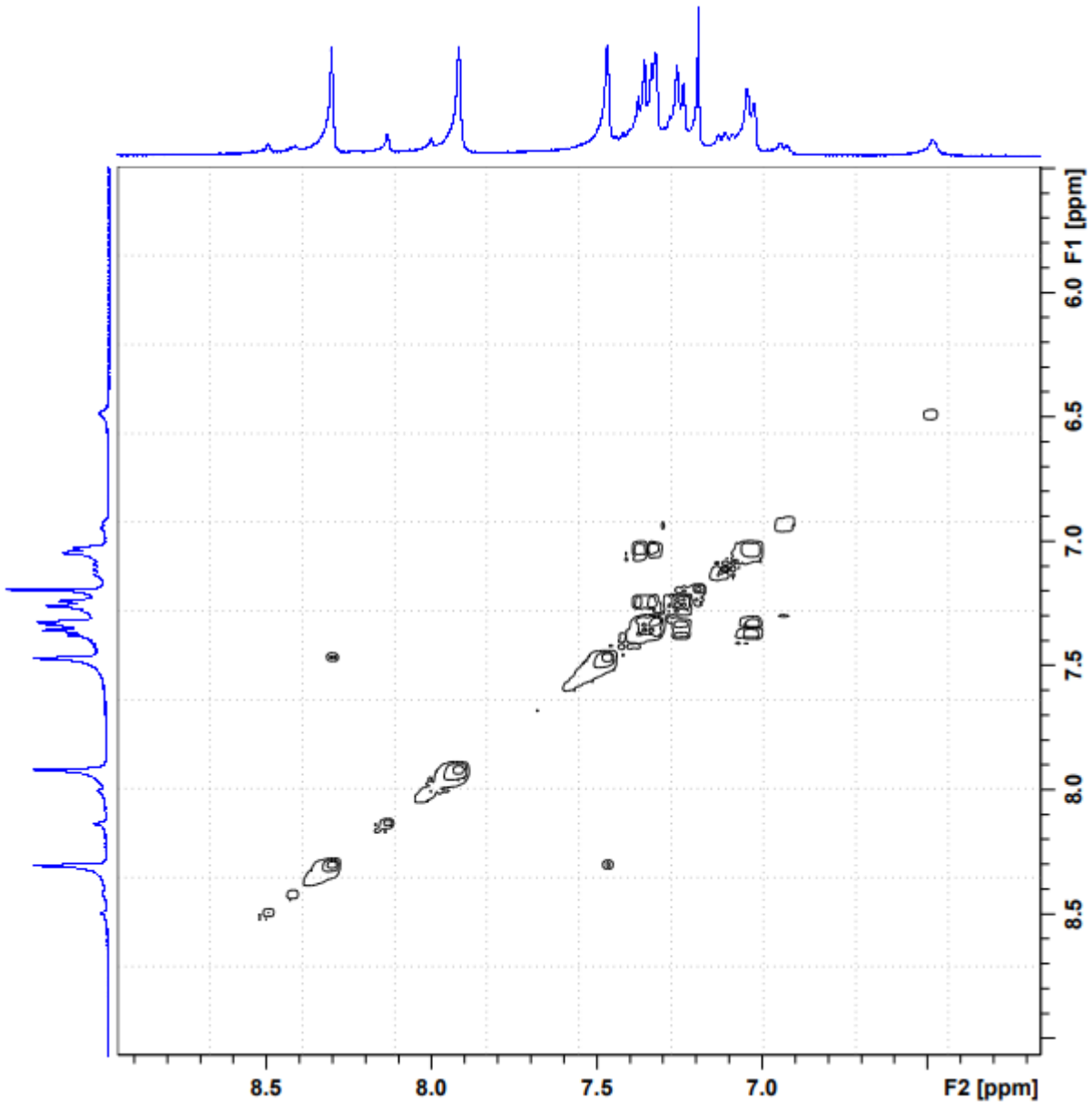

Figure 114. The COSY (expanded) spectrum of compound **153 d**

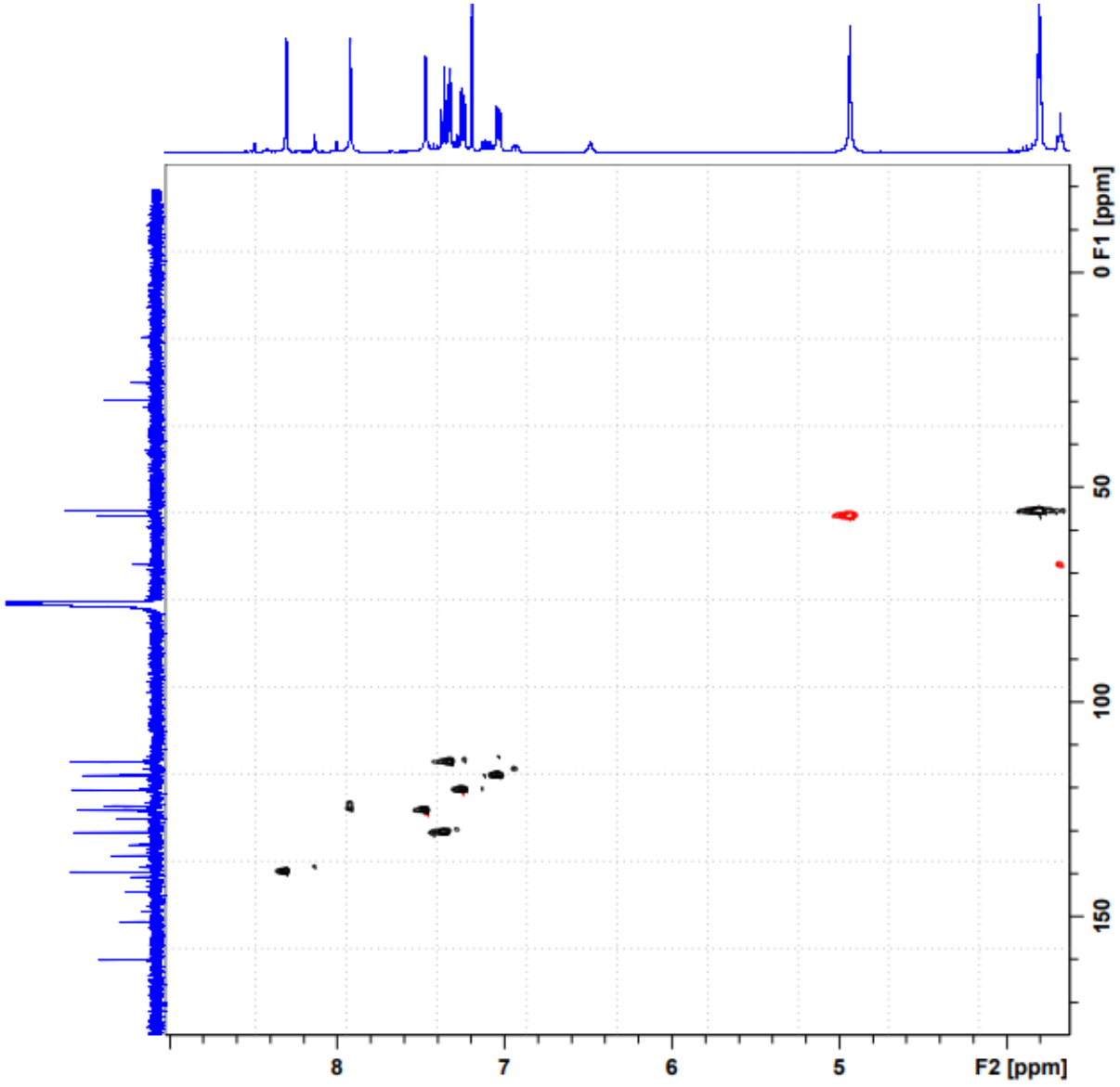

Figure 115. The HSQC spectrum of compound **153 d**

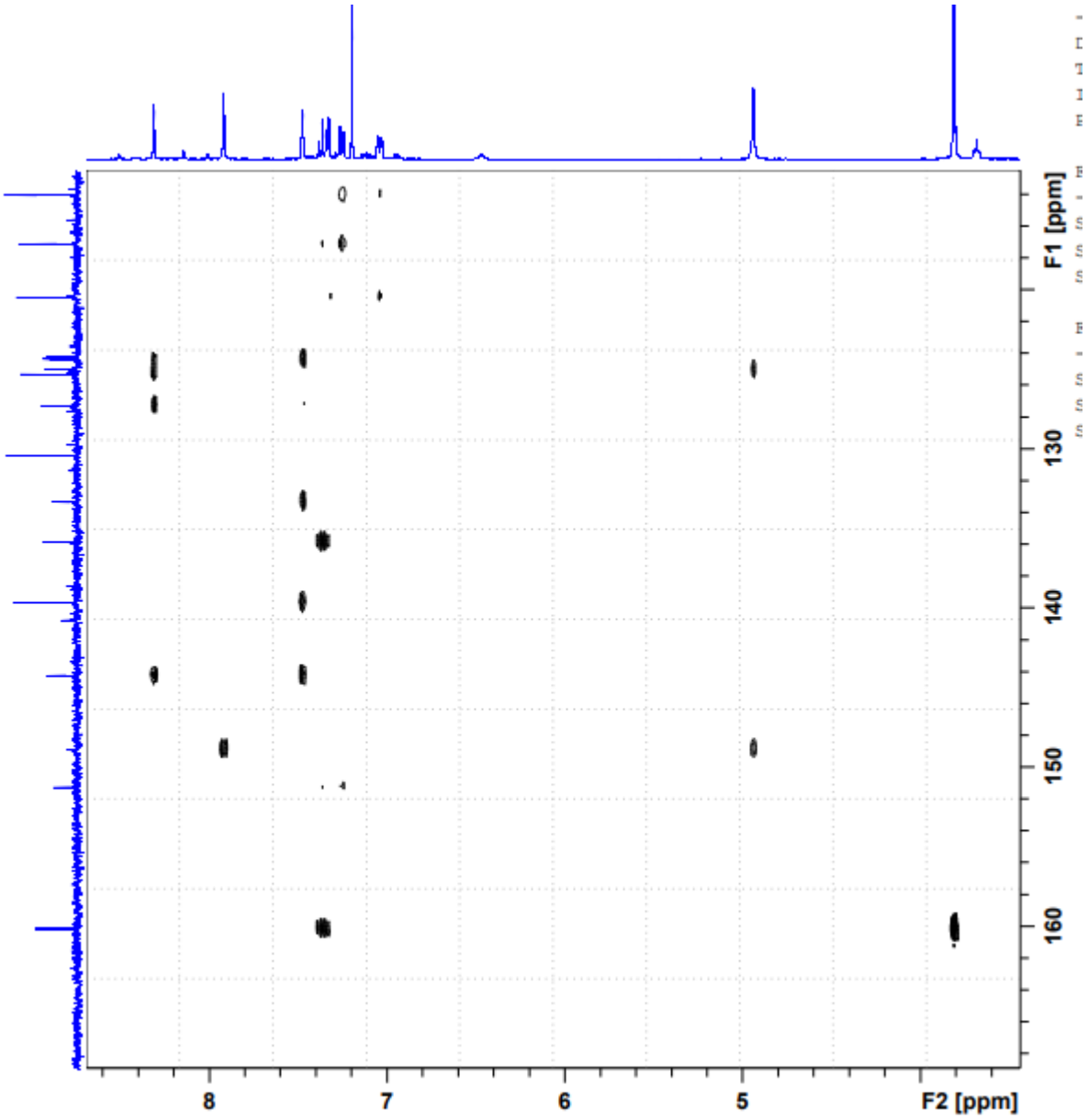

Figure 116. The HMBC spectrum of compound **153 d**

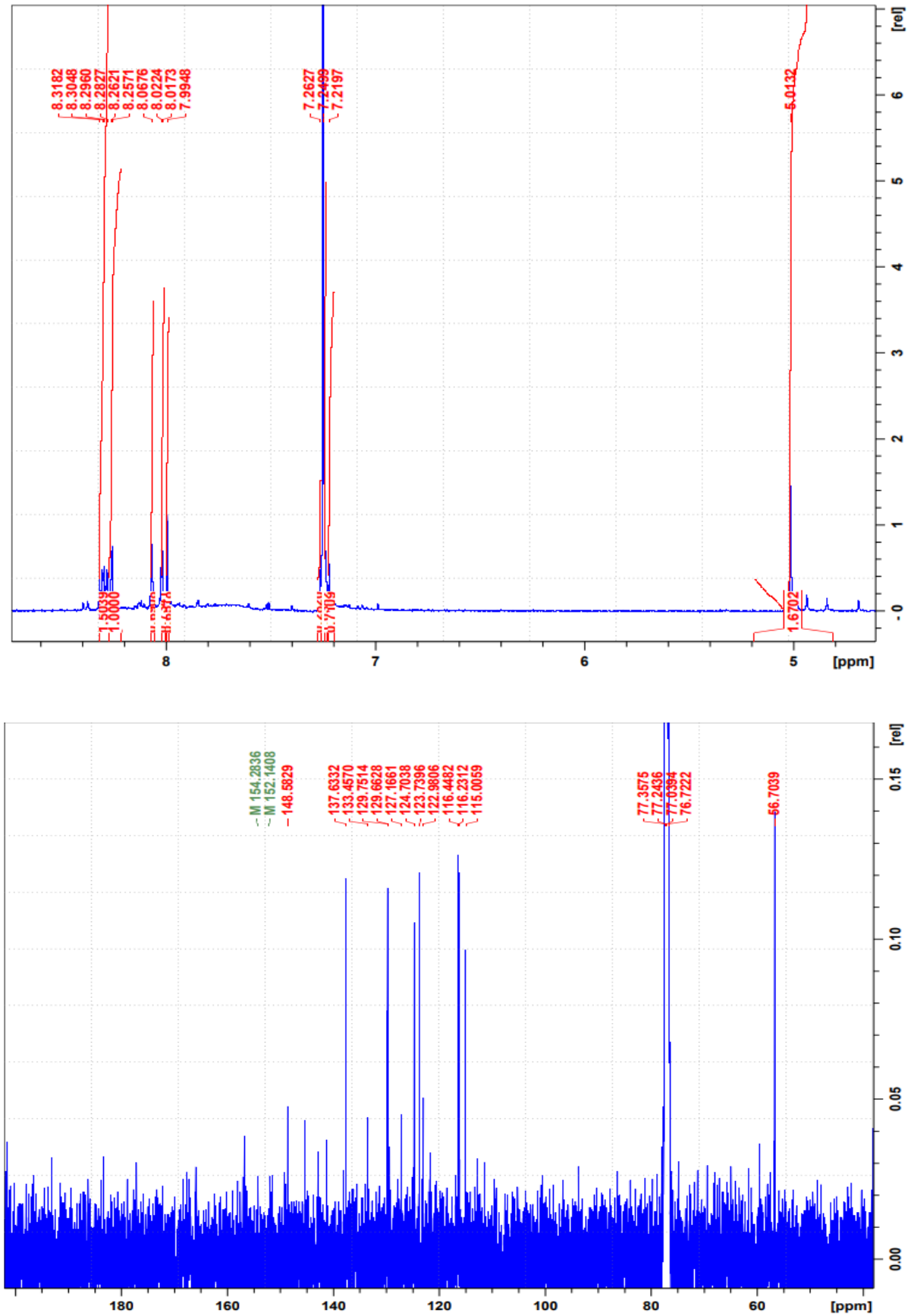

Figure 117. The 1H NMR spectrum of compound **153 e**

Figure 118. The 13C NMR spectrum of compound **153 e**

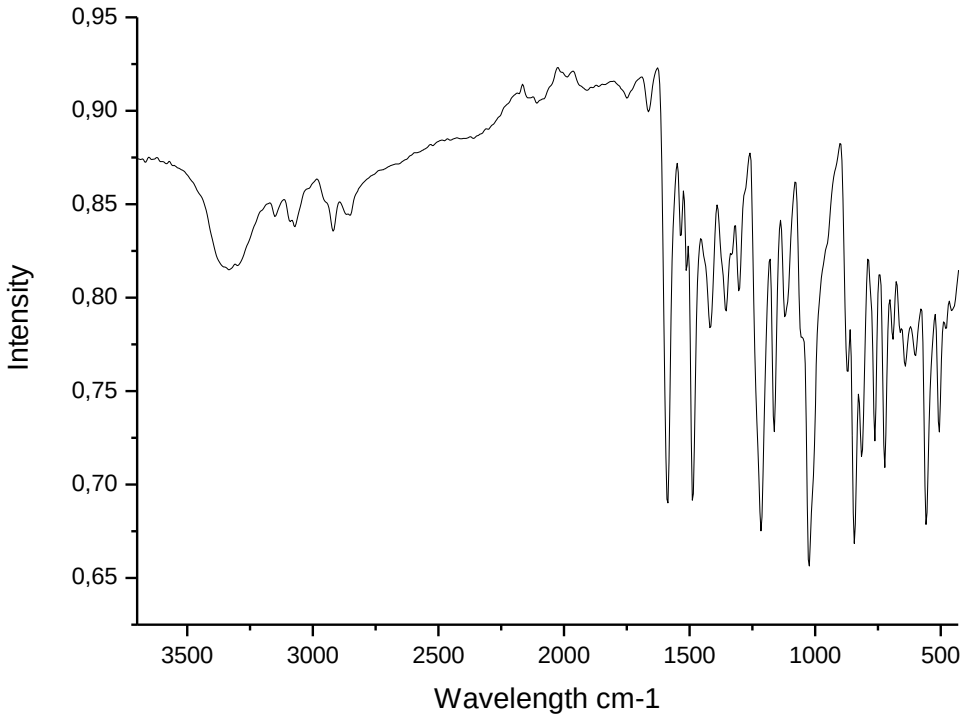

Figure 119. The FTIR spectrum of compound **153 e**

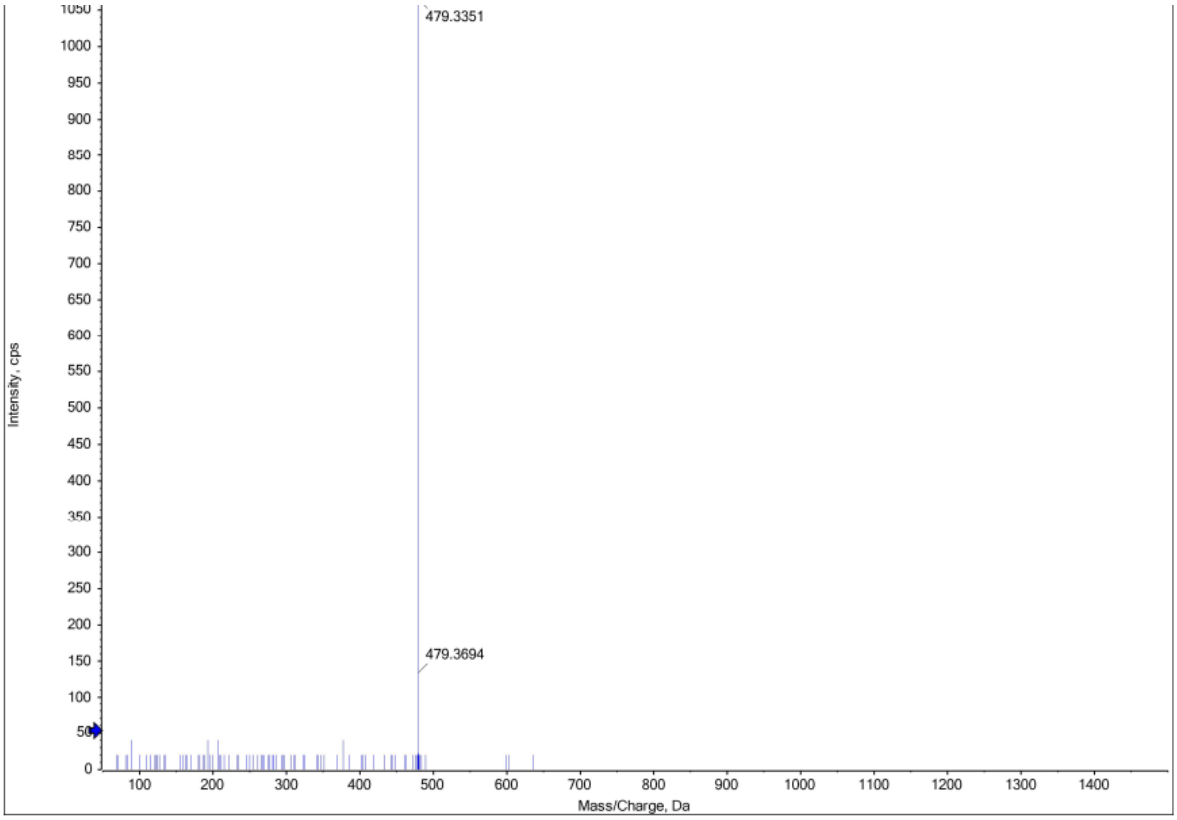

Figure 120. The HRMS spectrum of compound **153 e**

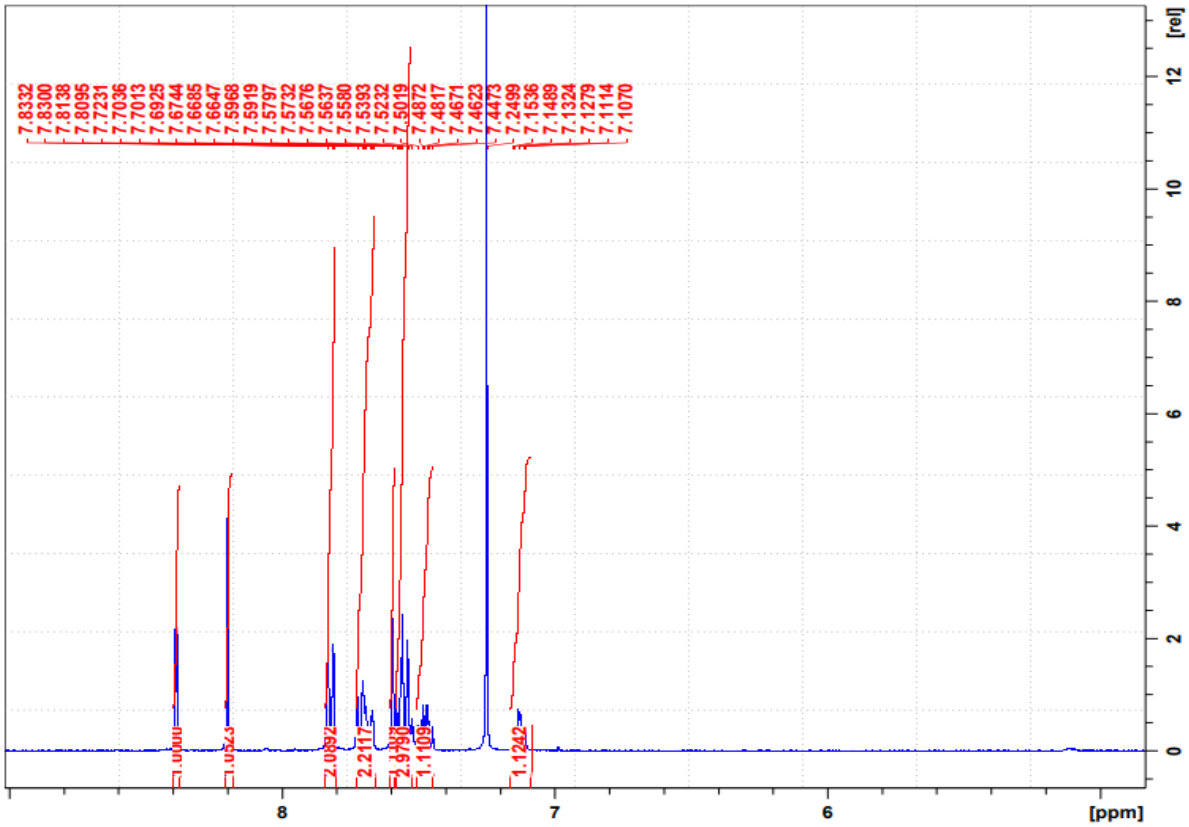

Figure 121. The ^{1}H NMR spectrum of compound **153 f**

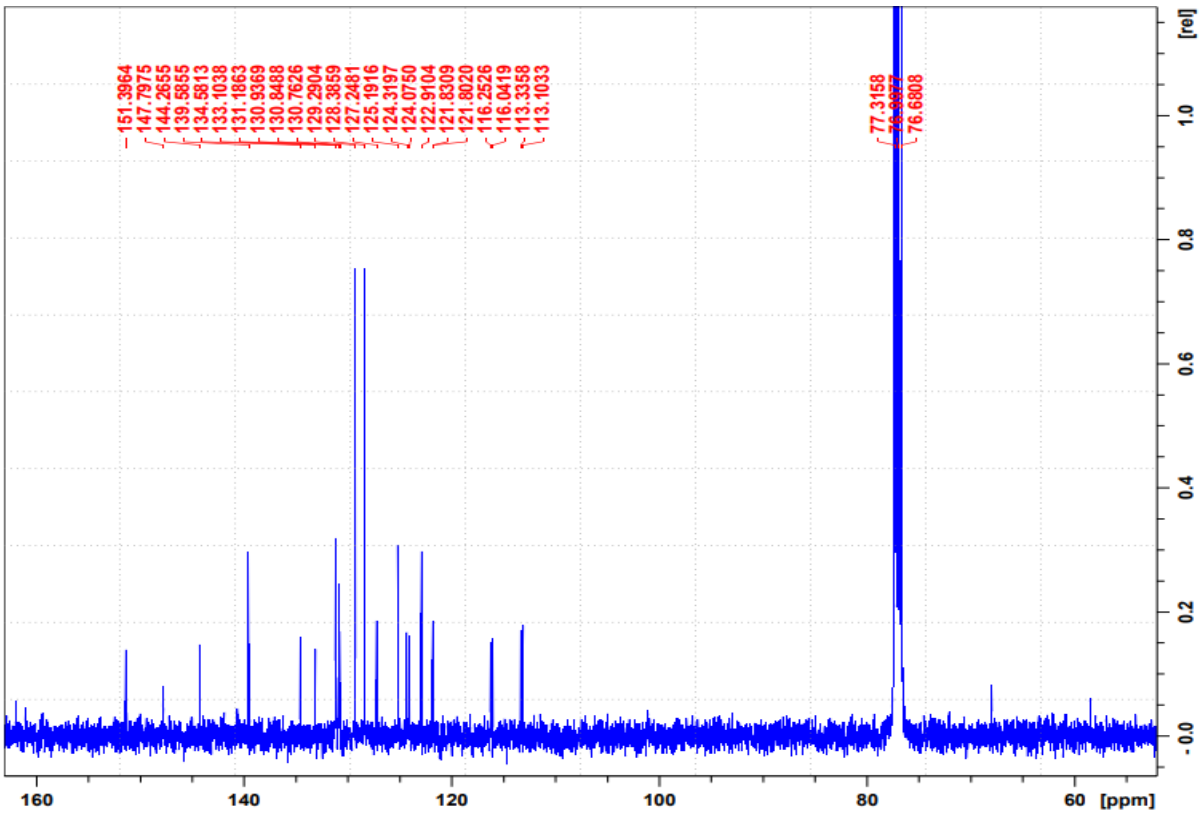

Figure 122. The ^{13}C NMR spectrum of compound **153 f**

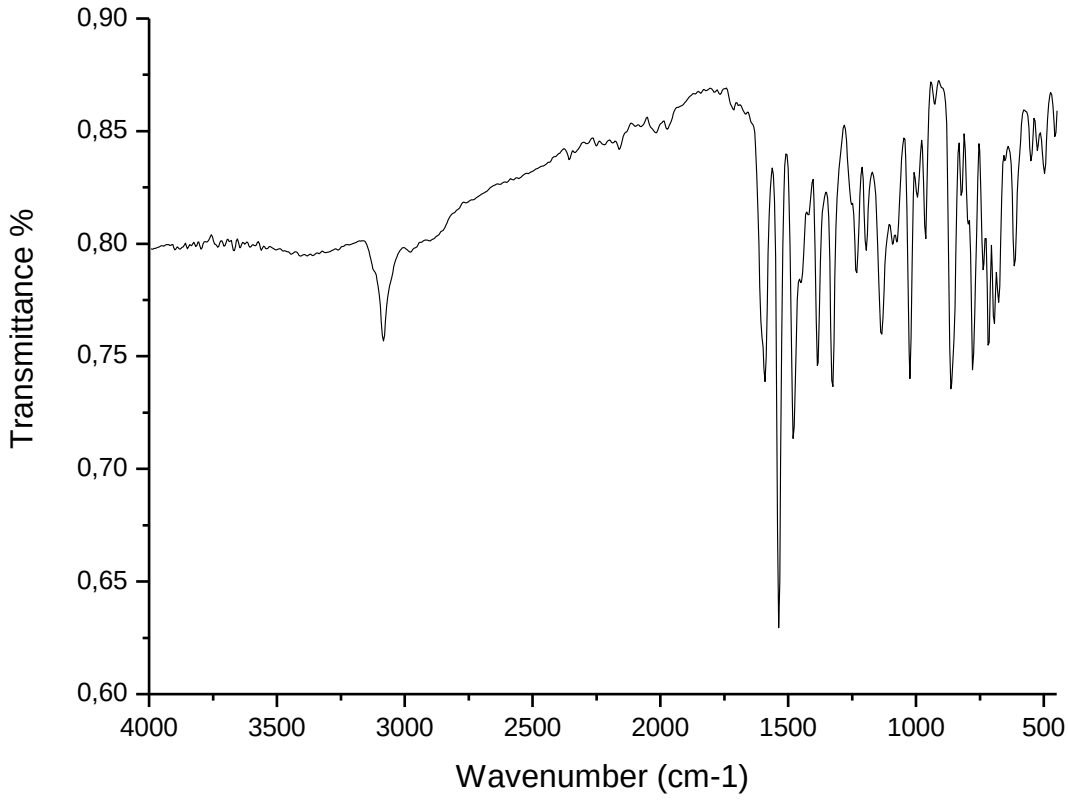

Figure 123. The FTIR spectrum of compound **153 f**

Figure 124. The HRMS spectrum of compound **153 f**

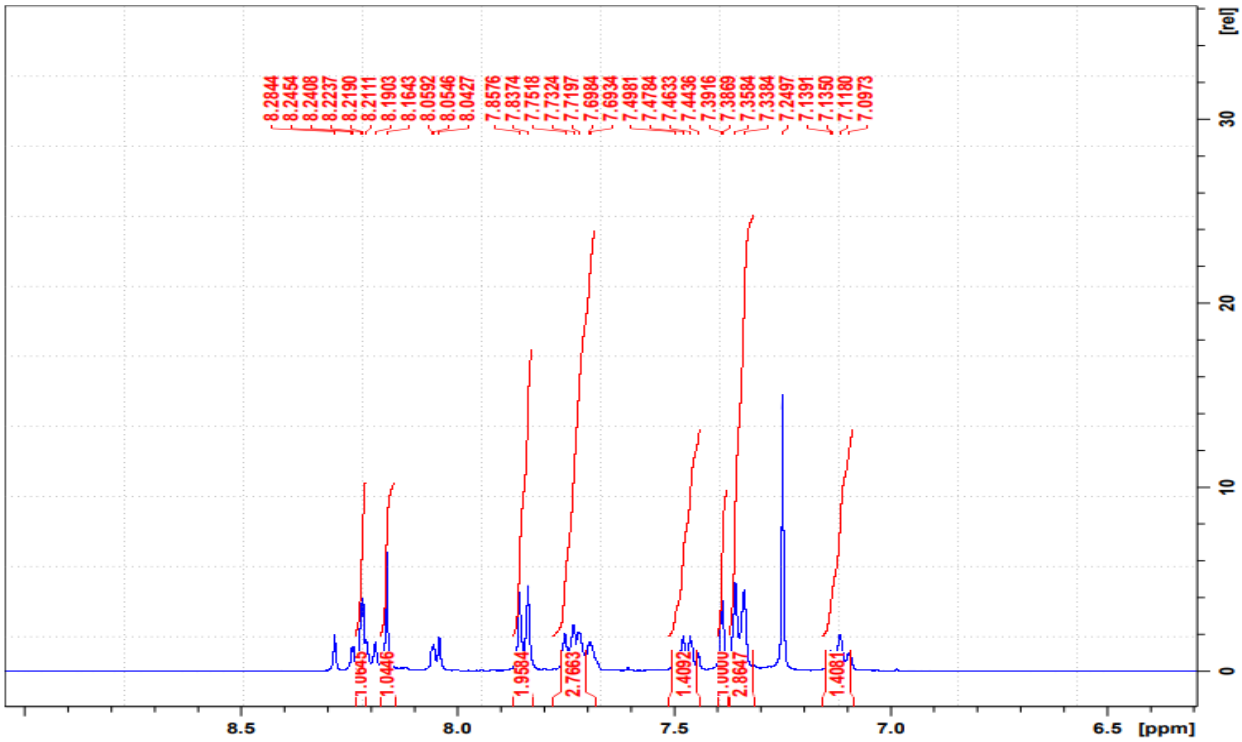

Figure 125. The ^{1}H NMR spectrum of compound **153 g**

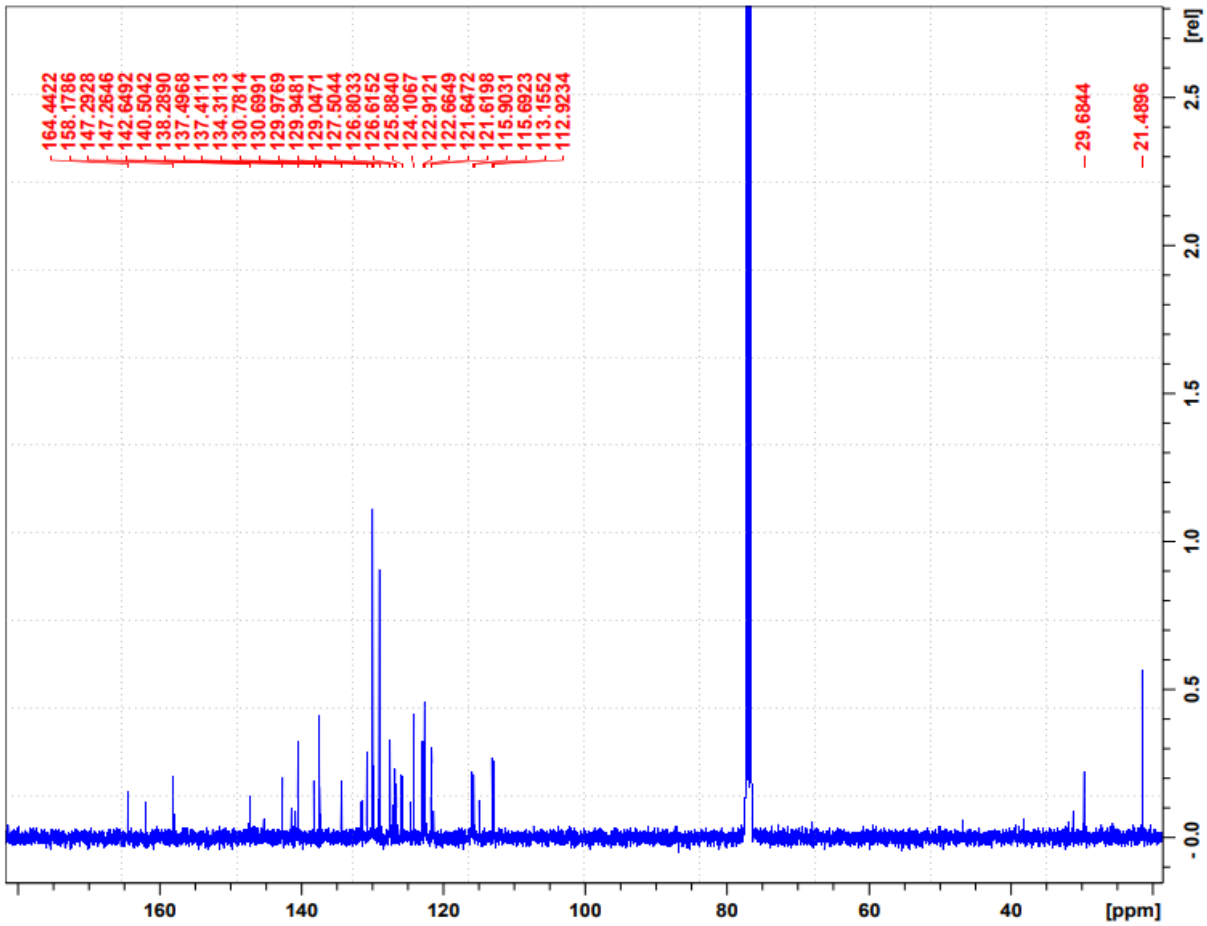

Figure 126. The ^{13}C NMR spectrum of compound **153 g**

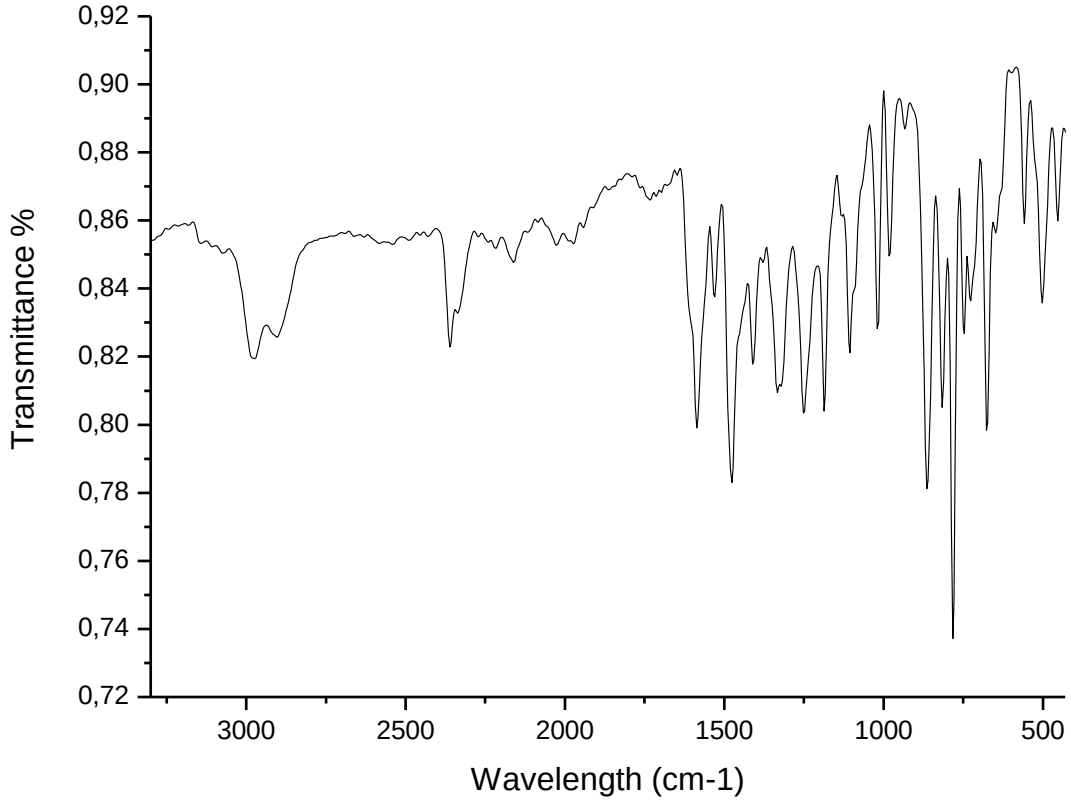
0,92
0,90
0,88
0,86
0,84
0,82
0,80
0,78
0,76
0,74
0,72
Transmittance %
3000
2500
2000
1500
1000
500
Wavelength (cm-1)

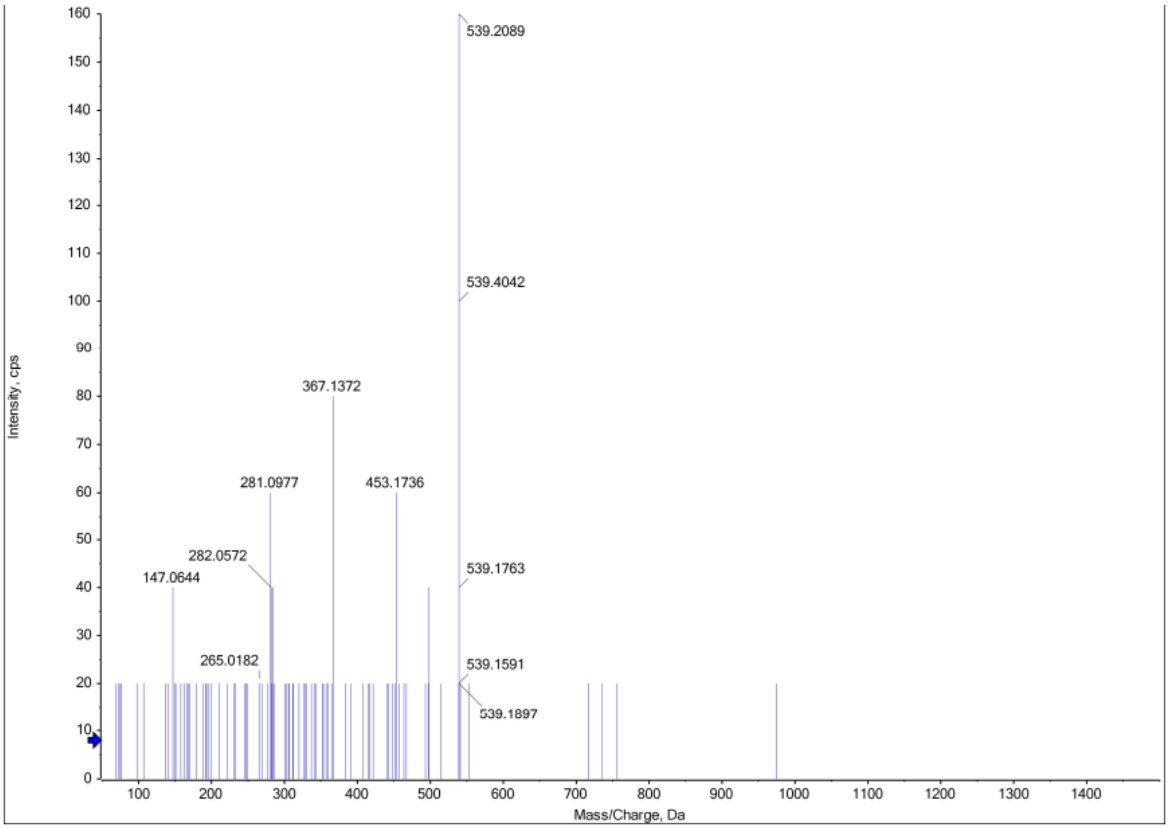

Figure 127. The FTIR spectrum of compound **153 g**

Figure 128. The HRMS spectrum of compound **153 g**

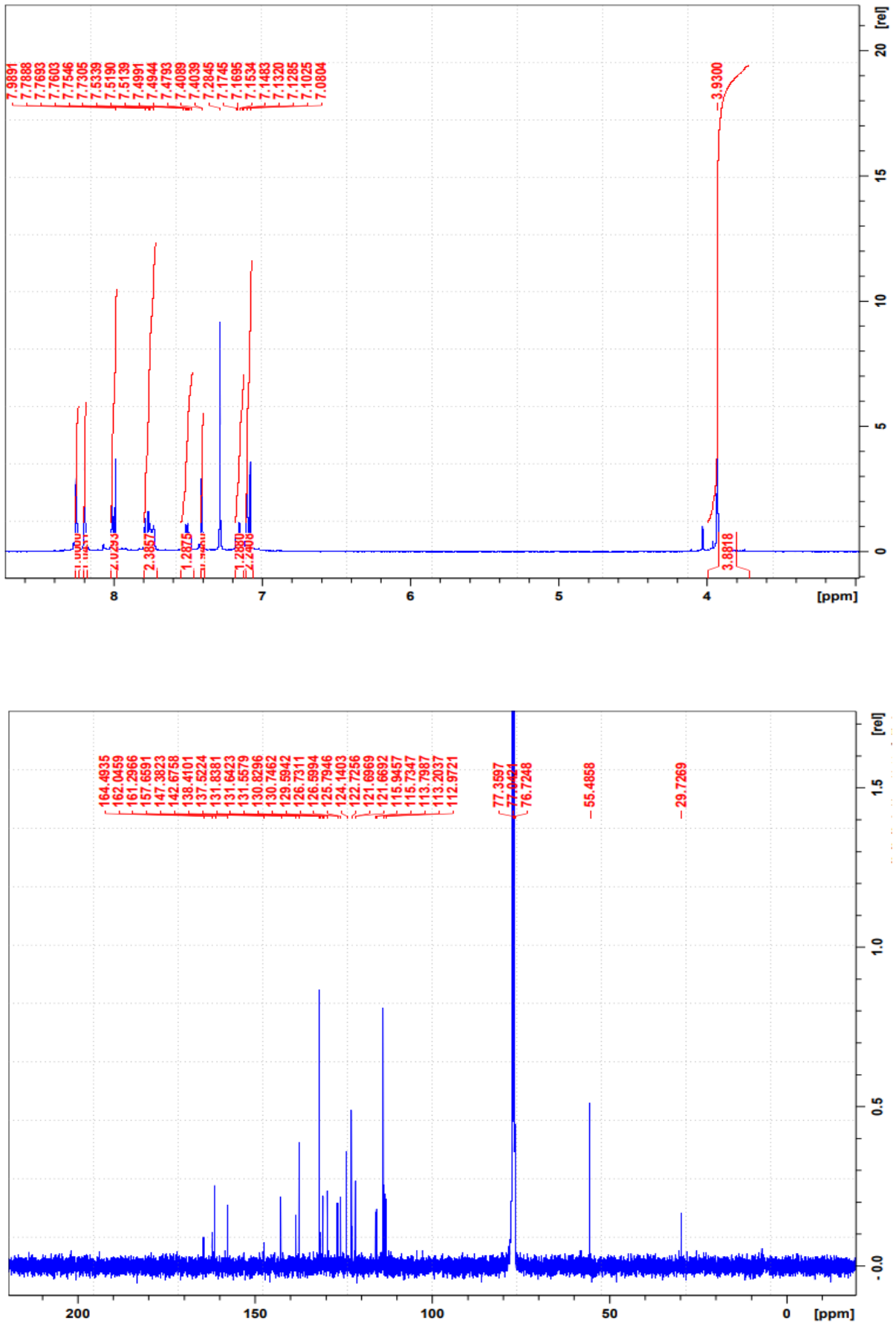

Figure 129. The ^{1}H NMR spectrum of compound **153 h**

Figure 130. The ^{13}C NMR spectrum of compound **153 h**

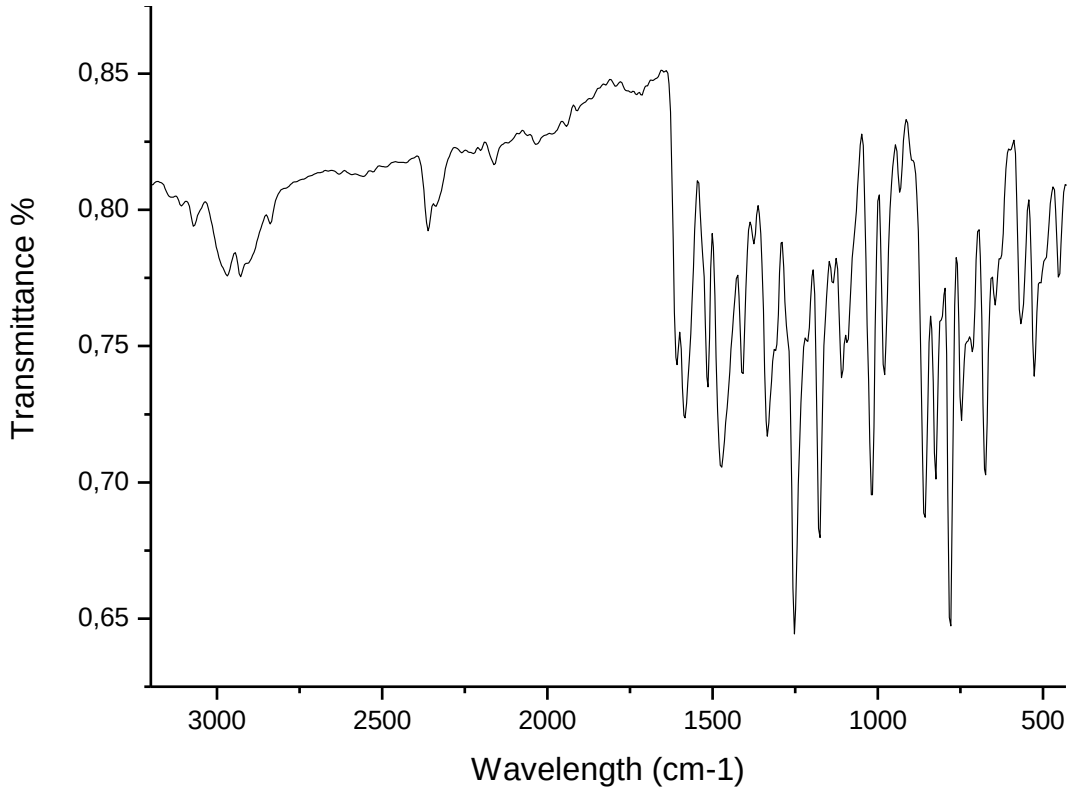

Figure 131. The FTIR spectrum of compound **153 h**

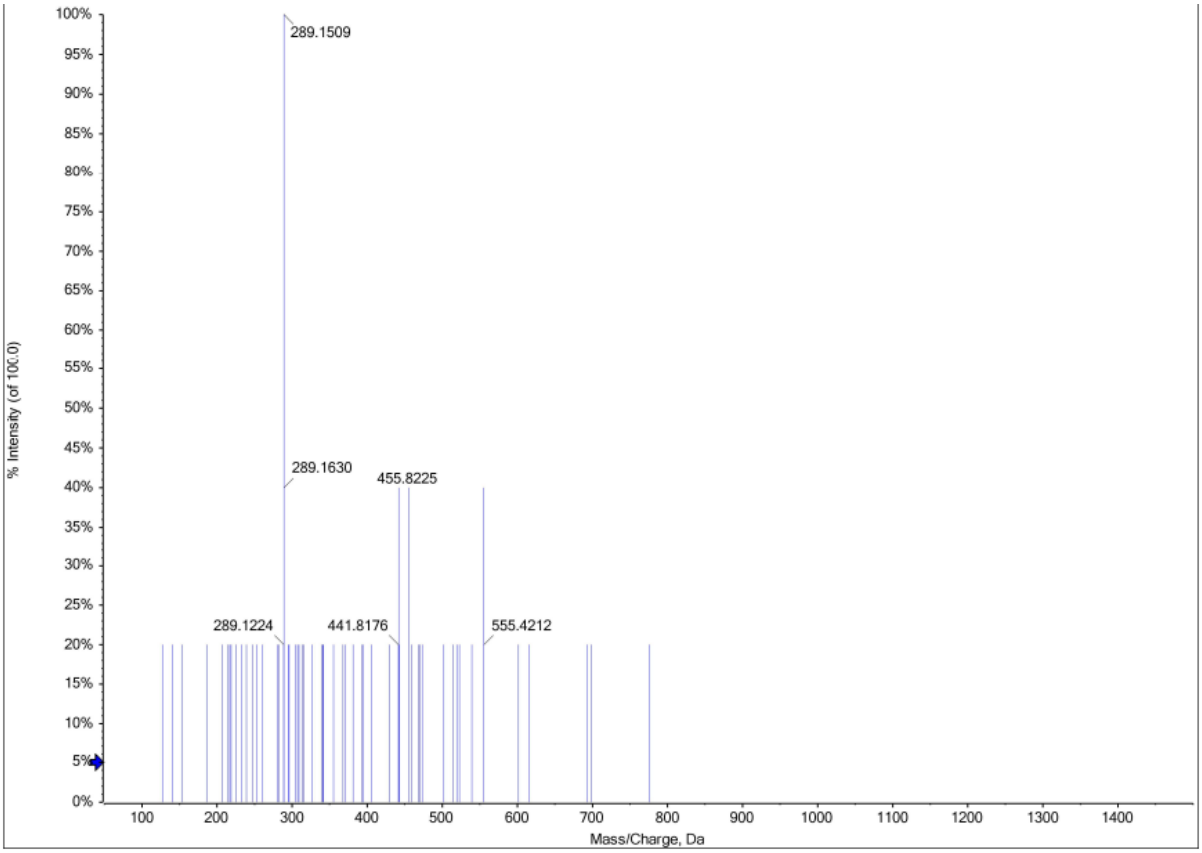

Figure 132. The HRMS spectrum of compound **153 h**

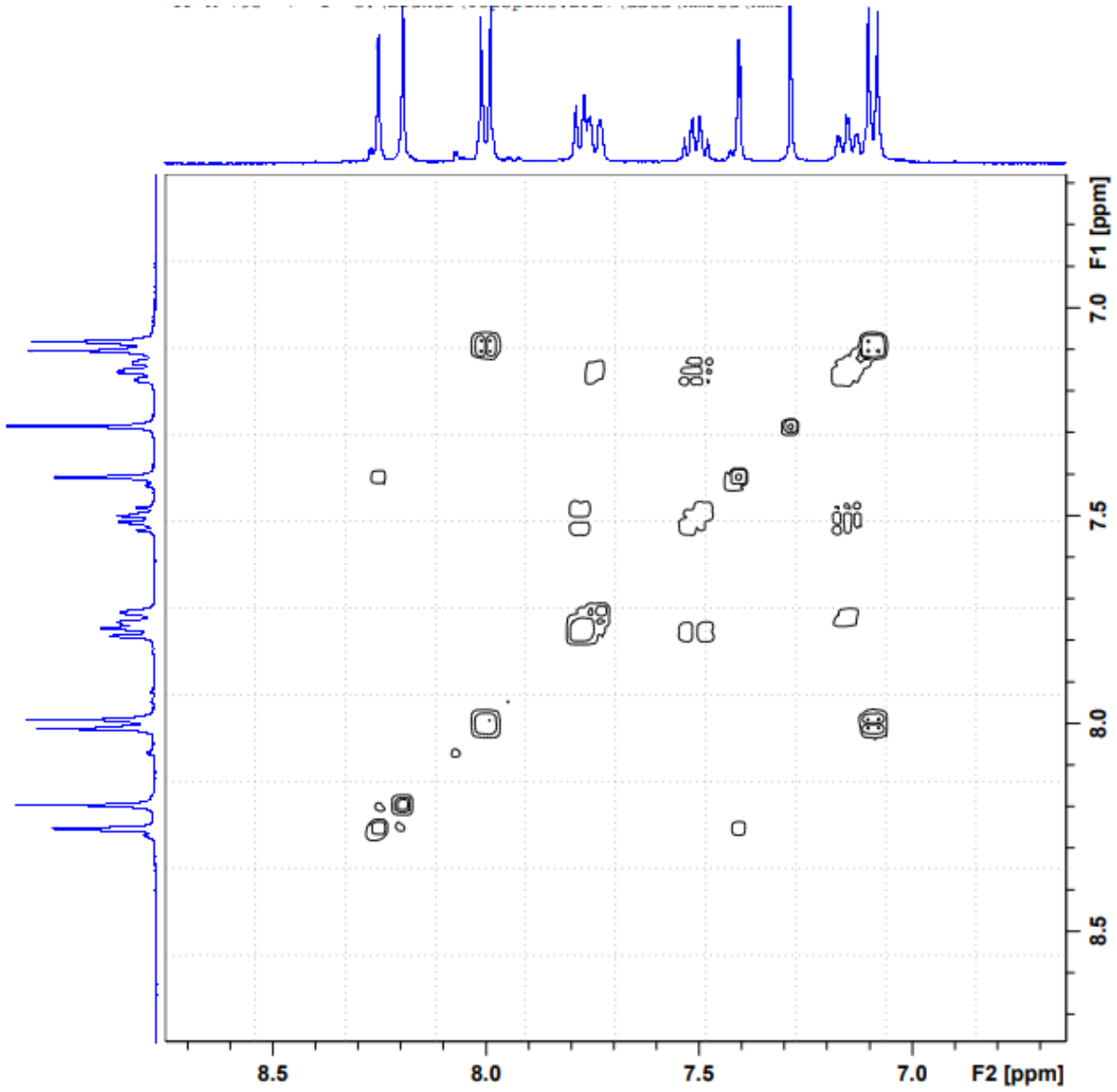

Figure 133. The COSY spectrum of compound **153 h**

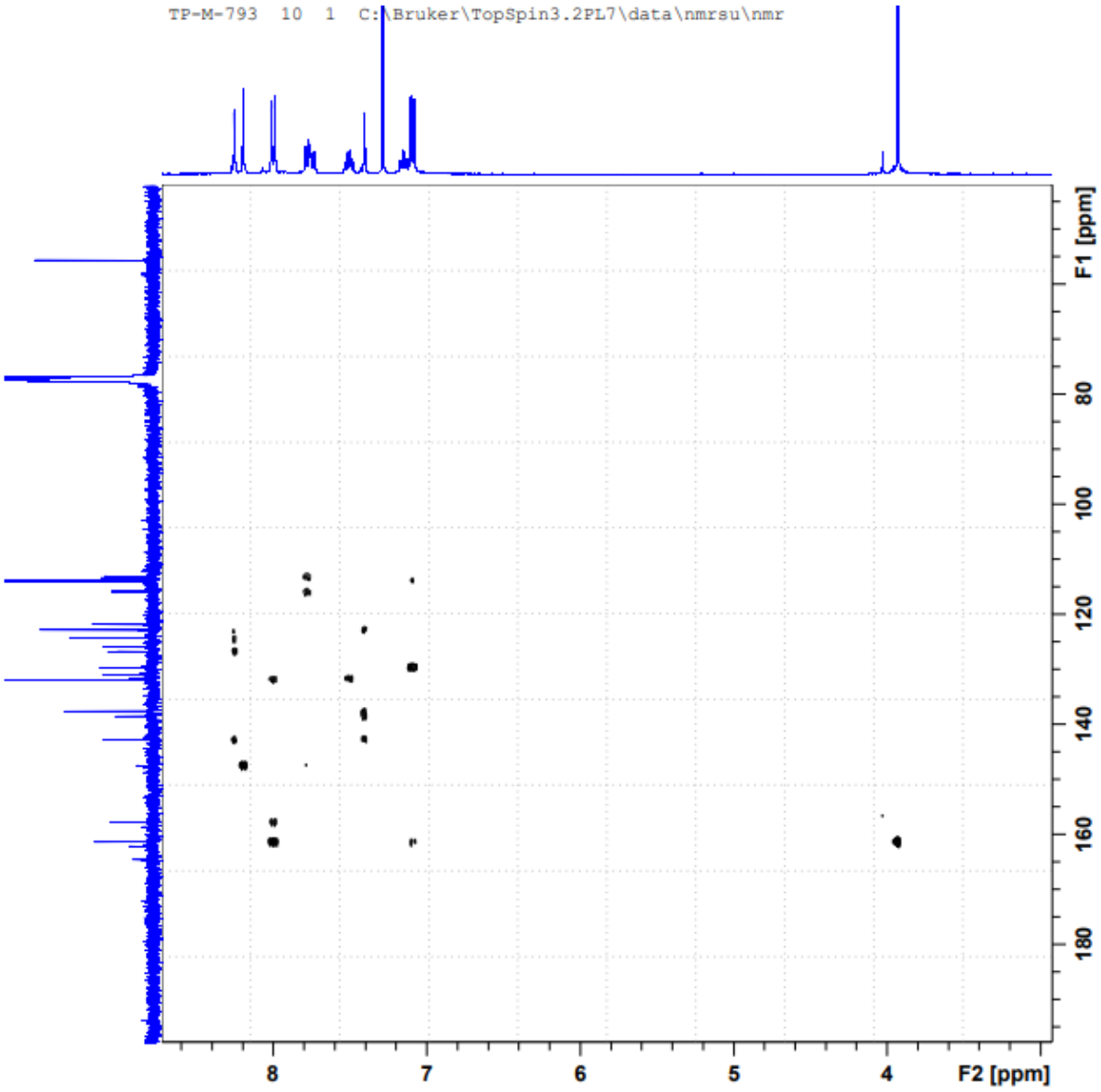

Figure 134. The HMBC spectrum of compound **153 h**

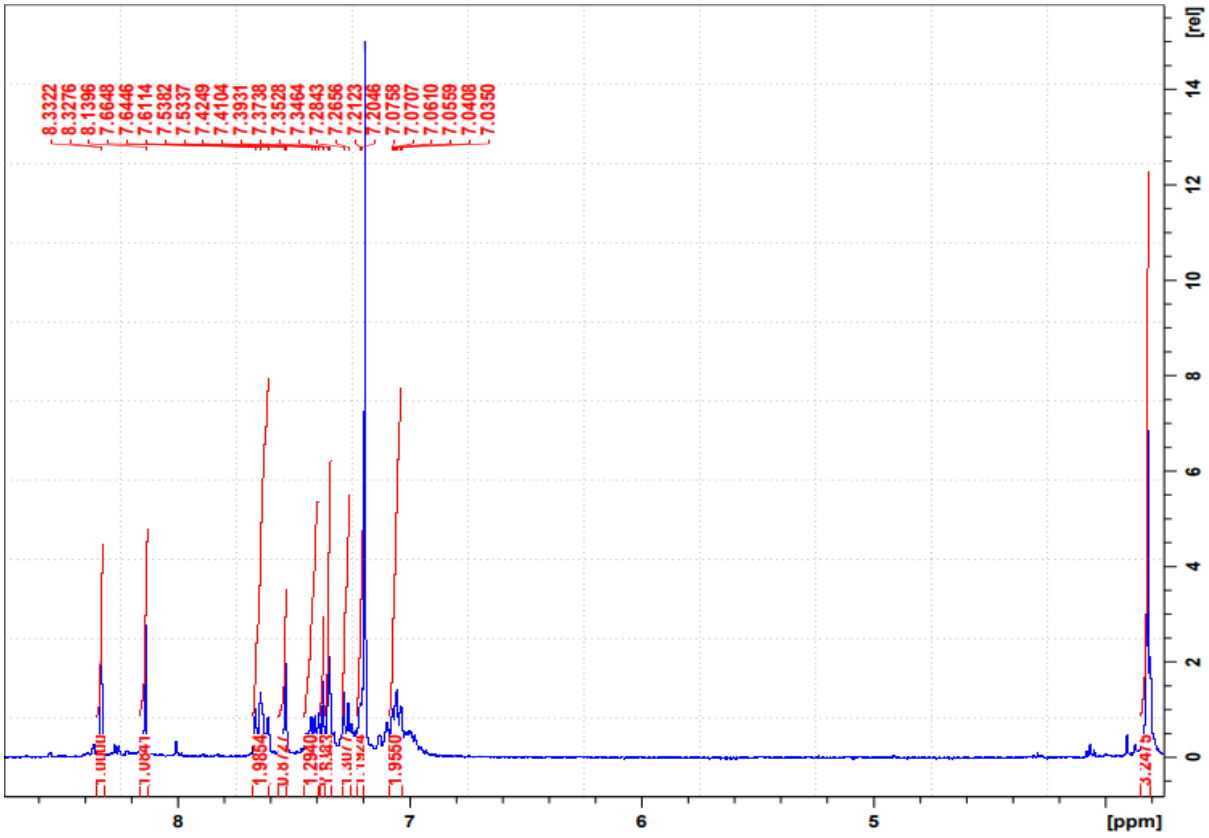

Figure 135. The ^{1}H NMR spectrum of compound **153 i**

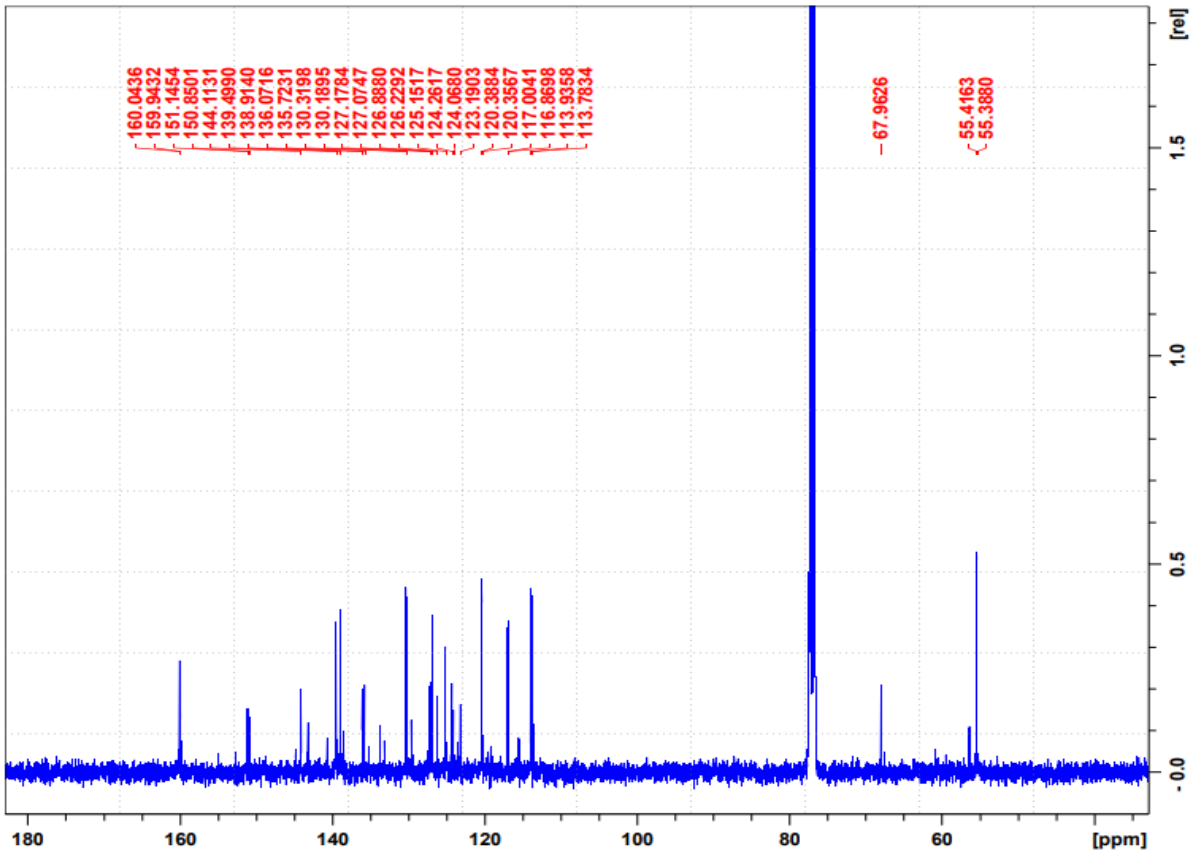

Figure 136. The 13C NMR spectrum of compound **153 i**

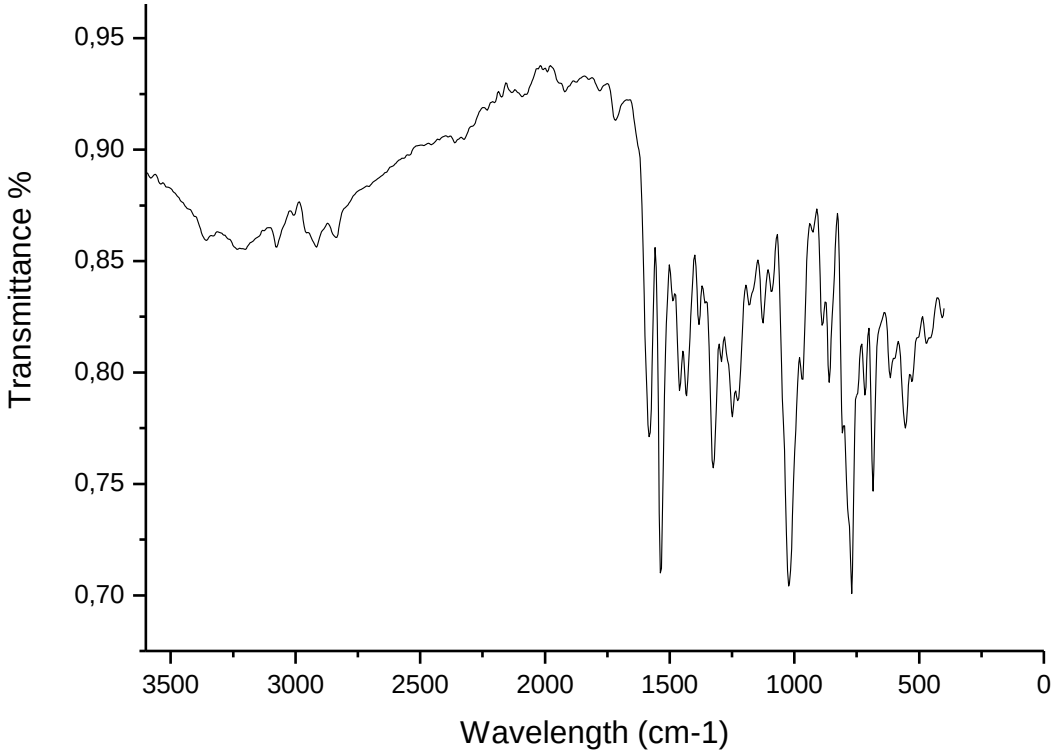

Figure 137. The FTIR spectrum of compound **153 i**

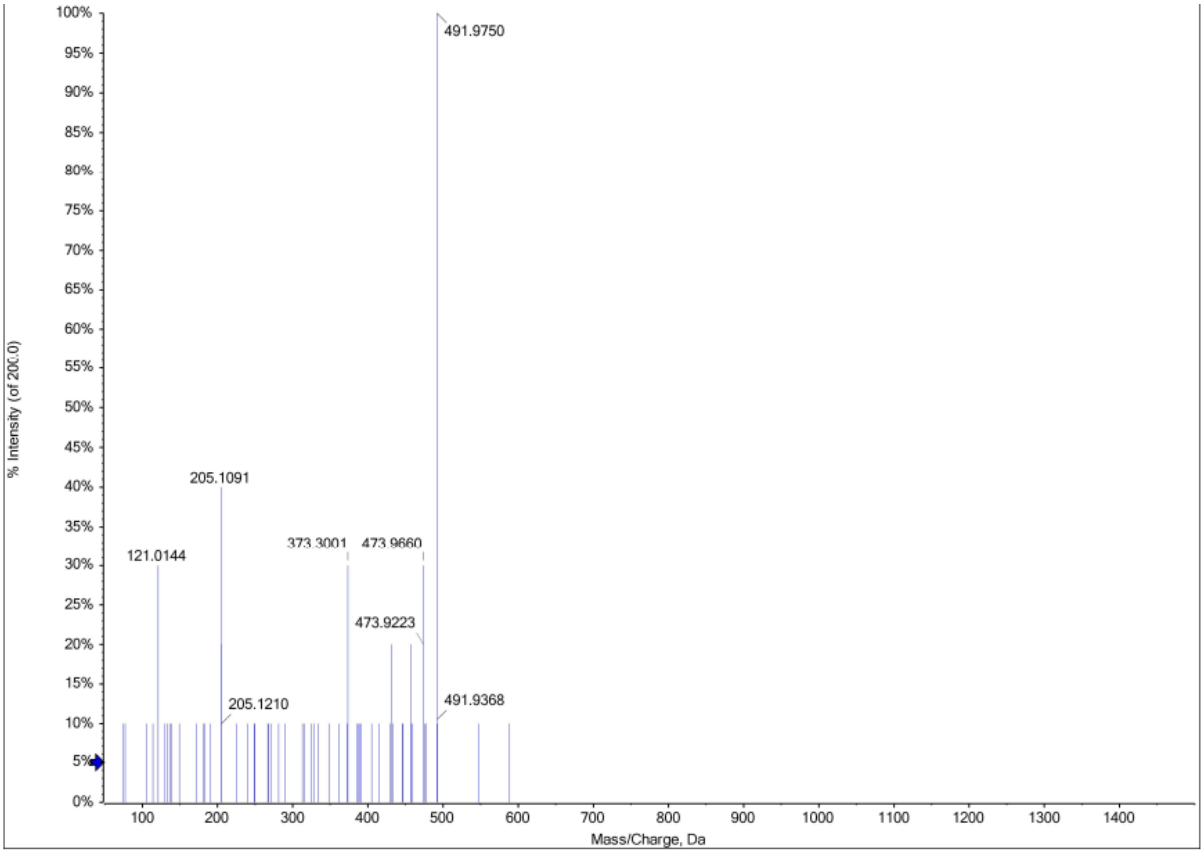

Figure 138. The HRMS spectrum of compound **153 i**

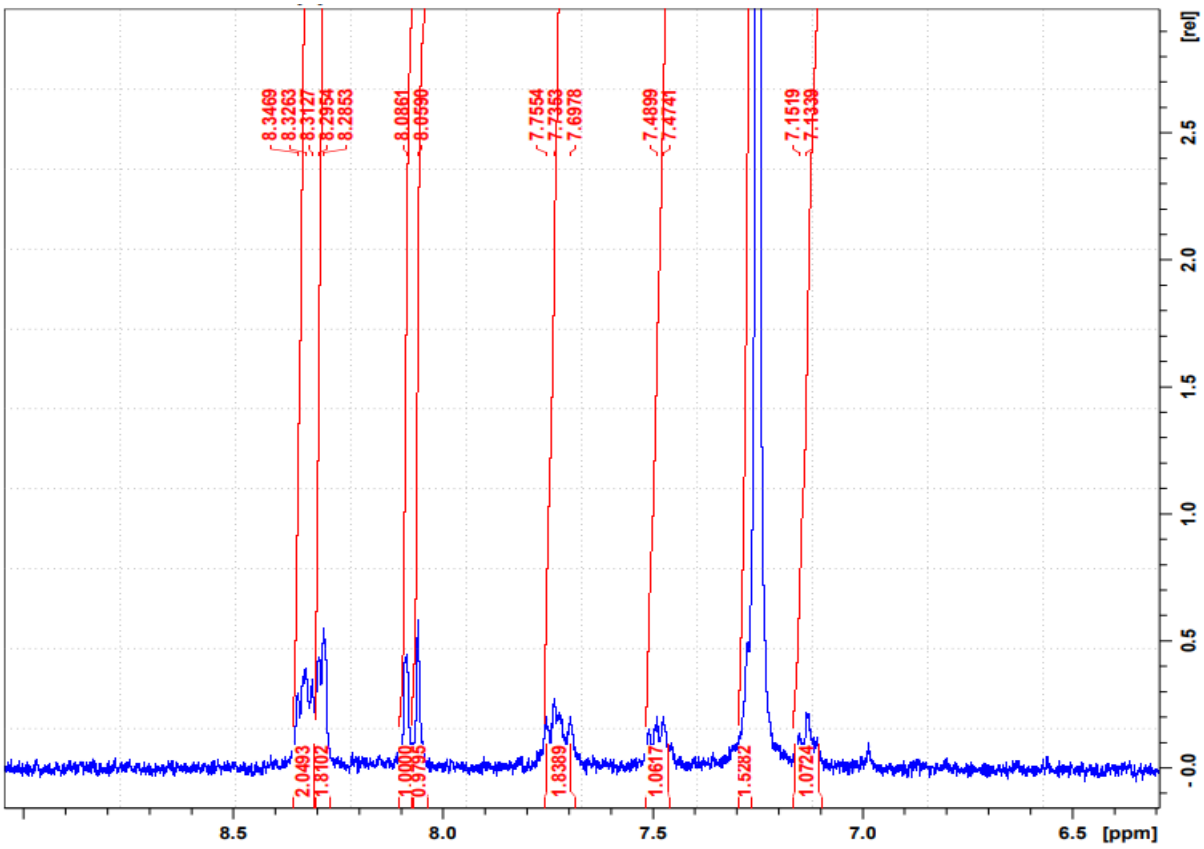

Figure 139. The ^{1}H NMR spectrum of compound **153 j**

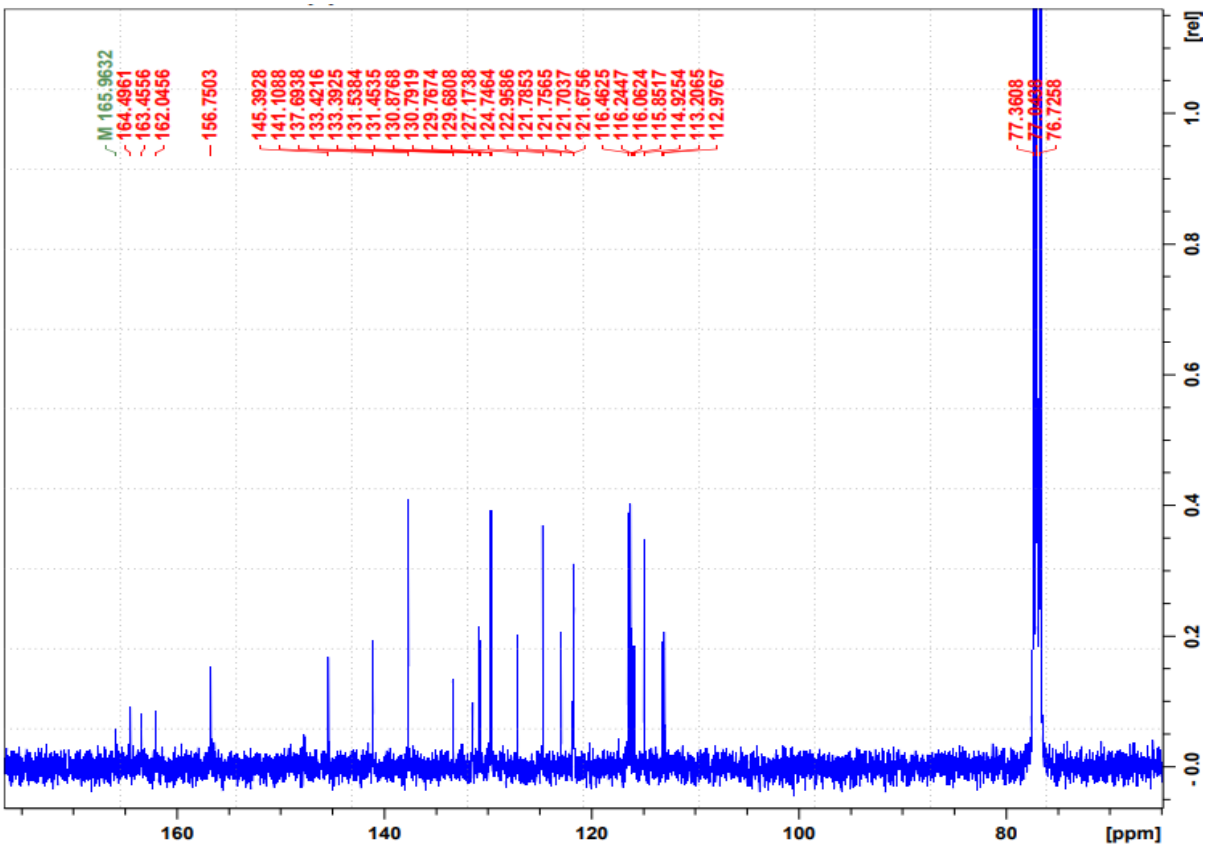

Figure 140. The ^{13}C NMR spectrum of compound **153 j**

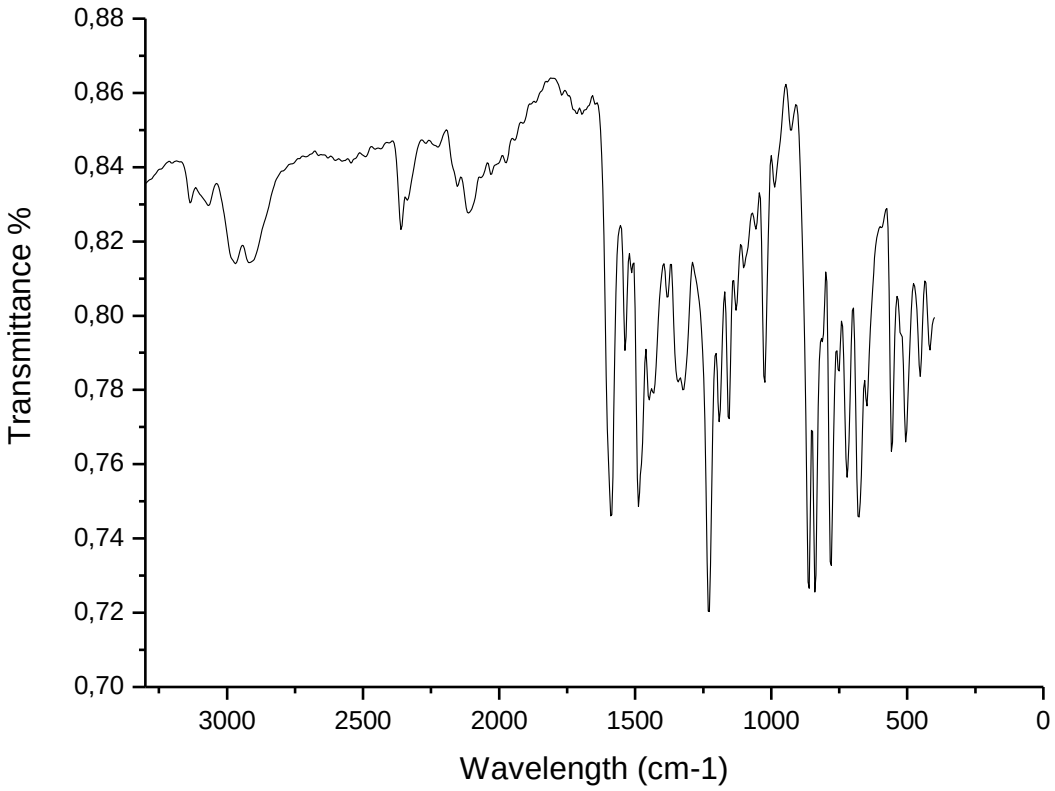

Figure 141. The FTIR spectrum of compound **153 j**

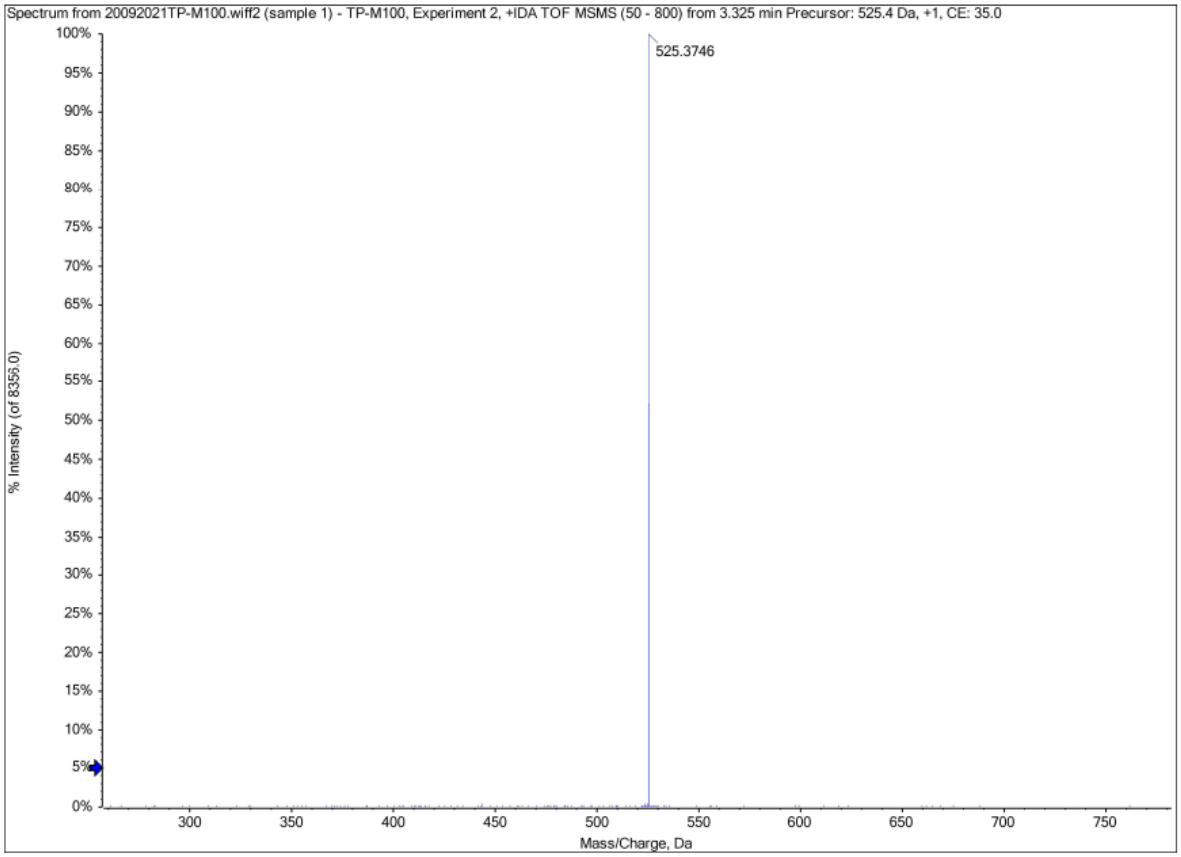

Figure 142. The HRMS spectrum of compound **153 j**

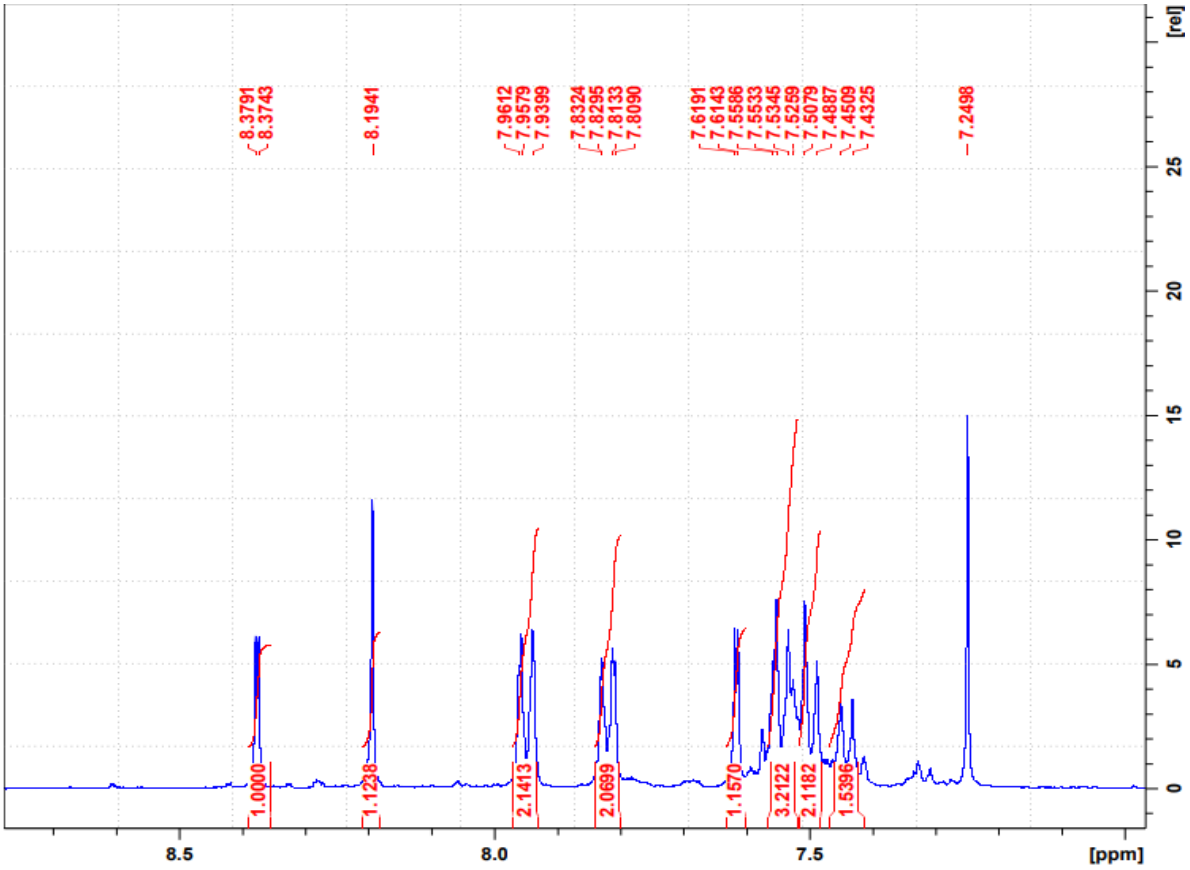

Figure 143. The ^{1}H NMR spectrum of compound **153 k**

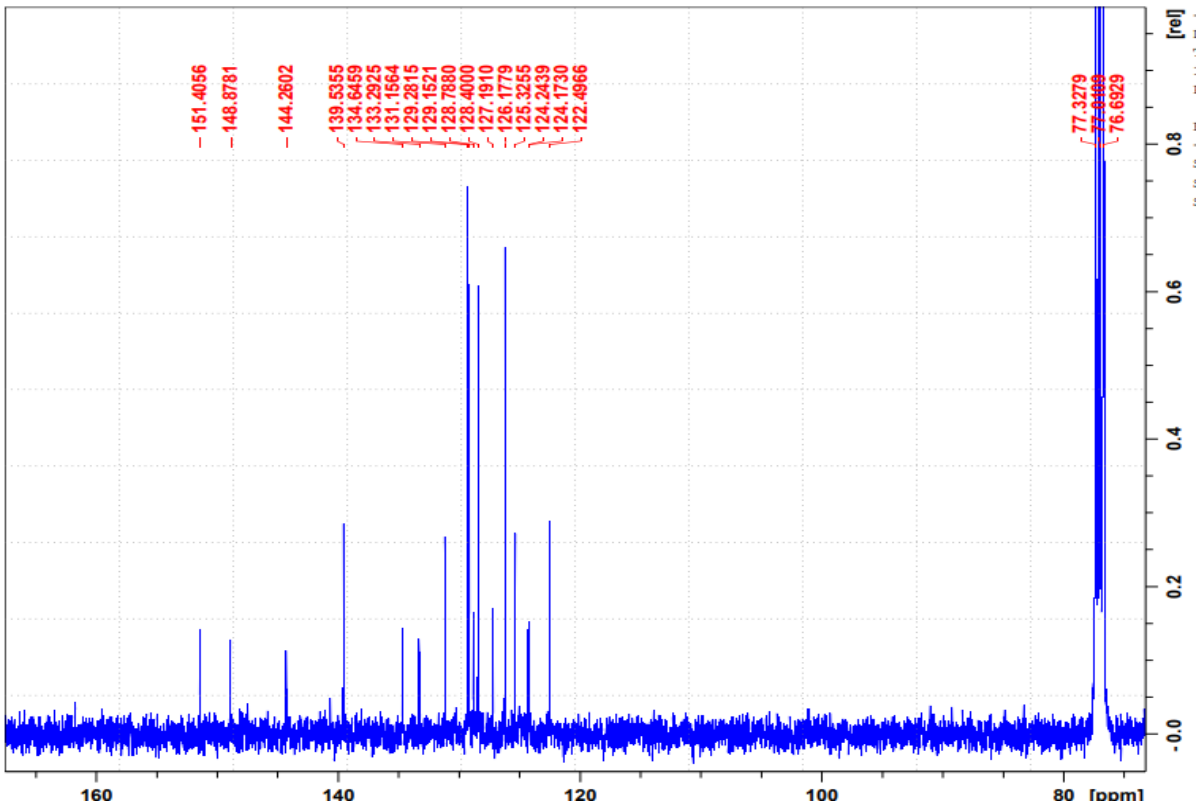

Figure 144. The ^{13}C NMR spectrum of compound **153 k**

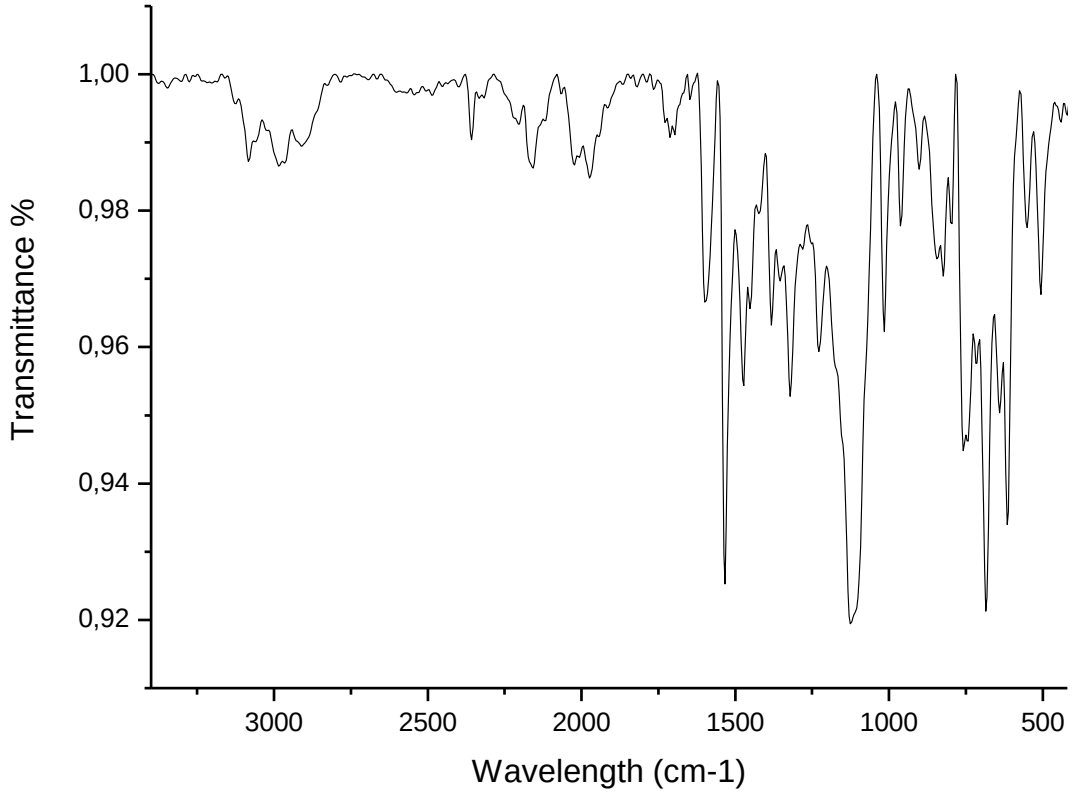

Figure 145. The FTIR spectrum of compound **153 k**

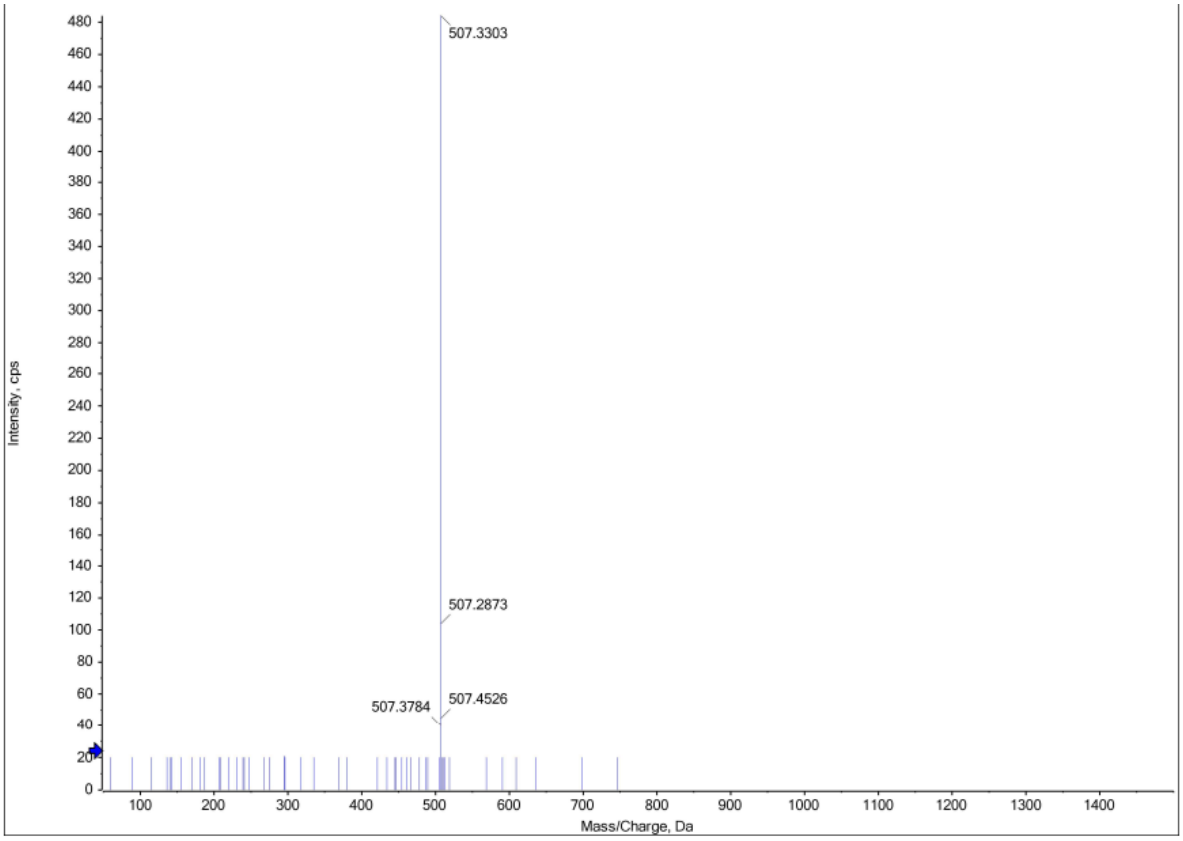

Figure 146. The HRMS spectrum of compound **153 k**

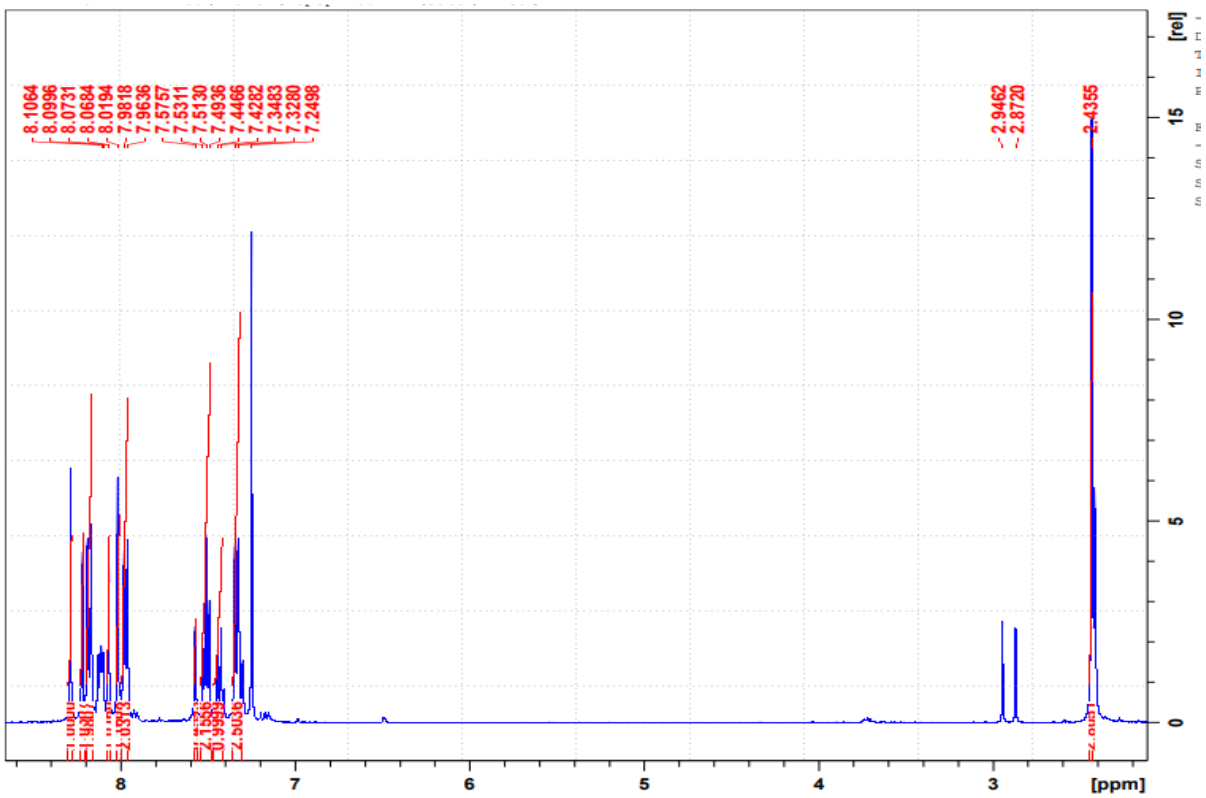

Figure 147. The ^{1}H NMR spectrum of compound **153 l**

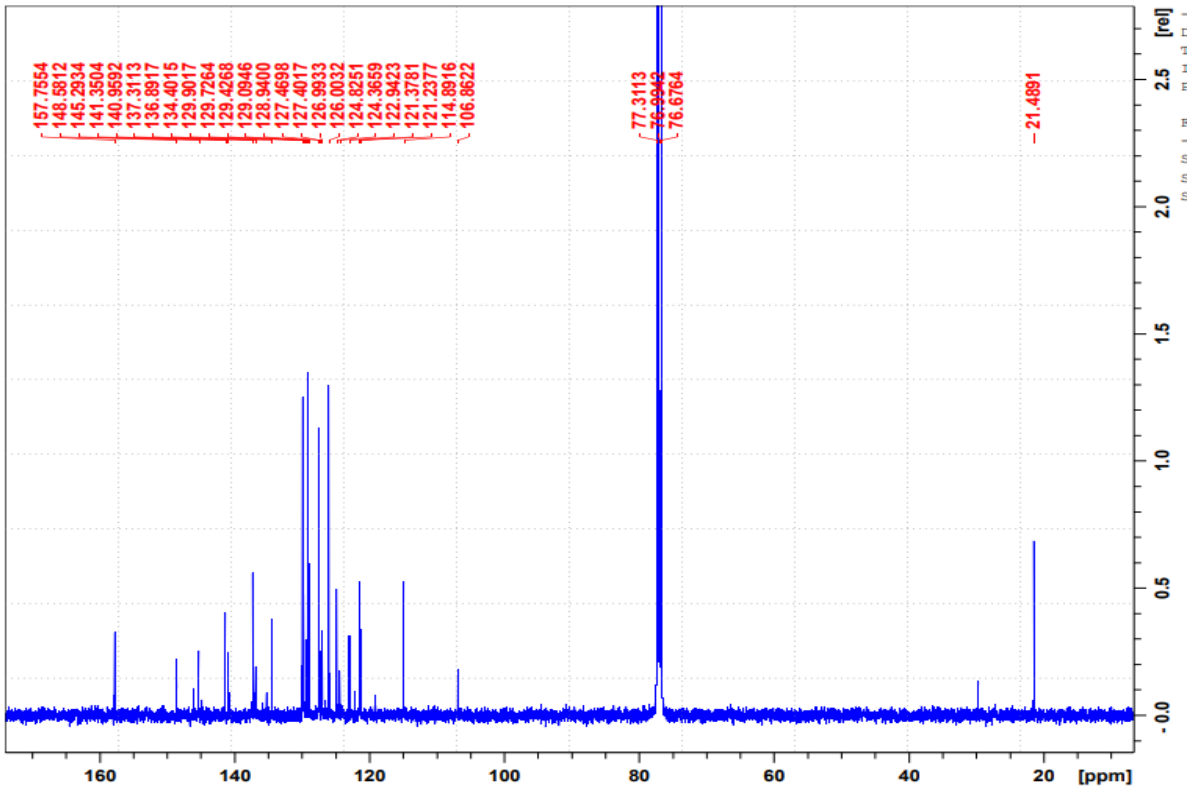

Figure 148. The ^{13}C NMR spectrum of compound **153 l**

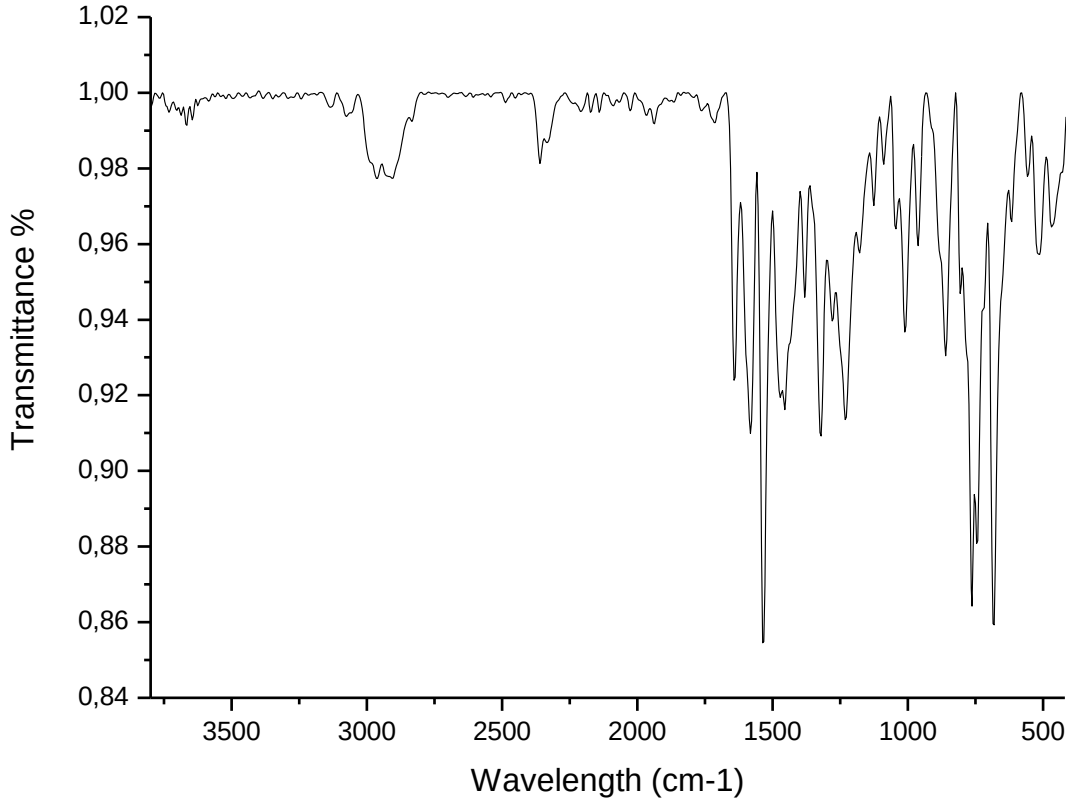

Figure 149. The FTIR spectrum of compound **153 l**

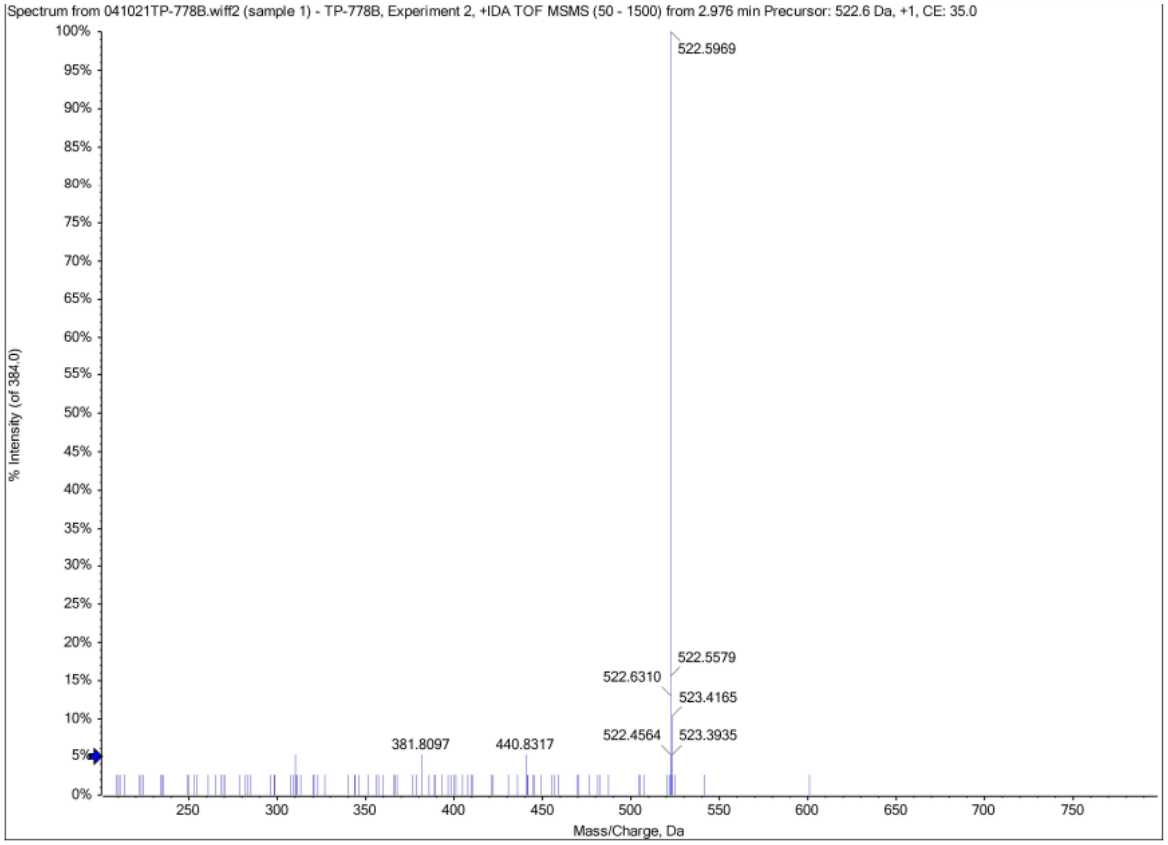

Figure 150. The HRMS spectrum of compound 153 l

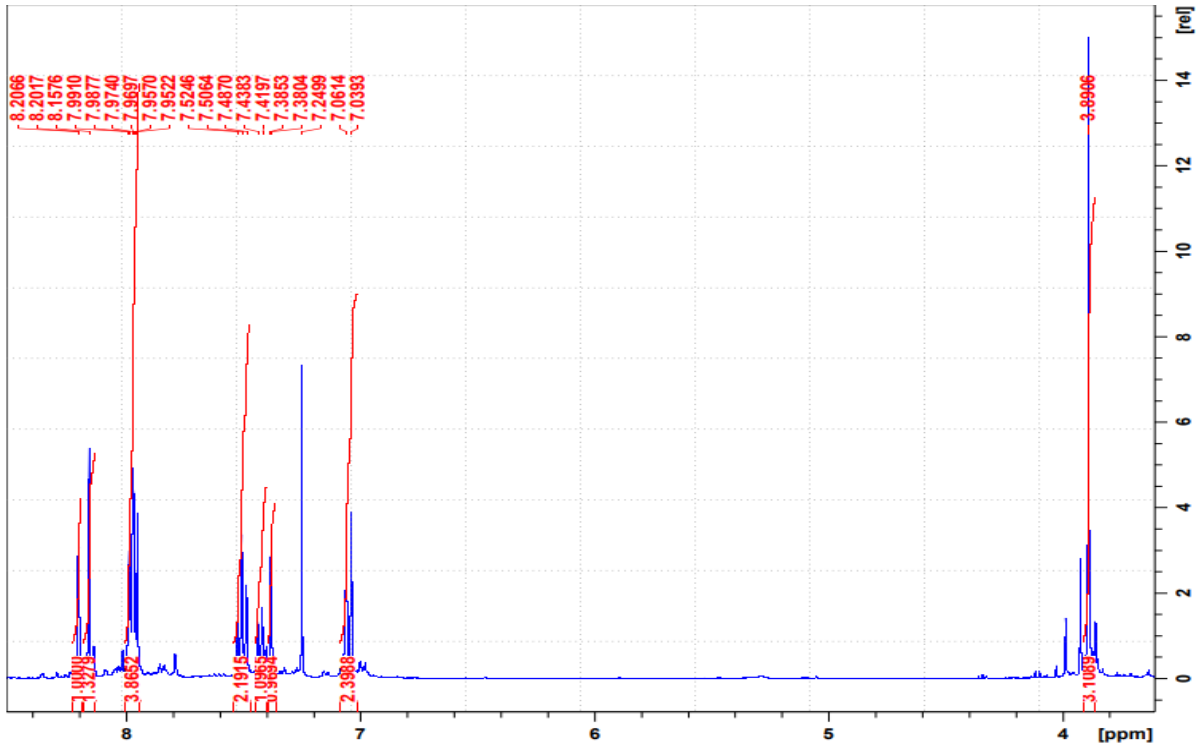

Figure 151. The ^{1}H NMR spectrum of compound **153 m**

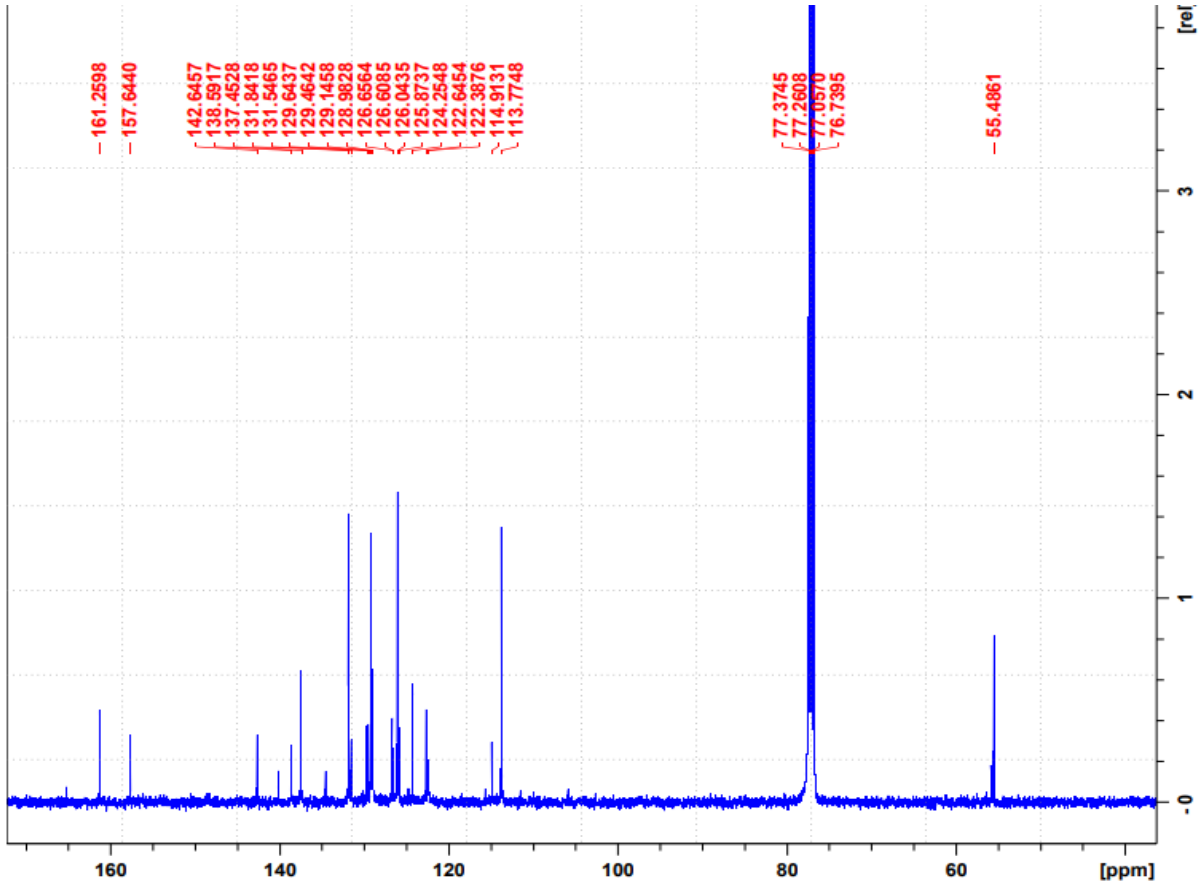

Figure 152. The ^{13}C NMR spectrum of compound **153 m**

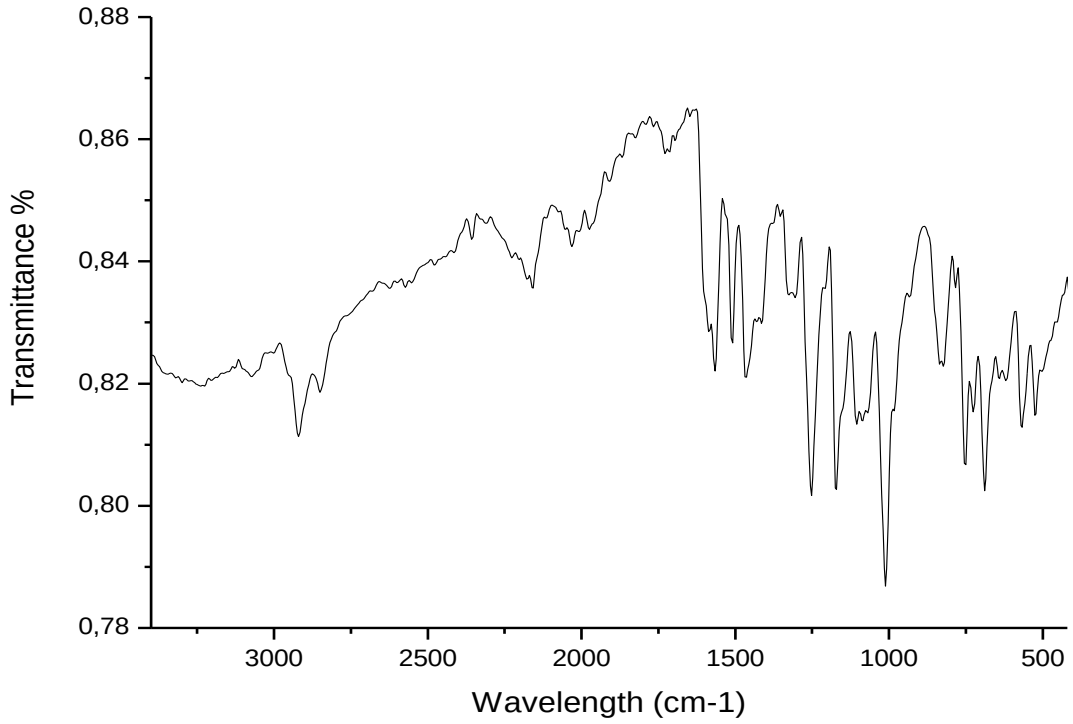

Figure 153. The FTIR spectrum of compound **153 m**

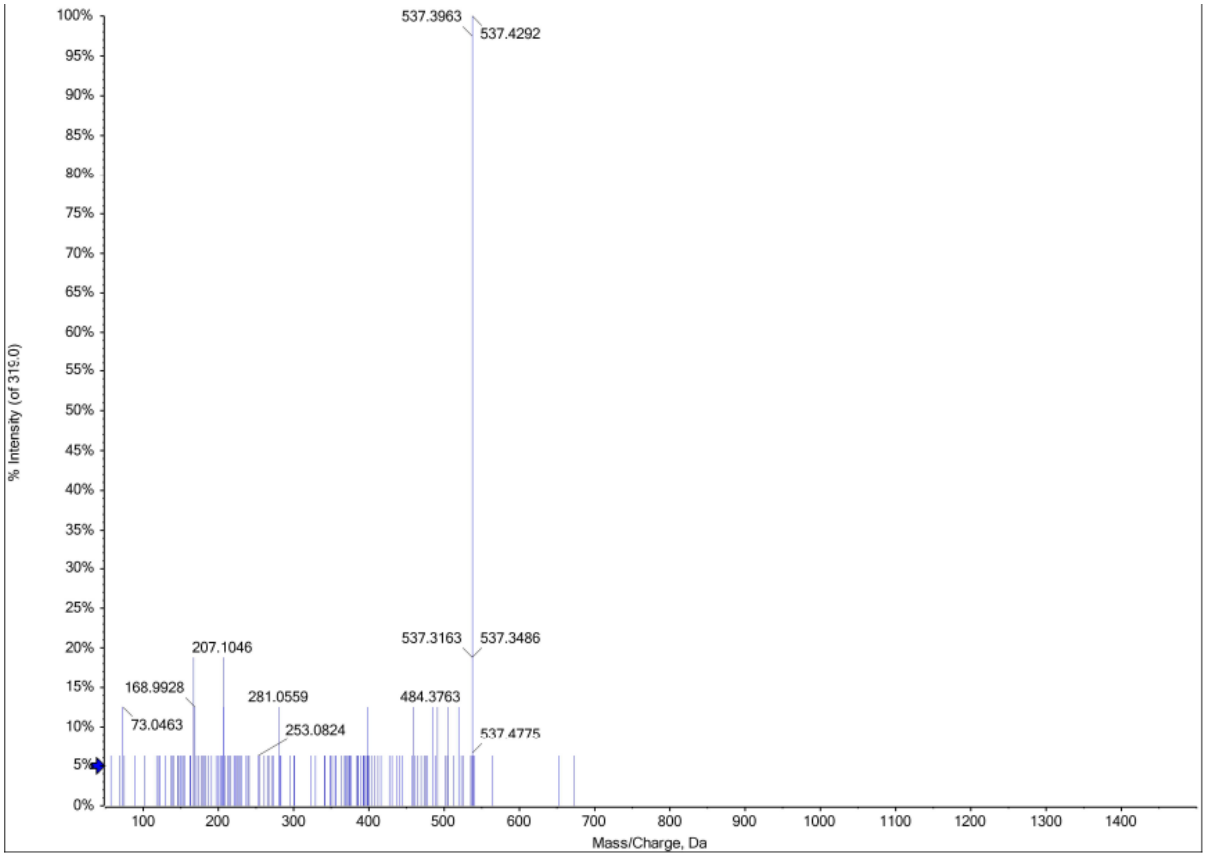

Figure 154. The HRMS spectrum of compound **153 m**

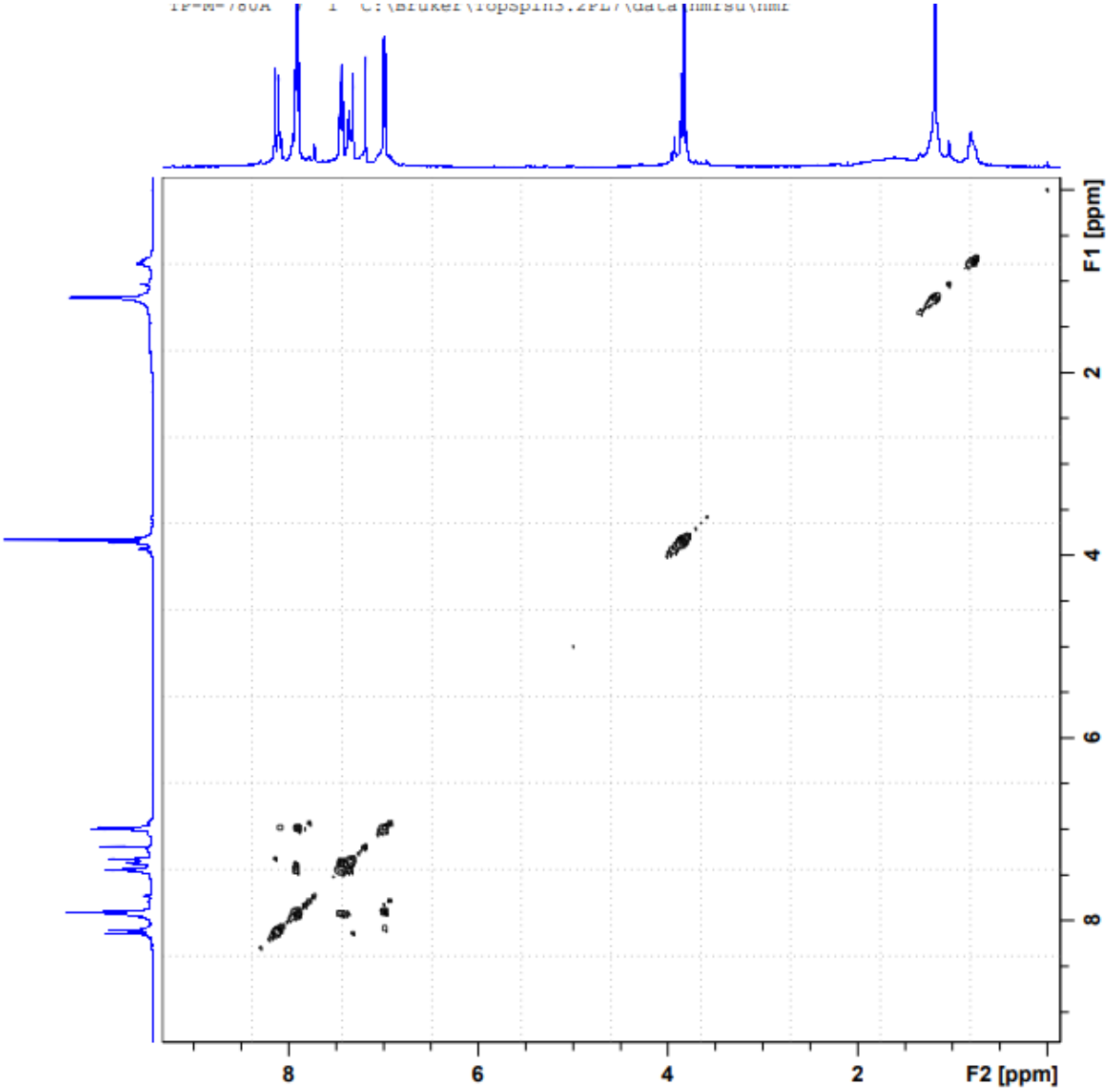

Figure 155. The COSY spectrum of compound **153 m**

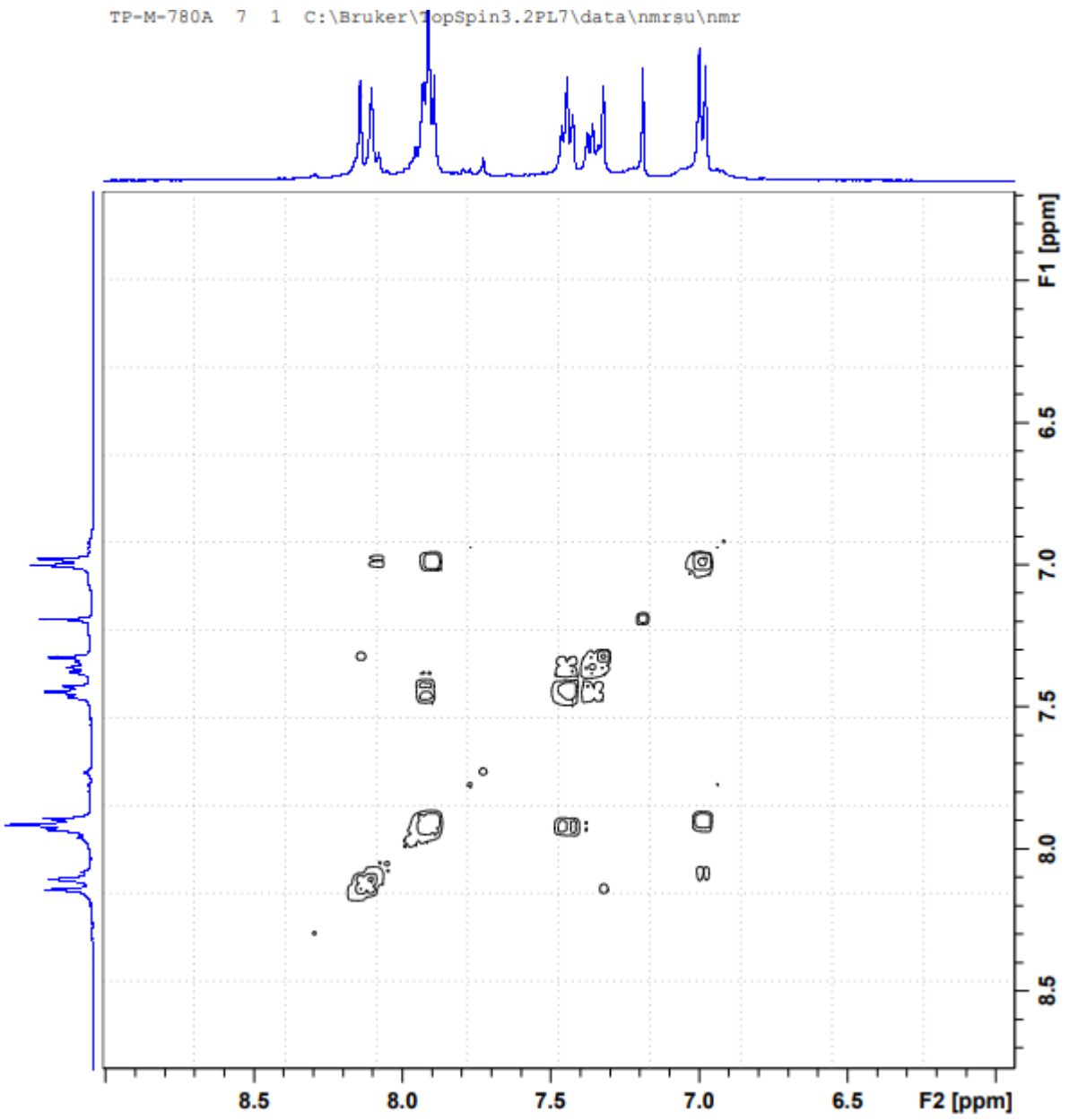

Figure 155. The COSY (expanded) spectrum of compound **153 m**

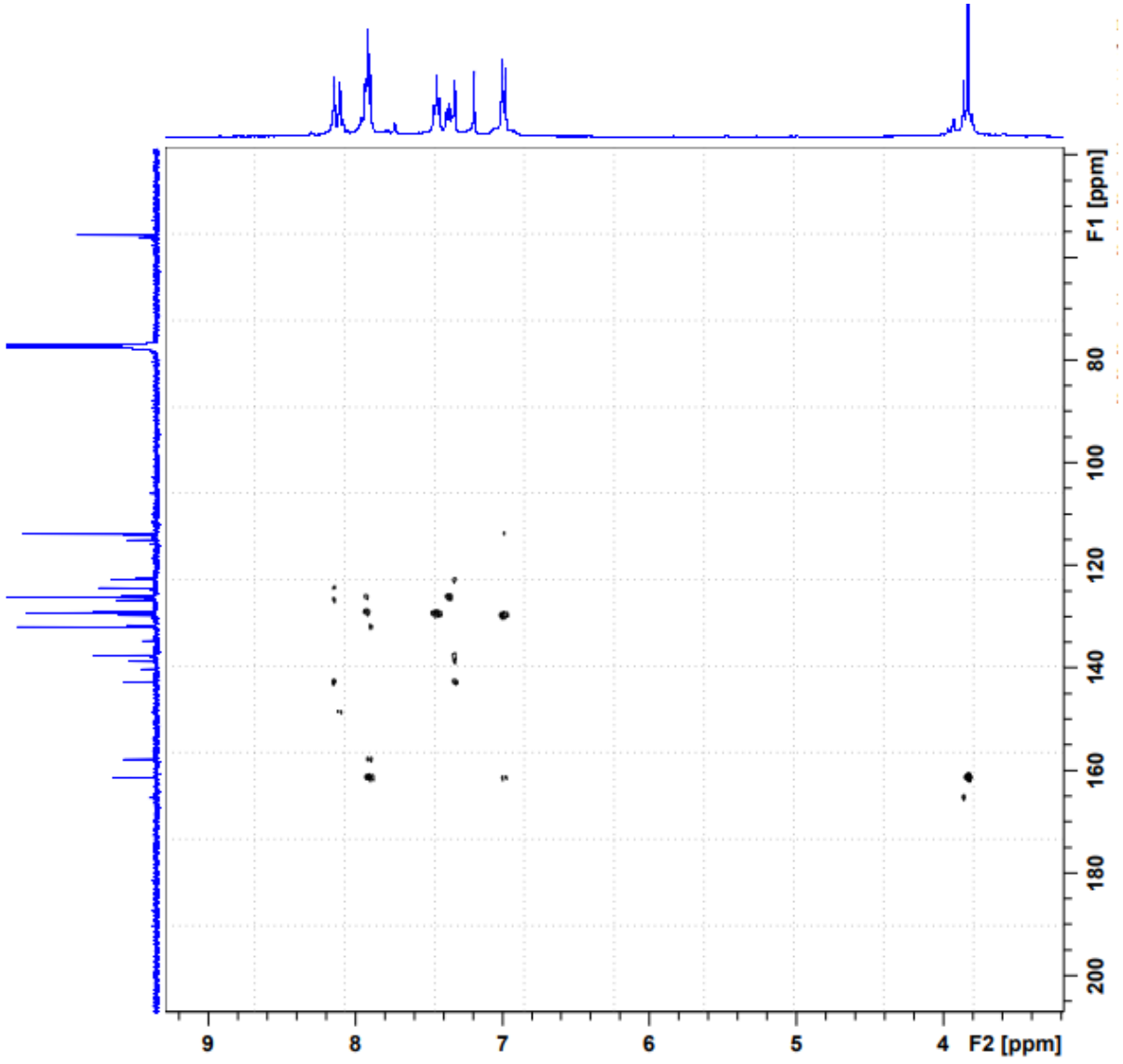

Figure 156. The HSQC spectrum of compound **153 m**

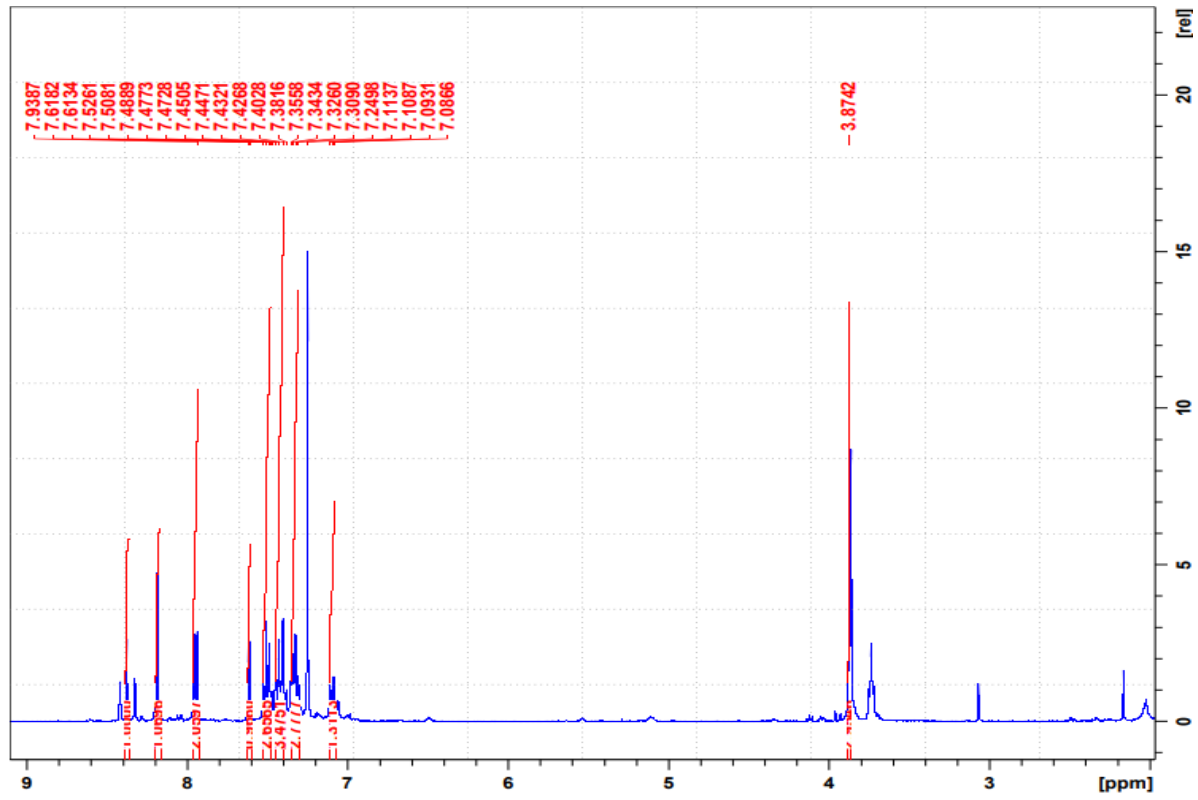

Figure 157. The ^{1}H NMR spectrum of compound **153 n**

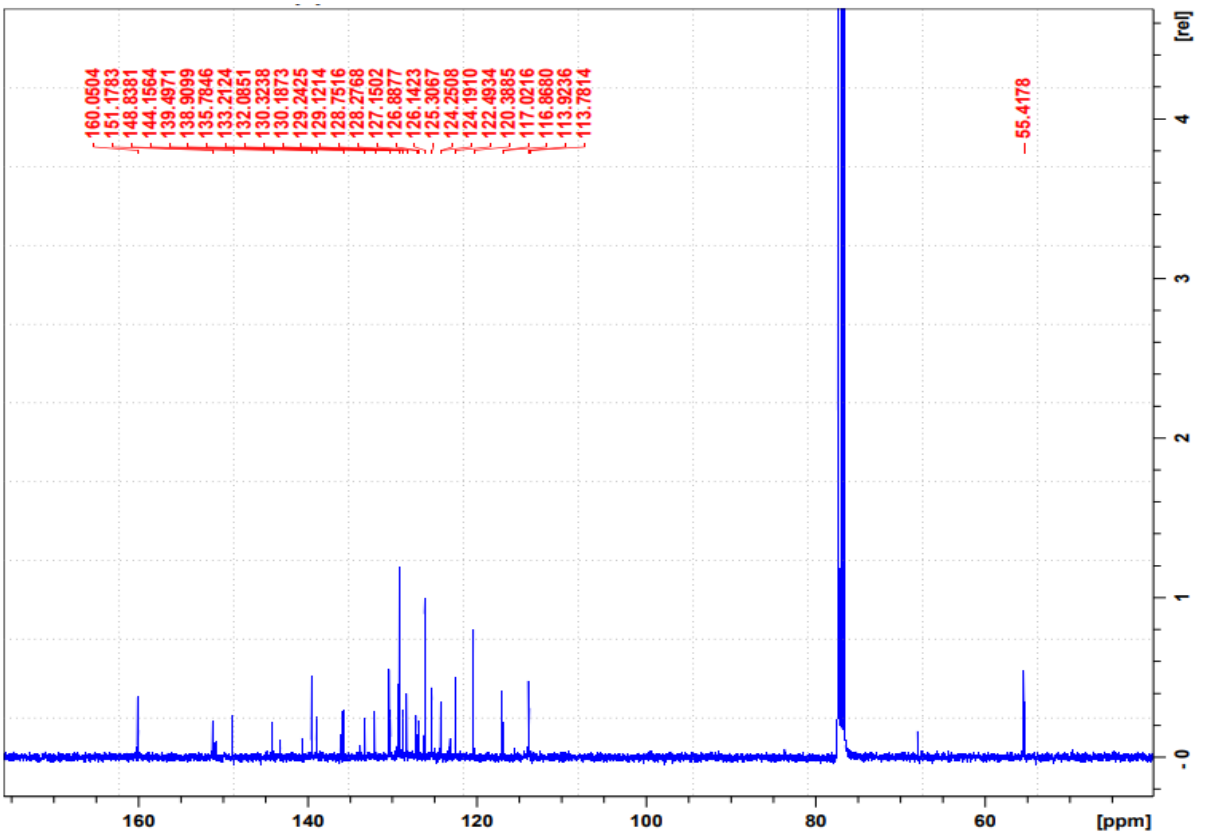

Figure 158. The ^{13}C NMR spectrum of compound **153 n**

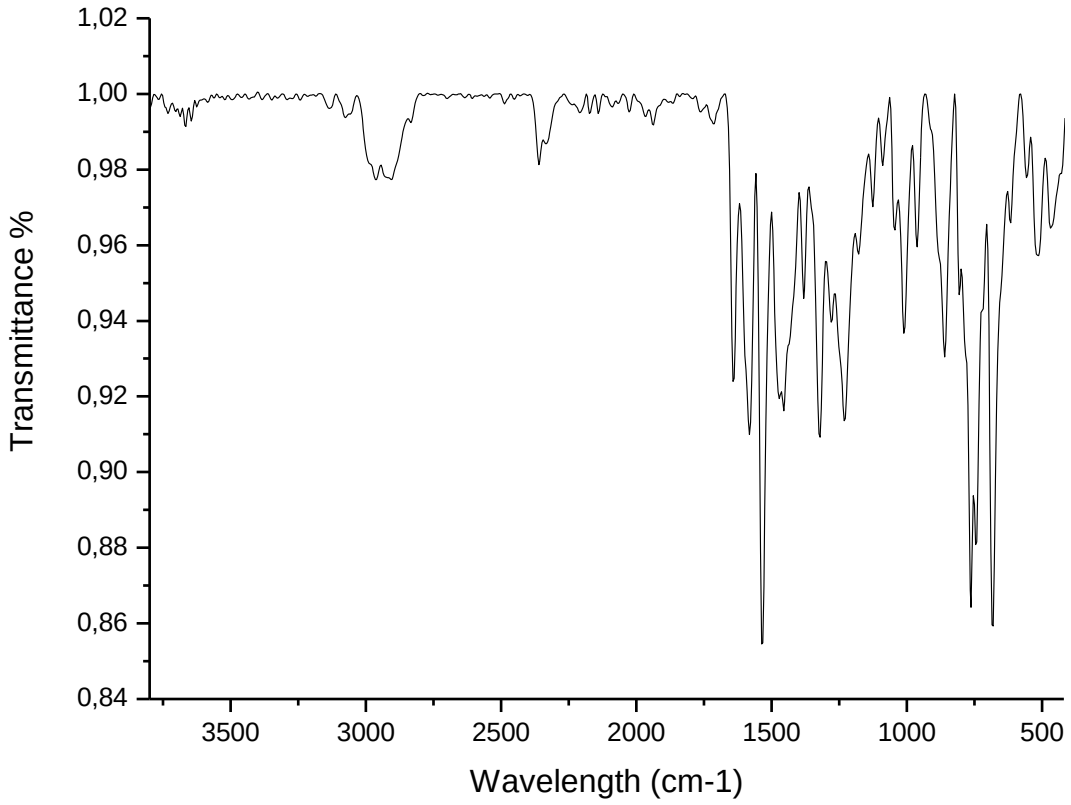

Figure 159. The FTIR spectrum of compound **153 n**

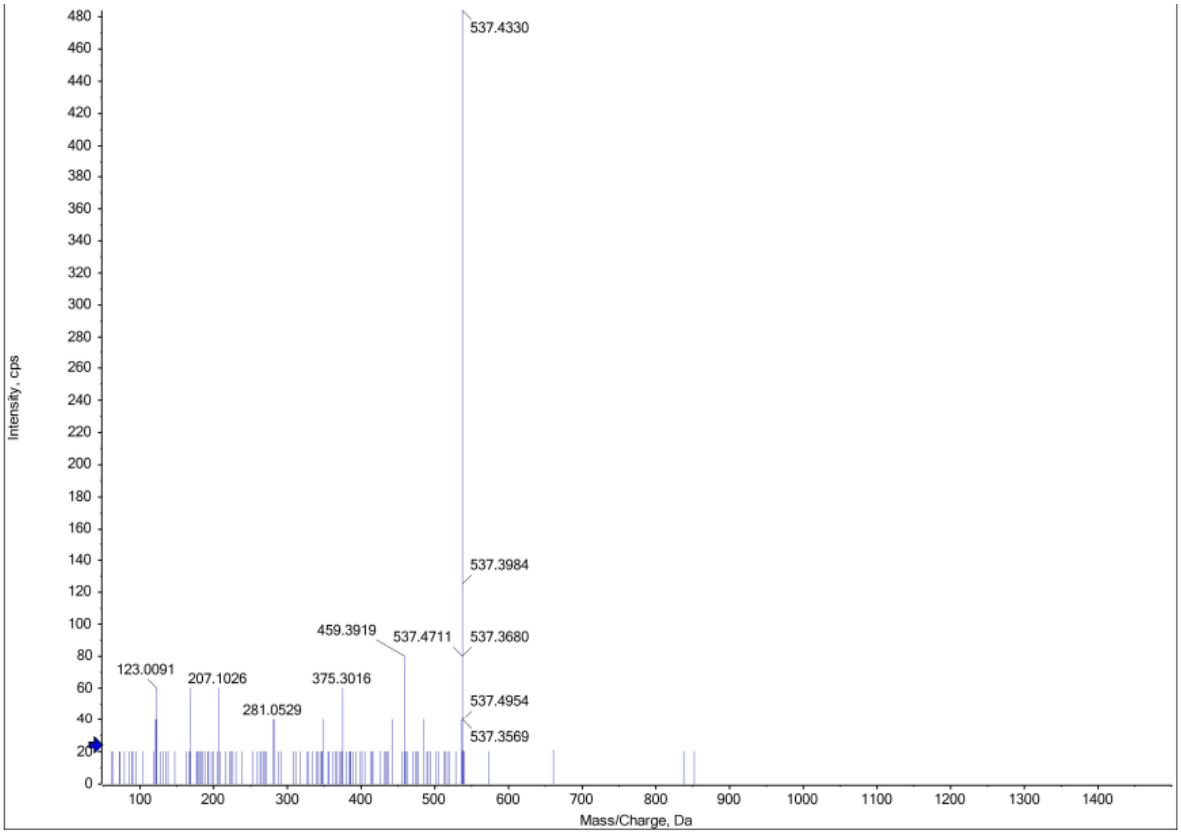

Figure 160. The HRMS spectrum of compound **153 n**

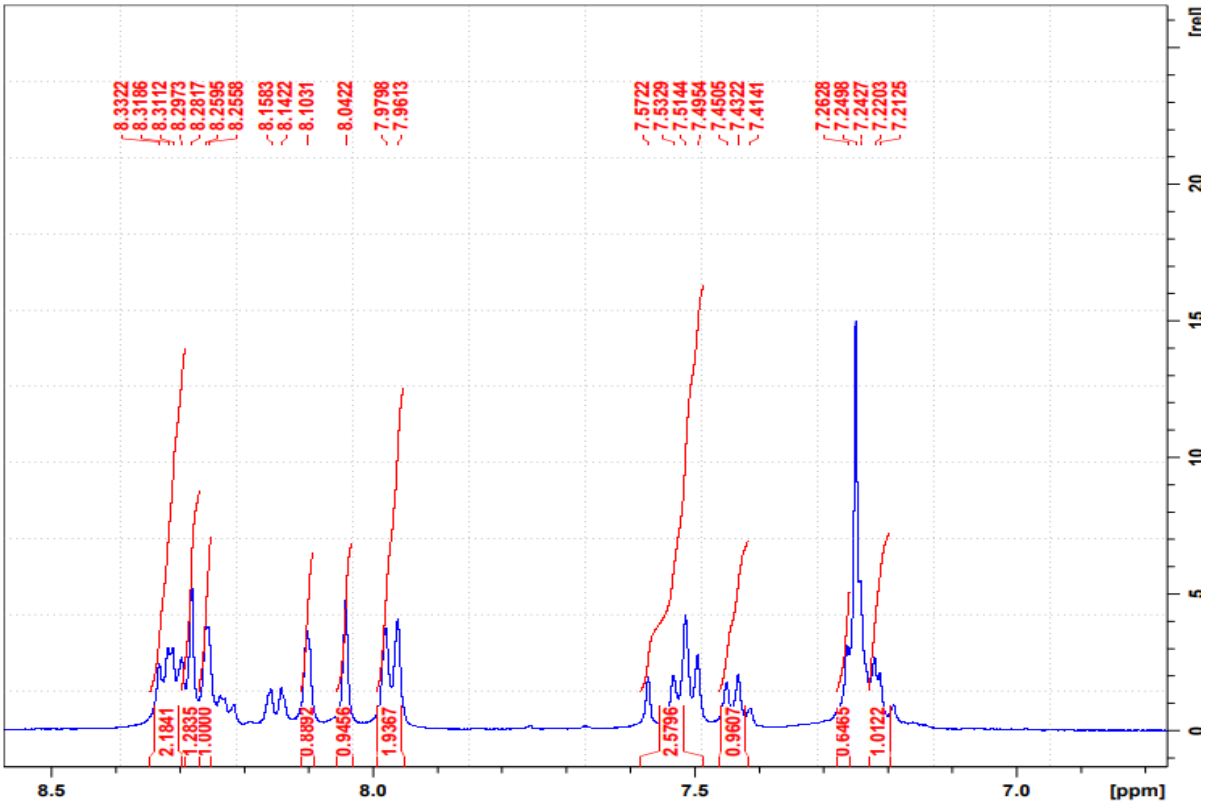

Figure 161. The ^{1}H NMR spectrum of compound **153 o**

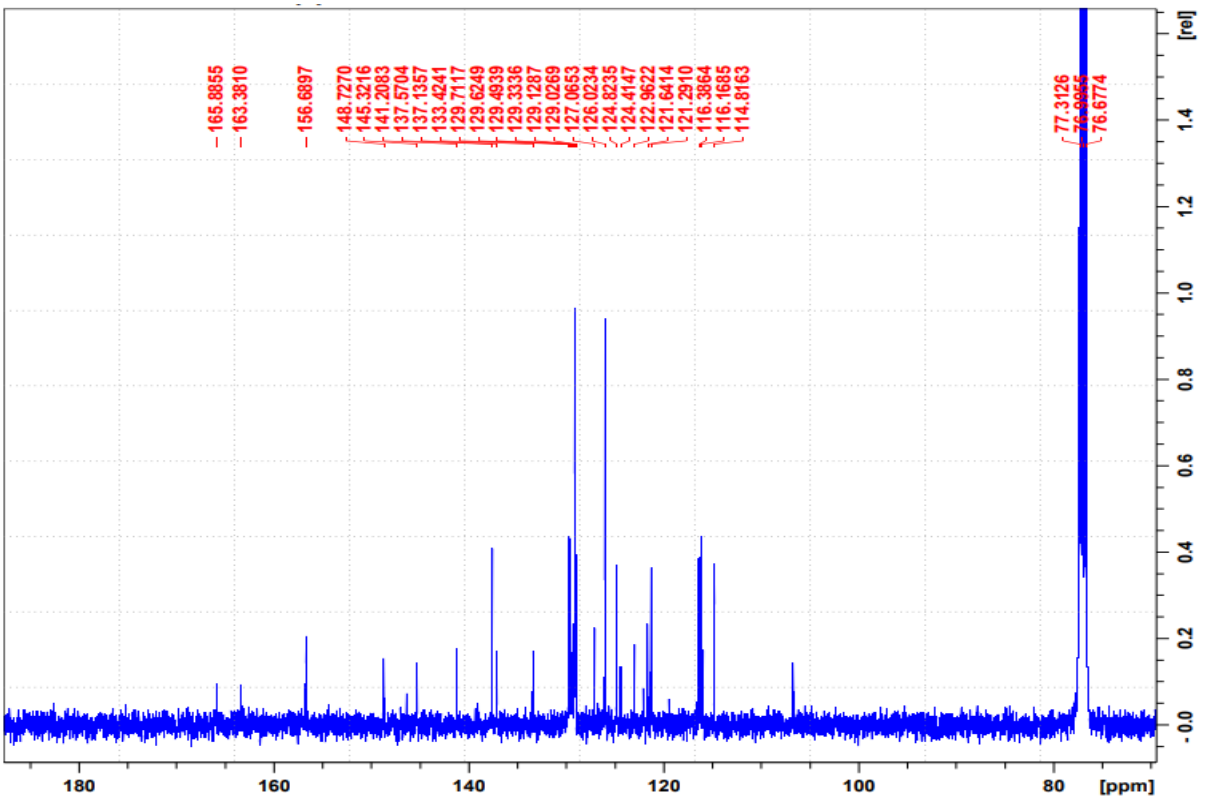

Figure 162. The ^{13}C NMR spectrum of compound **153 o**

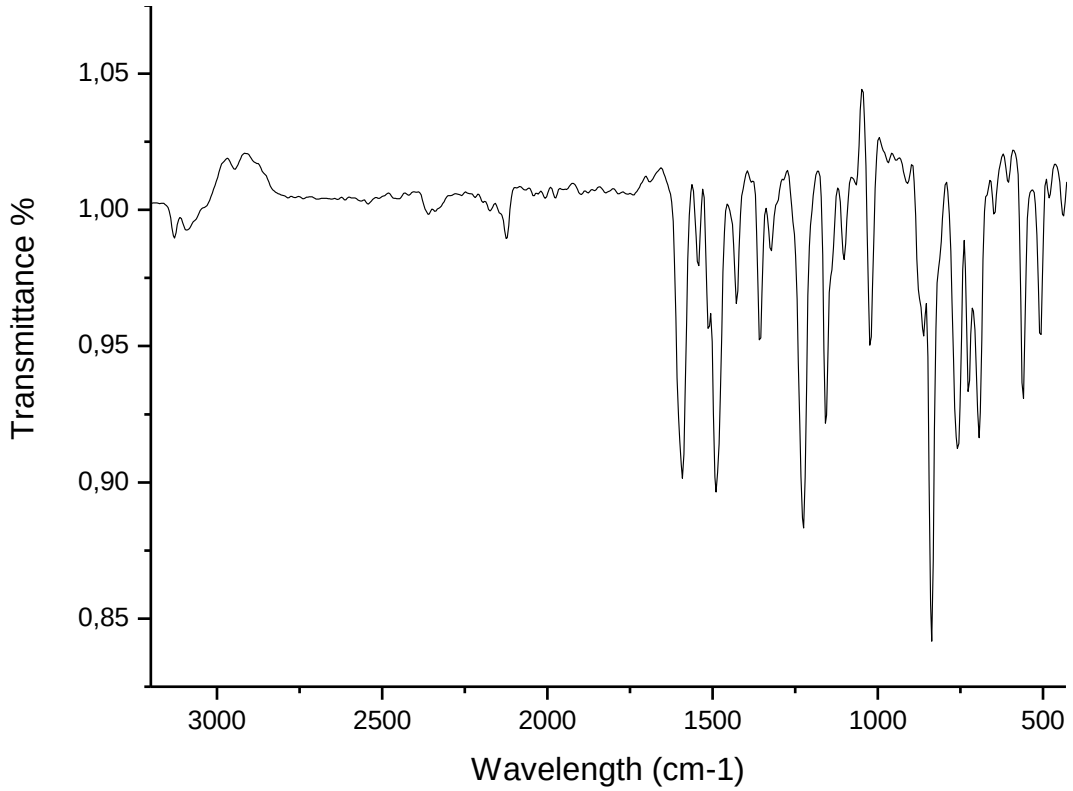

Figure 163. The FTIR spectrum of compound **153 o**

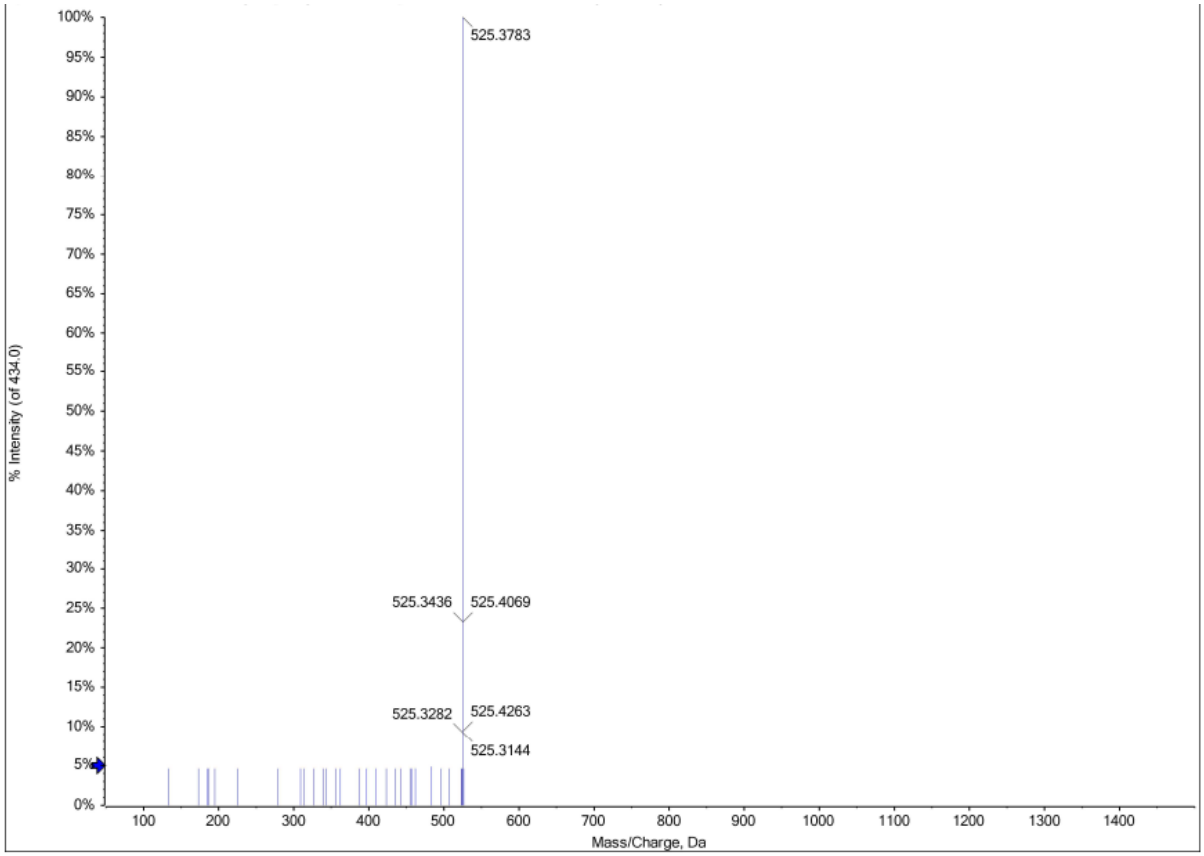

Figure 164. The HRMS spectrum of compound **153 o**

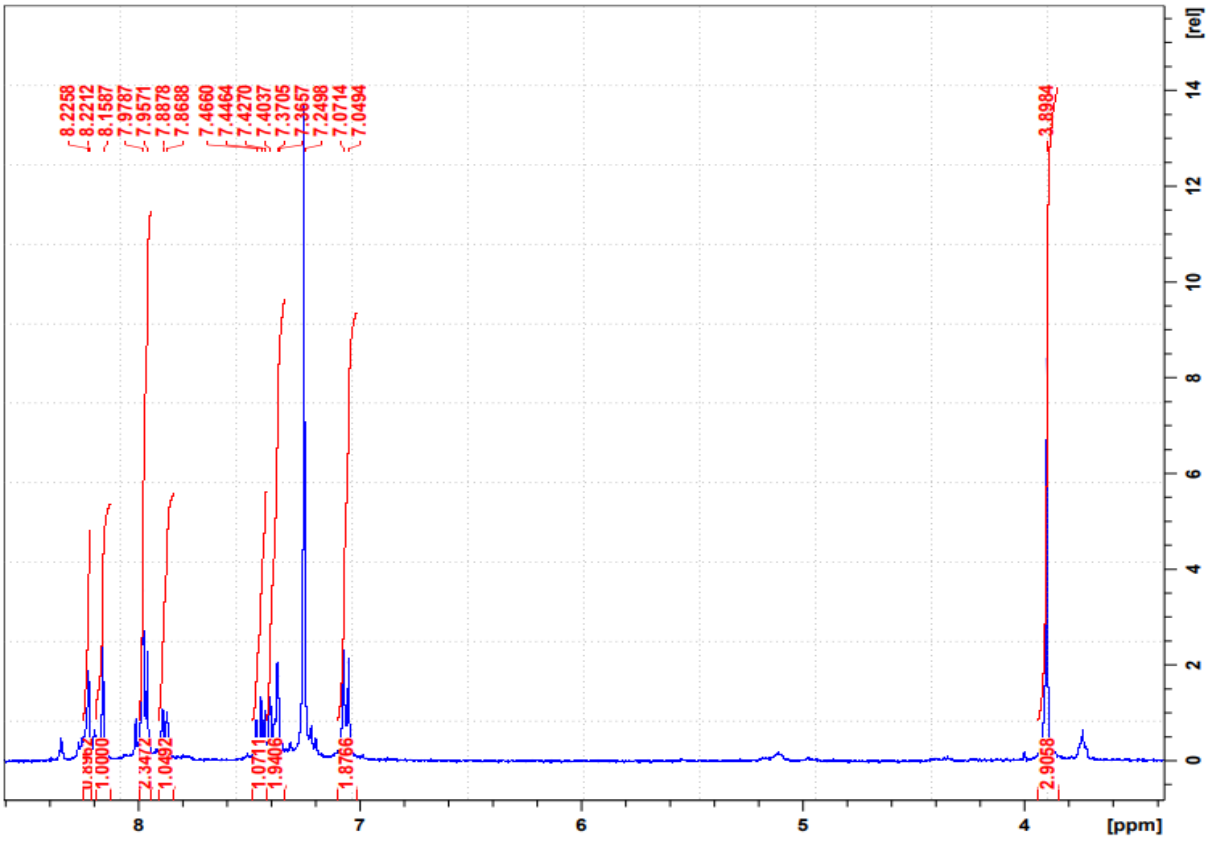

Figure 165. The ^{1}H NMR spectrum of compound **153 p**

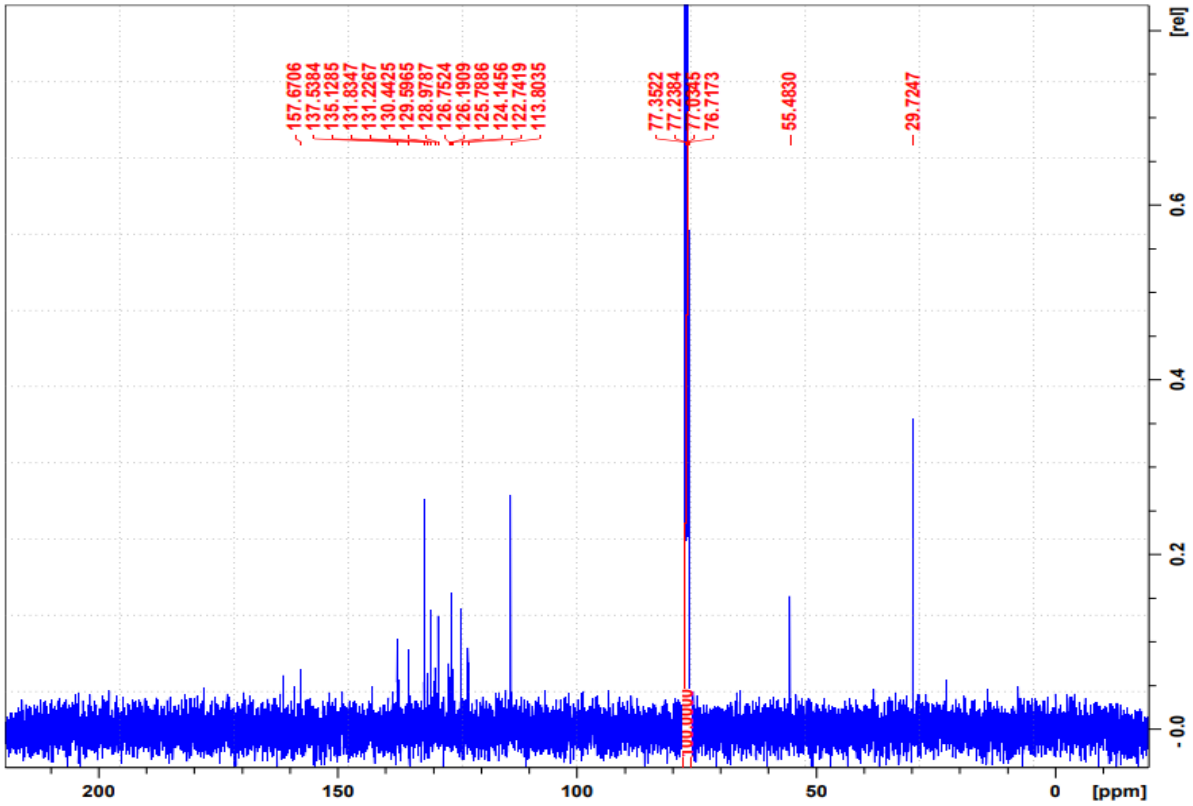

Figure 166. The ^{13}C NMR spectrum of compound **153 p**

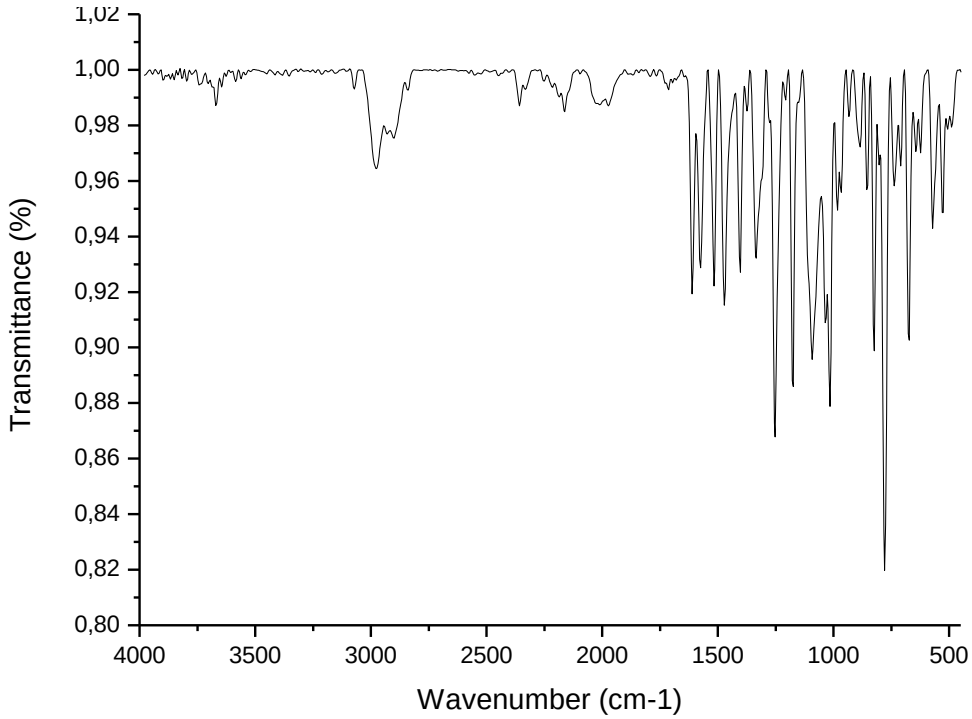

Figure 167. The FTIR spectrum of compound **153 p**

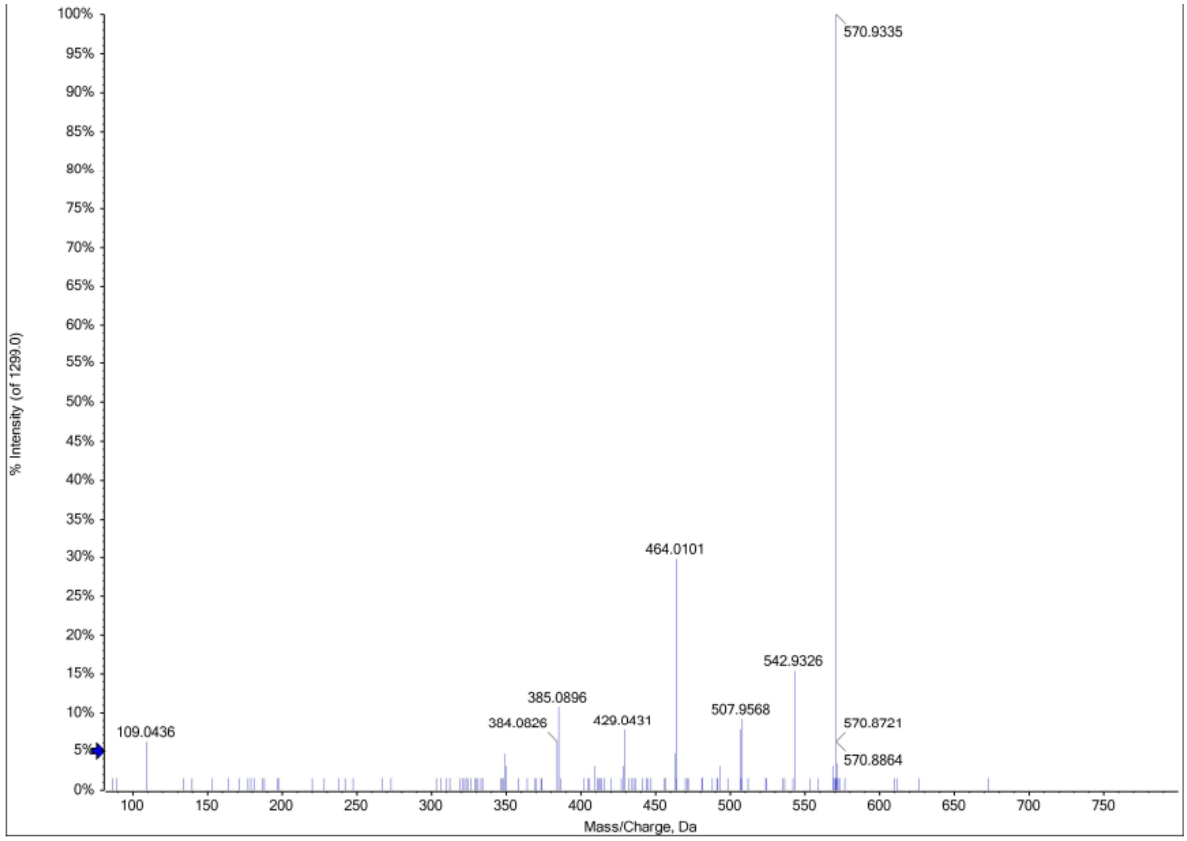

Figure 168. The HRMS spectrum of compound **153 p**

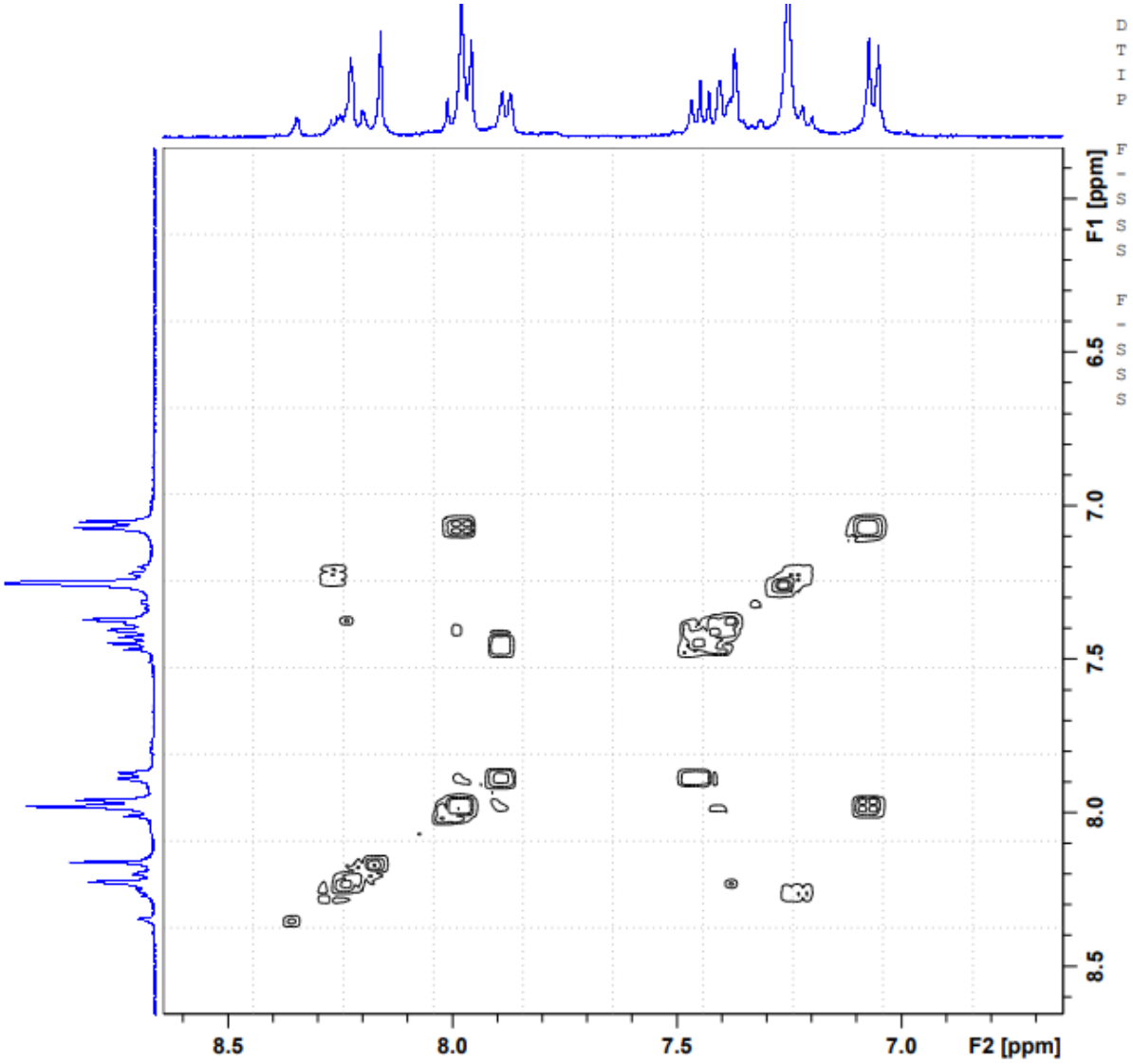

Figure 169. The COSY spectrum of compound **153 p**

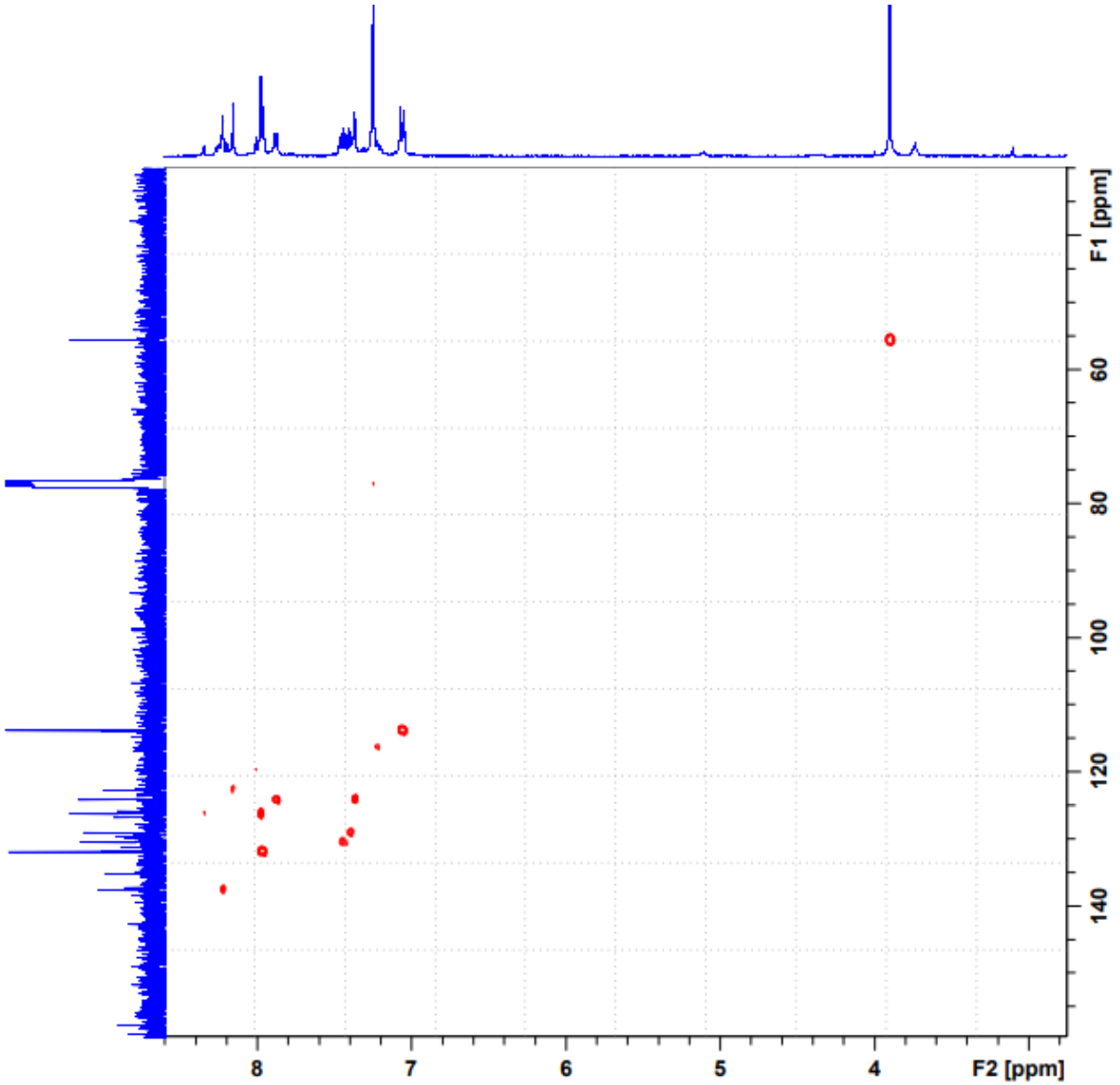

Figure 170. The HSQC spectrum of compound **153 p**

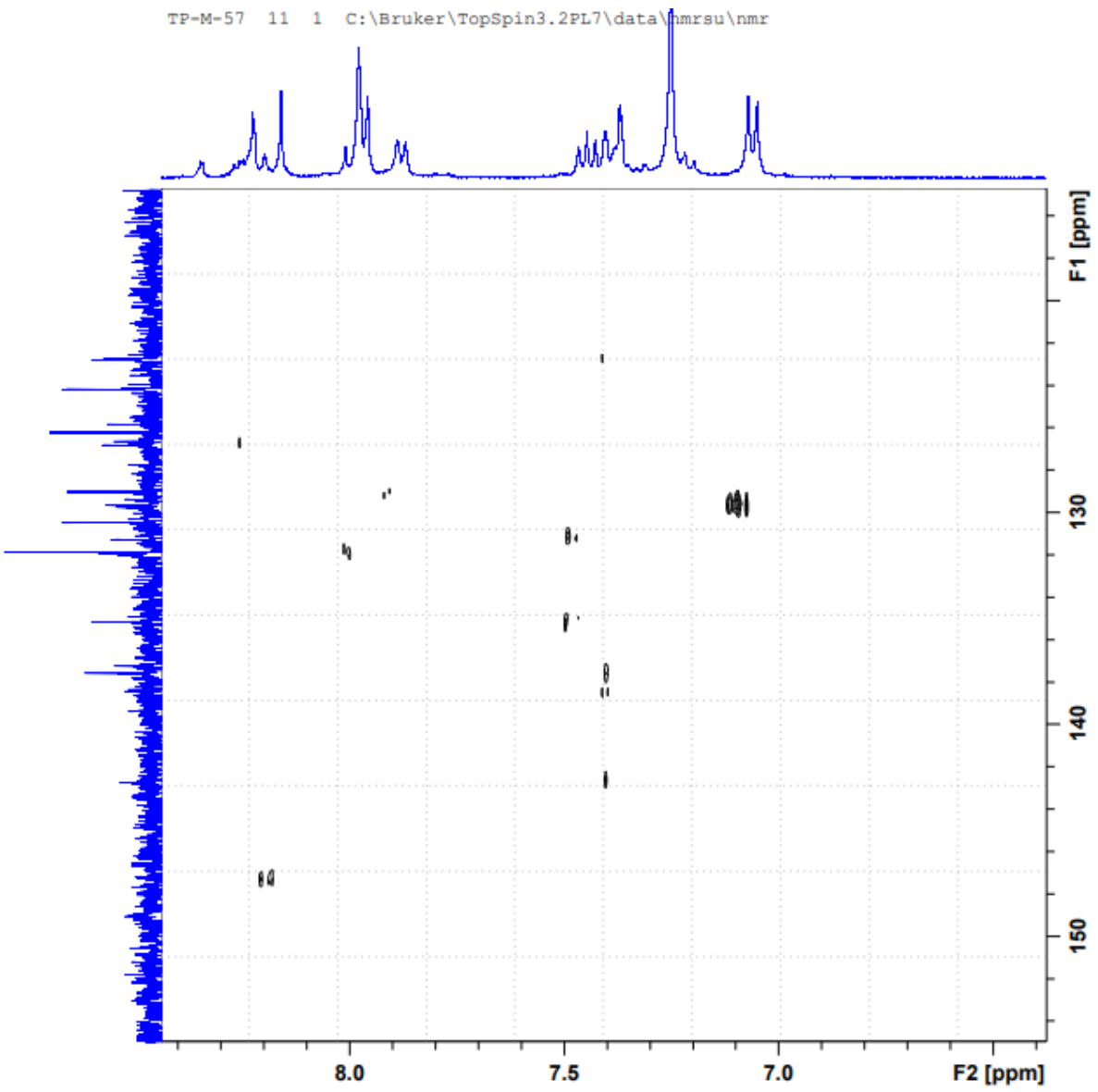

Figure 171. The HMBC spectrum of compound **153 p**

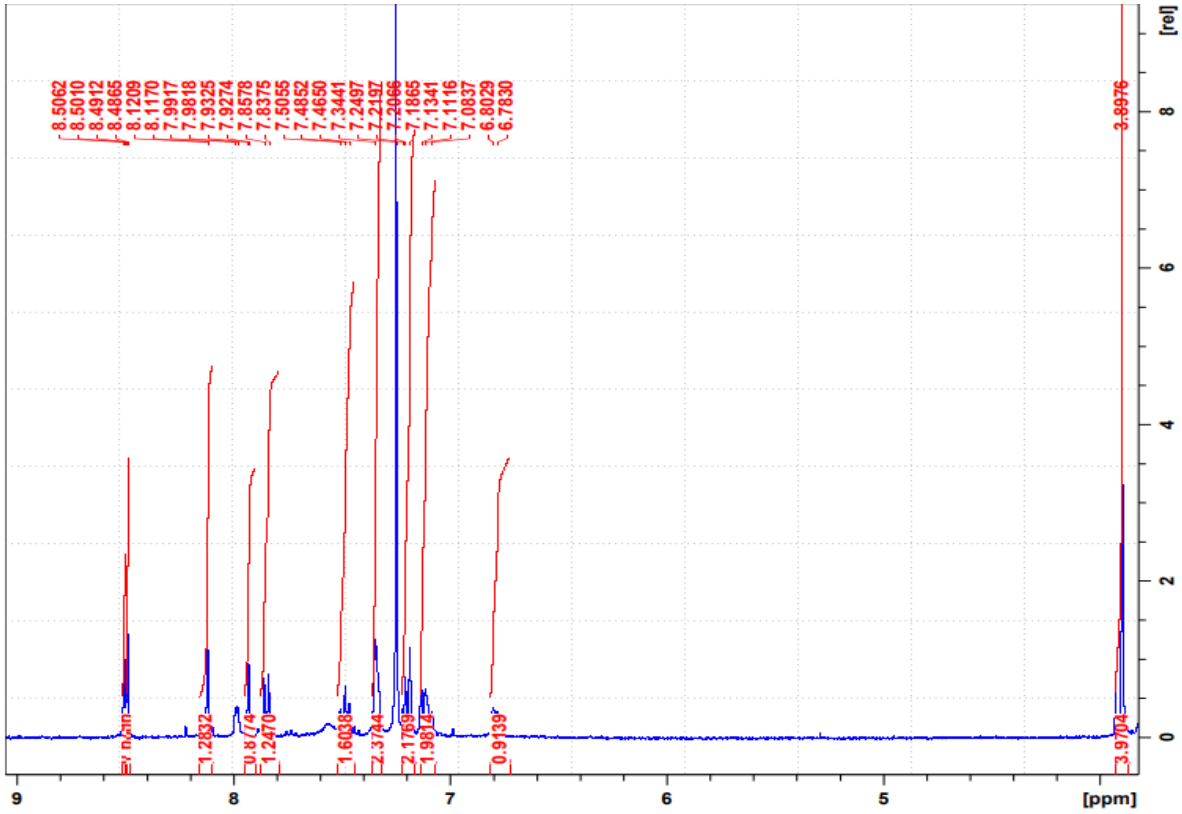

Figure 172. The ^{1}H NMR spectrum of compound **153 q**

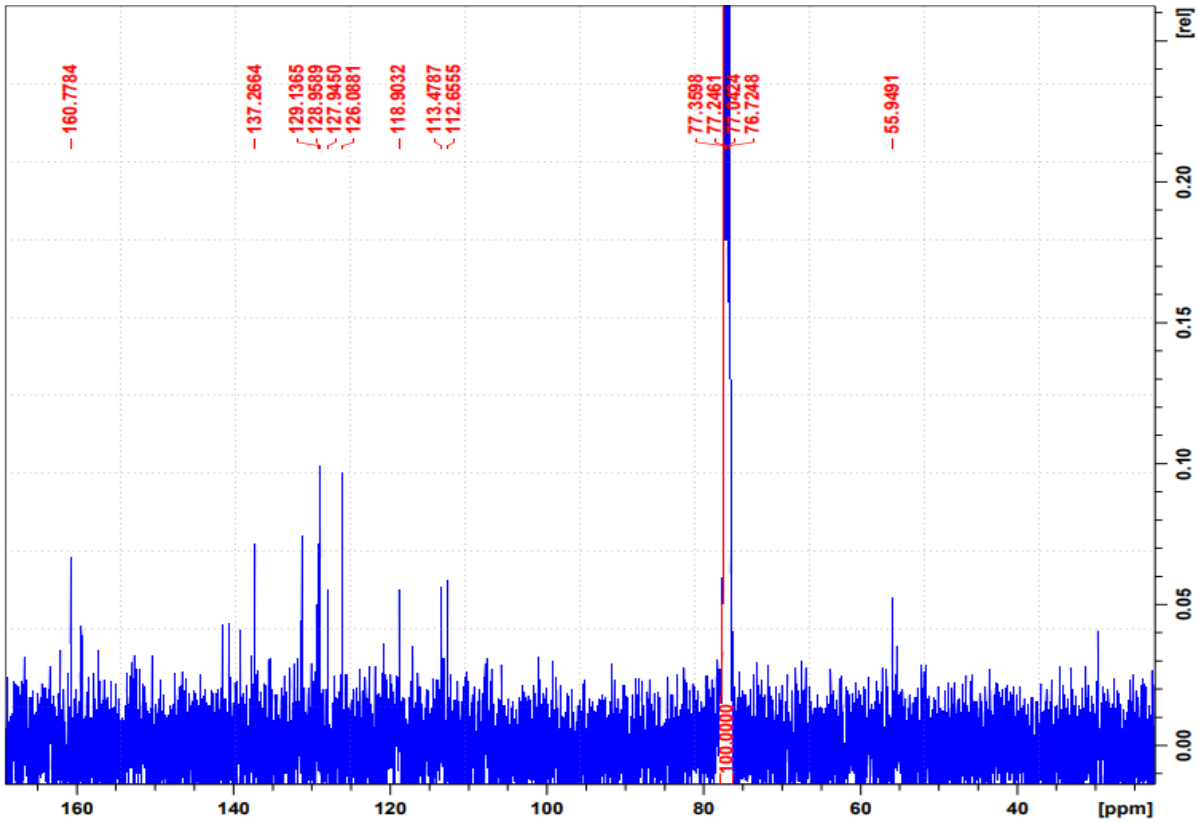

Figure 173. The ^{13}C NMR spectrum of compound **153 q**

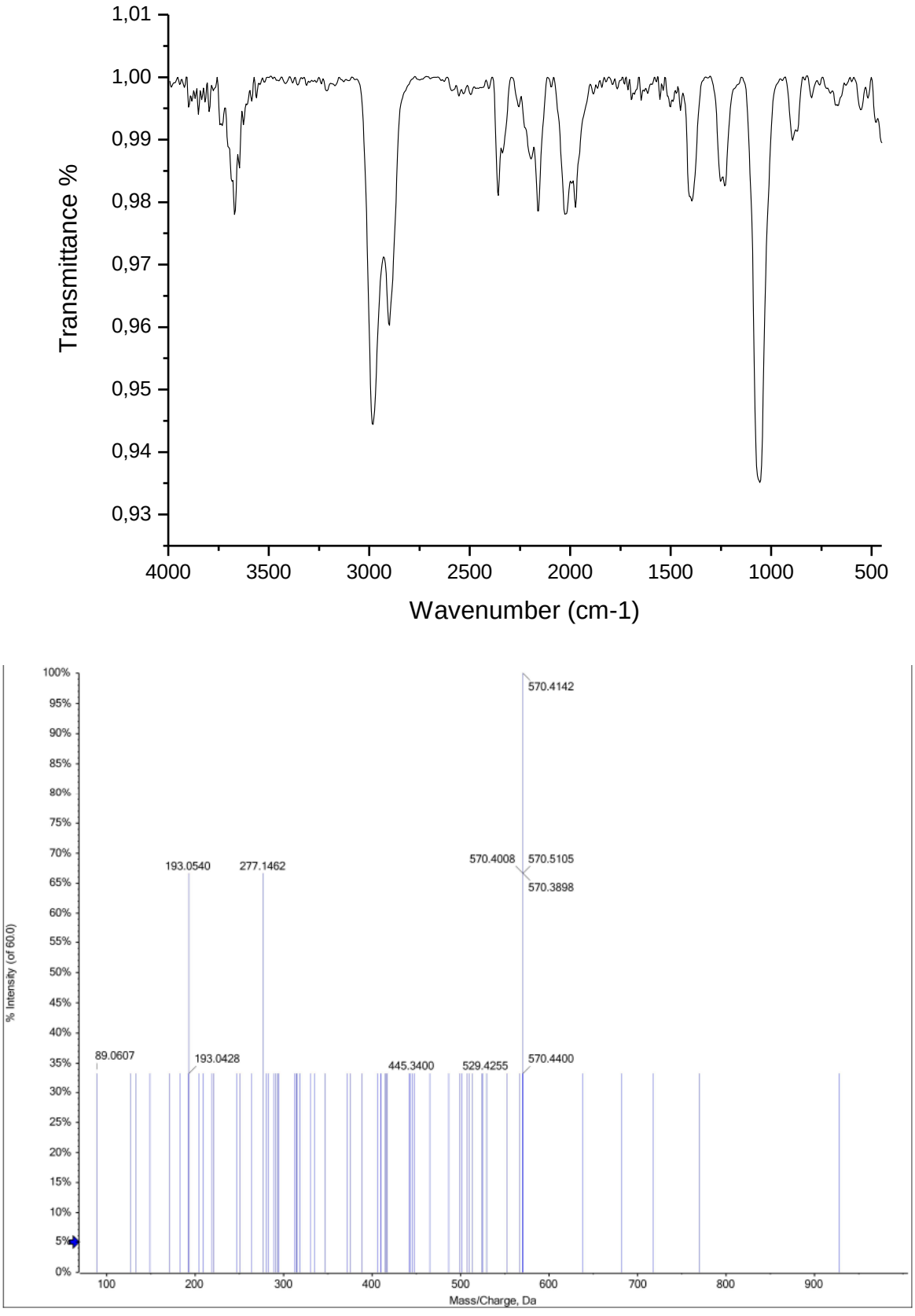

Figure 174. The FTIR spectrum of compound **153 q**

Figure 175. The HRMS spectrum of compound **153 q**

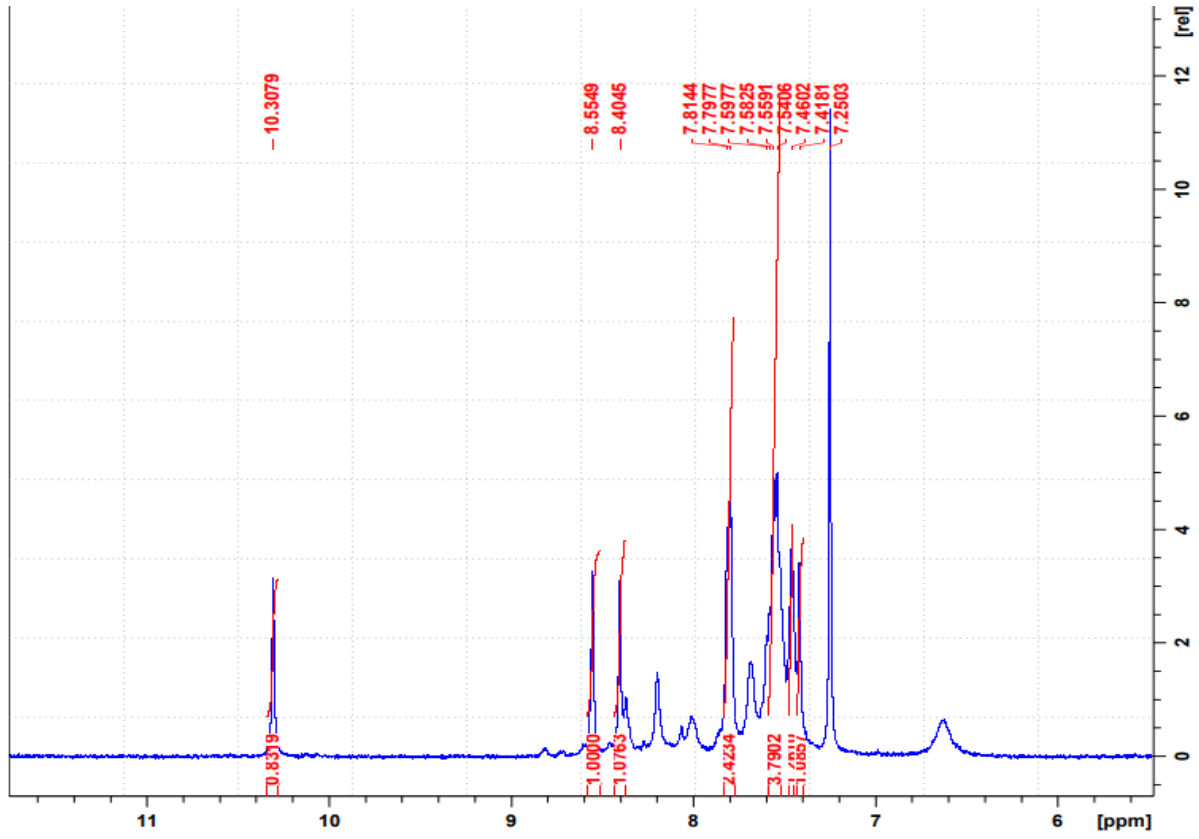

Figure 176. The 1H NMR spectrum of compound **154 a**

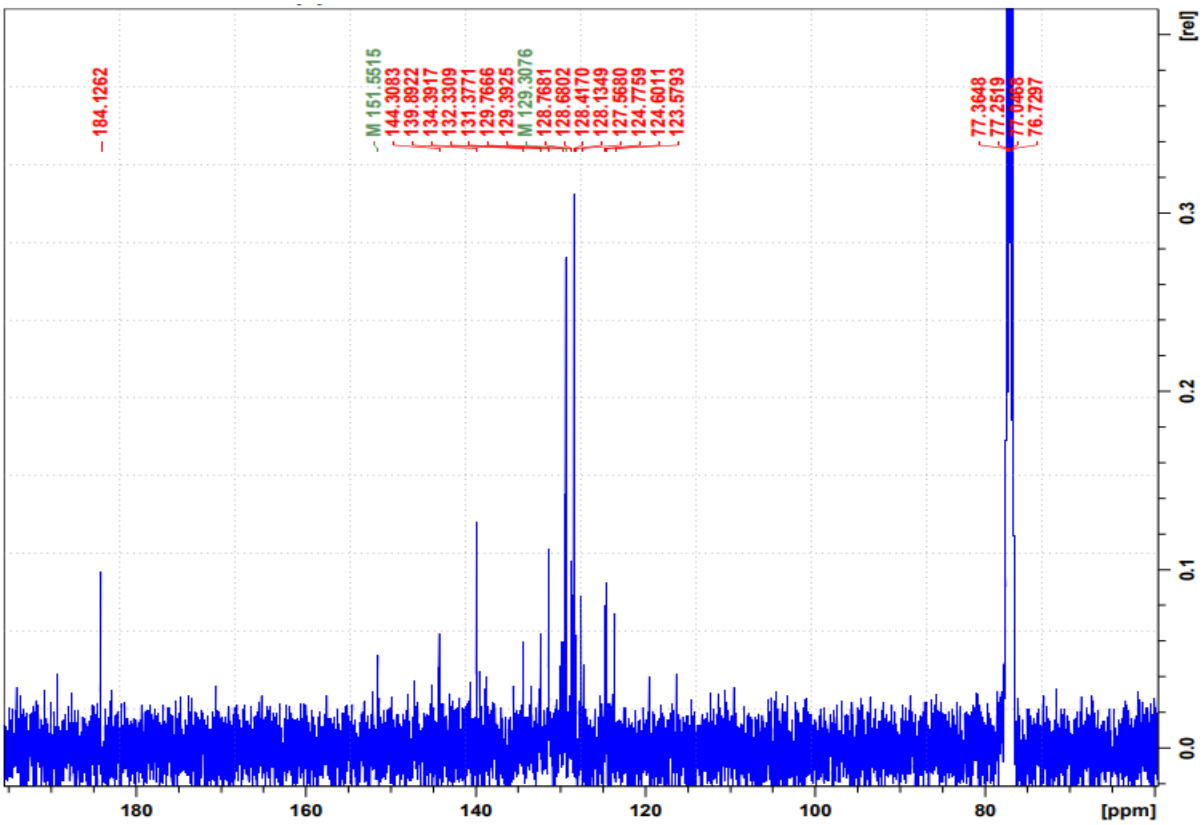

Figure 177. The ^{13}C NMR spectrum of compound **154 a**

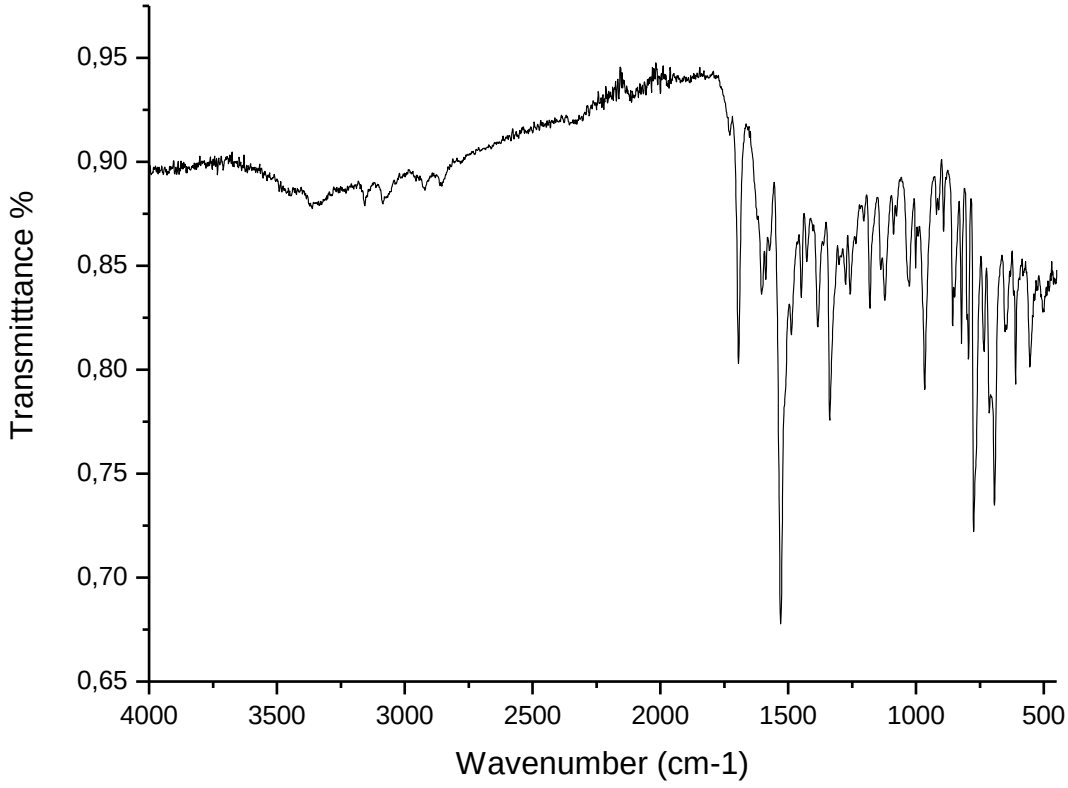

Figure 178. The FTIR spectrum of compound **154 a**

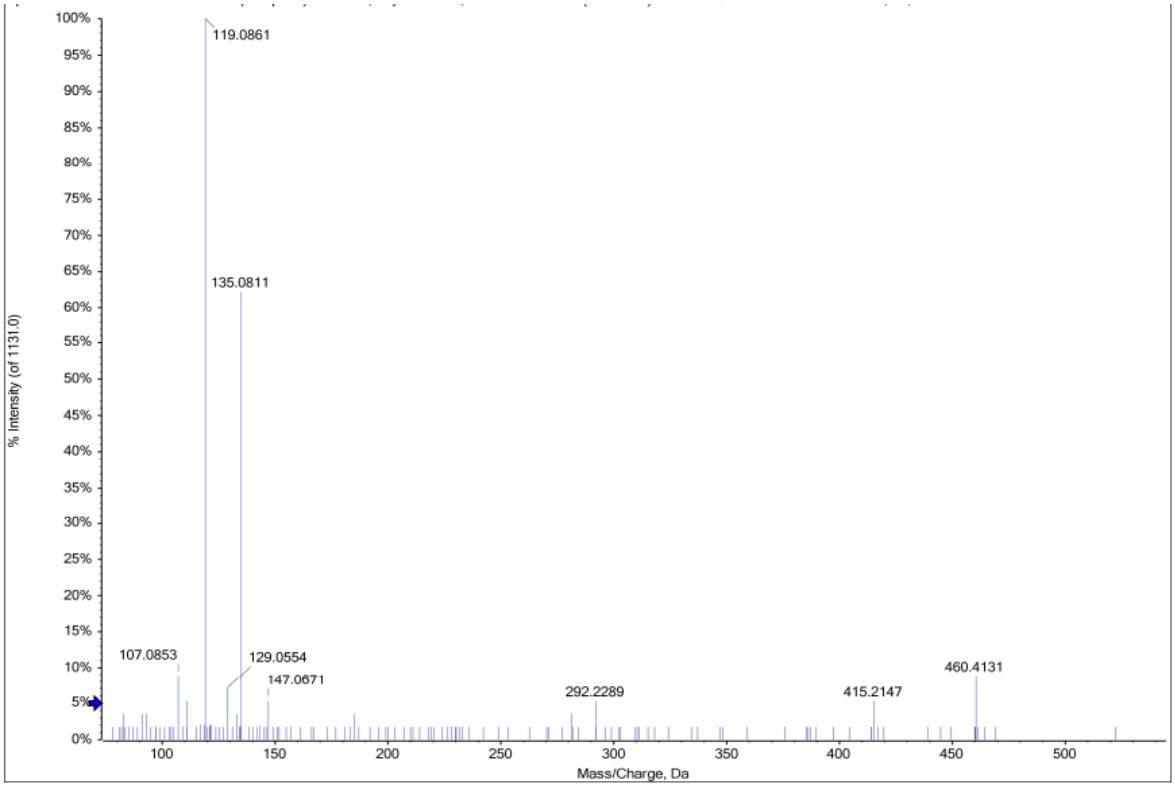

Figure 179. The HRMS spectrum of compound **154 a**

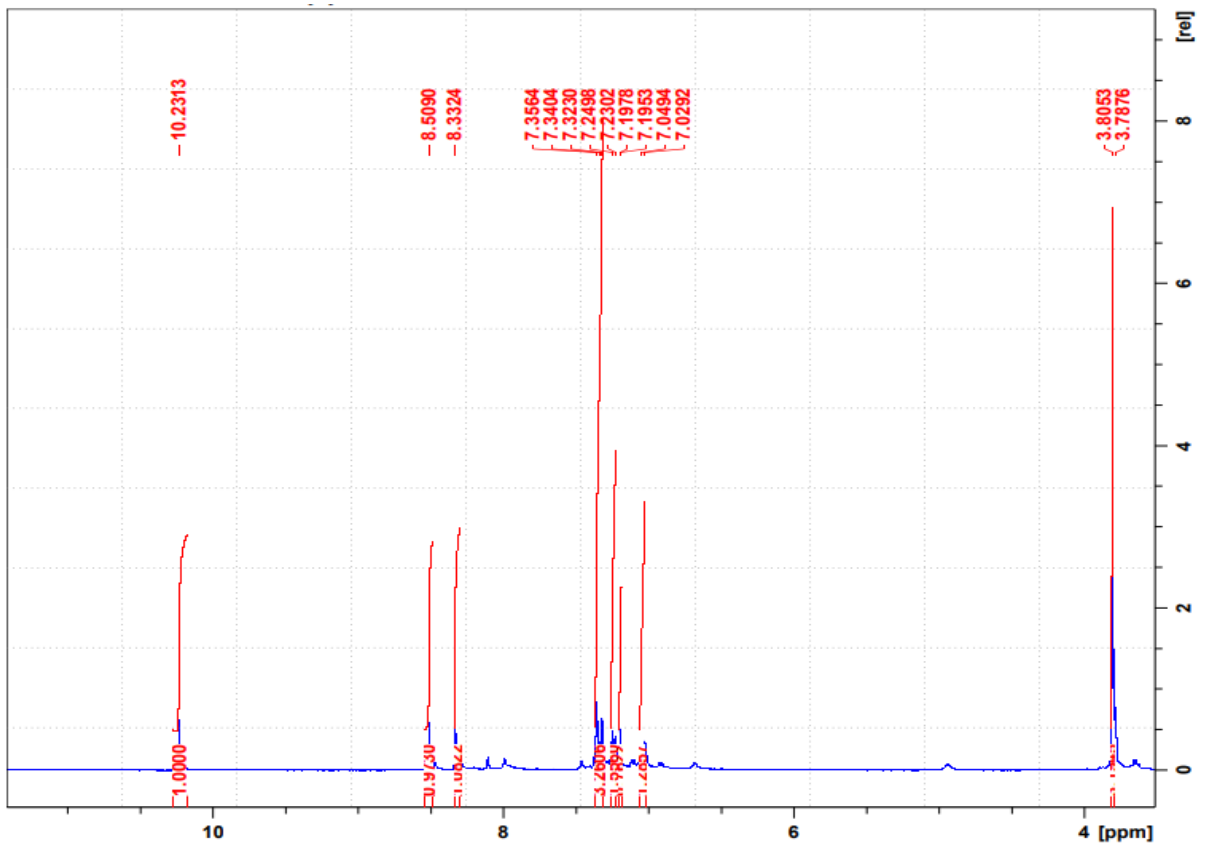

Figure 180. The ^{1}H NMR spectrum of compound **154 b**

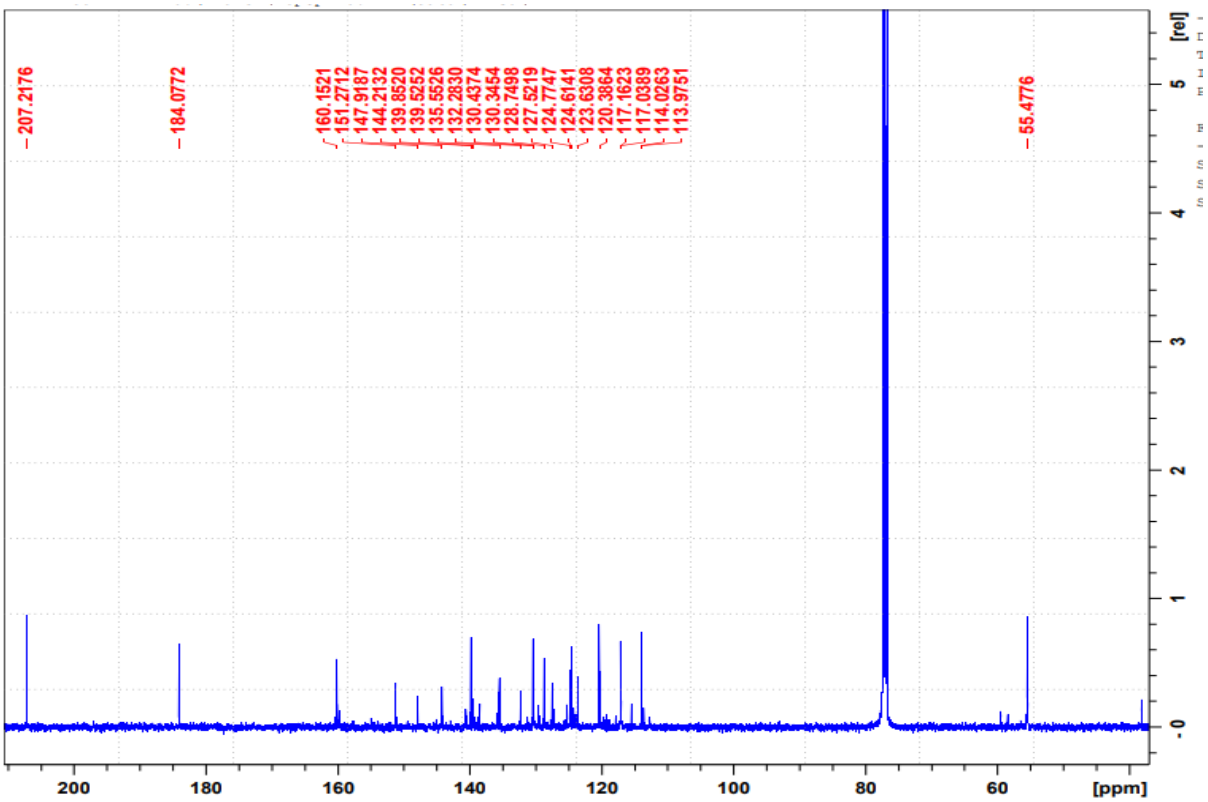

Figure 181. The ^{13}C NMR spectrum of compound **154 b**

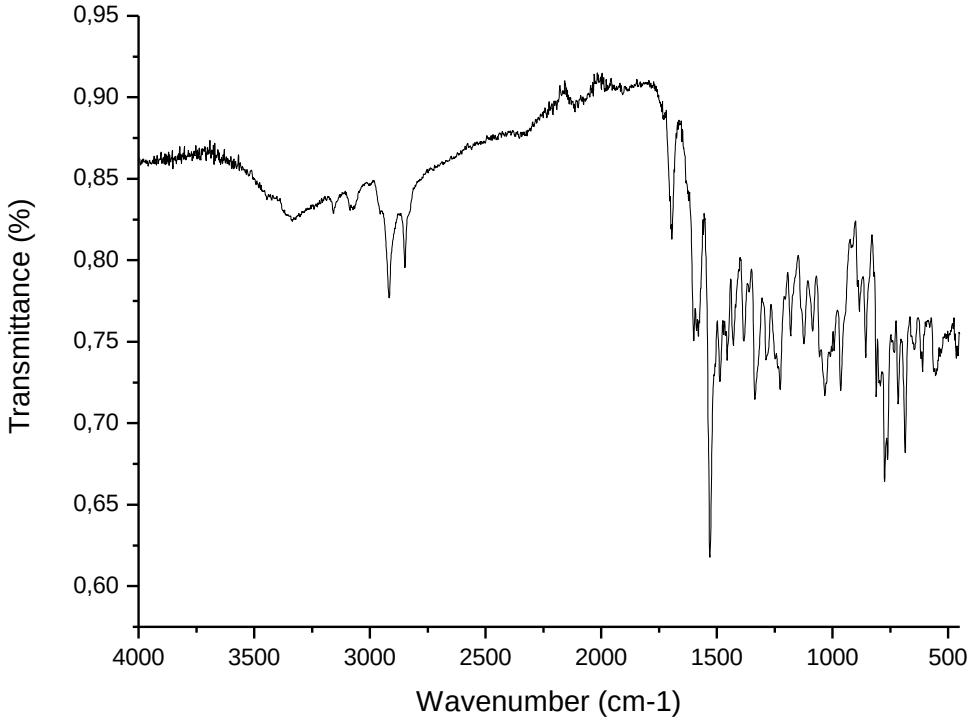

Figure 182. The FTIR spectrum of compound **154 b**

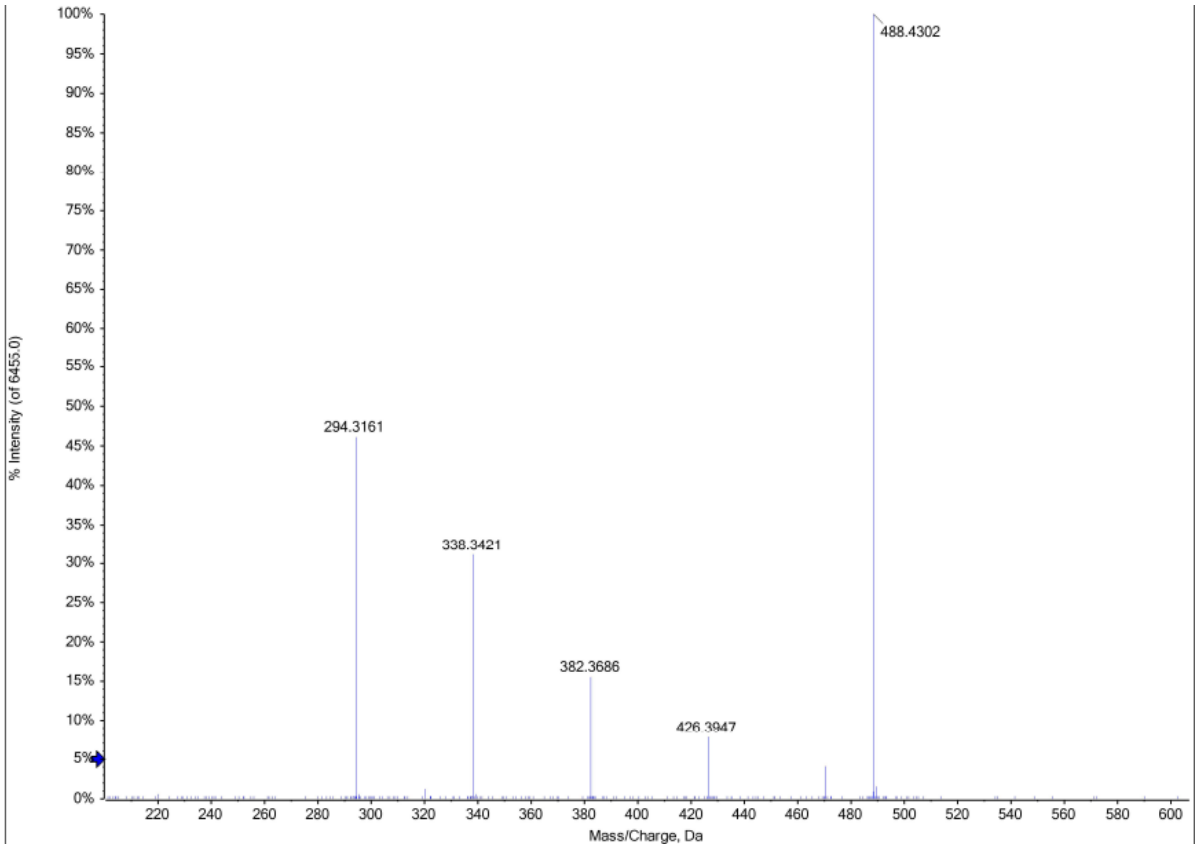

Figure 183. The HRMS spectrum of compound **154 b**

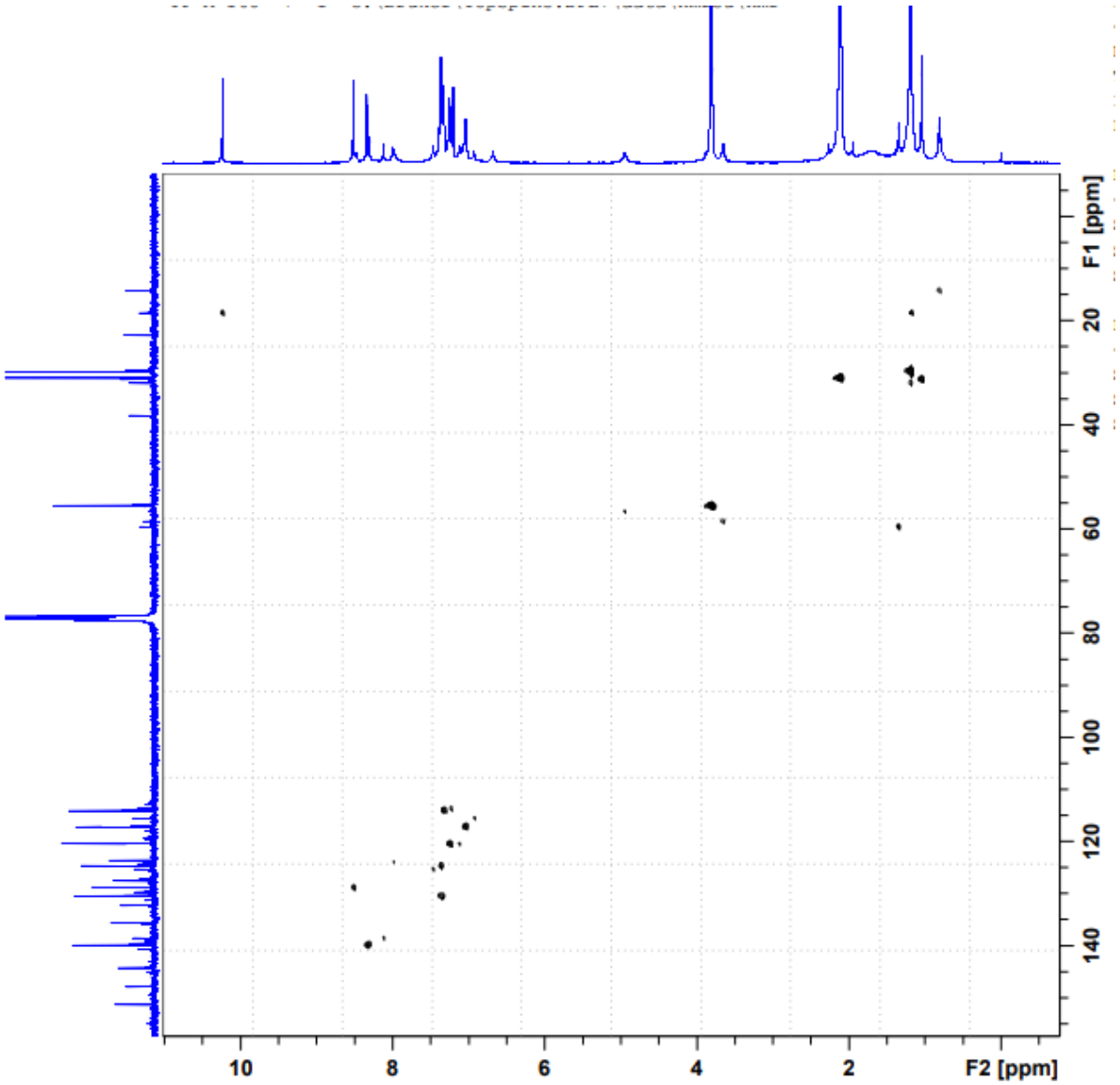

Figure 184. The HSQC spectrum of compound **154 b**

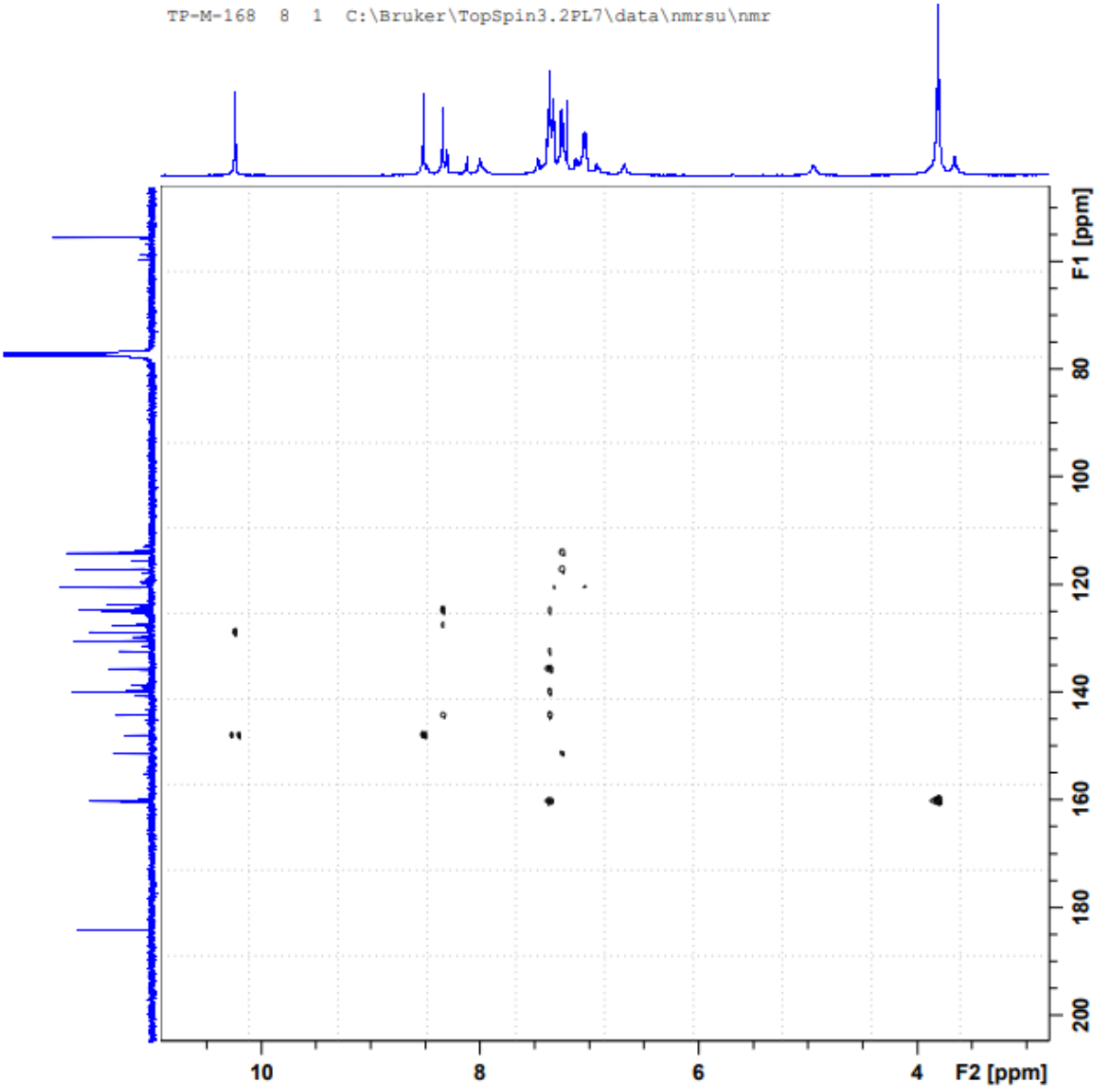

Figure 185. The HMBC spectrum of compound **154 b**

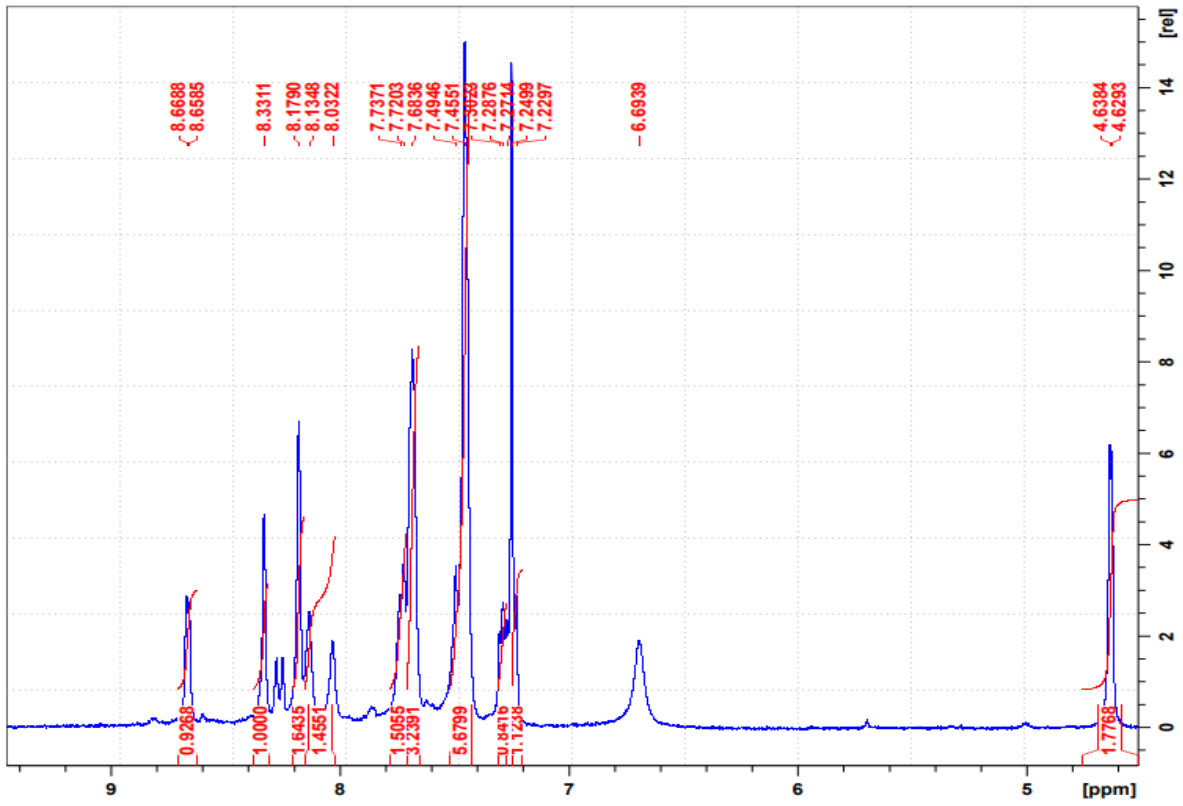

Figure 186. The ^{1}H NMR spectrum of compound **155 a**

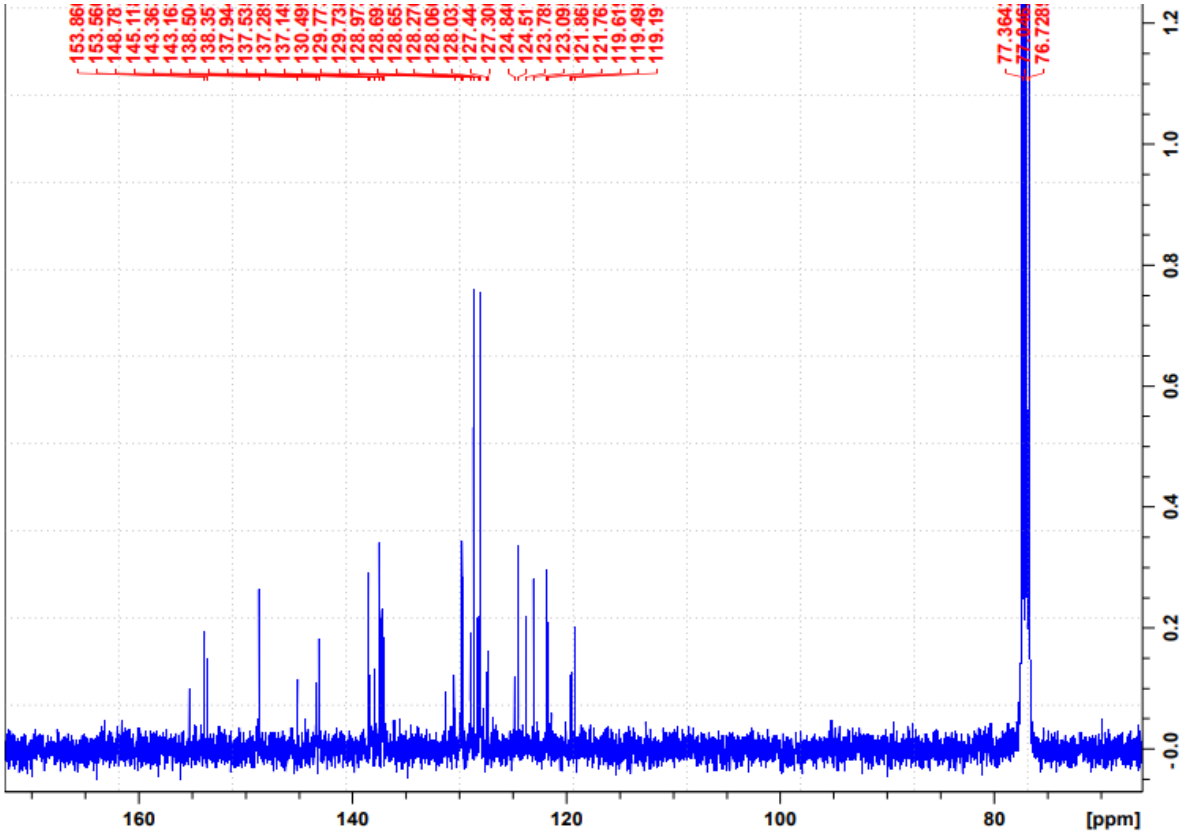

Figure 187. The ^{13}C NMR spectrum of compound **155 a**

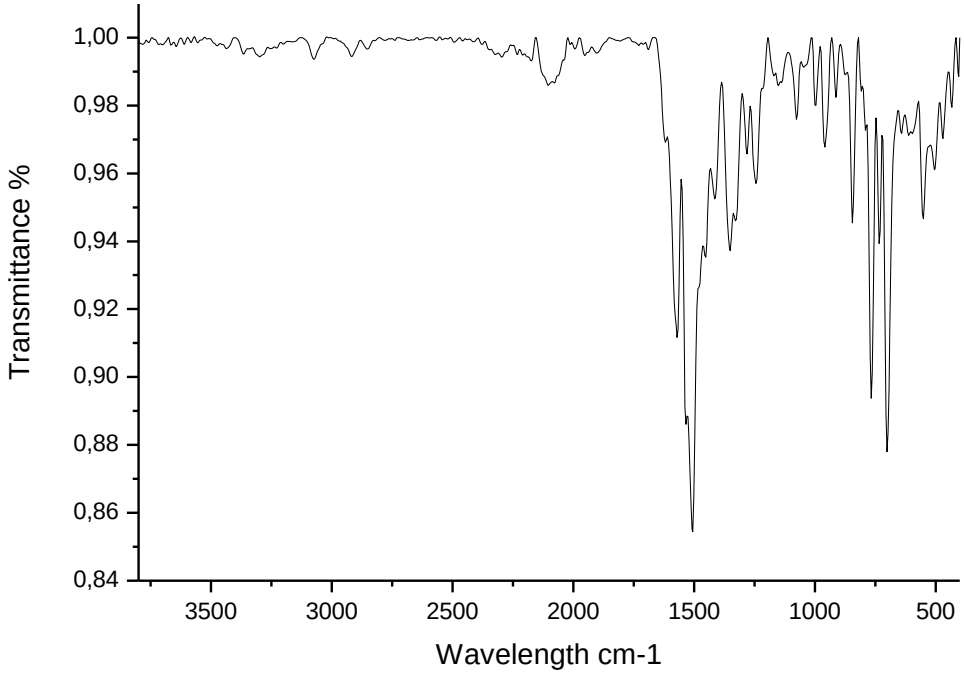

Figure 188. The FTIR spectrum of compound **155 a**

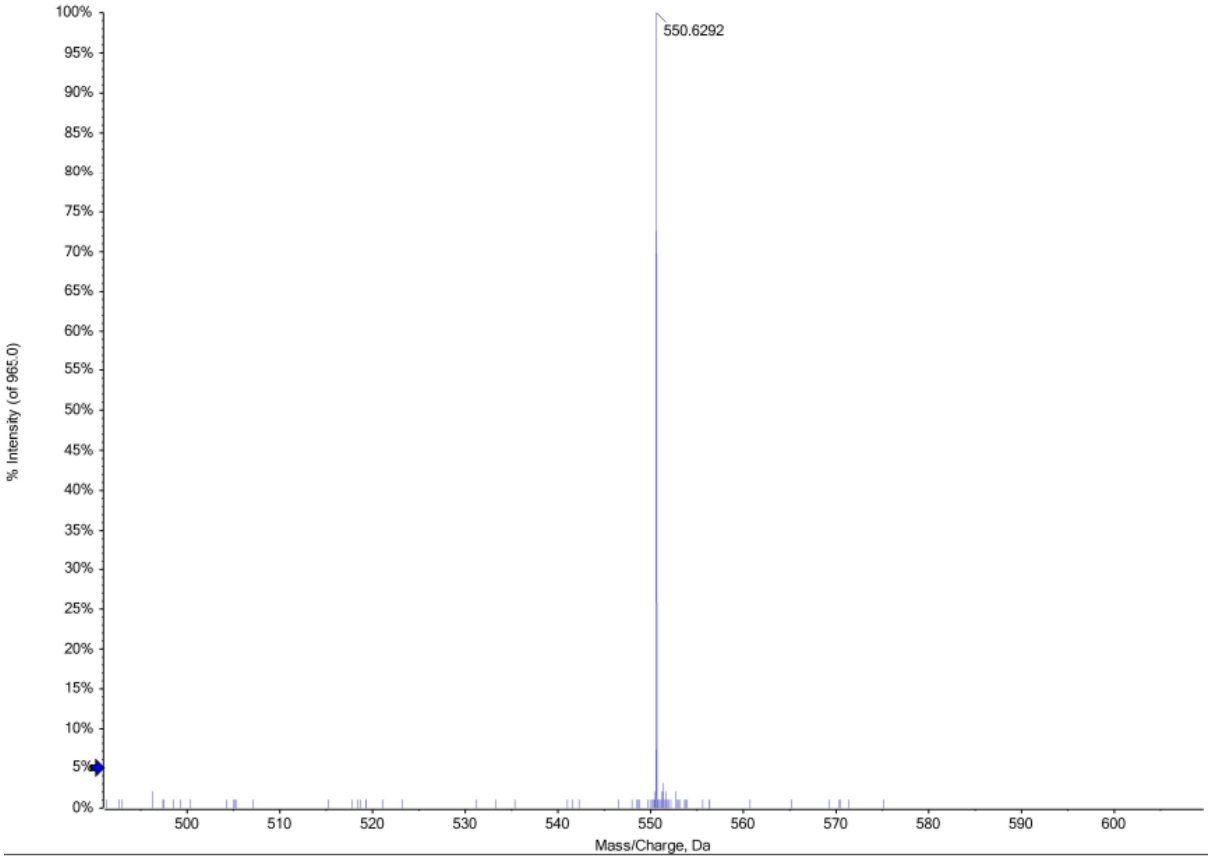

Figure 189. The HRMS spectrum of compound **155 a**

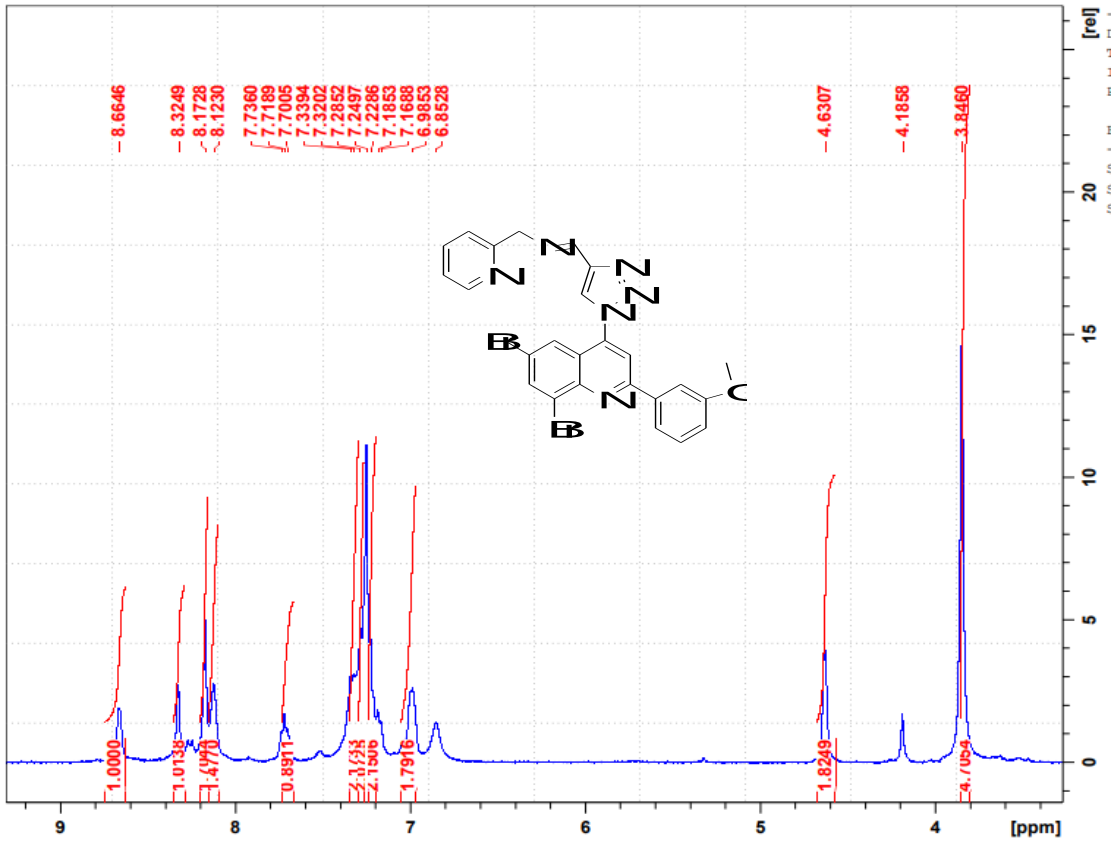

Figure 190. The ^{1}H NMR spectrum of compound **155 b**

Figure 191. The ^{13}C NMR spectrum of compound **155 b**

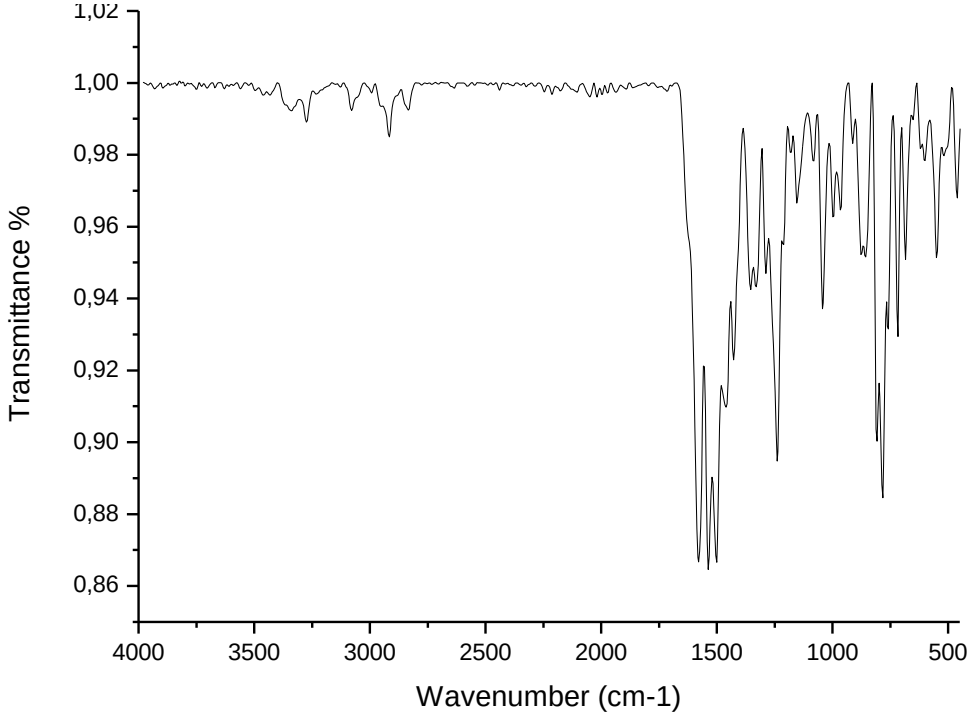

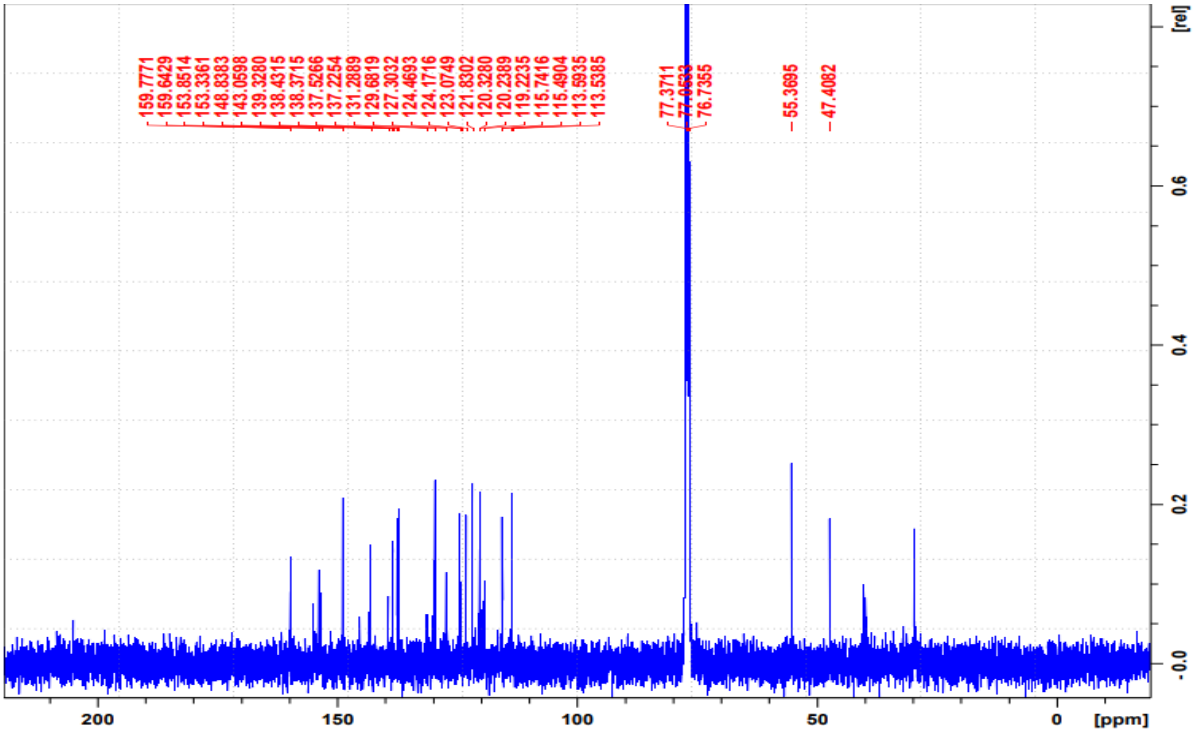

Figure 192. The FTIR spectrum of compound **155 b**

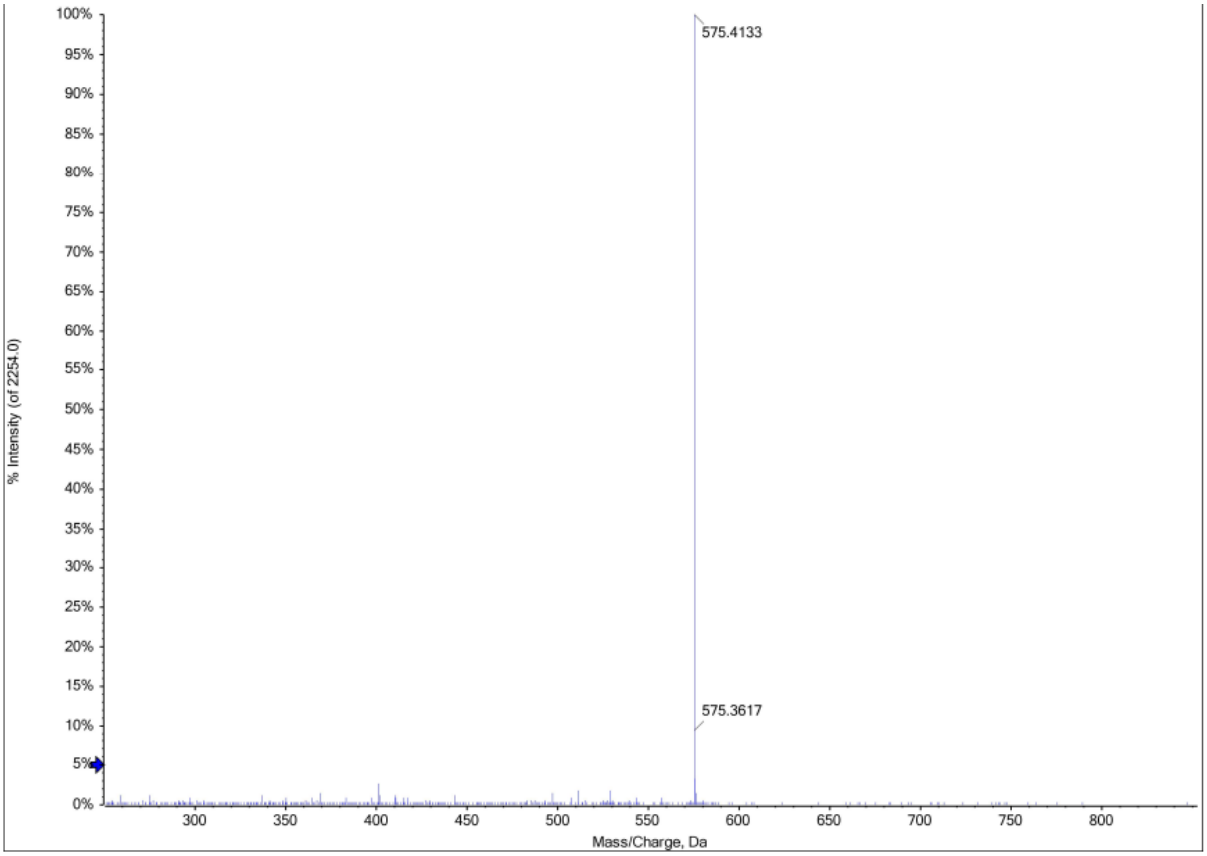

Figure 193. The HRMS spectrum of compound **155 b**

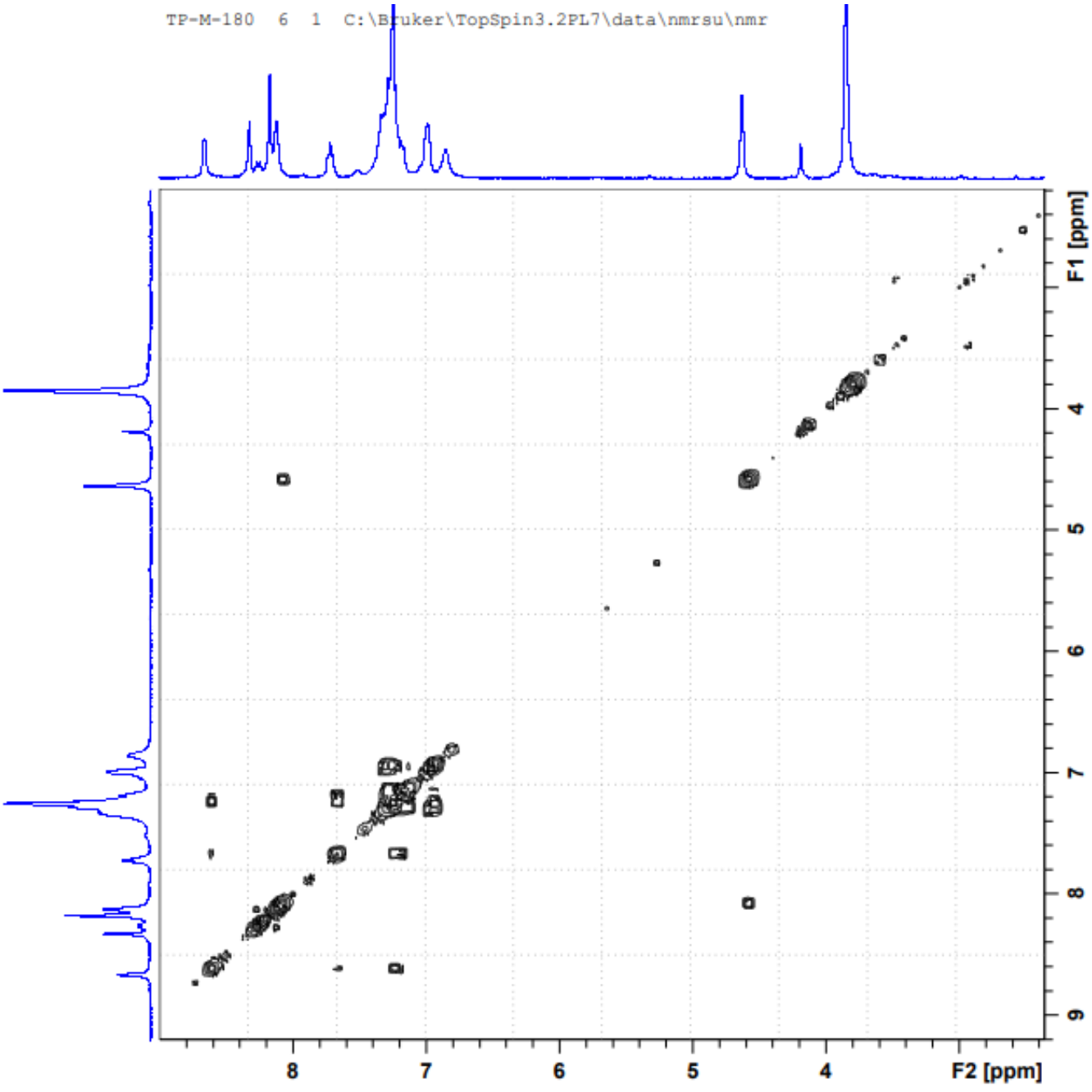

Figure 194. The COSY spectrum of compound **155 b**

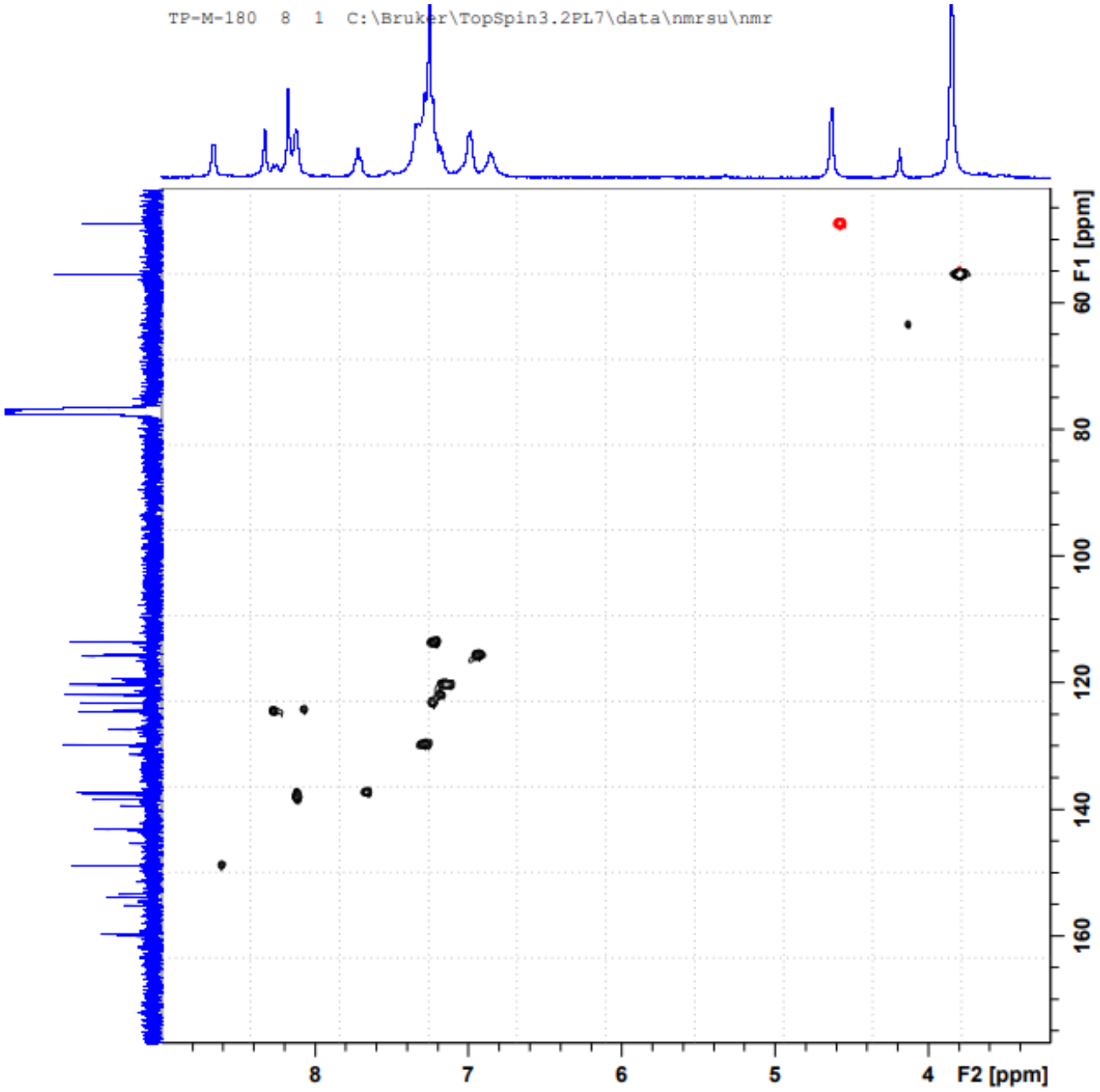

Figure 195. The HSQC spectrum of compound **155 b**

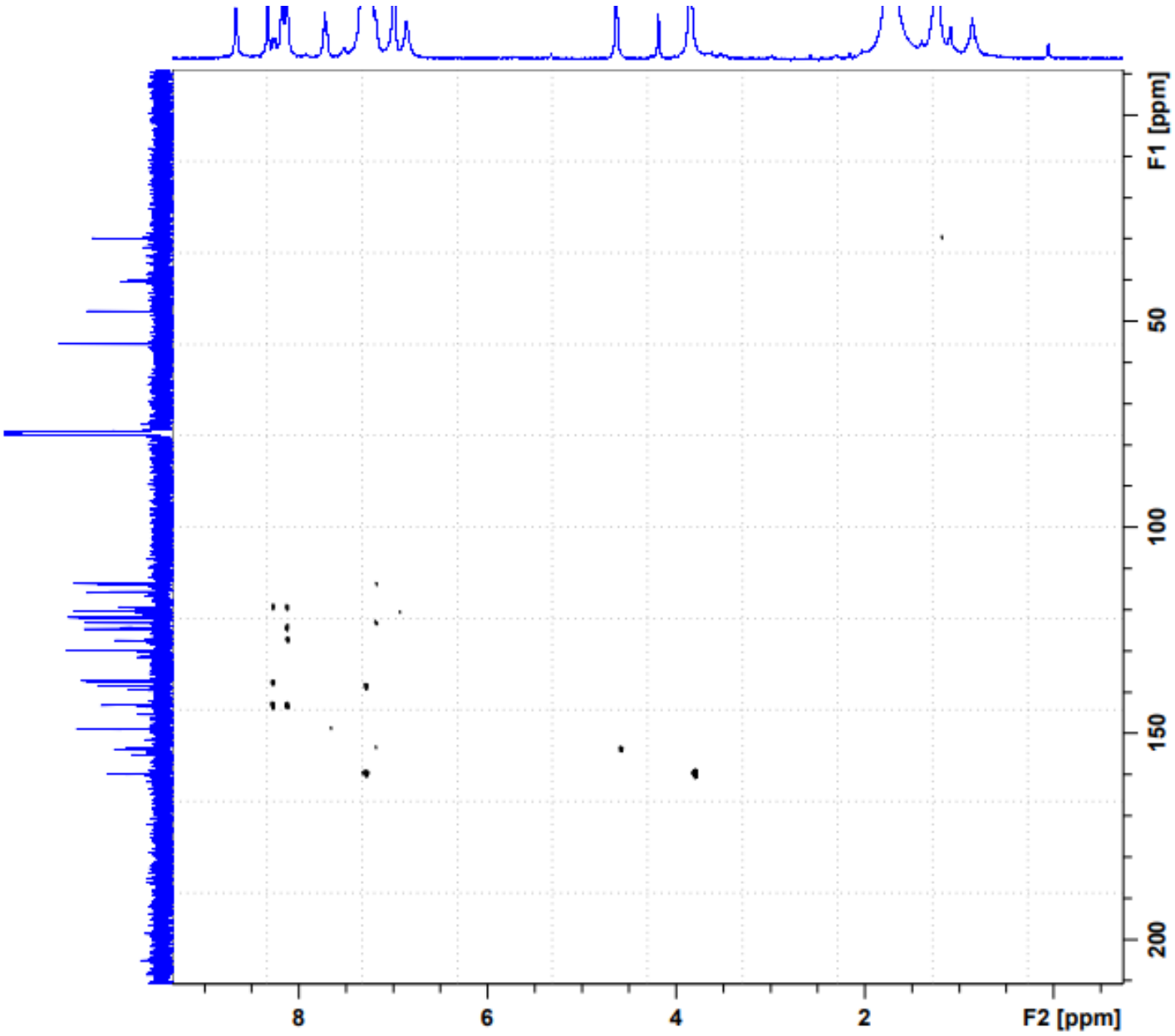

Figure 196. The HMBC spectrum of compound **155 b**

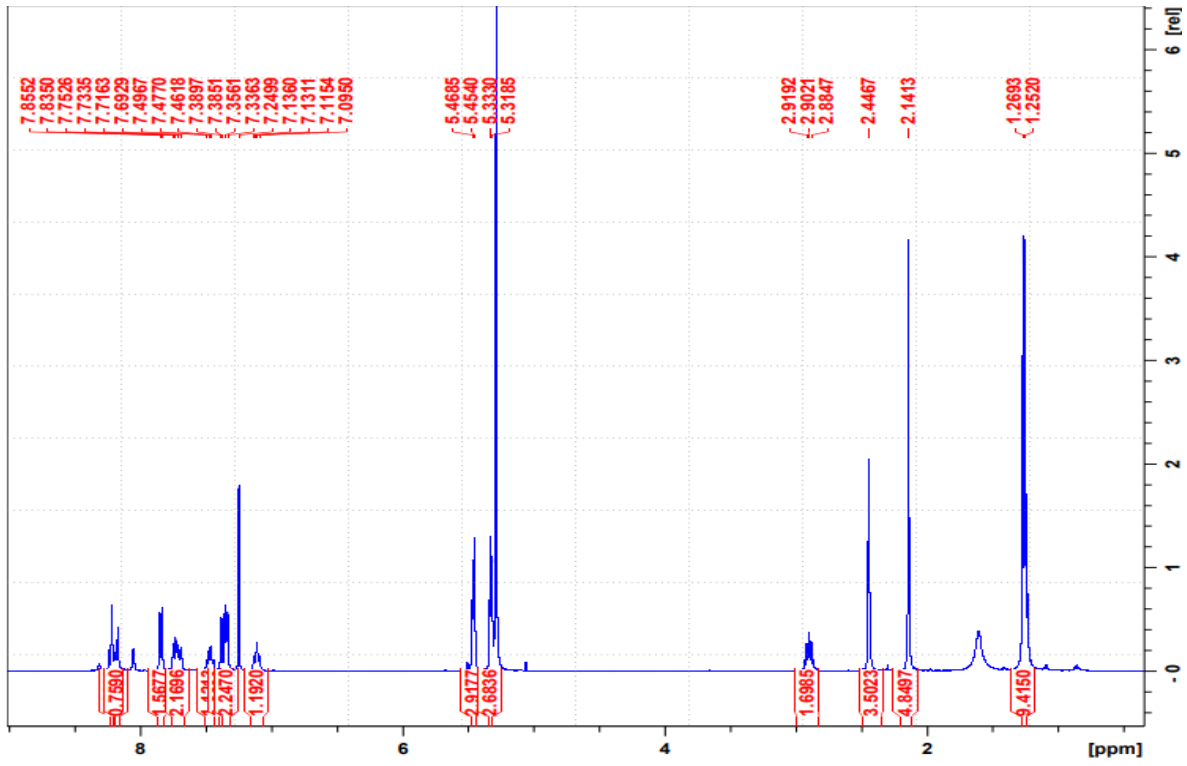
7.8552
7.8350
7.7526
7.7335
7.7163
7.6929
7.4967
7.4770
7.4618
7.3897
7.3851
7.3561
7.3363
7.2499
7.1360
7.1311
7.1154
7.0950
5.4685
5.4540
5.3330
5.3185
2.9192
2.9021
2.8847
2.4467
2.1413
1.2693
1.2520
0.7590
1.5677
2.1696
2.2470
1.1920
2.9177
2.6836
1.6985
3.5023
4.8497
9.4150
8
6
4
2
[ppm]
6 [rel]
5
4
3
2
1
-0

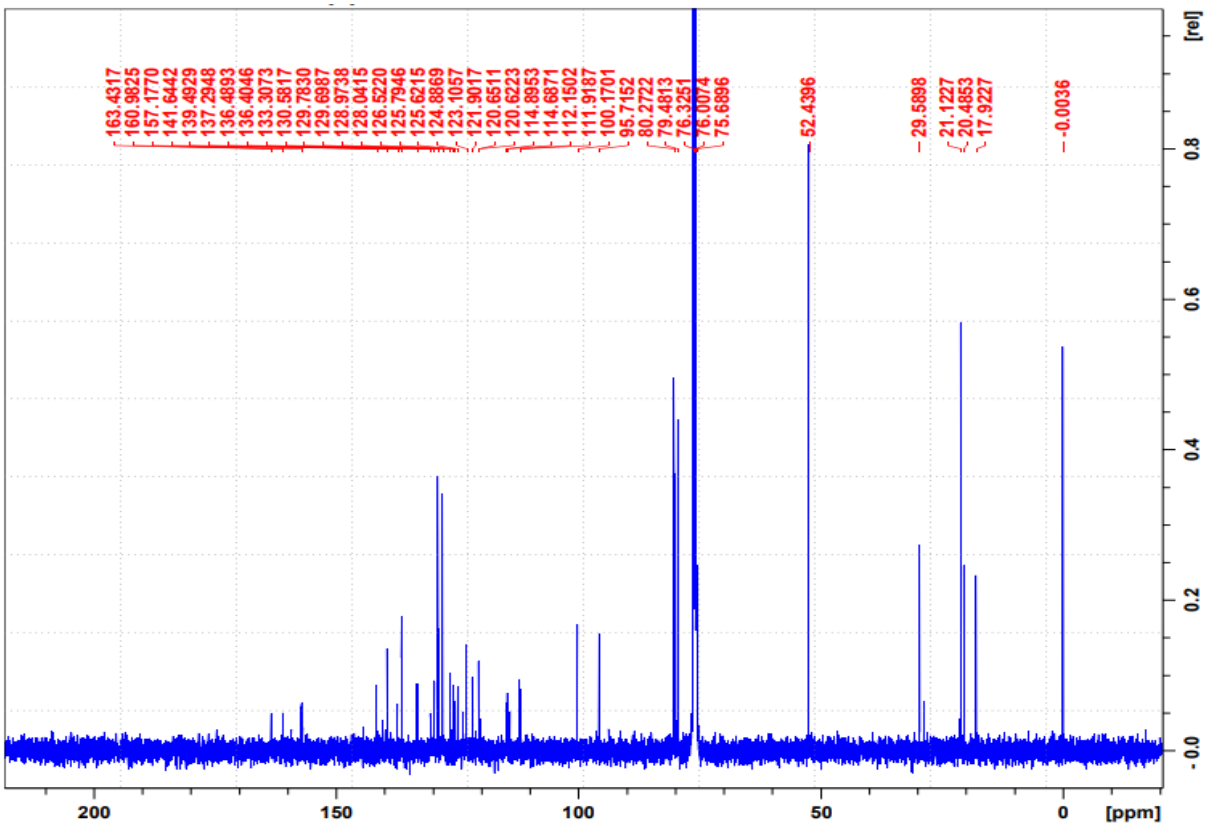

Figure 197. The ^{1}H NMR spectrum of compound **156 a**

Figure 198. The ^{13}C NMR spectrum of compound **156 a**

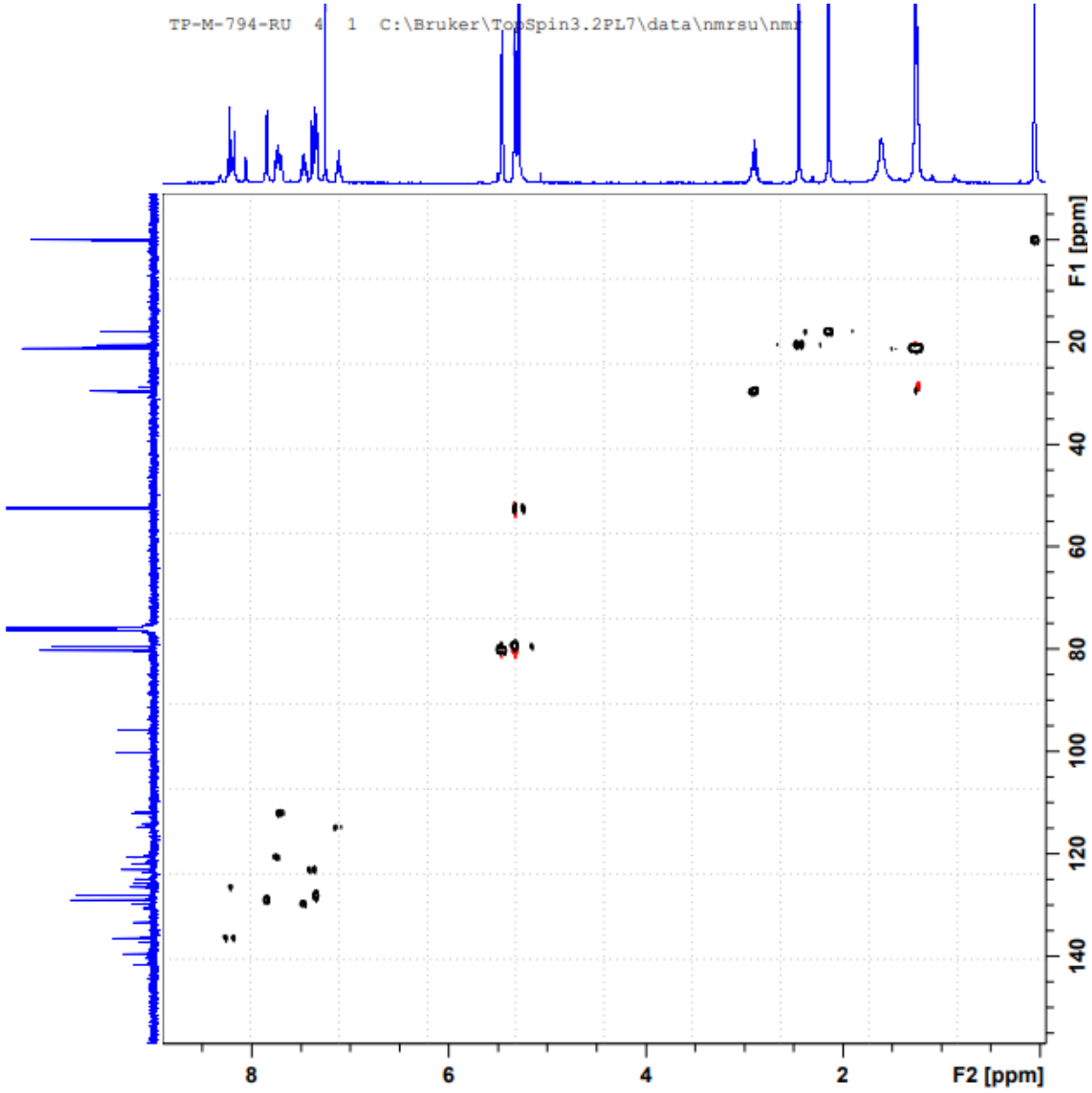

Figure 198. The HSQC spectrum of compound **156 a**

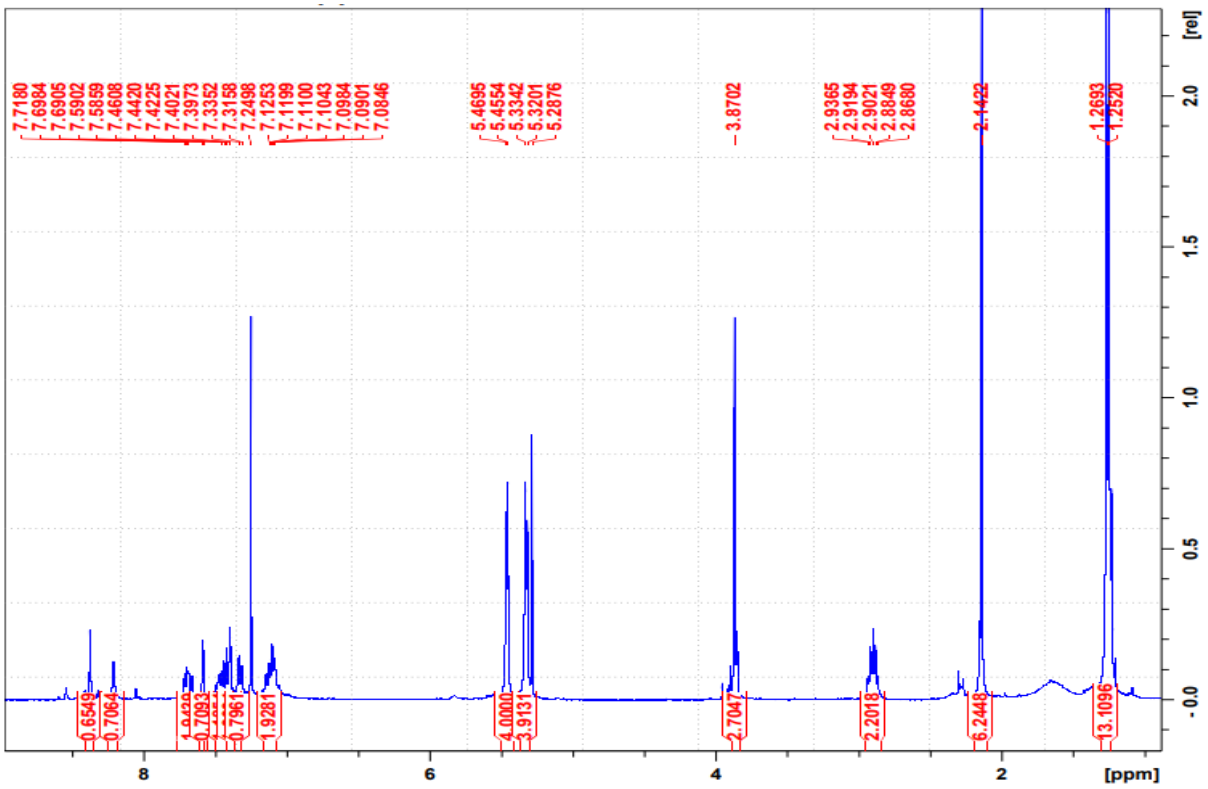

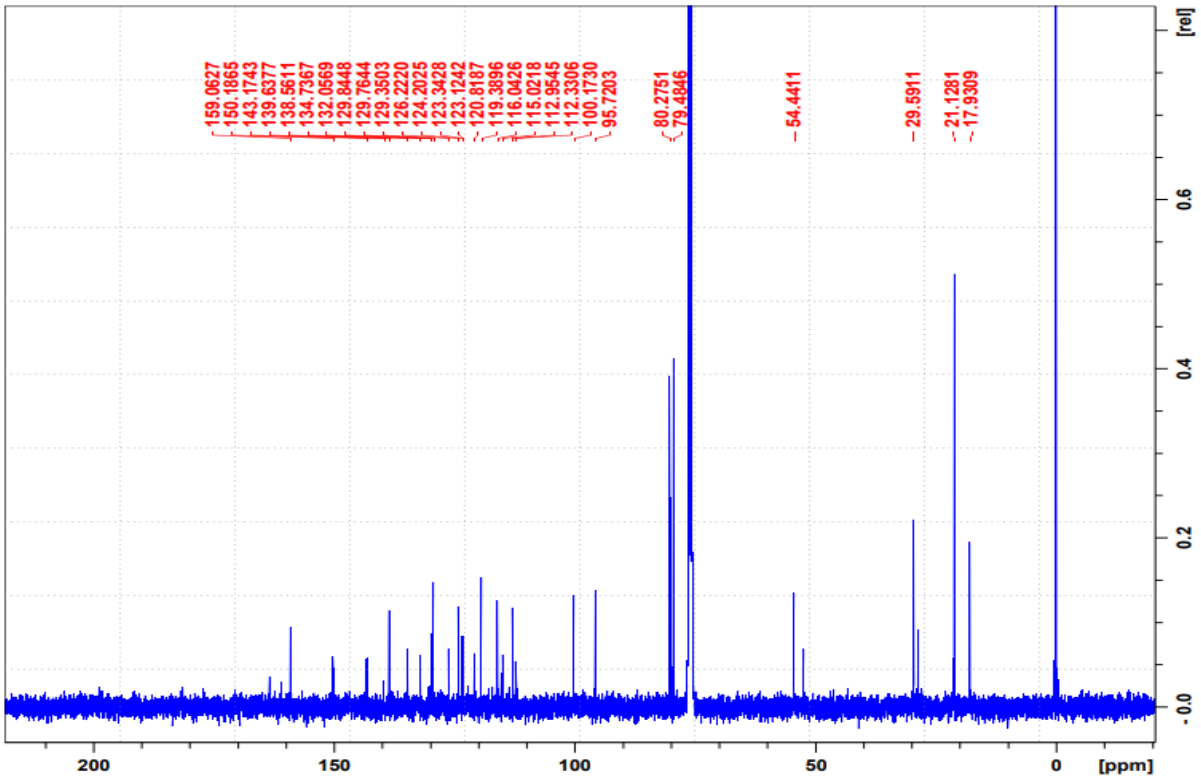

Figure 198. The ^{1}H NMR spectrum of compound **156 b**

Figure 199. The ^{13}C NMR spectrum of compound **156 b**

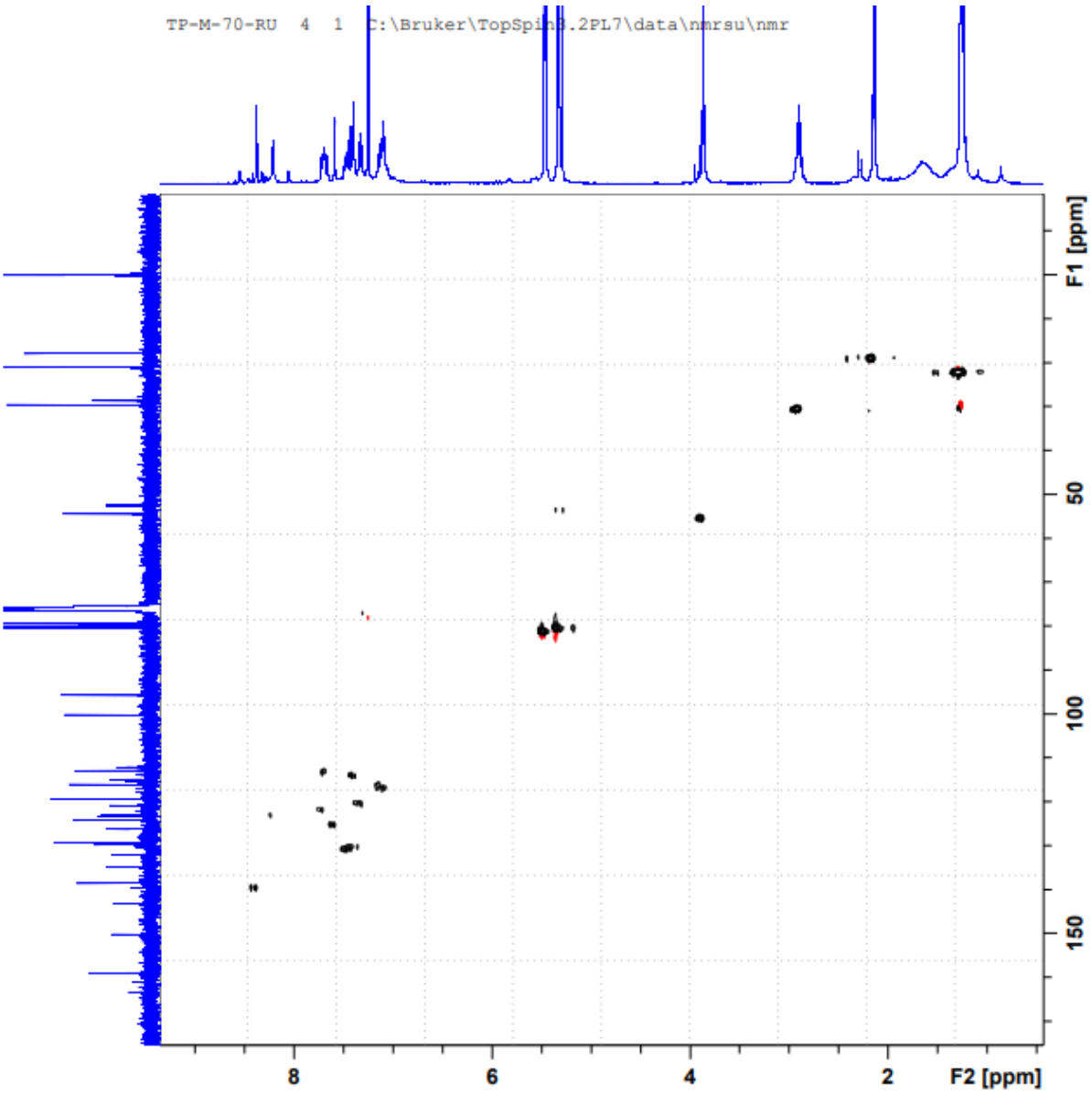

Figure 200. The HSQC spectrum of compound **156 b**